MODELLING SEAFARING IN IRON AGE ATLANTIC EUROPE

KARL SMITH

Kellogg College

Supervised by Rick Schulting & John Pouncett

A thesis submitted in two volumes in partial fulfilment of the requirements of Oxford University for the degree of Doctor of Philosophy.

Volume I

November 2020

Acknowledgements

I would like to thank the following people who made this thesis possible:

My supervisors John Pouncett and Rick Schulting, for their tireless help and support at every stage of the preparation of this thesis. My parents and grandparents Annette & Jaime Smith, John & Liv Mahlum, and Jim and Aida Smith, for their indefatigable support. Rachel Pope and Rich Mason, who share the blame with the rest of the PEN crew for introducing me to the British Iron Age. Emma Slayton, for her encouragement and support in building the navigation model. Beth Hodgett and Caroline Palmer, for monitoring simulations during my occasional absences from the computer lab. And my brother Calvin, for keeping me sane through the long, weird summer of 2020.

Abstract

The extent to which a European 'Atlantic Zone' was connected by maritime links in the Iron Age is debatable, as direct evidence is fragmentary and no accounts from contemporary inhabitants of Atlantic Europe survive. This thesis contributes to this debate by developing a new navigation model and deploying the model in the western English Channel. This thesis seeks to understand (1) whether proposed routes across the Channel would have been viable and whether other alternatives may have existed, (2) whether or not promontory forts could have been used as landmarks for navigator, and (3) how aspects of navigation – such as speed potential, landmarks, and ability to read conditions – may have affected Channel crossings. The model developed for this analysis is a fully agent-based model, in which simulated navigators follow a set of instructions without input from a human operator. A model that allows simulated ships to go off-course and potentially *not* reach their destinations can be used to evaluate routes in terms of risk and reliability.

The main analysis here consists of a comprehensive survey of simulated Channel crossings from March-September 2018. The results of this analysis suggest that crossings were most successful in brief windows, critique pre-existing schemes of Channel crossing, and evaluate whether certain coastal 'nodes' may have been more or less useful as points of departure across the Channel. Case studies focus on (1) the identification of a Continental node 'corresponding' to Hengistbury Head, and the potential of Guernsey as a 'staging port' for northbound voyages; (2) the connection between Iron Age settlements at Le Yaudet and Mount Batten, and the relative effects of parameter inputs to the model; and (3) the visibility of landmarks at the end of the Cornish and Breton

peninsulas. These results demonstrate the value of the model for future analysis and its potential for further development.

Table of Contents

Volume I

Acknowledgements **1**

Abstract **2**

Table of Contents **4**

Chapter 1: Introduction to Atlantic Europe **13**

1.1: Introduction 13

1.1.1: What is ‘Atlantic Europe’? 13

1.1.2: Iron Age Climate, Weather, and Sea Level in Atlantic Europe 15

1.2: Maritime Connectivity in Archaeological Literature 17

1.2.1: Developing Archaeological Perspectives 17

1.2.2: Establishing Maritime Links 19

1.2.3: Invasion, Migration, and Diffusion 22

1.2.4: From ‘Routes’ to ‘Approaches’ 24

1.3: Coastal Settlement in Atlantic Europe 28

1.3.1: Promontory forts as an ‘Atlantic Type’ 29

1.3.2: Promontory Fort Interpretation 31

1.3.3: Promontory Forts as Trading Sites 33

1.3.4: Promontory Forts as Sacred Places 35

1.3.5: Promontory Forts as ‘Theatres of the Sea’ 38

1.4: Research Questions 40

1.4.1: How Viable are Western Cross-Channel Routes? 40

1.4.2: Were Promontory Forts Landmarks? 41

1.4.3: How Did Navigation in the Western Channel Work? 43

1.5: Thesis Structure 44

Chapter 2: Seafaring and Navigation 47

2.1: Introduction 47

2.2: Iron Age Seagoing Ships 47

2.2.1: Ship Design in the Iron Age 48

2.2.2: Reconstruction and ‘Seaworthiness’ 49

2.2.3: Log Boats 50

2.2.4: Hide Boats 52

2.2.5: Plank Boats 55

2.2.6: Parameterising an Iron Age Seagoing Ship 58

2.3: Navigation in the Iron Age 60

2.3.1: Reconciling Definitions of ‘Navigation’ 60

2.3.2: Navigation and Pilotage as Sciences and Arts 61

2.3.3: Distinguishing Navigators from Seafarers 63

2.3.4: Dead Reckoning and ‘Natural Navigation’ 64

2.3.5: Navigation by Seas and Winds 65

2.3.6: Navigation by Natural Features 67

2.3.7: Navigation by Anthropogenic Features 69

2.3.8: Navigation by Animal Behaviour 70

2.3.9: Navigation by Celestial Bodies 73

2.3.10: An Iron Age Navigational Method 75

Chapter 3: Seafaring Models in Theory and Practice 77

3.1: Methods for Modelling Navigated Routes 77

3.1.1: Velocity Prediction Programs 77

3.1.2: Least Cost Path Analysis 78

3.1.3: Applying the LCP in Archaeological Analyses 80

3.1.4: Isochrone Modelling 81

3.1.5: Agent-based Modelling 83

3.2: Issues with Modelling Movement over Water 84

3.2.1: Integrating Four-Dimensional Data 85

3.2.2: Using Hydrodynamic Data as Proxies for Terrestrial Datasets 86

3.2.3: Building an Accumulated Cost Surface from Hydrodynamic Data . 88

3.2.4: Incorporating 'Qualitative Costs' 90

3.2.5: Optimality and Navigation 92

3.2.6: Agent-Based Modelling as an Alternative to ACS-Based Analysis 95

Chapter 4: Building the Navigation Model 97

4.1: Introduction 97

4.2: Inputs, Parameters, and Outputs 98

4.2.1: Model Inputs 99

4.2.2: Model Parameters 101

4.2.3: Model Outputs 103

4.3: Script Architecture 104

4.3.1: Stage 1 - Parameter Reading and Extraction 105

4.3.2: Stage 2 - Parameter 'Reckoning' 107

4.3.3: Stage 3 - Visibility Analysis 109

4.3.4: Stage 4 - Strategy Selection 113

4.3.5: Stage 5 - Heading Selection 114

4.3.6: Stage 6 - Path Calculation 117

4.3.7: Completion and Failure Conditions 117

Chapter 5: The Main Analysis (Western English Channel) 120

5.1: Introduction 120

5.2: Research Design: Parameter Survey 120

5.2.1: Parameter Sweeping 120

5.2.2: Description of Simulations 122

5.2.3: Ship Parameterisation 123

5.2.4: Landmark Selection 126

5.2.5: Constraints on Parameter Sweeping 129

5.3: Research Design: Study Area and Coastal Nodes 130

5.3.1: Coastal Nodes in the Western Channel 131

5.3.2: Identifying Coastal Nodes 132

5.3.3: Node-to-Node Path Distance Calculation 133

5.4: Research Design: Environmental Data 134

5.4.1: Environmental Data Gathering 135

5.4.2: Selecting Departure Times from Tide Data 137

5.5: Model Outputs and Data Processing 139

5.6: Main Analysis: Results 140

5.6.1: Speed and Success Rate as Criteria 141

5.6.2: Speed and Success Rate by Date 142

5.6.3: Speed and Success Rates by Node 146

5.6.4: Speed and Success Rates by Route 149

5.6.5: Track Density 151

5.6.6: Landmark Sightings 152

5.7: Main Analysis Discussion 154

5.7.1: Discussion of Sailed Routes 154

5.7.2: Discussion of Landmarks 157

5.7.3: Model Performance 158

Chapter 6: Case Study 1 (Hengistbury – Gulf of St. Malo) 159

6.1: Introduction 159

6.1.1: Archaeological Context 160

6.2: Analysis Results 160

6.2.1: Average Speed / Success Rates per Day 161

6.2.2: Average Speed / Success Rates per Node 162

6.2.3: Average Speed / Success Rates Per Route 163

6.2.4: Visibility Results 164

6.2.5: Vessel Parameterisation Results 165

6.2.6: 'Reckoning' Results 166

6.2.7: Track and Visibility Density Analysis 166

6.3: Discussion 168

6.3.1: Parameter Effects 168

6.3.2: Routes and Trading Links along the Hengistbury-St. Malo Axis .. 171

Chapter 7: Case Study 2 (Lannion – Plymouth) 173

7.1: Introduction 173

7.1.1: Archaeological Context 173

7.2: Results 175

7.2.1: Overall Average Speed / Success 175

7.2.2: Track Density Analysis 176

7.2.3: Landmark Visibility Analysis 178

7.2.4: Estimation Results 179

7.2.5: Leaving Time Results 180

7.2.6: Vessel Parameterisation Results 182

7.3: Discussion 183

7.3.1: Parameter Comparisons 184

7.3.2: Routes and Trading Links along the Plymouth-Lannion Axis 186

Chapter 8: Case Study 3 (Brest – Penzance) 190

8.1: Introduction 190

8.1.1: Archaeological Context 191

8.2: Results 194

8.2.1: Success Rates 196

8.2.2: Vessel Speed 197

8.2.3: Leaving Times 198

8.2.4: Visibility 199

8.2.5: Sailed Routes 201

8.3: Discussion 202

8.3.1: Different Routes for Bigger Ships? 203

8.3.2: Directionality and Landmarks 204

8.3.3: Conclusions 206

Chapter 9: Discussion 208

9.1: Research Questions and Answers 208

9.2: Interpreting Analysis Results 209

9.2.1: Cross-Channel Routes 209

9.2.2: Landmarks and Promontory Forts 213

9.2.3: Parameters and Outcomes: Temporal Parameters 215

9.2.4: Parameters and Outcomes: Parameterisation and 'Reckoning' 217

9.3: Future Research in the Channel 220

9.3.1: Improving Ship Parameterisations 220

9.3.2: Testing Coastal Routes 221

9.3.3: Landmark Identification and Visibility 222

9.3.4: Expanding Visibility Analyses of Promontory Forts 223

9.3.5: Casting a Wider Parameter Net 224

9.4: Future Development of the Navigation Model 226

9.4.1: Topographic and Environmental Data 226

9.4.2: Seakeeping and 'Failure Conditions' 230

9.4.3: Long-Range Planning and Embedded Simulations 231

9.4.4: Time to Wait and Rest 233

9.5: Concluding Remarks 234

Bibliography 236

Volume II

Table of Contents 1

List of Figures 2

Figures 6

List of Tables 75

Tables 76

Appendix I: Promontory Fort Catalogue 97

Appendix II: Natural Prominence Catalogue 117

Appendix III: Case Study 3 Simulation Plots.....171

Chapter 1 : Introduction to Atlantic Europe

1.1: Introduction

The western English Channel – the area for which simulations were performed in support of this study – is best understood as part of a set of interconnected waterways along Europe's western coast. Narratives of prehistoric movement, contact, and settlement have generally been focused on western Europe's Atlantic margin in its entirety rather than on a single component, a reasonable approach given the archaeological consensus that Atlantic waters served as a medium for inter-regional contacts throughout prehistory (see, for example: Bowen 1972; Cunliffe 2001; Henderson 2007). This chapter begins with an introduction to the 'Atlantic Zone' as a defined area and as an archaeological construct, and traces its genesis in archaeological literature. Promontory forts (also known as cliff castles, raths, duns, castros, and barred forts) are also discussed in this chapter, as they have been identified as an 'Atlantic' site type and form a large component of analyses for this study. The focus of this chapter is on archaeological literature – reviews of the geography and hydrology of the English Channel are reserved for Section 5.4. This chapter concludes with the presentation of the research questions addressed by this thesis, and a summary of its structure.

1.1.1: What is 'Atlantic Europe'?

Atlantic Europe is defined by the sea, but the definition itself is usually based on characterisation of the land. A strictly geographic definition of Atlantic Europe consists of watersheds draining into the Atlantic Ocean and its associated European waterbodies: the Norwegian Sea, the North Sea, the English Channel, the Irish / Celtic Seas, and the

Bay of Biscay. This area corresponds roughly with the 'temperate oceanic' described by the Köppen-Geiger classification system (Peel et al. 2007), with the exception of Iceland and southern Iberia. The 'Atlantic biogeographical region' defined by the European Environment Agency is based on these two data sources (see Figure 1.1). Archaeologists, however, have tended to define Atlantic Europe more narrowly, excluding areas draining into the Norwegian and North Seas and placing the border between 'Atlantic Europe' and 'Northern Europe' around northern Scotland and southeast England. In Christer Westerdahl's map of European 'coastal zones', the Atlantic Zone is divided into eight zones based on shipbuilding traditions and a methodology inspired by Braudel's *longue durée* (Westerdahl 2000, 13-14; see Braudel 1995, and Figure 1.2, left).[1] Meanwhile Jon Henderson's definition of Atlantic Europe follows the distribution of Iron Age settlement types, in that it excludes the 'hillfort dominated zone' in south-central England and the 'hillfort-dominated zone' in north-west England / south-east Scotland (Cunliffe 2005, 73-75, see Figure 1.2, right). There appears to be no universally-accepted definition of 'Atlantic Europe' in archaeological literature, and there is some debate as to the utility of the concept in general (see Henderson 2007, 21). Since the primary focus of this thesis is on waterways and coastal areas, the term is used here as a shorthand for: coastal areas in western Scotland and England, in Ireland, along the English Channel, along the coast of

[1] Or nine zones, including the northwest coast of Ireland. It is unclear whether southwestern Iberia and the inner Bay of Biscay are distinct zones. Coastal transport zones Figure 1.2 are, according to Westerdahl, "an expression of a kind of navigation which is 'hugging the coasts'" (2000, 15). He also envisions 'zones of the open sea', which are left unmapped (ibid.).

the Bay of Biscay, and along the coast of Galicia. This area provides the setting for the various theories of Iron Age coastal movement and settlement discussed in this chapter.

The coastline of Atlantic Europe is heavily indented. At a very large scale, the coastline is broken up by the Bay of Biscay, the English Channel, the Irish Sea, and the Celtic Seas. The headlands that are defined by these bodies of water are associated with the Caledonian and Cantabrian mountain systems and the Armorican and Galician massifs (Koster 2005, 4-6). Richard Bradley describes Atlantic Europe as "a series of projecting promontories of land linked by areas of sea" (1997, Fig. 2.1). At a smaller scale, portions of the Atlantic European coast are marked by a multitude of bays, coves, fjords, and other restricted waterways. In these areas coastal erosion has produced rocky, heavily-indented coastlines (Gómez-Pujol et al. 2014). The rocks of Atlantic Europe are particularly mineral-rich. Gold, copper, tin, iron and lead deposits are found in southern and central Atlantic Europe (see Figure 1.3), and the extraction and transportation of these minerals would have served as an impetus for sea travel within the waters of Atlantic Europe (Henderson 2007, 88).

1.1.2: Iron Age Climate, Weather, and Sea Level in Atlantic Europe

Atlantic Europe occupies a latitudinal range similar to the maritime Canadian provinces, yet experiences far milder winters than those portions of North America. Warmer conditions in Atlantic Europe are driven by the interaction of the North Atlantic Current (an extension of the Gulf Stream) with southwesterly winds that prevail within the region (see Seager et al. 2002). The winds that regulate climate along Europe's Atlantic coast also bring rain and stormy weather, which can be dangerous for ships under sail. Many passages along the Atlantic coast are still considered dangerous by modern

sailors; for Iron Age sailors using square rigs these waters would have been even more perilous in poor conditions (see Section 2.2.2).

By the end of the Iron Age, climate and weather conditions would have been slightly colder than those of today, by approximately 0.5 degrees Celsius (Henderson 2007, 38). The climate of Atlantic Europe was in flux throughout the Iron Age, as temperatures and precipitation rates recovered from a period of climate deterioration that occurred at the Late Bronze Age – Early Iron Age transition (see Bell 1996). The timing and scale of this 'deterioration' in particular regions of the Atlantic Zone is still a matter of debate (see, for example, Straker et al. 2012), but in general lower temperatures and more frequent rainfall would have become more common throughout the Atlantic Zone. It is possible that these climatological changes could have resulted in more stormy weather off the Atlantic coast (Lamb 1982, 144-5). Henderson speculates that if increased rainfall and lower temperatures did result in stormier weather it would help to explain the reduced contact between Atlantic Scotland and Continental Europe between 600-200 BC (2007, 38).

Maritime contact may have also been disrupted by marine transgressions over the course of the Iron Age. Sea levels are estimated to have risen by around one or two metres throughout the Atlantic Zone during the Iron Age, to a level approximately one metre lower than that of the present day (Turner 1981: 261-264). As with climatological changes, sea level rise differs by region within the Atlantic Zone (see Heyworth & Kidson 1982, Robinson 2007), and it is difficult to assess the degree to which rising sea levels would have affected maritime connectivity. Although estuaries and other potential harbours may have been affected by encroaching seas, the scale of this process is unlikely to have been sudden or cataclysmic. Given the likelihood that Iron Age mariners would

have been more than capable of launching and landing without formal waterside structures (McGrail 1998, 267-8), it seems likely that rising sea levels would have led to the selection or abandonment of specific landing or launching places rather a wholesale re-evaluation of maritime routes. Rising sea levels probably had a greater effect on coastal sites, many of which are under threat from coastal erosion today.

1.2: Maritime Connectivity in Archaeological Literature

This section traces archaeological interpretation of maritime contacts within Atlantic Europe from the inception of the discipline to the present day. Early work on the subject is generally pessimistic about the potential for prehistoric voyaging in general (Mackinder 1902), although mid 20th-century authors occasionally invoked prehistoric mariners in order to explain the movement of people and artefacts, especially across the English Channel (Crawford 1921; Fox 1959; Hawkes 1940, 1966). Reassessments in the latter half of the century produced a 'diffusionist' school of thought emphasising the potential for 'western seaways' as corridors easily accessible to prehistoric mariners (i.e. Crawford 1936; Bowen 1969, 1970, 1972). More recently, diffusionist theories have been incorporated into the wider 'Atlantic Façade' or 'Atlantic Zone' framework (see Cunliffe 2001), and have become the subject of criticism and calls for re-evaluation of the role of the seas in connecting and separating communities (Henderson 2007).

1.2.1: Developing Archaeological Perspectives

The first accounts of navigation in Atlantic Europe come from Classical sources. The earliest known descriptions of seafaring in the Channel are fragments from the *Massiliot Periplus*, which was written in the 6th Century BC and are believed to survive

in the 4th Century AD *Ora Maritima* (Hawkes 1977). Similarly, the voyages of the Greek sailor Pytheas around 325-320 BC were recorded in a now-lost periplus, and is known from later references in Strabo's *Geography* (1.4 & 7.3; see also Hawkes 1977) and Pliny's *Natural History* (4.30.16) in the 1st Century AD. Diodorus Siculus (5.21) and Pliny (*Natural History* 10.166, 4.104) also left accounts of coastal voyages in the Atlantic in the 1st Century, focused mainly on the sources of raw materials in the northern seas. These Classical authors were particularly interested in sources of tin, which were identified with Britain (see Section 1.1.1). The only first-hand account of seafaring in Atlantic Europe comes from Caesar, who described the ships of the Armorican Veneti and complimented their seamanship and navigational skill (*The Gallic War* 3.8-3.13). Caesar also mentions that the Gallic *Belgae* had crossed the Channel and settled in Britain (*The Gallic War* 2.14). These comments by classical authors – particularly Caesar's account of the *Belgae* – had a profound effect on antiquarian and early archaeological conceptions of movement along western Europe's Atlantic seaboard.

As archaeology developed into a scientific discipline around the turn of the 20th century, it drew theories and frameworks from adjacent fields in order to explain the distribution of archaeological material on either side of the Channel. Mackinder's *Britain and the British Seas* (1902) is ambivalent about whether the 'Narrow Seas' between Britain and the Continent encourages or prevents travel between the two shores, claiming that on one hand that "Narrow Seas are the strong natural frontier of Britain, but at all times they have been freely traversed, and the islanders have been neighboured by the peoples of the opposite shore", and on the other that "it is, however, not infrequently suggested that they [British people] have lost by the seas which have held them apart from one another and impeded fusion." (1902, 15-17). The balance of opinion in *Britain and*

the British Seas is that the waterways surrounding Britain have acted as barriers. In some cases the conclusions that Mackinder is driven to are contradictory. For example Mackinder argues that the strait between Scotland and Ireland ensures the 'insulation' of the latter (1902, 21), despite the strong linguistic and historical connections that exist between the two. Likewise, the margins of Brittany are described as "a broken, dangerous coast, though one full of harbours", similar to Cornwall in that they are "peopled by the same Celtic race, driven to bay at the land's end" (1902, 19). Mackinder casts the sea as both the entryway into Britain and an extension of its 'frontier', and as a barrier to entry that is only navigated by people under some sort of external pressure.

The ambivalence apparent in *Britain and the British Seas* likely stems from the historical context in which the work was written. Writing at the beginning of the 1900s, Mackinder's view of history over the past century would have been dominated by global, maritime empires for which the movement of goods by sea was both laden with risk and absolutely essential. Victorians were preoccupied with the dangers of seafaring despite (or perhaps because of) the important role that it played in the maintenance of their society (Wooding 1996, 3). Meanwhile, Henderson (2007, 12) argues that antiquarians' high regard for the Roman Empire – ostensibly a 'land-based power' – resulted in a focus on terrestrial links as a result. Insofar as prehistoric sea voyages were considered by antiquarians and early archaeologists they were imagined to be brief trips across the narrowest straits, rather than long voyages.

1.2.2: Establishing Maritime Links

The characterisation of sea travel in the remote past as a dangerous alternative to terrestrial movement persisted beyond the development of archaeological methods. The

publication of 'The Distribution of Early Bronze Age Settlement in Britain' by Crawford in 1912 – credited as the earliest paper suggesting prehistoric overseas routes connecting western Britain with the Continent – places emphasis on overland routes and portages as part of a system of movement that includes passages in the Irish Sea and the Channel. In arguing against an overland route across Cornwall, for example, he assumes that the peninsula "would not have been rounded by early navigators without sufficient cause" (1912, 197). Crawford's particular interest was in the distribution of golden *lunulae* in the British Isles and further south, and in this context he identified the harbours at Cherbourg, Weymouth, Christchurch and Southampton as potential points of departure across the Channel (1912, 197). In a later article, Crawford asserts that although the presence of Continental artefacts at British sites is not necessarily evidence of trade, "they may legitimately be used as evidence of intercourse, and the circumstance of their discovery seems to imply that the intercourse was peaceful" (1913, 643). Contemporary work on Bronze-Age artefacts by Breuil in the Paris Basin also focused more on distribution of material as evidence for movement than on the mechanisms driving that movement.[2] Excavations at Hengistbury Head (near Christchurch) by Bushe-Fox in 1911 and 1912 produced ceramics with "continental parallels", which led Bushe-Fox to interpret the site as a maritime port based on the quantity of these imported ceramics (1915, 9).

During the interwar years emphasis began to shift away from peaceful trade as an explanation for the apparent movement of artefacts within Atlantic Europe. A further

[2] Published in a series of papers entitled "L'âge du bronze dans le bassin de Paris" in the journal *Archaeologie*, 1900-1909.

publication by Crawford in 1921 attributed the Llyn Fawr hoard to Celtic invaders from the Alps (Wheeler 1921, 191-2). By the 1930s, the concept of 'culture' in archaeology led to more frequent identifications between groups of materials and people with which they associated (see Childe 1930). Archaeologists considering maritime routes in the Channel during the 1930s were largely concerned with their potential relationship to the 'Belgic invasion' of Britain mentioned by Caesar in *The Gallic War* (2.14; see Bushe-Fox 1925, Hawkes & Dunning 1930). Meanwhile, the extensive expeditions of Sir Mortimer Wheeler and Katherine Richardson in 1936-9 in Normandy and Brittany, while firmly anchored in Classical narratives of invasion, provided clear archaeological evidence for parallels between the promontory forts of south-western Britain and north-western France (see Section 1.3). Writing of the reported inhabitants of Brittany during the Gallic Wars, Wheeler and Richardson state that the "intimate relationship between the Veneti and the accessible parts of Britain in the pre-Caesarian era, combined with the similar topography of the Cornish and Breton coasts, provides the perfect context for that identity of habitat and fortification which the archaeological evidence has demonstrated" (1957, 7). The focus on invasion and migration as a means of introducing material and ideas to the British Isles in turn had lasting effects on the interpretation of sites along Britain's Atlantic coastline.

Sir Cyril Fox's *The Personality of Britain* (1959) contained the first published map of potential prehistoric sea-routes around the British Isles (see Figure 1.4). Fox's distinction between 'Continental' and 'Atlantic' routes followed Mackinder's division of the English Channel into western and eastern zones – Fox placed the boundary between the two at the Bill of Portland. Fox's routes generally favoured overland passages through promontories rather than voyages around them – Cornwall, Pembrokeshire, and the Llyn

Peninsula are all depicted in Figure 1.4 as starting / ending points for contact rather than as points along a longer route. A map of 'western sea routes' published by Crawford in 1936 also shows a clear preference towards short crossings, to the point that the route from Calais to St. George's Channel involves an overland route from a tributary of the Thames (Figure 1.5). This skepticism survives in more recent work by R. Davis (1997), who argues that crossings of the English Channel west of Normandy would have been prohibitively difficult for Iron Age ships (see Section 2.2.6).

1.2.3: Invasion, Migration, and Diffusion

Concerns about the possibility of overseas travel faded as more archaeological evidence was compiled. Evidence in support of maritime contact included the discovery of Iron Age boats at Brigg, Hasholme, and Hjortspring (McGrail 2001, 172-178; see Sections 2.2.3 & 2.2.5). The compilation of new archaeological material into large-scale distribution maps was also used to challenge views of the seas as barriers to movement. The maps constructed by Crawford, Childe, and Fox were based primarily on the distribution of artefacts (combined with some consideration of the 'natural' paths across waterways). Since these authors inferred the movement of people between Britain and the Continent from the distribution of artefacts, changes in material culture were taken to indicate periods of disruption or invasion (Fox 1959). The shift from 'invasion' to 'migration' in the work of Hawkes (1931, 1942, 1959) opened up the possibility of (relatively) peaceful exchange while continuing to treat new materials and ideas as foreign innovations introduced to the British Isles from outside. Childe also subscribed to the invasion hypothesis in *Prehistoric Communities of the British Isles*, but described

a series of small invasions along "devious routes" rather than a few larger invasions across the Strait of Dover (Childe 1940, 228; Wilkes 2004, 42).

By the 1970s, both 'migration/invasion' theories and 'sea as a barrier' theories were beginning to show cracks. It was the latter that began to collapse first, resulting in a flood of scholarship emphasizing the role of overseas travel in distributing ideas and material. The recognition that seaways (as they were termed) could have been viable routes was still rooted in contemporary theories of migration and displacement (see Henderson 2007, 18-19), and also looked to artefact distributions as the ultimate source of evidence for maritime trade. In a paper delivered to the Cambrian Society's 'The Irish Sea Province in Archaeology and History' conference in 1970, Bowen wrote that "it is important to realize that our increased knowledge of the use of the seaways has been acquired not so much from archaeological excavation, but by the mapping of the location of archaeological finds and sites on an extensive scale" (1970, 13). In a series of other works (Bowen 1969, 1972, 1977), Bowen expanded Crawford's conception of the 'western seaways' to include the entirety of the European Atlantic coast from Shetland to Galicia (Bowen 1970; see Figure 1.6). Bowen constructed these dense networks of routes based on distributions of material throughout Atlantic Europe. This approach to mobility turned Mackenzie's approach to movement on its head – Bowen argued that "no longer does the sea divide and the land unite; the seas unite the lands around their shores, while the mountains and boglands of inland territories divide one culture from another" (1970, 14). Bowen's formulation of the western seaways adhered to Hawkes' 'ABC' system for interpreting Iron Age sites that was itself based in invasion theories that were already undergoing re-evaluation (c.f. Clark 1966, Hawkes 1966).

If we accept that the events of the early 20th century influenced invasion and migration theory, then it is equally likely that developments in the post-war world affected the subsequent development of diffusionist theory. Radio communication and radiolocation were quickly and widely adopted during the Second World War (when radar stations would be built on many of the coastal sites discussed here), and the ability to locate and communicate with ships at sea at further distances from the coast improved their ability to navigate. The debut of the first numerical weather forecasts in the 1950s (Harper et al. 2007) also reduced the chances of ships being surprised by foul weather. These innovations had lasting effects on the practice of navigation (discussed in Chapter 2). The work of Bowen and other diffusionists (see for example Hawkes 1940, Alcock 1963; Lewis 1958 in the context of early Medieval voyages) were less concerned with the circumstances – weather, wind, crews, etc. – or theoretical context of maritime travel than with the delineation of the routes themselves. At the time, there were good grounds for optimism when considering the capabilities of prehistoric mariners: new evidence from wreck sites revealed that prehistoric ships were more capable than previously thought (see Section 2.2), while the work of anthropologists and experimental archaeologists in the Pacific (i.e. Malinowski 1922, Heyerdahl 1950) likely inspired optimistic evaluations of the capabilities of ancient mariners. In his 1970 paper, Bowen triumphantly invoked Childe's claim that "We may picture these grey seas as bright with Neolithic Argonauts as the western Pacific is today" (Childe 1946, 36).

1.2.4: From 'Routes' to 'Approaches'

Wider developments in Iron Age studies over the next several decades did little to challenge or confirm the existence of maritime routes in the 'western seaways'. In

terms of trade and exchange, the development of core-periphery models and reactions against them (cf. Kristiansen et al. 1987; Renfrew & Cherry 1986) made useful contributions to the debate over the nature of prehistoric maritime contact without being overly concerned about where routes of contact may have been. Henderson notes that the development of processual archaeology "by its very nature did little to further the 'western seaways' debate" (2007, 20), as archaeologists became more open to attributing archaeological changes to local innovation and less focused on diffusionist frameworks. Although discussion of specific routes continued (see Cunliffe 1978, 1982, 1983, 1987, 1988, 1990, 1992, 1997; McGrail 1983; Cunliffe & Galliou 2000; Burns et al. 1996; Cunliffe & de Jersey 1997; Cunliffe et al. 2004-2007; Cunliffe 2015), the role of 'Atlantic Seaways' in linking the shores of western Europe was minimised in processual studies, which tended to focus on specific parts of the Atlantic Zone. Noel Fojut's 1982 "geography of Shetland Brochs" is a good example of this type of regional study. Fojut played down the effects of contact on Iron Age Shetland, and argued that the coastal location of brochs followed the coastal distribution of arable land (which, in turn, he attributed to increased peat formation over the course of the Iron Age (1982, 42-43)). Fojut argued that brochs served as foci for "small communities, often in isolated areas, making the most of their local resources and occasionally indulging in trade for luxuries or scarce goods" (1982, 52). Similarly, the study of maritime links was not high on the list of priorities enumerated by post-processual archaeologists. While post-processual emphasis on individual engagement with archaeological places and materials has been hugely influential in developing new perspectives on landscapes and sites (see Section 1.3.4), this theoretical turn prompted little discussion of the 'western seaways'. Whereas debates over terrestrial movement have continued throughout (c.f. Stančič et al. 1995,

Llobera 2000, Tilley 2010), the character of purported voyages in Atlantic Europe has not attracted much attention.

There are several exceptions to the trend away from large-scale studies of prehistoric maritime mobility in Western Europe, besides McGrail's aforementioned paper on Channel crossings. Cunliffe's 2001 book *Facing the Ocean* represents a hugely important synthesis, incorporating evidence from the end of the Ice Age to the 16th Century. Cunliffe argues for a view of western Europe's coastline as an 'Atlantic Façade' – a term proposed originally in a 1963 paper by Pierre-Roland Giot, who used it to define a deliberately vague area ("une zone à délimitation floue et fluctuante" (1963, 3)) consisting of Atlantic Europe and portions of the Western Mediterranean. The terms 'Atlantic Façade' and 'Atlantic Zone' became heavily identified with the Iron Age Atlantic through Cunliffe's work (Cunliffe 1997, James 1999). Cunliffe's formulation of Iron Age seaways in *Facing the Ocean* focuses on coastal 'nodes' such as Dublin Bay while leaving the connections between these nodes open-ended (2001, 61-2). Cunliffe's focus on coastal 'nodes' carries on in the work of Eileen Wilkes in identifying coastal nodes in southern England (2004, 2007), and prehistoric landing places (Bradley et al. 2016). Cunliffe suggests specific routes within smaller geographic contexts (i.e. 2001, 54), but characterises the Atlantic Zone as a whole in terms of 'approaches' and 'corridors', while suggesting specific routes only in the context of particular sites or coastlines (2001, 349-404).[3] In the maps reproduced in Figure 1.7, Cunliffe (and John Koch) distinguish between routes and general zones of exchange; their 'cognitive

[3] This approach reflects the characterisation of Bronze Age seaways as nested zones developed by Brun (1991).

geography' replaces routes with 'approaches' to 'narrowing seas' (Cunliffe & Koch 2010, Fig. 1.4).

The widespread acceptance of the Atlantic Zone in archaeological literature is possibly due to its vague formulation, which allows it to accommodate different interpretations of maritime contact. To start with, the use of the term 'corridor' rather than 'route' avoids arguing for *direct* long-distance contact while leaving a door open for the possibility that long-distance voyages may have taken place. Whether the existence of an "interlocking chain of contacts" (Waddell 1991, 29) in the Iron Age Atlantic is functionally different to the long-distance connections proposed by diffusionist scholars remains a matter of debate (Wooding 1996). The term 'façade' can also be read in different ways depending on one's perspective. For those that 'look in' at Europe the concept of a façade implies a collection of architectural elements organised around a single theme and structure, whereas for those 'looking out' at the Atlantic the term signifies elements that are exterior to the structure and may be purely decorative (see Henderson 2007, 25).

Jon Henderson's *The Atlantic Iron Age* (2007) stands out in recent literature for its criticism of the 'Atlantic Zone' framework. Henderson describes the book as an attempt "to bridge the gap between the macro-diffusionist scale and more geographically limited processualist studies" (2007, 22) by comparing analyses at different spatial and temporal scales – an approach that has inspired the design of this research programme. Henderson places particular emphasis on the creation of local and regional identities in Iron Age Atlantic Europe through the construction and adaptation of settlements. He argues that discontinuities in material culture and settlement types between parts of the Atlantic Zone constitute evidence for lack of contact between these areas. In *The Atlantic*

Iron Age the development of Atlantic maritime contacts over the course of the Iron Age is characterised as (1) a reorganisation following the collapse of Bronze Age exchange networks, (2) decrease in contacts between 'inner' and 'outer' Atlantic Zones following the development of 'hillfort dominated zones' in eastern Scotland, north Wales, and south-central England around 600 BC, and (3) the resumption of inter-Zone contacts in the Late Iron Age, with Armorica serving as a 'gateway' to the British Isles (2007, 285-8; see Figure 1.8).

1.3: Coastal Settlement in Atlantic Europe

Coastal settlement in Atlantic Europe took many forms and types. In Britain, most of the Atlantic Zone falls within Cunliffe's zone of 'strongly defended homesteads', which he identifies with Cornwall, Devon, western Wales and the northern and western coasts of Scotland (2005, 74). Henderson's boundary for Atlantic Europe in Figure 1.2 appears to follow the boundaries of this zone. If the entirety of the English Channel is included, then the Atlantic Zone also encompasses Cunliffe's 'hillfort dominated zone', which stretches from northern Wales to Dorset and Kent (ibid.). Iron Age settlements along the Atlantic coast tend to take the form of small, defended sites – *castros* in northern Spain (Fanjul Peraza 2004), 'cliff castles' in Cornwall and Wales (Sharpe 1992; Herring 1994, 2000), raths and duns in Scotland and Ireland (Lamb 1980; Ralston 1980; Raftery 1994; Redmond 1995; Cotter 2000), and *éperons barré* in northwest France (Wheeler & Richardson 1957; Bender 1986, Maguer 1996). Larger promontory forts are scattered throughout Atlantic Europe, but are especially well-represented in the inner reaches of the English Channel (see Wheeler & Richardson 1957; Cunliffe 1978, 1988, 2015).

As this study is primarily concerned with prehistoric navigation, coastal settlements are crucial in that they may have been places of departure or arrival, and insofar as they may have been used as landmarks. Rather than attempting a detailed review of coastal settlement within Atlantic Europe (for which see Henderson 2007), the following section focuses on a particular site-type – the coastal promontory fort. These sites are likely candidates for all of the functions described above, and are found throughout the Atlantic Zone. Their obscurity in archaeological literature relative to inland sites provides an opportunity to contextualise their landscape setting through maritime-based assessment (see analyses in Chapters 5-8).

1.3.1: Promontory forts as an 'Atlantic Type'

Promontory forts are also referred to as 'raths', 'duns', 'castros', 'cliff castles', and 'barred forts'. Unlike other settlement site-types associated with the Atlantic Iron Age, promontory forts can be found throughout the Atlantic Zone (Cunliffe 2001, 362; see Figure 1.9).[4] Whereas the distribution of brochs, wheelhouses, and souterrains is confined to particular parts of the Atlantic Zone (see Henderson 2007), promontory forts are found along the coasts of Atlantic Europe from Shetland to northern Portugal (Lamb 1980; see Henderson 2007, 151; *ibid*. 242). Promontory forts are found both on coastlines and further inland (see Figure 1.10) – for the sake of convenience the term 'promontory fort' is used to refer specifically to the coastal variety in this study. Promontory forts are defined by the Royal Commission of Ancient and Historic Monuments as enclosures "formed by erection of defences across the landward end of a promontory" (RCAHMS

[4] Cunliffe also identifies *chevaux-de-frise* as found throughout the Atlantic Zone (2001, 362).

1988, 30). Relatively few promontory forts have been excavated, so dating them is problematic. Based on artefact scatters, comparisons with other sites, and the few radiocarbon dates available, it appears that the earthworks that delimit promontory forts date to the Iron Age – except in the case of western Ireland, where these sites are Medieval (Cotter 2000). Some Iron Age promontory forts may also have earlier origins (see Section 1.3.4). Like hillforts, promontory forts vary widely in their size and complexity. The area enclosed by earthworks in promontory forts varies considerably – a few are larger than 100 hectares but the majority of promontory forts enclose fewer than 10 hectares' worth of headland.[5] Separation from the mainland is achieved in some cases by a single ditch and bank, in others by multivallate systems of earthworks, and in others by built structures (see Figure 1.11). The scale of earthworks range from small banks across narrow approaches to impressive ramparts and stone-cut ditches. Different rates of erosion along the coastlines where promontory forts are found make it estimating the *original* size of some promontory forts difficult without detailed documentation or geological analysis (see Pollard et al. 2020).

Although promontory forts are located throughout the Atlantic Zone, using that distribution as evidence for maritime contact is problematic. The existence of promontory forts as a site type at all is questionable, given the wide variety in their construction, layout, and setting (see Sharpe 1992, Nowakowski 2011, 39). As Henderson points out, the concept of separating the tip of a promontory from the mainland is equally likely to have originated within communities as to have been introduced from elsewhere (2017, 128). Furthermore, the category of 'promontory fort' encompasses both coastal sites and

[5] For examples in the English Channel, see Appendix I.

'inland promontory forts', which are located mainly along inland river systems. Although trade need not have occurred at the coastline, the grouping of coastal promontory forts with similar sites situated much farther inland makes it more difficult to classify this type of site as necessarily involved in maritime trade. If we restrict ourselves to 'coastal promontory forts', however, several problems remain. First of all, very little direct evidence for trade has been recovered from the vast majority of known coastal promontory forts. Ceramic evidence is limited in Ireland, Wales, and southern Scotland for the Iron Age (Haselgrove & Pope 2007; Haselgrove & Moore 2007), which restricts the formulation of chronologies for these areas and consequently the interpretation of promontory forts (Cunliffe 2005, 120).

1.3.2: Promontory Fort Interpretation

The development of archaeological interpretations of promontory forts has followed a similar path to interpretations of maritime trade in the Atlantic Zone. This section reviews how early interpretations of promontory forts as redoubts built to repel pirates and/or foreign invaders have been challenged by theories that integrate these sites into wider economic frameworks, and by interpretative methods that prioritise individuals' experiences at / interactions with sites (see below, but cf. Wheeler & Richardson 1957, 4-8; Cunliffe & de Jersey 1997; Giles & Cripps 2012). It is likely that promontory forts were built for a variety of reasons and served multiple roles in the lives of the people that interacted with them. However a good understanding of the roles that these sites *may* have played – one of the projects of this study – has the potential to serve as the basis for further investigation of the site-type.

Early interpretation of promontory forts followed Classical sources closely, particularly the first-century BC accounts of Julius Caesar and Diodorus Siculus' *Library of History* (5.19-40). In the first case, Caesar mentions settlements on promontories in the context of military campaigns against the Veneti people in Brittany, and claims that their 'oppidae' were "placed at the furthest end of tongues [of land] and promontories" (*The Gallic War* 3.12.1). Caesar goes on to describe how the Romans struggled to besiege these strongholds only for their victims to escape in ships to another promontory. The identification of promontory forts *as* forts based on this testimony was applied to sites on either side of the Channel. As more promontory forts were excavated and dated, the project of interpreting them became a project of identifying the people who had 'brought' them there. For example Aileen Fox, in a 1958 paper, notes similarities between hillforts and promontory forts in Cornwall and northern Spain and conjectures whether these similarities could be explained by a migration event from the Iberia following the Roman conquest of the peninsula (Frere et al. 1961, 53). Although Fox also posits that these similarities may reflect similar responses to the Atlantic climates of southern Britain and northern Spain, she identifies the former as "probably of Atlantic origin" (Frere et al. 1961, 55). The presence of promontory forts in Atlantic Scotland was, similarly, held to be the result of subsequent migration from the English southwest (Lamb 1980, 69). Whereas Fox's Iron Age migrants were characterised as refugees or merchants, other scholars adopted a much more militaristic view, which in turn influenced their interpretations of promontory forts. In a paper on the origins of Welsh hillforts published in 1971, for example, E.H. Savory asserted that "in Central Europe ... we can find a tradition of military earthwork building in the Bronze Age, the normal expression of which is the promontory fort" (1971, 259). Meanwhile, other archaeologists rejected

promontory forts as evidence of migration from the continent while continuing to stress their defensive potential. For example Paul Ashbee describes promontory forts in the Isles of Scilly as "defended areas, dominating separate tracts of land" that "could well reflect the bellicose territoriality of indigenous early Scillonians" (Ashbee 1974, 293). Autochthonous or not, the interpretation of promontory forts as defensive structures is durable and persists to the present day.

1.3.3: Promontory Forts as Trading Sites

A second strand of Classical sources used to contextualise promontory forts identify Britain as a source of tin that was carried across the Channel by Gallic merchant-ships. Diodorus Siculus, in an account believed to be based on that of Pytheas, identifies the source of British tin as a tidal island near an 'ἀκρωτήριον' ('promontory') called 'Belerion' (*Library of History* 5.21-22). It is difficult to establish the scale implied by the word 'ἀκρωτήριον' (which indicates a 'highest point' or 'extremity', and can indicate either a promontory or a peninsula), although the general consensus has been to identify it with Cornwall in general (see Penhallurick 1986). The identification of 'Belerion' with Cornwall is described in more detail in Chapter 8. Although the site that Diodorus describes in his account is not as clearly identifiable with promontory forts as the same from Caesar's account, his location of the source of tin on the coast rather than further inland cemented their association with trans-Channel trade in the minds of early archaeologists. Promontory forts became identified as 'gateway communities' (Hirth 1978) involved in the transport of goods between developed areas further inland. Curiously, these interpretations stressed the importance of promontory forts as centres of

trade whilst maintaining a conception of coastal areas as a 'hinterland' – connected to yet remote from the Classical world.

Relatively few coastal promontory forts have been excavated to date, and as such the evaluation – and dating – of these sites is often based on stray finds and comparisons to similar sites (see Henderson 2007, 131-2). As more promontory forts have been surveyed and excavated, however, the blanket interpretation of promontory forts as emporia has become more difficult to support. More recent excavations of smaller promontory forts have failed to find direct evidence for long-distance trade, and have tended to see these sites as integrated with local economic systems rather than as 'gateways'. Excavations at Maen Castle, at Land's End, found that the site was integrated with Iron Age field systems (Herring 1994). At Porth y Rhaw, Pembrokeshire, Crane and Murphy suggest that the promontory fort was "at least as densely occupied" as inland sites during the Early and Middle Iron Age, and that the Late Iron Age hiatus observed at Porth y Rhaw echoes results from these other sites (Crane & Murphy 2010, 91, see also Mytum 2013). In a later paper, Ken Murphy argues that the results of the aforementioned excavations at Trevelgue Head and Porth y Rhaw, in addition to results from Dale Head, Pembrokeshire (Benson & Williams 1987) and Baròna, Galicia (Martens & Carrión Marco 2011) suggest that "a specialised economy may have been a feature of these sites, with the inhabitants controlling and using coastal and maritime resources as well as inland agricultural land" (2018). In this case the function of promontory forts may not have been too different to that of hillforts.

There is some direct evidence for metal production and long distance trade at some Iron Age promontory forts. Excavations at Hengistbury Head and Le Yaudet, in particular, produced clear ceramic evidence that these sites were involved in cross-

Channel trade (Cunliffe et al. 2004-2007, Cunliffe & Galliou 2000, 2016). Excavations at Mount Batten and St. Michael's Mount found less overwhelming ceramic evidence (a single non-local sherd in both cases), but also resulted in the recovery of metal ingots, suggesting that they were at least involved in the production and aggregation of resources (Cunliffe 1988, Herring 2000). Similarly, a reanalysis of the results of the 1939 excavations at Trevelgue Head on Cornwall's north coast found evidence of 'non-local' ceramics and glasswork, as well as for on-site production of iron ingots – possibly for export (Nowakowski 2011, 391). Evidence for tin production at Land's End in the 3rd and 4th centuries AD has been found at Botallack Head, approximately 1.5 kilometres from the promontory fort at Kenidjack Castle (Lawson-Jones 2013). While metal production at coastal sites is not necessarily evidence that trade took place, it at least suggests trade as a possibility at these sites.

1.3.4: Promontory Forts as Sacred Places

In Cornwall in particular, increased attention to smaller groups of promontory forts (in particular Russel 1971) has called attention to the variability in promontory forts' size and landscape setting.[6] The differences between sites has been grounds for skepticism of interpretations of promontory forts as defensive or trading sites, from Molly Cotton's 1959 suggestion that "it might be profitable to approach a study of ... Cornish sites as individual unit[s] ... rather than [as] a homogenous group" (1958-9, 114), to Adam Sharpe's suggestion that archaeologists may "have been treating as a single group a collection of sites which have no more in common than their location and apparent form"

[6] Although see Lamb 1980, Peraza 2004 for similar observations elsewhere in the Atlantic Zone.

(1992, 65-7), to Jacqueline Nowakowski and Henrietta Quinnell's conclusion that "the considerable variety in shape, form and size of the cliff castle in Cornwall means that these sites can not be treated as a single type" (2011, 393). Although the variety in promontory fort location and form has been used to argue that these sites could have had no specialised function (see next section), others have argued that the liminal location of coastal promontory forts supports an interpretation of these sites as local monuments or sacred places.

Sharpe's 1992 paper on the promontory fort at Treryn Dinas, West Penwith, laid the foundation for interpretations of promontory forts as 'sacred places'. Treryn Dinas is a small bivallate promontory fort (approximately 3 hectares in size) located on the southern side of Land's End, most of which is occupied by granite rock formations (Herring 1994, 50-54).[7] In his paper Sharpe calls attention to other smaller promontory forts which are not well-suited as defensive works or as harbours, noting that the promontory forts at Treryn Dinas, Kenidjack Head, Giant's Castle (in the Isles of Scilly), Gunnard Head, and Tubby's Head all enclose small, rocky headlands in not-particularly-defensible positions (1992, 67). Sharpe is at pains to distinguish such sites from other promontory forts with large internal areas, and suggests that these smaller promontory forts may have served as local landmarks, created by 'demarcating' a prominent topographic feature with ditches and banks in a manner similar to that of Neolithic tors (1992, 65-7). By modifying existing landscape features, Sharpe posits that these

[7] Amongst these is a logan, or 'rocking' stone, recognised since at least the 19th century as a curiosity and identified by Christopher Tilley and Wayne Bennett as a possible focus of prehistoric worship (2001, 359).

promontory forts were the result of communities building identities out of features that were already prominent in the landscape. Sharpe's critique echoes R. G. Lamb's identification of "small strengths" – a subset of promontory forts including Gote o'Tram, Caithness, Burgh Head, Orkney, and Castle of Sand Geo, also on Orkney. Lamb notes that "it is difficult to imagine that such insignificant sites could have contained the manpower necessary to defend them" (1980, 68).

The association between promontory forts and possible non-secular activity is not directly attested, but hinted at by the presence of other religious and funerary monuments at promontory forts along the English Channel. In Morbihan, promontory forts from which Iron Age material was recovered were in association with a Bronze Age tumuli at Camp du Lizo á Carnac, Bronze Age burials and a Neolithic dolmen at Pointe du Blair en Baden, and a megalithic tomb at le Torche en Plombeur (Giot 1995, 278). Roman temples are thought to have been built at Giant's Castle in the Isles of Scilly (Ashbee 1974, 218) and at Le Pinacle on Jersey (Kinnes & Hibbes 1988, 70-3). In the Iron Age, it is also possible that headlands (or outcrops thereupon) enclosed by some promontory forts may have themselves been the focus of these sites. Natural features such as springs and bogs have been identified as sacred locations by archaeologists and in Classical sources (Cunliffe 2005, 566-70, Bradley 2000, Webster 1995). Cunliffe points out that many promontory forts were repurposed as Christian holy places during the Medieval Period, and speculates that promontory forts could have been "special places used by Atlantic communities to help articulate their relationship with the sea" (2001, 363). This attitude has been embraced by Tilley & Bennett, who describe the promontory fort at Treryn Dinas, West Penwith, as "a series of fantastic rock formations with towers and pinnacles,

some of which resemble menhirs, solution basins, and the famous logan or rocking stone ... If the Iron Age wall defended anything, it was these stones" (2001, 359).

1.3.5: Promontory Forts as 'Theatres of the Sea'

The view of promontory forts expressed in more recent work sees promontory forts as a set of enclosed sites linked more by their basic form and landscape setting than by a common function (cf. Henderson 2007 141-2; Herring et al. 2010, 178-183; Giles & Cripps 2012). Building on the observations of Sharpe (1992), they point out that counterexamples can be found for blanket interpretations of promontory forts. Henderson, following Bradley (2005), notes that promontory forts may have been built to serve multiple purposes – for example as both refuges and as local landmarks (2007, 140).[8] Following Cotton's suggestion that each promontory fort could be considered as an 'individual unit', calls for further excavations to gather evidence for or against the interpretations described in previous sections have become a common refrain (see Henderson 2007, 137; Nowakowski & Quinnell 2011, 393; Herring et al. 2016, 184).

Although attention to the location and setting of promontory forts is not new (Wheeler and Richardson memorably describe promontory forts as "eyries of deep-sea sailors ... suspended in an enduring sea-mist between the mournful screaming of the sea-birds and the relentless crashing of the breakers" (1957, 5-7)), older works tended to use

[8] The proximity of promontory forts in parts of the Atlantic Zone such as Cornwall also provides the opportunity that the same people may have used different promontory forts for different purposes. The promontory forts at Maen Castle and Treryn Dinas, for example, are separated today by approximately half a day's walk along the Southwest Coast Path.

the setting of promontory forts to suggest that a common set of activities may have taken place there.[9] In their paper on the promontory forts of Cornwall Giles & Cripps refer to promontory forts as 'theatres of the sea', on the basis that "their frequently dramatic use of space and orchestration of movement, and the very special sense of liminality created between land and sea, would have coloured and influenced every event and activity which took place on these promontories" (2012, 20). Rather than being the setting for a set of common activities, this conception of promontory forts sees their setting as the element that these sites have in common.

By making the landscape setting of promontory forts central to their interpretation, the 'theatres of the sea' approach raises several interesting questions. What common features do the landscape settings of promontory forts have? Can particular settings be taken as evidence for one of the interpretations described above? Are differences in landscape and experiential setting between different promontory forts sufficient to argue for different categories within this site-type? There are several different paths that approach answers to these questions. One of these encompasses 'phenomenological' surveys along the lines of Tilley & Bennett's 'archaeology of supernatural places' (2001). Another follows regional visibility studies such as the ones contained in this thesis (and also in the author's MSt research on promontory forts in Pembrokeshire (Smith 2016)). Finally, large-scale syntheses such as Lock & Ralston (forthcoming) may also serve as a basis for answering these questions. This thesis addresses them in the context of navigation, which is the subject of Section 2.2.

[9] See also Sharpe (1992), Tilley & Bennett (2001).

1.4: Research Questions

This chapter has briefly reviewed archaeological literature concerning maritime movement in Atlantic Europe, and the interpretation of coastal promontory forts in light of those larger-scale interpretations. Within these debates there is broad agreement on several important topics, which in some cases papers over a lack of specific evidence. For example archaeologists generally agree that there was an 'Atlantic Zone' in the Iron Age in which voyages took place, but disagree about the length, duration, and continuity of those contacts (see Section 1.2.4). In the case of promontory forts, archaeologists agree that the remote and liminal setting of these sites would have structured how people would have engaged with them, but different examples of remoteness or liminality are presented as evidence that these sites were defensive, monumental, pragmatic, etc. (see Section 1.3). The research questions described below have been crafted to advance these debates by exploring a specific context – that of a navigator at sea – and relating that context to the interpretations that have been discussed in earlier sections of this Chapter.

1.4.1: How Viable are Western Cross-Channel Routes?

As we have seen, the topic of travel along 'routes' or 'corridors' within the Atlantic Zone has been a frequent point of contention, with a great deal of discussion testing whether 'seaways' ought to be the focus of archaeologists' attention (Henderson 2007, 19-20). The shift from strictly delineated routes to 'zones of interaction' shown in Figures 1.4-1.8 addresses some of the points raised in this debate, while leaving others unsettled. This thesis aims to inform our understanding of the English Channel – a 'zone of contact' in Cunliffe (2001) and Henderson's (2007) models – by asking: how

successful and efficient would western Channel crossings have been in general, and in particular along routes already proposed by archaeologists?

This thesis answers this question by building a descriptive, agent-based model to simulate the navigation of sailed voyages (Chapter 4), and deploying it throughout the Channel on voyages between coastal 'nodes' (see Chapters 5-8).[10] This allows proposed routes to be tested against the full set of plausible cross-Channel routes. The directionality of sailed routes is of particular interest, since winds and tides can conspire to make inbound sailings from ports easier or more difficult than arrivals (see McGrail 1983). Archaeological models of contact based on artefactual similarities (i.e. Cunliffe 1988; Cunliffe & De Jersey 1997) can be used to suggest direct routes between sites, when in fact the material may have arrived via a less direct route. Investigating the success of cross-Channel voyages can, at the very least, evaluate the assertion that the western Channel would have been too difficult for Iron Age mariners to cross (see Davis 1997), and that crossings would have occurred at the relatively narrow waters between Calais and Dover, or between Poole and Cherbourg. By establishing the Western Channel as perhaps a zone of easy contact, or possibly as a dangerous province only to be attempted occasionally by skilled crews, this thesis seeks to inform this debate and others concerning the nature of maritime contacts within Iron Age Atlantic Europe.

1.4.2: Were Promontory Forts Landmarks?

Landscape setting is crucial to the interpretation of promontory forts. The inaccessible situation of some promontory forts has been used to interpret them as

[10] For discussion of nodes in particular, see Section 5.3.2.

refuges, the position of others near natural harbours is taken as evidence that they may have been emporia, and the natural grandeur of other promontory forts has been used to suggest that they may have been sacred places (cf. Wheeler & Richardson 1959; Cunliffe 1988; Tilley 2001). Aside from the presence of earthworks, the setting of coastal promontory forts as 'theatres of the sea' may in fact be one of the only features that these sites hold in common (Giles & Cripps 2012). As analysis of the landscape setting of coastal sites tends to be from a terrestrial perspective (but see Robinson 2007 for an exception), this study aims to provide crucial context for these sites by answering the question: could promontory forts have served as landmarks, and how would they have appeared to navigators attempting to cross the Channel?

In this study this was accomplished by performing visibility studies as part of the normal course of simulations (see Section 4.3.3), and by comparing the results of simulations that use archaeological sites as landmarks to the results of simulations where natural prominences are used instead (see Section 5.2.4). The visibility of prehistoric monuments has been widely used to aid their interpretation (see Wheatley & Gillings 2000), although systematic studies of views from the sea have been less common in the Atlantic region. Study of the visibility of promontory forts from the point of view of a particular practice – in this case navigating – addresses some of the concerns raised by Tilley (1994) and Bender (1997): that analytic studies of visibility surpass 'embodied' perception and therefore fail to appreciate how monuments relate to their landscape and the people that they engage with. Assessing the visibility of these sites also addresses the coherence of the 'promontory fort' site-type, by testing whether these sites are seen in similar ways despite differences in their construction. The main problem in using coastal promontory forts' landscape setting to determine their function is that general evaluations

of their prominence, or isolation, or visibility can be used to support multiple interpretations. The fact that a promontory fort is highly visible, for example, could indicate that it was meant to be a point of reference for merchants approaching from the open sea; or that it was situated in order to advertise the status of the community that built it; or that it was located in a place that people in the wider landscape could monitor and withdraw to easily. By testing the visibility of promontory forts specifically from the perspective of an Iron Age mariner, this thesis seeks to discover whether this first proposition is likely or not.

1.4.3: How Did Navigation in the Western Channel Work?

In Atlantic Europe, maritime links have been proposed as a mechanism that explains the movement of materials, 'peoples', and ideas within this area during the Iron Age (see Section 1.2). Despite the enthusiasm with which scholars have promoted sea-routes as an important component of Atlantic Europe, little has been written about the components of *that* mechanism – that is to say how voyages would have been planned, where they could have launched from, whether they were likely to go off course or not, or how they would have navigated. The few papers that have been published on Iron Age navigation (McGrail 1988, Davis 1997) focus on travel times and visible distances. However these factors are contingent upon other considerations, such as weather, wind, daylight, obstacles, the design of the ship, and the knowledge and skill of the navigator. The navigation model described in Chapter 4 is designed to account for all of these conditions as parameter inputs to the model, and the analyses detailed in Chapters 5-8 test the performance of this model under different parameter combinations (Section 5.2.1). The final research question under consideration in this thesis is: which of these parameters

has the greatest effect on the outcomes of simulated voyages? Is ship design, the ability to navigate, the timing of voyages, or the ability to read local conditions paramount?

Besides contextualising the voyages that would have been the basis for maritime contacts in the Iron Age, making these comparisons gives us a window into the choices that prehistoric mariners may have faced. These voyagers would have surely weighed the speed of their ships versus their experience at sea, for example, or considered whether a short crossing in unpredictable weather was preferable to a longer crossing along a different route. Investigating the relative parameter effects in the results of the model helps us understand these trade-offs in the context of specific passages and routes, which in turn informs assessments of the navigability of Atlantic waters in the Iron Age.

1.5: Thesis Structure

This thesis addresses the research questions listed above by developing and deploying an agent-based model of prehistoric navigation in the western English Channel. Developing such a model demands an understanding of archaeological evidence for seafaring in the Atlantic Zone, a working knowledge of the principles of navigation, and a survey of existing models and techniques. As such, the structure of the remainder of thesis is as follows:

- Chapter 2 reviews evidence for Iron Age seafaring and discusses prehistoric methods of navigation. As no Iron Age seafaring ships have been identified in the archaeological record, the first half of this chapter is concerned with establishing what the the capabilities of these ships may have been. The second section seeks to establish a working definition of the term ‘navigation’ as applied to Iron Age seafarers.

- Chapter 3 reviews and critiques computational models for movement over water. This chapter argues for a descriptive approach over more deterministic modelling techniques, as a method to more realistically model navigation as defined in the previous chapter.
- Chapter 4 describes the design of the model used in this analysis. The general architecture of the model is discussed, and each component step of the simulation is described in detail.
- Chapter 5 describes the Main Analysis, which simulates voyages across the Channel over a seven-month study period. A general overview of the study area (the western English Channel) is offered, and datasets gathered in support of this analysis are reviewed. Finally, the results of the Main Analysis are presented and discussed.
- Chapter 6 describes Case Study 1, which tests routes to and from Hengistbury Head from possible points of departure suggested by Cunliffe & De Jersey (1997). The potential of southern nodes as ports corresponding to Hengistbury Head is discussed, as is the potential for multi-node routes.
- Chapter 7 describes Case Study 2, which tests routes between the archaeological sites at Le Yaudet and Mount Batten (corresponding to the Lannion and Plymouth nodes (see Cunliffe 1988)). This analysis involves a broad sweep of parameter inputs to the model; relative parameter effects and the results of simulations are the main object of discussion.
- Chapter 8 describes Case Study 3, which tests routes between the Brest and Penzance nodes using 3D visibility analysis and a more conservative vessel parameterisation. Discussion focuses on the potential value of coastal sites as first

and last points of contact, and on the possibility that changes in ship design in the Iron Age may have precipitated a change in the configuration of cross-Channel routes.

- Chapter 9 reviews the results and discussions from the Main Analysis and case studies in order to address research questions listed above. The model is evaluated and suggestions for further research and improvements to the model are made.

Volume II of this thesis contains figures and tables referenced in the text, as well as three Appendices. These Appendices contain: (I) a catalogue of archaeological sites used as landmarks; (II) a catalogue of natural prominences used as landmarks (see Section 5.2.4); (III) a collection of plots showing the full results of Case Study 3 (Chapter 8).

Chapter 2 : Seafaring and Navigation

2.1: Introduction

The research questions that motivate this thesis are posed from the point of view of a navigator. To understand how navigators would have selected routes, understood promontory forts, and estimated the risks and rewards involved in Channel crossings requires an understanding of both the practice of navigation and the ships that prehistoric navigators would have sailed on. This chapter provides crucial context by reviewing evidence for seagoing ships in Iron Age Atlantic Europe, and by exploring the practice of navigation and how may it may have functioned within this context. Discussion of ships' seakeeping qualities and speed potential directly informs analyses in Chapters 5-8 by forming the basis for vessel parameterisations within the model (see Section 5.2.3), and the 'working definition of navigation' proposed at the end of this chapter (Section 2.3.10) is used to critique existing computational movement models (Chapter 3) and to develop the navigation model used in this analysis (Chapter 4).

2.2: Iron Age Seagoing Ships

No investigation concerning seafarers would be complete without a discussion about the ships that carry them. The design of ships determines not only the cargo that can be carried and the speed that can be attained, but also serves as both an essential point of reference and a setting for all the actions of mariners. Navigation relies on the navigators' knowledge of their ship's capabilities. If monuments placed along the coastline constitute a 'seascape' meant to be appreciated by mariners, then the ship dominates the 'near distance' and helps determine what is viewed. An understanding of

the abilities and limitations of Iron Age ships is essential to the development of an adequate navigation model.

There is a great deal to be said about the particular characteristics of prehistoric ships – in particular the methods by which they were constructed, the appearance of different design features, and the goods that they might have carried (see, for example: Marsden 1997; McGrail 1998, 2001; Robinson & Wilson 2011). As the purpose of this chapter is to inform the design of a navigation model, the focus here is on issues relating to the seakeeping qualities of Iron Age ships. In particular, this section discusses what speeds these ships may have achieved in Atlantic waters by reference to archaeological reconstructions and replicas.

2.2.1: Ship Design in the Iron Age

The central obstacle to the discussion of seafaring ships in Iron Age Atlantic Europe is the lack of direct material evidence for these ships. Instead, historical sources, artistic representations, and comparisons with ships from other periods must serve as the basis for such a discussion. Since the focus of simulations in this work is on English Channel crossings, this section pays particular attention to those types of vessels that are thought to have been capable of these and other long-distance journeys.

In Seàn McGrail's seminal book *Ancient Boats in Northwest Europe*, five basic types of boat are identified for their use or potential use in the prehistoric Atlantic. These are: rafts, bark boats, logboats (dugouts), hide boats, and plank boats (McGrail 1998). The first two boat types on this list are not represented in the archaeological record, although McGrail points out that prehistoric people would have had the necessary materials and tools to make them (1998, 53; ibid. 88). The third ship type in the list,

logboats, are well-represented in the archaeological record (see McGrail 1978), but are unlikely to have been used in long voyages on the open sea. The final two types, skin boats and plank boats, are the most likely to have been involved in these types of voyages, but unfortunately material evidence for both of these in the Iron Age is lacking (see Figure 2.1). In both cases inferences from ships dating to other periods forms the basis of archaeologists' assumptions about the seagoing ships of the Iron Age and their capabilities.

2.2.2: Reconstruction and 'Seaworthiness'

The reconstruction of excavated ships may involve the construction of small-scale and full-scale replicas, but more often consists of numerical analysis in consultation with principles of naval architecture (see McGrail 1998, 192-204). These numerical reconstructions have the advantage of providing standard figures by which to judge ships, while requiring far less time and money to produce than scale models or full-size replicas. 3D models and software such as ORCA are particularly useful in producing these models (see Berry et al. 2019). The results of these models, however, are not necessarily an accurate reflection of the seaworthiness of the ships being modelled. The 'seaworthiness' or 'seakeeping qualities' of a ship are defined both by the ship's intended purpose, and by the ship's response to conditions that are encountered on voyages for said purpose (Lloyd 1991). Since the focus of this analysis is on seagoing ships, reconstructions that only test the performance of vessels under ideal conditions (i.e. calm waters) may not be good guides to their seaworthiness. Accordingly, the purported seaworthiness of archaeologically reconstructed ships is a matter of much debate (see for example McGrail 2007).

Important considerations in determining the seaworthiness of a vessel include: the shape of the hull and the presence of a keel; the ship's ability to withstand stress from wind and water; for paddled craft the amount of energy required to drive the boat, and for sailed craft the position of the mast and the configuration of sails (the 'rig'); the amount of freeboard (the distance from the waterline to the upper edge of a ship's hull) under different loads; the ability to steer; and the ability to dock, anchor, or land.

2.2.3: Log Boats

A 'basic logboat' consists of a hollowed-out tree trunk, which can be shaped or added to in order to create a useable boat. Logboats have been found throughout Atlantic Europe dating back to the Mesolithic (Andersen 1994; McGrail 2001, 172). The only boats found in Atlantic Europe known to date to the Iron Age are logboats: a since-destroyed logboat recovered from Brigg (North Lincolnshire) in 1888, a logboat recovered in several fragments from Poole Harbour in 1964 (McGrail 1978, 254-60), a logboat recovered from Hasholme near the Humber estuary in 1984 (Milett et al 1987), and a logboat found at Must Farm during excavations from 2009-2018 (Knight et al. 2019, 647).[11] These boats were built by hollowing out felled old growth oak (*Quercus sp*.). The ends of the log were then sealed with transom boards in the stern, and by either reducing the log to create a taper in the bow or else building a separate assembly in order to seal

[11] It is possible that the Brigg logboat has an earlier date than indicated in Figure 2.1. Radiocarbon dates based on surviving samples and from timbers recovered from a re-excavation of the site produced dates of 680 and 593 BC ± 100 years (McGrail & Switsur 1975, 194), which would place it in the Iron Age. However dates from samples of the original may be compromised by materials used to conserve the boat before it was destroyed in a fire in 1942 (ibid. 194-195).

off the bow (see Figure 2.2). The size to which logboats could be built was limited by the availability of timber. The Poole logboat measured 10 metres, and could have carried a maximum crew of 18 (Berry et al., 35-45).

It is generally assumed that logboats would have been paddled, which would have necessitated a large crew for long-distance voyages. There is tentative evidence for a mast step in the Poole logboat, although McGrail points out that the rectangular socket in question could have also been fitted with a towing bollard (1978, 256). If logboats were equipped with sails, then they may have been capable of making longer journeys. The use of sails would also have reduced the number of crewmembers needed and increased the amount of space available for cargo. Evidence for extension and more conclusive evidence for sail propulsion would have to come to light to support this hypothesis, however.

It is unlikely that any of the attested Iron Age logboats recovered in the Atlantic Zone were used on coastal or open-sea voyages. The Poole logboat was likely restricted to the Poole estuary (McGrail 1978, 256-7), and a recent reconstruction (Berry et al. 2013, 35-85) of the ship found that the vessel was "signifigantly less stable than originally believed" (ibid., 84). McGrail notes several methods that can be used to improve the seaworthiness of logboats – including extending the sides and 'pairing' logboats to create a multihull craft – but these improvements remain in the realm of possibility in the context of Iron Age voyages (McGrail 1998, 56).

The Hasholme and Brigg logboats were both considerably larger than the Poole logboat (at c. 13 and 14.75 metres, respectively), and the Hasholme logboat is estimated to have had a freeboard of 0.31 metres when fully loaded (McGrail 2001, 176; McGrail

1978, 168; Millett et al. 1987, 134). Millett suggests that the size of these vessels may have been a statement of prestige rather than a strategy for increasing their seaworthiness (although these goals are not incompatible); and the presence of 'eye sockets' on the bows of both boats may lend credence to this theory (Millett 1987, 127, McGrail 2001, 177). The Must Farm boat has yet to be reconstructed, but its location far from the sea suggests against its use as a coastal vessel – perhaps along the same lines as the Poole logboat.

2.2.4: Hide Boats

Hide boats are built by stretching animal hide over a frame or skeleton in order to form the hull. The suggestion that they were used in the Iron Age Atlantic is largely based on references to hide boats in Classical and medieval sources (Pliny, *Natural Histories* VII-206; Solinus *Polyhistor* XXIII; Avienus *Ora Maritima*), and the continued use of hide boats in Ireland, Scotland and Wales from the medieval period until the 19th and 20th centuries (McGrail 1998, 186). The closest thing to direct evidence for hide boats in the Iron Age comes from a boat model recovered with a several gold artefacts in 1896 from a field in the townland of Broighter in Ireland (see Figure 2.3). The Broighter boat model has been dated to the first century BC based on its association with other objects in the hoard – particularly a La Tène torc (Farrell & Penny 1975, 15) Unfortunately, the hull of the Broighter boat was crushed by a plough prior to its discovery, and was afterwards sent to a goldsmith in Dublin for restoration (Neill 1993, 24-5).[12] The reconstructed hull is

[12] After being found, items from the hoard were washed in an open sink at the farm belonging to the men who uncovered it. Ken Neill records a quote from Maggie Nicholl, a maid at the farm at the time, who later recalled that "it is quite possible that some small objects may have been washed down the open drain, for it was not then known that the finds were of gold and no great care was taken in their cleansing"

rounded with little sheer, and measures 18.4 x 7.6 cm with a depth of 4.9 cm – if the scale of the model is accurate then the length of the ship it represented would have been approximately 15.25 metres (Farrell & Penny 1975, 20).[13] The model was equipped with nine oars on each side, a spar and a grapnel, rowing thwarts, a mast and yard, and a steering oar on the port side (Farrell & Penny 1975, 19-20). Most scholars have equivocated as to whether it represents a hide boat or some other type, considering the circumstances of its recovery, the fact that it was more likely an ornament than a realistic representation of a boat, and the fact that no other Iron Age boat models are known to exist from the Iron Age Atlantic region (see Lethbridge 1950, 76; Marsden 1972, 118; Farrell & Penny 1975, 21; c.f. Bowen 1972, 36-41). McGrail considers that the Broighter boat was 'likely' a hide boat, and addresses concerns over the boat's size and seaworthiness by referencing the experimental hide boat *Brendan* (McGrail 1998, 186-7; see Figure 2.4). Although the *Brendan* is not directly comparable to the Broighter boat and used technologies that would have been unavailable in the Iron Age, it proved to be sufficiently seaworthy to cross the Atlantic (Severin 1978).

The main advantage to hide boats over other types of boat is that these can be built quickly without using materials like old-growth timber or metal fittings that may be hard to obtain – this may have been an especially important consideration in cleared, windswept portions of Atlantic Europe. Although hide boats may not have been as

(1993, 24). It is possible therefore that some details (such as a possible second steering oar (see Farrell & Penny 1975, 24)) were lost at this stage; however it is impossible to know for certain.

[13] Farrell & Penny suggest that a scaled version of the Broighter Boat would measure 50 feet (15.25 metres), but also note that modern curraghs rarely exceed half of that length (1975, 20).

durable or long-lasting as logboats or plank-built ships, ethnographic records (see, for example, Pedersen 1986) and Severin's experience on the *Brendan* suggests that they would have been capable of surviving long periods in rough seas. The light construction of these ships would have made them more vulnerable to hazards, but would have also allowed them to approach shallow landing places and reduced the amount of effort necessary to stow and launch them from above the tide-line. Although it is difficult to say how they may have sailed (the *Brendan* was equipped with fore- and aft-sails and used a more modern rig, whereas the Broighter boat shows a single square rig placed amidships), navigators on hide boats may have experienced a high degree of leeway (the degree to which the course of a ship is deflected by the wind). However hide boats can be equipped with keels or similar 'longitudinal members' (McGrail 1999, 182). The existence of plank keels on ships in the Atlantic Zone is hinted at in Caesar's memoirs, where his soldiers construct hide boats with plank keels "of the kind that his knowledge of Britain a few years before had taught him" (C.B.C. 1.54). Some protection against drift could also have been provided by steering oars – the long steering oars depicted in the Broighter Boat may have fulfilled such a function, as they did on the *Brendan* (McGrail 1997, 242; Severin 1978, 258-259).

Although there is no direct evidence for these ships, references from Classical sources and the existence of the Broighter boat suggest that hide boats would have been in use in the Iron Age. McGrail considers that hide boats could have been involved in long-distance voyages in the Iron Age, based on their durability and seakeeping qualities (1983, 300). Given that hide boats are relatively cheap and easy to produce, these types of ship may be a good candidate for further archaeological reconstruction and testing.

2.2.5: Plank Boats

Plank boats are built in a variety of ways; in the context of the Iron Age two plank-built traditions are relevant. These are Bronze Age sewn-plank boats, and 'Romano-Celtic' boats dating from the 1st to 4th centuries AD. It is unclear how late traditions of sewn-plank boat building persisted and how early ships of the Romano-Celtic type began to be built, given that there is no archaeological evidence for Iron Age plank-built ships in Atlantic Europe. Equally, whether or not the transition was gradual or abrupt, or distributed evenly around the Atlantic Zone is a matter of speculation. As such both sewn-plank boats and Gallo-Roman boats will be treated as different types of vessel for the purposes of this thesis.

In the first case, sewn-plank boats are characterised by planks laid flush with and fastened to one another with organic fibres. Sewn-plank boats are reinforced with transverse timbers and slotted cleats, and caulked with moss (Van de Noort et al. 2014, 292). Evidence for sewn-plank boats in Atlantic Europe comes from two sources: Bronze Age plank boats found in Britain, and the Hjortspring boat recovered from a bog in southern Denmark. Although the Hjortspring boat dates to the Iron Age (see Bojesen-Koefoed et al. 2003), it is unlikely to have belonged to a boatbuilding tradition originating in Atlantic Europe. Sea trials for a fully-reconstructed Hjortspring boat achieved speeds of 7-8 knots, using a trained rowing crew.[14] Bronze Age sewn-plank boats, meanwhile, have only been found in Britain (see Figure 2.1). The remains of three of these sewn-plank boats are sufficiently intact to enable the creation of models and replicas (Van de

[14] See: https://www.hjortspring.dk/w_old/sailing_y2k_2.htm

Noort et al. 2014, 292). As there is no evidence for masts associated with sewn-plank boats, presumably they would have been powered by oars or paddles. A reconstruction of the Dover boat with a flat bottom estimated a 'comfortable speed' of 5 knots over long periods with a full crew (Roberts 2004, 206), although Crumlin-Pederson has argued that the Dover boat's hull was more rounded and has called for re-evaluation of the reconstruction (2006). While some authors have called for a reassessment of the capabilities of sewn-plank boats (see Van de Noort 2006), the consensus amongst archaeologists is that sewn-plank boats were mainly used for inland and limited coastal voyages. For example, environmental evidence from the Dover boat suggests that it was not primarily a seagoing vessel (as timbers do not appear to have been damaged by marine organisms), nor was it confined to the Dour estuary (sediments were found in the hull that 'did not originate in Dover (Clark 2004, 312)). However there has lately been a push to reconsider their capacity for longer voyages, given that they are theorised to have played a role in long-distance Bronze Age exchange (cf. Coates 2005, Van de Noort 2006; McGrail 2007). Sewn-plank boats can certainly be built to complete long-distance voyages – sewn-plank ships were used to complete Indian Ocean crossings relatiely recently (see Agius 2002).

In the second case, the term 'Romano-Celtic' refers to boats found in western and central Europe dated to the period from the 1st to the 4th century AD (McGrail 1975, 139). The primary characteristics of this shipbuilding tradition are large, closely spaced framing timbers faced with flush planking attached with thick nails that bend around the interior of the hull like staples (ibid. 140; see Figure 2.5). McGrail further divides Romano-Celtic boats into two subgroups: one consisting of keel-less, flat-bottomed boats which are interpreted as 'lake, river and canal boats'; and another consisting of boats with rounded

sides, keels and end-posts, a frame-first design, and with sailing rigs that would have enabled them to sail 'by and large', which are interpreted as seagoing vessels (McGrail 1995, 143). The second category is of interest here; it consists of Blackfriars 1, St. Peter Port 1, and the Barland's Farm boat (see, respectively: Marsden 1994, Rule & Monaghan 1993, Nayling & McGrail 2004). Blackfriars 1 and St. Peter Port 1 are both substantial ships with closed decks, and would have been capable of long-distance journeys with cargo (Millar 2002, 53). Whereas the Barlands Farm boat measured 11.40 metres in length (ibid. xvii), the St. Peter Port 1 ship is estimated to have been 25 metres long (Rule & Monaghan 1993, 127). The Barlands Farm boat is interpreted as primarily a coastal and estuarine ship, although it is also noted that the ship "was a good all rounder" that "could even have crossed St George's Channel to Ireland in the right weather" (Nayling & McGrail 2004, 216). As far as propulsion is concerned, mast steps have been found on all three seagoing Romano-Celtic ships found to date, in all cases set one third from the bow (i.e. well ahead of amidships). This raises the possibility that these ships used fore-and-aft sails rather than a square rig – a digital reconstruction of the Barlands Farm boat suggests that better performance would have been achieved with a (fore-and-aft) lug sail rather than a square sail (Nayling & McGrail 2004, 191-2; see Figure 2.6). Based on this reconstruction the top speed of the Barlands Farm boat is estimated at 7.6 knots with a load of 7 tonnes, and 7.8 knots with a load of 4 tonnes (ibid. 187). A reconstruction of Blackfriars 1 suggested that in "normal circumstances" the ship's top speed could have been 7 knots, and that the ship could have achieved 9-10 knots in "ideal conditions" (Marsden 1994, 89). Unfortunately no complete reconstructions of Barlands Farm 1 and St. Peter Port 1 have been made. It is possible that their increased size would have allowed for a larger sail and faster speeds, but without a reconstruction this is purely conjectural.

Of the plank boats discussed in this section, only the Romano-Celtic variety are widely assumed to have been seafaring vessels. It is entirely possible that the Bronze Age sewn-plank boatbuilding tradition was carried into the Iron Age in parts of the Atlantic Zone, and that innovations in this tradition influenced the development of Romano-Celtic ships. However there is no direct evidence for this, and we should be careful not to leap to conclusions about what such an 'intermediate' ship would have been capable of.

2.2.6: Parameterising an Iron Age Seagoing Ship

This section has surveyed four very different boatbuilding traditions (five including the Hjortspring boat) that span two millennia. Of all the boats mentioned here, the remains of only three have been found in Atlantic Europe (as defined in Section 1.1.1). As such any statements as to the general seaworthiness and performance of Iron Age ships must be speculative. Taking this into consideration, it seem likely that logboats were used in rivers and the inner reaches of estuaries, sewn-plank boats were used as ferries and in short coastal voyages, and longer voyages by sea would have been undertaken in hide boats or possibly in the plank-built precursors to Gallo-Roman ships. Although shorter overseas passages may have been possible by oar, these voyages would have been very difficult over longer stretches of open water. For example at a speed of 5 knots (the rowing speed suggested for the Dover Boat), passage across the Strait of Dover (c. 18 nautical miles) would have required four hours of paddling, whereas the passage across the western entrance to the Channel (c. 100 nautical miles) would have required part of the voyage to be completed by drifting – or else 20 hours of continuous paddling. This is to say nothing of conditions at sea, which would have been challenging for logboats and sewn-plank boats as we currently understand them through reconstructions.

It is generally assumed that sailed ships in the Iron Age Atlantic Zone would have been equipped with square rigs (McGrail 1988, 220), possibly along the lines of the configuration represented by the Broighter Boat. However archaeologists are divided on the extent to which ships with square rigs are able to sail into-wind. R. Davis suggests that into-wind sailing is impossible for square-rigged ships, based on Severin's observation that the *Brendan's* leeway compensated for speed gains made by sailing to windward (Severin 1978, 266; Davis 1997, 129). However the *Brendan* was a replica of a skin boat without a prominent keel, carried a small crew (crews can compensate for leeway by paddling), and used modern mast- and sail-configurations. Lindsay notes that the square-sails used in Classical Mediterranean ships would have been obstructed by stays and other rigging found on modern ships, and could therefore have been braced at a closer angle to the wind (2012, 143). McGrail makes a somewhat less conservative estimate of the capabilities of Iron Age ships in his 1983 paper on Channel crossings:

> ...the indigenous, prehistoric open boat could not sail closer to the wind than 7 points, a sector of 15½° centred on the wind ... with a 1 point leeway for a planked boat ... and a 2 point leeway for a skin boat. ... maximum speed in ideal conditions might be as much as 7 kts for a boat of 7-m waterline length of 9 kts for one of 12 m (McGrail 1983, 300).

McGrail's estimates were used to derive parameterisations for simulated ships in the analyses described in this thesis. Given the maximum speeds identified in the survey here, this characterisation of a hypothetical Iron Age ship seems appropriate. Although Blackfriars 1 may have achieved a faster speed in ideal conditions, it was also substantially larger. Until more ships are excavated and more reconstructions / replicas are constructed, it provides a good working basis for the development of an Iron Age ship parameterisation within a computational model (see Section 5.2.3).

2.3: Navigation in the Iron Age

An estimation of the capabilities of Iron Age ships is necessary to model the voyages of prehistoric people, but in order to model those voyages faithfully some thought must be given to *how* these ships were conducted across the waters of Atlantic Europe. To model Iron Age voyages requires an understanding of how Iron Age mariners would have navigated – how they would have been able to fix their position, what points of reference they could have used, and how reliable the systems that they relied upon were. The initial part of this section expands on this definition by examining how the concept of 'navigation' has developed in more recent history. Subsequent sections describe techniques that prehistoric mariners could have used to navigate. In the final section of this chapter a method of Iron Age navigation is proposed, based on two of these techniques: navigation by natural and anthropogenic landmarks (or 'dead reckoning'). This proposed set of methods informs the discussion of computational models in Chapter 3, and the development of the navigation model described in Chapter 4.

2.3.1: Reconciling Definitions of 'Navigation'

The term 'navigation' was once synonymous with 'seafaring', but since the 16th Century it has come to refer specifically to practices for guiding ships at sea.[15] Perhaps because of this history, definitions of the term tend to vary over time. Navigation is defined differently by different authors, from the conservative: "the art of conducting a ship from port to port" (Chapman 1956, 449), to the specific: "the duty of a navigator is

[15] Harper, D. *navigation*. Online Etymology Dictionary. Available at: https://www.etymonline.com/search?q=navigation. Accessed October 6, 2020.

to find and record the position of his ship frequently" (Kells et al. 1943, 102), to the general: "navigation is all about applying knowledge of the world around us – and above us – to get to a particular destination through unknown or featureless territory" (Denny 2012, 119). These differences in definition reflect different contexts in which navigation is imagined as taking place. In the three examples above, the first is from a practical handbook for yachters, the second is from a U.S. Navy manual on navigation, and the third is from a chapter on prehistoric seafaring in a history of navigation.

To a certain extent the differences between these definitions follow from the development of navigation into a scientific discipline. Needham has divided the development of navigational techniques into stages: non-instrumental navigation, quantitative navigation, and mathematical navigation (1971, 555). The methods of navigation described in this chapter are all non-instrumental – McGrail places the advent of quantitative navigation at the end of the 14th century AD (1998, 275). Since little can be said for certain about the specifics of navigation in the Iron Age Atlantic Zone, this study defines navigation generally as: a collection of heuristic techniques used to determine the position of a ship at sea, in order to guide the vessel to a destination.

2.3.2: Navigation and Pilotage as Sciences and Arts

A distinction between 'navigation' and 'pilotage' is frequently found in navigational literature. This distinction is partly based on practical differences between pilots and navigators, and partly on the development of 'navigation' as a branch of science. In general, pilotage tends to refer to types of navigation that rely on local knowledge and the prediction of conditions, whereas 'navigation' generally refers to techniques that reference a vessel's position to extra-terrestrial bodies or the earth's

magnetic field. Whether or not this distinction is meaningful in the context of prehistoric Atlantic Europe is an open question, but it should be considered before describing navigational techniques in detail.

Today, pilots and navigators belong to two separate professions – navigators are part of a ship's crew and help guide their vessel between ports, whereas pilots work at a particular harbour or waterway in which they guide other ships. Over time navigation has become particularly associated with the open ocean whereas pilotage is associated with inshore waters. In particular, navigation by landmarks is usually considered to fall within the domain of pilotage, since landmarks can be difficult to read without local knowledge. In the same vein, knowledge of 'local conditions' such as the location of reefs and sandbars, the timing of tidal streams, and the prediction of weather are more often placed in the domain of pilotage. Their proximity to the shore means that pilots are able to navigate by landmarks, and by soundings where possible. By contrast, 'navigation' is generally understood as navigation on the open sea where no landmarks are visible. In this context navigation is understood as a means for fixing a vessel's position analytically: relative to groups of stars, or a compass bearing, or a constellation of satellites.

The dividing line between navigation and pilotage is fuzzy. There is a considerable amount of overlap in the techniques used by navigators and pilots, to the extent that Kells et al. state that "the basic principles of piloting apply to all navigation" (Kells et al. 1943, 128). There is also overlap in the areas in which they are applied – knowledge of current and wind patterns can be used to guide a vessel out of sight of land (see Section 2.3.5, below), and a compass can be used to guide a ship when in sight of land. The development of quantitative and mathematical navigational techniques has served as a wedge between these two practices, as these techniques largely benefitted

navigators in unknown waters – in particular long-distance voyagers of the past several centuries. Scientific navigation makes finding one's way in every part of the world equally 'easy', whereas techniques that rely on specific types of knowledge and experience still require a person who has those faculties. Seán McGrail acknowledges this difference when he describes pilotage as an "art and science", and remarks that "navigation is now regarded as a science but has not always been so; until relatively recently it was also an *art* [emphasis his]" (1998, 275). Since the advent of 'navigation-as-a-science' falls after the close of prehistory, in the remainder of this work the term "navigation" refers to any method for fixing position, regardless of whether it falls within the traditional provinces of 'navigation' or 'pilotage'.

2.3.3: Distinguishing Navigators from Seafarers

Sailors in the Iron Age Atlantic likely did not distinguish between pilotage and navigation on the grounds of art vs. science, but this does not mean that similar professional distinctions did not exist in prehistory. The closest parallel in documentary sources comes from the mid-first-century A.D. *Periplus of the Erythean Sea*, where the author describes fishermen employed as guides to river entrances in India (Casson 1989, 78). Certainly local pilots could have been used in the Iron Age Atlantic Zone, in which case they would have been able to provide detailed knowledge of local conditions to crews from faraway shores.

Although navigation requires many of the same skills and information as seafaring, it is not necessary for every crew-member to be a navigator. However many of the skills necessary to be an effective sailor are also used in navigation. In particular, being able to evaluate weather and sea state is crucial in both cases. Seafarers need to be

able to evaluate the direction / strength of currents, winds etc. in order to keep their ship afloat and moving. For the navigator, these phenomena may help indicate position. By the same token, being able to predict when and where these phenomena occur gives seafarers the opportunity to prepare for good or bad conditions, and gives the navigator another point of reference.

2.3.4: Dead Reckoning and 'Natural Navigation'

The following sections discuss possible navigation techniques that could have been used in the Atlantic Zone, calling attention to local conditions were possible. As mentioned in Section 1.1.2, sea levels and weather regimes in this area during the Iron Age would have been similar to those of today. Geological modelling suggests that sea levels in the English Channel were up to 6 metres lower in the Late Iron Age than today, which is inside the modern tidal range (Heyworth & Kidson 1982). Weather is more difficult to model – based on general assumptions it appears that weather patterns in north-western Europe have been similar since c. 1000 BC (Lamb 2011).

The navigational techniques described in the following sections have all been described as methods for non-instrumental navigation (see Gatty 1958), as opposed to scientific approaches that rely on instruments and accurate charts. Since prehistoric voyagers in the Atlantic Zone probably lacked both of these, most of their navigational techniques would have been 'natural', with one exception. This exception is the process of dead reckoning, which uses an assessment of a vessel's speed along a known course in order to estimate position along that course. Mariners would have had to rely on observational methods to gauge speed, such as: comparing a boat's progress with the position of the sun, using established measurements of a 'day's sail', and measuring the

position of bow waves along the hull of the boat (McGrail 1998, 282).[16] They would have also had to rely on the sun or stars to gauge time under sail, or else on their own sense of time. It is important to note that dead reckoning is generally considered to be an inaccurate method of navigation – even when assisted by chronometers and speedometers – since inaccuracies can compound on long voyages, and dead reckoning does not take current and wind drift into account (see Chapman 1956, 344a-344b). These parameters can be difficult to judge (see Section 4.3.2), reducing the accuracy of dead reckoning. If dead reckoning was used by Iron Age navigators in the Atlantic Zone, it was almost certainly combined with other navigational techniques, such as those described below.

2.3.5: Navigation by Seas and Winds

The interplay of atmosphere and hydrosphere that produces currents is extremely complex, but these interactions can be used to navigate where they result in predictable, observable phenomena. Currents, swell, and tidal streams are distinct phenomena with different origins, which means that they can be compared with one another in order to estimate position. Doing so requires the ability to detect these phenomena, and a mental map that places them in relation to oneself.

Ocean currents are caused by the motion of the earth in combination with changes in ocean salinity and temperature. The rotation of the earth and the resultant Coriolis force acts on the oceans to create gyres in the open ocean. Temperature gradients between the planet's poles and tropics also create patterns of oceanic circulation. Western Europe is

[16] In circumstances where a second bow wave is created, the further back on the hull it occurs the faster the vessel is moving.

dominated by the North Atlantic Current, a branch of the Gulf Stream (see Section 1.1.2). Ocean currents can be difficult to detect from the surface, especially in coastal waters where other types of current may be more noticeable.

Swell is caused by wind blowing over long stretches of exposed water. Since swell is caused by a force on the surface of the water, it can be easier to detect aboard ship. The strength of swell depends on the force of the wind and the distance that the wind blows over the sea (fetch). If swell can be distinguished from other currents at sea, then it can be used to orient a navigator. Disturbances or lack of swell can also indicate that the vessel has passed within the lee of nearby land.

Tidal streams are caused when the earth's tides are obstructed by land. Tidal forces drive water onto land once or twice daily at the flood tide; this water drains away again at the ebb tide. Tidal streams are the currents produced by this cycle. Tides themselves are caused by the displacement of water by the gravitational pull of the sun and moon. Both of these bodies exert gravitational force on the oceans, causing oceanic bulges beneath the sun / moon and on the opposite side of the earth. Spring tides are produced when solar and lunar tidal forces align, and neap tides are produced when solar tidal forces partially 'cancel out' the moon's gravitational influence. Because both the sun and moon act as tide-generating bodies, the intensity and frequency of tides is driven by orbital characteristics. To an observer on the surface of the earth, solar tides occur every twelve hours (twice per rotation), whereas the interval between lunar tides is approximately 12 hours and 25 minutes (Talley et al. 2011, 239).[17] The timing of high

[17] This is because the moon orbits in the same direction that the earth rotates.

and low tides therefore shifts throughout the year. Both the earth and the moon also follow elliptical orbits, which affects the amount of pull the oceans feel from the moon and sun at different times of year. Although tidal forces are very predictable, the interaction of these forces with the coast can be difficult to predict. The two dominant tidal regimes are diurnal (one high tide per day) and semidiurnal (two high tides per day). Tides along the eastern Atlantic coast are semidiurnal, and tidal streams cause the most noticeable currents in enclosed waters such as the English Channel. Figure 2.7 shows the average current velocity in the English Channel based on data obtained for this study (Section 5.4). Particularly strong tidal streams can be found near Alderney, the Île d'Oessant, and the Isles of Scilly. Since these streams behave predictably, they can be used for navigation. Tidal streams can be predicted from experience, or from a system that relates them to other phenomena (i.e. the phases of the moon). McGrail (1998) notes that classical sources ascribe a "good working knowledge of astronomy ... with particular emphasis on the moon" and that "such learning would have had direct application to direction finding at sea and to tidal prediction" (1998, 277).

2.3.6: Navigation by Natural Features

Both terrestrial and marine topography can be used to navigate. Terrestrial features can be used to navigate when the location of those features is known, and having sets of known features – landmarks – allows navigators to orient themselves relative to landmark alignments. Although the sea bed is not visible, it can be used to navigate by taking soundings. Both of these navigational techniques could have been used in the English Channel during the late Iron Age.

In the first place, indented coastlines along the Atlantic Zone contain many natural features that could have been used as landmarks (see Davis 1997; Section 5.2.4). Prominent places such as points, rocks, and hills can be seen from far away in clear weather. Colour contrasts also aid visibility, in particular in the case of chalk landscapes and coastal islands befouled by sea birds. Distance from a landmark can be roughly estimated by observing its size in the navigator's field of view. If a landmark has a distinctive shape, then it may be possible to work out the direction relative to a navigator. These methods may not be particularly accurate, especially at long distances. Another way to navigate by landmarks is to reference landmark alignments. If two landmarks are seen to line up, then a navigator who is aware of the landmarks' location can assume that he or she is somewhere on a line defined by those locations. In Shetland, where this system of navigation was used by fishermen into the 20th century, these lines are known as 'meids' (Simpson 2010). Figure 2.8 shows how meids can be used to work out position and to define particular areas of sea. Navigation by meids is useful because its practitioners can fix their positions very accurately, however this accuracy is contingent on the coverage of meids over the waters that one intends to sail. Poor visibility in cases of bad weather can also make navigation by landmarks difficult, creating an incentive to establish other 'backup' meids.

In the second place, soundings can be used to navigate when the composition of the seafloor is known. Sounding involves lowering a weighted object (a lead) attached to a line from the deck of a ship until the lead rests on the seafloor. The length of the line can be used to estimate the depth of the seafloor, and sediment that adheres to the lead when brought back onboard can be used to estimate a ship's location. The texture and composition of sediment brought up by a lead can indicate specific areas or the general

characteristics of a coastline. For example, clay-silt may indicate the presence of an estuary nearby. Sounding lines had been in use in the Mediterranean since the 5th century BC, and it is possible that by the Late Iron Age they were being used by sailors in the Atlantic (McGrail 1998, 276). McGrail estimates that the maximum depth of sounding lines recovered in the Mediterranean were approximately 50 or 100 metres – a depth limit which encompasses most of the inshore waters of the Atlantic Zone Section (see Section 5.4).

For both of these types of navigation, detailed local knowledge is essential. Natural landmarks can be easily mistaken for one another – particularly in poor weather – which means that relying on only a few landmarks can lead to disaster. Navigation by meids may be more accurate, but still requires the navigator to build up a mental map of alignments and the waters to which they correspond. Navigation by taking soundings requires a very detailed knowledge of the composition of the sea floor for it to be used on its own, especially given that similar sediments may be found in different areas or spread across a very large area.

2.3.7: Navigation by Anthropogenic Features

The method for navigation by anthropogenic features is essentially the same as the methodology for navigating by landmarks in the previous section (i.e. by using dead reckoning and meids). In this case, however, the landmarks that are used are designed in order to be visible and in order to convey information to sailors. This may include creating markers with distinctive shapes, colouring markers brightly or so as to create contrast, setting markers so that they intersect a viewer's horizon line, or placing lights on a marker in order to make it visible at night. The modern lighthouse is a good example of these

techniques in action. Most lighthouses are designed as towers, which can be seen from far away and which intersect the horizon. They are often painted white, which creates a colour contrast with land behind it, or in alternating white and black stripes. At night, the beam of a lighthouse makes it clearly visible to ships.

Whether or not Iron Age seafarers created features for the purpose of standing as landmarks is uncertain. However, coastal sites meet several of the criteria mentioned above. Many Iron Age promontory forts are placed in very visible locations that can be seen from great distances. The earthworks associated with these sites give them distinctive shapes, and when viewed from a distance serve to separate the sites from the rest of an observer's skyline. Ramparts and exposed soil at these sites would have created colour contrasts that would have made them more visually prominent – especially in the predominantly-chalk soils on Britain's southern coast. There is some direct evidence for signal fires at promontory forts (Pouncett & Schulting 2012), and the potential of hillforts as links in a signalling network has been explored in other parts of Britain (Robinson & Soper 2011).

It is important to recognise that the landmarks used to navigate may include natural and anthropogenic features. In Shetland, for example, meids were often based on alignments between a prominent hill and an especially visible structure (often a white house – see Simpson 2010). Coastal features could have been used in the same way by Iron Age navigators.

2.3.8: Navigation by Animal Behaviour

The behaviour of animals can be used as a navigational aide, although it is generally not treated as such in navigational literature. Animals have been observed

navigating by landmarks, smell, and sight; as well as by dead reckoning and celestial bodies (see below). Some animals – in particular certain fish and bird species – are able to orient themselves within the earth's magnetic field, which they use to navigate (Howard 2018; Scanlan et al. 2018). The behaviour or presence of these animals can be used to navigate, if the navigator is sufficiently familiar with their habits.

It is difficult to say which animal behaviours would have been useful to Iron Age navigators, as the subject has received little scholarly attention. Fish were apparently underexploited in the Iron Age North Sea (Dobney & Ervynck 2007), but this does not necessarily mean that this was also the case in the Atlantic Zone or that fish behaviours were unfamiliar to people living on the shores of either body of water. It is probably safe to assume that the behaviour of seabirds was familiar to people who lived near and made their living on the shore, however. These people would have likely followed seabirds to schools of fish, and may have hunted them or raided their nests for eggs. The observations they collected for these purposes could have also helped them navigate. For example, they may have associated increasing numbers of 'inshore' seabirds with nearby land. Gulls, for example, are land-based birds, and typically stay within 80 kilometres of the coast.[18] Gulls are inter-tidal feeders and scavengers; their main sources of food are beaches and estuaries (where they find molluscs, urchins, starfish, and seaweed), the nesting grounds of other birds (where they steal eggs and hatchlings), and human settlements (where they scavenge waste). Because gulls get most of their food from terrestrial sources, navigators who observe increasing numbers of gulls may assume that they are nearing land. Conversely, the presence of a wide-ranging seabird such as the

[18] Although they are known to follow boats – particularly trawlers – outside this range (Gatty 1958, 197).

Great Skua (whose range covers most of the North Atlantic) is not necessarily a sign that a nearby ship is close to land. Some birds have specialised behaviour that may indicate the direction of land; in the Channel the most useful seabirds for this purpose would have been puffins and shearwaters.[19] During the breeding season (early summer), these birds alternate between their nests and feeding groups that 'raft' on the open sea. Puffins and shearwaters depart their rafts at dawn or dusk to return to their nests, so the direction in which they fly at these hours can be taken as the direction of land (see Gatty 1958). The use of captive birds to find land is probably the oldest attested method of navigation at sea – it is referenced in the *Epic of Gilgamesh* in the late second millennium BC, where the protagonist uses doves, sparrows, and ravens to find land after a flood (George 2000, 93-4).

Methods of navigation that follow animals or make inferences from their behaviour require a working knowledge of their behaviour in order to use reliably, and then may provide limited information about one's location. Harold Gatty, writing in a guide to 'natural navigation', writes that "it is absolutely necessary to take into account the law of averages ... no evidence from bird numbers at sea should be regarded as conclusive, unless it involves more than a handful of observations of several different species or unless it is coupled with indications from other natural signs" (Gatty 1958, 175). However we should not discount navigation by animals as a potential type of navigation used in Iron Age voyages because we consider it to be unreliable, and bear in mind that the use of animals for navigating has been confirmed in other parts of the world.

[19] See Robinson (2007, 185-6) for lists of birds present on the Scilly Isles during the 1st and 2nd millenniums BC.

The aforementioned *Periplus of the Erythean Sea*, for example (see Section 2.3.3), records that for ships bound for the Sinthos River "an indication to those coming from the sea that they are already approaching land in the river's vicinity are the snakes that emerge from the depths to meet them" (Casson 1989, 73). In the Pacific, Gladwin (1970) identifies animal behaviours as part of navigational knowledge on the Micronesian island of Puluwat. In this case navigators compiled 'inventories' of animals that were through to signal different approaches to islands in the twenty-eight directions specified by the constellations that make up the Puluwat 'compass'. According to a skeptical Gladwin, a sample of 'sealife' around the island of Puluwat consists of birds and fishes in various arrangements, as well as a whirlpool that "really exists" (1970, 204). While the Puluwatis acknowledged that sealife was only rarely sighted; nevertheless they counted it as an important component of their system of navigation (Gladwin 1970, 204-208).

2.3.9: Navigation by Celestial Bodies

The position and course of the sun, and of stars in the nights sky can be used to navigate. The course of the sun is determined by the orbital characteristics of the earth, which means that its position can be predicted from repeated observations. In the northern hemisphere, the sun points due south at midday. At night, stars appear to revolve around the earth's axis of rotation. Stars that occur near this axis may appear stationary relative to an observer from earth, whereas stars falling near the horizon will be seen to rise and set. Like the sun, stars point in consistent directions when they have reached their apogee. Stars that have apogees close to the horizon are particularly useful for navigation at sea, if the direction of their rising is known. Figure 2.9 illustrates how stars appear to move from the perspective of a navigator.

There are several important advantages to navigation by celestial bodies. Although the position of stars does move over time, these changes take place over hundreds or thousands of years. The 'north star' Polaris, for example, would have been around ten degrees from the celestial pole in the Late Iron Age.[20] However since the courses of stars are essentially stable over the timespan of several human generations, they can be used to build durable systems of navigation that can be easily transferred to other parts of the hemisphere. Celestial navigation is widely attested to in literary sources – Homer has Odysseus navigating by stars in the *Odyssey* (5.271-74; see Mark 2005, Theodossiou *et al.* 2011) – and has is widely cited as a potential form of prehistoric navigation (see Davis 1997; McGrail 1998, 280-281; Cunliffe 2001, 81-84).

The obvious downside to navigating by the sun and the stars is that the navigator can only make useful observations of the sun at high noon and of the stars at night. Cloudy or misty weather can also prevent navigators from using celestial bodies to navigate. In the context of the Atlantic Zone (particularly northern portions), this makes celestial navigation problematic. In the first place, visibility in the Channel is variable. An analysis of Meteorological Office records for the English Channel (see Section 5.4.1) suggests that good visibility ought to occur roughly twenty percent of the time (see Meteorological Office 1940). Since celestial navigation requires small sections of the sky to be visible at precise moments, the effect of scattered clouds on ship being navigated by the stars may be more than the effect of the same ship navigating by a set of nearby landmarks. The high number of mixed reports also demonstrates how changeable visibility conditions in the Channel can be. In the second place, sailing at night can be risky – especially when

[20] In classical antiquity the star Beta Ursae Minoris was closer to the celestial pole (see Dicks 1970).

close to shore. Accordingly, navigating by the stars would have required careful planning in order to avoid making landfall in darkness.

2.3.10: An Iron Age Navigational Method

All of the navigational techniques that have been described so far share two important features. First of all, these techniques require detailed knowledge in order to work effectively. Although many of the processes that underpin these systems are regular and predictable, they can also be extremely complicated and difficult to predict – especially without understanding the mechanics of the system involved. It is not likely that people in the Iron Age understood that the moon's gravitational pull creates tides on earth, but they probably did understand that the moon was somehow responsible based on years or possibly generations' worth of observations. Navigators needed to acquire this knowledge through teaching or personal experience, and also needed to be skilled in applying this knowledge to actual conditions at sea. Secondly, these techniques are not always reliable – both in the sense that they cannot always be used, and in the sense that they do not always produce the same amount of useful information. Navigation by stars is impossible on overcast days, navigation by landmarks is difficult in areas where the shoreline lacks relief, and the presence of seagulls is not particularly enlightening when the length of the crossing is half of their maximum range. Navigators would have relied on combinations of these techniques rather than a single one, both in order to limit the chances of having no techniques available in poor conditions, and in order to enhance the accuracy of their predictions. Navigation using multiple techniques produces predictions that are more than the 'sum of their parts', since the results of one technique can be used to inform the results of another technique. If each technique suggests different sets of

possible positions, the navigator can compare these sets to make a more accurate assessment. Using multiple techniques also reduces the risk that unreliable observations affect the final assessment too much.

The type of navigation that Iron Age mariners would have used in the Atlantic Zone is best understood as a collection of heuristics which they would have used in combination in order to estimate their position, rather than a single method. In waters that they were familiar with they likely used natural and anthropogenic landmarks when they were visible, and when these could not be seen they would have relied on observations of the sun and stars, currents, local wildlife, and an estimate of their progress according to a 'reckoned' course. Since the actual knowledge that they carried about these conditions is lost to us, we cannot say how these different navigational techniques stood in relation to each other in their own minds. To return to the island of Puluwat, Gladwin notes "the other remarkable thing about sealife inventories is that navigators seem to take them seriously" (1970, 204). Gladwin found that navigators admitted that sealife was rarely observed in predicted locations, but insisted that when it was observed it was a useful navigational aide. This example should serve as a caution against ranking the navigational techniques of a prehistoric people based on their presumed practicality or utility. This being said, the model here places its focus on the two navigational techniques that would have been most useful to Iron Age mariners in the Atlantic Zone: dead reckoning and navigating by landmarks.

Chapter 3 : Seafaring Models in Theory and Practice

3.1: Methods for Modelling Navigated Routes

Although route-finding methods for terrestrial environments are common in GIS, this well-trod path disappears at the water's edge. Methods for modelling movement over water fall into four general categories: velocity prediction programs, least-cost-path analyses, routing analyses, and agent-based models. Although there is some overlap between these methods, they reflect different approaches to maritime movement: from hydrography, from topographic analysis, from marine forecasting, and from archaeological/anthropological models, respectively. The following sections describe how each of these methods is used to model the movement of ships over water, and how these analyses have been used in archaeological analysis. Published archaeological models are few and far between (see Slayton 2018, 55-57), and of these only a few address voyages where sailing is the primary method of propulsion. Because sailing models are so few, this section includes analyses that focus on rowed/paddled voyages and drift voyages where these methods use techniques that could also be used to simulate sailed vessels.

3.1.1: Velocity Prediction Programs

The performance of sailed craft are characterised in hydrodynamic literature as 'velocity prediction programs', or VPP (Milgram 1997). These programs use parameters of naval architecture to predict a ship's velocity under all angles of attack under 'ideal' conditions (i.e. flat water). Although VPPs can be useful for understanding the theoretical capabilities of archaeological watercraft, they are somewhat less useful at modelling

sailed voyages. Because VPPs are usually used to analyse and fine-tune sailing yachts, they are not designed to predict performance in sub-optimal conditions. For the same reason these programs assume that ships being modelled have design features common to modern sailing boats (such as Bermuda rigs and projecting keels) that would not have been found on Iron Age boats.[21] Navigation is not addressed at all within these models, since their main purpose is to optimise performance rather than simulate routes. The proprietary nature of most VPPs, however, is the main impediment to their use in an archaeological study, as this makes them more difficult to incorporate into other computational environments. Even if an 'archaeological VPP' were to be developed, modellers may struggle to gather the necessary data to make accurate predictions. To calculate resistive forces acting upon a hull requires a 3D model of that hull, which may be difficult to generate where direct evidence for ships is lacking – as in the Iron Age Atlantic (see Section 2.2).[22]

3.1.2: Least Cost Path Analysis

The most common computational method for simulating movement over water is least cost path (LCP) analysis (see Davies & Bickler 2013, 216-7; Slayton 2018, 55-7). LCP algorithms are designed to find the most efficient route between two known points, and are common in archaeological movement analysis. Tools for generating LCP are

[21] Examples of (proprietary) VPPs include: Sailfish (http://techsail.com/); AHVPP (http://www.aerohydro.com/products/marine/ahvpp.htm), and HydroComp (https://www.hydrocompinc.com/).

[22] In this analysis general parameterisations were used rather than a 3D model, but it is possible to generate speculative models and quantify their performance in a VPP (see Section 9.3.1).

widely available in GIS programs, including ArcGIS, GRASS, and R.[23] Archaeological LCP analyses generally follow three steps: cost surface generation, accumulated cost calculation, and path calculation.

In the first step, raster inputs are combined in order to create a cost surface that represents the amount of resistance (in terms of time, energy, or some other metric) to travel through the cell in question. Topographic data (i.e. elevation models and derivatives) are the most common basis for building archaeological cost surfaces. Other data sources used to build ACS include landcover, visibility, and features representing corridors or impediments (Herzog 2014). The two main challenges for archaeologists generating cost surfaces are correctly modelling cost for anisotropic surfaces (surfaces where the cost of moving through a cell differs with the direction of movement), and in combining multiple cost surfaces into a single raster for computing cost accumulation. In the first case, Tobler's Hiking Function (Tobler 1993) is the most commonly-used method for generating a cost surface from elevation, slope and aspect. The ArcGIS Path Distance Tool also calculates anisotropic costs using the same three inputs.[24]

In the second step, the cost surface is evaluated against an origin point in order to create an accumulated cost surface (ACS). The ACS is generated by computing the cost of moving from that cell to cells within a set neighbourhood, starting with the origin and

[23] See, respectively: https://pro.arcgis.com/en/pro-app/tool-reference/spatial-analyst/cost-path.htm, https://grass.osgeo.org/grass78/manuals/r.cost.html, and https://cran.r-project.org/web/packages/leastcostpath/vignettes/leastcostpath-1.html.

[24] See: https://desktop.arcgis.com/en/arcmap/10.3/tools/spatial-analyst-toolbox/understanding-path-distance-analysis.htm

spreading to the extent of the dataset. LCP algorithms used in GIS programs follow Dijkstra's Algorithm (1959), which converts cells in a raster to points in a weighted graph (see Herzog 2014). Links between nodes are weighted based on adjacency and the type of window used in the spreading algorithm, and during this spreading process the backlinks between nodes are stored. These backlinks are used to construct a pathway.

In the final step, a pathway is generated from the ACS. Herzog (2014) points out that some GIS packages use drainage algorithms rather than the full implementation of Dijkstra's Algorithm to avoid having to track backlinks. The full implementation, however, is supported by both ArcGIS and GRASS, and involves tracing backlinks from the destination point back to the point of origin. The end result of this process is the creation of a pathway that is maximally efficient, according to the terms of the ACS.

3.1.3: Applying the LCP in Archaeological Analyses

LCP is usually presented in reviews and manuals as the go-to method for modelling terrestrial movement. As such archaeologists interested in applying LCP analysis to maritime contexts have had to come up with solutions and workarounds for some of the assumptions implicit in the process. Cost surface generation has been a particularly difficult issue, since many maritime 'costs' are anisotropic, and no widely-accepted "boating function" exists. Where archaeologists have developed their own alternatives, they tend to be narrowly research-focused. For example: Gustas & Supernant (2017) use Tobler's Hiking Function without modification, ignoring travel times produced in the output so that they can focus on the pathways themselves as a component of site likelihood. Livingood (2012) adapts Tobler's Hiking Function to historic and modern canoeing datasets in a custom script in order to create cost surfaces. Leidwanger

(2011, 2014) uses the ArcGIS *Path Distance* tool to calculate costs, by treating the heading of a ship moving into a cell as the horizontal relative moving angle, and using values derived from average wind speeds as a 'vertical factor' (2011, 109).[25] Indruszewski & Barton's (2008) method for generating maritime ACS avoids these problems by using a 'wildfire spreading' tool to model the effect of wind (see Figure 3.1).

3.1.4: Isochrone Modelling

The isochrone method for modelling vessel routes was originally developed by Richard W. James (1956) as a practical method for plotting courses by hand using basic ship parameters and wave charts. This method consists of constructing vectors representing possible ship courses, adjusting the lengths of those vectors to reflect the distance achievable in 24 hours along the heading, and joining the endpoints of those vectors to create an isochrone representing the potential location of the vessel in 24 hours. James' procedure iterates by constructing an arc centred on a destination point tangent to the curve defined by the isochrone, and selecting the point of intersection as a starting point in the next iteration (1956, 52). This method was developed into a computational 'modified isochrone method' by Hideki Hagiwara (1989), who treats the isochrone method as a process of 'discrete optimisation'. Hagiwara's method involves generating isochrones by generating and evaluating course-vectors at regular intervals, and selecting a vector based on its distance from the starting point as the starting point in the next iteration. Hagiwara's modified method then traces a path backwards from the destination through isochrone vertices in order to find the most efficient path.

[25] See: https://desktop.arcgis.com/en/arcmap/10.3/tools/spatial-analyst-toolbox/path-distance.htm

A recent push by Jan Hildenbrand (2015), Jan Chrisoph Athenstädt (2018), and Emma Slayton (2018), has developed the modified isochrone method further by optimising the generation of isochrones to avoid obstacles and 'loops', using ACS in evaluating course-vectors, and modelling the effect of leeway by adding an offset to course-vectors. These processes have been developed into GIS tools that have been used to simulate canoe travel in the Greater Antilles (Athenstädt 2018, Slayton 2018). Hildenbrand's model generates course-vectors dynamically (rather than at fixed intervals, as in Hagiwara's method) by attempting to construct a new vector within a set interval if an obstruction is in the way (Figure 3.2). He also includes a process for removing overlapping isochrone points that 'loop' around islands. The tool developed by Slayton and Athenstädt calculates vessel speed by using a canoeing speed function and an ACS – essentially using least-cost paths to generate course-vectors – and applying a vector offset based on the speed and direction of the wind.

The modified isochrone tools developed by Athenstädt, Hildenbrand, and Slayton avoid many difficulties in implementing maritime movement analyses in GIS by implementing the process in a custom program whose results can be easily converted into GIS datasets (Slayton 2018, 78). Although producing a model outside of established GIS tools is more difficult (the model developed for this thesis encountered many of the same problems addressed by the isochrone method), the reward is a model that engages with hydrodynamic parameters directly instead of treating them as terrestrial proxies (see Section 3.2.2).

3.1.5: Agent-based Modelling

Agent-based modelling (ABM) is a method of simulation in which a system is modelled as a collection of autonomous parts. These parts are analogous to real agents in that they are programmed to act as individual units within the remit of the simulation (Lake 2014). Agents are placed in a simulated environment and are given rulesets for interacting with that environment and (usually) other agents. Research using ABM observes the behaviour of agents whilst varying rulesets and/or environmental parameters in order to test claims about the system. ABM has been promoted as a means to address some of the perceived shortcomings in more formal mathematical models, such as: reduction to a single scale of analysis, reliance on small or simple parameter sets, absence of individual behaviour as a model input, and the difficulty of incorporating qualitative data (Ferber 1999).

Agent-based modelling is not new in archaeology but has become much more popular in recent years (Lake 2014, Cegielski & Rogers 2016). This increase has been attributed to practical factors such as increased availability of processing power, the development of ABM software tools such as NetLogo, and an increase in interdisciplinary studies with fields in which ABM is more common.[26] The development of ABM approaches to navigation and maritime movement has occurred in fits and starts over the past several decades, as researchers have begun to use ABM methods as components within more traditional models. The model developed by Irwin et al. (1990) to investigate the Polynesian colonisation of the Pacific, for example, was not presented as an ABM but

[26] See: https://ccl.northwestern.edu/netlogo/.

shared some key features – in particular rulesets that determined how vessels interacted with different types of winds, and rulesets determining when and how the vessels were able to navigate. Callaghan & Scarre's analysis of Neolithic seaways (2009) shared many of the same features, although it was not fully computational as it requires the user to select a sailing 'strategy' for the iteration of the model. The strategy selected by the user guides the simulation of the vessel's movement by reference to a precomputed table of expected vessel speeds under 'various wind conditions' (2009, 361). For the purposes of their research Callaghan & Scarre's model recorded voyage durations for simulated routes, and considered voyages to be successful if they made landfall at their intended destination. The model developed by Davies & Bickler is a genuine ABM, using NOAA weather records in a simulation that involves NetLogo, R, and Google Earth (2013, 218). As with the model developed here (see Section 4.3), Davies' and Bickler's model uses a polar diagram to calculate sailing speeds under different wind conditions, and lets navigators choose between navigation by dead reckoning and navigation by latitude.

3.2: Issues with Modelling Movement over Water

Since LCP-based approaches are well established in archaeology, and have been deployed in archaeological analyses of movement over water, one might reasonably ask why coding-heavy approaches such as the isochrone method or the development of a new ABM is necessary. In order to answer the research questions in this study, a LCP seafaring model would have to fulfil two conditions – that the LCP can simulate movement over water in sufficient detail to make it useful for this analysis, and that the LCP can be used to simulate *navigation* in addition to movement over water. This section discusses the challenges that LCP analyses face in fulfilling these two requirements in order from 'least

problematic' to 'most problematic'. Overcoming these problems ultimately requires either the production of new cost functions, modifying or coordinating the LCP process with custom code, or ignoring important aspects of navigation in favour of a purely quantitative analysis. None of these options is appealing: generating new cost functions falls outside the scope of a typical archaeological research project, custom code is already required to develop isochrone- and ABM-models, and qualitative factors are extremely important to the practice of navigation at sea.

3.2.1: Integrating Four-Dimensional Data

The first difficulty in using LCP analyses to simulate navigation lies in the dynamic nature of hydrodynamic and/or aerodynamic (hereafter referred to as 'environmental') data sources. The fact that environmental parameters vary over time is a practical problem for LCP analyses in which terrestrial data inputs such as elevation and aspect are replaced by environmental datasets such as current speed and direction. Using a single set of environmental observations to build an ACS assumes that the currents, winds, etc. that they represent are constant throughout the voyage, when this is rarely the case. Overcoming this problem comes either at the expense of data resolution or ease-of-use. In the first case, some archaeologists have time-averaged environmental data in order to produce an ACS (see for example Liedwanger 2014), generally in order to produce datasets representing 'prevailing' currents or winds. Although this allows an entire voyage to be simulated in a LCP, it removes potentially important variation in the data and limits analysis to time-scales at which a factor can be said to be 'prevailing'. The isochrone method avoids this problem by treating each stage of a journey as a separate LCP analysis, generating new cost surfaces every 3 hours in the case of Slayton's analysis

(2018, 67). Although this effectively addresses the problem of incorporating four-dimensional data it comes with an increased computational load, as each voyage is built out of a chain of LCP analyses rather than a single one.

The flexibility of agent-based models makes it simple to incorporate four-dimensional datasets, as these models iterate over timesteps rather than over cells in a raster. Moreover, designing an ABM for seafaring allows for environmental datasets to be read natively, without necessarily having to interpolate or convert them into other formats. In the end, the challenge of incorporating four-dimensional data precludes 'out-of-the-box' LCP studies where averaging environmental parameters is not appropriate, such as in areas where there is considerable variation in these factors, or for studies focused on shorter voyages.

3.2.2: Using Hydrodynamic Data as Proxies for Terrestrial Datasets

Calculating maritime costs has been the subject of some debate, as can be seen by the variety of solutions mentioned previously. The simplest approach has been to use existing cost-surface-creation tools by using maritime data (in particular wind and current data) as proxies for terrestrial datasets such as slope maps and aspect maps. For example, Newhard et al. (2014) and Liedwanger (2015) have argued that wind is similar to slope in that it either helps or hinders travel through an area depending on the direction of travel. In both cases ESRI tools are used to generate cost surfaces from hydrodynamic inputs for which 'slope' and 'aspect' have been generated. The main problem with this approach is that the effect of wind on a sailed vessel is not well-represented by a continuous function. The relationship is in fact discontinuous, as sailing into a vessel's dead zone removes *all* 'assistance' from the wind. Since cost functions are generally continuous (Herzog 2014),

discontinuities in input datasets present a problem for modellers that must be addressed. Another important difference between slope and wind is illustrated by cases where there is no wind (i.e. where the 'wind slope' is zero). In this case, following LCP logic, one surmises that the wind provides neither cost nor benefit for travel through the area. In reality, being becalmed prevents a sailed vessel from moving at all.[27] Although slope and wind may be similar, the problem here is that walkers and sailing ships interact with slope and wind in fundamentally different ways. Slope does not power the movement of walkers, but wind does power the movement of sailing ships. Using current as a proxy for terrestrial datasets raises different, and possibly more difficult issues. Current is different to both wind and slope in that it is both in motion and the medium in which a ship moves.[28] This means that the cost to move from one cell to another in a current-based cost surface may be negative, in cases where the strength of the current is greater than the maximum speed of the vessel. This premise violates Dijkstra's Algorithm (Dijkstra 1959), which is implemented in most GIS LCP routines. This is important for navigation modelling purposes because navigators will often take currents into account when selecting a course, attempting to offset the force of currents in order to reach their destination.

[27] One could argue that sailors may have had alternate methods of propulsion (such as rowing) for windless situations, providing a 'base speed' which wind conditions could either improve or reduce. Neither Newhard (2014) nor Liedwanger (2015) makes this case, however.

[28] Although wind is also a medium in which a ship moves, it exerts much less force on a vessel if sails are not raised.

These problems become more acute at finer resolutions, which perhaps explains why they are often left unaddressed (see Herzog 2014). For example, a hypothetical study in which the resolution of inputs is fifty nautical miles and wind/current vectors are averaged across the course of a month is unlikely to run into the problem of negative costs, because foul streams or similar extreme conditions would likely be 'averaged out' of the input datasets. Similarly, a study in which inputs are probabilistic – for example, where wind is represented by the percent chance that a strong wind will occur in the area – avoids the 'zero slope' problem by assuming that a ship will be able to travel into wind so long as the percent chance of an oncoming wind is less than one hundred. As more detailed environmental data becomes available, the limitations of LCP will become even more of a barrier to making effective use of these datasets in a movement model.

The problem here is not necessarily with the practice of using hydrodynamic data as proxies for terrestrial data, but with equating terrestrial movement with seafaring. When the logic of a GIS tool is not consistent with the logic of the practice under consideration, new approaches are necessary (see Lock & Pouncett 2010, 2017). In a LCP context, problems of modelling seafaring in a GIS environment can be addressed by developing new methods for cost-calculation and accumulation.

3.2.3: Building an Accumulated Cost Surface from Hydrodynamic Data

In order to build an ACS without relying on existing tools, modellers require a process for creating cost surfaces, and a process for combining those surfaces into a single ACS. The diversity of LCP-adaptations for maritime movement modelling reflects the diversity of seafaring technologies and techniques. Although evaluations of Tobler's Hiking Function under different conditions have led to the development of new functions

(see for example Irmischer & Clarke 2018), it is generally accepted that a model that describes modern walkers describes walkers in archaeological contexts reasonably well. The same cannot be said for ships, especially when considering factors such as hull design and rig. Since calculating cost surfaces for ships can be problematic using terrestrial methods, archaeologists have tended to base custom cost-designation procedures on experimental data, usually by referencing a table of calculated or observed speeds under different conditions, or else by deriving a cost function from a set of observations. Allocating cost from experimental data avoids the methodological problems raised in previous sections, while limiting the applicability of these methods to contexts in which ships and environmental conditions are similar to those of the original research. As a consequence, models based on experimental data are more likely to become restricted to areas in which research goals overlap (particularly in the Mediterranean and the Pacific). Cost functions developed for maritime LCP analysis, by contrast, are more widely applicable but tend to be simplistic. The procedure for the ORBIS Roman network model, for example, estimates travel times by representing the effect of wind on a sailing vessel as *time = function1(wind velocity) / function2(wind velocity)*, and characterising the effect of wind angle of attack on vessel speed using the (continuous) cosine function (Meeks 2105, Arcenas 2015).[29] Although this approach is easily transferrable, its extremely general characterisation of ship parameters makes it less useful in addressing the research questions of this study.

[29] The ORBIS method was not included in previous sections as it is designed to estimate travel time over pre-determined rather than navigated routes (Meeks 2015).

Difficulties in combining different types of environmental cost surfaces into a single dataset present further challenges to building ACS for maritime movement modelling. Archaeological LCP analyses almost always use a single environmental parameter to generate cost surfaces (with the notable exception of Indruszewski & Barton (2008)). The use of a single cost surface is usually justified either by citing regional conditions (for example: weak currents in the Mediterranean (Liedwanger 2013, 99-100)) or by arguing that only one parameter is significant from the standpoint of research questions. In the first place, accepting that some contexts are 'modellable' and others are not places an arbitrary limit on archaeological analysis. In the second place the argument that navigation and seafaring can be modelled accurately based on a single parameter advances a grossly oversimplified view of navigation and seafaring (see Chapter 2). The model developed for this analysis considers four discrete environmental parameters (wind, current, tide, and weather; see Section 5.4), to say nothing of parameters that *could* be incorporated into future versions of the model (see Section 9.4). Models that weight hydrodynamic and aerodynamic costs against one another (Slayton 2018) have the potential to widen the number of parameters that can be incorporated into an ACS, and this approach is likely the way forward within a LCP environment.

3.2.4: Incorporating 'Qualitative Costs'

Combining environmental factors into an ACS is difficult, but achievable given a sound enough understanding of conditions and the vessel in question. However, adding qualitative costs to an ACS is not straightforward. The main problem is characterising qualitative factors as 'costs'. In the context of navigation, qualitative parameters include factors such as the visibility of landmarks, the approachability of beaches, the potential

for good or foul weather, and the location of an area or object in a person's mental map. Because these phenomena are not themselves directly observable by others, they must be approached through proxies. Sandy beaches with shallow shelving and protection from the wind are arguably 'good' landing places, and GIS analyses can be used to apply physical criteria to characterise landscapes and seascapes as having good or poor landing places.[30] This exercise becomes harder when the criteria used to evaluate qualitative costs are less clear. The potential for good or poor weather is particularly difficult to parameterise both because there are many different ways of forecasting the weather (for example: different types of cloud, changes in atmospheric pressure, and previous experience) and because people are not necessarily consistent in predicting it accurately. The main problem with incorporating qualitative parameters into ACS, however, is that these parameters may not have simple (or any) relationships with cost-of-travel. Travellers who want to remain hidden, for instance, do not find it any more difficult to traverse an area because they want to avoid being seen. In fact, they may want to move through visible areas quickly in order to avoid detection, in which case from an ACS standpoint one might be tempted to reduce the cost of moving through highly visible areas. In reality decisions about navigation (and many other things) hinge on an evaluation of the risks and rewards of different courses of action based on the affordances that the decider recognises in their environment (see Turvey 1992, Gillings 2012). ACS-based approaches that integrate qualitative data essentially invent affordances in order to model their effect on pathfinding. Although all modelling is speculative, taking this

[30] See, for example: Wilkes (2004) in the context of this work, Gustas & Supernant (2017) in the context of LCP analysis.

approach demands a great deal of care. Gustas & Supernant (2016) use a number of different parameter weights in generating ACS for their analyses of canoe travel in the Pacific Northwest, grouping variables as 'cultural', 'environmental', and 'physiological'. Research of this type has the potential to develop a basis for arguing for relationships between certain qualitative parameters and cost-of-travel. However in this case much more work would need to be done to establish the validity of proposed relationships.

Given that the issue with parameterising qualitative parameters as costs lies in the potential lack of a relationship between the two, accumulating two qualitative-parameter-cost surfaces compounds the problem. If the relationship between parameters and costs is not demonstrable, then how can they be combined? Moreover in cases where movement is affected by two important qualitative variables – say 'being unobserved' and 'keeping a landmark in sight', which one should take precedence? These questions are difficult to answer, and it is telling that the isochrone method avoids these questions entirely by using quantitative parameters to generate its ACS, and using the results of LCP analyses to choose a path. However the qualitative nature of navigation precluded this approach in the development of a navigation model in this analysis. In an ABM, navigation can be modelled by approximating navigational methods with a set of rules, and creating rulesets that determine whether certain navigational methods are used and how much the results of these methods affect decisions made by the agent. This approach avoids the concept of cost entirely, and all the problems attendant on it.

3.2.5: Optimality and Navigation

This thesis advances the argument that navigation should be understood as a collection of heuristics or methods which can be used in combination with each other,

rather than a single method (see Section 2.3.10). Methods of navigation may work at different levels of accuracy under different conditions. By employing several methods at the same time, navigators attempt to eliminate uncertainty in their measurements. This is important because conditions at sea can be difficult to read correctly and predict robustly. A good navigator will not only be able to make good observations and predict conditions accurately, but also know when different methods of navigation are more or less accurate and whether the results of these methods can be trusted. The challenge for LCP- and ACS-based simulations of navigation is reconciling the multi-heuristic nature of navigation with a computational process premised on finding the optimal path between two points. The argument that LCP analysis is sufficient for modelling navigation essentially assumes that the routes that people travel are maximally efficient, or at least trend towards maximal efficiency over time (Herzog 2014). Anyone who has been lost in a poorly-signposted airport, hospital, government office, etc. will be able to dispute this assertion, so the notion of maximal efficiency tends to go hand-in-hand with the assumption that people in the past had a near-perfect understanding of their environment. This second assumption is implicit in LCP analyses, where it is represented by an ACS in which all costs are precisely defined, and a path is computed based on an evaluation of *all* values. Although the isochrone method addresses issues of multidimensional data and cost calculation raised in previous sections, it still likens pathfinding to an 'optimisation process' (Hagiwara 1989). While this hypothesis is arguable in terrestrial contexts, it is often untenable in maritime contexts.

In the first case, challenges involved in reading and forecasting environmental conditions make it difficult for the inexperienced navigator to decide which course is the 'optimal' course. Some conditions at sea may be predictable, whereas others may change

suddenly at short notice. In terrestrial contexts, people may be able to optimise their behaviour once they have spent enough time in a landscape to understand how that landscape affords movement – say by avoiding large hills. It can be more difficult to cultivate a similar understanding at sea, especially if conditions are unstable. If we equate the surface of the sea directly with the surface of the land, we should wonder whether people would eventually optimise paths within their neighbourhood if the hills around them were constantly (and occasionally unpredictably) reconfiguring themselves.

The second problem with optimisation as applied to seafaring is that it assumes a body of knowledge about local conditions which is accurate and widely accessible. However in the context of this study such an assumption would be presumptuous. Information on the optimality of sea-routes is lost whenever a voyage fails catastrophically – mariners who go down with their ships do not get the opportunity to share the details of their course. A second problem with assuming a common pool of maritime knowledge in a community is the existence of social impediments to the exchange of information within or between those communities. Gladwin (1970) found this to be the case in Puluwat, where navigators were separated into several 'schools' with their own sets of methods (Section 2.3.8) Although we are unlikely to ever discover whether the Iron Age Channel has similar institutions, we should at least consider the possibility that navigational knowledge was not widely distributed throughout Atlantic Europe.

Although efficiency was surely a factor in the decisions that navigators would have made as they planned their voyages, it would be wrong to say that it would have been the *only* factor in their decision-making process. Other social or practical factors also influence these decisions. ABM has the potential to address these factors and

incorporate them into the decision-making process, guiding the actions of agents in the model. Abandoning assumptions of optimality also has practical dividends for an ABM model. Whereas the isochrone method generates a new isochrone from each vertex in the preceding isochrone in order to select the most efficient path, an ABM can be designed to select a heading based on other criteria that do not require as much validation or data processing.

3.2.6: Agent-Based Modelling as an Alternative to ACS-Based Analysis

The application of LCPs to the contexts of maritime travel and navigation illustrate how the strengths of a GIS tool can become weaknesses when used outside of the context for which they were designed. Assertions that 'wind is the equivalent of slope' are oversimplified and mask the simple fact that land and sea behave very differently when traversed. Although modelling maritime movement – and in particular sailing – requires factoring in both hydrodynamic and aerodynamic data, LCP currently lacks a simple and robust means for doing so. Factoring other parameters into an ACS is similarly difficult, especially since these parameters must be characterised as costs regardless of whether they are actually experienced as such. Finally, the fact that LCP is optimised to find maximally efficient routes is problematic when research goals are not focused on optimality – as in this study. It fails to satisfy both criteria laid out at the beginning of this section (Section 3.2), in that it does not represent maritime navigation particularly well and it does not incorporate marine data well at small scales. The isochrone method avoids several of these problems by linking isochrones with LCPs, while leaving the selection of the final path to a separate process. The methods developed by Hildenbrand (2015) and Slayton (2018) / Athenstadt (2018) also improve on previous LCP approaches by

allowing for courses to be offset to represent the effect of current drift. However the integration of current and wind data into ACS is situational in the isochrone method as currently formulated. Problems of combining hydrodynamic and aerodynamic costs in an ACS limit its application to types of seafaring where wind and current are important factors – in particular sailing.

Developing an ABM to describe maritime movement and navigation allows us to dispense with the concept of 'cost', which has been the root of most of the issues raised in this section. ABM allows for the modelling of navigation as it has been characterised in previous chapters: as a collection of heuristic processes that are used in combination to decide upon a course of action. The model developed for this analysis uses values representing qualitative and quantitative parameters as inputs to a process of decision-making designed to resemble the process of navigation, without having to derive 'costs' for these variables. Although it requires the development of a new GIS tool, this task is no less herculean than the development of new cost functions, ACS-creation methods, or path-selection methods that would be necessary to model navigation at sea using LCPs or the isochrone method. The next section discusses the development of this ABM model and the process that it uses in modelling sailed voyages.

Chapter 4 : Building the Navigation Model

4.1: Introduction

This chapter describes the navigation model that is used in this thesis. This navigation model is a descriptive, agent-based model, designed expressly for the purpose of modelling Iron Age seafaring according to the requirements that have been the subject of the first several chapters of this work: it uses parameterisations derived from Iron Age ships (Section 2.3.10), incorporates dynamic datasets (Section 3.2.1), and does not impute unrealistic abilities or knowledge to simulated navigators (Section 3.2.5). Each of these design features are discussed in this chapter.

This model is written in Python 2.7 – Python is an accessible and open-source platform, in which ESRI's geoprocessing tools are implemented as a library (ArcPy). This library allows ArcGIS tools to be run within a Python environment – the script uses tools from ArcGIS version 10.4.1. The script uses a combination of existing geoprocessing tools and custom tools developed specifically for the purposes of the ABM. Custom tools for this script were developed either to perform functions for which there were no tools in the ArcGIS toolbox, or where relying on ArcGIS tools would have made the script less efficient. The process for determining intermediate visibility (see Section 4.3.3), for example, operates in the same way as the 'Visibility 2' tool in ArcGIS, but only for subsets of points rather than an entire array. Table 4.1 contains a list of GIS functions developed for this analysis, indicating where they incorporate existing geoprocessing tools. The model also uses the following two open-source external Python libraries: the

NetCDF4Python is used to read environmental datasets, and the PyEphem ephemera library in order to determine times for sunrise and sunset.[31]

The model is run through a basic GUI, which prompts the user to select input and output directories, specify parameter sets, and gives the user the option to overwrite existing results. This GUI was designed to allow others to monitor simulations for the analyses described below. Once all menus in the GUI have been completed, preliminary results are displayed on the console (see Figure 4.1). The results from each simulation are placed in a separate folder in the output location, named according to an ID supplied with input parameters. The following section discusses these model inputs, parameters, and outputs in more detail. Subsequent sections describe the process by which navigation is simulated by this program.

4.2: Inputs, Parameters, and Outputs

The following sections review data inputs the model, the parameters that users may set in order to deploy the model, and the data outputs that the model produces. In order to reduce the amount of processing as much as possible (see Section 9.4), data inputs and outputs are formatted as text files wherever possible. Separate scripts were used to generate parameter files, aggregate output logs, and generate GIS geometry objects from said logs. These scripts are listed in Table 4.2.

[31] For NumPy and PyEphem documentation see <http://www.numpy.org/> and <https://rhodesmill.org/pyephem/>, respectively.

4.2.1: Model Inputs

The main challenge in designing the model was determining which datasets – and accordingly which environmental parameters – should be used by the model. The list of datasets used by the model is conservative, for several reasons. To begin with, some data is anachronistic or does not exist at scales necessary to perform analysis. Sandbanks, for example, are common in parts of the Western Channel and almost certainly would have served as navigational hazards and aides – however sandbanks can shift rapidly over short time-scales, and predicting where they may have been located at any point in the Iron Age would have to involve a complicated geological analysis. Datasets were also excluded where they were not interoperable with other available data. For example using wave heights to simulate the heel angle of a ship requires information about the shape of the ship's hull, which would be a matter of speculation (see Section 2.2.2), so wave data was not used in order to avoid making unnecessary assumptions. The datasets selected for use by the script are:

Wind / Current / Tide Data: The model accepts environmental datasets formatted as NetCDF (Network Common Data Form) files. NetCDF is a machine-independent data format commonly used in environmental modelling. It is a multidimensional array in which each data 'bin' can contain values for several variables over a range of times. The script is written to retrieve wind direction and velocity from one NetCDF file, while current direction / velocity and tide height are retrieved from another NetCDF file.

A Speed Diagram: A tabular speed diagram represents the capabilities of ships in the model. Speed diagrams are commonly used to optimise sailing ships – they represent the expected speed of a vessel relative to an angle of attack against an oncoming wind. The tabular version used by this script contains an expected speed value in metres per second for each degree increment between 0° (on a run) and 180° (into wind).

A Raster DEM: Since the height of an observer in visibility studies is tied to tide height, the DEM used in this study is a composite of a terrestrial elevation model and a bathymetric model.[32] The DEM used in analyses for this thesis has a vertical resolution of 1 metre and a horizontal resolution of 30 metres.

Landmark Polygons / Grids: Point grids and polygon extents are used to represent landmarks in the model. The double-representation of landmarks as points and polygons speeds up visibility analysis functions within the model.

Visibility Records: The model uses a table identifying maximum visibility ranges for specific regions and dates in the study period.

[32] Terrestrial DEMs do not represent topography below sea level – therefore bathymetric data is needed to supplement a terrestrial DEM when a simulated ship is below sea level (i.e. at low tide).

These records are used to calculate maximum visible distances. Since the visibility table in this study was gathered from the UK Shipping Forecast, a raster map of forecast areas is also referenced by the script.[33]

Obstacle Polygon Features: Potential obstacles are represented by polygon features, which are used to calculate path distance. These include any islands or rocks which the simulated ship is meant to avoid.

Study Area Polygon Feature: A polygon that defines the outer limit of the study area. This polygon is used to constrain the model to the area for which environmental datasets are available.

4.2.2: Model Parameters

Links to each of these data sources must be supplied in a configuration file which is used to run the model. A full list of input parameters is shown in Table 4.3, however for the sake of simplicity those parameters relevant to this discussion of the model are listed below:

ID Code: A unique identifier for the simulation.

[33] Specifically, Shipping Forecast data was gathered by writing a web scraper for reports published by the BBC at <http://www.bbc.co.uk/weather/coast_and_sea/shipping_forecast>.

Route Coordinates: Coordinate pairs representing an origin and destination point for simulated vessels, as well as names for each. These names are used to aggregate the results of the script.

Visibility Settings: These settings enable or disable different levels of visibility analysis (see Section 4.3.3).

Output Settings: These settings enable or disable the generation of script outputs, including navigation and visibility logs, and plots of simulation tracks (see Section 4.2.3).

'Reckoning' Settings: 'Reckoning' is constrained to overestimation and underestimation ranges. These ranges take the form of two-element lists, where both elements are integers that represent percentages. These integers represent the minimum and maximum percent of 'real' values that will be added / subtracted during the 'reckoning' stage (see Section 4.3.2).

Simulation Date: A date string representing the date on which the simulation is set to start. This string is used to select the appropriate NetCDF arrays.

Starting Time: An integer representing the hour (0-23) at which the simulation is set to start. The minimum iterable time for the script is one hour.

The model operates by iterating through parameter files – accordingly one parameter file per simulation is needed. A custom script was written to generate these files (see Table 4.2, Section 5.5).

4.2.3: Model Outputs

One advantage of building a custom model is that values used in functions within the model can be easily recorded and collected without having to perform extra analysis on finished products. This script accomplishes this by creating text 'logs' in the output directory when the script initialises, and writing values of interest to these logs at each timestep. The script produces four types of logs, as well as a plot that summarises the results at each timestep:

Navigation Logs: These text files record variables relevant to the progress of the vessel across timesteps. Navigation logs record environmental parameters at each timestep as well as the location of the vessel and the heading selected. A full list of variables recorded in navigation logs can be found in Table 4.4.

Visibility Logs: These text files record visibility values per sighting over the course of the simulation. These logs record, for each landmark found to be 'visible' by all enabled layers of visibility, the vessel location, timestep at which the landmark was visible, and the number of points in the landmark point grid determined to be 'visible'.

Track Plots: These plots track the operation of the script per timestep. These plots were used to evaluate the performance of the model during the development stage, and show nearby landmarks, real and 'reckoned' heading envelopes (Section 4.3.2, 4.3.5), and the selected heading. In this analysis these plots were used to check

results at a glance; data used in the following chapters was produced from navigation and visibility logs.

Benchmarking Logs: These text files record the amount of processing time used by different modules. They are optional outputs.

Report Logs: These text files record the details of errors that cause the model to fail prematurely (see Section 4.3.7). These logs record error messages passed from other tools as well as a list of data inputs. These were used in the development of the script, and were also used in analyses to identify simulations to exclude from general averages.

Sample logs and plots produced by the script are shown in Figure 4.3.

4.3: Script Architecture

Figure 4.2 shows the basic structure of the navigation model. At each whole-hour interval ('timestep') after a specified starting time (1) 'environmental parameters' are retrieved from input datasets, (2) headings are generated, (3) a visibility analysis is performed, (4) a heading is selected, (5) a path is computed for an hour's travel along the selected path, and (6) the selected path is checked to determine whether the simulated vessel has reached its destination. These stages repeat until the simulated vessel reaches its destination, suffers a catastrophic failure, or runs out of time. At each stage the vessel's position, local environmental variables, visibility analysis results, and selected headings are recorded as variables, as well as in the output logs. The following sections trace the operation of the script through these stages.

The navigation model uses a number of custom functions, which are listed in Table 4.1. In general, functions are called in the order that these functions' outputs are needed by the model. For example environmental datasets are used by all modules, so the module that loads these datasets is placed first. The Python / ABM structure of this model allows modules within the script to use datasets and variables that have been created or modified by other modules. This makes the script more flexible and efficient, but also more difficult to describe in a narrative. A chart of the basic process followed by the script is shown in Figure 4.2.

These descriptions use several terms with specific meanings in the context of this model. To begin with, the word 'vessel' is used to refer to the 'agent' in the model – that is to say the simulated navigator. 'Origin' and 'destination' refer to the position of the vessel at the beginning of the simulation, and the vessel's intended final destination. By contrast, the terms 'start point' and 'end point' refer to the vessel's position at the beginning and end of each one-hour timestep. In order to simulate the effects of different levels of knowledge and ability on the success of voyages, the script modifies certain environmental and spatial parameters. Therefore it is also necessary to distinguish between 'real' values that are collected directly from datasets, and values that are 'reckoned' by the script. The model 'reckons' values by modifying them by a random percentage within the estimation ranges set by the user.

4.3.1: Stage 1 - Parameter Reading and Extraction

The script's first stage gathers variables from the inputs listed in Section 4.2.1. To summarise: the script uses tables derived from tidal observations, the Shipping Forecast; a set of raster DEMs and masks; and NetCDF files. In the first case retrieving values from

these files is trivial, since these tables are stored as text (.txt) and comma-separated-value (.csv) files. Values from rasters are collected using the *Get Cell Value* tool to extract values from cells overlapping a set of input coordinates.[34] For small datasets such as the Shipping Forecast mask the script reads the entire raster image into memory, whereas for the DEM the script extracts portions of the raster image to memory for future sampling. Retrieving values from NetCDF files is more complicated, and required the development of a custom script tool (see Table 4.2). This is due to the structure of NetCDF files in general, and the NetCDF files used in this study in particular. NetCDF files consist of a multidimensional array, in which the centre of each 'bin' in the array is georeferenced by a set of coordinates. Unlike a multidimensional raster, the bins in a NetCDF file are not necessarily regularly spaced. This was found to be the case in many of the SHOM files, where the latitudinal separation of bins was found to be slightly less than the bins' longitudinal separation. Attempts to convert these NetCDF files into rasters using ArcMap's *Make NetCDF Raster Layer* function failed, because the function assumes that bins in an input NetCDF file are regularly spaced.[35] To solve this problem, a custom script tool was written to retrieve the value from a given dimension of a NetCDF at a certain time with geographic coordinates closest to an input set of coordinates. To accomplish this the script tool extracts an array of coordinates for a time-slice of the NetCDF, finds the array indices of the coordinate pair closest to the input coordinates, and retrieves a value from the NetCDF at the determined indices (see Figure 4.4). The script uses this

[34] See: https://desktop.arcgis.com/en/arcmap/10.3/tools/data-management-toolbox/get-cell-value.htm.

[35] See: https://desktop.arcgis.com/en/arcmap/10.3/tools/multidimension-toolbox/make-netcdf-raster-layer.htm

tool to gather the following variables from the input NetCDFs: current direction and velocity, wind direction and velocity, tide height, and shipping forecast area.

4.3.2: Stage 2 - Parameter 'Reckoning'

The 'real' values gathered in the first stage are then modified by the script in order to produce 'reckoned' values. This is done by selecting a random percentage within ranges defined by the 'underestimation range' and 'overestimation range' parameters set by the user, and adding or subtracting that percentage of the 'real' value to the value itself. 'Reckoning' values serves two main purposes: reflecting the difficulty of reading conditions at sea, and representing dead reckoning faithfully. In the first case, conditions at sea can be difficult to read. Conditions at sea would have been determined through a combination of navigators' judgement and experience, which can vary in both detail and precision. In some cases conditions may not even be directly observable. This can also be the case with terrestrial navigation – for example, one could criticise a terrestrial movement model that assumes that agents can *always* judge slope and aspect perfectly on the grounds that atmospheric and environmental conditions (fog, darkness, land-cover, near-sightedness – to name a few) may compromise that judgement. Using constrained randomness to 'reckon' environmental parameters acknowledges that maritime navigation can be imprecise, and gives the modeller an opportunity to investigate this dynamic by varying experience parameters (see Chapters 6-8) rather than ignoring it. 'Reckoning' environmental parameters also prevents the difference between 'navigation by landmarks' and 'navigation by dead reckoning' from being lost in the script. If 'real' values are used at all stages of the simulation, then the effect is that navigation by dead-reckoning would be perfectly accurate and therefore exactly as useful as navigation by

landmarks. Since this is clearly not the case (see Section 2.3.4), simulating dead reckoning requires a mechanism for performing the 'reckoning' – expressed in this model by modifying 'real' values.

Once 'reckoned' values have been generated, the script computes how far along a set of headings the vessel expects to travel. Figure 4.5 shows a simplified version of this process. First, a set of unit vectors is created for a full turn at an angular resolution of one degree. Then the script finds the angle defined by each unit vector and a NetCDF-derived vector representing the direction and speed of the wind at the vessel's location. This value is then compared with a table representing a polar diagram for the vessel. This table references angles of attack (vessel angle relative to wind, i.e. the computed interior angle) with expected speed under sail.[36] The script then multiplies the magnitude of the unit vector with the value found in the polar diagram table. Finally, a vector representing the speed of the current is added to the modified unit vector. The result of this series of operations is a 2D radial array in which the length of each vector represents the theoretical maximum distance that the vessel could achieve along the heading under given environmental conditions. This array does not take obstacles into account, however, and in order to address this vectors are compared against a set of Polygon objects representing 'obstacles' (i.e. islands, shoals, and gaps in environmental datasets). By trimming vectors

[36] This method is similar to those of the ORBIS model (Arcenas 2015), and the seafaring model underpinning Philbin-Briscoe et al.'s 'serious game' of Mediterranean seafaring (2017). New methods for generating an ACS in ArcGIS now use a similar method to calculate 'horizontal cost factors' in the *Distance Accumulation* tool (https://pro.arcgis.com/en/pro-app/tool-reference/spatial-analyst/distance-accumulation.htm).

in the heading array where they intersect obstacles, and converting the remaining endpoints into vertices in a Polygon object, a ‘heading envelope’ is produced for the vessel’s starting location. This envelope represents the area in which the vessel is expected to be within an hour based on ‘reckoned’ environmental values. The script then checks whether the destination point is within this heading envelope. If so, then the simulation is completed (since the vessel is assumed capable of reaching its destination within an hour), and if not the script proceeds to the next stage.

4.3.3: Stage 3 - Visibility Analysis

The script uses three methods for establishing and quantifying ‘visibility’: (1) a simple Euclidean-distance calculation based on the observer position and the centre of the target feature, (2) a plan-view visibility analysis based on a skyline, and (3) an optional 3D visibility analysis based on a radial sampling array. These methods are referred to hereafter as ‘layers’ of analysis, since they build upon one another in order to produce a final quantification of the visibility of a landmark. For example the observer-landmark distance calculated in the first layer of analysis is used to determine the maximum extent of the skyline in the second layer, and the projective extent of the skyline generated in the second layer is used to constrain the radial array generated in the third layer of analysis. As a part of the visibility analysis, each landmark in the input dataset is subjected to analysis by the first layer; those landmarks that are designated ‘visible’ are analysed in the second layer, and those that are ‘visible’ in the second layer of are then passed on to the third layer. This structure prevents resources from being wasted on attempting to measure the visibility of landmarks that are outside the maximum visible range, or

attempting to quantify the apparent size of landmarks that are completely obscured by terrain.

The first layer of visibility analysis consists of a simple test of Euclidean distance from the observer point (the simulated vessel's real position) to the centre-point of the selected feature. The script checks this distance against the maximum visible distance as defined by the Shipping Forecast (Section 5.4.1). In order to determine this distance the script consults a table containing transcripts of the Shipping Forecast gathered for the study area / period. The shipping forecast predicts visibility according to four categories: Very Poor, Poor, Moderate and Good (see Table 4.5). In some cases the shipping forecast predicts multiple visibility conditions, or qualifies its prediction within areas. In these cases, the script selects the 'best' visibility conditions. If the vessel-landmark distance is less than or equal to the maximum visible distance according to these conditions, then the landmark is counted as 'visible'. The landmark is then added to a list of landmarks to be investigated in the next layers of analysis.

The second layer of visibility analysis tests the 2D or 'plan-view' visibility of a landmark from the position of a simulated vessel. Whereas the first layer of visibility analysis does not take topography into account, this layer of analysis tests whether or not an observer's view of a given landmark is obstructed by intervening topographic features (hills, ridges, etc.). This is accomplished in the script by collecting the spatial parameters of the input feature from a set of points representing that feature, creating a skyline specifically for said feature, and testing whether points in the grid are 'inside' or 'outside' the skyline. To begin with, landmarks in the script are described by (1) a polygon feature representing the extent of the site, and (2) a grid of points distributed regularly within that extent. The script calculates the horizontal angles defined by these points, and selects a

pair of angles that 'define' the site in plan view. These values are then used by the script as inputs to the ESRI *Skyline* tool.[37] This tool takes an input 3D point and a 3D surface, and constructs a polyline defining the horizon from the observer's position. Skylines can be constrained by limiting 'starting' and 'ending' angles, and crucially by setting a 'maximum distance' to which the skyline will be calculated. In order to determine visibility in plan view, the script creates a skyline limited to the angular extents extracted from the landmark point-grid, with a maximum distance limited to the Euclidean distance calculated in the first visibility analysis layer. Each point in the original landmark point-grid is then tested to determine whether it is 'inside' or 'outside' the skyline. Figure 4.6 shows a set of hypothetical scenarios using this method. In each sub-figure, the 'landmark' is represented by a regular grid of points. In the first case, the skyline generated for the target landmark runs along a ridge between the observer and the target landmark. Since all points in the point-grid intersect (and are therefore 'outside') the skyline, the feature is designated as 'not visible'. In the second example the skyline runs through the landmark because the landmark lies on an area that defines an observer's horizon, and is designated as 'visible' because it has grid-points 'inside' the skyline. Finally, in the third example the skyline runs through the feature because the 'maximum distance' parameter of the skyline has been set to the observer-landmark distance. In this final case the feature has grid-points inside its skyline, and is therefore identified as 'visible'.

In order to determine whether landmarks are or are not visible, only the first two layers of visibility analysis are required and strictly necessary to guide the ABM. These

[37] See: https://desktop.arcgis.com/en/arcmap/10.3/tools/3d-analyst-toolbox/how-skyline-works.htm

two layers answer the basic question: 'is the potential landmark within sight of the vessel?'. In order to determine whether landmarks are *more* or *less* visible, the script uses a third layer of visibility analysis to quantify the 'projective extent' or 'apparent size' – the amount of an observer's field of view that an object occupies – for landmarks that have passed the other two layers. This measure of visibility differs from the results of a 'viewshed' in that according to the logic of a viewshed the same object is the same 'percent visible' whether it is 2 metres or 2 kilometres away from the observer, as long as the angle between the object and the observer is the same and no other objects obstruct it (see Figure 4.7 for an illustration). While it is not simply the case that 'things that look bigger are more visible' (visibility is also affected by lighting, colour contrast, and other optical effects; see Higuchi (1983)) the apparent size of an object is at least an intuitive property of that object. One does not need any other information about something that occupies most of his or her field of view to confirm that the object 'looks big'. By contrast, the knowledge that most of the area of a viewed object is visible requires some knowledge about how much of the area of the object is visible.

The analysis used to quantify apparent size builds on previous work by archaeologists in developing 'radial arrays' (Pouncett 2013), and also runs parallel to efforts in other fields to develop 3D rendering approaches within GIS (see, for example, Batty 2001, VanHorn & Muserinjohn 2010, and Lonergan & Hedley 2014). The process used to measure apparent size is similar to the processes of 'ray-casting' and 'ray tracing' used in computer graphics packages, in which an image is generated by examining the interaction of a 3D scene with sets of 'rays' emanating from an observer point and a light source. This process used here is much simpler: the 3D scene in question is a DEM surface, and only one array is used. As in Layer 2, a point-grid representing a feature is

used to determine the minimum and maximum horizontal and vertical angles for which an observer-target array is to be generated. This array is then intersected with a DEM terrain surface with the 'Intersect 3D Line with Surface' tool in order to produce a set of intersection points. Figure 4.8 shows the results of a hypothetical array-DEM intersection, in profile view. Since each ray in the array may intersect the terrain surface multiple times, the script checks all points and preserves only those points closest to the observer along each ray. These points represent the visible extent of a feature, as shown in Figure 4.9 where their coordinates have been transformed into 'projective' space (i.e. space within an observer's visual field). The 'visible area' returned by this layer of analysis is a count of these 'first-intersection' points. This measurement serves as the basis the selection of navigational strategy.

4.3.4: Stage 4 - Strategy Selection

If a valid heading envelope is generated and the simulation is not yet successful, the script attempts to select the heading that will move the vessel closest to where the script 'reckons' that the destination is, based on the results of the visibility analysis. If at least two landmarks are recognised as 'visible' by the desired level of visibility analysis, then the script assumes that the simulated navigator is aware of its position. The threshold for how many landmarks must be seen before the vessel can use them to establish position is set at two in order to streamline the script. Requiring only one landmark is not sufficient, because even though being able to see a known object can help a navigator establish where they are *in general*, it is not always helpful in establishing a vessel's precise position. Two landmarks can be used to obtain a fix, which can be used to locate a navigator if distances to both landmarks are known, or along a meid if the landmarks

align. As described in Section 4.3.3, the more landmarks there are the more alignments are possible and the more accurate estimates of position are. The model used in these analyses requires two landmarks to be visible before making simulated navigators aware of their position; this threshold is also discussed in Section 9.3.3.

If fewer than two landmarks are 'visible', then the script compares the positions of the 'real' and 'reckoned' end-points from the previous timestep and applies the same offset to the destination point to create a 'reckoned' version. This 'reckoned' destination point is then used in the next stage to select a heading. Therefore the script assumes that navigators have good knowledge of their surroundings, but may not be able to reference that knowledge to the position of their destination. To paraphrase Terry Pratchett, according to this process simulated navigators are secure in their own position while the rest of the world is 'lost' around them.

4.3.5: Stage 5 - Heading Selection

After generating a heading envelope and establishing the real or 'reckoned' position of the destination point, the script then selects the heading that will move the vessel closest to the destination's presumed position. To accomplish this the script considers each vertex in a given heading envelope and selects the vertex with the least path distance to the presumed location of the destination. Path distance (not to be confused with the ArcGIS *Path Distance* tool) differs from Euclidean distance in that path distance measures the distance from Point A to Point B while avoiding a set of obstacles, or adhering to a set of routes. Although the heading envelope is clipped to a set of obstacles in a previous stage, it is still necessary to calculate path-distance for each vertex in order to keep the vessel from becoming trapped in indentations in the coastline where the outlet

is further away from the destination than the vessel. Figure 4.10 illustrates this ‘dead end’ problem. In this scenario a vessel that has arrived at the mouth of a bay that is oriented on a vessel-destination point axis. Calculating the Euclidean distance for each vertex to the destination point and selecting for the least distance leads the vessel to enter the bay, from which (according to these rules) it will never return. Using a path-distance calculation, however, prevents this scenario from occurring: a vessel finding itself in the same bay will find when calculating distances for each vertex that this value includes the distance necessary to exit the bay and sail around the coast.

There are several methods for calculating path-distance. Least cost paths, which were discussed in Section 3.1.2, are the best-known within archaeology. Least cost paths were not implemented in the script because they would have required a considerable amount of ‘pre-baking’. Essentially separate LCP analyses would have had to have been to be performed for each point-to-point combination in a grid covering the Western Channel, and the results of these datasets would have had to be collected into a new dataset to be consulted by the script. For smaller areas of interest this approach may be expedient and accurate, but for the study area considered in this research programme a more efficient solution was necessary. Therefore the script implements parts of a ‘convex path’ algorithm to determine the distance from vertices in a heading envelope to the destination. This algorithm (see Hong 2015 for the full implementation) computes path distance by constructing a vector from a start point for an end point, iterating through polygon obstacle features, and replacing sections of the vector with portions of convex hulls created for each obstacle feature. These substitutions are accomplished using

ArcGIS' *Polygon* and *Polyline* operations.[38] For each obstacle polygon that intersects a start-end polyline, a convex hull for that polygon is created using the 'convexHull' method. This convex hull is then split into two sections along the start-end polyline. The larger section is discarded, and the vertices of the smaller polygon are extracted to points. These points are then checked for intersection with the start-end polyline, and points that do not form part of this line are discarded. Those points that remain are added to a dictionary, and when all obstacles have been processed the script constructs a vector line object connecting all points in the point dictionary. Figure 4.11 illustrates the convex path algorithm used in this script. In the first part of this figure, two polygon features (representing islands) intersect a start-end polyline. In the second part, convex hulls are constructed for each obstacle feature, and are split into larger and smaller sections by the start-end polyline. Vertices selected from these split polygons are symbolised by hollow circles, and all other vertices (filled circles) are discarded. Finally, in the third part of the diagram a new line is drawn between preserved points.

To select a heading from vertices in a heading envelope, the script repeats this convex-path algorithm using heading envelope vertices as starting-points and the presumed destination location as an endpoint. The length of each convex path is then measured, and the vertex with the least path-distance to the presumed destination is selected. The heading corresponding to that vertex is recorded by the script. This heading serves as the basis for the actual vessel simulation performed by the script.

[38] See: https://desktop.arcgis.com/en/arcmap/10.3/analyze/arcpy-classes/polygon.htm, and https://desktop.arcgis.com/en/arcmap/10.3/analyze/arcpy-classes/polyline.htm (repsectively).

4.3.6: Stage 6 - Path Calculation

The simulation module draws upon functions and variables from the previous steps in order to simulate vessel travel over the course of the timestep. Functions from the Data Access module are used to read the 'real' environmental values from the appropriate NetCDF datasets. The same function that compares potential headings with current and wind vectors to produce a heading envelope is used on the heading selected by the Heading Selection module. The only substantial differences between the 'Simulation' and 'Heading Generation' modules are (1) only a single heading – the heading selected by path-distance comparison – is used, and (2) environmental variables are not modified in any way. This makes the result of this module a simulated path for a vessel under real conditions, along a heading that has been generated and selected based on a set of 'reckoned' conditions.

If the iteration of the steps described above is completed, then the simulated endpoint for the selected heading becomes the new start point for another iteration of the model. Iteration continues until 'success' or 'failure' conditions are met.

4.3.7: Completion and Failure Conditions

The model contains one condition for success, and several conditions for failure. In the first place, in early versions of the model simulations were counted as 'successful' when the endpoint of the selected heading fell within a certain distance of the destination point. This became a problem when simulated vessels passed close to the destination while overshooting it. To fix this problem simulations are held to be successful if the destination point falls within the heading envelope generated at Stage 2. Since the edges

of the heading envelope represent the maximum distance achievable in an hour, any point within that heading envelope is theoretically achievable.

The first failure condition results from a pre-determined maximum number of timesteps elapsing since the start of the simulation. This time limit was included in the script in order to limit the amount of processing necessary to complete analyses. In trial runs of the model, simulated vessels were occasionally swept out into the Atlantic, where they spent many iterations either stuck against the edge of the study area or else were unable to navigate back to land for lack of landmarks. None of the test runs that iterated over more than 48 hours reached their destinations, so a cut-off was introduced to the script to mark simulated voyages over a given threshold as 'failed'. Other failure conditions are manifested as errors in the script, which cause the simulation to stop. Every possible effort was made to eliminate bugs in the script that caused simulations to fail. Although nearly all of these bugs were eventually fixed, a few relating to memory usage could not be eliminated before simulations for the Main Analysis began. In these cases no navigation log was produced; simulations without a navigation log were excluded from datasets described below (instead of being marked as 'failed runs'), since the reason for their failure could not be determined. Two of these error cases, however, are allowed to interrupt the iteration of the script because they are analogous to actual conditions that would end or interrupt a sailing voyage. The first case occurs when the vessel enters an area for which there is no data. Since the boundaries of the environmental datasets in this study are well away from the area of interest, conditions in which this error arises are always more than 48 hours away from the destination and therefore not 'salvageable' by the script. The second case occurs when a heading envelope is generated without vertices (i.e. as an empty geometry). In this case there is no heading which the model can select

that will place the ship within the navigable area. This situation is analogous to a real navigator being forced ashore by the current or the wind.

It should be noted that being forced ashore is not necessarily a ‘failure’, and in fact can be part of a strategy for avoiding poor conditions. Nevertheless, because the model does not incorporate data about the ‘approachability’ of coastlines, in order to err on the side of caution simulated voyages that are forced ashore are counted as failures. Likewise voyages that strayed outside the footprint of input datasets are classified as ‘failures’. As a final note, although the definition of ‘success’ or ‘failure’ are fairly strict within the script, the fact that detailed logs are produced for each iteration of the script means that reanalysis of the data can be used to test different criteria for success – for example: proximity to the coastline belonging to the vessel’s destination. This possibility is explored in the analyses that follow (see Sections 5.6.2, 7.2.2, and 8.2.1).

Chapter 5 : The Main Analysis (Western English Channel)

5.1: Introduction

Whereas the previous three chapters have focused on problems of naval architecture, navigation, and computer analysis, in this chapter we return to Atlantic Europe. This chapter describes the 'Main Analysis' in support of this thesis: a comprehensive sweep of cross-Channel routes and sailing dates totalling some 88,000 simulations. As the three case studies described in following chapters use the same input datasets as the Main Analysis, the first half of this chapter is dedicated to a survey of those data inputs, as well as a brief description of the study area (see Figure 5.1). The remainder of the chapter presents the results from the Main Analysis, and discusses them briefly.

5.2: Research Design: Parameter Survey

This section returns to the input parameters of the navigation model, which are listed and described briefly in Section 4.2.2. The following sections outline the strategy used to define parameters for simulations in support of the Main Analysis, and describes the assumptions and datasets that were used to derive these parameters. Since several of these parameters are also used in the case studies reported in Chapters 6-8, the discussion of said parameters here is also relevant to those other analyses.

5.2.1: Parameter Sweeping

The basic approach taken in the analyses presented below is 'parameter sweeping'. Parameter sweeping is a common technique used in computer science to

evaluate and optimise models (see Samples et al. 2005; Chirigati et al. 2012). Parameter sweeping involves running a model multiple times over a wide range of parameter sets in order to determine which parameter combinations produce the best results. Although the purpose of this study is not to search for optimal paths across the Channel, the parameter sweeping approach is useful because its results can be used to investigate how much of an effect different parameters have on the outcome of a simulation.

The wide range of parameters included in the final model for this analysis precluded a full parameter sweep – testing each unique combination of parameters – on account of the large number of simulations that this would have required. For example, the study period consists of 212 days between March and September 2018, twenty-two coastal nodes in the UK, ten coastal nodes in France, and three sets of landmarks. Vessel parameterisations, 'reckoning', and sailings per day can be varied at will, but using a modest number of parameterisations for each would have resulted in:

	212	Days in Study Period
	22	Northern Nodes
	10	Southern Nodes
	3	Sets of Landmarks
	5	Vessel Parameterisations
	5	Estimation Ranges
X	3	Sailings per Day
	10,494,000	Total Runs

Assuming an average speed of two minutes per run, completing this many simulations would have taken approximately ten years of continuous processing on the four computers that were originally available for this study. Since not enough time or

processing power was available to perform a full parameter sweep two strategies were used to make the most out of the available resources. Firstly, criteria were developed to limit the extent of some parameters to reasonable ranges. Secondly, the hypothetical 'complete' analysis was divided into three smaller analyses designed to sweep for particular parameters. This section describes how the navigation model's parameter space was limited and divided in order to perform the analyses in the following sections.

5.2.2: Description of Simulations

In general, the parameter spaces of all four analyses can be described as (1) simulations for each date in the study period along cross-Channel routes identified in Section 5.3, using all landmarks, perfect reckoning, and a single ship type; (2) multiple daily simulations for voyages inbound and outbound from a single node over the period of a week, varying landmark datasets; (3) multiple daily simulations for a single cross-Channel voyage on a single day, varying reckoning and ship type; and (4) multiple daily simulations for a single Cross-Channel voyage, varying reckoning and ship type and using 3D visibility analysis in order to record the visibility of sites. Table 5.1 shows the number of simulations performed for each analysis, as well as the number of varied parameters for each. The average speed for analyses was around 2 minutes per simulation where 2D visibility was used to determine landmarks. Simulations that used advanced

visibility took significantly longer – from 20 minutes to several hours – depending on how many landmarks were sighted.[39]

5.2.3: Ship Parameterisation

As described in Section 4.3.2, the performance of ships is represented in the model by a speed diagram, which represents the expected speed under sail of a ship as a curve relative to vessel's angle of attack. In order to construct a speed diagram for the analyses described here it was necessary to define both the magnitude of the curve (relating performance to speed) and the shape of the curve (relating performance to angle of attack).

Determining vessel speed under sail for Iron Age vessels is a difficult task, since analytical techniques for doing so rely on measurements that the archaeological record does not afford. Hydraulic curves and naval architecture coefficients, for example, can only be used when the shape and dimensions of the boat in question are known. Without measurements from excavated ships these measurements cannot be taken. Experimental evidence is also lacking, since reconstructed boats from other periods such as the Hjortspring boat and the Ferriby boats are paddled craft, and in any case were likely designed to be inshore boats (Fenger & Lumbye-Hansen 2000, Vagn Valbjørn et al. 2000, Van de Noort et al. 2014). Since direct evidence for sea-going ships in the Late Iron Age Channel is fragmentary, the ship parameterisations used in these analyses follows Seán

[39] Simulations that used 3D visibility analysis were run in the background on a laptop PC while drafting sections of this thesis (see Chapter 8). As such processing times recorded for these simulations are likely longer than the same for other simulations, which were run across 4 desktop PCs over a longer timespan.

McGrail's (1983) 'deduction' of the seagoing properties of an Iron Age Channel-crossing vessel. McGrail assumes that Channel-crossing ships would have had:

1. Lengths of 7-12 metres, and been propelled by a single square sail.
2. Broad sides with 'flattish' bottoms and rounded bilges, in order to make room for cargo, add stability and make landfall on beaches and estuaries.
3. Upcurved bows and sterns, and enough freeboard to withstand rough waters.

Based on these assumptions, McGrail suggests that:

> Although maximum speed in ideal conditions might be as much as 7 kts for a boat of 7-m waterline length or 9 kts for one of 12 m, classical documentary evidence and the performance of recent boats and experimental replicas lead to the conclusion that, on a typical cross-Channel voyage, the average speed made good towards the destination for all points of sail would have been *c*. 2 ½ kts. ... with generally fair winds the average speed could have been 5 kts. (McGrail 1983, 300).

These values were used as upper and lower bounds for the parameterisation of ships in simulations.

Defining the shape of a speed curve for an Iron Age ship was similarly complicated by a lack of material evidence. The only comparable archaeological reconstructions that offer points of comparison are the *Brendan* reconstruction (Severin 1978, see Section 2.2.4), and replicas of later Viking craft (see, for example: Crumlin-Pedersen 1986). Although both used square sails they are problematic in their construction and rigging. The *Brendan* was a reconstructed skin boat, and as such probably had a much greater leeway than a plank boat would have had; in addition it was equipped with a foresail in addition to a mainsail (Severin 1978). Viking ships are

technologically very different from the types of plank boats that are supposed for the Channel, and would have had much better performance. A further complicating factor is the use of modern rigging in archaeological reconstructions, which improves their performance. The risk of introducing anachronisms into the model by using these speed curves as templates was judged to be less than the risk of misrepresenting vessel performance by generating arbitrary (i.e. mathematical) curves for the purposes of the analysis presented here. Therefore the shape of speed curves used in these analyses were adjusted from speed curves generated by the *Roar Ege*, a reconstruction of the Viking ship Skuldelev III. Skuldelev III has been interpreted as a 14-metre trading vessel dated to *c*. 1040 AD (Crumlin-Pederson 2002). Figure 5.2 shows the speed curve for the *Roar Ege* compared to a speed curve for a modern sailboat.[40] The shape of the speed curve used in these analyses was further altered by changing the cutoff point at which the vessel makes no headway when sailing into-wind, also known as the 'dead zone'. Again, McGrail's estimates were useful here, as he predicts that the dead zone for Channel-crossing boats extended to 78.75° on either side of an oncoming wind. The shape of the speed curve from the *Roar Ege* was combined with the speed estimates given by McGrail to define the speed diagrams shown in Figure 5.2.

Unfortunately, in building speed diagrams a unit conversion error resulted in maximum speeds being overestimated in the speed diagrams used in the Main Analysis, Case Study 1, and Case Study 2. These high speed values can be seen in Table 5.2, which shows all speed diagrams used in this study and the maximum and average speeds

[40] For speed curves, see https://www.vikingeskibsmuseet.dk/en/professions/education/exercises/the-speed-diagram/; http://www.albinvega.co.uk/ (respectively).

expected from each. This error resulted in the '7-metre' and '12-metre' parameterisations having top speeds of 10.56 and 13.76 knots, respectively.[41] As such these parameterisations better represent later Iron Age or Romano-Celtic ships (although even these are unlikely to have achieved such high speeds) than the smaller hide or plank-built boats imagined by McGrail in his analysis. Severin reports that the *Brendan* achieved speeds of over 12 knots "comparatively frequently in heavy weather and high seas" (2005, 265) and reached "close to 20 knots" in extraordinary circumstances (2005, 115), although we should remember that the *Brendan* was a speculative replica of a medieval ship that incorporated modern design features. Case Study 3, which was run after the error was discovered, uses speed diagrams based on the speed profile of the *Roar Ege*, with values corresponding to McGrail's predictions. Comparisons between the results of Case Study 3 and the other analyses with respect to vessel parameterisation are discussed in Section 9.2.4.

5.2.4: Landmark Selection

All analyses below are based on two sets of potential landmarks: a set of coastal sites and a set of coastal prominences. The first set of landmarks is based on archaeological catalogues and desk-based assessment. The second is based on an analysis of topographic data (using a DEM) using a local relief model (LRM; see Section 5.2.4). Figure 5.3 shows the distribution of both sets of potential landmarks. For both sets of

[41] For reference: the corresponding speeds kilometres per hour for the '7-metre' and '12-metre' parameterisations is 19.57 km/h, and 25.48 km/h.

landmarks it was necessary to use a set of criteria to decide whether or not to include potential sites / prominences in the final dataset.

In the case of sites, in preparation for the development of the model a full survey of Iron Age settlements in southern England and northwest France was conducted using published sources in order to identify promontory forts. These included published inventories (Bender 1986, Maguer 1996, Wheeler 1957), the Atlas of Hillforts of Britain and Ireland (Lock & Ralston 2017), and the GéoBretagne GIS warehouse (see https://cms.geobretagne.fr/). In the latter two cases databases were queries specifically for 'promontory forts' or 'éperons barrés'. These sites were then further selected by proximity to the coastline in order to exclude inland promontory forts from the final dataset. For each site remaining in the dataset, an extent was drawn in Google Earth using satellite imagery and archaeological reports (where available) as a guide. These extents were then clipped to conform to the coastline. This process resulted in a set of 97 landmarks based on coastal promontory forts. Details of these landmarks are given in Appendix I.

In the case of coastal prominences, identifying potential natural landmarks was aided by the Database of British and Irish Hills (DBIH), an online resource compiled by hillwalkers.[42] The DBIH includes coordinates for hills in the database as well as measurements of their local prominence. The DBIH database was used to evaluate a set of local-relief models run on the combined topographic-bathymetric DEM created for visibility analysis. The local relief model used for this purpose consists of smoothing the

[42] http://www.hills-database.co.uk/.

topographic surface by replacing the value of each target cell with the average value of all cells within a circular neighbourhood centred on the target cell, and subtracting this smoothed elevation model from the original DEM (see Hesse 2020, Kokalj et al. 2013). This results in a map of local prominence, where positive values represent areas that are higher than their surroundings and vice versa. This analysis used the ArcGIS *Focal Statistics* and *Raster Calculator* tools to generate LRMs.[43] To identify an appropriate window size for the generation of a final LRM, a series of twenty-one local relief analyses using different neighbourhood sizes were generated, and the results of each were checked against recorded prominence values for summit points collected from the DBIH. Figure 5.4 shows the accuracy of LRM analyses with different window sizes in predicting drop values recorded by the DBIH. An LRM with a neighbourhood size of 45 cells (1,350 metres) was selected as the basis for a set of natural landmarks based on its high accuracy in identifying hundred-metre prominences in the DBIH database. To generate this dataset, the raster LRM output was passed through a filter (using the 'SetNull' method within the *Raster Calculator* tool) in which all cells with prominence greater than 100 metres was given a value of 1, and all other values were eliminated. This raster was then converted into a set of polygons, for which internal rings (internal polygon 'holes') were eliminated. These polygons were then further culled by selecting only those that occurred within one kilometre of the coastline. Each of these polygons was then given a unique ID for identification by the script. Appendix II contains records of these landmarks.

[43] See: https://desktop.arcgis.com/en/arcmap/10.3/tools/spatial-analyst-toolbox/focal-statistics.htm, https://desktop.arcgis.com/en/arcmap/10.3/tools/spatial-analyst-toolbox/raster-calculator.htm

5.2.5: Constraints on Parameter Sweeping

Defining estimation ranges for parameter 'reckoning' for analyses was impeded by a lack of useful data for determining those figures. Although several studies have carried out experiments using GPS to test the ability of participants to navigate on land (see: Irmischer & Clarke 2018, Souman et al. 2009), no similar studies have been published for navigation at sea. Documentary sources are not any more helpful – while ships' logs contain data that can easily be converted into ranges, it is extremely difficult to locate logs where the navigator did not use instruments. Although anthropologists have sailed with navigators who navigate without instruments, they have not (understandably) attempted to check these mariners' work by comparing the real and presumed locations of the ships they sailed on. As such, the estimation ranges used in the analyses here are arbitrary.

To establish the bounds of estimation ranges, this study starts from the assumption that navigators in the Channel were competent sailors and seafarers. Although it is possible that navigators in the prehistoric Channel were drawn from a pool of people who were not conversant with the practicalities of seafaring, this seems unlikely and flies in the face of virtually all published discussion of the subject. Although the argument that Iron Age sailors were skilled because they were able to complete long voyages runs the risk of becoming circular, the argument that they were completing shorter voyages (i.e. across the Channel) between specific landing places suggests a measure of competence. On these grounds, then, the maximum amount of over- and underestimation used by the script was set at 60 % for Case Study 2, and 50 % for Case Study 3. In practical terms, this means that a simulated navigator might misjudge the quarter from which a wind blows, but would not mistake an oncoming wind from a following wind. In the second

place, in all analyses the lower bound for both over- and underestimation is set at zero (that is to say, at perfectly accurate estimation). Since randomness is not an ideal way to represent the intersection of skill with the vagaries of perception, it seems arbitrary to constrain the estimation ranges to a lower bound. Doing so would also conflict with the first assumption by preventing simulated navigators from ever 'reckoning' a value accurately.

Since the values used to guide reckoning in the script are somewhat arbitrary, great care was taken in their application to analysis. In the Main Analysis no environmental values were 'reckoned', so that the results of these analyses assume that simulated navigators were able to read the seas accurately.[44] Sets of estimation ranges were used to 'reckon' environmental values in all three Case Studies.

5.3: Research Design: Study Area and Coastal Nodes

Early in the design of this study, it was concluded that it would not be feasible to test maritime connections throughout the Atlantic Zone due to a lack of environmental data with high spatial and temporal resolution. The results of the navigation model improve as the temporal resolution of environmental inputs is increased (see discussion in Section 9.4.1); generating environmental datasets for the Atlantic Zone at hourly resolutions would have required access to proprietary data or else the development of new weather models. Since neither were available over this course of study, the western

[44] It was especially necessary to ensure that no misestimation occurred in the Main Analysis, as the results from the Main Analysis were used to select sailing times for the three Case Studies (Chapters 6-8).

English Channel was selected as a study area for these simulations. This section discusses coastal nodes within the study area.

5.3.1: Coastal Nodes in the Western Channel

The decision to locate all analyses in the western Chanel rather than all along its length was based on the availability of datasets and the geography of the Channel itself. To begin with, data coverage ruled out simulations in the eastern Channel. The study area of the Main Analysis corresponds to the area in which all three datasets shown in Figure 5.5 overlap. There are still grounds for limiting analysis to the western side even if data were available, based on the research questions and the limitations of the navigation model. In the first place, there are fewer promontory forts and local prominences in the eastern end of the Channel than in the west (out of 97 sites identified, only 9 are located east of the Isle of Wight), making simulations of navigation by landmarks in the eastern Channel more tenuous. The shorter crossings in the east also mean that ships crossing the eastern Channel will not be out of sight of land for significant periods of time. Finally at the eastern entrance to the Channel the distance from Britain to the mainland narrows to around 35 kilometres, a crossing which one would expect to complete in around 2-3 hours. Since the navigation model in these analyses operates on timesteps at one-hour intervals, results from an analysis of the crossing here would be less useful for assessing the process of navigation, as simulated navigators would only have to make ‘decisions’ at one or two timesteps.

5.3.2: Identifying Coastal Nodes

In order to keep the number of simulations feasible, it was necessary to develop a set of criteria for selecting origin and destination points for simulations. Identifying every possible landing and launching place along the coasts of the Western Channel would have resulted in a huge number of origins and destinations, and in any case would be anachronistic if based on modern charts or terrain datasets. Selecting origin and destination points for analysis was greatly aided by the work of Eileen Wilkes (2004, 2007) in identifying coastal 'nodes' along the UK south coast. Based on desk-based assessment and excavation of selected sites, Wilkes suggests the following criteria for potential Iron Age coastal nodes (see 2004, 125):

- Convenience to travelled routes, and favourable diurnal tides.
- Access to inland waterways.
- Nearby landmarks, and an identifiable break in the cliff-line to indicate a harbour.
- Shelter from winds and locations for anchoring and/or mooring.
- Capacity for storage and settlement around the harbour.
- Presence of Iron Age material at the site, including 'formal waterside constructions' such as jetties, piers, or ramps (see Wilkes 2007).

Using these criteria, Wilkes identified forty potential coastal nodes along the southern coast of the UK. Several of these nodes are located close together, and given the limited coverage of inshore areas in environmental datasets (see Section 9.4.1) placing equivalent nodes within the waters of the Channel would have resulted in several sharing locations. By combining adjacent nodes twenty-two of Wilkes' proposed nodes west of the Bill of Portland were selected to serve as nodes in the Main Analysis. Wilkes' nodes at Falmouth,

Topsham, and Wembury Bay were excluded. On the opposite coast, Wilkes' criteria were used to identify possible landing places along the northern coasts of Brittany and Normandy. For this purpose the UK Hydrographic Office Channel Pilot (2005) was consulted in order to determine a potential node's approachability and potential for anchorage. The Channel Pilot was also used to assess potential landmarks and identifiability from the sea, and to evaluate sets of cultural and natural landmarks generated for analysis (see Section 5.2.4). The identification of Iron Age activity at prospective nodes was based on the proximity of Iron Age sites identified in the survey that identified promontory forts within the study area Section (see Appendix I). Figure 5.6 shows nodes identified by Wilkes along the northern shore of the study area and potential coastal nodes identified by the author on the Channel's southern shore.

5.3.3: Node-to-Node Path Distance Calculation

The selection / identification of coastal nodes resulted in a set of twenty-two northern nodes and ten southern nodes, for which there are two hundred and twenty possible cross-Channel combinations. However not every combination of nodes produces a plausible cross-Channel route. For example a direct passage from Nacqueville to Penzance would be more of a voyage along the Channel than across it, and a navigator attempting such a voyage would be more likely to navigate along the coast and then cross the Channel from a more convenient node (or vice versa) than to plot a course directly to their destination. To limit node-pairings to only those that are located opposite one another, a distance-limit of 250 kilometres path-distance was imposed on possible combinations. The process used to compute path-distance is identical to the process used in the navigation model to estimate the distance from vertices on a heading envelope to a

destination point (see Section 4.3.5). As a result of this selection process, the total number of routes tested in The Main Analysis was 418.

5.4: Research Design: Environmental Data

Currents and tides in the English Channel can be variable, especially within channels between islands and the mainland. However in general the set of currents is towards the North Sea, and the prevailing wind is southwesterly. McGrail notes that wind-driven currents in the English Channel are not particularly strong, but flow fairly consistently from the south-east (McGrail 1998, 265). The tide range is particularly wide in the English Channel, reaching upwards of 5 metres in some areas. This section describes datasets used to represent environmental conditions in the model. Nearly all of the English Channel is less than 100 metres in depth, with the exception of the Hurd Deep. The extent of inshore waters with depth less than 50 metres varies within the English Channel – in general shallow waters extend further from the coast in the eastern Channel than in the western approaches. Figure 5.7 shows the areas of seafloor within the 50 and 100 metre depth contours for the western Channel. The shallower waters within the Channel result in strong currents near the coast and between the mainland and offshore islands, necessitating detailed environmental datasets.

In order to generate parameters for simulations in analyses it was also necessary to collect other environmental data, including: visibility forecasts for zones within the study area, sunrise and sunset times per node, and the time of high and low tide per node. These datasets are also discussed in this section.

5.4.1: Environmental Data Gathering

The main factor in selecting the time window for analysis was the availability of environmental data. A time window was selected to 'bracket' a possible midsummer sailing season by several weeks. Conditions at sea in the Channel can be hazardous in winter, and this factor is compounded by the lack of light in the winter at that latitude. Therefore the study period was limited to a window of 212 days between the 1st of March and the 30th of September, 2018.[45]

The analyses presented below use hydrodynamic forecasts from the French *Service Hydrographique et Océanographique de la Marine* (SHOM) to represent current speed / direction as well as tide height.[46] Weather forecasts from the AROME model published by the French National Centre for Meteorological Research are used to represent wind speed and direction. All of these forecasts are made available on a weekly rolling basis from the SHOM web portal. The NetCDF files that contain these forecasts are large – 1.6 gigabytes per day - and as such SHOM does not provide a method for downloading these files in bulk. In order to collect these datasets a custom Python script was written to download them remotely as they were published, and this script was used weekly during the months March-September to download hydrodynamic datasets to an external drive. At the end of the study period this data was checked for completeness and a series of requests were made to the SHOM database to collect datasets that had been missed. One of the files downloaded from SHOM was unusable due to file errors, and the

[45] Excluding dates for which data was unavailable.

[46] See: https://data.shom.fr/affichage.

date corresponding to that file (August 19) was excluded from analysis. The spatial extent of input datasets also posed a challenge, as the coverage of inshore waters varied from dataset to dataset. In some cases large areas of data were missing.[47] However areas of no data only blocked direct routes in one case (St. Peter Port, see Section 6.1), and even then the gap was short enough that most simulations were able to cross it in a single timestep.

The other source of weather data for these analyses was the Shipping Forecast, which was used to determine visibility distances. Like SHOM, the Shipping Forecast does not archive its reports online. Therefore another script had to be written to collect the daily forecast from its online source and record visibility information in tabular form.[48] Once forecasts had been collected for the entire study period, another script was written in order to process Shipping Forecast predictions. Assessments of visibility in the Shipping Forecast can indicate different conditions in different areas (i.e. 'good in SW, poor elsewhere'), or changing conditions ('moderate in the morning changing to poor'). In order to attach a single prediction to each day in the study period, the script used to process these records searched each forecast for the keywords 'good', 'moderate', and 'poor', and assigned the most optimistic prediction to the date.[49] It is possible on these grounds that data derived from the Shipping Forecast overestimates the potential for visibility. Because Shipping Forecasts were only available on the day that they were

[47] Areas that were not represented include: the mouth of the Sélune river at the head of the Gulf of St. Malo, waters between the Isle of Wight and the British mainland, and waters between St. Peter Port and the island of Herm in the Channel Islands.

[48] See: https://www.umr-cnrm.fr/spip.php?article120&lang=en.

[49] So that, for example, the record 'generally good with poor in NE and the morning' would be classified as 'good'. Likewise 'overall poor but with good spells' would also be classified as 'good'.

published, collecting them automatically was more difficult and resulted in several holes in the dataset that could not be filled. Shipping forecasts could not be gathered for the first two days in the study period (March 1-2), and these two days are excluded from the analysis.

5.4.2: Selecting Departure Times from Tide Data

For the Main Analysis, simulating more than one sailing per route would have caused the number of necessary runs (more than 88,000) to expand far outside the realm of the practical. Therefore it was necessary to develop a criteria for selecting leaving times for each day and origin node tested by the Main Analysis. Using a universal leaving time would have been problematic because it would have ignored local conditions which may have caused catastrophic failure. This would have carried a significant risk of misidentifying nodes as impractical or dangerous. Therefore it was decided to base leaving times in the Main Analysis on the state of the tides and the elevation of the Sun.

With respect to tides, it was assumed that navigators would have preferred to depart on a flood tide (after high tide). There are several advantages to launching on a flood tide: ships that are beached or stored on land can be launched more easily when the water is closer, receding tides can be used to carry ships out of estuaries, and higher waters can sometimes make reefs and other hazards passable. Since the navigation model operates on time steps at hourly intervals, it was decided to base leaving times on the first hour after high tide. To find this hour for each day-node combination in the parameter space, a Python script was written to scrape tide data from online forecasts.[50] This script

[50] Specifically, from https://tides4fishing.com.

produced tables identifying high-tide hours for each day-node combination included in simulations for the Main Analysis.

With respect to sunlight, it was assumed that Iron Age mariners would have preferred to launch during the day. Since tides are driven by the moon, the time of high and low tide varies throughout the year, so that the first high tide for a given day in the Channel may be before or after dawn. Although on certain days sailors may have been able to launch before dawn during the full moon, it was decided not to consider the moon as a source of light.[51] A Python script was written to calculate the time of sunrise for each day-node combination (using the PyEphem library) to serve as a basis for selecting sailing times. Tables produced with this script were compared with the compiled tide tables to select the final leaving times for simulations in the Main Analysis. The leaving time for these simulations represents the hour (rounded forward) of the first high tide after dawn.

Although basing leaving times on tides is better than selecting a universal departure time, it still carries risk of biasing the analysis against nodes where local conditions demand a particular launching time, or where tides are not the main factor in a sailors' decision to launch. As such, it was decided to vary sailing times in Case Studies 2 and 3 in order to gauge their effect on the results of simulations. Eleven sailing times were tested in both of these analyses. These leaving times were selected by bracketing the 'first time after dawn' time by five hours, performing simulations for each hour.

[51] Moonlight does not penetrate cloud cover as well as sunlight, and given the variability of weather in the Channel the ability to see at night on a full moon is not guaranteed.

5.5: Model Outputs and Data Processing

Since the navigation script produces navigation and visibility logs as text files, the 'Output Aggregator' script (see Table 4.2) was used to generate datasets from the results of the Main Analysis. For navigation logs, each log was summarised into a single entry in a database for the corresponding simulation. Simulation input parameters and success values were transferred to this database, and the number of timesteps iterated over was calculated for each input log by totalling the number of entries. For visibility logs, which record sightings per voyage, each sighting was incorporated into a separate database which was then queried in order to produce summaries. The Python script used to accomplish this also served as a data validator, checking simulation configuration files for errors. Some variables that were not included in navigation simulator logs but were deemed necessary for analysis were computed by this script. For example, 'days from start' was not included as an output parameter in navigation logs, but proved to be useful in assessing the data and in constructing figures presented below – on these accounts a 'days from start' parameter was calculated by the aggregation script and added to the output dataset.

The aggregation script was designed to output: a text file containing the results of log summarisation, point features denoting the location of landmark sightings, and polyline features tracing the course of simulated voyages. The attribute tables for the point and polyline features contained fields linking features to the UIDs for the simulations to which the features related. These datasets constitute the 'analysis results' discussed in the following sections.

5.6: Main Analysis: Results

The Main Analysis was intended to perform a complete parameter sweep of coastal nodes and leaving dates within the study period, in order to answer large-scale questions about Channel crossings. To start with, performing simulations for all dates was used to address the possibility of a 'sailing season', which is generally assumed to have been in mid-to-late summer. More successful simulations during these periods than in the spring and autumn months would support this proposition, and defining a sailing season in terms of weeks or days would provide useful context for characterising Channel crossings. Next, the Main Analysis was designed to test the validity of coastal nodes and the viability of routes between them. Identifying voyages to or from particular nodes as more successful than their neighbours has important implications and raises the potential of those nodes' involvement in cross-Channel trade. Where routes within the Channel have already been proposed and modelled, simulating voyages along these routes using the model developed here allows an opportunity for mutual evaluation. Finally, the results of the Main Analysis were used to formulate Case Studies 1-3. By selecting routes and favourable dates from the results of the Main Analysis, the parameter spaces of these analyses were reduced to manageable sizes.

The Main Analysis tested 418 routes over 212 days, with one voyage simulated per route per day. The ship parameterisation corresponding to McGrail's '7-metre' vessel, and a set of landmarks consisting of both coastal promontory forts and natural prominences were used for all analyses. No misestimation ranges were used in simulations for the Main Analysis. This resulted in a total of 88,616 simulations. Of these, 6,702 (7.56 %) simulations failed because of script errors (see Section 4.3.7) and

produced no navigation or visibility logs. These failed simulations are not included in the averages shown below. The results of these analyses are summarised here in tables and charts that reference coastal nodes and potential landmarks identified in Appendices I and II. Although distances are given in kilometres below, speeds are described in knots in order to make comparison with other research easier.

5.6.1: Speed and Success Rate as Criteria

Describing a route or a node or particular sailing date as 'likely' requires a set of criteria for deciding whether associated simulations were successful or not. This in turn requires a workable definition of 'success' – in this case in the context of Iron Age Channel crossings. Just as there are many potential reasons why people prefer certain routes on land – for example they may be familiar, or avoid unpleasant places, may afford good viewpoints or provide access to special resources – there are many potential reasons why Iron Age mariners may have decided to embark upon a particular route. This analysis focusses on two particularly important components of successful voyaging: time under sail and likelihood of completing a crossing. Mariners would have considered both of these (and still do) when setting sail across the Channel. Before proceeding, it bears repeating that the navigation model does not allow for catastrophic failure (see Section 4.3.7), and that therefore 'failure' in the context of these results does not necessarily indicate the loss of a simulated vessel (see Section 6.3.1, below).

Travel time is a straightforward measure of the success of a voyage. Sailing can be hard work, and with a limited amount of supplies on board Iron Age mariners would have preferred shorter voyages to longer voyages in general. Weather in the Channel can be variable, and making the crossing quickly reduces the risk of unexpected conditions

complicating the voyage. If navigators were making long-distance trips within the Atlantic Zone, then the time taken to cross the Channel would have had to fit within those schedules. However, when deciding where to cross the Channel the estimated speed of the crossing was likely secondary to the likelihood of making the crossing successfully. There are many risks involved in navigation and in seafaring, some of which result in delay and some of which can result in catastrophic failure. The possibility of losing ships and lives must surely have been a major part of navigators' decisions to favour some routes over others. One assumes that they would have sought to minimise risk even if it meant accepting longer travel times.

5.6.2: Speed and Success Rate by Date

Figure 5.8 shows the average speed for simulated routes across all days in the study period. Speed was calculated by dividing the number of timesteps that simulations took to successfully complete voyages by the path distance between points.[52] Since the Channel widens in the west, vessel speed proved to be a better method for comparing the results of all simulations than using the amount of time elapsed. The average speed of all successful simulated voyages across the Channel was 4.83 knots with the highest and lowest weekly averages being 6.56 and 3.40 knots. These averages accord very well with McGrail's prediction that for Channel crossings "with generally fair winds, the average speed could have been 5 knots" (1983, 300). The monthly average speed for simulated voyages is stable, with April, June and November being slightly better than the other months in the study period. Weekly averages show slightly more variability, and it is

[52] That is to say, the shortest distance between nodes that avoids obstacles – see Section 4.3.5.

interesting that the highest weekly averages are at the beginning and end of the study period. Daily averages suggest alternating 1-2 week periods where simulated voyages either exceed or fall under the general average by around 1 knot. The extent to which an increase of 1 knot decreases travel time depends on the width of the Channel at the crossing point – for a voyage of 50 nautical miles (the approximate distance from Nacqueville to Portland) an increase of 1 knot saves an hour and forty minutes, whereas an increase of 1 knot on a voyage of 130 n.m. (the approximate distance from Brest to Penzance) reduces the travel time by four hours and twenty minutes. For voyagers attempting to cross longer routes the expectation of better crossing times would have been important. In the spring and autumn, shorter days would have made these differences more important.

Success was calculated by dividing the number of simulations that completed successfully by the number of runs for which no script errors occurred. Because the Main Analysis involved so many simulations and because there was not enough time to re-run analyses, runs that caused unknown failures in the script were excluded from the dataset rather than counted as failures. The general success rate for simulated ships in this analysis is 60.17 %, a pessimistic figure. Figure 5.9 shows monthly, weekly, and daily success rates for simulations from the Main Analysis. The monthly averages appear to fit the expected profile for a sailing season – better chances in early and late summer with a fall-off in the autumn – although the overall differences between these probabilities are fairly modest. That being said, if we take the overall average at face value then even small improvements in one's chances of making it across the Channel would be worth pursuing. The graph of weekly success rates shows that success rates are more variable with respect to speed with time, and reveal that the high success rates in July are the result of a

particularly successful week (week 19) followed by several weeks that were close to the general average. Likewise, the low success rate in August results from two weeks in the month during which simulations performed very poorly. The daily averages shown in the third graph of Figure 5.9 best illustrate the high variability of success rates. Unlike the daily speed averages, which were all fairly close to the average, rates of success on individual days within the study period ranged from 100 % on Day 10 to 0 % on Day 172. Also, unlike daily speed averages, consecutive days with high success rates were rare within the study period. Assuming a success rate threshold of 80 %, there were only six instances with successful voyages on consecutive days within in the study period, only one of which spanned more than two days (from July 11-14). The overall pattern is characterised by a handful of days with relatively high rates of success followed by either a week or half a week of poor success rates.

The low overall success rates for simulations in the Main Analysis is interesting, and other sections discuss possible causes for this low rate (see Section 9.2.1). One possibility that was investigated in the context of the Main Analysis is that voyage 'success' is defined too narrowly. For the purposes of the navigation model, 'success' is achieved when the simulated navigator passes within one kilometre of their destination point. This means that simulations that cross the Channel but are unable to reach their intended destination are marked as failures. To test the degree to which this feature of the model was affecting success rates, navigation logs produced by the Main Analysis simulations were reanalysed in order to find the point at which simulated track was closest

to the opposite coast.[53] Simulations where tracks passed at least one kilometre away from their intended coastline were considered to have made landfall, and were considered to be successful in this reanalysis. Figure 5.10 shows landfall-success rates compared with the original success rates. Although there is an improvement when considering landfall as success – the average success rate rises to 69.58 % – the gains are not evenly distributed throughout the study period. In the weekly and daily averages in Figure 5.10 rates of success which were already high are not particularly improved by using landfall as a success criterion. With the exception of Weeks 3-4 (in late March), most improvement in success rates occurs on days directly before or after already-successful days.

Since the daily averages for both speed and success rate appear periodic, a useful comparison can be made between them. Figure 5.11 shows both of these in the same graph, where speed and success rate are charted as percentages of the greatest value in the series. What is striking about this graph is the degree to which periods of quick passage and high success rate alternate. The two variables have a moderate inverse correlation, with Pearson correlation coefficient (r) of -0.55). Interestingly, the areas where quick crossings correspond with high success rates are late May, mid-July and late August. Based on the results of this analysis, it would appear that if a single 'sailing season' is said to exist in the study period then its midpoint is at the beginning of July and its length is not much more than three to four weeks. If the possibility of a second sailing season is to be considered then late May is a good candidate for a 'spring sailing season'

[53] That is to say, the coastline on which the vessel's destination was located. Simulated voyages that failed to make the Channel but achieved landfall on the coast from which they launched were counted as failures.

based on monthly averages. The weekly and daily averages, however, tell a different story. Although simulations in July performed very well overall, there were still periods in the middle and at the end of that month where the success rate for simulations was barely forty percent. At the same time, the only day for which all simulations were successful was in mid-March (Day 10). The daily averages for success rates suggest that the best times to make a Channel crossing are periodic several-day periods where a navigators' chance of reaching their destination is high or – if out by a day or two – their chance of making the opposite coast is reasonable. The 'best' times to sail, according to the criteria laid out above, are where these windows of opportunity align with conditions that facilitate a speedy crossing.

5.6.3: Speed and Success Rates by Node

Table 5.3 shows speed and success rate averages for each node. These averages are further divided into inbound and outbound averages – speeds and success rates for voyages arriving at and departing from each node, respectively. Table 5.3 also shows the difference between averages for inbound and outbound voyages. This difference is important when considering the viability of coastal nodes within a larger transport network, where ships can be launched and landed at different nodes. For example, the low average success rate for a node could result from high numbers of failed outbound voyages and successful inbound voyages – in which case the node could still have served as a port of arrival for ships crossing the Channel. With this in mind, the values in Table 5.3 were used to classify nodes into groups according to their average speeds, chances of success, and inbound / outbound differences for both factors. The criteria used to make this classification is summarised in Table 5.4, and the classified nodes are shown in a map

of the Channel in Figure 5.12. The categories into which nodes are classified are as follows:

Generally Successful: Voyages calling at these nodes outperformed other nodes both in terms of success rates and average speeds. These nodes are Anse de Kernic, Budleigh Salterton, Morlaix, Sidmouth, and St. Malo. For all of these nodes the overall speed was higher than the general average, and overall success rates were higher than the general average. Moreover, the difference between inbound and outbound speeds and success rates for these nodes was less than the corresponding general averages. Three of these successful nodes are located on the southern shore of the Channel – Morlaix and Anse de Kernic are both in northwest Brittany and St. Malo is located at the head of the gulf of the same name. The two successful nodes on the northern shore of the Channel are located next to another in the centre of Lyme Bay.

Quick & Unsuccessful: Voyages to and from these nodes were relatively unsuccessful but also relatively quick; the nodes at Brest, Fowey, Le Légnét, Lulworth Cove, Mevagissey, Penzance, Poole, Portland, Rivière de Lannion, Salcombe, Teignmouth, and Topsham fall into this category. This is the largest category, and contains nodes throughout the Channel. The node at Brest is of particular interest here, as

it had by far the lowest average success rate of all nodes (35.36 %), but also the second-highest average speed (4.58 knots).

Slow & Successful: Voyages arriving at and departing from these nodes were relatively slow, but were more successful than the overall average. These nodes are Aber Wrac'h, Bigbury Bay, Christchurch, Dartmouth, Kérivoas, Kimmeridge Bay, Le Trieux, Nacqueville, Seaton, St. Peter Port (North and South), and Torquay. Only one of these nodes (Bigbury Bay) is on the northern shore of the Channel, and the rest are distributed all along its southern coast. This category includes several nodes that have been suggested as launching / landing places in archaeological literature – Christchurch, Nacqueville, Le Trieux and St. Peter Port – which are all investigated in greater detail in Analysis 2.

Successful but Imbalanced: Voyages starting and finishing at these nodes were more successful than the average, but showed a high difference between inbound and outbound speeds and success rates. Three nodes were identified as 'successful but imbalanced': Mothecombe, Plymouth, and Porthallow. All three of these nodes occur in Start Bay on the northern shore of the Channel. In all three cases the bias was towards outbound voyages both in terms of speed and success rates. It should be noted that high differentials between inbound

and outbound speeds / success rates do occur in other categories described above, particularly in the ‘quick and successful’ category.

Generally Unsuccessful: Two nodes underperformed in terms of general speed and success averages in simulated voyages: Helford and Mullion. These two nodes are adjacent to each other on either side of Lizard Head on the northern shore of the Channel. Both of these nodes also had much higher chances of success on outbound voyages than on inbound voyages.

5.6.4: Speed and Success Rates by Route

Although general averages by node are a good place to start, more useful observations can be drawn by investigating each route simulated, averaged across all days in the study period. Figure 5.13 and Figure 5.14 show speed and success rate averages by route in a road atlas-style chart, with nodes on the southern coast of the Channel displayed on the X axis and nodes on the northern coast on the Y axis. Nodes are arranged in sequence from west to east on both axes, so that the axis from the lower left to the upper right of the graph corresponds roughly with a line due east from the entrance of the Channel. In Figure 5.13, interestingly some of the fastest speed values correspond to routes diagonally across the Channel, for example from Lulworth Cove to Kérivoas and Morlaix, and from Helford to Nacqueville. An additional set of routes for which generally good speeds were made good exists in the centre of the Channel, particularly between the Start Point area and the western Gulf of St. Malo (in particular Le Légnét-Fowey and -Mevagissey). Speeds for Brest and St. Peter Port, which appeared low in general averages,

were generally low across tested routes. Success rates for individual routes (Figure 5.14) tended to follow the general averages more closely. Diagonal routes associated with high speed values were not identified as more successful in these averages. Instead, the fastest average speeds for diagonal voyages was along a Morlaix – Portland axis, and from Le Légnét to nodes in Start Bay, however neither of these routes is associated with a high percentage of successful voyages.

As with nodes, the difference between the results of voyages travelling north and south on each route may have had a bearing on how those routes were used. Figure 5.15 and Figure 5.16 show differences in speed and success rate for each tested route. Although speed differences were relatively minor for these routes, most (91.4 %) had faster average speeds for southbound voyages than for northbound voyages. The routes with the highest speed difference were mostly associated with nodes on the southern shore of the Channel, particularly St. Malo and Le Légnét. Success rate differences were much less skewed towards a particular direction of travel. However, there appears to be a clear divide in the data based on the orientation of the route: routes that cross the Channel directly (i.e. from the node of origin to the nearest opposite node) have low success rate differentials in the western end of the study area, and high success rate differentials at the eastern end. Voyages bound for the southeast from the northern shore of the Channel tend to have more successful northbound voyages than southbound, but the opposite is true for routes bound for the southwest. Simulations for the node at Le Trieux, for example, were 10 % more successful in a northbound direction for routes to / from Seaton, but 24 % more successful in a southbound direction for routes to / from Penzance. Routes involving Brest, Le Légnét, and St. Malo were exceptions to this trend, and showed consistently higher chances of success for simulations of southbound voyages.

5.6.5: Track Density

The coordinates given at each timestep in navigation logs produced by the model were used to create polyline features corresponding to each simulated voyage. Since the navigation model chooses endpoints based on a path distance algorithm rather than straight-line distance (see Section 4.3.5), the polylines produced by the aggregation script do not correspond exactly to the routes that simulated vessels take when near obstacles (i.e. near land). To separate the actual simulated course of a vessel from the polyline produced by joining coordinates from navigation logs, from this point the term 'track' is used to refer exclusively to the latter. This dataset were used to generate line-density analyses, which assigned values to cells in a raster based on how many tracks pass through the cell. Figure 5.17 and Figure 5.18 (respectively) show the results of line-density analyses for all tracks produced by the model for the Main Analysis, and all simulations that were successful.

The most obvious feature of both track-density plots is the corridor running from the Riviere de Lannion node to the Start Point headland (approximately midway between the Salcombe and Dartmouth nodes). Although the route appears to be diagonal in Figure 5.17 and Figure 5.18, this results from the map projection (ETRS 1989); the two nodes are nearly on the same line of longitude (see Section 7.1.1). Other areas of high traffic include the immediate vicinity of each node, and areas where tracks are obstructed by headlands. These last areas include Lizard Head, Start Point, the Bill of Portland, and Cap de la Hague, and the coastline between the nodes at Brest and Aber Wrac'h. The distribution of all tracks is largely confined to the interior of the western Channel. Although some tracks do reach the western edge of the navigable area (and would therefore end up in Atlantic), no simulated tracks reached further than the Seine Bay in

the east. In the south only a few reached the southern border of the navigable area, which would have resulted in their entering the Bay of Biscay. In the north, no simulated voyages reached the northern edge of the navigable area, which corresponds to the border between the Channel and the Irish Sea. Although some simulated tracks passed by the Scilly Isles and north of Land's End, these do not appear to have travelled more than 20 kilometres north of the peninsula. The distribution of *successful* ship tracks is more constrained still: no tracks reach the northern, southern, or eastern limits of the navigable area, and only a few reach the western end. Only a handful of tracks extend north of the Scillies and Land's End, and the difference between the western extent of all simulation tracks and successful simulation tracks is approximately 25 kilometres.

5.6.6: Landmark Sightings

Although the Main Analysis was not designed to test the hypothesis that coastal promontory forts could have served as landmarks – one set of landmarks containing both sites and natural prominences was used for all simulations – visibility logs produced by the simulations are still useful and provide the basis for some simple comparisons. Visibility logs produced by simulations were processed by counting the number of sightings for each landmark per log, and combining those counts into a single dataset consisting of 2.25 million sightings. This dataset served as the basis for the evaluation of landmarks in this analysis. Overall, archaeological sites accounted for 13 % of total sightings. When normalised by the number of sites in each category, the average number of sightings per archaeological site accounts for 33 % of the general average. These percentages apply both for successful and unsuccessful voyages. Figure 5.19 shows these values. The visibility of landmarks appears to be driven less by the type of landmark than

by its location in the Channel. Figure 5.20 shows the locations of landmarks from the Main Analysis, graded by the number of sightings recorded by simulations. The most visible landmarks are located on the southwestern coast of present-day Devon, Cap de la Hague, Guernsey, and Sept-Îles. All of these locations correspond with areas of high traffic identified by line density analysis of simulation tracks Section 5.6.5. The total number of sightings for each archaeological site considered as a landmark is given in Table 5.5. Also included in this table are the number of sightings for successful and unsuccessful voyages, and the maximum number of sightings for all landmarks within a five-kilometre radius of the site. For cultural landmarks that were sighted by simulations in the Main Analysis, slightly more than half were at least 5 kilometres from a landmark with at least 2,500 sightings, and just over one-third were the most-sighted landmark within 5 kilometres.

Figure 5.21 shows the results of a density analysis for points from which sightings were made. The results of this analysis follow the results of the ship-track density analysis described above in that the highest density is observed in the vicinity of Start Point. However, the area of especially dense sightings extends beyond Start Point to the east and the west, as far as Seaton and Mevagissey, respectively. Sightings on the southern shore of the Channel are relatively sparse, with the entrance to the Rade de Brest, the immediate coastline between Kérivoas and Lannion, and the approaches to St. Peter Port included in the areas of highest concentration / density.

5.7: Main Analysis Discussion

5.7.1: Discussion of Sailed Routes

In the Main Analysis, the departure date parameter had the greatest effect on the outcome of simulations, rather than the choice of node or route. Several days in the study period had success rates of 100 %. By contrast, the highest success rate for a single route (St. Peter Port to Portland) was 77.9 %. Likewise weekly average speeds in the study period averaged over 6 knots, higher than the average speeds broken down by node and route. These results suggest a sailing regime for the Iron Age Channel in which the most important factor is not where the crossing is made but when it is attempted. The high speeds and success rates associated with 'diagonal' routes across the Channel also suggests that navigators would have had a wide range of options when planning their crossings. For most nodes, there is no single 'obvious' destination node on the other side of the Channel, but rather a selection of destination nodes. This suggests that although coastal nodes may have been the best landing places along the shores of the western Channel, other smaller landing places may have also played a role in cross-Channel contacts.

Based on the results of the Main Analysis, several nodes and routes warrant special attention: routes from the Rade de Brest in western Brittany, routes from Lannion to Start Point, and routes from the Gulf of St. Malo / Channel Islands to the shores of south-central Britain. To a certain extent the issues raised with these routes apply to others within the three areas that they define: a western area consisting of the entrance to the Channel, a central area corresponding to the northern coast of Brittany and the southern coast of Britain between Lizard Head and Lyme Bay, and an eastern area composed of

the remaining coast of south-central Britain and the Gulf of St. Malo. The following paragraphs discuss these regions, and routes within each are tested in following Case Studies (Chapters 5-8).

Routes across the entrance to the Channel were associated with the lowest success rates, particularly those associated with the node at Brest. Success rates for routes originating and terminating at Brest were approximately half of those associated with the most successful nodes. Given that the Rade de Brest is a superb natural harbour, has many Iron Age sites nearby, and is identified as part of late Iron Age exchange networks by McGrail (1988) and Cunliffe & De Jersey (1997), it is difficult to argue that it was an unlikely departure point for cross-Channel navigators. A possible explanation for these low success rates is that the Chenal du Four is notoriously difficult to navigate (UK Hydrographic Office 2005, 236), perhaps to the point that the procedure used by the navigation script failed to successfully negotiate it (see Case Study 3, Section 8.2.5).[54] However, a closer look at the results of simulations for Brest suggests that rather than being a generally unsuccessful node, the periods during which voyages were successful were brief and relatively infrequent. For simulated voyages originating at Brest, simulations were 100 % successful on 30 days (c. 14 % of the study period). Bearing in mind that average vessel speeds for routes involving Brest were higher than average (as they were for Penzance, on the opposite coast of the Channel), the results here suggest that voyages from Brest could have been successful so long as they were timed properly.

[54] The navigation model is designed to react to conditions rather than anticipating them. See Section 9.4.3 for further discussion.

Routes in the central Channel were dominated by the axis between the headland north of the Lannion node and Start Point. This cross-Channel axis is readily apparent in track-density graphs, as can be seen in Figure 5.18. The high density of ship tracks here may result from the fact that the headland at Lannion is almost due south of Start Point (the deviation between the two is less than one minute of arc; see Section 5.6.5). Voyages under generally favourable conditions may have been able to follow the British coast to Start Point from nodes to the east, and been able to run due south until reaching Lannion (and vice versa). The fact that this behaviour does not occur around other headlands in the study area suggests that the density of routes here does not result from an error in the script, rather that this route was particularly effective. Case Study 2 (Chapter 7) focuses on this axis specifically in order to test parameters relating to navigators' experience and ship type.

Evaluating routes in the eastern portion of the study area was complicated by the nearness of the St. Peter Port and Nacqueville nodes relative to other nodes on the southern shore of the Channel. Both are situated much further north than other Continental nodes, to the extent that the distance due north from Nacqueville is about the same as the distance due south to the head of the Gulf of St. Malo. It was therefore surprising that average speeds for both the Nacqueville and St. Peter Port nodes were lower than average. The strong currents that run around the Channel Islands may be one of the causes of long voyages. For example the Alderney Race, which runs between the island of Alderney and the Cotentin Peninsula, appears to have been attempted by many voyages making landfall at St. Peter Port and Nacqueville. Currents preventing vessels from making headway while landmarks are still in sight would be consistent with the slow speeds and high success rates associated with these nodes. Also of interest in this part of

the study area are the large imbalances in success rates between inbound and outbound voyages. The Nacqueville and St. Peter Port have higher success rates for voyages bound for nodes directly opposite on the northern shore of the Channel, while the opposite was true for the nodes of St. Malo and Le Légnét. Given that all of these nodes are considered as possible points of departure for ships bound for the entrepot at Hengistbury Head (see Case Study 1 (Chapter 6) for further discussion), the imbalances in success rates for these nodes hint at the possibility that trade routes developed to take advantage of these circumstances.

5.7.2: Discussion of Landmarks

In the Main Analysis, coastal promontory forts were sighted three times less frequently than natural prominences, even while controlling for the relative frequencies of cultural / natural landmarks and the success of voyages. The simplest possibility is that archaeological sites were not especially useful as landmarks in these simulations. Sites that were frequently sighted occur in close proximity to natural landforms that were also sighted often in simulations. Since both types of landmarks were used in all simulations, comparing the relative number of sightings does not necessarily tell us whether crossings would have been successful if another set of landmarks were used. Case Studies 2 and 3 (Chapters 7-8) address this possibility by running simulations using separate landmark sets.

Although the results of this analysis do not support the interpretation of coastal promontory forts as landmarks, they could indicate that some of these sites may have been useful as stopping places. If the most important factor affecting the success of a crossing is the leaving date, then one of the strategies that navigators may have adopted

would have been to wait for the most advantageous day before setting out across the Channel. Crews returning from the opposite shore would have required somewhere to wait. In this case coastal promontory forts are less important for their visibility from the shore than for their vantage point to read conditions at sea. This possibility will be taken up in later sections.

5.7.3: Model Performance

Unfortunately, the results here are based on more optimistic parameterisations of vessel speed than McGrail used in his analysis (see Section 2.3.10), and on those grounds comparisons between the results should be understood as tentative. Table 5.6 shows travel times predicted by McGrail's Channel-crossing model (1983, 330) compared with results from the Main Analysis. Although maximum speeds allowed in the Main Analysis are higher than those predicted by McGrail, the results from the Main Analysis fall comfortably within the ranges defined by McGrail, who predicted separate travel times for vessels assuming average speeds of 2.5 and 5 knots. For those routes held in common between the Main Analysis and McGrail's model, average speeds suggested by the model were 4.57, 4.47, and 5.10 knots. Despite the higher predicted speeds, average travel times predicted by the model were longer than those predicted by McGrail (by 6.7 hours, 3.5 hours, and 4.4 hours respectively) but higher than averages McGrail predicts for ships with an average speed of 2.5 knots. This likely results from the fact that McGrail assumed relatively direct crossings with some displacement, whereas ships in simulations were counted as 'successful' so long as they reached their destination irrespective of whether they followed the most direct course. Discussion of differences between the results of the navigation model and McGrail's 1983 analysis is continued in Section 9.2.1.

Chapter 6 : Case Study 1 (Hengistbury – Gulf of St. Malo)

6.1: Introduction

Case Study 1 tests voyages connecting the Christchurch node – which corresponds to the Iron Age promontory fort at Hengistbury Head – with nodes along the Gulf of St. Malo and the Cotentin Peninsula. While Hengistbury Head is widely recognised as an Iron Age centre of trade, a corresponding centre of trade on the southern shore of the Channel has yet to be identified (see De Jersey 1993; Cunliffe 1978; Cunliffe & De Jersey 1997, 57-67; Wilkes 2004; Henderson 2007, 210-211). St. Peter Port, Guernsey, has also been suggested as an intermediate node on potential sea-routes to / from Hengistbury Head (De Jersey 1993). This case study evaluated 7 nodes (including both St. Peter Port North and St. Peter Port South) and 16 routes tested in this analysis.[55] Simulations were run once per day for a period of one week, from July 8 – July 14. Estimation ranges were varied in this analysis, at intervals of 5 %, 15 %, 30 %, and 60 %. Two vessel parameterisations were used, based on the lower and upper bounds of McGrail's speculative Channel-crossing craft (see Section 2.2.6). Taken all together, this amounted to 1,792 simulations, which were run over three weeks. Navigation and visibility logs produced by these simulations were processed by the same aggregation scripts used in the Main Analysis.

[55] The waters between the islands of Guernsey and Herm are not covered by environmental datasets, so it was necessary to create 'northern' and 'southern' St. Peter Port nodes.

6.1.1: Archaeological Context

Material evidence for cross-Channel trade is well attested, although no more so than at Hengistbury Head (Cunliffe 1978). The volume of ceramic evidence for exchange at Hengistbury Head, coupled with the supposition that other 'entrepots' along the southern coast of Britain likely existed (Wilkes 2004, Cunliffe & De Jersey 1997) suggests the existence of developed trading networks between *Armorica and Britain*. Although the evidence for Hengistbury Head as a major trading centre is clear, attempts to identify a 'corresponding' centre of trade on the southern side of the Channel have met with more difficulty. Although the settlement at Alet, near St. Malo (see Dos 1969) has been suggested as a possible complement to Hengistbury Head, a review of ceramics by De Jersey (1993) suggests a later, Gallo-Roman date for the site. In the same paper, De Jersey points out that ceramic evidence in the Gulf of St. Malo is concentrated in the south, with a lack of evidence for trade from the western edge of the Bay of St. Brieuc to Le Yaudet at the mouth of the Riviere de Lannion (1993, 331). De Jersey suggests the Bay of St. Brieuc as a possible alternative point of departure for northbound traders, whom he envisions stopping in the Channel Islands to consolidate their cargoes and replenish their supplies before continuing to Hengistbury Head. This hypothesis is further developed in *Armorica and Britain* (1997), where Cunliffe and de Jersey also suggest Nacqueville as another possible complement to Hengistbury Head, based on the presence of ceramics and the proximity of the Cotentin Peninsula to the south coast of England.

6.2: Analysis Results

The following sections report the results of simulated voyages in Case Study 1. These results are based on a total of 1,792 simulations, all of which completed without

encountering unexpected errors. As with the Main Analysis, the range of parameters used is discussed along with the results in the following sections.

6.2.1: Average Speed / Success Rates per Day

Simulations were run for 7 days (July 8-14) corresponding to Week 19 in the Main Analysis. Simulations along the routes tested in this case study (See Section 6.1) were all successful during this week in the Main Analysis. The results of these simulations therefore correspond to sailings within the most favourable 'window' identified in Section 5.6.2, and are likely not representative of the results of voyages as a whole. As such the success rates overall in Case Study 1 are higher than those of the Main Analysis, with simulations in Case Study 1 being on average 69 % successful compared to the average success rate of 60 % in the Main Analysis. The average speed for simulations in this case study is 4.39 knots, with averages just under 4 knots for the first five days of the study period and averages of 5.5 and 5.8 knots on the final two days. Average speeds in this case study are slightly lower than the Main Analysis' averages for these routes (see Section 5.6.4).

Figure 6.1 shows averages speeds and success rates per day in the study period. Average speeds over the period fell within a range of 4-5 knots; Days 3 and 6 were the best days in the study period in terms of average speed. The lowest and highest average success rates per day were 53 % and 80 %, respectively; success rates were initially high on Day 1, fell until Day 4, and fell again until the end of the study period. It is interesting that days with high speeds occur after peaks in success rates, although it is difficult to tell whether the two are linked given the time period that is represented by this case study.

6.2.2: Average Speed / Success Rates per Node

Table 6.1 shows average speeds and travel times for nodes included in this study. Because of a gap in environmental datasets, St. Peter Port is represented in this analysis as two nodes, St. Peter Port North and St. Peter Port South. In Figure 6.2 averages are given for both of these nodes, and as combined ('overall') averages – values for St. Peter Port North correspond to northbound voyages, and values for St. Peter Port South represent southbound voyages.[56] Imbalances in inbound/outbound speeds and success rates were pronounced for the Christchurch node and for southern 'mainland' nodes (St. Malo, Le Trieux and Le Légnét). In these cases, voyages southbound from Britain and the Channel Islands performed much better than simulated ships launched in the opposite direction. The southern mainland nodes also had very low average outbound success rates – for these nodes outbound voyages were approximately half as successful as inbound voyages. The opposite was true for the Christchurch node, although both inbound and outbound averages were higher than those of the southern mainland nodes. The St. Peter Port (Overall) and Nacqueville nodes, by contrast, show smaller imbalances in inbound / outbound success rates. Both of these nodes show a slight bias towards outbound voyages.

Average vessel speeds are strongly correlated with success rates in Case Study 1, with a Pearson correlation coefficient of 0.97. Again, the best average speeds were

[56] Representing St. Peter Port in this way avoids confusion since – unlike all other nodes – the relationship between 'northbound / southbound' and 'inbound / outbound' is not 1:1 for this node. St. Peter Port is the only node tested in this analysis that simulated 'inbound-southbound', 'inbound-northbound', etc. voyages. This fact is obscured by general averages when presented next to averages for other nodes.

accomplished by voyages outbound from the Cristchurch node, and inbound to the St. Peter Port North and southern mainland node. The nodes at St. Peter Port (Overall) and Nacqueville had relatively low average speeds, but the differences between inbound and outbound speeds were much less than for other simulations.

6.2.3: Average Speed / Success Rates Per Route

Case Study 1 tested routes between the Christchurch node and all southern nodes (Nacqueville, St. Peter Port, St. Malo, Le Trieux and Lé Légnet), as well as routes from St. Peter Port to the three southern nodes in the Gulf of St. Malo. The route from St. Peter Port to Nacqueville was not tested, as it is not suggested by De Jersey (1993) or Cunliffe & De Jersey (1997).[57] Average speeds and success times for these routes are shown in Figure 6.2. These averages are further divided into northbound and southbound categories. As with averages per node, average speeds and success rates are better overall for southbound voyages. Unlike the node averages, however, average speeds and success rates per route differ from each other. Simulations were completed unusually quickly for two routes: Le Légnét to Christchurch and St. Peter Port to St. Malo. These two routes had average speeds of 6.73 and 8.46 knots (respectively) for successful voyages, almost twice as fast as averages for other nodes. In consequence, the route from Le Légnét to Christchurch is associated with faster average speeds for northbound ships than for southbound, while the opposite is true for other nodes. When considering average speeds

[57] The navigation model would have also dealt poorly with the short distance from Nacqueville to St. Peter Port, producing simulations lasting only a few timesteps (see Section 5.3.1).

the route with the lowest difference between northbound and southbound speeds is Nacqueville.

6.2.4: Visibility Results

Case Study 1 used two sets of landmarks, one corresponding to natural prominences and the other corresponding to archaeological sites. Speed and success averages per landmark type are shown in Figure 6.3. In general, natural prominences made better landmarks than archaeological sites, increasing chances of success by 8-28 percentage points on average. This advantage is not repeated for average speeds, which remained fairly constant (within 0.35 knots) for all routes. Although average speeds were better with sites as landmarks, the differences were not large enough to build a convincing case that they served as better landmarks than natural prominences in this context. No routes had higher success rates with sites as landmarks, however simulations along the Christchurch-Nacqueville and Christchurch-Le-Trieux routes fared particularly poorly with sites as landmarks. This suggests that voyages from Le Trieux tended to pass along the western coast of Guernsey without sighting the promontory forts on its northeastern and southeastern corners. Similarly, differences in success rates for the Christchurch-Nacqueville route may be explained by simulated ships' being unable to sight Vaux du Catel, on the opposite side of the Jobourg Peninsula from the Nacqueville node. The finding that different sets of landmarks affected simulated voyages' chances of success much more than they affected their speed suggests that – for the week simulated, at least – the Channel crossing along these routes was fairly straightforward. Few successful voyages strayed far enough from the most efficient path that they skewed speed averages, although many voyages simply failed to complete.

In terms of sightings, the island of Sark and nearby islands (Breqhou, L'Etac, and Herm) were amongst the most visible sighted landmarks. Cunliffe & Durham (2020) have argued that Sark could have played an important role in maritime exchange networks in prehistory, and the results of this case study appear to confirm its visual prominence – at least to an Iron Age navigator. Although Sark has many promontories, no promontory forts have been identified on the island. The promontory fort at Jerbourg, at the southeast corner of Guernsey, sits across from Sark and was the most-sighted promontory fort in this case study. Jerbourg sits at the southern entrance to St. Peter Port harbour; as Table 6.2 shows, the most-cited promontory forts in this analysis were located close to coastal nodes. Hengistbury Head, curiously, was the fifth-most sighted promontory fort in this analysis. Considering that the values in Table 6.2 represent the raw number of sightings in all analyses, and that most simulations in this case study started from or were bound for Hengistbury Head (or else St. Peter Port), it was expected that this site would have been the most-sighted archaeological landmark. The fact that it was not perhaps reinforces its interpretation as a coastal emporium, rather than as a landmark.

6.2.5: Vessel Parameterisation Results

Two vessel parameterisations were tested in this Case Study – one for a ship with a maximum speed of 13.76 knots and one for a ship with a maximum speed of 10.56 knots (see Section 5.2.3). Speeds and success rates averaged by ship type are shown in Figure 6.4. Reassuringly, average speeds and success rates were higher for the 13.76-Knot vessel than for the 10.56-Knot vessel for all routes tested. Average speeds and success rates were higher for the 13.76-Knot parameterisation for routes from St. Peter Port and Nacqueville to / from Christchurch, while the same were higher for the 10.56-Knot parameterisation

for routes from St. Peter Port to nodes on the Gulf of St. Malo. The suggestion that smaller boats would have been more suitable for shorter voyages in the Gulf of St. Malo while larger ships would have been better suited to Channel crossings is also reassuring.

6.2.6: 'Reckoning' Results

Four ranges for misestimating – or 'reckoning' – environmental values in simulations were used in this analysis. To accomplish this values were manipulated by a random constant but constrained to within 5 %, 15 %, 30 %, or 60 % of their original value. Figure 6.5 shows average speeds and success rates for each of these misestimation ranges. Overall, voyages were generally successful even with poor reckoning. The lowest and highest chances of success for a voyage allowing for 60 % misestimation were 46.4 % and 75 % - figures that compare favourably with success rates from the 10.56-Knot ship parameterisation. However, the difference in success rates between simulations using 5 % and 60 % misestimation is in the order of 15-20 % for all routes. The greatest difference between adjacent misestimation values is between simulations using 5 % and 15 % misestimation. As with vessel parameterisations, average speeds for successful voyages remained fairly stable across misestimation values in Case Study 1. Although simulations for some routes (Christchurch to Nacqueville, St. Malo, and Le Légnét) were actually faster when 'reckoned' at 30 % and 60 % than at 5 % and 15 %, the differences between different misestimation values were small (<0.5 knots).

6.2.7: Track and Visibility Density Analysis

Track densities were computed using the same process as the Main Analysis, and at the same resolution (100 metres). As such the same caveat that tracks produced by the

ship represent links between iterations in the model rather than the actual paths of simulated vessels applies to these results. Figure 6.6 and Figure 6.7 show track densities for all routes and for successful routes, respectively. Figure 6.8 shows track density for successful voyages from Hengistbury Head to Continental nodes, and vice versa (i.e. voyages that do not start or stop in the Channel Islands). The extent of routes in all figures suggests that simulations performed in this case study were fairly efficient – no tracks lead beyond Start Point in the west, nor beyond Brighton in the east.

Since the number of voyages in Case Study 1 is small, densities associated with each can be described in detail. The route from Nacqueville to Christchurch is straightforward, with most voyages heading due north or northeast and arriving directly at their destination. Routes from Christchurch to nodes in the Gulf of St. Malo all run through the Channel Islands. The clearest concentrations of tracks in the Channel Islands in Figure 6.8 run from St. Malo along the eastern coast of Jersey, and from Le Trieux / Le Légnét past the west coast of Guernsey. When routes originating in the Channel Islands are included, the difference between the Le Trieux / Le Légnét - Guernsey - Christchurch route becomes more distinct from the Christchurch - Jersey - St. Malo route. When all tracks are considered (see Figure 6.6), areas where unsuccessful voyages can be seen mainly in the middle of the Gulf of St. Malo south of Guernsey and Sark, and along the north-western coast of Normandy. In the first case this appears to be because vessels failed to make headway against the wind (the 'hatching' in the track density plot suggests repeated tacking), whereas in the second case the proximity of failed voyage tracks to the coast suggests that the script was unable to find a path forward that did not run into land.

In addition to track density, sighting density was also computed for Case Study 1, and the results are shown in Figure 6.9. Areas where most sightings occur consist of the

approach to Christchurch (which is unsurprising considering the density of tracks in that area), as well as areas associated with failed tracks. Again, this probably results from simulations attempting to tack against an oncoming wind, which would result in being able to make several sightings from similar positions over the course of the simulation. Sightings occur continuously between Nacuqeville / St. Peter Port and Christchurch, which suggests that landmarks could have been visible at all stages of a cross-Channel journey along these routes.

6.3: Discussion

6.3.1: Parameter Effects

A wide range of parameters were used in Case Study 1 in order to evaluate their relative contributions to successful voyages. In order to compare the effects of parameters on the results of simulations in this case study, the average speeds and chances of success for simulations under different parameter values were calculated; the results are shown in Figure 6.10. If the effect of a parameter on simulations as a whole is measured as the difference between success rates for the ‘best’ and ‘worst’ parameters in a parameter set, then the parameter with the greatest effect on simulations in Case Study 1 is reckoning, for which the difference between the ‘best’ and ‘worst’ misestimation ranges was 18.53 %. The same difference for landmarks was 15.18 %, and for vessel parameterisations the

difference was 10.27 %. These figures should be treated with caution given that these parameter sets are not directly comparable.[58]

The speed of a vessel is not directly related to a navigator's ability to fix their position, rather faster speeds reduce the amount of time spent out of sight of land and therefore reduce the amount of error that accumulates in positions calculated by dead reckoning. As such, it makes sense that vessel parameterisation had the least effect on simulation success rates in terms of difference between the 10.56-Knot and 13.76-Knot vessels. The greatest effect of ship parameterisation was – unsurprisingly – on average vessel speed. The difference between the two general averages was 1.15 knots, less than might have been expected given that the difference between the two parameterisations' maximum speeds is 2 knots. Since only two parameterisations were used comparison is difficult – this is addressed in Case Study 2. Additionally, the effect of vessel parameterisation may be influenced by the fact that the navigation simulator assumes that ships are invincible – the only conditions that result in catastrophic failure are running out of time and being forced onto land (see Section 4.3.7). Real ships are not invincible, and as such the effects of vessel size on overall success rates are almost certainly understated.

Whereas a single set of landmarks was used in the Main Analysis, simulated voyages in this case study used either natural prominences or archaeological sites as landmarks. Given that these landmark sets differ in their location and density throughout the study area, it was expected that their effect on the results of Case Study 1 would be

[58] In the sense that no explicit relationship between, say, 'maximum ship speed' and 'ability to recognise conditions at sea' is suggested.

more pronounced. It is possible that the effect of landmark sets on success rates was depressed by the location of sailed routes. Three out of eight routes were set in the Gulf of St. Malo, where vessels along these routes would have been able to maintain sight of land. Of the remaining five, two routes (Christchurch to St. Peter Port and Christchurch to Nacqueville) are shorter than the others due to the northerly location of the latter two nodes. It is possible that navigation was less important to the success of simulations in Case Study 1 because voyages were shorter and therefore less likely to go off-track. The difference between average speeds achieved by simulated vessels navigating by both sites and natural prominences supports this interpretation. Navigation by coastal site actually resulted in faster travel times (by a slim 0.16 knots), suggesting that although navigation by landmarks was more likely to result in success, both navigation strategies were equally efficient. The fact that navigation by natural prominences resulted in more successful voyages but no advantage in efficiency suggests that tracks followed by successful voyages using both types of landmark were similar.

Finally, the effect of reckoning environmental conditions on the outcomes of simulations in Case Study 1 resembled the effects of landmark sets, in that less misestimation resulted in more successful voyages but not in accordingly faster speeds. Although the misestimation ranges are not equally sized the relationship between misestimation and success rate is linear in the results of this case study, with each percentage point of possible misestimation corresponding with a drop in the average success rate of 0.34 %. The fact that this relationship is linear, let alone the shallow slope of the line, is surprising. Again, this may result from most simulations being able to sight landmarks along their entire route, and therefore not relying on 'reckoned' values at all.

The observation that the ability to read conditions at sea does not have a strong influence on the outcome of voyages is also taken up in Case Study 2 (see Section 7.3.1).

6.3.2: Routes and Trading Links along the Hengistbury-St. Malo Axis

The results of this analysis appear to confirm Cunliffe and de Jersey's hypothesis in general – that Guernsey could have served as a useful departure point for voyages across the Channel. Success rates for simulations between Christchurch and St. Peter Port are high for southbound voyages and compare very favourably with northbound success rates for the three nodes at the base of the Gulf of St. Malo. The track-density around Guernsey, Herm, and Sark is high even when tracks passing through St. Peter Port are eliminated, and the results of simulations suggests that voyages from Le Trieux and Le Légnét pass along Guernsey's western coasts. With regards to the node at Nacqueville, which was proposed as a possible departure point for Hengistbury Head, simulations from this node performed well, although they were hampered somewhat by a lack of landmarks near the node itself. The main advantage associated with the Nacqueville node is its high northbound success rate (79.5 %), which was the best out of all routes tested in the case study. This suggests that Nacqueville may have been a good place to launch from in order to get to Hengistbury Head, but perhaps not an easy port to return to.

The results of this case study do not strongly support the Bay of St. Brieuc as an obvious alternative to St. Malo. Although northbound success rates were slightly better for the Le Légnét node, at 27.7 % this rate was only 5.5 % better than that of St. Malo (33.2 %). Average speeds associated with this node were also high, particularly northbound speed. Like Nacqueville and St. Peter Port, Le Légnét has lower success rates than St. Malo while being better situated as a point of departure. Le Trieux, at the western

end of the Gulf of St. Malo, has more balanced success rates, and reasonable average speeds.

The higher southbound speeds and success rates observed in nearly all simulated routes also underline the importance of Nacqueville and St. Peter Port to navigators crossing the Channel under these conditions. However the fact that southbound voyages were generally quick and successful suggests that the links between coastal nodes need not have been bidirectional. Although a vessel in this study sailing from St. Malo to Christchurch would have dramatically increased its odds of completing its journey by first sailing to St. Peter Port rather than sailing directly (50.9 % success rate vs. 23.2 %), they would have found the odds of success for a direct passage back to St. Malo (90.2 %) roughly equal to the odds of a passage from St. Peter Port to St. Malo (92.0 %). The main advantage of breaking a southbound passage in the Channel Islands in this case study is the extremely high 8.46-knot average speed achieved by voyages bound from St. Peter Port to St. Malo; however average speeds from Christchurch to St. Peter Port (5.07 knots) is less than the average speed of a direct passage (5.26 knots). Given that track-density plots indicate a well-travelled route from St. Malo along the east coast of Jersey, this may well indicate a return route from Hengistbury Head. If this is the case then trade in the Gulf of St. Malo may have tended in a clockwise direction, since the chances of success increase from St. Malo to Le Légnét, and from Le Légnét to Le Trieux. This possibility in turn marks sites along these routes, in particular Jerbourg, Le Catel de Rozel, and Vaux du Catel, as potential landmarks or stopping places.

Chapter 7 : Case Study 2 (Lannion – Plymouth)

7.1: Introduction

Case Study 2 focussed on a single pair of routes between the nodes at Plymouth and Lannion. This route is suggested by Cunliffe & de Jersey (1997) as a possible crossing point, based on material evidence from the site at Le Yaudet. The main purpose of this case study, however is to investigate relationships between 'reckoning' ranges, vessel parameters, and leaving times. 'Reckoning' ranges were varied in Case Study 1, but because other parameters were not as widely varied few comparisons could be made. Only two vessel parameterisations were tested in Case Study 1, which provided useful context for interpreting those simulations but made evaluating the parameters themselves difficult. Furthermore, leaving times were not varied in either Case Study 1 nor in the Main Analysis – in both those cases leaving times were based on the time of the first flow tide after sunrise. Case Study 2 was designed to investigate these parameters in more detail by varying all three widely for simulations using a single pair of routes – northbound and southbound from both Plymouth and Lannion – on a single date in the study period using a single set of landmarks combining natural prominences with archaeological sites. The date selected for simulations (May 20, 2018; Day 80) was chosen based on the results of the main analysis, where voyages on this date perform especially well.

7.1.1: Archaeological Context

The potential for a set of routes connecting northern Brittany with Devon and Cornwall is suggested most strongly by excavations at Le Yaudet, in western Côtes-

d'Armor. Le Yaudet occupies a peninsula at the outflow of the river Léguer into the Baie de la Vierge, a small stretch of water enclosed by peninsulas that empties into Lannion Bay. The origins of the site at Le Yaudet are likely Bronze Age, and the earthworks that separate the peninsula from the mainland have been attributed to the Late Iron Age (Cunliffe & Galliou 2000, Cunliffe 2004, Guigon 2007). Excavations at the site from 1991-2002 recovered ceramic evidence for maritime trade, in particular sherds from Dressel I amphorae as well as small amounts of ceramic manufactured in Britain (Cunliffe et al. 2004-2007, 371). In particular, Cunliffe identifies the clay from which British imports to Le Yaudet were made as originating in Devon (Cunliffe & de Jersey 1997, 52). Based on the provenance of imports to Le Yaudet, Cunliffe and de Jersey suggest Mount Batten, in Plymouth Sound, as a possible departure point for southbound voyages across the Channel. They note that Plymouth Sound provides good anchorage and access to inland waterways. It is also located roughly due north from Le Yaudet (Cunliffe & de Jersey 1997, 52). If Mount Batten was not itself the launching place for ships bound for Le Yaudet, then Cunliffe et al. suggest that Plymouth Sound was the most western potential port, with Hengistbury Head marking the eastern limit of this area (2004-2007, 371).

The immediate vicinities of the Lannion and Plymouth nodes contain several sites identified as potential landmarks. Besides Le Yaudet, the Lannion node sits opposite the promontory forts at Pointe de Primel and Île Callot, approximately 25 kilometres to the west. These sites are located to either side of the Morlaix node, which is associated with an estuary that contains three other Iron Age enclosures and potential landmarks (Le Voallas, Lavallot, and Belair). The stretch of coastline between the Lannion and Anse de Kernic nodes has no natural prominences identified by LRM analysis, and so all potential

landmarks in the area are archaeological sites. Meanwhile, the immediate vicinity of the Plymouth node is dominated by Rame Head, which sits at the entrance to Plymouth Sound.[59] Rame Head is a distinctive promontory, and was the most-sighted landmark associated with archaeological remains in the Main Analysis. The nearest coastal sites to Rame Head are Bolt Tail Camp and Bantham Camp to the southeast, and Dodman Castle approximately 45 kilometres due east. The vicinity of Plymouth Sound contains many natural prominences, particularly along the stretch of coast between Looe and St. Austell, and along the western side of Start Point.

7.2: Results

Case Study 2 involved 2,420 simulations in total. None of these simulations encountered unexpected errors, so all 2,420 were included in the datasets presented in the following sections. The following sections describe the results of these simulations as they relate to parameters varied in the case study; the form of these parameter sets and the results are presented in each section.

7.2.1: Overall Average Speed / Success

The overall speed for simulated voyages in Case Study 2 was 4.5 knots; average speeds for northbound and southbound voyages were both close to the general average at 4.8 and 4.1 knots, respectively. The overall success rate in Case Study 2 was 62.2 %, a

[59] Mount Batten itself could have served as a landmark, although its status as a promontory fort is questionable. It is not included in the Hillforts Atlas (Lock & Ralston 2017), and historic development of the peninsula has likely erased any earthworks that may have been there (see Cunliffe 1988).

low value but not unexpected given the wide variation of other parameters in the case study. Since only two nodes and one date were used in Case Study 2, comparison between the two should not be used to evaluate the viability of the route; however such a comparison is useful for evaluating the results of this case study. On average, voyages from Plymouth to Lannion were about half as successful as voyages in the opposite direction (42 % vs. 82 %), but were on 0.18 knots faster (4.48 knots vs. 4.30 knots). The high number of northbound voyages in Case Study 2 contrasts with the results of Case Study 1 (where most successful voyages were southbound), and with general averages reported in the Main Analysis, where southbound voyages along Plymouth-Lannion routes were 1 % more successful in directional averages. General averages are shown in Table 7.1. The average voyage duration for successful simulations was 24 hours and 24 minutes – much lower than the 32 hours suggested by Cunliffe & de Jersey (1997, 371). The use of very optimistic vessel parameters (see Sections 5.2.3 & 7.2.4) in addition to Cunliffe & de Jersey's conservative assumed average speed of 2.5 knots likely accounts for this difference. For northbound voyages the average travel time was 23:39, and for southbound voyages the average time was 26:09.

7.2.2: Track Density Analysis

Figure 7.1 and Figure 7.2 show ship tracks for all simulations in Case Study 1 and for successful simulations, respectively. In general, simulated voyages were either direct or else were carried to the west before sighting land and completing the passage by navigating along the coast. No simulated voyages strayed beyond Start Point or the headland north of the Lannion node in the east, and only a few passed Land's End or the Chenal du Four in the west. Simulated voyages that made landfall west of Lizard Head

(in the north) and the Anse de Kernic node (in the south) were all unsuccessful. Density plots for northbound and southbound voyages (Figure 7.3 and Figure 7.4) show that Channel crossings fell into two categories: direct passages taking a direct route from one node to the other, and crossings that made landfall to the west of their destination node and were able to travel along the coast until the destination was reached. Southbound voyages were almost all direct – an expected result given that northbound voyages from the Lannion node in the Main Analysis were very tightly clustered (Section 7.2.2). Although a few made landfall further along the coast, most that failed to arrive directly at the Lannion node made landfall at the western edge of the Bay of Lannion. By contrast, successful northbound voyages were more likely to be carried west over the course of the crossing. Some simulations were carried slightly to the west, re-joining the main 'stream' shortly before arriving at the Plymouth nodes. Other voyages were carried further west, making landfall within Mounts Bay and sailing up the coast to arrive at the Plymouth node.

When comparing track densities from successful and failed simulations it is important to remember that 'success' as discussed in these analyses is defined narrowly as 'reaching a pre-set destination point'. However, other criteria for 'success' are possible, and it is possible that under some conditions Iron Age mariners would have thought their voyage 'successful' even if they did not reach their intended destination (see Sections 5.6.2 & 7.3.2). With this in mind, concentrations of ship tracks around Lizard Head, Dodmun Point, and Fowey are interesting given the close proximity of coastal nodes and promontory forts to these concentrations of routes. In the particular case of Lizard Head, three coastal promontory forts are located on the south-eastern corner of the headland and one is located in the northeast near the Helford node. These three smaller sites face an

area of high ship track density in Figure 7.4, created by vessels attempting to make Plymouth after having made landfall. On the southern coast of the Channel, most unsuccessful voyage tracks stick close to the shoreline, and the areas with the most track density along the shore correspond to the Anse de Kernic and Kerivoas nodes.[60]

7.2.3: Landmark Visibility Analysis

Rather than test cultural and natural landmarks independently, a single set containing both types of landmarks was used in this case study. This was done in order to limit the number of simulations and to take into account the general lack of natural prominences identified in the Breton coast in the between the Lannion and Anse de Kernic nodes. Table 7.2 lists the number of sightings per landmark used in Case Study 2, and Figure 7.5 shows the results of a density analysis for sighting locations. The most frequently-sighted landmarks in the case study were Pointe de Primel and Rame Head – which are located directly opposite and at the entrance to their respective coastal nodes. Sightings on the northern shore of the Channel were concentrated on the coast between the Lizard and Start Point. Within this area, the stretch of coast from Dodman Castle to Bolt Head contained landmarks with the most sightings. The site at Dodman Castle was sighted particularly frequently, as were the coastal sites at Black Head and Bolt Tail Camp. There were fewer sightings on the southern shore of the Channel in this case study, due in part to the aforementioned lack of natural prominences near the Lannion node. As such, the most frequently-sighted landmarks were the coastal promontory forts at Pointe de Primel and Île Callot, and the natural prominences at Île-Grande and Île-Renote. Le

[60] The Morlaix node is close enough to the Lannion node that most successful voyages also pass nearby.

Yaudet was not well-sighted, despite being situated at the entrance to the river for which the Lannion node is named; as a point of comparison, it was sighted slightly less frequently than the small promontory fort of Little Dennis on the eastern side of Lizard Head.

The distribution of sightings amongst these landmarks fits well with track-density results for Case Study 2. Nearly all successful northbound simulations were confined to the stretch of Channel between the Lizard and Start Point, and southbound voyages from Plymouth tended to proceed south-southwest for 20-30 kilometres before turning south towards the opposite coast. The number of sightings most likely reflects a combination of these two factors. In the south, coastal sites with the most sightings fall along the route that most simulated vessels took into the Lannion node.

7.2.4: Estimation Results

Eleven estimation ranges were used in Case Study 2 in order to 'reckon' locations when out of sight of land. These ranges were set at intervals of five percent between zero percent (no under- or over-estimation) and fifty percent (values were allowed to be over- or underestimated by a factor of up to 1.5). Table 7.1 shows average speeds and success rates per estimation range. The effects of estimation ranges on voyage speed and success were largely as expected: success rates and average speeds decreased with higher estimation ranges. Allowing 50 % misestimation decreased the average speed of all successful voyages by 1.17 knots, with less than 0.25 knots of difference between the amount of speed lost on southbound and northbound voyages. The effects of poor reckoning were more pronounced on success rates in the case study – misestimation ranges of 50 % decreased the percentage of successfully completed voyage by 25.91 %.

As with average speeds, the difference between success rates for ‘best’ and ‘worst’ reckoning for southbound and northbound voyages were small (25.45 % vs. 26.36 %, respectively).

Southbound speeds and success rates were much lower than the same measures for northbound voyages for all estimation ranges tested. Given that speeds and success rates decreased for both groups of voyages at similar rates, it is unlikely that this difference is caused by estimation parameters.

7.2.5: Leaving Time Results

Several points should be made with regard to the interpretation of the effects of leaving times on simulations in Case Study 2. First of all, high tide at Plymouth on the simulation date was at 04:24 at Plymouth and at 04:30 at the Lannion node. Secondly, the time of nautical twilight (counted as sunrise by the script) was 03:46 for both nodes on the date for which simulations were run. The navigation model rounds sunrise times to the nearest hourly timestep, therefore the ‘first high tide after dawn’ time that would have been selected in the Main Analysis and Case Study 1 was 04:00. Simulated voyages starting before 04:00 would have not been allowed to sight landmarks until twilight. Given these points, one would predict that voyages before dawn would be generally unsuccessful, and that successful voyages would follow the ebbing tide. These results are borne out by overall averages for different sailing times, but northbound and southbound averages complicate this interpretation. Northbound voyages launched before 06:00 were overwhelmingly successful – more than 98 % of voyages during this period completed successfully – but that percentage fell swiftly to 20.9 % over the next four hours. By contrast, southbound averages rose fairly steadily from a low of 1.8 % successful sailings

for ships departing at 23:00 the previous day, to a high of 77.3 % successful sailings for vessels departing at 07:00, falling back down to 61.8 % success rates for 09:00 departures. Although average speeds for northbound and southbound voyages appeared to follow the same trend, differences between the two were comparatively minute. For example, the difference between average speeds for northbound and southbound ships leaving at 23:00 was 1.9 knots, which pales in comparison to the 97.3 % difference in success rates for the same start time. The greatest difference between northbound and southbound speeds was 2.5 knots, which was observed in ships departing at 02:00.

The magnitude of the difference between northbound and southbound success rates is surprising. Conditions specific to the day used in the simulation may be responsible, although this is unlikely given that it identified as a successful day in the Main Analysis. Given that high tide was predicted for similar times at both nodes on this day, differences in launching time between the two nodes also seems unlikely as an explanation for the difference – although it is likely the cause of the decline in success rates for northbound voyages. The timing of daylight can also be eliminated as a possible cause, since northbound and southbound success rates begin to decline / increase at the same leaving times, and the difference in average travel times is only 1 hour and 30 minutes. A northbound departure at 23:00 and a southbound departure at the same hour would both arrive at night. After eliminating these factors, the most likely explanation is that conditions on the northern coast of Brittany were not favourable for the day simulated. If we expand our definition of ‘successful voyages’ to include journeys that reach the opposite shore, then the overall percentage of successful southbound voyages rises from 43 % to 83 %. Therefore the effect of starting time on the results of this case

study should be interpreted as the chances of simulated vessels arriving directly at their destinations, rather than their chances of making the crossing.

7.2.6: Vessel Parameterisation Results

Ten vessel parameterisations were used in Case Study 2, and results of analyses using these speed diagrams can be seen in Table 7.1. These parameterisations were created by adjusting the speed curve for the '5-metre average' parameterisation designed for the Main Analysis (see Section 5.2.3) by a set of equal intervals, so that the average predicted speed for each parameterisation differed from its neighbour by 0.2 knots. Unfortunately, the same conversion error that overestimated average speeds in the Main Analysis and Case Study 1 resulted in vessel parameterisations having upper speeds greater than McGrail's predicted range for Iron Age ships (7-9 knots; see again Section 5.2.3). Maximum speeds for the vessel parameterisations used by simulations in this case study varied from 10.6 to 14 knots. As such, the results from the most conservative parameterisation are the most directly comparable with the types of vessels that McGrail suggests would have been used to cross the Channel. As in the Main Analysis, however, the high maximum speeds in vessel parameterisations do not appear to have resulted in ridiculously high average speeds (i.e. > 7 knots). Differences between the overly optimistic parameterisations used here and parameterisations more in line with McGrail's predictions are investigated in Case Study 3 Section (Chapter 8).

Vessel parameterisation had the greatest effect on voyage length – as expected – with simulated ships using the 'best' parameterisation achieving average speeds 1.68 knots faster than simulated vessels referencing the 'worst' speed curve. The speed gain achieved for northbound voyages (2.08 knots) was more than double the same measure

for southbound voyages (0.82 knots). Since speed averages were calculated using records for successful runs only, this finding lends weight to the conclusion that conditions at sea on the day used in the simulation favoured northbound voyages. The effect of vessel parameterisation on success rates is less straightforward. Average success rates under parameterisations with higher maximum speeds do not trend upward, as expected, but rather increase and decrease within a 57 %-67 % range. Success rates for northbound voyages follow a similar pattern, whereas success rates for southbound ships actually decrease as the expected average speed of vessel parameterisation is increased. The most likely reason for this decrease is the difficult approach to the Lannion node. The navigation model always selects the heading that it 'believes' will move the simulated vessel closest to the destination point. In other words the navigation model will always follow a tack for at least one timestep before changing tack, and will never short-tack (perform many tacks in quick succession) unless forced to by obstruction. Short-tacking can be an effective way to make progress in enclosed spaces such as Lannion Bay, while taking more time between tacks increases the risk of going aground.

7.3: Discussion

This section discusses the results of this case study in light of its two main aims: to perform a wide sweep of model parameters in order to evaluate which have the greatest effect on the success of Channel Crossings, and to evaluate the potential connection between the Lannion and Plymouth nodes. These objectives are addressed in the following sections.

7.3.1: Parameter Comparisons

Figure 7.6, Figure 7.7, and Figure 7.8 show speeds and success rates under different combinations of the three parameter sets discussed in the preceding sections: estimation, leaving time, and predicted average speed. These charts are colour-coded by value, so that the interaction between parameter combinations can be more easily seen. Comparing how these parameters affect one another helps understand how they affect outcomes in the model.

The chart comparing average speeds for combinations of estimation ranges and leaving times (Figure 7.6) has the highest values in the lower left corner, corresponding with little-to-no under- or overestimation and the earliest leaving times. There is a clear gradient in this plot, with earlier leaving times compensating for higher levels of misestimation and vice versa. The comparison of success rates along the same lines in Figure 7.6 does not follow this pattern: the best success rates correspond to later leaving times combined with less misestimation. There is no clear gradient in this success rate plot, with the worst chances of success occurring with combinations of high misestimation and later sailing times, and earlier sailing times and less misestimation. Curiously, voyages were more successful at earlier sailing times when more misestimation was allowed. This may result from the time of arrival being more important than the time of departure in the success of a simulated voyage.

The speed comparison charts in Figure 7.7 for estimation ranges and vessel parameterisation show a gradient weighted towards vessel parameterisation. Speeds are highest for combinations of low misestimation and high average speed, however vessel parameterisations that allowed for higher speeds were able to achieve good speeds when

allowing for more misestimation. Since ‘speed’ in the context of this case study is a measure of route distance (rather than travelled distance) in comparison to travel time (see Section 5.6.2), the observation that ships with higher maximum speeds were able to complete voyages faster despite using poor estimation is interesting. Simulated ships that stray off course spend more time at sea and therefore decrease their speed relative to the fixed path-distance between nodes. The fact that the effect of vessel parameterisation compares favourably to that of reckoning suggests that simulated ships capable of faster average speeds were able to make up for the time that they may have spent deviating from the most efficient path. The corresponding comparison chart for success rates is again more difficult to interpret than its counterpart. In this case the best success rates are more strongly identified with better reckoning, although the best success rates are actually associated with good reckoning and slower predicted average speeds. This may be a result of the navigation model facing difficulties in modelling inshore sailing, as has been mentioned. Although the gradient in this chart is less clear, it would appear that estimation ranges had a greater effect on success rates in this case study than did vessel parameterisation.

Finally, Figure 7.8 compares start times and vessel parameterisations in terms of average speeds and success rates. The comparison chart for average speeds shows that earlier leaving times are associated with faster average speeds. As in Figure 7.7, the best speeds are associated with leaving times before high tide. The three best vessel parameterisations were able to achieve respectable average speeds of 4.32-5.21 knots at the later leaving times, while the most conservative parameterisation was not associated with high speeds at any of the simulated leaving times. In the corresponding comparison chart for success rates, leaving time clearly has the greatest influence on success rates.

The highest success rates are associated with departures at and just after high tide, whereas leaving times at either end of the range have low success rates. Combinations with success rates of over 80 % are split evenly between the four 'best' parameterisations and the three 'worst'.

Figure 7.9 summarises the comparisons that have been made in the preceding paragraphs of this section. In terms of vessel speed, ship parameterisation proved to be the most effective parameter. Simulated vessels that were able to achieve higher speeds were able to maintain those speeds despite starting at inopportune times and being more liable to spend time at sea recovering from coming off-course. Regarding success rates, however, vessel parameterisation was less effective than the time of departure – and the relative effectiveness of reckoning vs. vessel parameterisation and reckoning vs. departure time were difficult to characterise. However, estimation ranges were slightly more effective than vessel parameterisations, in that simulations allowing for small amounts of misestimation were generally successful in combination with all vessel parameterisations, while the opposite was not true. Likewise leaving times appear to be more effective than vessel parameterisation in determining success in simulations, as the highest success rates are associated with a few specific leaving times. This suggests that leaving time, rather than reckoning, was the parameter that most influenced the success of simulations in this case study.

7.3.2: Routes and Trading Links along the Plymouth-Lannion Axis

The results of this case study support the claim that the route between Mount Batten and Le Yaudet is tenable, and suggest that this connection may have been even stronger than suggested by Cunliffe and de Jersey. Although southbound success rates

were poor overall, nearly all southbound failures reached the opposite shore of the Channel and could have conceivably landed at Morlaix or another nearby node. If we consider a 'sea route' as a link between two stretches of coastline rather than between two coastal nodes, then the link between the Lannion area and the Plymouth area was very strong for the simulated voyages in this case study. The best evidence supporting this link are the concentration of ship tracks, especially for southbound voyages. The fact that relatively few simulated ships strayed far from these tracks is impressive, especially considering that some of these simulations had misestimation ranges of up to 50 %. Northbound voyages were less concentrated, but voyages that became off-course were mostly able to recover before passing Lizard Head. Moreover, comparison between vessel parameterisation and estimation ranges suggests that these detours did not overly affect the speed of passage.

Although Cunliffe identifies Mount Batten as the westernmost possible port from which ships bound for Le Yaudet may have embarked, the results of this study suggest that voyages connecting the Plymouth and Lannion nodes would have spent most if not all of their time in waters west of these two nodes. Although voyages were only simulated for one route, none of the tracks for these voyages passed east of Start Point. Instead, voyages that did not follow a direct route were contained within the waters between Lizard Head and Plymouth in the north, and between the nodes at Anse de Kernic and Lannion in the south. These results suggest a reconsideration of the links that Mount Batten and Le Yaudet may have had with the wider Channel. Rather than thinking of Mounts Bay as the western extent of a zone of contact that ends at Hengistbury, perhaps we should consider it to be located near the eastern extent of a zone that extends to Lizard Head. Rather than think of Le Yaudet as a port that may have relied on Guernsey to handle

its cross-Channel trade, we should think of it as part of a collection of ports in north-central Brittany in contact with the proposed Mount Batten-Lizard Head 'zone'.[61] While we should not lose sight of the results of the Main Analysis (where voyages from Lannion to ports east of Start Point were very successful), the results of this analysis at least suggest that direct contact between these nodes is plausible.

The inverse relationship between average success rates and speeds in the comparison between vessel parameterisation and leaving times (Section 7.3.1) is of particular interest in this study. As with the main analysis, where certain routes were faster but less likely to succeed, the results of this case study hint at the decisions that Iron Age sailors would have made when deciding when to launch. In this case, the launch time that best balances risk and reward is within an hour of the first high tide after dawn. This result is encouraging, as it suggests that leaving times in the Main Analysis and the other case studies are reasonable. The results of this case study also reinforce the Main Analysis' conclusion that the timing of voyages is crucial to their success. Measured by average speeds and success rates, the vessel parameterisation and leaving time parameters proved to be the most effective predictors of high performance in this case study. Although the day for which simulations were run in this analysis had generally good conditions, differences in success rates and speeds for different leaving times were dramatic. Additionally, in 'better' formulations of vessel parameterisation / leaving time were able compensate for the effects of poor reckoning. Although some of the reason for this may

[61] This hypothesis is provisionally supported by the results of Case Study 1, where the chances of completing voyages successfully increased for nodes located further west along the Gulf of St. Malo (see Section 6.2.2).

be geographic (Lizard Head, for example, seemed to play a large role in redirecting wayward simulations), the results here suggest that Channel crossings along this route were relatively easy to accomplish, but difficult to time correctly.

Chapter 8 : Case Study 3 (Brest – Penzance)

8.1: Introduction

Case Study 3 was planned as an investigation of the western margin of the Channel, and was to consist of c. 2,000 simulations testing a single route between Brest and Mounts Bay. Unfortunately these simulations were scheduled for the spring of 2020, and were curtailed substantially by the COVID-19 pandemic. In response to this crisis the number of simulations in Case Study 3 was revised down to 180, of which 38 were completed in time to be included in this thesis. Rather than abandon this case study entirely, a different approach was developed in order to interrogate these partial results. Instead of looking at simulations in aggregate, as has been done in the previous case studies, this section presents the results of each simulation individually, and draws preliminary conclusions by detailed analysis of the courses taken and landmarks spotted. The use of 3D visibility analysis (see Section 4.3.3) in this case study aids in this approach, as it allows sites to be compared with one another both in terms of the number of sightings made over the course of the simulation, and in terms of the 'apparent size' of the fort (see Section 4.3.3).

The results of Case Study 3 suggest that conditions in the western Channel are challenging enough that ship design and skill at estimating conditions at sea were particularly important. These results are especially important considering that this case study used ship parameterisations that follow McGrail's estimates for an Iron Age boat – whereas the Main Analysis and Case Studies 1 and 2 used parameterisations with unrealistically high maximum speeds (see Section 5.2.3). Voyages that were easily completed using faster parameterisations in the Main Analysis (see Section 5.6) struggled

to approach their intended destination using slower parameterisations in this study. This raises the possibility that the larger, sturdier ships of the Late Iron Age (see 2.2.5) could have been capable of traversing the mouth of the Channel while other, slower ships could not.

8.1.1: Archaeological Context

The western approaches to the Channel encompass the waters between the southwest coast of Cornwall and the northwest coast of Brittany. The Channel is at its widest between Land's End and Finistère, at approximately 185 kilometres. Both of these peninsulas afford access to waters beyond the Channel – voyagers from the northern coast of Cornwall can reach south Wales and the Irish Sea, while the southern coast of Brittany provides access to the Bay of Biscay and the Gironde estuary. Groups of islands lie off the western coasts of Brittany and Cornwall; both groups of islands afford protection to mariners attempting to cross the headland, while also creating channels of fast-moving water that are difficult to navigate (see United Kingdom Hydrographic Office 2005). The Île d'Oessant is the largest island off the west coast of Brittany, and there are several islands between the Île d'Oessant and the mainland. The Isles of Scilly are located west-southwest of Land's End, Cornwall, and consist of an archipelago of small islands. Both regions are assumed to have been involved in wider prehistoric trade and exchange; coastal voyages from Brittany south to the mouth of the Gironde are assumed by McGrail (1983) and Cunliffe (2001), and Cornwall has long been considered a possible departure point for Wales, Ireland, and other coastal areas along the Irish Sea (see Bowen 1972, 1977; Cunliffe 2001).

As mentioned in Section 1.3.3, classical authors were particularly interested in the western Channel as the source of metals, particularly tin. Strabo reports that the 4th century explorer Pytheas identified the 'Osismii' as a people inhabiting a "promontory that projects quite far out into the ocean" (Strabo *Geography* 4.4.1); the names 'Osismii' and 'Ouexisame' have been identified with the Île d'Oessant (also known as 'Ushant' (Cunliffe 2001, 304)). Descriptions of the tin trade survive in the works of Pliny (*Natural History* 4.30) and Diodorus Siculus (*Library of History* 5.22). Pliny mentions that the "island called Mictis is within six days' sail of Britannia, in which tin is found; and that the Britons sail over to it in boats of osier, covered with sewed hides". Diodorus Siculus goes into more detail, suggesting that:

> The inhabitants of Britain who dwell about the promontory known as Belerion are especially hospitable to strangers and have adopted a civilized manner of life because of their intercourse with merchants of other peoples. ... they work the tin into pieces the size of knuckle-bones and convey it to an island which lies off Britain and is called Ictis; for at the time of ebb-tide the space between this island and the mainland becomes dry and they can take the tin in large quantities over to the island on their wagons. ... On the island of Ictis the merchants purchase the tin of the natives and carry it from there across the Strait to Galatia or Gaul... (*Library of History* 5.22)

Debate as to the possible location of Mictis/Ictis has been ongoing since the 19th century (see: Hawkes 1984; Cunliffe 1983). The promontory of Belerion is generally associated with Cornwall, and Ictis with St. Michael's Mount – a tidal island near the head of Mounts Bay. Other candidates include the Isle of Wight (based on the possibility that Pliny confused the names 'Mictis' and 'Vectis'), and the promontory at Mount Batten (see Section 7.1), Cunliffe 1983). Finally, it should be noted that the Veneti, whose description in Caesar's *The Gallic Wars* is used as circumstantial evidence for the construction of

plank-built ships in the Late Iron Age (3.13), are understood to have been the southern neighbours of the 'Osismii' of Finistère.

If these historic sources are credible, then voyages between the two shores would have presumably been common enough to encourage trade and 'hospitality' between the inhabitants on either side.[62] If these accounts are discounted, there still remains some evidence for cross-Channel trade. A tin ingot recovered from a shipwreck in Bigbury Bay (Devon) thought to be of prehistoric date appears to fit Diodorus Siculus' description of tin 'knuckle-bones' (Cunliffe 2001, 305). Herring (2001) suggests that prehistoric ceramics unearthed at St. Michael's Mount are 'not entirely local' and may be evidence for long-distance trade. Gary Robinson's study of prehistoric landscapes in the Scillies identifies both natural granite tors as well as passage graves and standing stones as navigational aids used by historic and modern navigators in the Isles of Scilly, and suggests that "the consistent placement of standing stones in relation to the sea and their visibility from the sea suggests that one of the functions of these monuments was to locate and orientate people on the sea" (2007, 127). Robinson also notes that these standing stones are sited on the eastern side of the archipelago (ibid.).[63] These strands of evidence suggest that a route across the mouth of the Channel may have existed, although the documentary sources are by far the strongest evidence.

[62] There is sufficient reason to doubt these commentators who (with the exception of Caesar) drew on the works of others writing centuries before when constructing their accounts (Henderson 2007, 9).

[63] Although this is not necessarily evidence for voyages arriving from Brittany – landmarks could also be set up to guide arrivals from Cornwall.

McGrail (1988) and Davis (1997) are divided as to whether Iron Age mariners would have been capable of crossing the mouth of the Channel. Davis has argued that it "would have been prohibitive to all but the most daring" on account of the high risk of sailing at night and the long time spent out of sight of land (1997, 133). McGrail's 1983 paper is more optimistic, and suggests two routes across the Channel entrance: from the Île d'Oessant to Mounts Bay, and from the Île d'Oessant to Plymouth Sound. For the former, McGrail estimates a crossing of 38 hours at an average speed of 2.5 knots, and a crossing of 19 hours at an average speed of 5 knots (1983 , 330). Considering the results of this case study (see Section 8.2.5), it is worth mentioning that McGrail also predicts a displacement of 6-17 nautical miles to the northeast for ships bound from the Île d'Oessant to Mounts Bay. The estimates that McGrail makes can serve as a baseline for interpreting the results of this case study, as the ship parameterisation here follows the estimates in his 1983 paper.

8.2: Results

The simulations presented in this case study represent a partial sweep of the following parameters: leaving time, landmark type, ship parameterisation, and estimation range. Because only 38 simulations were completed out of a planned 180, some parameter options are not represented in these simulations. Table 8.1 shows the number of simulations for each parameter combination out of the total. However, because parameter files for all simulations were generated in a separate Python script with a set of nested code loops, the simulations presented here represent a limited sweep for the first parameter to be iterated. The hierarchy of parameter loops in the parameter file assembly script is:

- Route
- Date
- Estimation Range
- Ship Parameterisation
- Landmark Type
- Leaving Time

Simulations 1-30 here represent a full sweep for the combination of the Brest-Penzance route and the ‘no misestimation’ parameter, while simulations 30-38 represent the beginning of the sweep for the Brest-Penzance route with an ‘up to 50 % over- and underestimation’ parameter. Three ship parameterisations were used in this case study, representing ships with top speeds of 5, 7, and 9 knots using the same speed curves used in other simulations. Two sets of landmarks were used in analyses, one representing cultural landmarks and the other natural prominences. Leaving times were set at one and two hour increments before and after the ‘first tide’ sailing time used in the Main Analysis, for a total of five hourly leaving times.

All simulations took place on the same day: June 8, or Day 98 in the Main Analysis (see Section 5.6.2). This date was selected on the grounds that it had the highest average success rate for both northbound and southbound voyages along the Brest-Penzance route in that analysis. All simulations in Case Study 3 also used the 3D visibility analysis technique (see Section 4.3.3). For each sighting the ‘apparent size’ of the landmark in square degrees was recorded in the simulation’s visibility log. Simulations tracks and sightings for each simulated route are shown in Appendix III. The complete set of simulated tracks is shown in Figure 8.1. Table 8.2 shows the total number of sightings and the average apparent size for landmarks.

8.2.1: Success Rates

No simulations performed in this case study successfully reached the Penzance node in the 48 hours allowed by the navigation simulation (although several made landfall on the opposite coast – see below). There were two main causes for failure. In the first case, some simulated ships encountered difficulties passing through the strait between the Île d'Oessant and mainland Brittany (or else opting to keep west of the Île d'Oessant entirely), reducing the amount of time available for the crossing. In the second case, ships that made the crossing often became 'stuck' in the waters between Land's End and the Isles of Scilly, and were unable to effectively tack against the wind in order to enter Mounts Bay. Only two simulations failed from being 'driven ashore', and these failures occurred shortly after leaving the Brest node.

Since the sample size in this analysis was small enough to permit close inspection of each simulation, a simple set of criteria was developed to compare these simulations relative to one another. Simulations that reached the coast of mainland Cornwall were counted as 'successful' runs, although they did not reach Penzance. Simulations that spent more than four hours tacking in the waters between Land's End and the Isles of Scilly were labelled as 'qualified successes', since they could have abandoned their goal of Penzance and presumably put ashore in the Isles of Scilly. Vessels that managed to sight the British coast but did not reach those coastal waters were designated 'potential successes', as they could have potentially reached Penzance (or in the Isles of Scilly) with a few more hours' run time. Simulated sips that failed to sight landmarks on the opposite side of the Channel were counted as 'failed' runs. Using these criteria only 3 simulations were successful, a further 14 were qualified successes, 10 were potential successes, and 11 were failures.

With such a small sample size, limited significance can be attached to correspondence between parameter combinations and the success of simulations. That being said, vessel parameterisations and misestimation ranges had the greatest effects on outcomes in this case study. First, simulations using the '5 knot maximum speed' parameterisation were unsuccessful – none of these were successes or qualified successes, and all failed runs used this parameterisation – while the '9 knot maximum' ship parameterisation performed slightly better than the '7 knot maximum' parameterisation. This is partly due to the 48-hour limit mentioned in the previous section (8.2.1), which prevented slower ships from completing journeys. Secondly, all of the simulations that allowed for up to 50 % misestimation were failures. Only 8 runs using this estimation range were completed, however, and caution should be exercised in drawing any inferences from these failures.

8.2.2: Vessel Speed

As no vessels successfully reached the Penzance node, it was not possible to calculate ship speed as in other analyses. Consequently a stretch of sea between Land's End and the Scillies was defined (see Figure 8.1), and the path distance from Brest to the centre of this area was calculated for the purposes of comparing simulations.[64] For simulations that were designated 'successes' or 'qualified successes', the time of completion was set at the point where the simulated vessel first entered this area. As such,

[64] More specifically: an axis was defined between the promontory forts at Maen Castle and Shipman Head was drawn in ArcGIS, the midpoint of that line was used to measure the path-distance to the Brest node, and a 10-kilometre buffer was generated in order to define this 'destination zone'.

the speeds for ‘successful’ simulations reflects the speeds achieved by simulated ships that reached the coast of Cornwall and would have at least had an opportunity to make landfall. Table 8.3 shows average speeds calculated for these simulations.

The three vessel parameterisations used in this Case Study were designed to more accurately reflect the estimates made in McGrail’s 1983 paper (see Section 2.2.6). It is therefore not particularly surprising that speeds for these simulations were slower than those of the Main Analysis and the other case studies. The overall average speed for simulations in Case Study 3 was 3.23 knots, compared to 4.84 knots in the Main Analysis, 4.39 kts for the other two case studies. The average speed for successful simulations along the Brest-Penzance route in the Main Analysis was 4.57 knots – lower than the overall average, but much faster than the average speed achieved by simulations in this case study. The average speed achieved by simulated ships in Case Study 3 is within McGrail’s 2.5-5 knot average speed range (1983, 300). These results provide an interesting contrast to the results of the Main Analysis, where average speeds were closer to those suggested by McGrail but maximum speeds were much higher. Possible causes for this relationship are discussed in Section 9.2.4.

8.2.3: Leaving Times

Earlier and later leaving times did not appear to have much of an effect on the outcome of results, although a possible effect may be obscured by the small sample size. Two out of the three ‘successful’ simulations departed at the leaving time determined by the Main Analysis. The results here appear to accord with those of Case Studies 1 and 2, where leaving times at or just after the Main Analysis leaving time produced the best results.

8.2.4: Visibility

In the simulation plots in Appendix III landmark sightings are symbolised by lines drawn from the location of the sighting to the landmark in question, graded by the apparent size of the landmark. Apparent size is measured in square minutes of arc by the navigation model, and is converted to square degrees of arc for the purposes of presentation. For reference, a 'square degree' is approximately the size that one's thumbnail appears when held at arms' length. The size of the human visual field, then, is approximately 50,000 square degrees (Sardenga & Shelly 2002, 253).[65] Table 8.2 contains the average apparent sizes of sighted promontory forts in square degrees. Figure 8.2 and Figure 8.3 show the relative apparent sizes of all tested landmarks at each end of the simulated route (Cornwall and Brittany, respectively).

The two landmarks that appeared largest to simulated navigators in this case study were both sites: Kermorvan and Pointe du Toulinguet. Both of these were much more visible than other landmarks – the average apparent size for all landmarks excluding these two sites is 2.28 square degrees. The large apparent size of both of these sites results from their location close to the Brest node. In the first instance, Kermorvan sits at the entrance to the Chenal du Four, which was used by 30 out of the 38 simulated vessels. In particular, simulated ships that held close to the mainland coast while navigating the channel passed close by Kermorvan. In the second instance, the Pointe du Toulinguet is situated approximately 5.5 kilometres southwest of the location of the Brest node. Although the

[65] This is a rough estimate based on the area of an ellipse with the semimajor and semiminor axes equivalent to the horizontal and vertical limits of human vision. The exact 'size' of individuals' field of vision varies from person to person and is not defined by hard edges.

site was highly visible, simulation tracks did not approach it as closely as Kermorvan, and as a result its average apparent size was roughly half that of Kermorvan. The next most visible landmarks in this case study were all natural prominences. The group of natural prominences with average apparent sizes of over 5 square degrees consisted of two promontories on either side of the Pointe de Toulinguet, the Pointe de Bachaol on the northern coast of the Île d'Oessant, and the Trevescan cliff just to the southeast of Maen Castle (in Cornwall). For simulations that used sites as landmarks, promontories on the northern side of the Île d'Oessant served the same purpose as Kermorvan – orienting vessels as they passed around the Île d'Oessant and neighbouring islands before they left sight of land. Landmarks with apparent size on average between 1 and 5 square degrees included promontory forts in Cornwall (Maen Castle, Carn Les Boel, Treryn Dinas), one promontory fort in the Scillies (Giant's Castle), and one promontory fort on mainland Brittany (Ile d'Yoc'h). Of these, Giant's Castle and Treryn Dinas were notable in that they served as the first 'points of contact' for simulated ships in approximately half of all simulations where sites were used as landmarks.[66] On the southern side of the Channel, the Île d'Yoc'h played a similar role as a last point of contact, and the Pointe de Raz at the end of Cap Sizun was also very visible to ships approaching the Île d'Oessant. Natural prominences on the Île d'Oessant and in the Isles of Scilly served a similar role for simulations where natural prominences were used as landmarks (see Appendix II).

It is also worth comparing the locations of highly-cited cultural landmarks with those that were only slightly visible or were not sighted in these simulations. Starting in

[66] Specifically, Treryn Dinas was sighted first 9/20 times where sites were used as landmarks; Giant's Castle was sighted 11/20 times under the same circumstances.

the south, of the four promontory forts on Cap Sizun only Pointe du Raz was highly visible – the other three (Castel Meur, Kergulan, and Castel Coz) were frequently sighted but did not appear to be very large. Likewise, Kastell Ac'h and Beg Monom on the northern coast of Finistère were frequently sighted but not visually imposing. Sites within the Rade de Brest other than Pointe du Toulinguet were either not sighted or sighted infrequently in these simulations. In Scilly, the promontory forts at Shipman Head and Burnt Hill were sighted but not particularly visible – as with Cap Sizun the promontory fort at Giants Castle was by far the most visible. On the mainland, Trereen Dinas and St. Michael's Mount marked the eastern extent of sightings. The fact that St. Michael's Mount was not particular visible is surprising, given that it is famously visible from the land within Mounts Bay – however the fact that no simulated ships managed to enter Mounts Bay likely explains its lack of visibility in this case study.

8.2.5: Sailed Routes

In the Main Analysis it was noted that very few voyages entered the waters around the Isles of Scilly, or passed north of Land's End (see Section 5.6.5). Figure 8.1 shows that for simulations along the Brest-Penzance route in the Main Analysis, more-or-less direct passages were the norm. Voyage tracks produced in this case study tell a very different story. This is partially due to the conditions on the day for which all of the simulations for this case study were performed. The highlighted track on the plot of Main Analysis tracks in Figure 8.1 represents the simulations corresponding to date used in the present case study – the simulation crossed the Chenal du Four diagonally, passing the northern corner of the Île d'Oessant and continuing northwest for a further 50 kilometres, before turning 90 degrees to starboard and continuing on that course until due south of

the Penzance node. The simulated ship was then able to continue more or less directly north to the node. Simulations for Case Study 3 began similarly, with most simulated ships trending northwest after leaving sight of the Breton coast, but none of these performed the same eastward turn. Instead, they continued north or northwest until they reached the waters off West Penwith or the Isles of Scilly. From there only a few simulated ships managed to make it make it to the mainland coast, after spending several timesteps performing a series of tacks.

A few failed runs hint at a possible alternative to the route followed by the Main Analysis simulation. Several Case Study 3 simulations (specifically: Simulations 04, 05, and 09) stayed close to the Breton coast after leaving Brest, turning away from the coast at the Île d'Yoc'h and setting a course due north. One of these three simulations managed to sight natural prominences on the Lizard before timing out (see 4.3.5, while the other three failed without sighting land. Had they continued on their courses, these ships would have entered Mounts Bay from the southeast, and would probably have been able to reach the node.

8.3: Discussion

Before moving on to the discussion of these results, it bears repeating that said the simulations performed in support of this case study represent a fraction of the runs that were originally intended. In particular, no southbound simulations were tested. Although the results of this case study are less useful for assessing the viability of the Brest-Penzance route, the 3D visibility analysis used here proved to be very useful in assessing the visual prominence of landmarks. On this account, the results of Case Study 3 provide important data and demonstrate the potential of the navigation model.

8.3.1: Different Routes for Bigger Ships?

Aside from the use of 3D visibility analysis, the greatest point of difference between Case Study 3 and other case studies presented here is that vessel parameterisations used in this analysis have much slower maximum speeds. Whereas varying vessel speed in Case Studies 1 and 2 resulted in shorter or longer voyages and a swing of 5-15 % in success rates, the impact of vessel speed on the results of Case Study 3 appears to have been much greater. The dog-leg route taken by the Main Analysis simulation (highlighted in Figure 8.1) used a ship parameterisation that allowed for a top speed of 14 knots, and this route proved impossible to follow for simulations in this case study using parameterisations with lower top speeds (5-9 knots). This suggests that the relationship between vessel speed and chances of success are more complex than indicated in the Case Studies, and that there may be a 'cutoff point' for certain approaches that precludes ships that cannot achieve sufficient speed from navigating those routes.

Simulations that were 'successful' made landfall just off of Maen Castle, near Land's End – a short walk from Sennen Cove, a sandy beach that could have served as a landing place. Maen Castle itself has been the focus of excavations which produced Early Iron Age pottery, and on that basis has been identified as an 'early site' by Herring (1994, 47). Although certainly not definitive, the association between a potentially Early Iron Age site and salvaged voyages using more conservative ship parameterisations raises the possibility that Maen Castle could have served as a landmark – or possibly as a destination – for ships that found themselves too far west of Mounts Bay. This example raises the possibility that the development of faster and more seaworthy ships would have expanded the range of possible sea-routes across the Channel – rather than simply making existing routes more efficient. This would have created opportunities for those who were able to

make more direct crossings – sailing along the coast would have required more detailed knowledge of hazards and conditions, taken more time, and possibly involved negotiations with locals. If we accept the accounts of Caesar and suppose that the ships of the Veneti were precursors to Romano-Celtic vessels, then it is possible that their reported control over trade with Britain was in part enabled by their ability to navigate more direct routes to the Cornish peninsula. Although this proposition is supported by a small number of simulations for a single day, the possibility that certain cross-Channel routes would have been substantially more difficult for earlier ships to navigate is intriguing. Performing more simulations under more conservative vessel parameterisations could help evaluate this possibility (see Section 9.3.5).

8.3.2: Directionality and Landmarks

In interpreting the results of this analysis it is particularly important to remember that the simulations completed in support of this case study were for northbound passages only. Although the simulations that were completed were not successful, this does not necessarily mean that voyages from Penzance to Brest simulated under the same conditions would have been successful. In light of these analyses the viability of the Brest-Penzance route appears to be doubtful, but in by no means disproven.

The results from northbound simulations are nevertheless interesting in that they may explain the different characters of the Île d'Oessant (and neighbouring islands, in this section referred to collectively as the Île d'Oessant) in the Iron Age. The Scillies and the Île d'Oessant are superficially similar in that they lie off the coast of their respective peninsulas, both of which are referenced in Classical sources and feature in proposed systems of maritime contact and trade (see McGrail 1983; Cunliffe 2001, 304; also

Section 8.1.1). Both groups of islands are similarly sized, and have indented coastlines and rocky shores.[67] Although one might expect to find promontory forts at least on the Île d'Oessant, evidence for Iron Age settlement is found inland (Le Bihan & Villard 2011). Meanwhile there are three known promontory forts in the Isles of Scilly. In simulations performed for this case study, these three promontory forts were all sighted, although the fort at Giant's Castle was by far the most sited archaeological site (with 228 sightings – see Table 8.2). This is likely due to its position at the southern end of the archipelago. It is possible that the other two promontory forts would be sighted by simulations testing navigation to Cornwall from locations further north (such as Ireland or Wales).

Had it been possible to complete all runs for this case study, an examination of the role of the Île d'Oessant in southbound voyages would have been useful in investigating this discrepancy. The results of completed simulations suggest that the mainland promontory forts of Kermorvan and Pointe du Raz were visible enough to serve as landmarks for simulations passing along the outside of the islands, as in Simulation 33. The distance from the Isles of Scilly to mainland Cornwall (c. 40 km.) is much greater than the distance from mainland Brittany to the Île d'Oessant (c. 20 km.), meaning that landmarks on the mainland may be out of visual range for ships passing through or around the Scillies. If one of the functions that promontory forts fulfilled was to serve as landmarks for the purposes of navigation at sea, then the results here hint at a possible explanation for their absence on the Île d'Oessant.

[67] The land area of the Scillies is roughly 22 square kilometres, whereas the land area of the Îsle d'Oessant and its neighbours is approximately 24 square kilometres.

8.3.3: Conclusions

Although Case Study 3 is not as extensive as other case studies in terms of the number of simulations performed or the range of parameters swept, the information that it provides is crucial to interpreting the results of other analyses. To begin with, it suggests that the results of ships with maximum speeds of below 10 knots can produce very different results – whether this is because of the conditions of the western Channel or because of the model, however, remains unknown. It would be worthwhile to test whether or not simulations using these slower ship parameterisations would produce different results in the contexts of Case Studies 1 and 2. This case study also demonstrates the potential both for the 3D visibility technique. By separating the number of sightings from the apparent size of potential landmarks, it was possible in Case Study 3 to identify sites like Giants Castle, Pointe du Raz and Kermorvan which were genuinely visually prominent from those that were frequently sighted but did not appear to be very large to simulated navigators. Analysis of a more comprehensive set of results could be used to develop more robust characterisations of the visual prominence of these sites, establishing a useful dialogue between theories of 'seascapes' (see Jerpåsen 2009) and terrestrial methodologies for assessing visual prominence (see Bernardini et al. 2013; Llobera 2001). Finally, the small sample size in this case study allowed for a detailed interrogation of simulation results that would not have been possible for other case studies (and certainly not for the Main Analysis).

Although none of the simulations performed for this case study were successful in the strict sense of reaching their destination node, creating a criteria for 'qualified' and 'potential' success was a useful exercise that could be developed into a more rigorous set of categories. This could be useful in future analyses, especially in contexts where the

odds of reaching an intended destination are low, but the risks of making landfall elsewhere are not too great. Considering how a navigation model might be designed in order to allow simulated navigators to make those sorts of decisions would likely lead to significant improvements to the model (see Section 9.4.4).

Chapter 9 : Discussion

9.1: Research Questions and Answers

In this chapter we return to the research questions posed in Section 1.4:

1. **How successful and efficient would western Channel crossings have been in general, and in particular along routes already proposed by archaeologists?**

   Voyages in the western Channel were not particularly successful overall, but certain routes afford opportunities for successful voyages better than others. Proposed routes in eastern and central sections of the study area could have been viable; however these routes may not have been bi-directional.

2. **Could promontory forts have served as landmarks, and how would they have appeared to navigators attempting to cross the Channel?**

   Promontory forts did not perform especially well as landmarks, but were highly visible. The partial results of Case Study 3 suggest that they could have played an important role as first 'points of contact' with the coast.

3. **Which parameter input to the model has the greatest effect on the outcomes of simulated voyages?**

   Sailing time had the greatest impact on success, but it is possible that vessel speeds outside the tested range could have had a great effect. The use of different landmark sets and estimation ranges had less of an effect than was expected.

This chapter discusses the wider implications of results from the Main Analysis and case studies for the characterisation of cross-Channel routes, the interpretation of promontory

forts as prominent sites and landmarks, and the balance of risk and reward for navigators in the Channel. The process of developing and deploying the model has also suggested a number of opportunities for further research in the Iron Age Channel, and for the future development of the navigation model.

9.2: Interpreting Analysis Results

The total number of simulations possible within the parameter space defined by the datasets gathered for this analysis and the navigation model presented here is enormous, potentially consisting of more than ten million possible simulations (see Section 5.2.1). In order to address this thesis' research questions as thoroughly as possible, selections from that parameter space were made, resulting in the Main Analysis and case studies presented in Chapters 5-8. These analyses targeted different sections of the western Channel, evaluated different parameter relationships, and tested different configurations of landmarks. This section brings the results of these analyses back together, in order to speak to the wider topic of seafaring in Iron Age Atlantic Europe.

9.2.1: Cross-Channel Routes

In all analyses, the chances of success for simulated voyages were surprisingly low. The overall average success rate in the Main Analysis was only 56 %. Given that the Main Analysis used a generous vessel parameterisation, these rates could have easily been lower had smaller craft been used in simulations. The low overall success rate could be a taken as a sign that Channel crossings were difficult and rarely successful (along the lines of Davis 1997). However we should also be aware that simulations that failed to reach their destination were not always complete failures. The results of Case Study 3 suggest

that ‘success’ can be measured in a number of ways – some voyages that the model marks as ‘failures’ could have been salvaged by attempting to reach another port, or by returning to their point of origin.

Taking low success rates as a sign that routes were not travelled presumes that prehistoric mariners attempted to minimise risk as much as possible – which was not *necessarily* the case. It is tempting to assume as a first principle that navigators prefer to reduce the risks involved in a voyage as much as possible. There are practical reasons for making this assumption: the time saved by plotting a risky course may be offset by the expenditure of effort, cargo, or even lives along the way. However, in making this assumption we should be careful not to project our modern sensibilities about transportation and seakeeping onto the past. To generalise: modern (particularly Western) societies expect maximum efficiency, and are also particularly intolerant to risk. These attitudes are supported by schemes of law, indemnity, and responsibility that exist at scales from personal to corporate to national to global.[68] If similar schemes existed in the Iron Age Atlantic Zone, then no record of them has come down to us. In a world where navigators were constrained by different sets of rules and customs, we should expect to find different attitudes towards risk. Rule & Monaghan’s description of the St. Peter Port 1 ship suggests an alternative state of affairs in the world of shipbuilding:

> Numerous minor constructional errors occur in the ship and a casual crudeness is evident wherever a watertight fit was not required. Although an element of planning went into its construction, there is an asymmetry about the structure which suggests a rather empirical

[68] Although, in fairness, these schemes are often circumvented in the name of efficiency – for example by registering a ship in a jurisdiction with lower taxes or less stringent safety regulations.

> approach to shipbuilding. This class of vessel fulfilled its function, which may have been all that the shipwrights required of it. (1993, 127)

Minor errors in the construction of St. Peter Port 1 may not have actually affected its safety, but we should remain open to the possibility that maximising safety (thereby minimising risk) was not the top priority for the builders of St. Peter Port 1, an by extension other Channel-crossing vessels. The relative speed and success of simulated voyages into and out of coastal nodes in this analysis suggests that different ways of calculating risk might have been at play in different areas of the Channel. In the Main Analysis nodes were separated into five groups based on the qualities of routes attached to those nodes. If we consider those routes that have been suggested by archaeologists and are best-supported by the archaeological record, the nodes that would have been involved in these routes fit different profiles. Four of the six nodes investigated in Case Study 1 were classified as 'slow but successful', with St. Malo ('generally successful') and Le Legnét ('quick and unsuccessful') serving as exceptions.[69] The route from Le Yaudet to Mount Batten, tested in Case Study 2, was between nodes classified as 'quick and unsuccessful' and 'generally unsuccessful', respectively. And the route identified by McGrail across the western mouth of the Channel involved two nodes classified as 'quick and unsuccessful'. If we accept both the characterisations from the Main Analysis and the archaeological / documentary evidence for exchange, then we should be open to the idea that prehistoric mariners' decisions to sail along certain routes may have been based on a combination of factors that included the chances of arriving safely at their destination,

[69] St. Peter Port North and St. Peter Port South are counted as the same node here, since they were both classified as 'slow an successful'.

rather than a combination of factors intended to maximise those chances. This distinction is subtle, but indicates a fundamental difference with potential implications for the rest of Atlantic Europe. An Atlantic Zone in which navigators were more willing to take risks is one with a greater potential for long-distance travel and, perhaps, the establishment of long-distance routes.

Returning to the Channel, it would appear that the routes proposed by Cunliffe and De Jersey for the eastern half of the study area (Cunliffe 1988; Cunliffe & De Jersey 1997) are plausible routes in light of the results of this study. These routes were mostly classed as 'slow but successful' in the Main Analysis – a good sign if one subscribes to the 'safety first' school of good seamanship. Case Study 1 found that Guernsey could have served as a stopping place for goods crossing the Channel, and that voyages from Nacqueville performed well despite there being few landmarks nearby. These results, however, suggest that voyages between the nodes identified by these authors may have involved a wider area – including other anchorages and coastal settlements. For example, in Case Study 1, the node at Le Trieux on the western edge of the Gulf of St. Malo was found to be the best departure node from mainland France to Britain; in Case Study 2 voyages bound for Plymouth were carried west as far as Lizard Head and were frequently forced to tack along the coast to reach their destinations; and in Case Study 3 the Scillies emerged as a crucial reference point for northbound voyages that missed the entrance to Mounts Bay. When we think of 'sea routes' between sites or anchorages, we should understand that voyages along these routes might make landfall at points along a long stretch of adjacent coast instead of imagining that their intended destination was their first sight of land. From the perspective of a mariner, the extent of potential landfall should be

included in the ‘vicinity’ of a coastal node, whether it is close or distant to the node itself in terms of kilometres or nautical miles.

9.2.2: Landmarks and Promontory Forts

In order to answer research questions concerning promontory forts, two different sets of landmarks were used in these simulations to establish whether or not these sites ‘make sense’ as landmarks, and how visually prominent these sites would have appeared to navigators. In the first place, the results of these analyses suggest that simulated ships could have used promontory forts as landmarks, although their odds of success would have improved by also navigating by natural prominences. In Case Study 1, simulations that used only promontory forts as landmarks were approximately fifteen percentage points less likely to reach their destination. To put the difference in average success rates between simulations using the two different types of landmarks into context: in the same analysis a similar average success rate range was found between simulations that used no misestimation and simulations where values could be misestimated by up to 30 %. Case Study 3 found that ‘successful’ voyages (voyages that made landfall on the Cornish Peninsula) were divided roughly evenly between simulations using promontory forts and natural prominences as landmarks. This suggests that promontory forts are unlikely to have been placed in order to serve as landmarks, or that if they were used as landmarks then they would have been used alongside natural prominences. The fact that travel times for successful voyages in Case Study 1 were nearly identical for simulations using both landmark types suggests that simulated ships that managed to reach their destinations while using sites as landmarks did not stray any further from the most direct course than ships that used only natural prominences as landmarks.

In the case studies, several specific promontory forts were found to be situated at areas of particularly high track density, or at 'inflection points' within a voyage. The promontory forts of the Channel Islands were found to be particularly useful reference points for ships stuck in the Gulf of St. Malo in Case Study 1. In Case Study 2 promontory forts on the eastern side of the Lizard appeared to play a role in redirecting simulations to Plymouth. And in the third case study the point at which potentially successful voyages turned away from the coast was marked by a promontory fort. These findings are interesting, and have the potential to be developed into new interpretations for the sites concerned. There are counterexamples, however, the best one being Hengistbury Head itself, which was not particularly well-sighted in Case Study 1 despite being the focus of most of the simulations in that analysis.

The second part of the research question under consideration here – how would promontory forts have appeared to navigators attempting to cross the Channel? – is more difficult to answer from the results of this study. The use of 3D visibility analysis in Case Study 3 effectively addressed these questions, as records of apparent size of a promontory fort could be compared with the number of sightings. This was used to identify promontory forts that were frequently sighted and loomed large in simulated crossings, such as Kermorvan, and to identify promontory forts that were uncommonly visually prominent despite being located near other promontory forts that were sighted a similar number of times (in particular Pointe du Raz). In the Main Analysis and Case Studies 1 and 2, however, counting the number of sightings was less useful in quantifying visual prominence, since the value used to establish visual prominence was the same for sites close by simulated ships as it was for sites kilometres away. In the Main Analysis promontory forts were not particularly well-sighted. The most-sighted promontory fort

(Rame Head) ranked 15th out of all landmarks (cultural and natural) in terms of total sightings. In the Main Analysis promontory forts were sighted approximately half as many times as natural prominences (Section 5.6.6), suggesting that not all of these sites were situated in order to be easily viewed by navigators. Of those promontory forts that were sighted, only one third were the most-sighted landmark within a five kilometre radius.

As promontory forts defied general characterisation in the other analyses in this study, detailed analysis along the lines presented in Case Study 3 presents the best pathway to evaluating individual sites' visual prominence and possible role as landmarks. A site-by-site analysis based on 3D visibility results fell outside the scope of this study, but is an excellent candidate for future analyses, both in the Channel and within the wider Atlantic Zone.

9.2.3: Parameters and Outcomes: Temporal Parameters

For a descriptive model, working out how different parameters interact within the model is both a challenging task and its own reward. The most widely varied parameters in this study were temporal, with 212 days tested in the Main Analysis, and up to 11 leaving times tested in Case Studies. This section discusses the effects of these temporal parameters on the results of the model – parameterisation and 'reckoning' parameters are discussed in the next section.

To begin with, the analyses performed here appear to confirm the 'received wisdom' that prehistoric mariners would have had to wait for ideal conditions before setting out (see Davis 1997). Timing was the most important parameter in these analyses, in terms of voyage success. Two parameters used in the analysis focused on the timing of

voyages: sailing date and sailing time. The first was the key parameter swept in the Main Analysis, and was also varied in Case Study 1. The second was varied in all Case Studies but not in the Main Analysis. The results of these analyses suggest that both of these parameters had huge effects on the success of simulated voyages. The range of average success rates per week in the Main Analysis study period was c. 39 %-85 %, about 10 % higher than the range of average success rates per simulated route (see Section 5.6.4). Success rates by day in the Main Analysis were extremely variable, with all simulated voyages being successful on some days, and all failing on others. Days with high success rates appeared periodically in the results of the Main Analysis, with sailing windows lasting no longer than a few days. The results of Case Study 1, which tested a full week, shows a pattern consistent with the results from the Main Analysis. On the first day tested in Case Study 1 the average success rate was c. 77 %, decreasing over the next two days to 62 %, before increasing again to 81 % on the following day and then decreasing over the next three days to 53 %. Although these sailing windows were more tightly clustered in midsummer, there was no long stretch of days where voyages were uniformly successful. These simulations indicate, therefore, that a summer 'sailing season' should be understood as a window of opportunity more likely to offer time windows for successful voyages, rather than a period over which voyages are likely to succeed.

In the Main Analysis, a single sailing time was used, set to the first hour after high tide and nautical twilight. This was based on the assumption that a flow tide would have helped mariners away from the coast and increase their odds of success. This assumption was tested in all three case studies, and the results confirm that it was correct. For Case Study 2, the earliest high tide was at 04:00, and the most successful leaving time overall was 06:00, with 04:00 and 05:00 coming close behind. The results for Case Study 3 are

not as easy to interpret, but of the three 'successful' simulations in that analysis two were launched at the earliest high tide. This suggests that the assumptions that informed the selection of the 'first daylight high tide' were correct: launching on a flood tide appeared to help simulated vessels avoid being forced ashore in the early stages of the simulation. If more complete and detailed inshore data becomes available, this hypothesis may be tested in more detail.

A final temporal parameter that was *not* varied was the amount of time given to complete a simulation: 48 hours. Although the average lengths of successful runs in the Main Analysis and Case Studies 1-2 were around 26 hours, the results of Case Study 3 suggest that for slower ships more time might have been necessary. In the Main Analysis approximately 25 % of all completed simulations ran out of time, and the percentage of successful voyages could be higher if simulations were to be run with a greater maximum duration. In Case Study 3, it appeared that those few simulations that were on track to reach their destinations would have been able to do so within an additional day. Since the 48-hour period covers two days and two nights (i.e. starts and ends around dawn), then extending simulations at least until sunset two days from launch seems reasonable.

9.2.4: Parameters and Outcomes: Parameterisation and 'Reckoning'

Interestingly, the average speed under sail achieved in the Main Analysis and Case Studies was well within the ranges that McGrail suggested, even though an error in transferring McGrail's estimates to a speed diagram in the setup for the Main Analysis resulted in most simulated ships having unrealistically high top speeds (see Section 5.2.3). One would expect simulations with a higher top speed to have similarly inflated average speeds, but this appears to have been the case in only a few contexts (such as the St. Peter

Port – St. Malo route in Case Study 1; see Section 6.3.2). The most likely explanation for this discrepancy is that the simulations presented here were not as efficient as McGrail imagined sailing ships to be in his model. The assumptions in McGrail's model allowed for a certain amount of displacement – he estimated that unfavourable winds resulted in, at most, a doubling of the amount of time required for the passage (1983, 331). No similar limit was placed on simulated vessels in this analysis – ships were counted as 'successful' if they reached their destinations regardless of how long the simulated ship had been at sea. Similarly, while McGrail quantified the amount of time spent out of sight of land, this information did not affect the progress of the vessel in this model, which used dead reckoning. Many simulations that became 'lost' without landmarks were nevertheless successful, but would have had longer voyage times as a result. This would perhaps explain the high maximum speeds and low average speeds reported in these analyses, as the design of the model does not compensate for overly high maximum speeds. To argue for the latter would be counterproductive – not to mention hypocritical given that descriptiveness has served as one of the pillars supporting the navigation model. The best way to approach the 'maximum speed' problem encountered in this thesis would be to perform additional simulations using the 'slower' ship parameterisations developed for Case Study 3.

We should not rush to any general conclusions based on comparisons between the results of Case Study 3, which was designed to test a single pair of routes on a particular day, and the results of the Main Analysis and other Case Studies. However the fact that none of the simulations in Case Study 3 were successful within the 48-hour simulation-length limit is interesting given that these simulations used ship parameterisations better suited to possible Iron Age craft. Given that results with the faster ship parameterisations

produced results broadly in line with McGrail, Cunliffe, and De Jersey's predictions for Iron Age routes (see McGrail 1983; Cunliffe 1988; De Jersey 1993; Cunliffe & De Jersey 1997), a re-evaluation with slower ship parameterisations could be revealing. Identifying the 'minimum maximum speed' at which these routes become viable would be especially interesting, as this could be used as the basis for determining whether reconstructed ships would have faced more or less difficulty in crossing the Channel.

The final parameter varied in these analyses represented the ability of simulated navigators to read conditions at sea by allowing them to under- or overestimate environmental values up to a user-selected threshold (see Section 4.3.2). Estimation ranges were varied in all three Case Studies, although the configuration of these ranges differed from case study to case study. The relationship between misestimation and simulation success was unexpected in that it appeared to be linear in both Case Studies 1 and 2 (see Sections 6.2.6 & 7.2.4). Here it was expected that there would be a sharp fall-off in success rates as misestimation ranges approached 50 %. As it happened simulations using the highest misestimation values used in Case Studies 1 and 2 (60 % and 50 %, respectively) had average success rates almost equal to those ranges (60.27 % and 51.82 %, respectively). These success rates are low, but not substantially lower than the average success rates using no misestimation in Case Studies 1 and 2 (78.79 % and 76.36 %, respectively). Whether the success rate of simulated vessels falls off for misestimation ranges of over 60 % remains to be seen. Simulations in Case Study 3 were meant to address this, but it was not possible to perform them.

9.3: Future Research in the Channel

The model developed as a part of this thesis is the first agent-based model to be deployed in the Iron Age Channel, so perhaps it was to be expected that the results of this study would raise a host of other questions about cross-Channel navigation and seafaring. The scope for potential analysis within the western Channel using this model is huge, especially if the navigation model is combined with another type of analysis. This section discusses potential research in the western Channel, involving both the application of the navigation model and studies that would contextualise or improve the results of the model.

9.3.1: Improving Ship Parameterisations

In the analyses presented here a fairly simple parameterisation for Iron Age ships was used. The decision to use a polar diagram to represent an Iron Age ship in the model was based on the scanty nature of the archaeological record with regards to these vessels (see Section 2.2). The recovery of more material would, naturally, be useful in developing more detailed ship parameterisations, but the production of more ship reconstructions would also be extremely useful. Reconstructions of St. Peter Port 1 in particular would be helpful in establishing what the 'upper bound' on the capabilities of a Late Iron Age ship might have been. Likewise reconstructions of curraghs (real or hypothetical) could be used to generate a more nuanced parameterisation. Gathering more detailed knowledge about the capabilities of Iron Age ships (especially their heeling angle and predicted freeboard in rough weather) would also enable changes to the navigation model to make it more accurate (see Section 9.4.2, below).

9.3.2: Testing Coastal Routes

When designing the model, it was decided not to test coastal pathways as (1) it would increase the number of necessary simulations to unworkable levels, (2) coastal hazards close to shore are not well-represented in the DEM used for analysis, and (3) the coverage of hydrodynamic datasets in inshore waters is patchy in certain parts of the study area (see Section 5.4.1). If these problems were to be addressed, then an analysis of coastal routes would serve as a useful complement to the analyses presented here. Section 9.3.3 (below) offers suggestions on how this might be accomplished, so this section will concern itself with outlining the potential dividends of such an approach.

To begin with, testing coastal routes would allow for archaeologically-proposed routes to be tested, along the same lines as this analysis. McGrail (1983) and Davis (1997) both suggest coastal routes as part of a wider schema of cross-Channel movement. Analysis 1, in this study, suggested that in the Gulf of St. Malo ships would have increased their odds of completing a northbound crossing successfully by sailing to Le Trieux of St. Peter Port before journeying on to Christchurch. An analysis of coastal routes between sites could test these hypotheses, and could also shed light on the placement of coastal nodes. Establishing the amount of time necessary to pass between nodes may reveal patterns in their distribution in terms of hours' or days' sailing. Just as this analysis identified disparities in northbound and southbound voyages across the Channel, an analysis of coastal passages could be used to identify disparities in eastbound and westbound passages. This information would be extremely useful in a future analysis of voyaging in the Channel.

Similarly, such an analysis could shed new light on the situation of promontory forts (as well as their visual prominence – see below). Case Study 3 found that promontory forts appeared to be situated at important points along simulation tracks – Kermorvan, for example, was placed just before the point where simulations most likely to reach Mounts Bay turned away from the coast. Although promontory forts did not prove to be especially useful landmarks for cross-Channel voyages, this may not have been the case for coastal voyages. A comparison between the usefulness of promontory-forts-as-landmarks in coastal and cross-Channel analyses would be especially useful in contextualising this analysis, and could form the basis for an interpretation of these sites' landscape setting if a significant difference is found.

9.3.3: Landmark Identification and Visibility

In these analyses Local Relief Models were used to identify natural prominences, in order to test whether these areas served better as landmarks than archaeological sites. Other methods for classifying 'natural landmarks' could also be used. Assessments such as Robinson's survey of Scilly (2007) could be replicated for other sections of the Channel, in order to identify likely landmarks. Such an approach would require a combination of fieldwork – and consultation with local mariners – in order to establish a likely group of natural landmarks. The danger in such an approach would be that the 'baseline' of natural landmarks established by such an analysis would reflect more recent historic navigational sensibilities to an unreasonable degree. Still, the results of the navigation model presented here based on such a set of landmarks would provide a useful point of comparison in this endeavour.

In Section 4.3.4, it was decided to set the number of landmarks that must be visible before the navigation model stops using dead reckoning at two. If this threshold was made into a parameter of the model then it would effectively become another 'experiential' parameter – analyses varying a 'landmark recognition threshold' could test (1) whether requiring more landmarks to be in view for navigators to find their position affects the outcomes of simulations, and (2) whether there are patterns in *which* landmarks are sighted under different thresholds. This would be useful both for developing the model and for furthering our understanding of the maritime visibility of coastal sites.

9.3.4: Expanding Visibility Analyses of Promontory Forts

In Case Study 3, testing the 3D visibility of promontory forts proved to be much more useful than basing their visibility on the number of sightings, since it is possible for sites that are not visually prominent to nevertheless receive a high number of sightings. Future analyses that use the navigation model would be well-served by using 3D visibility rather than the 2D approach used in the Main Analysis and in Case Studies 1 and 2 (see Section 4.3.3). Although the 3D visibility routine used in this analysis is processing-intensive, further development of the tool could make it more efficient, and changes to the way that landmarks are represented could also improve the speed of the model.[70] The processing power of personal computers has increased steadily over the years, and the development of GPU-oriented GIS tools have also contributed to gains in efficiency (see,

[70] For example, representing landmarks as a mesh rather than as a clipped raster would make it more difficult to use with ArcGIS tools, but would open the door to other methods of surface-intersection that may be more efficient.

for example, Stojanovic & Stojanovic 2013). ArcGIS Pro has also been built to better handle 3D analysis. There is good reason to be optimistic that 3D visibility analysis can be developed into a more efficient tool in the future, and that its deployment in simulations along the lines presented here would be very useful.

Further visibility analyses may also be useful in characterising the landscape setting of promontory forts. Analyses described in this thesis tested the visibility of promontory forts in a very specific way: from the perspective of a ship-bound navigator attempting a crossing across the Channel. Future analyses could inform this study by investigating the visibility of promontory forts by individuals with different perspectives – taking an approach similar to Driver's analysis of hillforts (2007). The visibility of promontory forts from the land is worth undertaking, both for its own sake and to provide a point of comparison with the results of this study. It is possible that some promontory forts are more visible to a navigator aboard ship than to a navigator on land. If this is the case, then it may be more appropriate to say that some promontory forts are 'theatres of the land' than 'theatres of the sea' (see Section 1.3.5). Such an analysis could take the form of a large-scale visibility analysis (see for example Gillings 2009), or else could test the visibility of promontory forts from points derived from a terrestrial navigation analysis.

9.3.5: Casting a Wider Parameter Net

Defining parameter ranges for analyses in support of this thesis proved to be a challenge. Since no comparable navigation models exist, the limits of 'reasonable' parameter ranges were first set by intuition, and later informed by the results of parameter sweeping. For example, it was assumed (based on the author's limited experience as a

sailor) that misestimation ranges of up to 60 % would result in unsuccessful voyages. However in Case Study 2 the relationship between estimation ranges and success rates appeared to be linear, and simulated navigators allowed to misestimate values up to 60 % were successful 60 % of the time in that analysis. Future analyses could contribute to this area of study by testing parameters outside of the ranges tested here, particularly in terms of misestimation ranges and maximum vessel speed. The results of Case Study 3 suggest that the relationship between maximum speed and success rates are *not* linear between parameterisations that allow for maximum speeds of between 5 and 12 knots. Understanding the nature of this relationship could shed a great deal of light on our understanding of Iron Age Channel crossings.

The suggestion that slower vessel speeds may have a significant impact on the success of voyages has been raised several times in the discussion sections of this thesis (see Sections 5.7.3, 6.2.5, & 7.2.6), and analyses using different vessel parameter sets are an obvious candidate for further analysis. The discrepancy between results from the Main Analysis and Case Study 3 Section raises the possibility that certain routes would have been navigable for Late Iron Age ships but not for Early Iron Age ships. If this is the case in such an analysis the implications for theories of contact would be manifold – based on such a conclusion, one could argue that the re-establishment of contacts in the Late Iron Age were driven by changes in ship design as much as they may have been by climatic or historical factors – a hypothesis that could be brought to bear directly on Henderson's work in the Northern Isles (2007). If no significant difference is observed in the performance of 'Early Iron Age' parameterisations versus 'Late Iron Age' parameterisations, then changes in ship design are less likely to have affected changes in Iron Age schemes of maritime contact.

Further analysis should seek to test environmental datasets outside the temporal range of this analysis – most of which pertain specifically to weather conditions in 2018. Although the development of these datasets is discussed below, testing the conclusions presented here based on datasets from other years would certainly be useful. If a wide range of data was available, and the character of data series could be classed in terms of favourability (i.e. as a 'stormy year' or a 'fair year'), a comparative study using such data series would be incredibly useful in furthering our understanding of how weather (and potentially climate) affects inter-Channel navigation.

9.4: Future Development of the Navigation Model

The following sections discuss possible improvements to the model and to the data inputs that have been used to run the analyses presented in Chapters 5-8. Many of these suggestions were formulated while interpreting the results of the Main Analysis and case studies. While the suggestions here are made with a view to improving the model's performance in these analyses, development along these lines would improve the navigation model generally, and could allow it to be deployed in waters outside the Iron Age Atlantic.

9.4.1: Topographic and Environmental Data

The topographic and environmental data used here proved to be particularly useful in simulating voyages. In particular the fine temporal resolution of wind and current forecasts gave simulated navigators 'time' to make decisions. Improving the detail and accuracy of environmental and topographic inputs to the model would further improve the quality of results, enable the simulation of coastal routes (see Section 9.3.2), and

potentially address the anachronisms implicit in using modern datasets to represent prehistoric conditions.

There are two main avenues for improving the datasets used in this study: improving the detail and extent of data, and addressing the anachronistic character of the conditions that these datasets represent. First, the scale of the datasets used to assemble the DEM used by the model left many smaller rocks, banks, and other offshore hazards unrepresented. Similarly, the environmental forecasts used in this analysis tended not to cover shallow inshore areas. These were the main factors in the decision to simulate cross-Channel rather than coastal routes, despite the fact that the latter undoubtedly took place and likely influenced which cross-Channel routes were used. Obtaining more detailed and comprehensive datasets would make it possible to test these routes, and improve the operation of the model when launching and landing. Secondly, the DEM and environmental data used in this analysis are both contemporary. As they represent the lay of the land and the set of the seas in the present, they are appropriate to the extent that conditions now broadly resemble conditions in the Iron Age (see Section 1.1.2). Climatic conditions, however, changed throughout the Iron Age, and rising sea levels since the end of that period have altered the coastline. Promontory forts have been particularly affected by coastal erosion, so that some sites may have once been much larger while others may have disappeared entirely. There are several promising avenues by which improvements to the datasets used here might be reached: interpolation from more detailed data, digitisation of historic maps and charts, and the development of independent erosion and weather models. These analyses are beyond the scope of the current thesis – however future research projects may be able to address them.

In the first case, the datasets used to generate the DEM in this analysis (the SRTM terrain model and the GEBCO bathymetry model) were both chosen because of their wide coverage. One can find much more detailed datasets for specific part of the coast, and it should be possible to stich these together to create a more detailed DEM. The main problem here is that this dataset would contain holes that would either have to be excluded from model's navigable area or filled using interpolation. The same is true for bathymetry – although detailed studies of inshore waters have been performed, these studies have usually been restricted to harbours and estuaries. Better-quality bathymetry would be very useful in creating an intertidal DEM. On the terrestrial side, if more large-scale projects such as the recent LiDAR survey of the Channel Islands are undertaken, then it may become easier to generate such a dataset.[71] As far as environmental data is concerned, this approach would involve collecting overlapping data from multiple weather models and developing a process for harmonising those results – not impossible, but certainly outside the capabilities of most archaeologists.

In the second place, generating a DEM from maps and charts would likely produce the best representation of offshore hazards, given that the interpretative work (i.e. judging what constitutes a hazard) that goes into creating these documents. Using historic maps to generate a DEM also addresses the anachronism issue. Gillings (2009) has used this approach in Alderney, where the modification of the island during WWII resulted (among other things) in modern elevation models failing to represent pre-war terrain. A similar approach could be useful, especially for coastal sites that have eroded significantly since

[71] See: https://www.jerseyheritage.org/news/digital-survey--new-heritage-sites-revealed-.

the inception of accurate topographic maps.[72] However there are drawbacks here as well. At a practical level, the task of digitising maps and charts for the entire western Channel would be gargantuan. The amount of detail in the resulting dataset would be conditioned on the detail of the maps used, which may be problematic if older maps are used. In the case of environmental data, digitising historic sources would result in a near-total loss of spatial and temporal detail. The analyses performed here would not have been possible had they used month-averaged wind roses as environmental inputs, so either modern environmental data would have to be used alongside historic terrain data, or else some process for interpolating historic environmental data would be required.

In both instances, one of the main difficulties in gathering data from other sources is the harmonisation of elevation data with environmental data. Winds, currents, hills and channels are part of a single system, and so modifying one element of the system while leaving the others unchanged is obviously problematic. A direct approach to this problem would be to undertake a new set of models, focused on sea conditions and coastal erosion in the Channel. Generating a weather model specifically for future analysis has the major advantage that it could be designed specifically to represent conditions in the Iron Age, and that the resolution and extent of data could be determined by the authors of the model rather than by the availability of existing data. The main obstacle – that it would be a large project that would require input from weather, climate, and geological specialists – is also an opportunity for interdisciplinary research.

[72] Although erosion occurring prior to the creation of said maps would still be represented in the datasets.

9.4.2: Seakeeping and 'Failure Conditions'

In the analyses performed here, the only conditions for failure were reaching the maximum number of timesteps allowed in the simulation (48 hours), and not being able to move without running aground. It does not, however, allow for catastrophic failure that results in the loss of the vessel. The primary reason that conditions for catastrophic failure were not added to the model for this analysis was that relevant parameters of naval architecture (heeling angle, freeboard, etc.) for Iron Age ships remain conjectural (see Section 2.2). Additionally, if 'failure conditions' had been included in this analysis as a parameter, they would have increased the parameter spaces of all analyses and thereby the number of necessary runs. Further development of the model could add failure conditions based on parameters such as wave height, wind strength, and heading angle. If coastal voyages are considered, then water depth could also be incorporated into a set of failure conditions representing ships running aground on sandbars, striking rocks, etc.

If more failure conditions are to be added to the model then some consideration should be given as to what would have constituted 'failure' in prehistoric navigation and how an agent-based model should incorporate the conditions under which failure could have occurred. Simply ending a simulation as soon as it encounters a failure condition effectively treats that condition as if it were an explosive mine – an impediment with a hard boundary that annihilates the vessel the moment that it is encountered. However catastrophic failure is often the result of a chain of decisions, and often the potential for disaster can be seen from links further up the chain. Occasionally storms *do* appear out of nowhere, often they are spotted and navigators are able to react to them. Although the spatial and temporal resolution of environmental data in this analysis is high, compared

to the timescales involved in seafaring it is very coarse. This should be taken into account before adding failure conditions to the navigation model.

After completing these analyses, the question "under what conditions is navigation impossible?" seems less productive than the question "how do navigators respond to challenging conditions?" In the Main Analysis success rates were contextualised by calculating how many simulated vessels made landfall on the opposite coast, whether or not they reached the nodes that served as their intended destinations. Case Study 3, by necessity, explored how 'failed voyages' can be thought of as qualified successes if they have another port to put into. Future versions of the model could incorporate responses to failure conditions by having the simulated navigators attempt to find a new port, or by having them attempt to return to their original port. Such a model could produce interesting results, especially if one were able to differentiate between ports of second, third, etc. resort from its results. Letting simulated navigators choose their own landing places could also allow the navigation model to be developed into a multiagent model.

9.4.3: Long-Range Planning and Embedded Simulations

Decisions made by the navigation model have a tendency towards being short-sighted. When headings are selected by the model, the heading that is selected is the one that the simulated navigator believes will move the ship closest to the destination *over the course of the next hour*. However as we have seen in Case Study 3, this can result in ships ending up in difficult circumstances and failing to reach their destinations. Giving simulated navigators a way to make long-range plans would address this issue. Models using the 'isochrone method' developed by Hildenbrand (2015) and Slayton (2018) /

Athenstädt (2018) already address this issue by performing a complete point-destination LCP analysis for each point in an isochrone before the selection stage. Implementing a similar approach in this model would require a separate simulation for each point in each heading envelope.

These embedded simulations would in effect represent the simulated navigator 'thinking through' the remainder of the voyage before selecting a point. However, there are practical and theoretical problems with implementing such an approach into the model. First, each run would involve much more processing to complete. The average time to complete a simulation in the Main Analysis was approximately 2 minutes, and simulations in this analysis iterated over 26 timesteps on average. Performing embedded simulations in the main analysis would have increased the processing time per simulation from two minutes to just under three days.[73] Secondly, using embedded simulations as a means of 'planning ahead' gives simulated navigators a potentially-unrealistic ability to predict future conditions. While the ability to predict conditions at sea is one of the marks of good seamanship, not all conditions are equally easy to predict. The timing of tides, for example, can be predicted well ahead of a voyage (see Section 2.3.5), whereas storms at sea can be sudden and unexpected. An implementation of embedded simulations would have to address these discrepancies – for instance, it would be possible to develop 'degrading' estimation factors for these simulations or to restrict embedded simulations

[73] For the purposes of this estimate it was assumed that 150 headings outside the dead zone would be tested, and that processing time scales linearly with the number of timesteps left in the run. The resulting equation is $\sum_{i=1}^{26}(i \times 150 \times (2 \div 26))$ = 4,050 minutes, or 67.5 hours.

to a few timesteps. This second of these options has the added benefit of reducing the amount of processing necessary to implement this system.

Future development of the model should address the lack of long-range planning, by implementing a system of embedded simulations or by creating a new system entirely. For example, the script could be modified to consult precompiled meteorological predictions, or heading selection criteria could be modified to prioritise or avoid certain areas. A system to implement long-range planning would need to be tested, and the results of these simulations can provide useful context for that evaluation. The framework used in this thesis could easily be used to effect such an analysis.

9.4.4: Time to Wait and Rest

The navigation model currently assumes that simulated ships with no viable points in their heading envelope must be 'driven ashore', and that the simulation that brought them to this point is a failure. However in reality it may be advantageous to shelter behind headlands when confronted with inclement weather (McGrail 1983), or in extreme cases to put to shore entirely. Future versions of the model could accommodate this by allowing ships to fix their location in cases where (1) they are in close proximity to a landing place or sheltered area, and (2) can make no more progress. It would also be possible to allow simulations to pause at a nearby node in poor conditions, and begin again on a subsequent day. Implementing such a system would likely require one of the types of 'forward planning' discussed in the previous section, since simulated navigators would need to have a basis for the decision not to continue. The model would also have to be supplied with a list of 'sheltered areas' and 'landing places', or else include a criteria for deciding whether simulated ships are near either of these.

An analysis that allows vessels to stop and start could provide useful to a study such as this. To start with, the anchorages / landing places at which simulated navigators choose to stop could be mapped, and their proximity to coastal sites could be plotted and analysed. Additionally, nodes could be evaluated based on their status as 'stopover points'. This metric would have be useful in an analysis such as Case Study 1, which was partly focused on the potential of Guernsey as a staging ground for ships bound for Hengistbury Head; and in Case Study 3, which suggested that sites in the Isles of Scilly might have been served as a port of last resort for simulated ships that failed to reach Mounts Bay.

9.5: Concluding Remarks

The philosophy behind the development of the navigation model used in this analysis has been to be as descriptive as possible. Instead of reducing 'navigation' to a few key components in order to build a model, the approach taken here was to replicate, as far as possible, the chain of decision-making that a real navigator would have made aboard ship. The results of the analyses in this thesis validate the descriptive approach – in each analysis the results of the navigation model made an important contribution to our understanding of the Iron Age Channel: by testing the links between known trading sites, by identifying promontory forts that may have played a role in directing ships at sea, and by providing a basis for comparing the parameters of seafaring.

This navigation model was developed for this analysis, but it is not limited to investigations of the Iron Age English Channel in the same way that other, tailored models are (see Section 3.1). This model is flexible – previous sections (Section 9.4) have illustrated the variety of ways in which different methods of navigation and datasets could

be incorporated into it. This versatility makes it transferrable to other modelling contexts. In this thesis the model is used to test Iron Age navigation, but it could also be used to test claims in other seafaring contexts. For example, debates over the seafaring potential of Bronze Age sewn-plank boats (see Section 2.2.5) could be addressed by the application of this model. It could equally be applied in an historic setting such as Viking navigation, the navigation model could be used to evaluate historical sources and engage with other seafaring models (such as Indruszewski & Barton 2008, or De Roo 2014). This thesis has demonstrated the navigation model's potential, but it will ultimately be through further applications that its full potential will be realised.

Bibliography

Agius, D. 2002. In the wake of the dhow: the Arabian Gulf and Oman. Reading: Ithaca Press

Alberti, G. 2017. TRANSIT: a GIS toolbox for estimating the duration of ancient sail-powered navigation. *Cartography and Geographic Information Science*, 45(6): 510-528.

Alcock, L. 1963. Celtic archaeology and art. In E. Davies (ed) *Celtic studies in Wales: a survey*, 78–135. Cardiff: University of Wales Press.

Andersen, E., Cumlin-Pedersen, O., Vadstrup, S., & Vinner, M. 1997. *Roar Ege: Skuldelev 3 skibet som arkaeologisk eksperiment*. Roskilde: Viking Ship Museum.

Andersen, S.H. 1994. New finds of Mesolithic logboats in Denmark. In C. Westerdahl (ed) *Crossroads in Ancient Shipbuilding*, 1–10. Oxford: Oxbow Books

Arcenas, S. 2015. ORBIS and the sea: a model for maritime transportation under the Roman Empire. ORBIS Working Papers. Available at: https://orbis.stanford.edu/assets/Arcenas_ORBISandSea.pdf.

Ashbee, P. 1974. *Ancient Scilly from the first farmers to the early Christians: an introduction and survey*. Newton Abbot: David & Charles.

Athenstädt, J.C. 2018. *Reconstruction and visualization of archaeological networks*. Ph.D. Universität Konstanz.

Bayliss, A., Groves, C., McCormac, C., Bronk Ramsey C., Baillie M., Brown D., Cook G., & Switsur R. 2004. Dating. In P. Clark (ed) *The Dover Bronze Age boat*, 250–255. Swindon: English Heritage.

Beck, H.E., Zimmermann, N.E., Mcvicar, T.R., Vergopolan, N., Berg, A., & Wood, E.F. 2018. Present and future Köppen-Geiger climate classification maps at 1-km resolution. Scientific Data 5(1): 180214.

Bell, M. 1996. Environment in the First Millenium BC. In T. C. Champion & J. M. Collis (eds) *The Iron Age in Britain and Ireland: recent trends*, 5–16. Sheffield: John Collis Publications.

Bell, M., Caseldine, A., & Neumann, H. 2000. *Prehistoric intertidal archaeology in the Welsh Severn Estuary*. York: Council for British Archaeology.

Bender, B. 1986. *The archaeology of Brittany, Normandy and the Channel Islands: an introduction and guide*. London: Faber and Faber.

Bender, B., Hamilton, S., & Tilley, C. 1997. Leskernick: stone worlds; alternative narratives; nested landscapes. *Proceedings of the Prehistoric Society* 63: 147–178.

Bennett, J. 2017. *Navigation: a very short introduction*. Oxford University Press.

Benson, D., & Williams, G. 1987. Dale Fort. *Archaeology in Wales* 27: 43.

Bernardini, W., Barnash, A., Kumler, M., & Wong, M. 2013. Quantifying visual prominence in social landscapes. *Journal of Archaeological Science* 40: 3946–3954.

Berry, J., Parham, D., & Appleby, C. eds. 2019. *The Poole Iron Age logboat*. Oxford: Archaeopress Archaeology.

Bojesen-Koefoed, I.M., Crumlin-Pedersen, O., Trakadas, A., & Vikingeskibshallen. 2003. *Hjortspring: a pre-Roman Iron-Age warship in context*. Roskilde: Viking Ship Museum.

Bowen, E.G. 1969. *Saints, seaways and settlements in the Celtic lands*. Cardiff: University of Wales Press.

Bowen, E.G. 1970. 'Britain and the British seas'. In *The Irish Sea province in archaeology and history*, 13–28. Cardiff: Cambrian Archaeological Association

Bowen, E.G. 1972. *Britain and the western seaways*. London: Thames and Hudson.

Bowen, E.G. 1977. *Saints, seaways and settlements in the Celtic lands 1st ed., reprinted with revised plates and second preface*. Cardiff: University of Wales Press.

Bradley, R. 1997. *Rock art and the prehistory of Atlantic Europe: signing the land*. London: Routledge.

Bradley, R. 2005. *Ritual and domestic life in prehistoric Europe*. London: Routledge.

Bradley, R., Rogers, A., Sturt, F., Watson, A., Coles, D., Gardiner, J., & Scott, R. 2016. Maritime havens in Earlier Prehistoric Britain. *Proceedings of the Prehistoric Society* 82: 125–159.

Braudel, F. 1995. *The Mediterranean and the Mediterranean world in the age of Philip II*. Berkeley: University of California Press.

Brun, P. 1991. Le bronze atlantique et ses subdivisions culturelles: essai de définition. In C. Chevillot & A. Coffyn (eds) *L'age du bronze Atlantique: ses faciès, de L'Écosse a L'Andalousie, et leurs relations avec le bronze continental et la Méditerranée*, 11–24. Beynac-et-Cazenac: Association des Musées du Sarladais.

Burns, B. 1996. *Guernsey: an island community of the Atlantic Iron Age*. Oxford: University Committee for Archaeology.

Bushe-Fox, J.P. 1915. *Excavations at Hengistbury Head, Hampshire, in 1911–12*. London: Society of Antiquaries of London.

Bushe-Fox, J.P. 1925. *Excavation of the late-Celtic urn-field at Swarling, Kent*. London: Society of Antiquaries.

Callaghan, R., & Scarre, C. 2009. Simulating the Western Seaways. *Oxford Journal of Archaeology* 28(4): 357–372.

Cambrian Archaeological Association. 1970. *The Irish Sea province in archaeology and history*. Cardiff: Cambrian Archaeological Association.

Casson, L. 1989. *The Periplus Maris Erythraei: text with introduction, translation, and commentary*. Princeton, NJ: Princeton University Press.

Cegielski, W.H., & Rogers, J.D. 2016. Rethinking the role of agent-based modeling in archaeology. *Journal of Anthropological Archaeology* 41: 283–298.

Chapman, C.F. 1956. *Piloting, seamanship and small boat handling*. 1956–57 ed. New York: Motor Boating.

Childe, V.G. 1930. *The Bronze Age*. Cambridge: The University Press.

Childe, V.G. 1940. *Prehistoric communities of the British Isles*. London: Chambers.

Chirigati, F., Silva, V., Ogasawara, e., de Oliveira, D., Jonas, D., Porto, F., Valduriez, P. Mattoso, M. 2012. Evaluating parameter sweep workflows in high performance computing. In *SWEET '12: Proceedings of the 1st ACM SIGMOD workshop on scalable workflow execution engines and technologies, May 2012*, 1–10. New York: Association for Computing Machinery.

Clark, G. 1966. The Invasion Hypothesis in British Archaeology. *Antiquity* 40(159): 172–189.

Clark, P. 2004. *The Dover Bronze age boat*. Swindon: English Heritage.

Coates, J. 2005. The Bronze Age Ferriby Boats: seagoing ships or estuary ferry boats? *International Journal of Nautical Archaeology* 34(1): 38–42.

Cotter, C. 2000. The chronology and affinities of the stone forts along the Atlantic coast of Ireland. In J. C. Henderson (ed) *The prehistory and early history of Atlantic Europe: papers from a session held at the European Association of Archaeologists fourth annual meeting in Göteborg 1998*.BAR international series, 117–154. Oxford: Archaeopress.

Cotton, M.A. 1958. Cornish cliff castles. *Proceedings of the West Cornwall Field Club* 2(3): 113–21.

Crane, P., & Murphy, K. 2010. The excavation of a coastal promontory fort at Porth y Rhaw, Solva, Pembrokeshire, 1995-98. *Archaeologia Cambrensis* 159: 53–98.

Crawford, O.G.S. 1912. The distribution of Early Bronze Age settlements in Britain. *The Geographical Journal* 40(2): 184.

Crawford, O.G.S. 1921. *Man and his past*. London: Milford.

Crawford, O.G.S. 1936. Western seaways. In *Custom is king: studies in honour of R. R. Marett*, 181–200. London: Hutchinson's Scientific and Technical Publications.

Crumlin-Pedersen, O. 1986. Aspects of Viking Age shipbuilding in the light of the construction and trials of the Skuldelev ship-replicas 'Saga Siglar' and 'Roar Ege'. *Journal of Danish Archaeology* 5: 209.

Crumlin-Pedersen, O. 2002. *The Skuldelev ships I: topography, archaeology, history, conservation and display*. Roskilde: Viking Ship Museum in cooperation with Centre for Maritime Archaeology of the National Museum of Denmark.

Crumlin-Pedersen, O. 2006. The Dover Boat—a reconstruction case-study. *International Journal of Nautical Archaeology* 35(1): 58–71.

Cunliffe, B. 1982. Britain, the Veneti and beyond. *Oxford Journal of Archaeology* 1(1): 39–68.

Cunliffe, B. 1983. Ictis: is it here? *Oxford Journal of Archaeology* 2(1): 123–126.

Cunliffe, B. 1990. Social and economic contacts between western France and Britain. In J. L'Helgouach (ed) *La Bretagne et L'Europe préhistoriques: mémoire en hommage à Pierre-Roland Giot.* Revue archéologique de l'ouest. Supplément, 2, Rennes: CNRS.

Cunliffe, B. 1992. Le Câtel de Rozel, Jersey: the excavations of 1988–90. *The Antiquaries Journal* 72: 18–53.

Cunliffe, B., & Durham, E. 2020. *Sark: a sacred island?: volume 1: fieldwork and excavations 2004-2017*. Oxford: Oxford University School of Archaeology.

Cunliffe, B., & Galliou, P. 2000. Britons and Bretons: some new evidence from Le Yaudet. *Archaeological Journal* 157(1): 200–228.

Cunliffe, B.W. 1978. *Hengistbury Head*. London: Elek.

Cunliffe, B.W. 1987. *Hengistbury Head, Dorset: volume 1, the prehistoric and Roman settlement, 3500 BC-AD 500*. Oxford: University Committee for Archaeology.

Cunliffe, B.W. 1988. *Mount Batten, Plymouth: a prehistoric and Roman port*. Oxford: University Committee for Archaeology.

Cunliffe, B.W. 1997. *The ancient Celts*. Oxford: University Press.

Cunliffe, B.W. 2001. *Facing the ocean: the Atlantic and its peoples, 8000 BC-AD 1500*. Oxford ; New York: Oxford University Press.

Cunliffe, B.W. 2005. *Iron age communities in Britain : an account of England, Scotland and Wales from the seventh century BC until the Roman conquest* 4th ed. London: Routledge.

Cunliffe, B.W. 2015. *Le Yaudet en Ploulec'h, Côtes-d'Armor : archéologie d'une agglomération : IIe siècle av. J.-C. - XXe siècle apr. J.-C.* Saint-Brieuc: Société d'émulation des Côtes-d'Armor.

Cunliffe, B.W., Galliou, P., & Boccard-Billon, M. 2004. *Les Fouilles du Yaudet en Ploulec'h, Côtes-d'Armor*. Oxford : University of Oxford, School of Archaeology.

Cunliffe, B.W., & de Jersey, P. 1997. *Armorica and Britain: cross-Channel relationships in the late first millenium BC*. Oxford: Oxford University Committee for Archaeology.

Cunliffe, B.W., & Koch, J.T. 2010. *Celtic from the west: alternative perspectives from archaeology, genetics, language and literature*. Oxford: Oxbow.

Davies, B., & Bickler, S.H. 2013. Sailing the simulated seas: a new simulation for evaluating prehistoric seafaring. In *Across Space and Time. Papers from the 41st*

Conference on Computer Applications and Quantitative Methods in Archaeology. Perth, 25-28 March 2013: 215-223.

Davis, P.R. 1997. Some navigational considerations of pre-medieval trade between Cornwall and north-west Europe. *Cornish Archaeology* 36: 129–137.

De Roo, Tessa. 2014. *The Viking Sea from A to B: charting the nautical routes from Scandinavia to the British Isles in the early Viking period using computer simulation.* Ph.D. Cambridge.

Denny, M. 2012. *The science of navigation: from dead reckoning to GPS*. Baltimore: Johns Hopkins University Press.

Dicks, D.R. 1970. *Early Greek astronomy to Aristotle*. London: Thames & Hudson.

Dijkstra, E.W. 1959. A note on two problems in connexion with graphs. *Numerische Mathematik* 1(1): 269–271.

Dobney, K., & Ervynck, A. 2007. To fish or not to fish? Evidence for the possible avoidance of fish consumption during the Iron Age around the North Sea. In *The later Iron Age in Britain and beyond*, 403–418. Oxford: Oxbow Books.

Dos, A. 1969. Cinq campagnes de fouilles archéologiques à la cité d'Alet à Saint-Servan-sur-Mer. *Annales de Bretagne* 76: 229–45.

Driver, T. 2007. Hillforts and human movement: unlocking the Iron Age landscapes of mid Wales. In A. Fleming & R. Hingley (eds) *Prehistoric and Roman landscapes*, 83–100. Macclesfield: Windgather.

Fanjul Peraza, A. 2004. *Los castros de Asturias: una revisión territorial y funcional*. Spain: Ayuntamiento de Teverga.

Farrell, A.W., & Penny, S. 1975. The Broighter Boat: a reassessment. *Irish Archaeological Research Forum* 2(2): 28.

Fenger, N.P., & Lumbye-Hansen, H. 2000. Reconstruction of the Hjortspring Boat - theoretical performance and initial test results. In *Down the river to the sea : proceedings of the Eighth International Symposium on Boat and Ship Archaeology, Gdańsk 1997*, 111–116. Gdańsk: Polish Maritime Museum.

Ferber, J. 1999. *Multi-agent systems: an introduction to distributed artificial intelligence*. Harlow: Addison-Wesley.

Finney, B. 1998. Nautical cartography and traditional navigation in Oceania. In D. Woodward & G. M. Lewis (eds) *The history of cartography, book three: cartography in the traditional African, American, Arctic, Australian, and Pacific societies*, 443–492. Chicago: University of Chicago Press.

Floyd, R.W. Nondeterministic Algorithms. *Journal of the ACM* 14(4): 636-644.

Fojut, N. 1982. Towards a geography of Shetland Brochs. *Glasgow Archaeological Journal* 9: 37–59.

Fox, C. 1959. *The personality of Britain: its influence on inhabitant and invader in prehistoric and early historic times* 4th ed. (New impression with amendments). Cardiff: National Museum of Wales.

Frere, S., Council for British Archaeology, & University of London. Institute of Archaeology. 1961. *Problems of the Iron Age in Southern Britain: papers given at a C.B.A. conference held at the Institute of Archaeology, December 12 to 14, 1958*. London: University of London, Institute of Archaeology.

Gatty, H. 1978. *Nature is your guide: how to find your way on land and sea* New Edition. Sydney: HarperCollins Distribution Services.

George, A.R. 2000. *The epic of Gilgamesh: the Babylonian epic poem and other texts in Akkadian and Sumerian*. London: Penguin.

Giles, M.C., & Cripps, L.J. 2012. Cliff castles and the Cornish landscape. In G. Tregidga (ed) *Memory, place and identity: the cultural landscapes of Cornwall*, 12–21. London: Francis Boutle Publishers

Gillings, M. 2009. Visual affordance, landscape, and the megaliths of Alderney. *Oxford Journal of Archaeology* 28(4): 335–356.

Gillings, M. 2012. Landscape phenomenology, GIS and the role of affordance. *Journal of Archaeological Method and Theory* 19(4): 601–611.

Giot, P.R. 1963. Les civilisations atlantiques du Néolithique à l'Age du fer. In *Colloque Atlantique Brest 11 September 1961*. Rennes: Laboratoire d'anthropologie et préhistorique de la faculté des Sciences.

Giot, P.-R. 1995. *Protohistoire de la Bretagne* 2nd ed. Rennes: Ouest-France.

Gladwin, T. 1970. *East is a big bird; navigation and logic on Puluwat atoll*. Cambridge: Harvard University Press.

Gómez-Pujol, L., Pérez-Alberti, A., Blanco-Chao, R., Costa, S., Neves, M., & Del Río, L. 2014. The rock coast of continental Europe in the Atlantic. *Geological Society Memoir* 40(1): 77–88.

González, J.M., Blas Cortina, M.A. de, & Villa Valdés, A. 2002. *Los poblados fortificados del noroeste de la Península Ibérica: formación y desarrollo de la cultura castreña : Coloquios de Arqueología en la Cuenca del Navia : homenaje al prof. Dr. José Manuel González y Fernández-Valles*. Navia: Parque Histórico del Navia.

Gustas, R., & Supernant, K. 2017. Least cost path analysis of early maritime movement on the Pacific Northwest Coast. *Journal of Archaeological Science* 78: 40–56.

Hagiwara, H. 1989. *Weather routing of (sail-assisted) motor vessels*. Ph.D. Technische Universiteit Delft.

Halbout-Bertin, D. 1975. Préliminaire à une étude de l'Age du Fer en Normandie : Inventaire et répartition des sites du Hallstatt et de la Tène. *Annales de Normandie* 25(4): 227–240.

Hamilton, S., & Manley, J. 2001. Hillforts, monumentality and place: a chronological and topographic review of first millennium BC hillforts of south-east England. *European Journal of Archaeology* 4(1): 7–42.

Harper, K., Uccellini, L.W., Kalnay, E., Carey, K., & Morone, L. 2007. 50th anniversary of operational numerical weather prediction. *Bulletin of the American Meteorological Society* 88(5): 639–650.

Haselgrove, C., & Moore, T. 2007. *The later Iron Age in Britain and beyond*. Oxford: Oxbow Books.

Haselgrove, C., & Pope, R. 2007. *The earlier Iron Age in Britain and the near continent*. Oxford: Oxbow Books.

Hawkes, C. 1931. Hill forts: a retrospect. *Antiquity* 12(46): 225–228.

Hawkes, C. 1959. The A B C of the British Iron Age. *Antiquity* 33(131): 170–182.

Hawkes, C. 1966. British prehistory: the invasion hypothesis. *Antiquity* 40(160): 297–299.

Hawkes, C., & Dunning, G. 1930. The Belgae of Gaul and Britain. *Archaeological Journal* 87: 150.

Hawkes, C.F.C. 1940. *The prehistoric foundations of Europe to the Mycenean age*. London: Methuen.

Hawkes, C.F.C. 1942. The Deverel Urn and the Picardy Pin: a phase of Bronze Age settlement in Kent. *Proceedings of the Prehistoric Society* 8: 26–47.

Hawkes, C.F.C. 1977. *Pytheas: Europe and the Greek explorers, a lecture delivered at New College, Oxford on 20th May, 1975, revised and amplified with ten maps*. Oxford: Blackwell, Classics Department for the Board of Management of the Myres Memorial Fund.

Hawkes, C.F.C. 1984. *Ictis disentangled: and the British tin trade*. Oxford: Blackwell.

Henderson, J.C. 2007. *The Atlantic Iron Age*. London: Routledge.

Herring, P. 1994. The cliff castles and hillforts of West Penwith in the light of recent work at Maen Castle and Teryn Dinas. *Cornish Archaeology* 33: 41–56.

Herring, P. 2000. *St Michael's Mount, Cornwall, reports on archaeological works, 1995-1998*. Truro: Cornwall Archaeological Unit.

Herring, P., Johnson, N., Jones, A.M., Nowakowski, J.A., Sharpe, A., & Young, A. 2016. *Archaeology and landscape at the Land's End, Cornwall: the West Penwith surveys 1980-2010*. Truro: Cornwall Archaeological Unit, Cornwall Council.

Herzog, I. 2014. Least-cost paths – some methodological issues. *Internet Archaeology* 36.

Hesse, R. 2010. LiDAR-derived local relief models – a new tool for archaeological prospection. *Archaeological Prospection* 17(2): 67–72.

Heyerdahl, T. 1950. *The Kon-Tiki expedition: by raft across the South Seas*. London: Allen & Unwin.

Heyworth, A., & Kidson, C. 1982. Sea-level changes in southwest England and Wales. *Proceedings of the Geologists' Association* 93(1): 91–111.

Higuchi, T. 1983. *The visual and spatial structure of landscapes*. Cambridge: MIT Press.

Hildenbrand, J. 2015. *Shortest path calculation on water surfaces*. M.A. University of Konstanz.

Hirth, K.G. 1978. Interregional trade and the formation of prehistoric gateway communities. *American Antiquity* 43(1): 35–45.

Hong, I. 2015. *Deriving an obstacle-avoiding shortest path in continuous space: a spatial analytic approach*. Ph.D. Arizona State University.

Howard, I.P. 2018. *Animal navigation*. Oxford University Press.

Indruszewski, G., & Barton, C.M. 2008. Cost surface DEM modeling of Viking Age seafaring in the Baltic Sea. In Bernard, F. & Dakouri-Hild, A. (eds) *Beyond illustration: 2D and 3D digital technologies as tools for discovery in archaeology, international series*, 56–64. Oxford: Archaeopress.

Ingold, T. 2000. Stop, look and listen! In *The perception of the environment: essays on livelihood, dwelling and skill*, 243–287. Abingdon: Routledge

Irmischer, I.J., & Clarke, K.C. 2018. Measuring and modeling the speed of human navigation. *Cartography and Geographic Information Science* 45(2): 177–186.

Irwin, G., Bickler, S., & Quirke, P. 1990. Voyaging by canoe and computer: experiments in the settlement of the Pacific Ocean. *Antiquity* 64(242): 34–50.

James, R.W. 1957. *Application of wave forecasts to marine navigation*. Ph.D. New York University.

James, S. 1999. *The Atlantic Celts: ancient people or modern invention?* London: British Museum Press.

Jerpåsen, G.B. 2009. Application of visual archaeological landscape analysis: some results. *Norwegian Archaeological Review* 42(2): 123–145.

Jersey, P. de. 1993. The early chronology of Alet, and its implications for Hengistbury Head and cross-Channel trade in the Late Iron Age. *Oxford Journal of Archaeology* 12(3): 321–335.

Johnson, N., & Rose, P. 1982. Defended settlement in Cornwall - an illustrated discussion. In D. Miles (ed) *The Romano-British countryside: studies in rural settlement and economy* Brit. Ser., 151–209. Oxford: BAR.

Kells, L.M., Kern, W.F., & Bland, J.R. 1943. *Navigation* 1st ed. New York: McGraw-Hill Book Company.

Kinnes, I., & Hibbs, J. 1988. *The dolmens of Jersey: a guide*. St. Helier: La Haule Books.

Knight, M., Ballantyne, R., Robinson Zeki, I., & Gibson, D. 2019. The Must Farm pile-dwelling settlement. *Antiquity* 93(369): 645–663.

Kokalj, Ž., Zakšek, K., & Oštir, K. 2013. Visualisations of lidar derived models. In D. Cowley & R. Opitz (eds) *Interpreting archaeological topography: airborne laser scanning, 3D data and ground visualisation*, 100–114. Oxford: Oxbow.

Koster, E.A. 2005. *The physical geography of Western Europe*. Oxford: University Press.

Kristiansen, K., Larsen, M.T., & Rowlands, M.J. 1987. *Centre and periphery in the ancient world*. Cambridge: University Press.

Lake, M.W. 2014. Explaining the past with ABM: on modelling philosophy. In *Agent-based modeling and simulation in archaeology*, 3–35. New York: Springer International Publishing Switzerland.

Lamb, H.H. 2011. *Climate: present, past and future*. Abingdon: Routledge.

Lamb, R.G. 1980. *Iron Age promontory forts in the northern isles*. Oxford: BAR.

Lawson-Jones, A. 2013. Discoveries along the North Land's End Pipeline. *Cornish Archaeology* 52: 197–222.

Le Bihan, J.-P., & Villard, J.-F. 2011. *Archéologie d'une île à la pointe de l'Europe: Ouessant*. Quimper: CRAF Quimper.

Leidwanger, J. 2014. Maritime networks and economic regionalism in the Roman Eastern Mediterranean. *Les nouvelles de l'archéologie* (135): 32–38.

Lethbridge, T.C. 1950. *Herdsmen & hermits: Celtic seafarers in the northern seas*. Cambridge: Bowes & Bowes.

Lewis, A.R. 1958. *The northern seas: shipping and commerce in northern Europe, A.D. 300-1100*. Princeton: University Press.

Lindsay, D. 2012. Olympias under sail, and other performance matters: a practical seaman's perspective. In B. Rankov (ed) *Trireme Olympias: the final report*, 142–144. Oxford and Oakville: Oxbow Books.

Livingood, P. 2012. No crows made mounds: do cost-distance calculations of travel time improve our understanding of southern Appalachian polity size? In *Least cost analysis of social landscapes: archaeological case studies*, 14. University of Utah Press.

Llobera, M. 2000. Understanding movement: a pilot model towards the sociology of movement. In G. Lock (ed) *Beyond the map: archaeology and spatial technologies*, 65–84. Amsterdam: IOS Press.

Llobera, M. 2001. Building past landscape perception with GIS: understanding topographic prominence. *Journal of Archaeological Science* 28(9): 1005–1014.

Lloyd, A.R.J.M. 1991. Seakeeping. *Philosophical transactions of the Royal Society: physical and engineering sciences (1990-1995)* 334(1634): 253–264.

Lock, G., & Pouncett, J. 2010. Walking the Ridgeway revisited: the methodological and theoretical implications of scale dependency for the derivation of slope and the calculation of least-cost pathways. In B. Frischer, J. Crawford, & D. Koller (eds) *Making history interactive: computer applications and quantitative methods in archaeology (CAA), proceedings of the 37th international conference, Williamsburg, Virginia, United States of America, March 22-26, 2009*, 191–202. Oxford: Archaeopress.

Lock, Gary, & Pouncett, J. 2017. Spatial thinking in archaeology: Is GIS the answer? *Journal of Archaeological Science* 84: 129–135.

Lock, G., & Ralston, I. forthcoming. *Atlas of Hillforts of Britain and Ireland*. Edinburgh: Edinburgh University Press.

Lonergan, C., & Hedley, N. 2016. Unpacking isovists: a framework for 3D spatial visibility analysis. *Cartography and Geographic Information Science* 43(2): 87–102.

Mackinder, H.J. 1902. *Britain and the British seas*. London: William Heinemann.

Maguer, P. 1996. Les enceintes fortifiées de l'Age du Fer dans le Finistère. *Revue Archéologique de l'Ouest* 13(1): 103–121.

Malinowski, B. 1922. *Argonauts of the western Pacific: an account of native enterprise and adventure in the archipelagoes of Melanesian New Guinea*. London: George Routledge & Sons.

Mark, S. 2005. *Homeric Seafaring*. College Station: Texas A&M University Press.

Marsden, P. 1972. Ships of the Roman period and after in Britain. In G. Bass (ed) *A History of Seafaring*, London: Thames and Hudson.

Marsden, P.R.V. 1994. *Ships of the Port of London: first to eleventh centuries AD*. London: English Heritage.

Marsden, P.R.V. 1997. *Book of ships and shipwrecks*. London: BTBatsford/English Heritage.

Martens, M., & Carrión Marco, Y. 2011. Iron Age and Roman woodworking in the northwest of the Iberian Peninsula. *Saguntum: Papeles del Laboratorio de Arqueología de Valencia* (11): 103–104.

McGrail, S. 1978. *Logboats of England and Wales with comparative material from European and other countries*. Oxford: British Archaeological Reports.

McGrail, S. 1983. Cross-channel seamanship and navigation in the late first millennium BC. *Oxford Journal of Archaeology* 2: 299–337.

McGrail, S. 1995. Romano-Celtic boats and ships: characteristic features. *International Journal of Nautical Archaeology* 24(2): 139–145.

McGrail, S. 1997. The boat fragments. In N. Nayling & A. Caseldine (eds) *Excavations at Caldicot, Gwent: Bronze Age palaeochannels in the Lower Nedern Valley*. Research report (Council for British Archaeology); no. 108, 210–217. York: Council for British Archaeology.

McGrail, S. 1998. *Ancient boats in North-West Europe: the archaeology of water transport to AD 1500* Corrected ed. London: Longman.

McGrail, S. 2001. *Boats of the world: from the Stone Age to medieval times*. Oxford: University Press.

McGrail, S., & Switsur, R. 1975. Early British boats and their chronology. *International Journal of Nautical Archaeology* 4(2): 191–200.

Meeks, E. 2015. The design and implementation of ORBIS: The Stanford geospatial network model of the Roman world. *Bulletin of the Association for Information Science and Technology* 41(2): 17–21.

Meteorological Office. 1940. *Weather in home waters and the north-eastern Atlantic.* London: HMSO.

Milgram, J. 1997. Hydrodynamics in advanced sailing design. In *Twenty-first symposium on naval hydrodynamics*, Washington, D.C.: National Research Council.

Millar, R. 2002. *The technology and economics of water -borne transportation systems in Roman Britain*. Ph.D. University of British Columbia.

Millett, M., McGrail, S., Creighton, J.D., Gregson, C.W., Heal, S.V.E., Hillam, J., Holridge, L., Jordan, D., Spencer, P.J., Stallibrass, S., Stevens, D., & Turner, J. 1987. The archaeology of the Hasholme Logboat. *Archaeological Journal* 144(1): 69–155.

Murphy, K. 2018. The Atlantic coast. *Internet Archaeology* (48).

Mytum, H.C. 2013. *Monumentality in later prehistory : building and rebuilding Castell Henllys hillfort*. New York: Springer.

Nayling, N., McGrail, S., Bell, M., Jones, P., & Roberts, O.T.P. 2004. *The Barland's farm Romano-Celtic boat*. London: Council for British Archaeology.

Needham, J. 1971. *Science and civilisation in China. Vol. 4, Physics and physical technology*. Cambridge: University Press.

Neill, K. 1993. The Broighter Hoard: or how Carson caught the boat. *Archaeology Ireland* 7(2): 24–26.

Newhard, J.M.L., Levine, N.S., & Phebus, A.D. 2014. The development of integrated terrestrial and marine pathways in the Argo-Saronic region, Greece. *Cartography and Geographic Information Science* 41(4): 379–390.

Nowakowski, J.A., & Quinnell, H. 2011. *Trevelgue head, Cornwall: the importance of CK Croft Andrew's 1939 excavations for prehistoric and Roman Cornwall*. Cornwall: Council.

Parcero Oubiña, C. 1995. Elementos para el estudio de los paisajes castreños del Noroeste peninsular/Elements for the study of Northwestern Iberian Iron Age landscapes. *Trabajos de Prehistoria; Madrid* 52(1): 127–144.

Parry, S., & McGrail, S. 1991. A prehistoric plank boat fragment and a hard from Caldicot Castle Lake, Gwent, Wales. *International Journal of Nautical Archaeology* 20(4): 321–324.

Peel, M.C., Finlayson, B.L., & McMahon, T.A. 2007. Updated world map of the Köppen-Geiger climate classification. *Hydrology And Earth System Sciences* 11(5): 1633-1644.

Penhallurick, R.D. 1986. *Tin in antiquity: its mining and trade throughout the ancient world with particular reference to Cornwall*. London: Institute of Metals.

Petersen, H. C. 1986. *Skinboats of Greenland*. Roskilde: National Museum of Denmark.

Philbin-Briscoe, O., Simon, B., Mudur, S., Poullis, C., Rizvic, S., Boskovic, D., Liarokapis, F., Katsouri, I., Demesticha, S., & Skarlatos, D. 2017. A serious game for understanding ancient seafaring in the Mediterranean Sea. In *2017 9th international conference on virtual worlds and games for serious applications (VS-Games)*, 1–5.

Pollard, E., Corns, A., Henry, S., & Shaw, R. 2020. Coastal erosion and the promontory fort: appearance and use during Late Iron Age and Early Medieval County Waterford, Ireland. *Sustainability* 12(14): 5794.

Pouncett, J., Schulting, R. 2012. Yellow Top, Paviland: geophysical survey of a promontory fort on the Gower Peninsula. Oxford: School of Archaeology, University of Oxford.

Pouncett, J. 2013. Expanding horizons: visibility, monuments and topography. In *Across space and time: papers from the 41st annual Conference of Computer Applications and Quantitative Methods in Archaeology (CAA), Perth, 25-28 March 2013.*, Perth.

Raftery, B. 1994. *Pagan Celtic Ireland: the enigma of the Irish Iron Age*. London: Thames and Hudson.

Ralston, I. 1980. The Green Castle and the promontory forts of north-east Scotland. *Scottish Archaeological Forum* 10: 22–40.

RCAHMS. 1988. *Argyll: an inventory of the ancient monuments 6 - Mid-Argyll and Cowal*. Edinburgh: HMSO.

Redmond, M. 1995. A survey of the promontory forts of the Kerry Peninsulas. *Journal of the Kerry Arcaeological and Historical Society* 28: 5–63.

Renfrew, C., & Cherry, J.F. 1986. *Peer polity interaction and socio-political change*. Cambridge: University Press.

Roberts, O. 2004. Reconstruction and performance. In P. Clark (ed) *The Dover Bronze age boat*, 189–210. Swindon: English Heritage

Robinson, D., & Wilson, A. 2011. *Maritime archaeology and ancient trade in the Mediterranean*. Oxford: Centre for Maritime Archaeology.

Robinson, E., & Soper, E. 2011. *The hillfort glow: An experiment to explore the intervisibility between ten hillforts across north east Wales and Cheshire and their connection with their local communities.* Clwydian Range Area of Natural Beauty Report. Available at: http://www.clwydianrangeaonb.org.uk/files/904476070-The %20Hillfort %20Glow- %20final %20report.pdf.

Robinson, G. 2007. *The prehistoric island landscape of Scilly*. Oxford: Archaeopress.

Roseman, C. 1983. *Pytheas of Massalia: a critical examination of the texts*. Ph.D. University of Washington.

Rule, M., & Monaghan, J. 1993. *A Gallo-Roman trading vessel from Guernsey: the excavation and recovery of a third century shipwreck*. Candie Gardens: Guernsey Museums & Galleries.

Russell, V. 1971. *West Penwith survey*. Truro: Cornwall Archaeological Society.

Samples, M., Daida, J., Byom, M., & Pizzimenti, M. 2005. In *Proceedings of the 7th annual conference on genetic and evolutionary computation, 25 June 2005*, 1791–1792.

Sardegna, J., & Shelly, S. 2002. *The encyclopedia of blindness and vision impairment*. New York: Infobase Publishing.

Savory, H.N. 1971. A Welsh Bronze Age hillfort. *Antiquity* 45(180): 251–261.

Scanlan, M.M., Putman, N.F., Pollock, A.M., & Noakes, D.L.G. 2018. Magnetic map in nonanadromous Atlantic salmon. *Proceedings of the National Academy of Sciences of the United States of America* 115(43): 10995–10999.

Seager, R., Battisti, D.S., Yin, J., Gordon, N., Naik, N., Clement, A.C., & Cane, M.A. 2002. Is the Gulf Stream responsible for Europe's mild winters? *Quarterly Journal of the Royal Meteorological Society* 128(586): 2563–2586.

Severin, T. 1978. *The Brendan voyage*. London: Hutchinson.

Sharpe, A. 1992. Treryn Dinas: cliff castles reconsidered. *Cornish Archaeology* 31: 65–68.

Simpson, C. 2010. *Water in Burgidale: Shetland fisheries in a pre-electronic age*. Lerwick: Shetland Amenity Trust.

Slayton, E.R. 2018. *Seascape Corridors. Modeling Routes to Connect Communities Across the Caribbean Sea*. Ph.D. Leiden University.

Smith, K. 2016. *Maritime perspectives on the coastal promontory forts of Pembrokeshire*. MSt. University of Oxford.

Souman, J.L., Frissen, I., Sreenivasa, M.N., & Ernst, M.O. 2009. Walking straight into circles. *Current Biology* 19(18): 1538–1542.

Stančič, Z., Dular, J., Gaffney, V., & Tecco-Hvala, S. 1995. A GIS-based analysis of later prehistoric settlement patterns in Dolenjska, Slovenia. In J. Wilcock & K. Lockyear (eds) *Computer applications and quantitative methods in archaeology 1993*, 161–164. Oxford: Tempus Reparatum.

Stojanovic, N., & Stojanovic, D. 2013. High–performance computing in GIS: techniques and applications. *International Journal Of Reasoning-based Intelligent Systems* 5(1): 42–49.

Straker, V., Brown, A., Fyfe, R., & Jones, J. 2012. Later Bronze Age and Iron Age environmental background. In C. J. Webster (ed) *The Archaeology of South West England, South West Archaeological Research Framework, Resource Assessment and Research Agenda*, 103–116. Taunton: Somerset County Council.

Talley, L.D., Pickard, G.L., & Emery, W.J. 2011. *Descriptive physical oceanography: an introduction* 6th ed. London: Elsevier Academic Press.

Theodossiou, E., Manimanis, V.N., Mantarakis, P., & Dimitrijevic, M.S. 2011. Astronomy and constellations in the Iliad and Odyssey. *Journal of Astronomical History and Heritage* 14: 22–30.

Tilley, C., & Bennett, W. 2001. An archaeology of supernatural places: the case of West Penwith. *Journal of the Royal Anthropological Institute* 7(2): 335–362.

Tilley, C.Y. 1994. *A phenomenology of landscape : places, paths and monuments*. Oxford: Berg.

Tilley, C.Y. 2010. *Interpreting landscapes : geologies, topographies, identities*. Walnut Creek: Left Coast Press.

Tobler, W. 1993. *Non-isotropic modeling*. Santa Barbara: National Centre for Geographic Information and Analysis.

Turner, J. 1981. The Iron Age. In I. G. Simmons (ed) *The environment in British prehistory*, London: Duckworth.

Turvey, M.T. 1992. Affordances and prospective control: an outline of the ontology. *Ecological Psychology* 4(3): 173–187.

UK Hydrographic Office. 2005. *Channel pilot*. London: United Kingdom Hydrographic Office.

Vagn Valbjørn, K., Rasmussen, H.P., & Jørgensen, J.A. 2000. Reconstruction of the Hjortspring Boat - philosophy, execution and initial result. In *Down the river to the sea : proceedings of the Eighth International Symposium on Boat and Ship Archaeology, Gdańsk 1997*, 103–110. Gdańsk: Polish Maritime Museum.

Van De Noort, R., Cumby, B., Blue, L., Harding, A., Hurcombe, L., Hansen, T.M., Wetherelt, A., Wittamore, J., & Wyke, A. 2014. Morgawr: an experimental Bronze Age-type sewn-plank craft based on the Ferriby boats. *International Journal of Nautical Archaeology* 43(2): 292–313.

Van de Noort, R., Middleton, R., Foxon, A., & Bayliss, A. 1999. The 'Kilnsea-boat', and some implications from the discovery of England's oldest plank boat remains. *Antiquity* 73(279): 131–135.

Van de Noort, V.D.N., & Van de Noort, R. 2006. Argonauts of the North Sea - a social maritime archaeology for the 2nd millennium BC. *Proceedings of the Prehistoric Society* 72: 267–287.

VanHorn, J.E., & Mosurinjohn, N.A. 2010. Urban 3D GIS modeling of terrorism sniper hazards. *Social Science Computer Review* 28(4): 482–496.

Waddell, J. 1991. The Irish Sea in Prehistory. *The Journal of Irish Archaeology* 6: 29-40.

Westerdahl, C. 2000. From land to sea, from sea to land: on transport zones, borders and human space. In L. Jerzy (ed) *Down the river to the sea : proceedings of the Eighth International Symposium on Boat and Ship Archaeology, Gdańsk 1997*, 11–20. Gdańsk: Polish Maritime Museum.

Wheatley, D., & Gillings, M. 2000. Vision, perception and GIS. In G. Lock (ed) *Beyond the map: archaeology and spatial technologies*, 1–27. Amsterdam: IOS Press.

Wheeler, M., & Richardson, K.M. 1957. *Hill-forts of northern France*. Oxford: Printed at the University Press by Charles Batey for the Society of Antiquaries, London.

White, D.A. 2015. The basics of least cost analysis for archaeological applications. *Advances in Archaeological Practice* 3(4): 407–414.

Wilkes, E. 2004. *Iron Age maritime nodes on the English Channel coast: an investigation into the location, nature and context of early port and harbours*. Ph.D. Bournemouth University.

Wilkes, E. 2007. Prehistoric sea journeys and port approaches: the south coast and Poole Harbour. In V. Cummings & R. Johnston (eds) *Prehistoric Journeys*, 121–130. Oxford: Oxbow Books.

Wooding, J.M. 1996. *Communication and commerce along the western sealanes AD 400-800*. Oxford: Tempus Reparatum.

Wright, E.V. 1990. *The Ferriby boats: seacraft of the Bronze Age*. London: Routledge.

Wright, E.V., Hedges, R.E.M., Bayliss, A., & Van de Noort, R. 2001. New AMS radiocarbon dates for the North Ferriby boats—a contribution to dating prehistoric seafaring in northwestern Europe. *Antiquity* 75(290): 726–734.

Wurzer, G., Kowarik, K., & Reschreiter, H. 2014. *Agent-based Modeling and Simulation in Archaeology*. New York: Springer.

MODELLING SEAFARING IN IRON AGE ATLANTIC EUROPE

KARL SMITH

Kellogg College, University of Oxford

Supervised by Rick Schulting & John Pouncett

A thesis submitted in two volumes in partial fulfilment of the requirements of Oxford University for the degree of Doctor of Philosophy.

Volume II

November 2020

Table of Contents

Volume II

Table of Contents 1

List of Figures.....2

Figures 6

List of Tables.....75

Tables 76

Appendix I: Promontory Fort Catalogue.....97

Appendix II: Natural Prominence Catalogue 117

Appendix III: Case Study 3 Simulation Plots.....171

List of Figures

Figure 1.1: The European Environmental Agency's 'Atlantic Geographical Bioregion' overlaid on areas with a Temperate Oceanic Climate. 6

Figure 1.2: Archaeological boundaries around and within Atlantic Europe proposed by Westerdahl (2000) and Henderson (2007). 7

Figure 1.3: Topography and 'metal rich zones' within Atlantic Europe. 8

Figure 1.4: 'Probable sea routes' to Britain proposed by Sir Cyril Fox, after (Fox 1959, Maps A & B). 9

Figure 1.5: Crawford's western sea routes, after Crawford (1936, 183). 10

Figure 1.6: Bowen's 'Western Seaways' (Bowen 1970, 19). 11

Figure 1.7: Cunliffe's (2001) map of Iron Age Exchange Systems (left) and a detail from a 'cognitive geography of the Atlantic Zone' in *Celtic From the West* (after Cunliffe 2001, Fig. 7.34; Cunliffe & Koch 2010, Fig. 1.4.). 12

Figure 1.8: Maps of schemes of contact proposed for the Atlantic Zone by Henderson, after (Henderson 2007, 286 & 296). 13

Figure 1.9: Areas with coastal promontory forts (after Lamb 1980, Fig. 1; expanded to include Spanish promontory forts (see Oubiña 1995, González et al. 2002, Fanjul-Peraza 2004). 14

Figure 1.10: Distribution of Promontory Forts in Britain and Armorica (after Wheeler & Richardson 1957; Halbout-Bertin 1975; Bender 1986; Lock & Ralston 2017; GeoBretagne). 15

Figure 1.11: "Multivallate promontory forts in Armorica and south-west England" (after Henderson 2007, Fig. 4.14, after Johnson & Rose 1982, Fig 10; Maguer 1996, 3). 16

Figure 2.1: Locations and dates for ships mentioned in the text. 17

Figure 2.2: Illustration of construction stages of the Poole Logboat (after Berry et al. 2019, 66). 18

Figure 2.3: Photographs of the Broighter boat model, after Farrell & Penny 1975, 16. 19

Figure 2.4: Plan of the hide boat Brendan (after Severin 1978, 258-259). 20

Figure 2.5: Reconstruction drawing of Blackfriars 1, showing hooked nails used to attach planks to strakes (after Marsden 1994, Fig. 69). 21

Figure 2.6: Model of the Barlands Farm boat (after Nayling et al. 2004, Fig. 8.3). Note that the replica has been fitted with a fore-and-aft sail rather than a square sail. 22

Figure 2.7: Strength of currents in the western Channel, based on hydrodynamic data used in simulations. 23

Figure 2.8: Illustration of the use of meids to obtain a fix (A) and to demarcate an area (B). 24

Figure 2.9: Illustration of the movement of stars and the sun as experienced by a voyager at sea, (after Bennett 2017, Figure 1). 25

Figure 3.1: Cost surface generated by Indruszewski & Barton; “lightest is lowest cost and darkest is highest cost” (after Indruszewski & Barton 2008, Ch. 5 Pl. 11). 26

Figure 3.2: Illustrations of the isochrone method (after Hagiwara (1989; left) and Hildenbrand (2015; right)). 26

Figure 4.1: Sample GUI (above), and console (below) from the navigation model. 27

Figure 4.2: A step-by-step diagram of the operation of the Navigation Model. 28

Figure 4.3: Sample model outputs. 29

Figure 4.4: Illustration of the process used to retrieve values from NetCDF files. 29

Figure 4.5: Illustration of the process used to generate headings. Note that the diagram is simplified: here rays are separated by 20°, whereas ray separation in the script is 1°. 30

Figure 4.6: Possible scenarios for site grid – skyline evaluation: (A) all points are obstructed by topography, (B) some points are obstructed by topography, and (C) skyline maximum distance intersects feature grid. 31

Figure 4.7: Comparison of a 2D viewshed (isovist) and a 3D rendering generated for the same scene. Note that according to the 2D image both pyramids are classified as ‘50% visible’. 31

Figure 4.8: Radial array – DEM surface intersection, shown in profile. 32

Figure 4.9: Results of radial array – DEM intersection transformed from Cartesian to projective coordinates. 32

Figure 4.10: Path-distance generation applied to the ‘dead end’ problem. 33

Figure 4.11: Demonstration of the convex path algorithm. Polygons representing obstacles are split by start-end line (I), and points are extracted from each smallest split feature (II, selected features are shaded). Points from the split features are then used to construct a path-distance line (III). 33

Figure 5.1: Map of the western Channel, showing waterways and landforms. 34

Figure 5.2: Speed diagrams for the *Roar Ege* in green, and a modern sailboat in red (after Mette Kryger, redrawn from Max Vinner, https://www.vikingeskibsmuseet.dk/en/professions/education/exercises/the-speed-diagram/). 35

Figure 5.3: Distribution of landmarks within the study area. 36

Figure 5.4: Accuracy of LRM analyses in identifying drop values from the DBIH database. 37

Figure 5.5: Environmental data coverages. 38

Figure 5.6: Nodes on the northern shore of the Channel identified by Wilkes (2004), and by the author. 39

Figure 5.7: P2-S1-Depth contours for the western Channel, based on bathymetry used in simulations 40

Figure 5.8: Average speed (in knots) for successful simulations along all routes in the Main Analysis, per day. Alternate months are highlighted. 41

Figure 5.9: Percentage of simulations for all routes that reach their destinations in the Main Analysis, per day. Alternate months are highlighted. 42

Figure 5.10: Percentage of simulations for all routes that reach their destinations (dark green) with the percentage of extra simulations that reach the opposite coast added (light green) in the Main Analysis, per day. Alternate months are highlighted. 43

Figure 5.11: Correlation between daily averages where success rates were high (green) and speed was high (orange), with periods of high coincidence (within 20 percentage points) highlighted. 44

Figure 5.12: Nodes classified according to average speed / success rates from the Main Analysis. 45

Figure 5.13: Average speed for routes simulated in the Main Analysis. Cells corresponding to slower routes are red, and cells matching faster routes are yellow. ... 46

Figure 5.14: Success rates for routes simulated in the Main Analysis. Cells corresponding to less successful routes are shaded dark green, and vice versa. 47

Figure 5.15: Difference in average speeds for routes simulated in the Main Analysis. Cells corresponding to more successful northbound routes are red, those corresponding to southbound routes are blue. 48

Figure 5.16: Difference in average success rates for routes simulated in the Main Analysis. Cells corresponding to more successful northbound routes are red, those corresponding to southbound routes are blue. 49

Figure 5.17: Results of line density analysis for all simulations. 50

Figure 5.18: Results of line density analysis for all successful simulations..... 50

Figure 5.19: Visibility results per landmark type. 51

Figure 5.20: Landmarks used in the Main Analysis, symbolised by number of sightings. 51

Figure 5.21: Density of landmark sighting locations in the Main Analysis. 52

Figure 6.1: Average speeds and success rates per day in study period. 53

Figure 6.2: Average speed and success values for Case Study 1. In the first tier, light and dark green indicate high and low success rates. In the second tier, orange and red indicate faster and slower speeds. In the third tier red indicates better northbound value, blue indicates better southbound value. 54

Figure 6.3: Average speeds and success rates, and differentials for landmark sets in Case Study 1. Routes are bidirectional (averaged across northbound and southbound voyages). In the first tier, light and dark green indicate high and low success rates. In the second tier, orange and red indicate faster and slower speeds. In the third tier red indicates better northbound value, blue indicates better southbound value. 55

Figure 6.4: Average speeds and success rates for ship parameterisations in Case Study 1. In the first column, orange and red indicate faster and slower speeds. In the second column, light and dark green indicate high and low success rates. 56

Figure 6.5: Average speeds and success rates for reckoning ranges in Case Study 1. In the first column, orange and red indicate faster and slower speeds. In the second column, light and dark green indicate high and low success rates. 57

Figure 6.6: Track densities for all simulations in Case Study 1. 58

Figure 6.7: Track densities for all successful simulations in Case Study 1..... 59

Figure 6.8: Track densities for successful simulations in Case Study 1, excluding simulations originating and terminating at St. Peter Port. 60

Figure 6.9: Sightings density for simulations in Case Study 1. 61

Figure 6.10: Comparison of general average success rates and speeds for parameter inputs to simulations in Case Study 1. 62

Figure 7.1: Ship track density results for all simulations performed for Case Study 2.. 63

Figure 7.2: Ship track density results for all successful simulations performed for Case Study 2. 64

Figure 7.3: Ship track density results for all successful northbound simulations performed for Case Study 2. 65

Figure 7.4: Ship track density results for all successful southbound simulations performed for Case Study 2. 66

Figure 7.5: Sighting density results for all simulations performed for Case Study 2..... 67

Figure 7.6: Average speeds and success rates for combinations of estimation ranges and leaving times in Case Study 2. Light and dark green indicate high and low success rates. Yellow and red indicate fast and slow speeds. 68

Figure 7.7: Average speeds and success rates for combinations of estimation ranges and vessel parameterisations in Case Study 2. Light and dark green indicate high and low success rates. Yellow and red indicate fast and slow speeds. 69

Figure 7.8: Average speeds and success rates for combinations of vessel parameterisations and leaving times in Case Study 2. Light and dark green indicate high and low success rates. Yellow and red indicate fast and slow speeds. 70

Figure 7.9: Summary of relative parameter effects in Case Study 2. 71

Figure 8.1: Simulated ship tracks for Case Study 3, and for the Brest-Penzance route from the Main Analysis. 72

Figure 8.2: Apparent size of landmarks sighted on the northern shore of the western Channel in Case Study 3..... 73

Figure 8.3: Apparent size of landmarks sighted on the southern shore of the western Channel in Case Study 3..... 74

Chapter 1 Figures

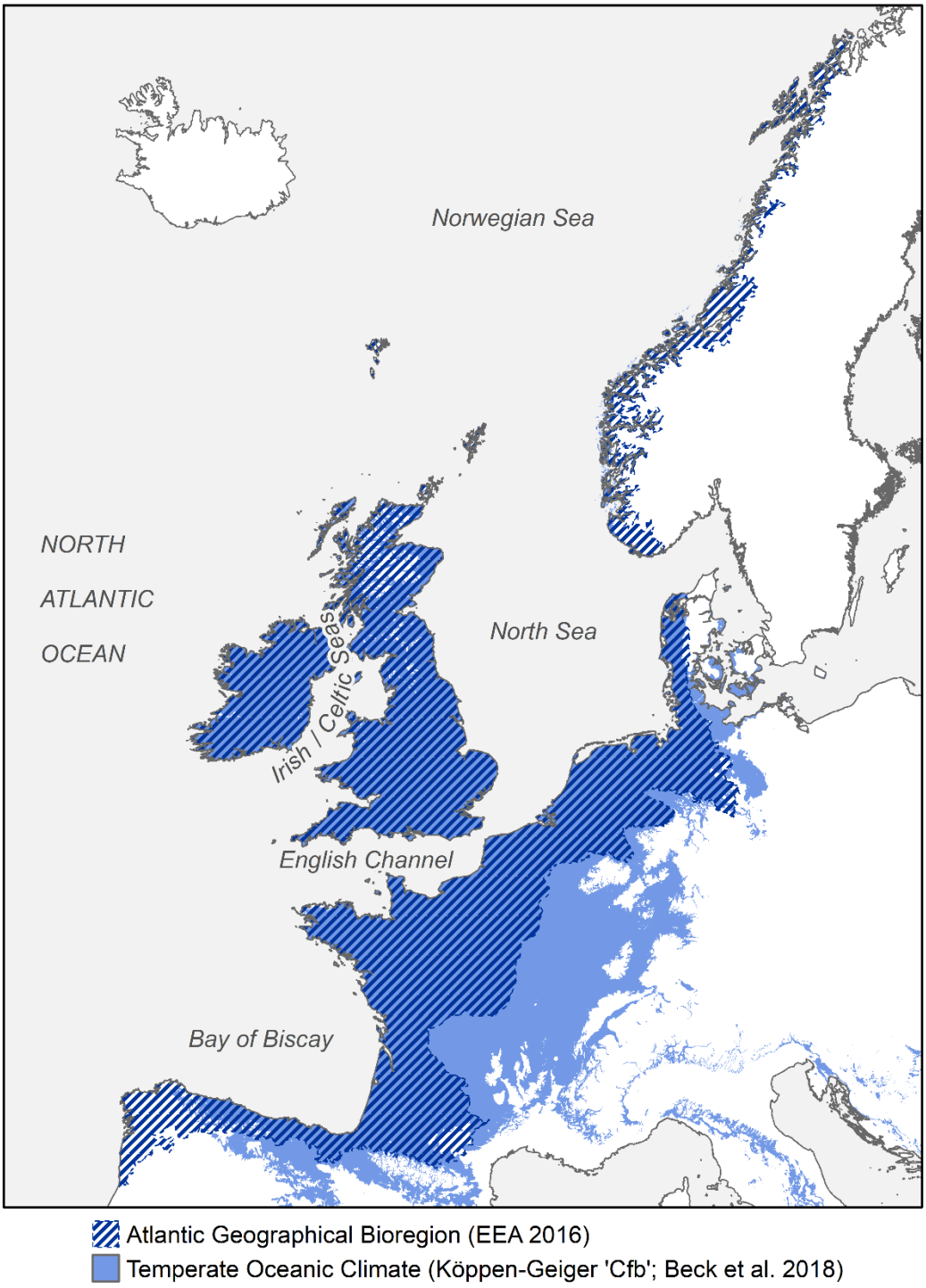
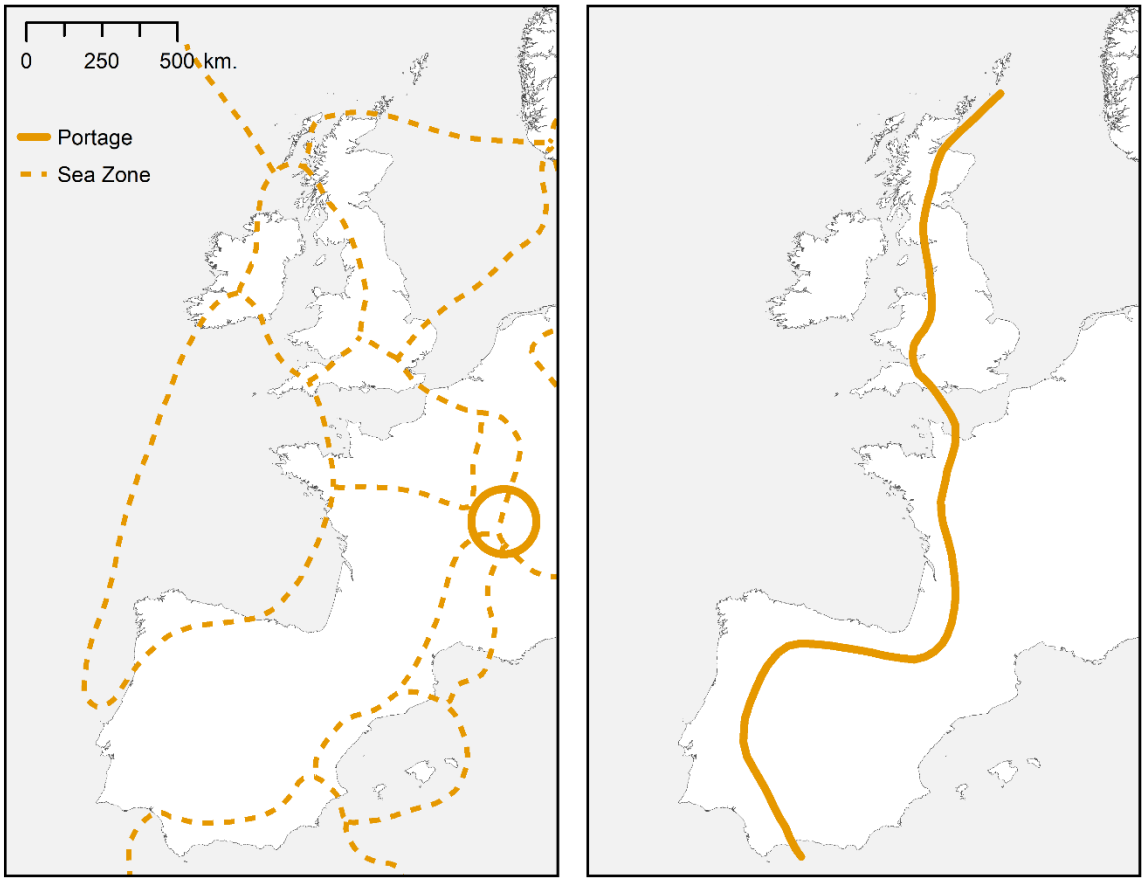


Figure 1.1: The European Environmental Agency's 'Atlantic Geographical Bioregion' overlaid on areas with a Temperate Oceanic Climate.



Detail of Westerdahl's "Coastal Zones of Europe" (2000)

Henderson's "Atlantic Europe" (2007)

Figure 1.2: Archaeological boundaries around and within Atlantic Europe proposed by Westerdahl (2000) and Henderson (2007).

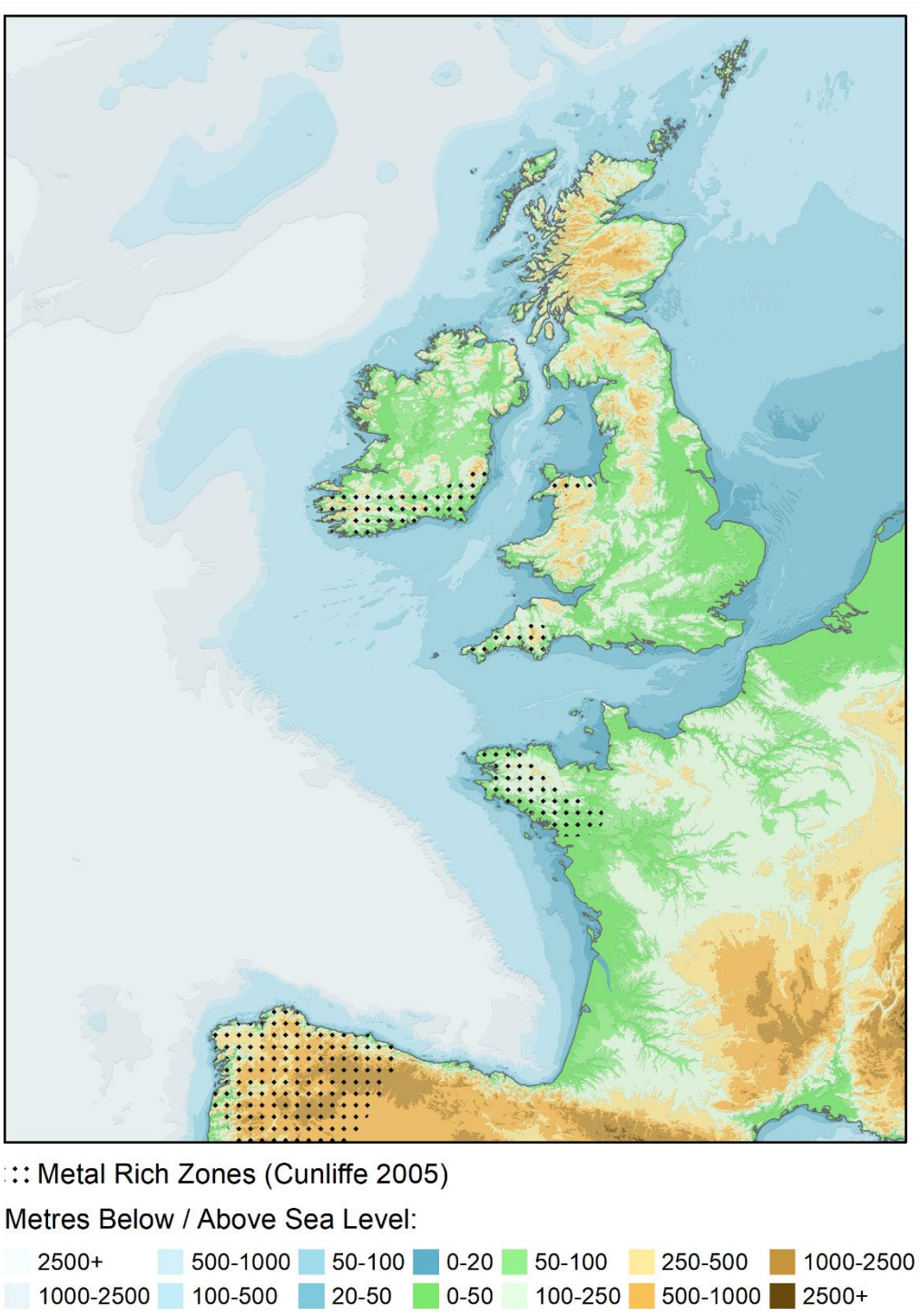


Figure 1.3: Topography and ‘metal rich zones’ within Atlantic Europe.

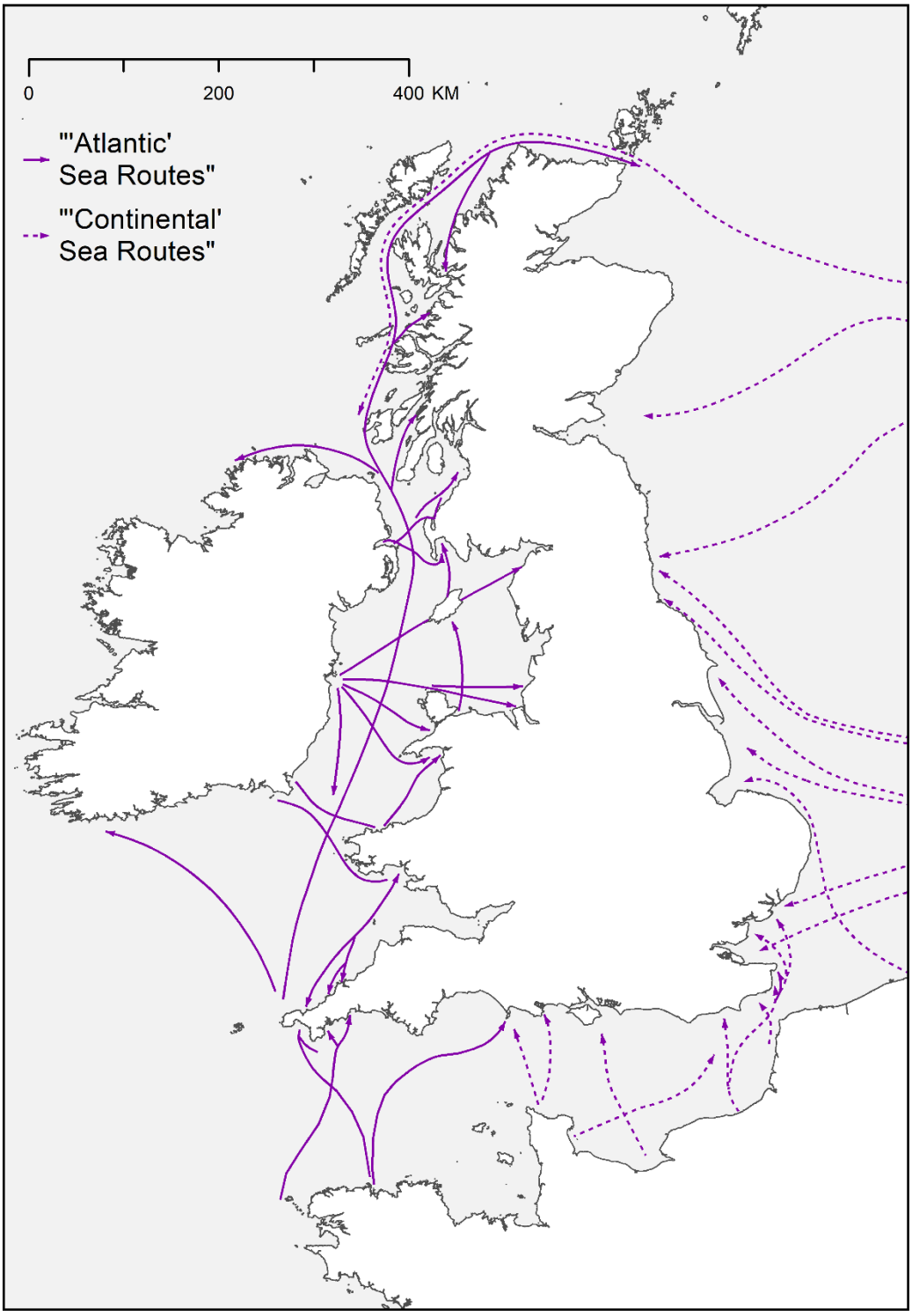


Figure 1.4: ‘Probable sea routes’ to Britain proposed by Sir Cyril Fox, after (Fox 1959, Maps A & B).

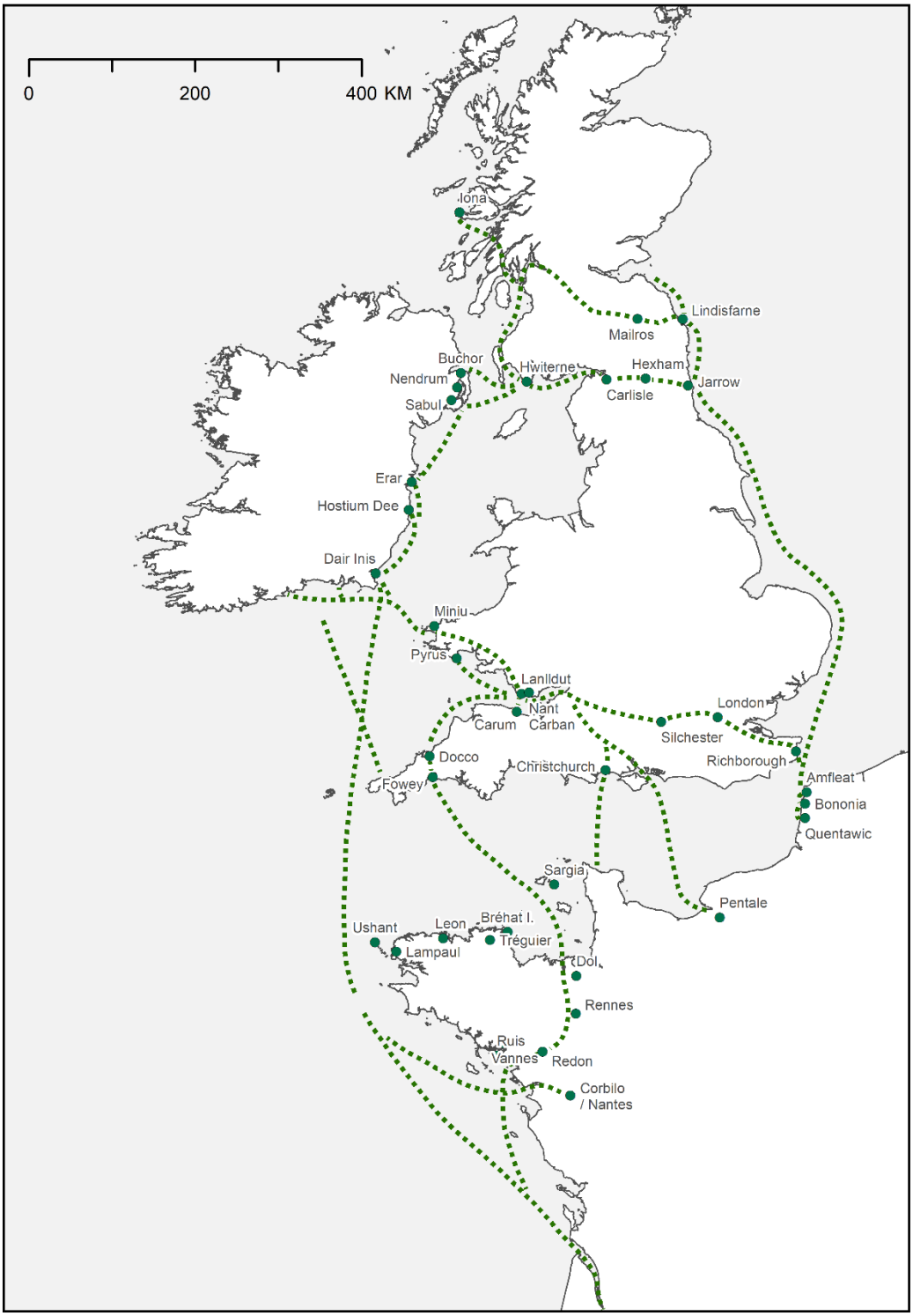


Figure 1.5: Crawford's western sea routes, after Crawford (1936, 183).

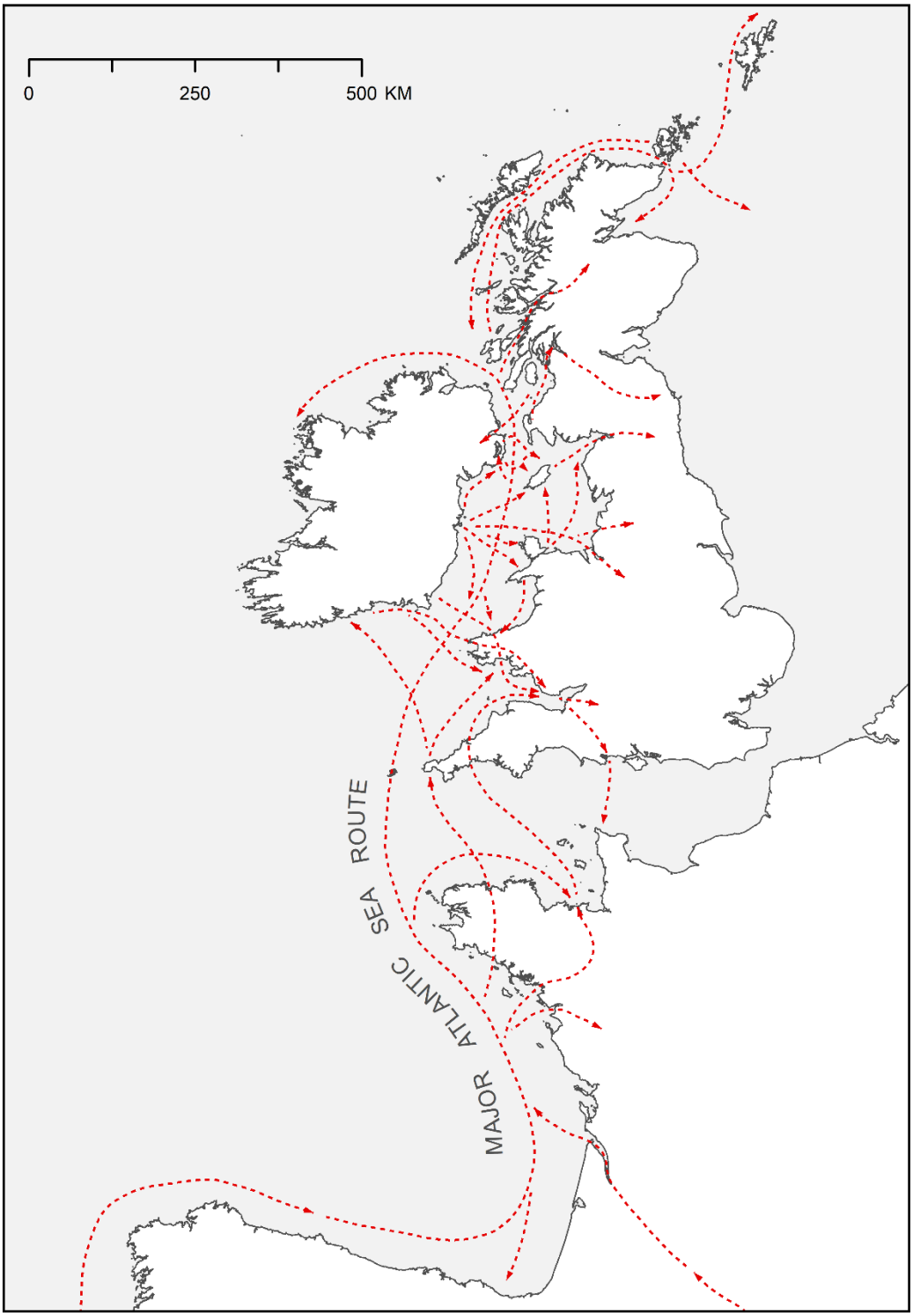
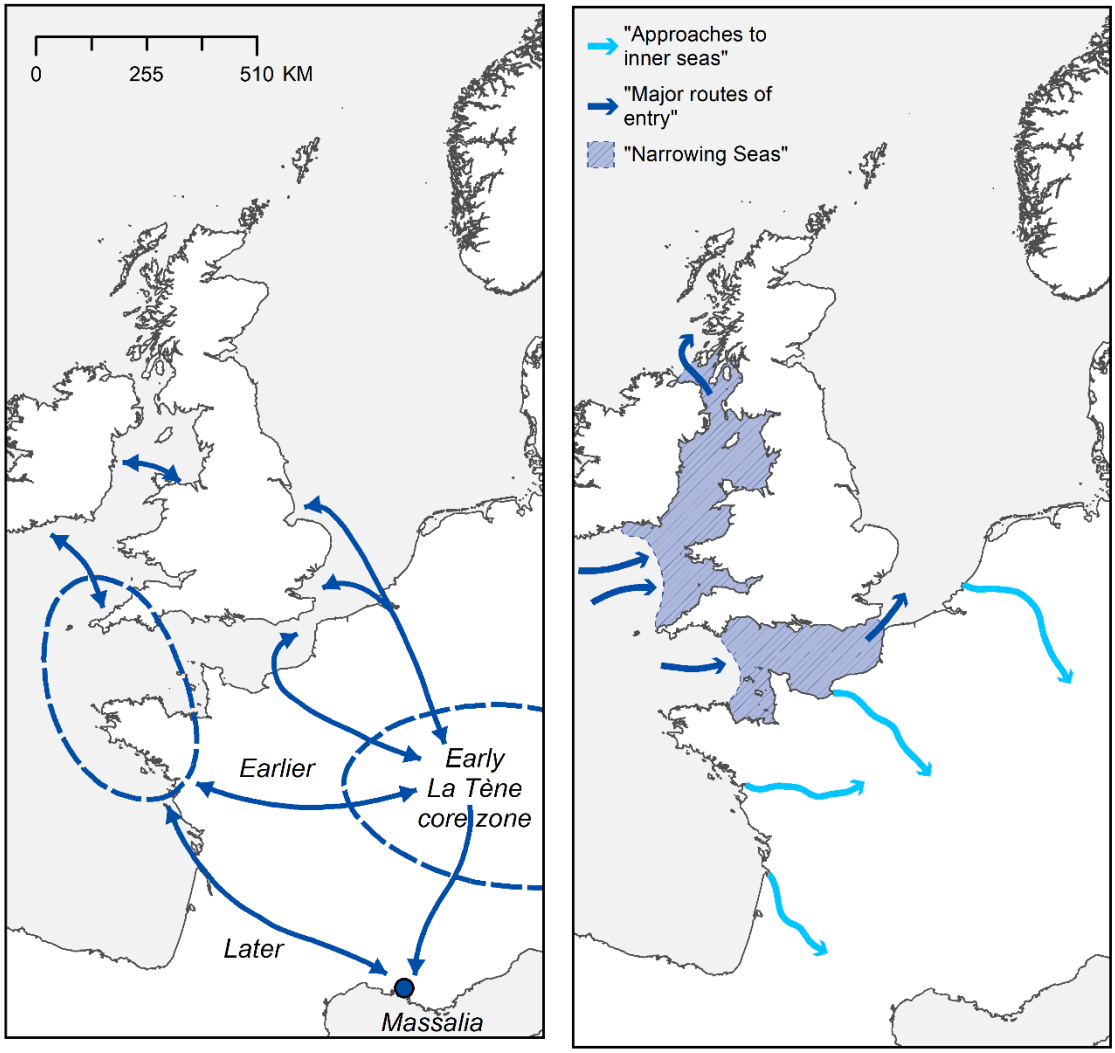


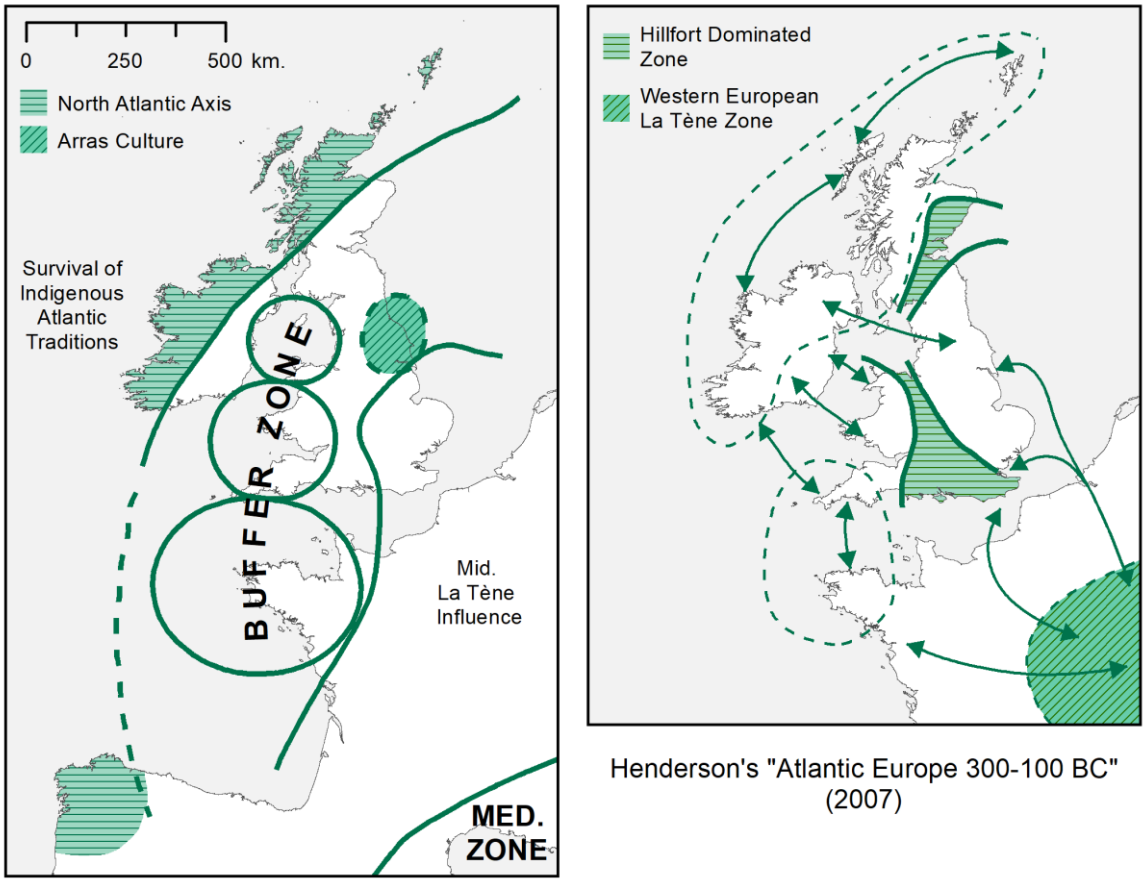
Figure 1.6: Bowen's 'Western Seaways' (Bowen 1970, 19).



Detail from "The Major Exchange Systems 500-200 BC" (Cunliffe 2001)

Detail from a "Cognitive Geography of the Atlantic Zone" (Cunliffe & Koch 2010)

Figure 1.7: Cunliffe's (2001) map of Iron Age Exchange Systems (left) and a detail from a 'cognitive geography of the Atlantic Zone' in *Celtic From the West* (after Cunliffe 2001, Fig. 7.34; Cunliffe & Koch 2010, Fig. 1.4.).



Henderson's "Spheres of interaction in the northern Atlantic Zone 600-100 BC" (2007)

Henderson's "Atlantic Europe 300-100 BC" (2007)

Figure 1.8: Maps of schemes of contact proposed for the Atlantic Zone by Henderson, after (Henderson 2007, 286 & 296).

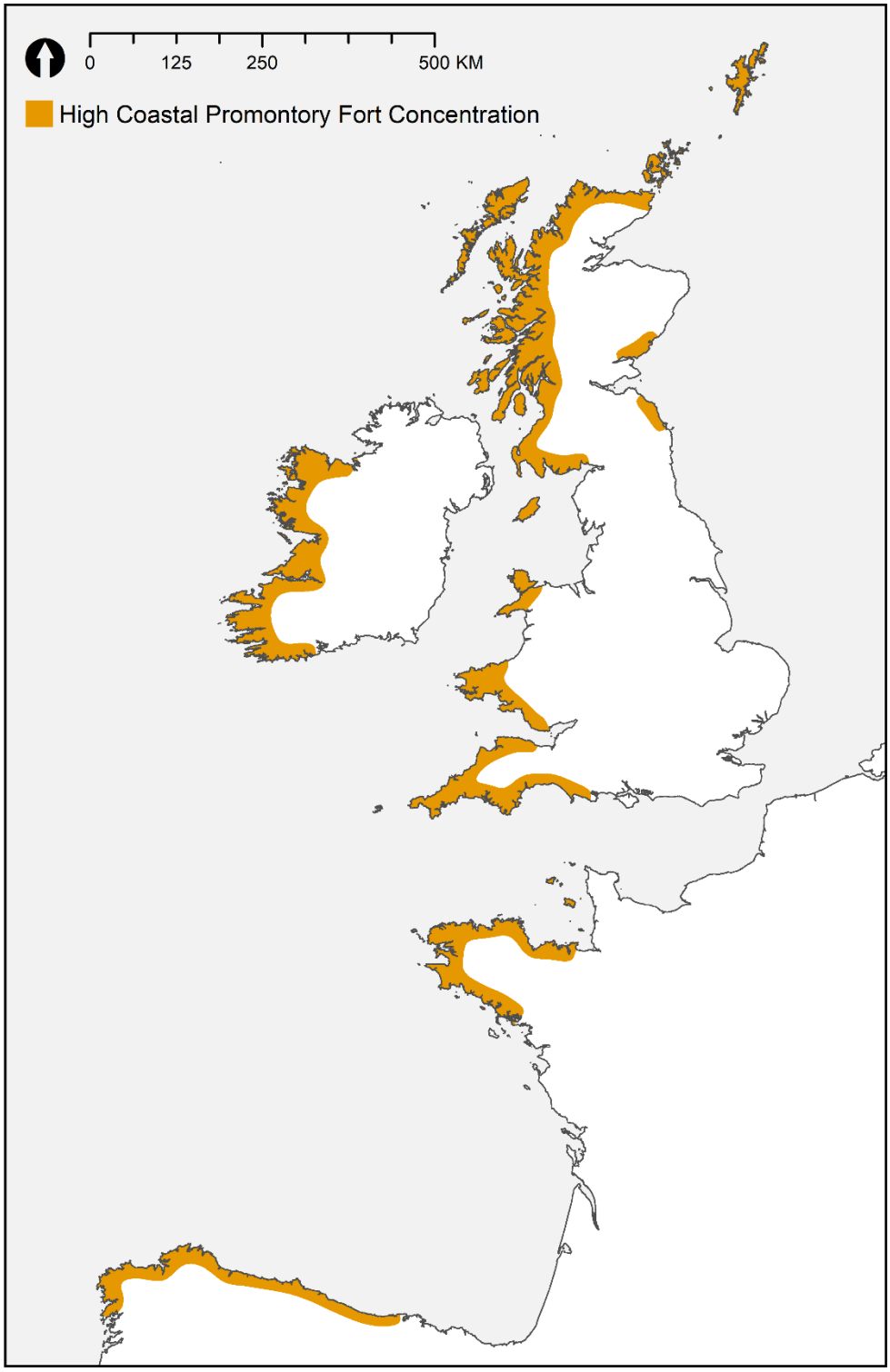


Figure 1.9: Areas with coastal promontory forts (after Lamb 1980, Fig. 1; expanded to include Spanish promontory forts (see Oubiña 1995, González et al. 2002, Fanjul-Peraza 2004).

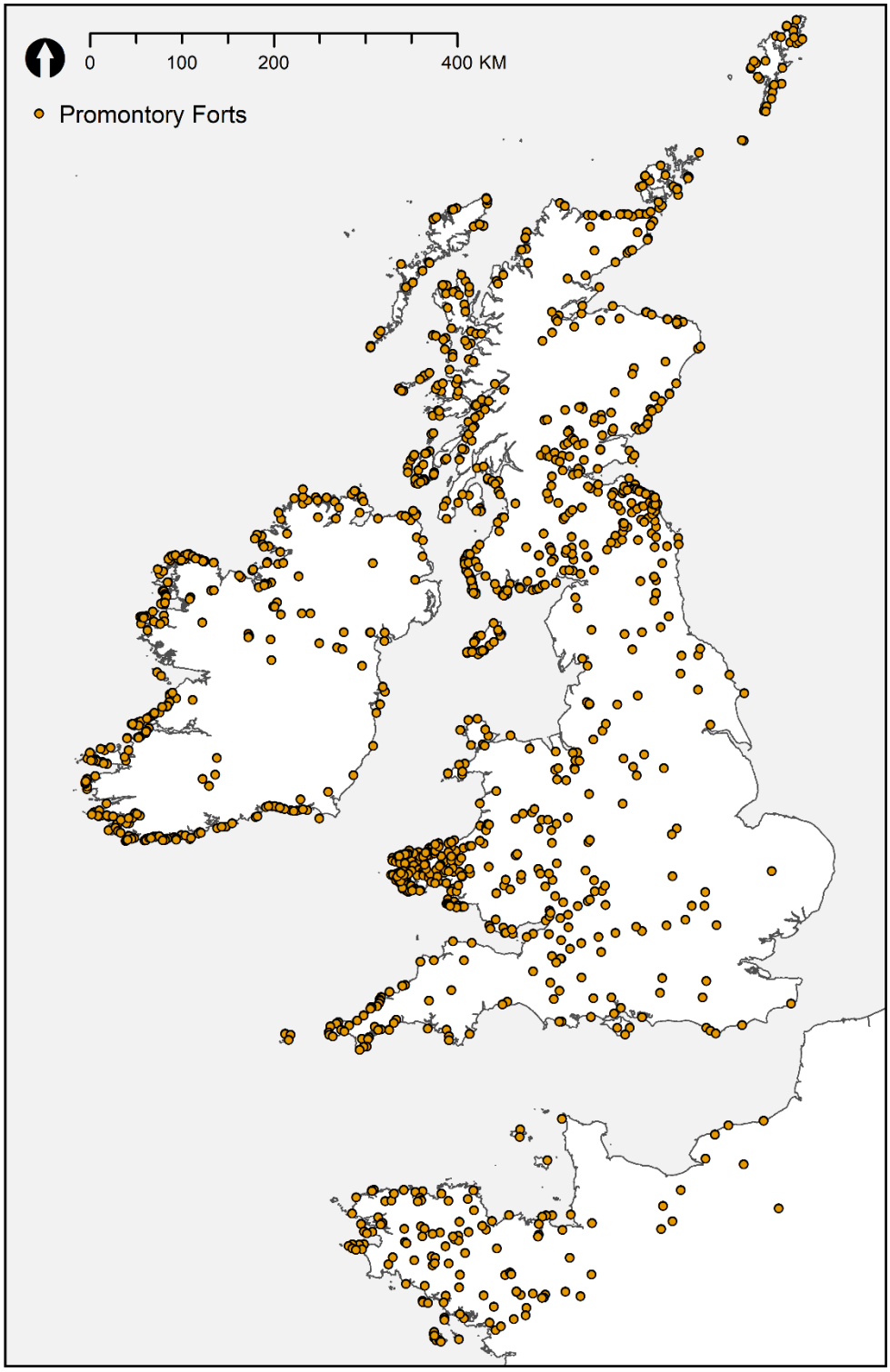
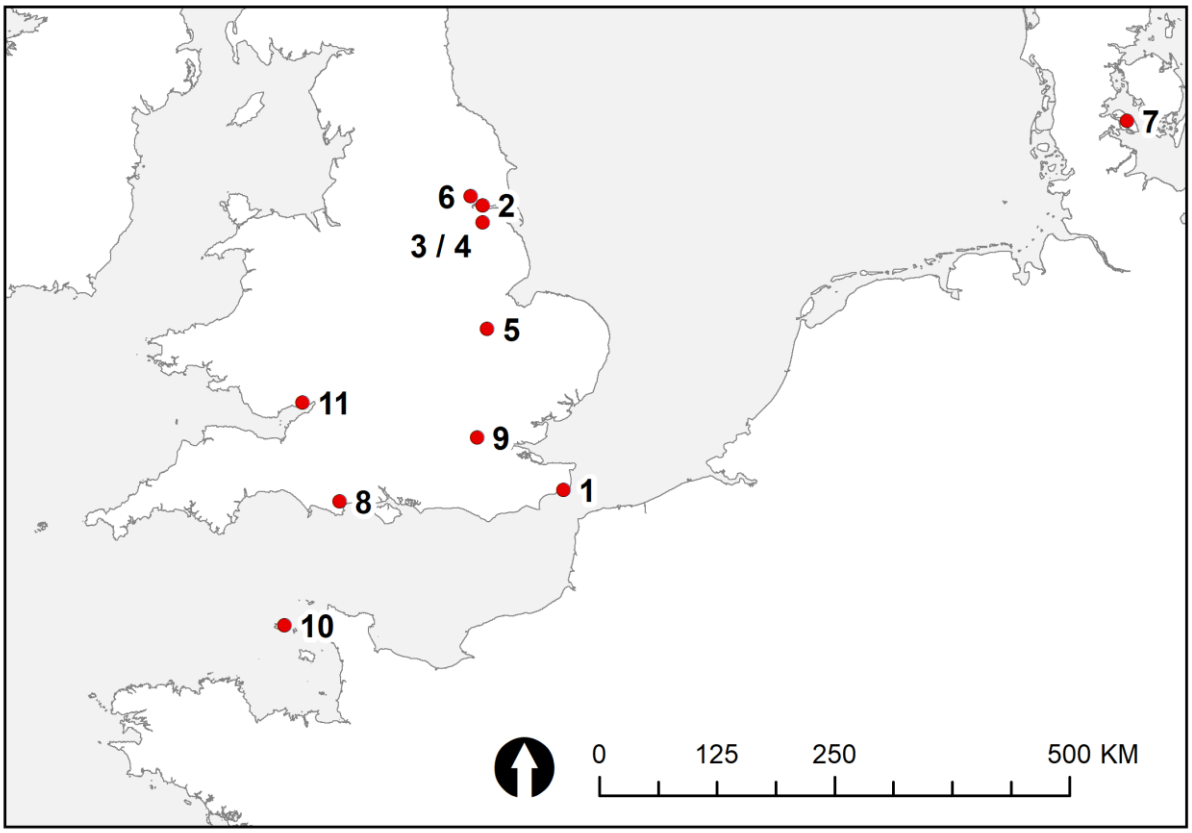


Figure 1.10: Distribution of Promontory Forts in Britain and Armorica (after Wheeler & Richardson 1957; Halbout-Bertin 1975; Bender 1986; Lock & Ralston 2017; GeoBretagne).



Figure 1.11: "Multivallate promontory forts in Armorica and south-west England" (after Henderson 2007, Fig. 4.14, after Johnson & Rose 1982, Fig 10; Maguer 1996, 3)

Chapter 2 Figures



No.	Name	Type	Date	Citation
1	Dover	Sewn Plank	1575-1520 BC	Bayliss et al. 2004
2	North Ferriby 1	Sewn Plank	1880-1680 BC	Wright et al. 2001
3	Brigg 'Raft'	Sewn Plank	825-760 cal BC	Switsur 1981
4	Brigg Logboat	Logboat	780-493 cal BC*	McGrail & Switsur 1975
5	Must Farm 1	Logboat	c. 800-400 cal BC	http://www.mustfarm.com/bronze-age-river/discoveries/
6	Hasholme	Logboat	699-323 BC	Millett et al. 1987
7	Hjortspring	Sewn Plank	c. 300 BC	Bojesen-Koefoed et al. 2003
8	Poole	Logboat	397-176 BC	Berry et al. 2019, McGrail & Swistur 1975
9	Blackfriars 1	Romano-Celtic	130-175 AD	Millar 2002
10	St. Peter Port 1	Romano-Celtic	c. 280 AD	Millar 2002
11	Barland's Farm	Romano-Celtic	279-c. 350 AD	Nayling & McGrail 2004

Figure 2.1: Locations and dates for ships mentioned in the text.

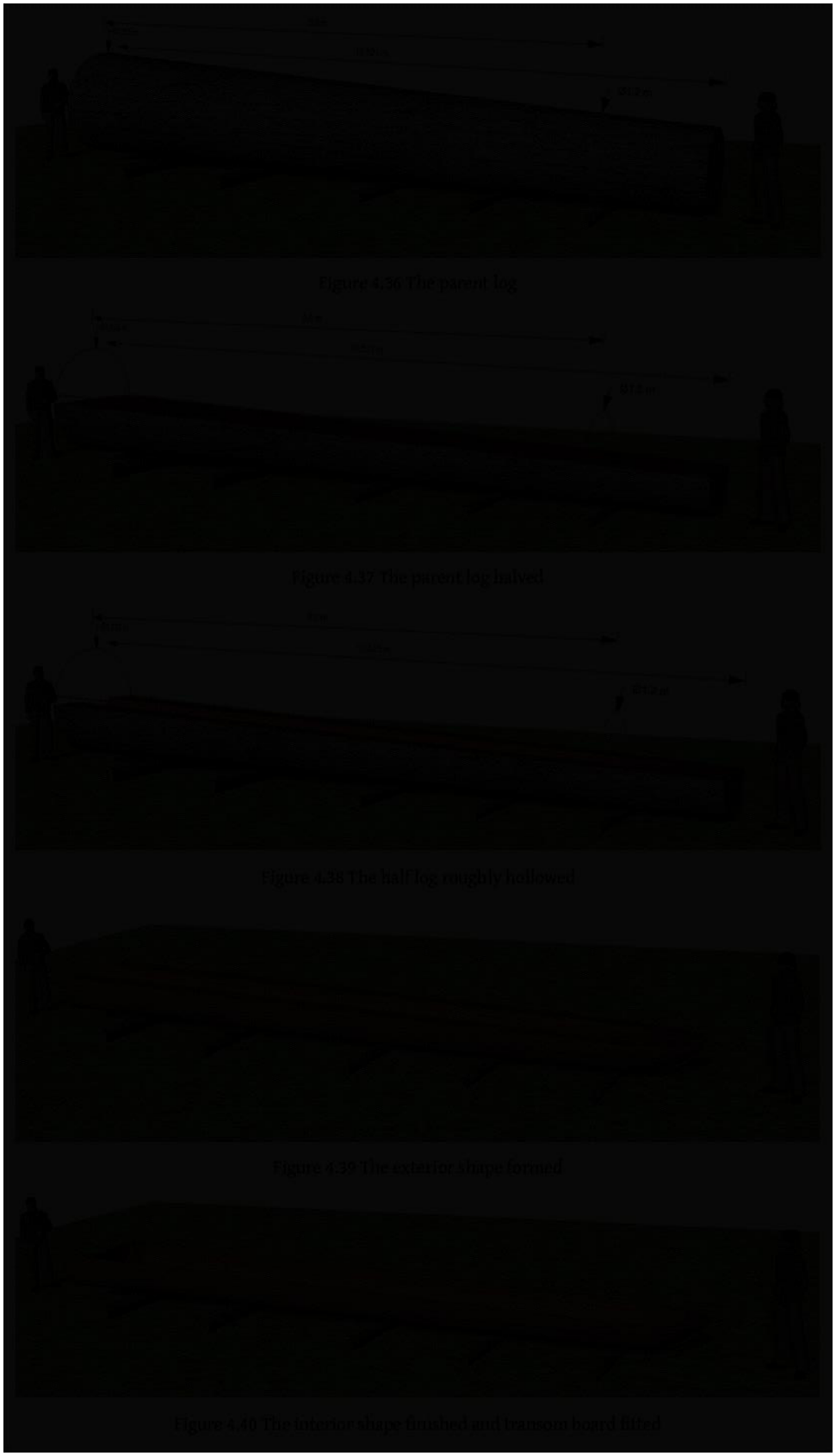


Figure 2.2: Illustration of construction stages of the Poole Logboat (after Berry et al. 2019, 66).

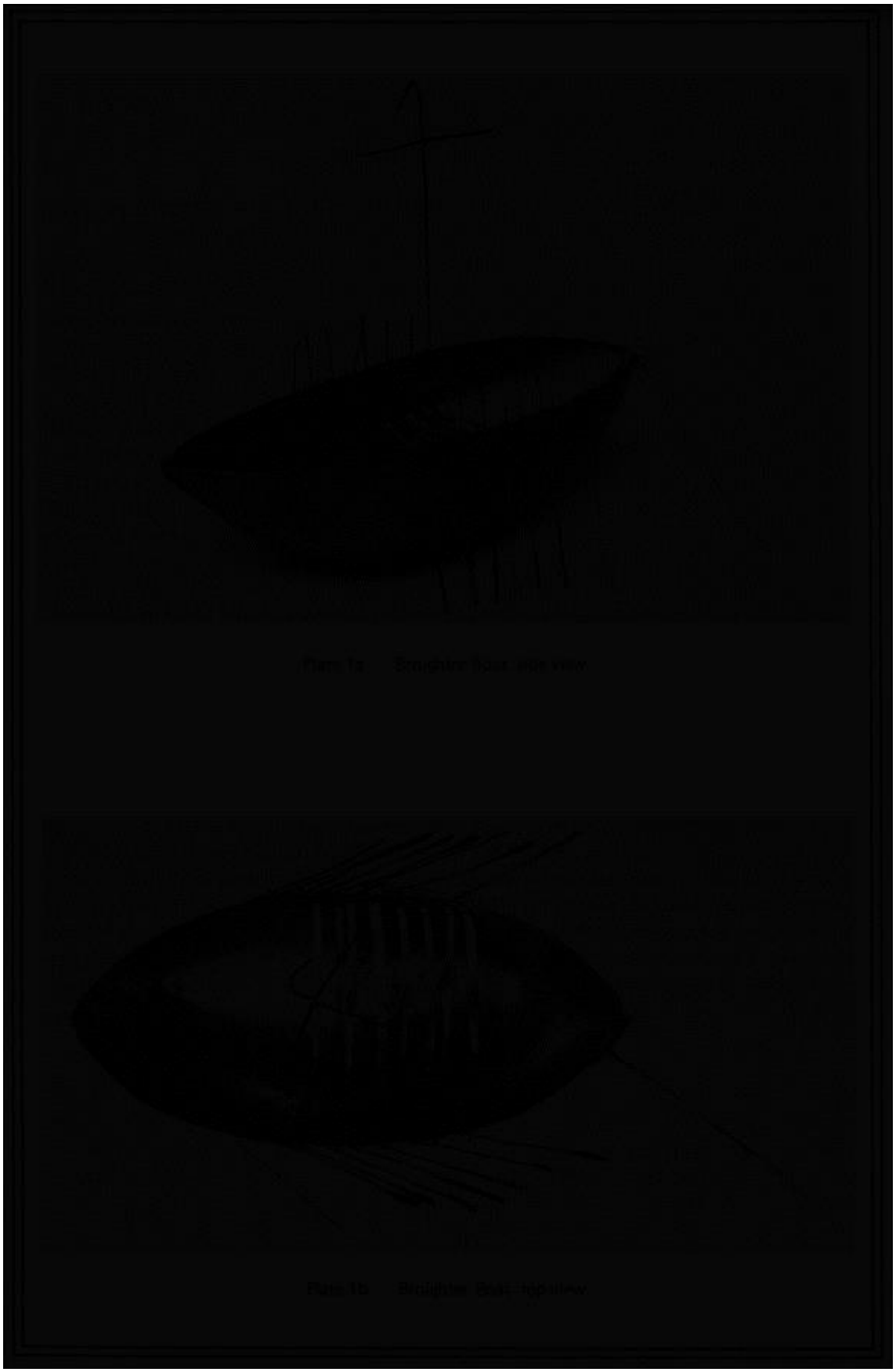


Figure 2.3: Photographs of the Broighter boat model, after Farrell & Penny 1975, 16.



Figure 2.4: Plan of the hide boat Brendan (after Severin 1978, 258-259).



Figure 2.5: Reconstruction drawing of Blackfriars 1, showing hooked nails used to attach planks to strakes (after Marsden 1994, Fig. 69).

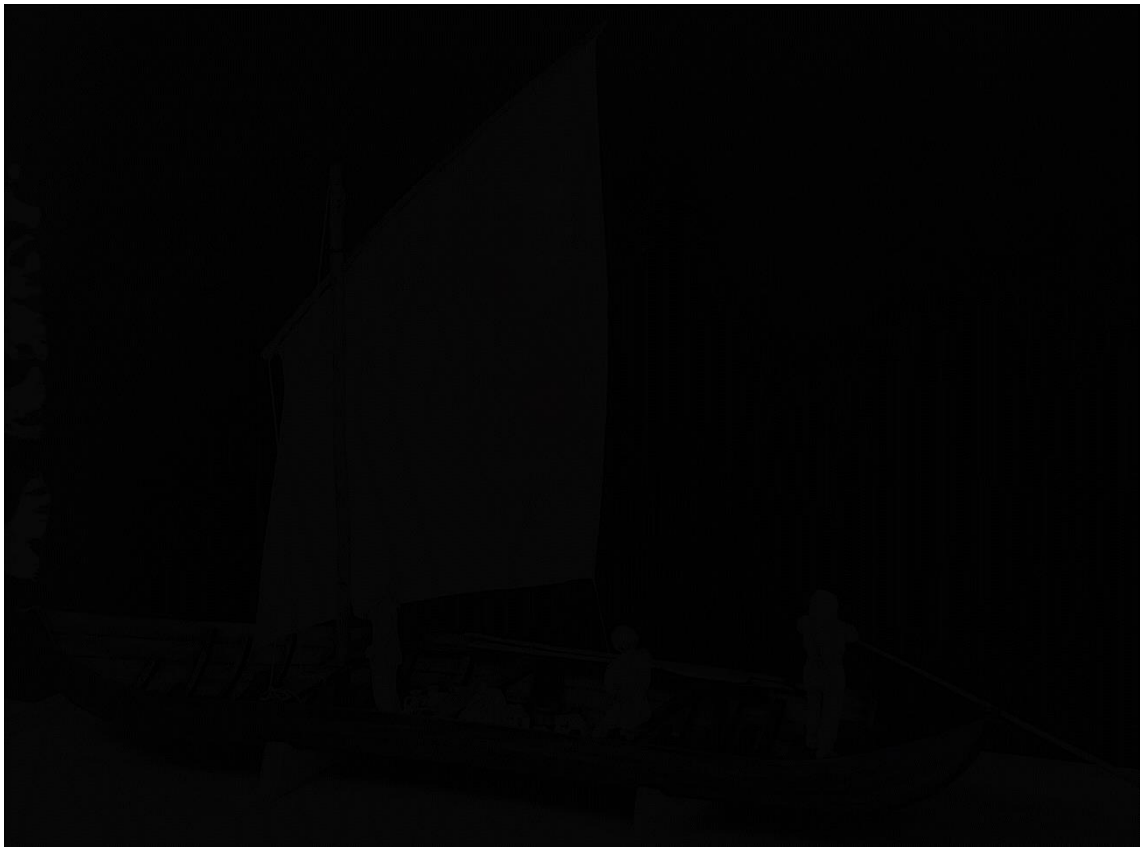


Figure 2.6: Model of the Barlands Farm boat (after Nayling et al. 2004, Fig. 8.3). Note that the replica has been fitted with a fore-and-aft sail rather than a square sail.

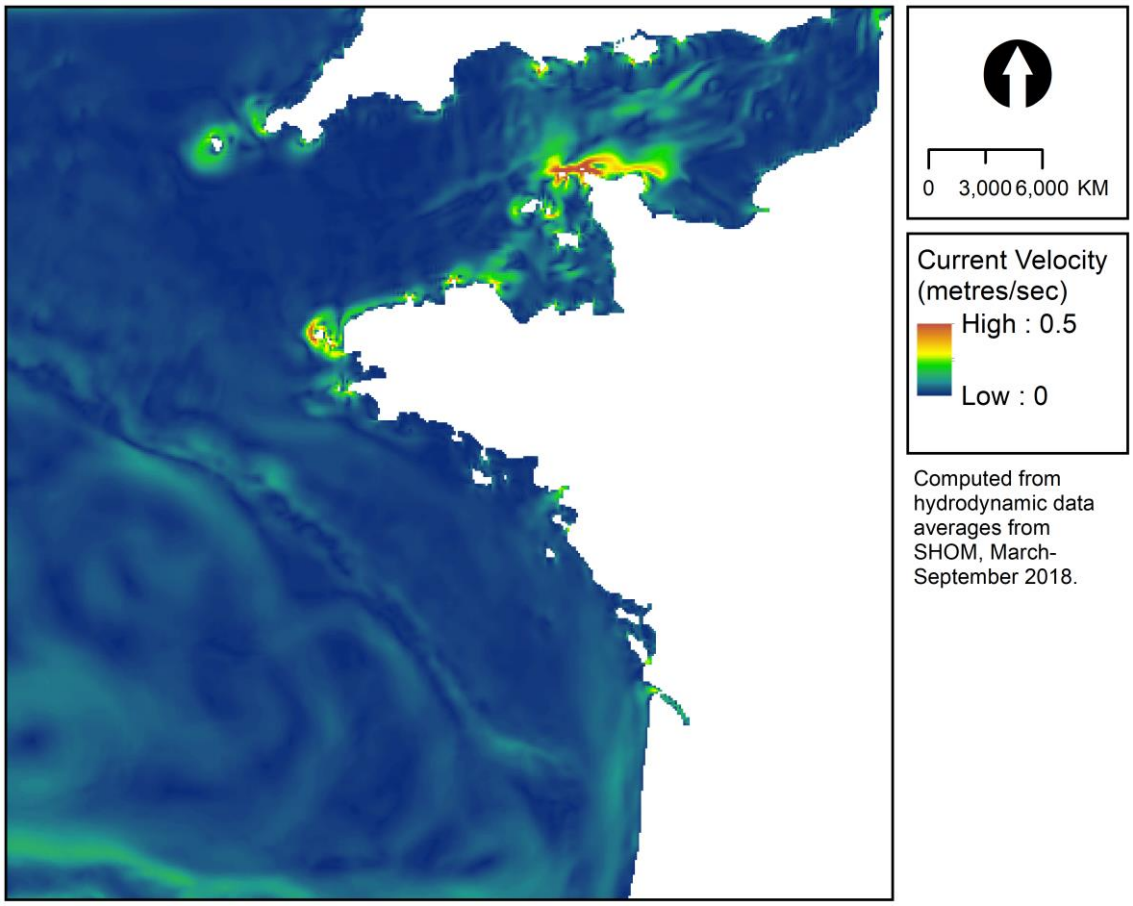


Figure 2.7: Strength of currents in the western Channel, based on hydrodynamic data used in simulations.

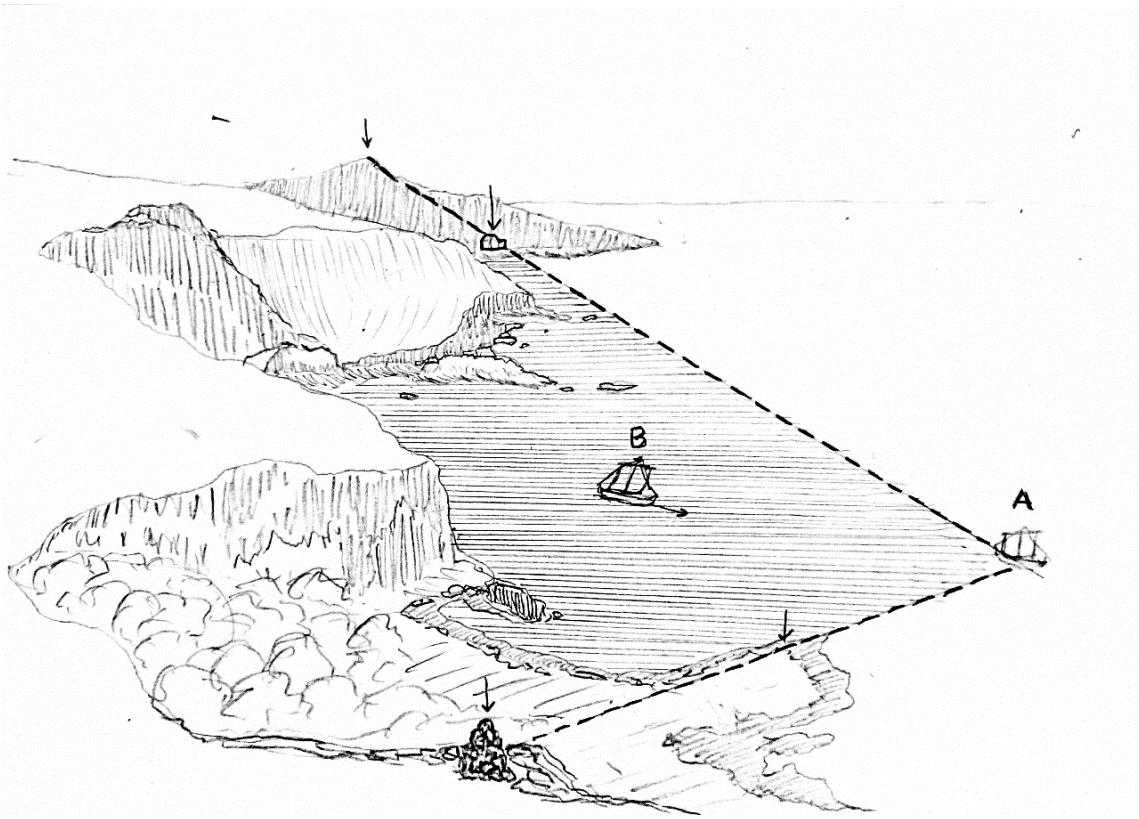


Figure 2.8: Illustration of the use of meids to obtain a fix (A) and to demarcate an area (B).

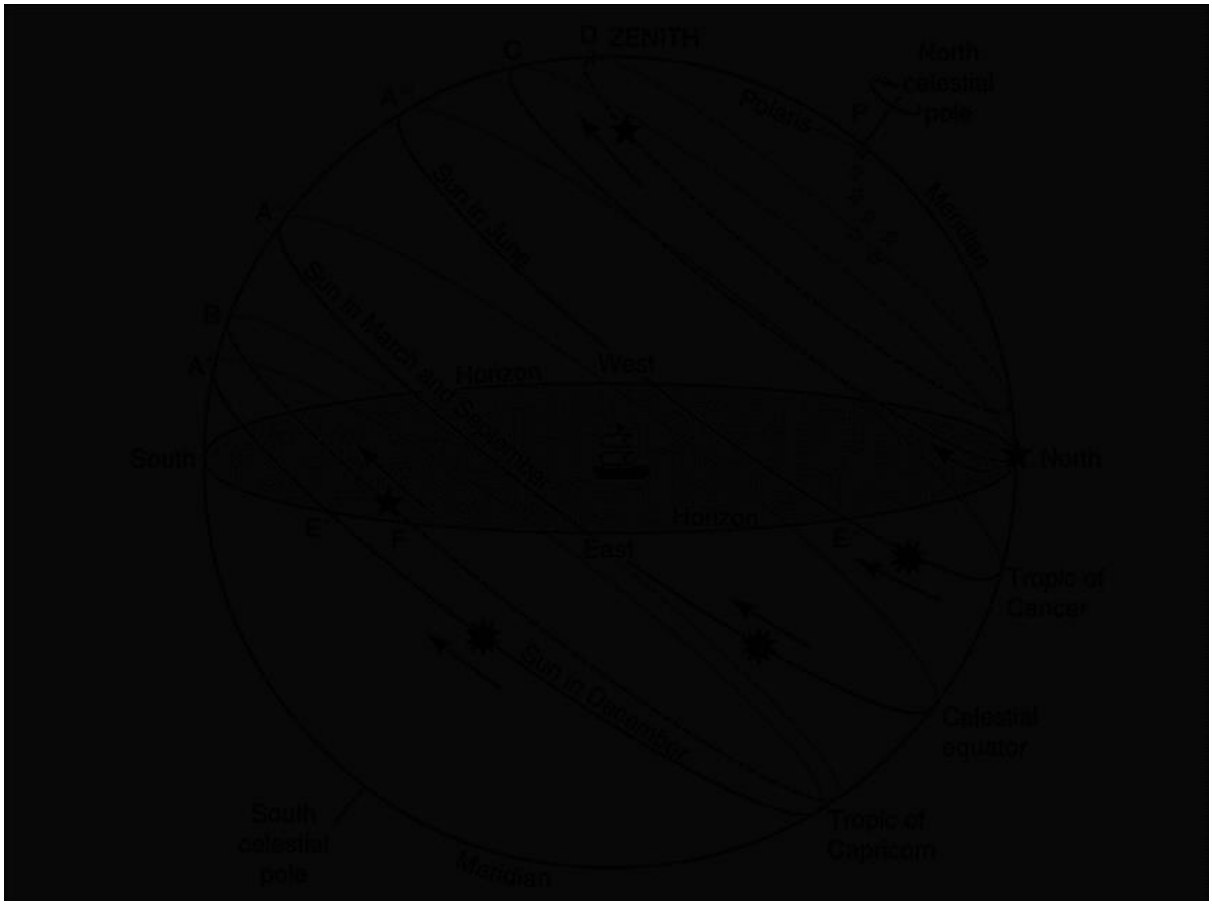


Figure 2.9: Illustration of the movement of stars and the sun as experienced by a voyager at sea, (after Bennett 2017, Figure 1).

Chapter 3 Figures



Figure 3.1: Cost surface generated by Indruszewski & Barton; “lightest is lowest cost and darkest is highest cost” (after Indruszewski & Barton 2008, Ch. 5 Pl. 11).

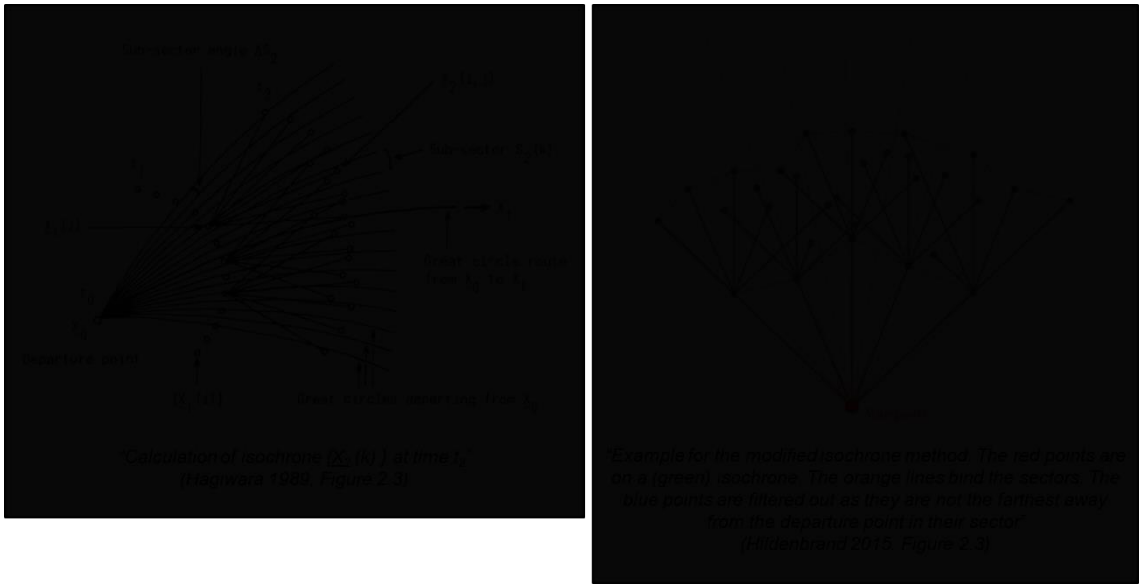


Figure 3.2: Illustrations of the isochrone method (after Hagiwara (1989; left) and Hildenbrand (2015; right)).

Chapter 4 Figures

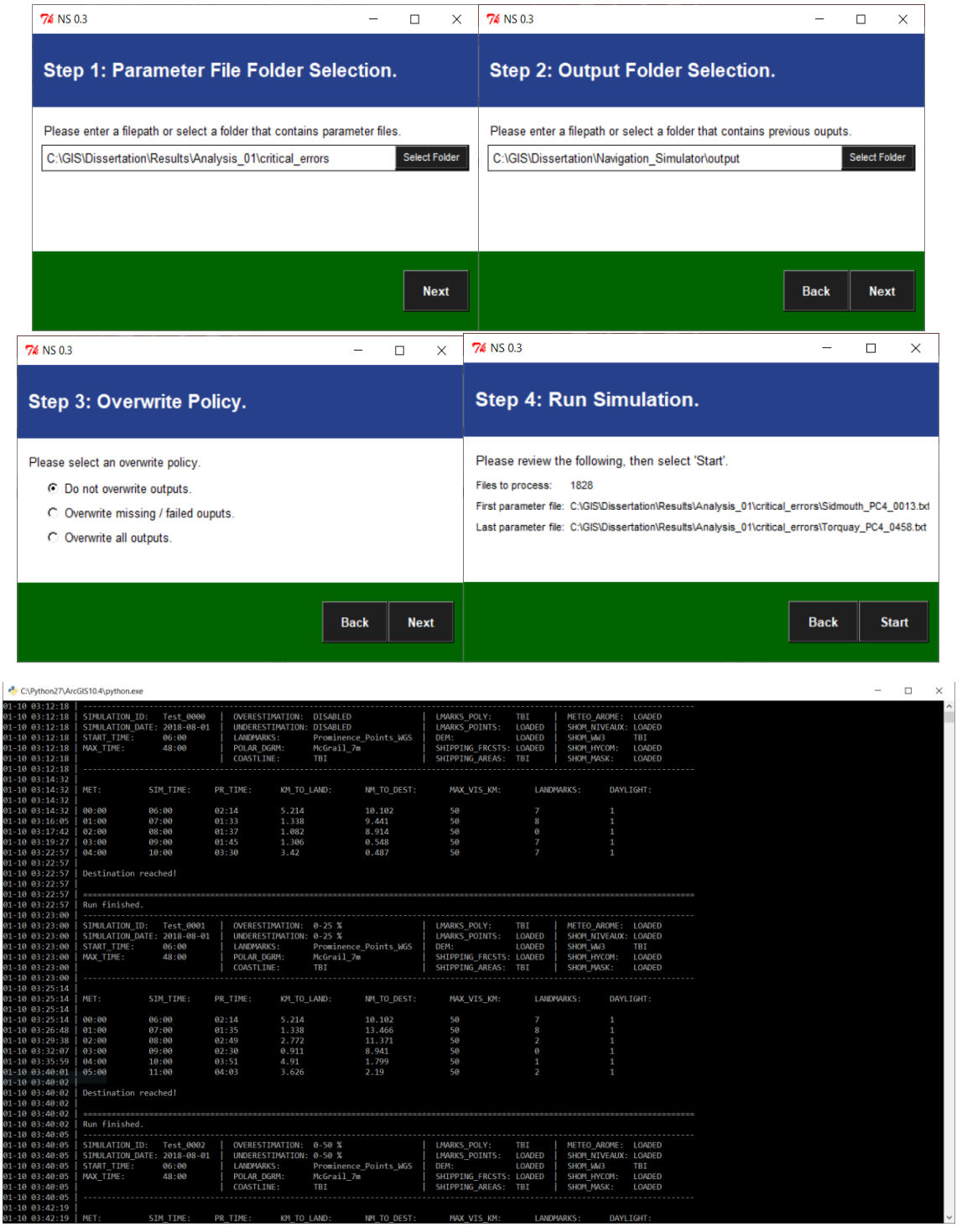


Figure 4.1: Sample GUI (above), and console (below) from the navigation model.

FOR EACH SET OF PARAMETERS:

1. IMPORT STATIC DATASETS
   Import & validates datasets with duration greater than 1 day.
2. GENERATE HEADING ARRAY
   Create 1-deg. vector array dictionary.
3. GENERATE TIMESTEP DICTIONARY
   Create dictionary containing Datetime objects representing 1-hour intervals.

4. FOR EACH DAY IN TIMESTEP DICTIONARY:

1. IMPORT NETCDF & WEATHER FORECAST.
   Import NetCDF / text files for simulation date.

2. FOR EACH HOUR IN DAY:

1. CHECK VISIBILITY CONDITIONS
   Check for daylight & retrieve maximum visibile distance.
2. VISIBILITY LAYER 1
   Cull landmarks by checking landmark-vessel distance.
3. VISIBILITY LAYER 2
   Cull landmarks that 'cross' skyline.
4. VISIBILITY LAYER 3
   Cull landmarks with no projective extent.
5. MODIFY DESTINATION POINT
   Modify location of destination to reflect outcome of visibility analysis.

6. FOR EACH HEADING:

1. SIMULATE W / 'RECKONED' CONDITIONS
   Simulate travel along heading.
2. COMPUTE PATH DISTANCE
   Compute path distance from heading endpoint to destination point.

7. SELECT HEADING
   Select heading with least path distance.
8. SIMULATE W / 'REAL' CONDITIONS
   Simulate travel along selected heading.
9. CHECK FOR SUCCESS
   Check endpoint against success / failure criteria.

5. OUTPUT
   Plot journey & write logs.

Figure 4.2: A step-by-step diagram of the operation of the Navigation Model.

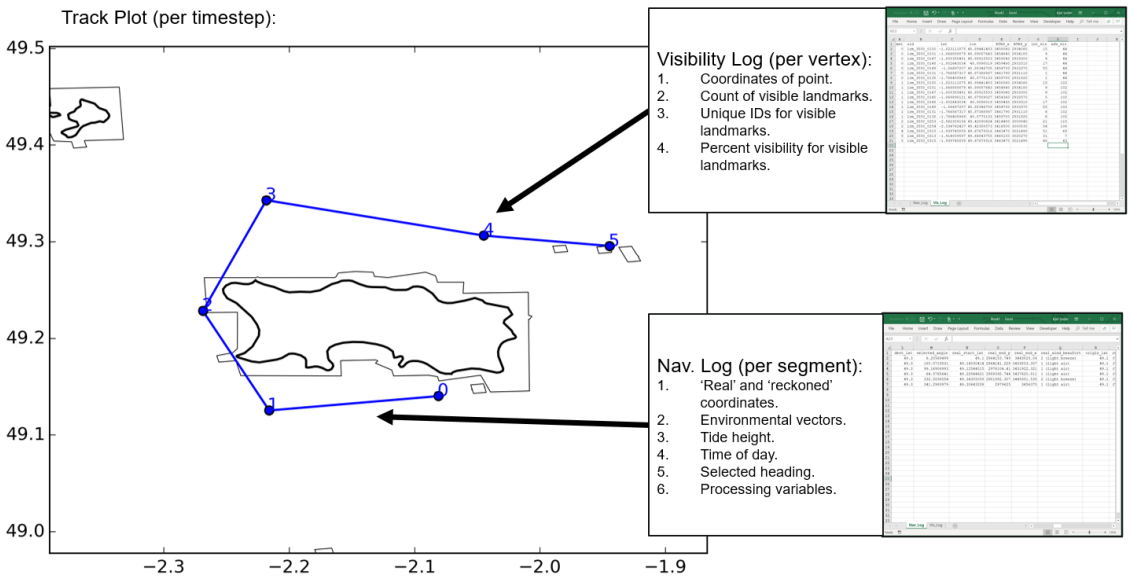


Figure 4.3: Sample model outputs.

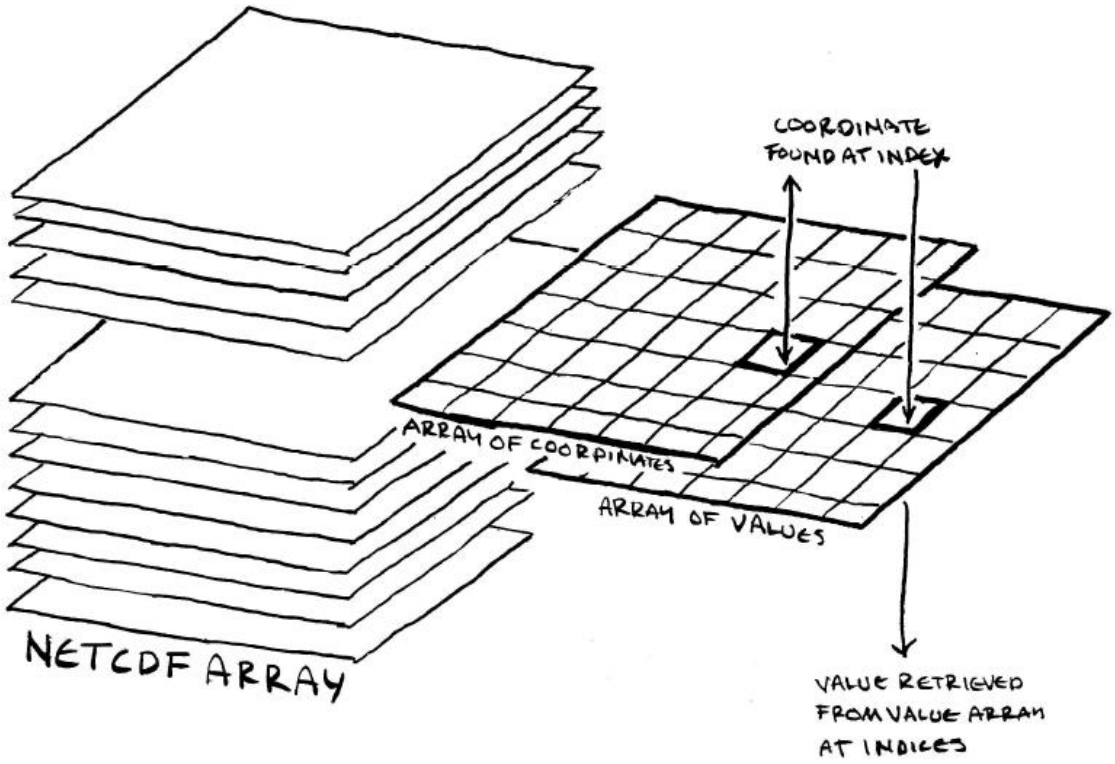


Figure 4.4: Illustration of the process used to retrieve values from NetCDF files.

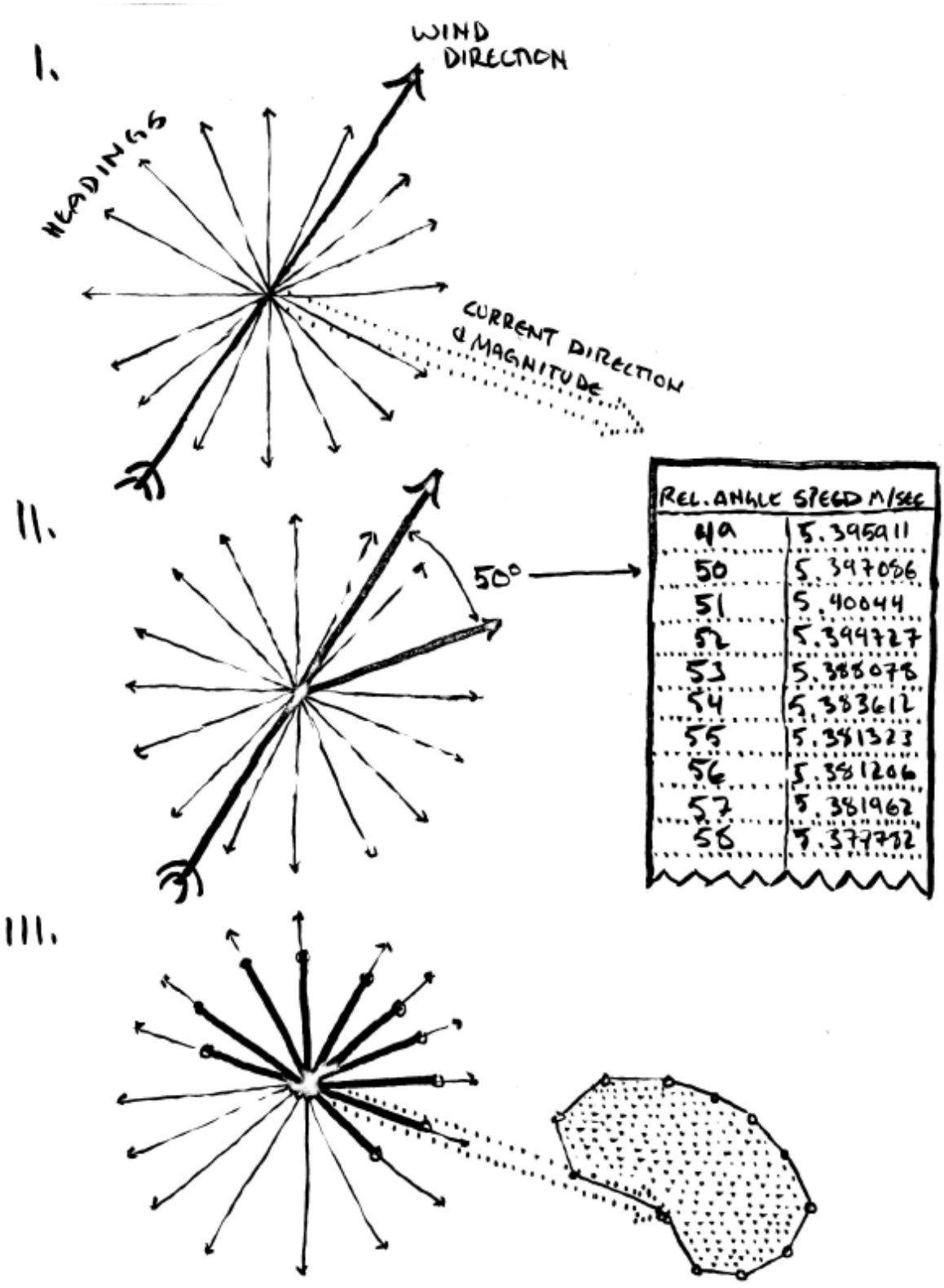


Figure 4.5: Illustration of the process used to generate headings. Note that the diagram is simplified: here rays are separated by 20°, whereas ray separation in the script is 1°.

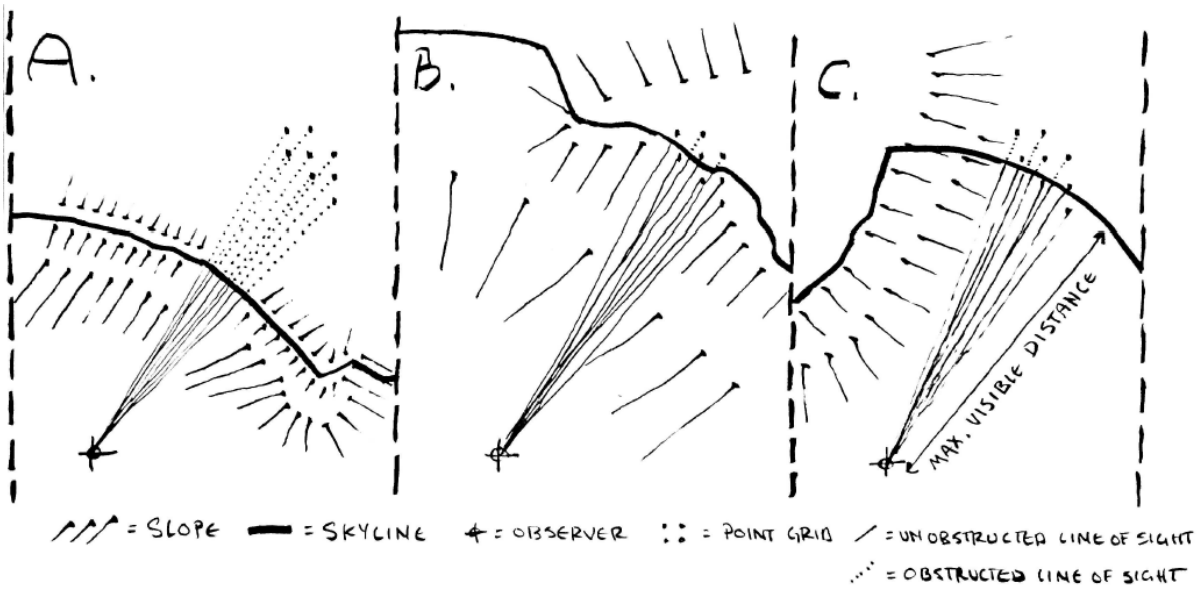


Figure 4.6: Possible scenarios for site grid – skyline evaluation: (A) all points are obstructed by topography, (B) some points are obstructed by topography, and (C) skyline maximum distance intersects feature grid.

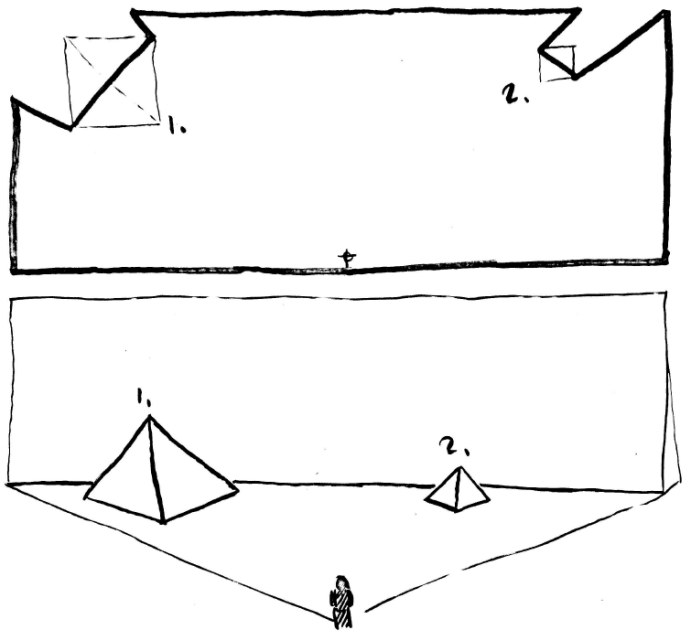


Figure 4.7: Comparison of a 2D viewshed (isovist) and a 3D rendering generated for the same scene. Note that according to the 2D image both pyramids are classified as ‘50% visible’.

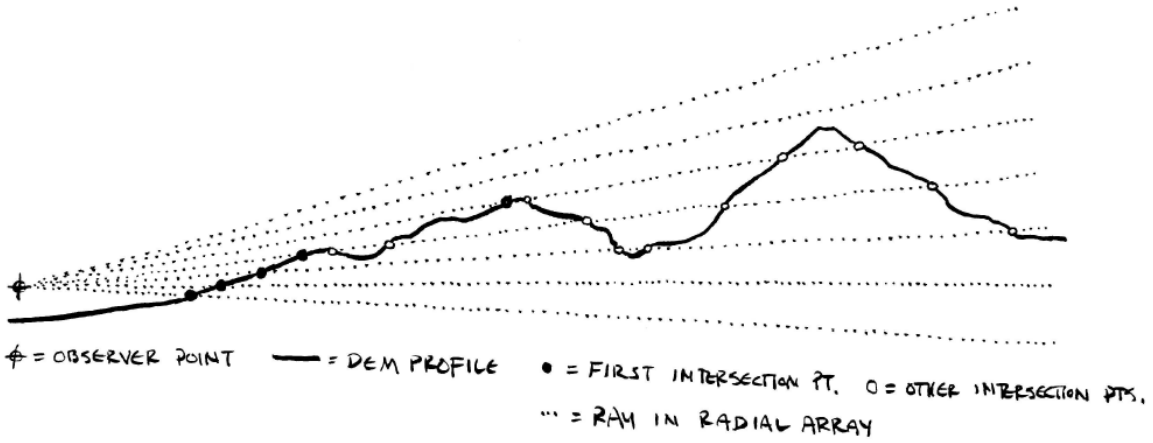


Figure 4.8: Radial array – DEM surface intersection, shown in profile.

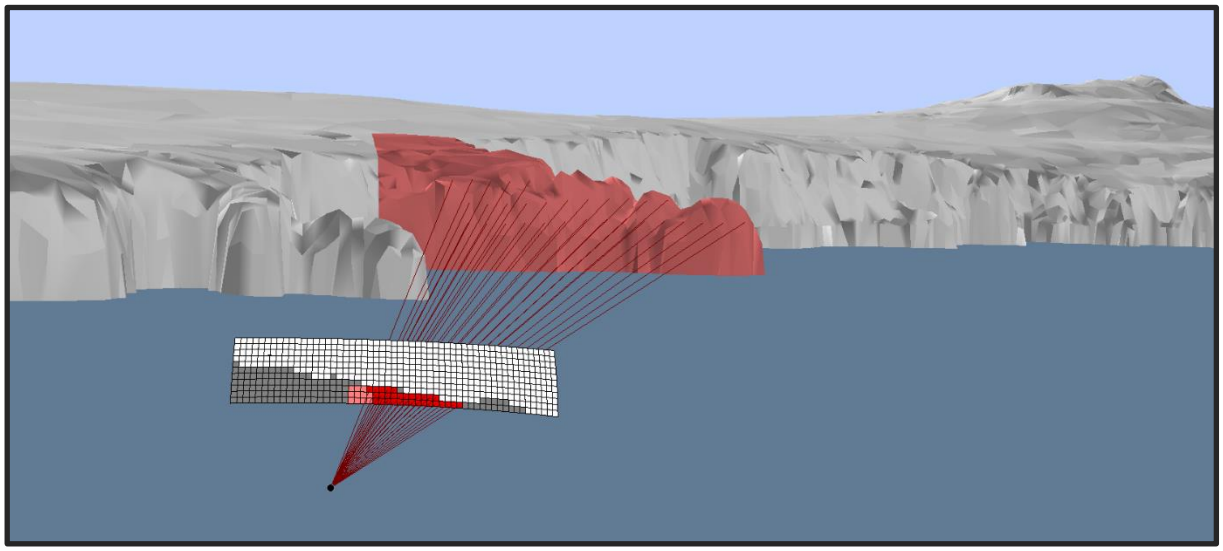


Figure 4.9: Results of radial array – DEM intersection transformed from Cartesian to projective coordinates.

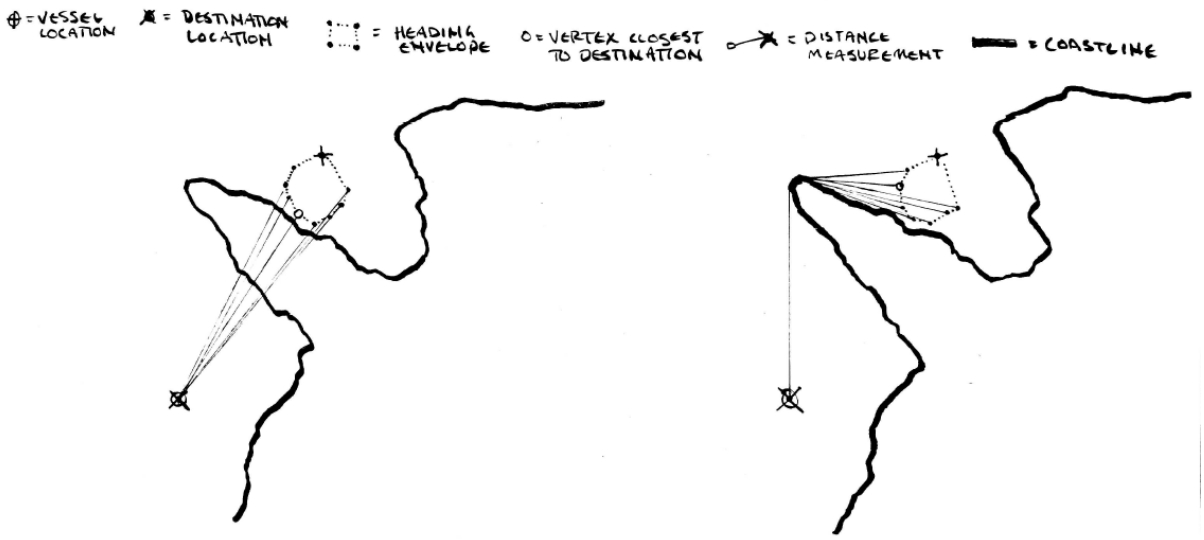


Figure 4.10: Path-distance generation applied to the ‘dead end’ problem.

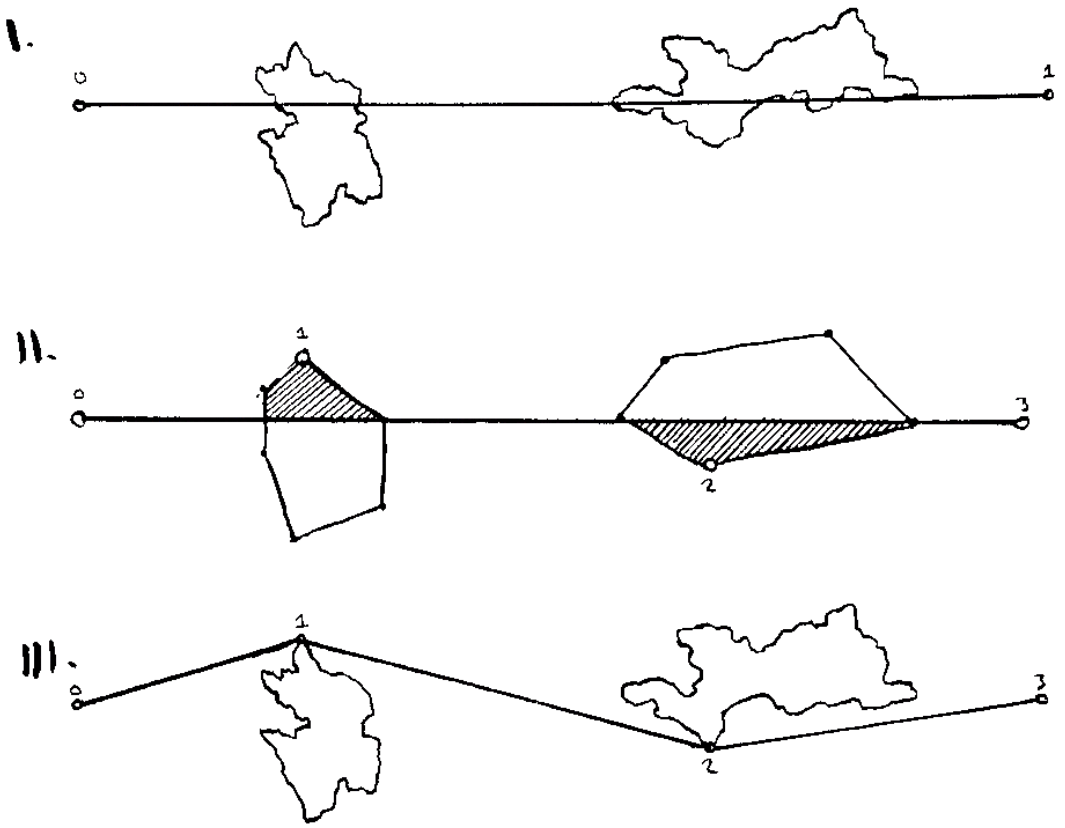


Figure 4.11: Demonstration of the convex path algorithm. Polygons representing obstacles are split by start-end line (I), and points are extracted from each smallest split feature (II, selected features are shaded). Points from the split features are then used to construct a path-distance line (III).

Chapter 5 Figures

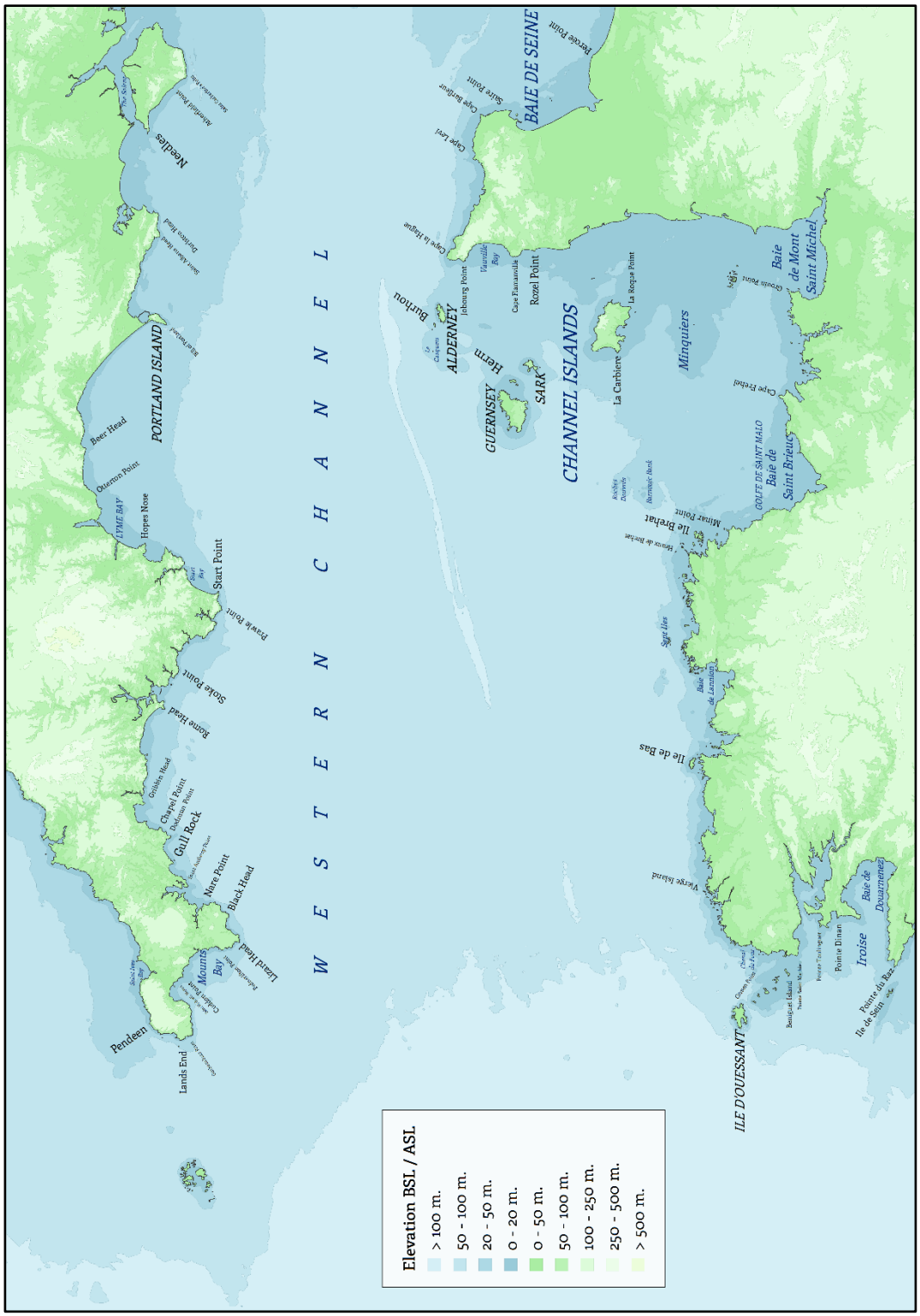


Figure 5.1: Map of the western Channel, showing waterways and landforms.

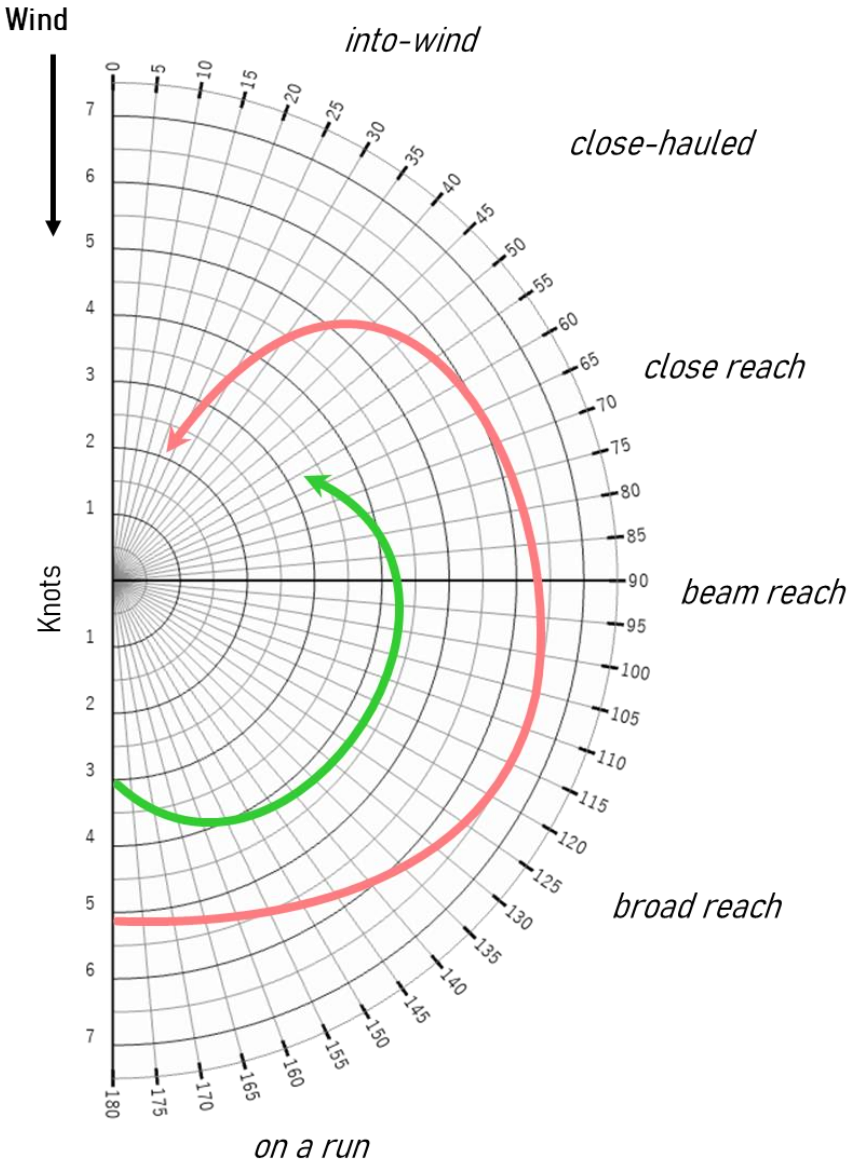


Figure 5.2: Speed diagrams for the *Roar Ege* in green, and a modern sailboat in red (after Mette Kryger, redrawn from Max Vinner, https://www.vikingeskibsmuseet.dk/en/professions/education/exercises/the-speed-diagram/).

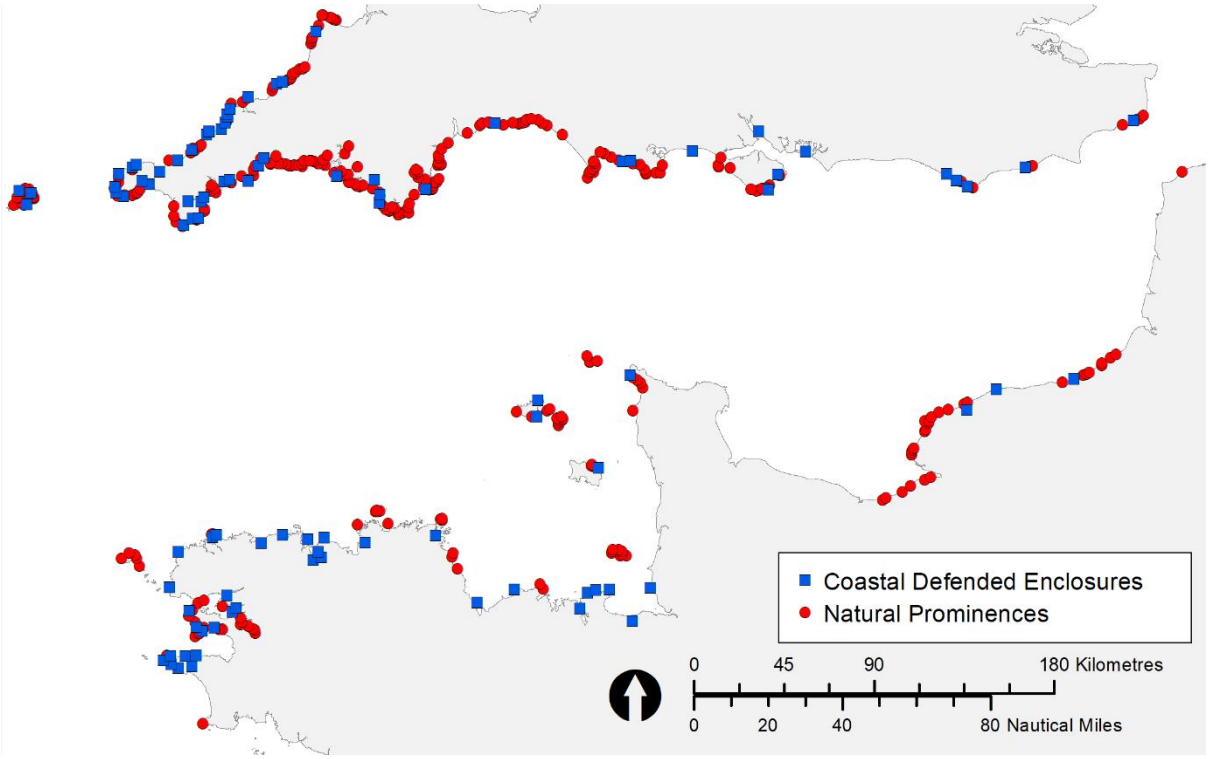


Figure 5.3: Distribution of landmarks within the study area.

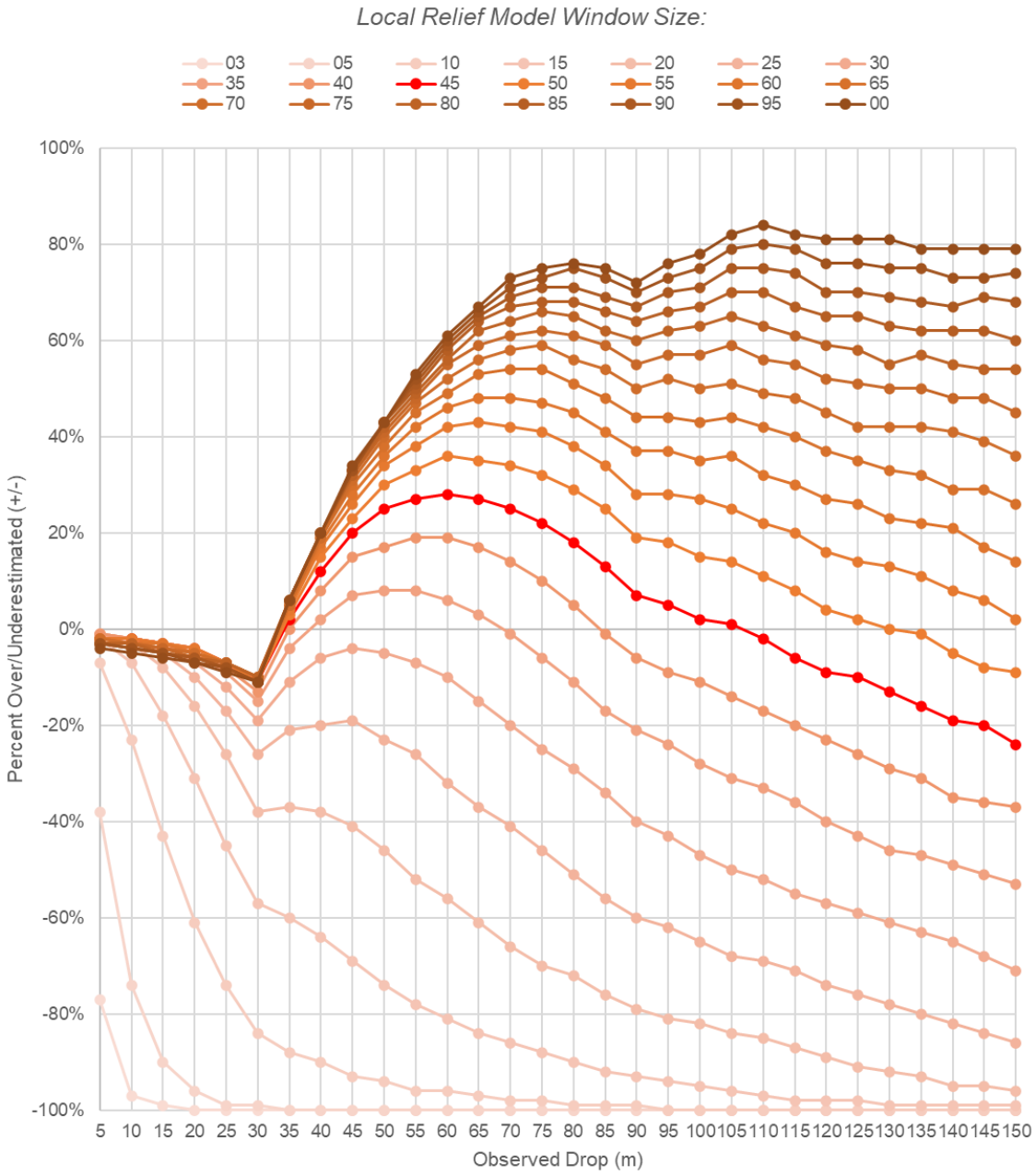


Figure 5.4: Accuracy of LRM analyses in identifying drop values from the DBIH database.

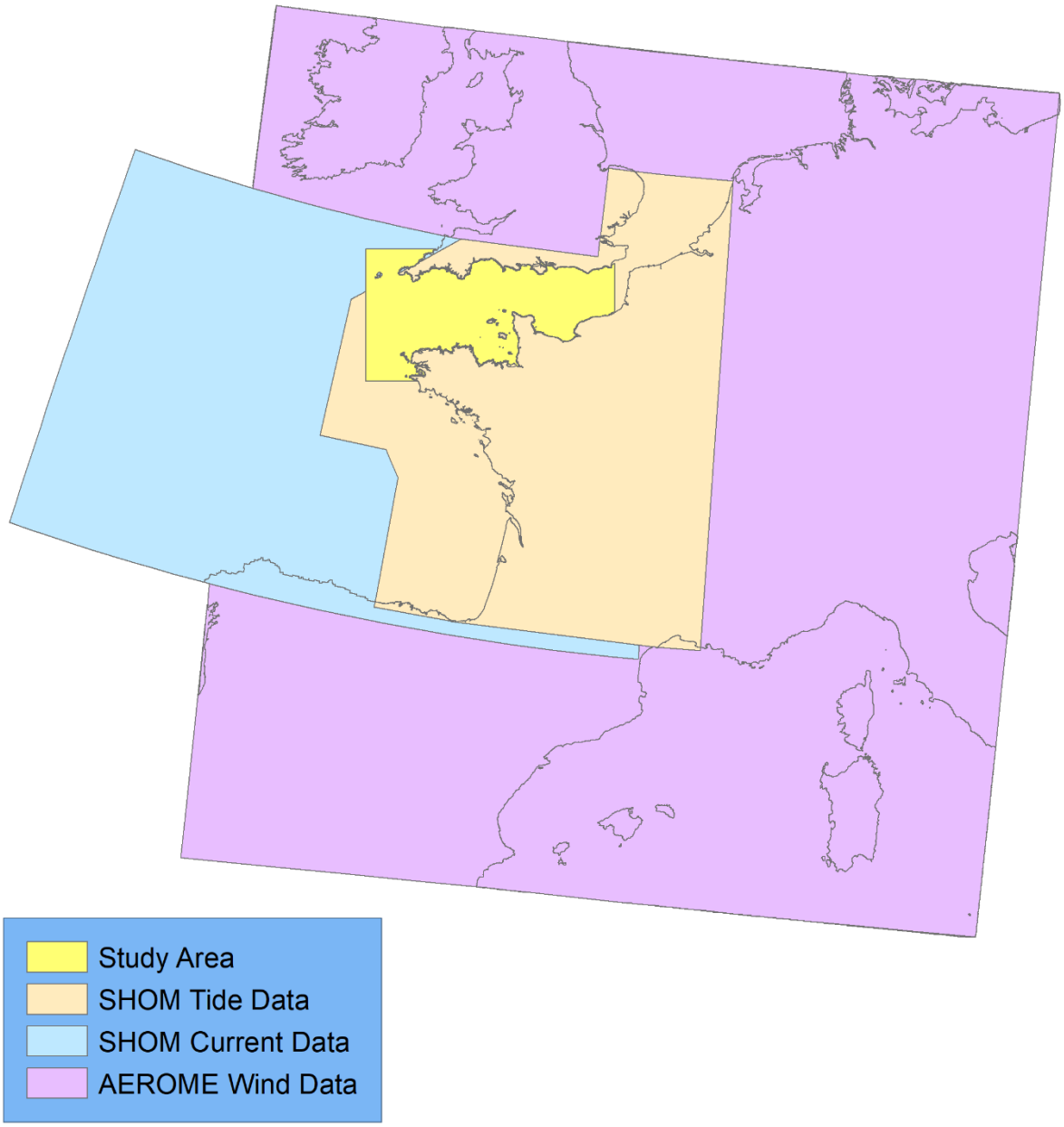


Figure 5.5: Environmental data coverages.

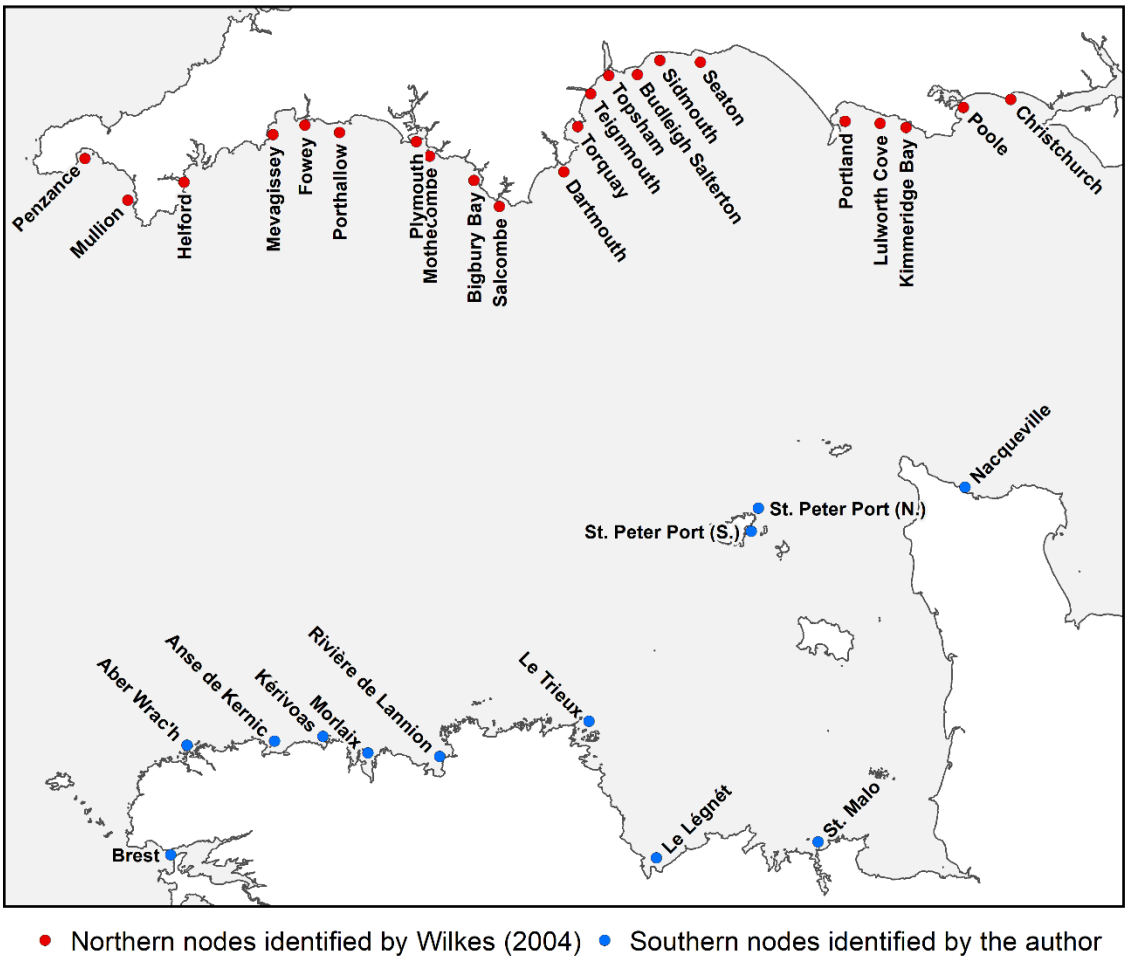


Figure 5.6: Nodes on the northern shore of the Channel identified by Wilkes (2004), and by the author.

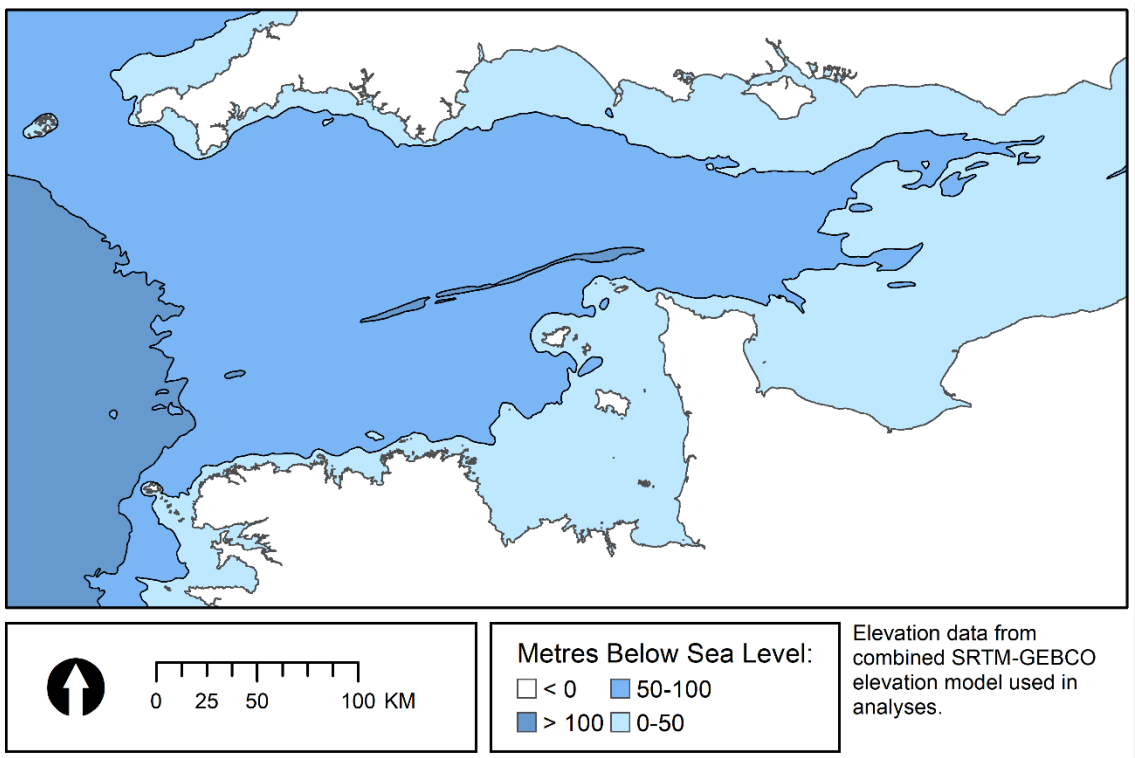


Figure 5.7: P2-S1-Depth contours for the western Channel, based on bathymetry used in simulations

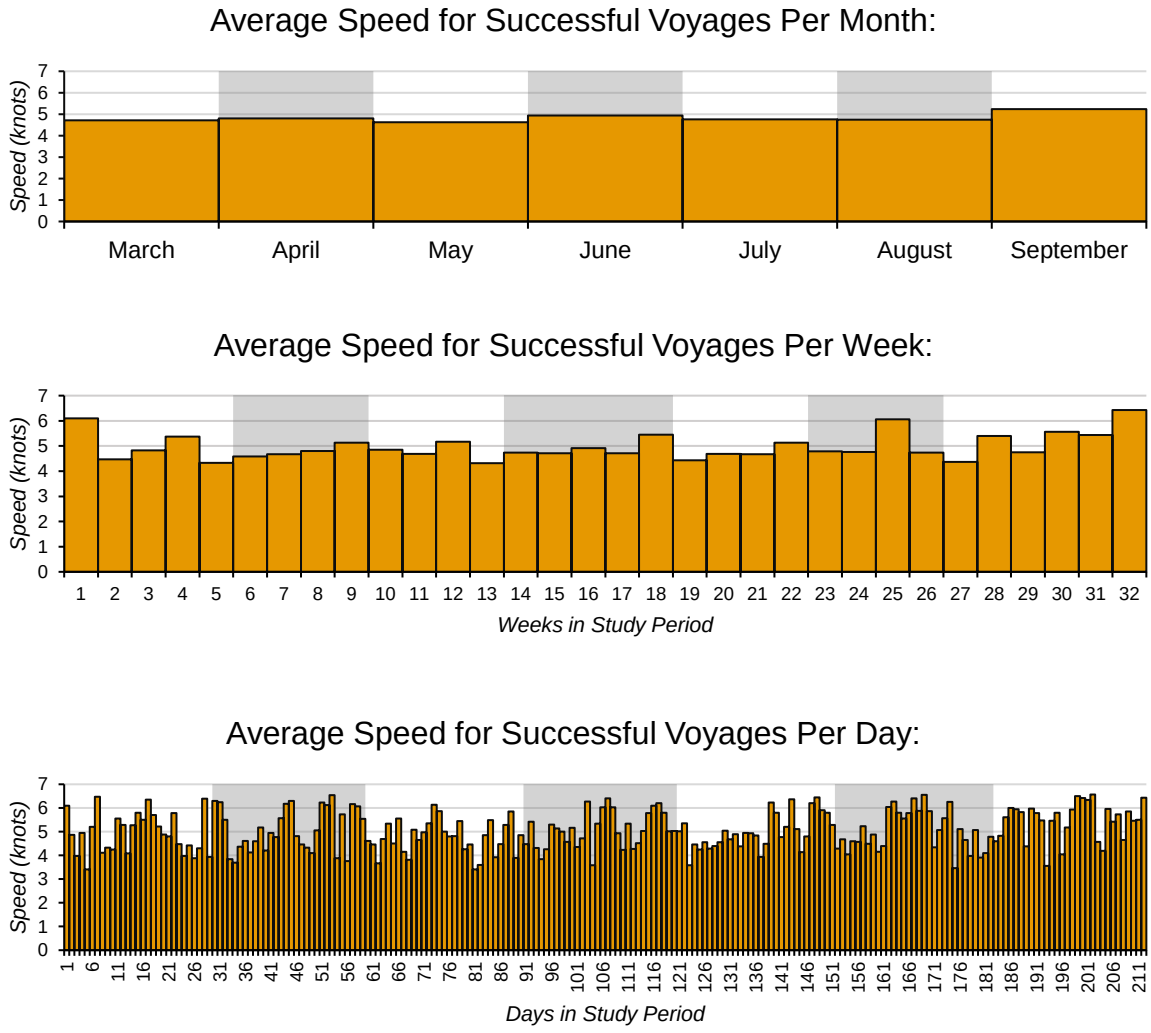


Figure 5.8: Average speed (in knots) for successful simulations along all routes in the Main Analysis, per day. Alternate months are highlighted.



Figure 5.9: Percentage of simulations for all routes that reach their destinations in the Main Analysis, per day. Alternate months are highlighted.

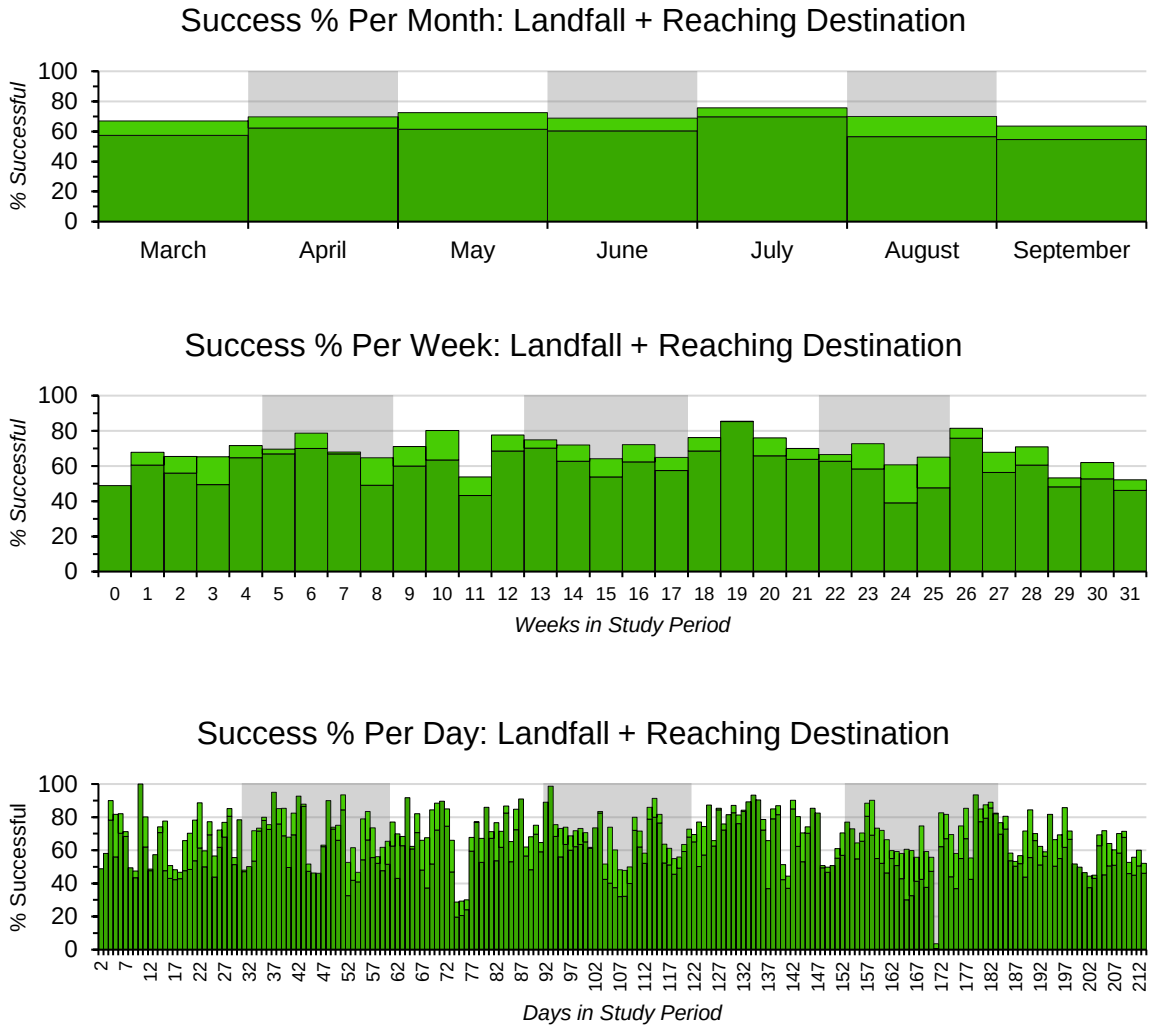


Figure 5.10: Percentage of simulations for all routes that reach their destinations (dark green) with the percentage of extra simulations that reach the opposite coast added (light green) in the Main Analysis, per day. Alternate months are highlighted.

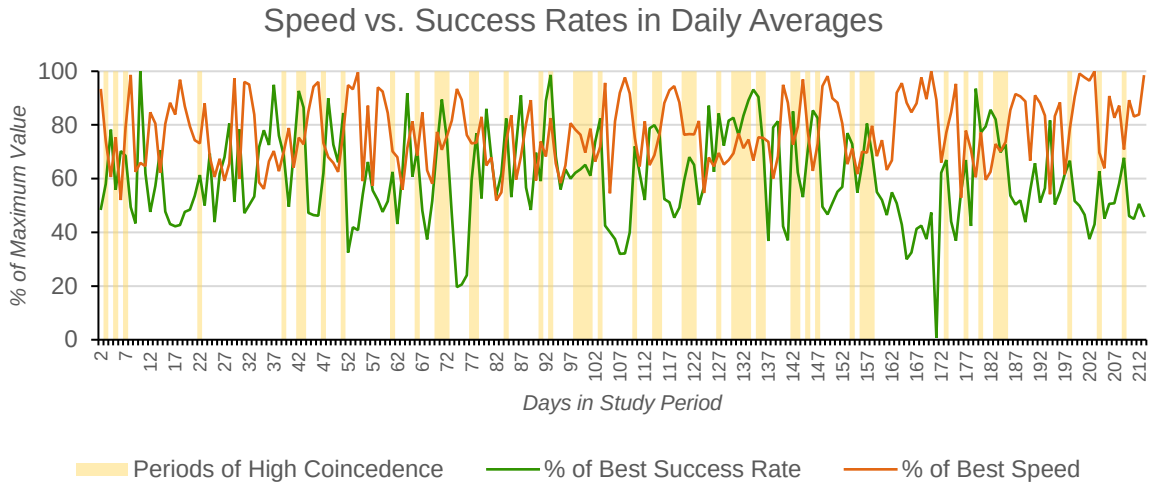


Figure 5.11: Correlation between daily averages where success rates were high (green) and speed was high (orange), with periods of high coincidence (within 20 percentage points) highlighted.

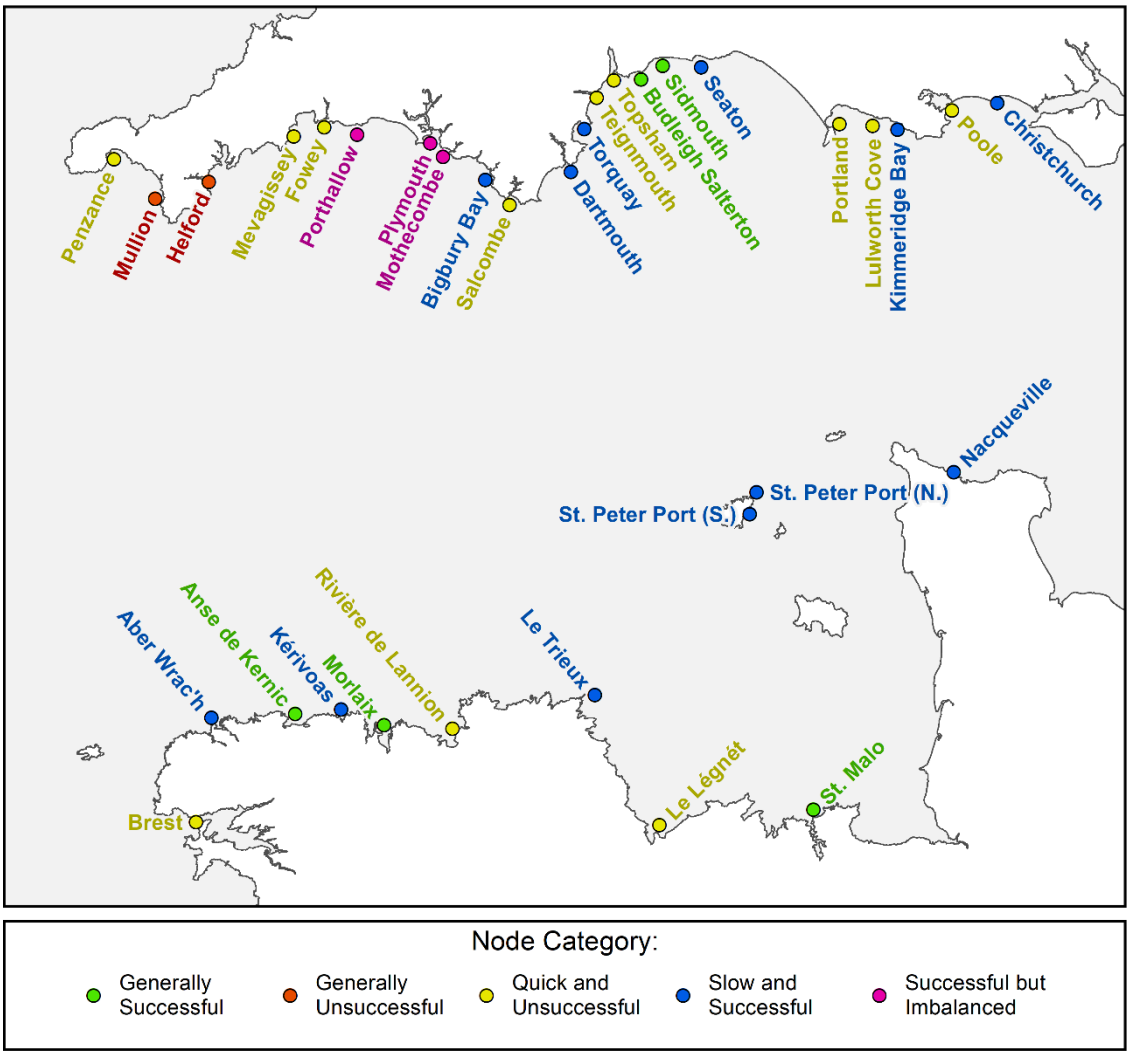


Figure 5.12: Nodes classified according to average speed / success rates from the Main Analysis.

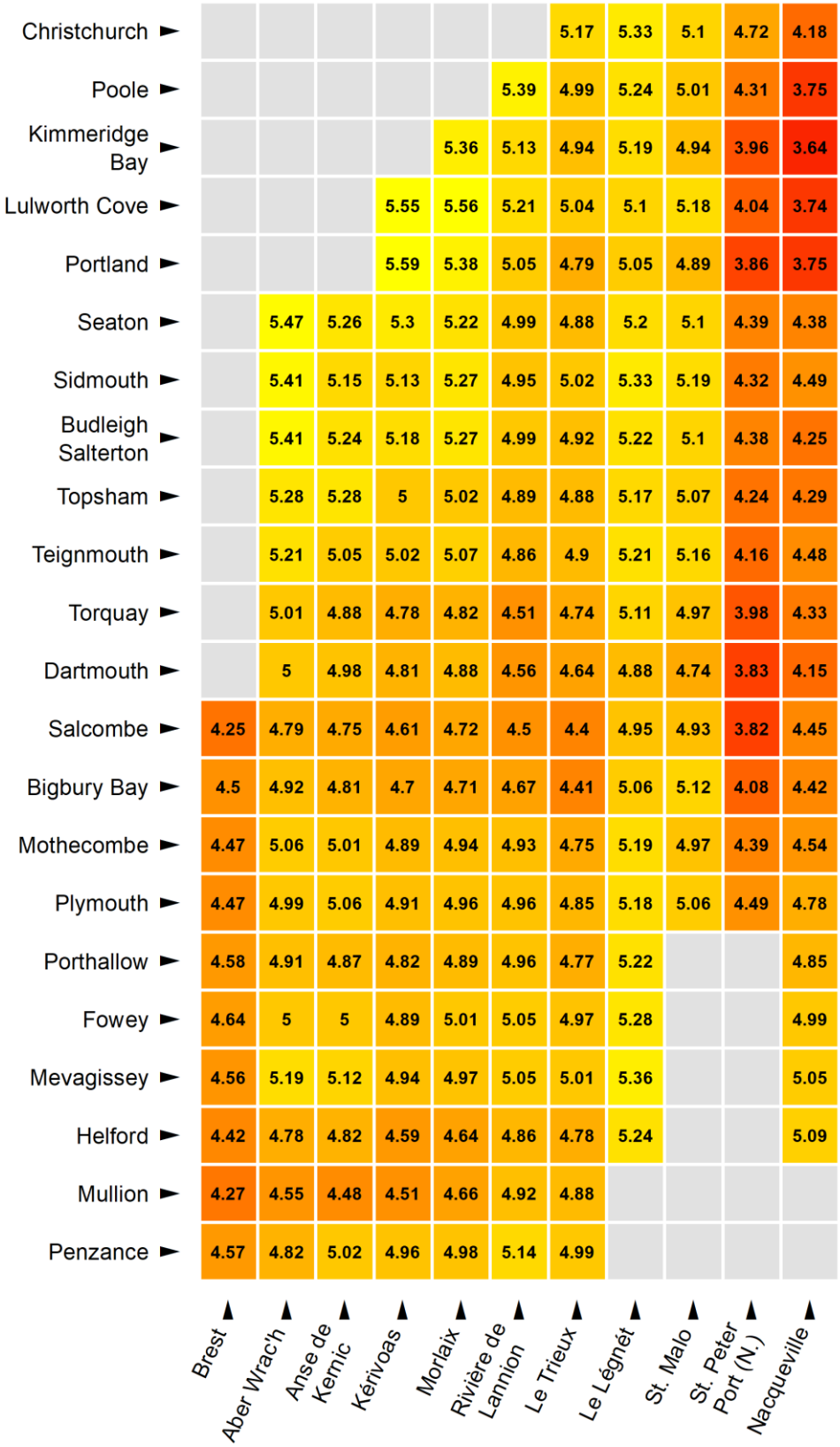


Figure 5.13: Average speed for routes simulated in the Main Analysis. Cells corresponding to slower routes are red, and cells matching faster routes are yellow.

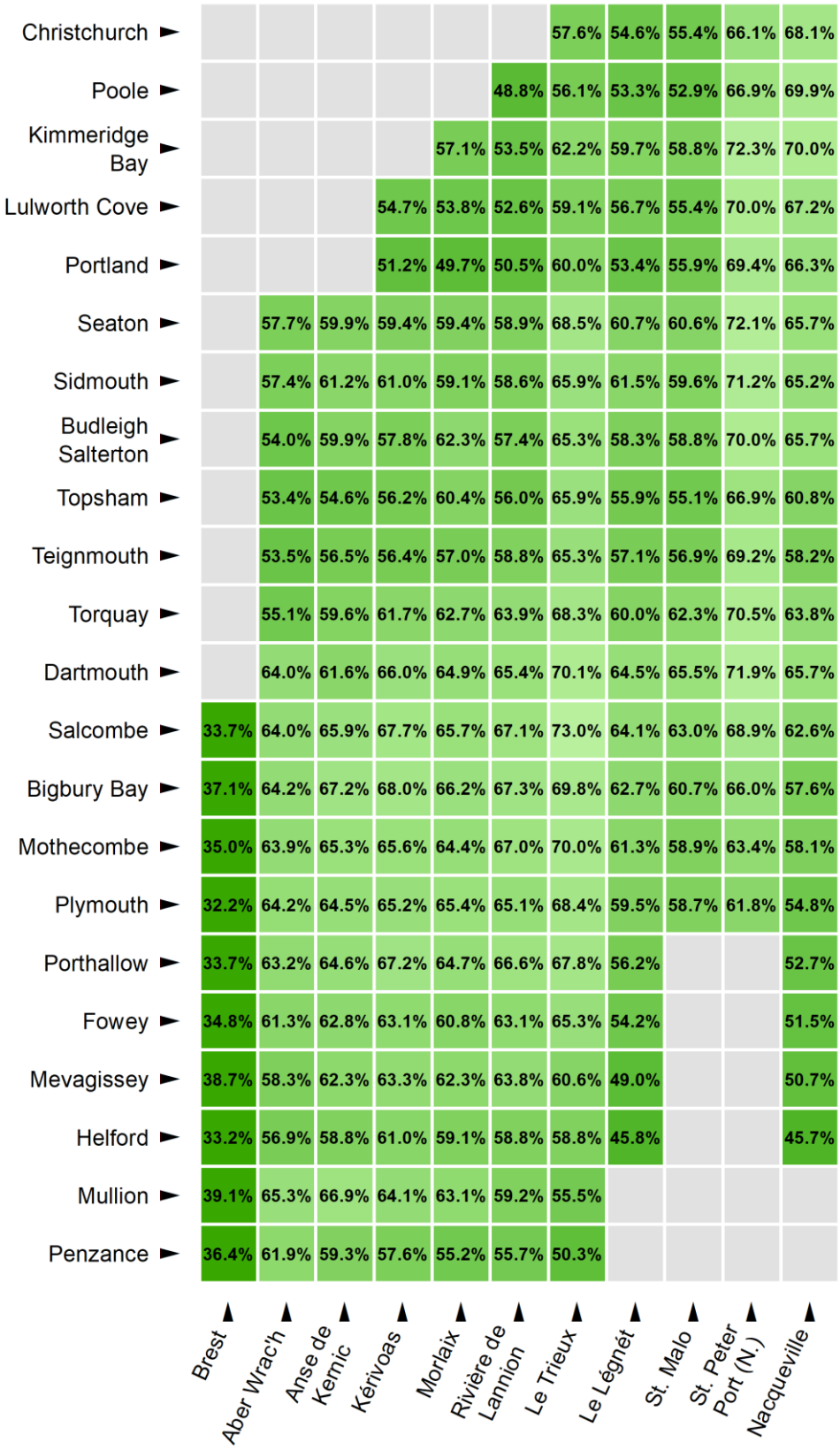


Figure 5.14: Success rates for routes simulated in the Main Analysis. Cells corresponding to less successful routes are shaded dark green, and vice versa.

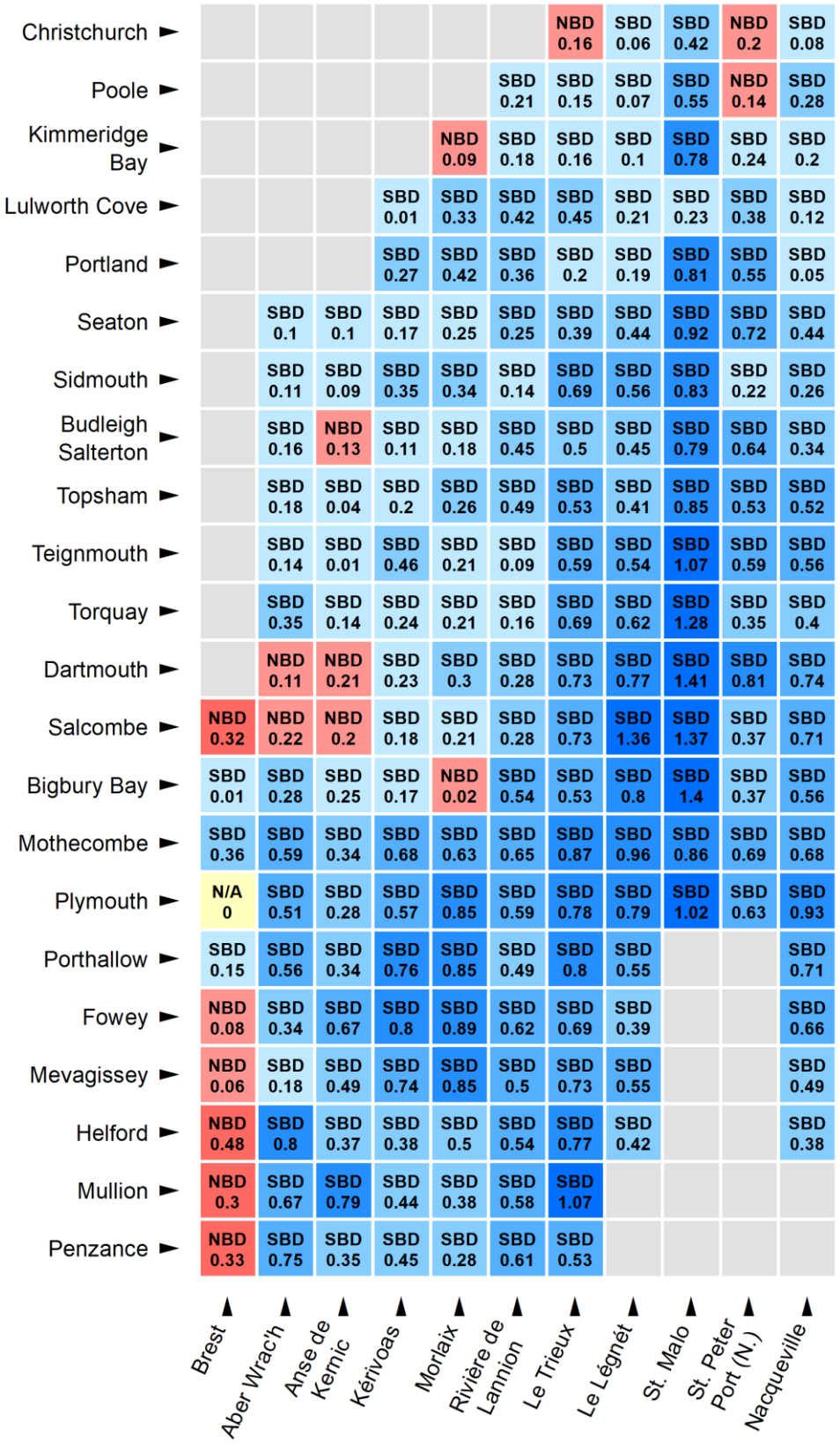


Figure 5.15: Difference in average speeds for routes simulated in the Main Analysis. Cells corresponding to more successful northbound routes are red, those corresponding to southbound routes are blue.

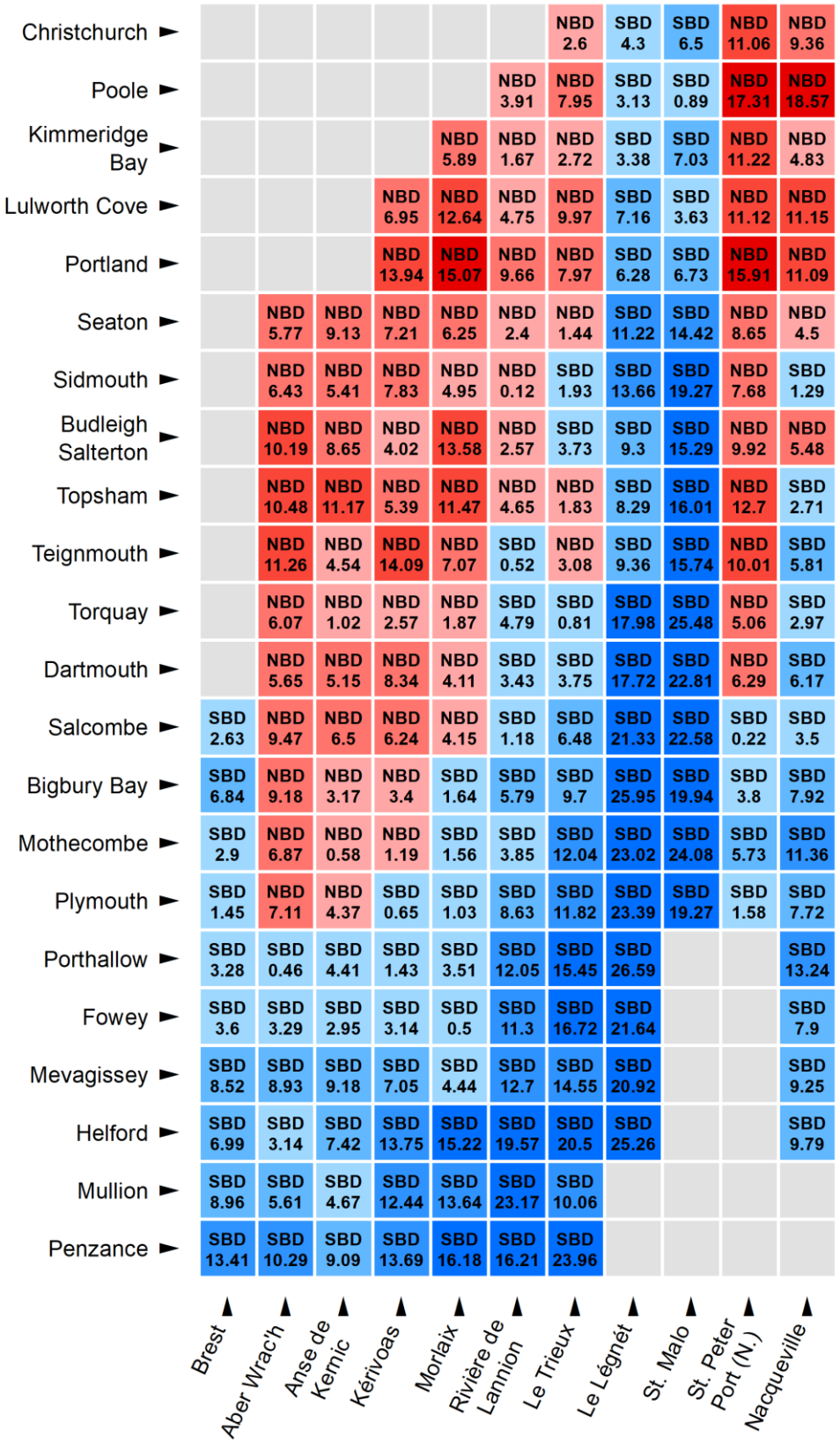


Figure 5.16: Difference in average success rates for routes simulated in the Main Analysis. Cells corresponding to more successful northbound routes are red, those corresponding to southbound routes are blue.

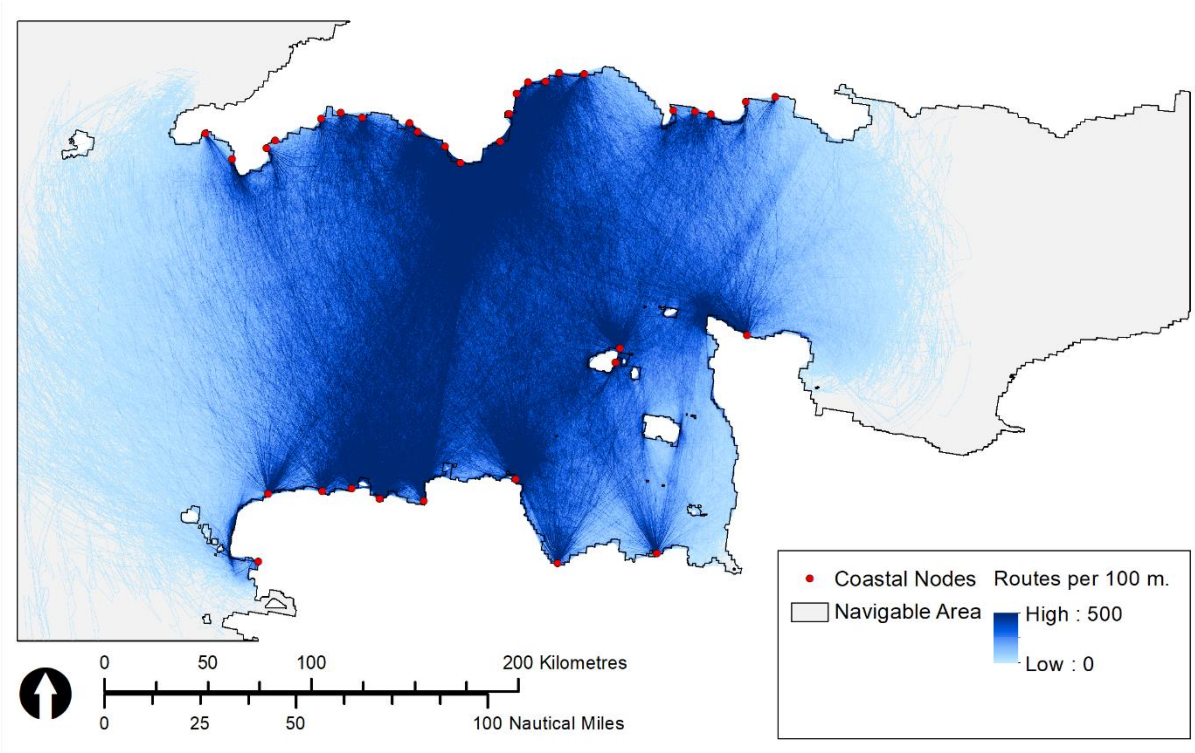


Figure 5.17: Results of line density analysis for all simulations.

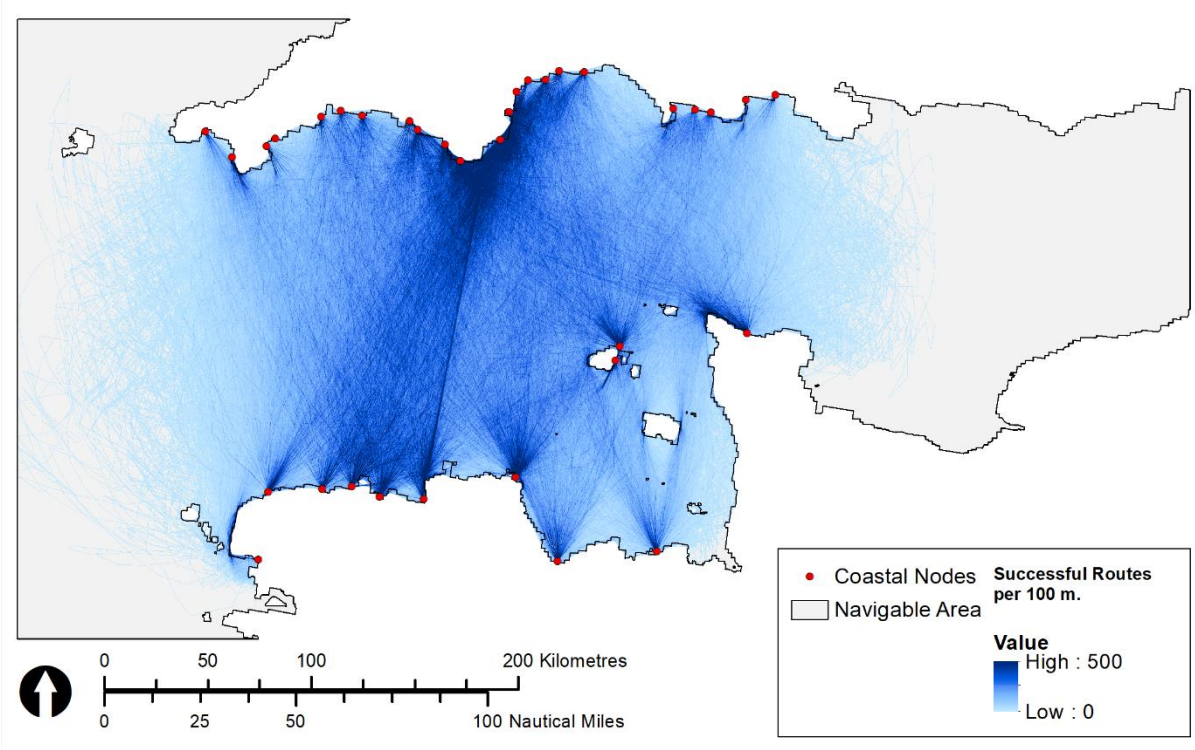


Figure 5.18: Results of line density analysis for all successful simulations.

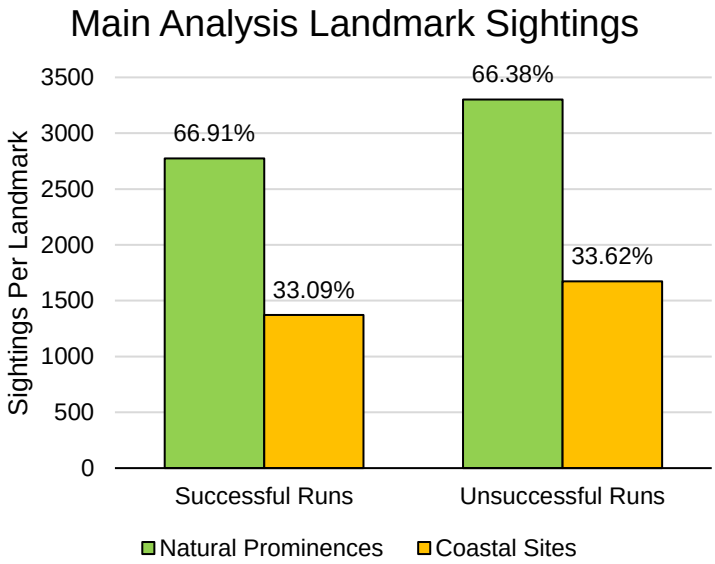


Figure 5.19: Visibility results per landmark type.

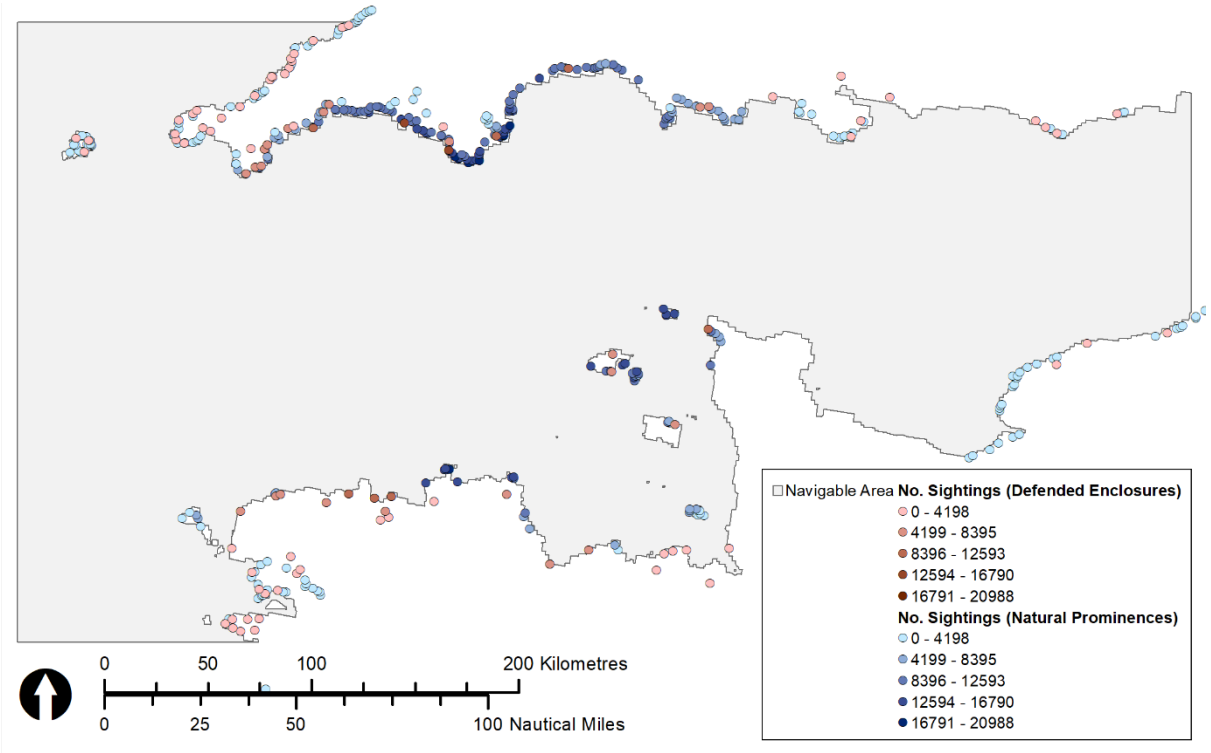


Figure 5.20: Landmarks used in the Main Analysis, symbolised by number of sightings.

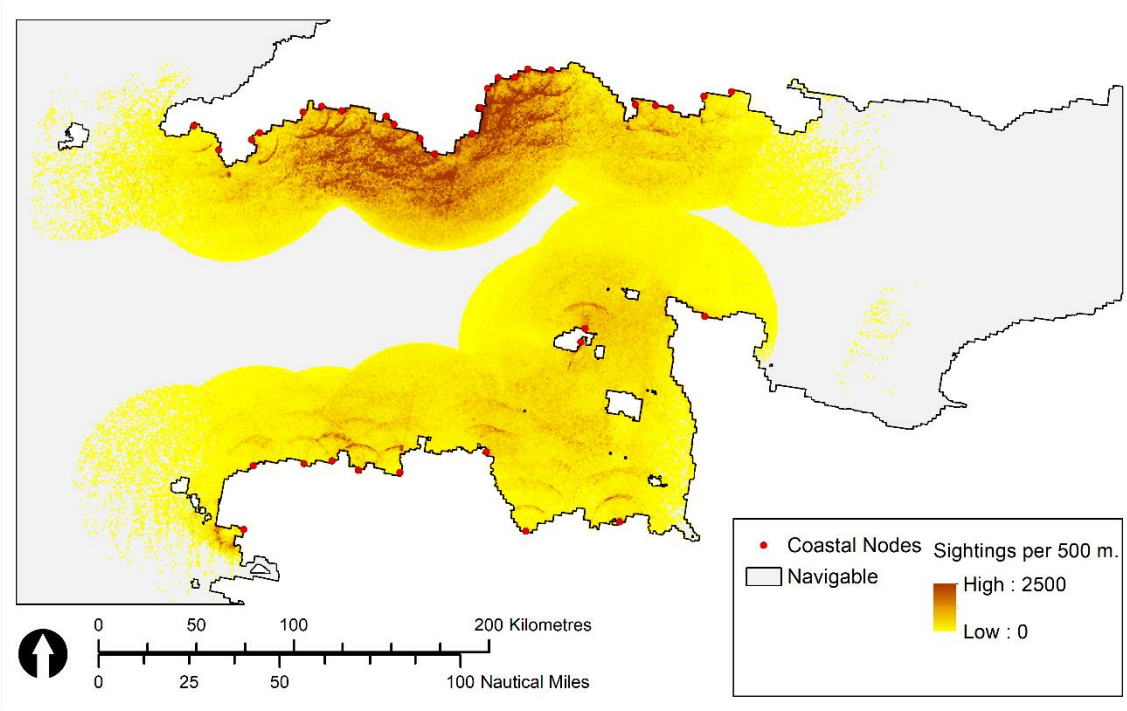


Figure 5.21: Density of landmark sighting locations in the Main Analysis.

Chapter 6 Figures

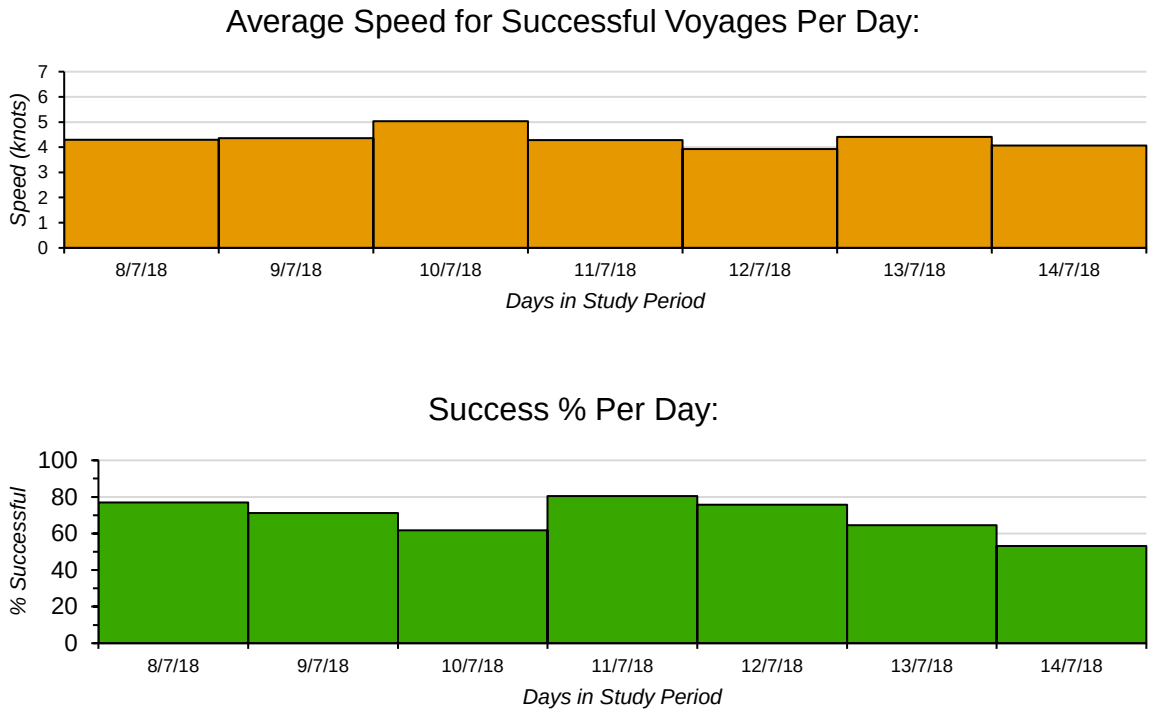


Figure 6.1: Average speeds and success rates per day in study period.



Figure 6.2: Average speed and success values for Case Study 1. In the first tier, light and dark green indicate high and low success rates. In the second tier, orange and red indicate faster and slower speeds. In the third tier red indicates better northbound value, blue indicates better southbound value.

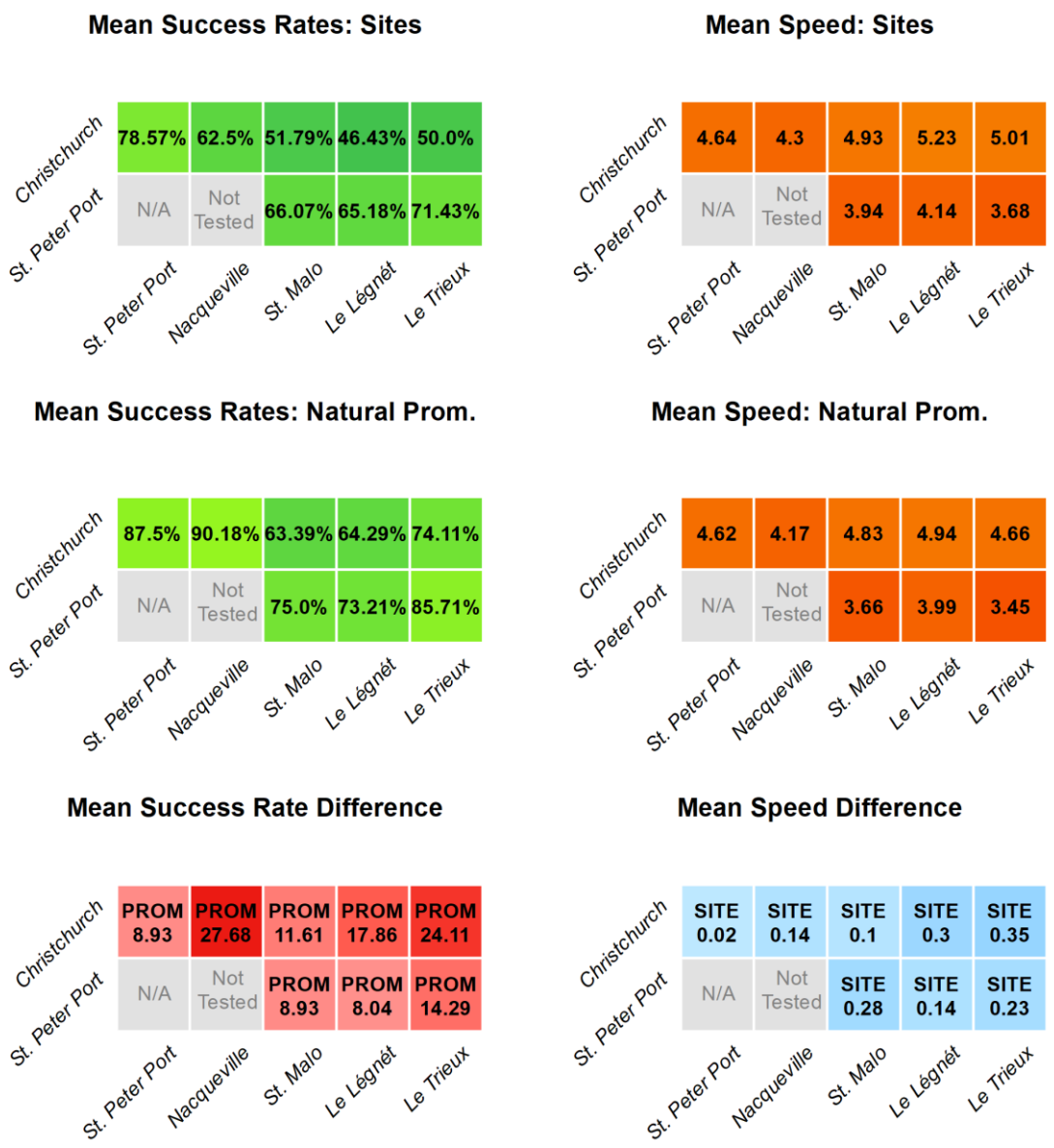


Figure 6.3: Average speeds and success rates, and differentials for landmark sets in Case Study 1. Routes are bidirectional (averaged across northbound and southbound voyages). In the first tier, light and dark green indicate high and low success rates. In the second tier, orange and red indicate faster and slower speeds. In the third tier red indicates better northbound value, blue indicates better southbound value.

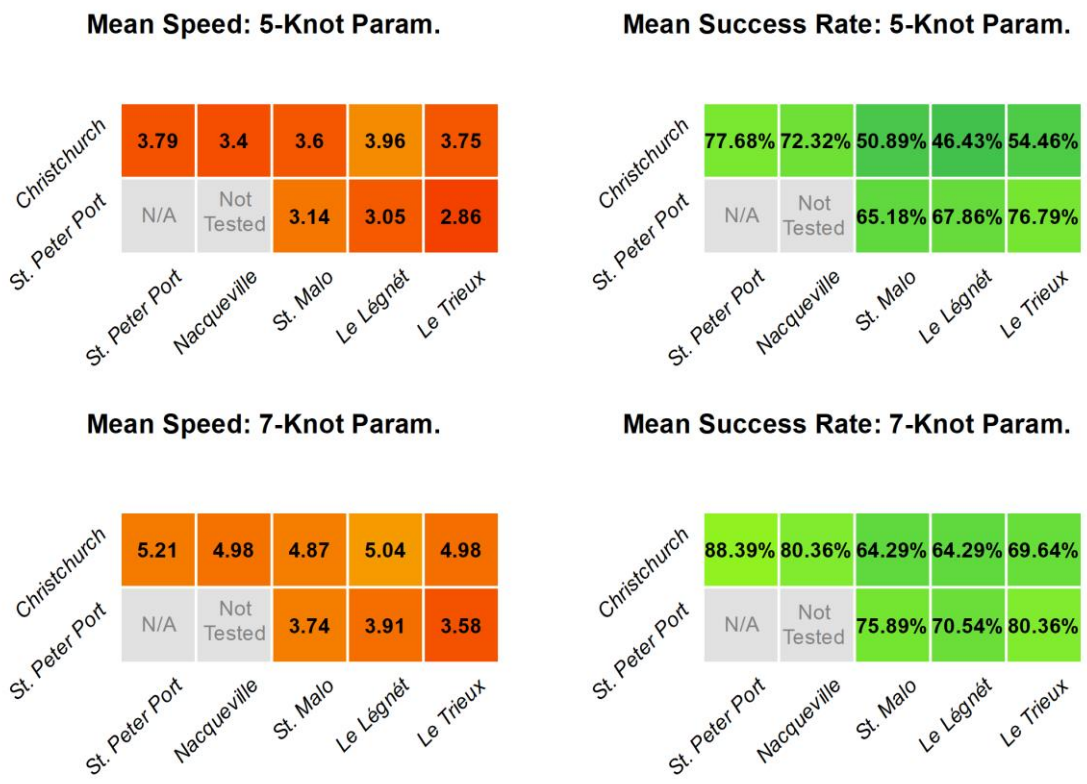


Figure 6.4: Average speeds and success rates for ship parameterisations in Case Study 1. In the first column, orange and red indicate faster and slower speeds. In the second column, light and dark green indicate high and low success rates.



Figure 6.5: Average speeds and success rates for reckoning ranges in Case Study 1. In the first column, orange and red indicate faster and slower speeds. In the second column, light and dark green indicate high and low success rates.

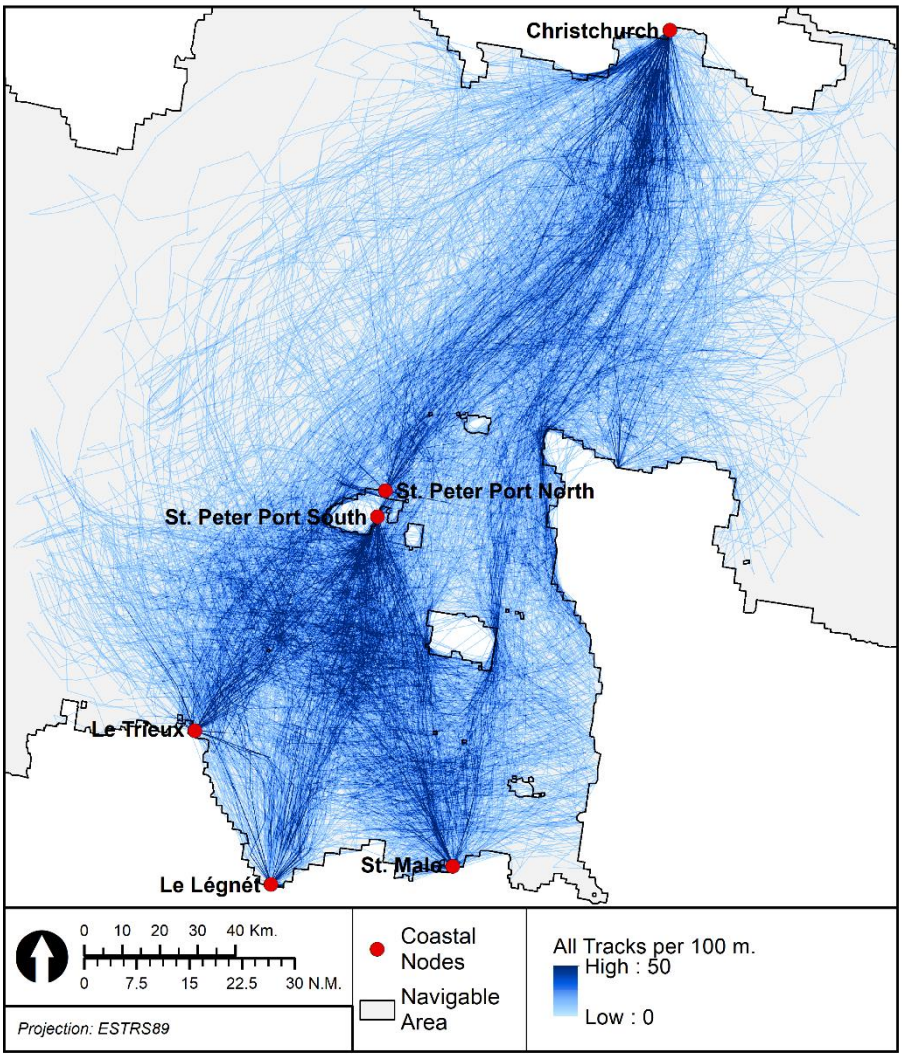


Figure 6.6: Track densities for all simulations in Case Study 1.

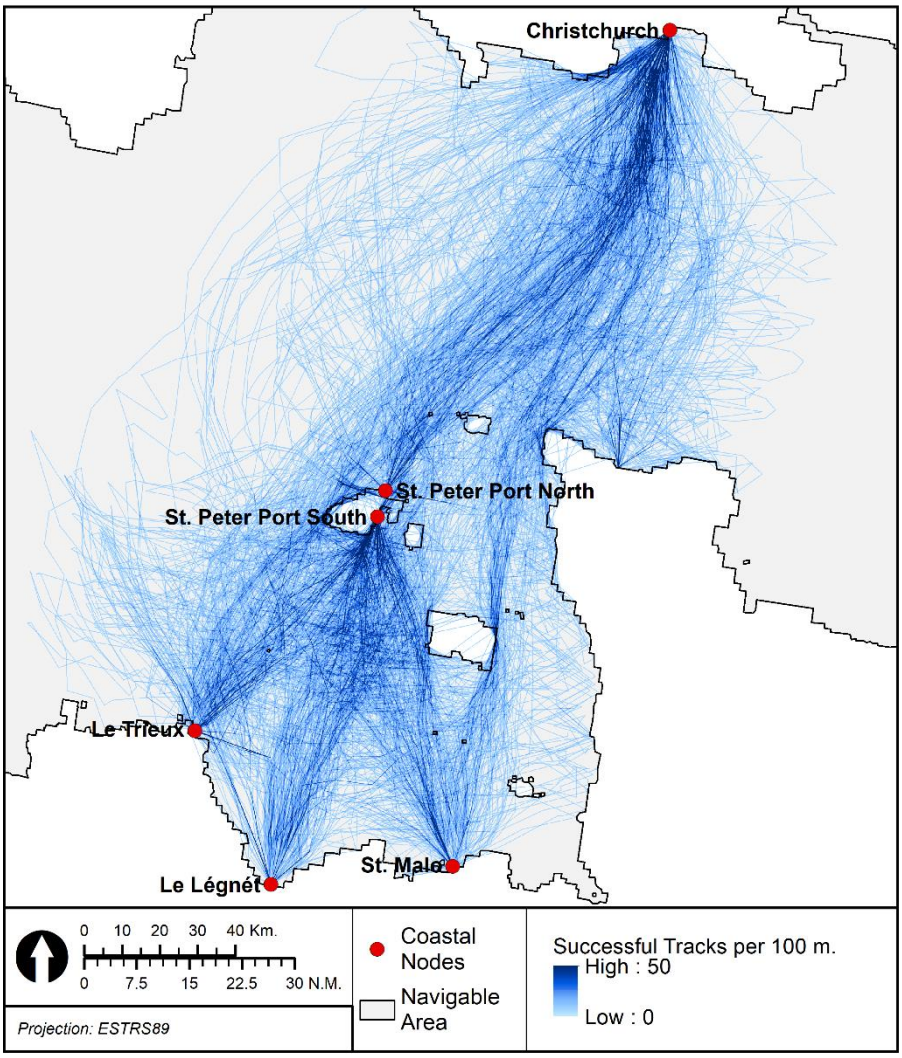


Figure 6.7: Track densities for all successful simulations in Case Study 1.

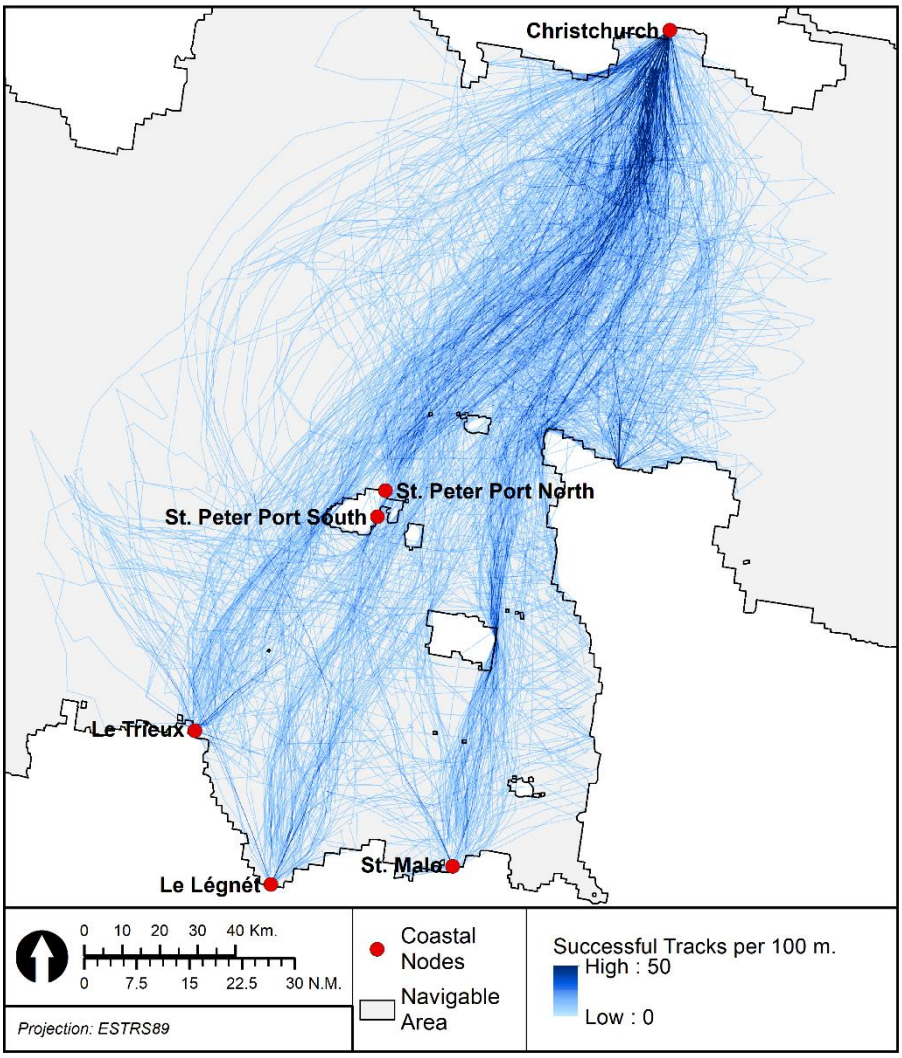


Figure 6.8: Track densities for successful simulations in Case Study 1, excluding simulations originating and terminating at St. Peter Port.

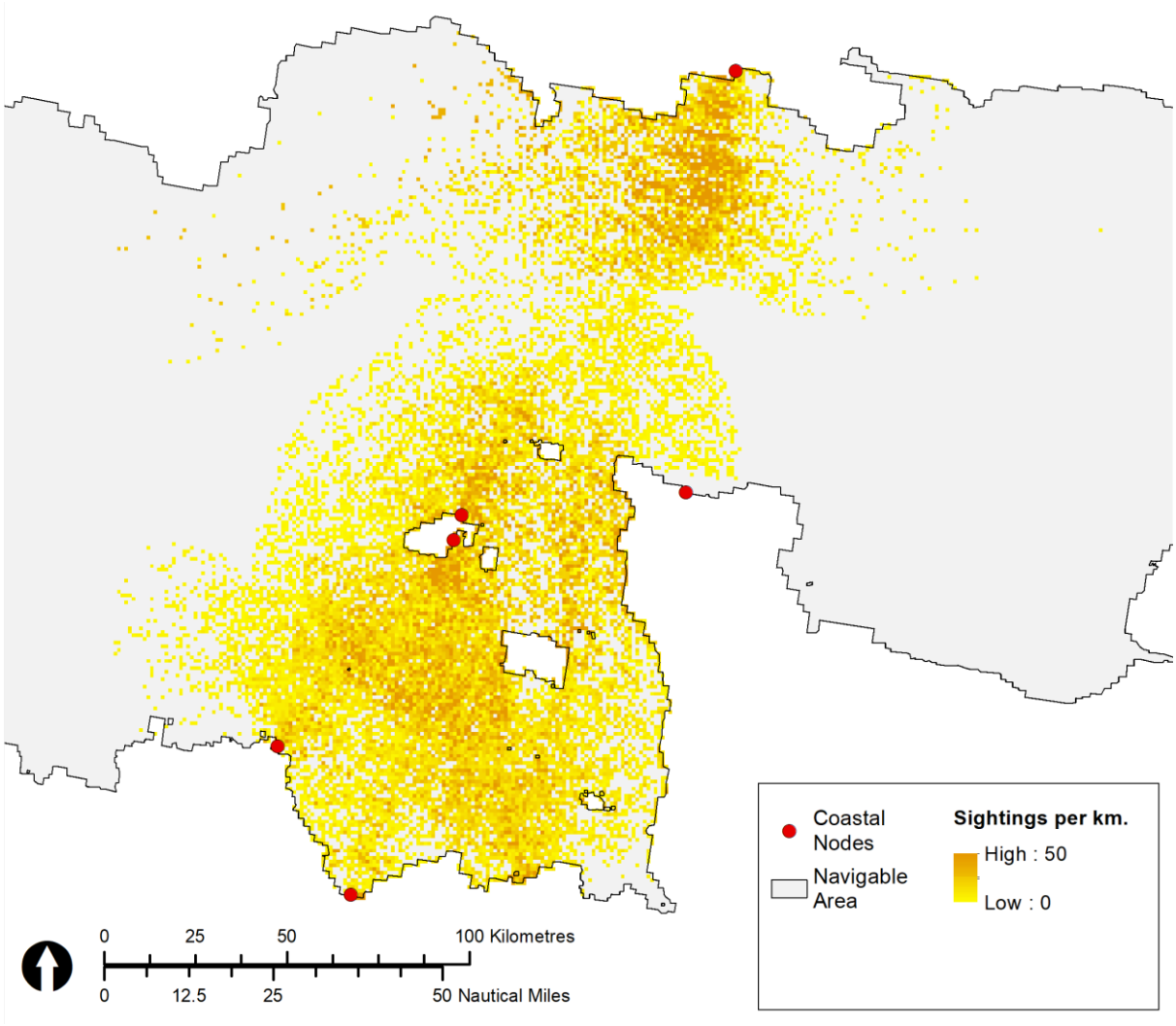


Figure 6.9: Sightings density for simulations in Case Study 1.

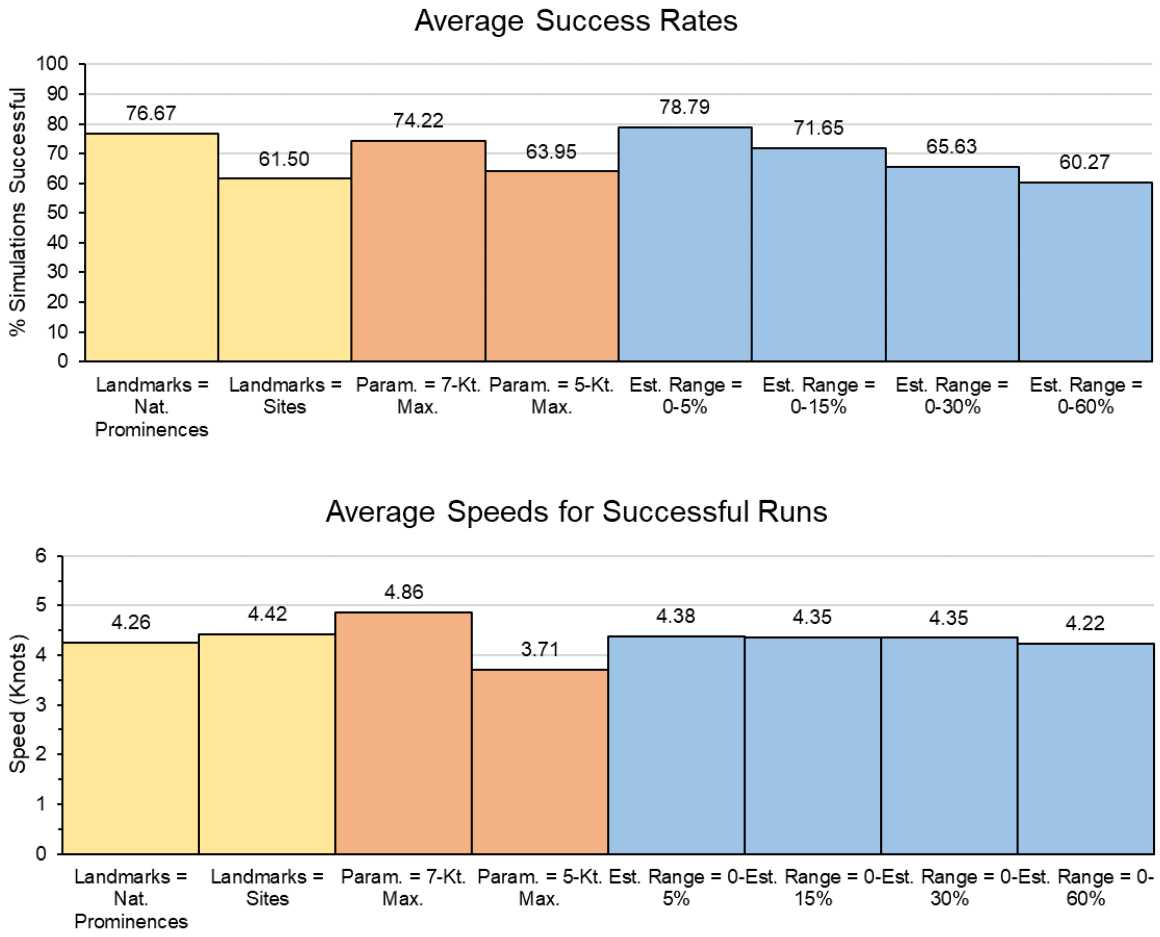


Figure 6.10: Comparison of general average success rates and speeds for parameter inputs to simulations in Case Study 1.

Chapter 7 Figures

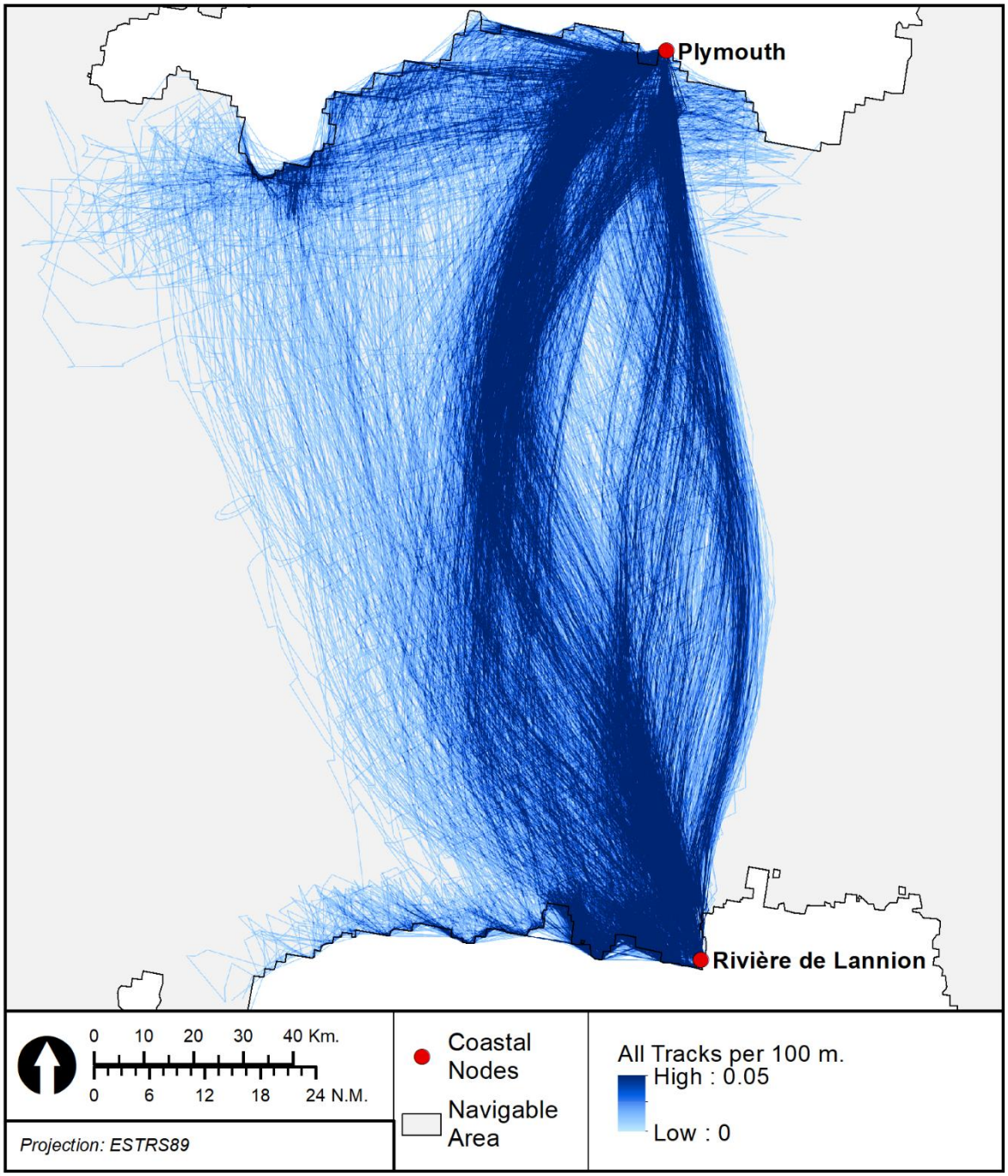


Figure 7.1: Ship track density results for all simulations performed for Case Study 2.

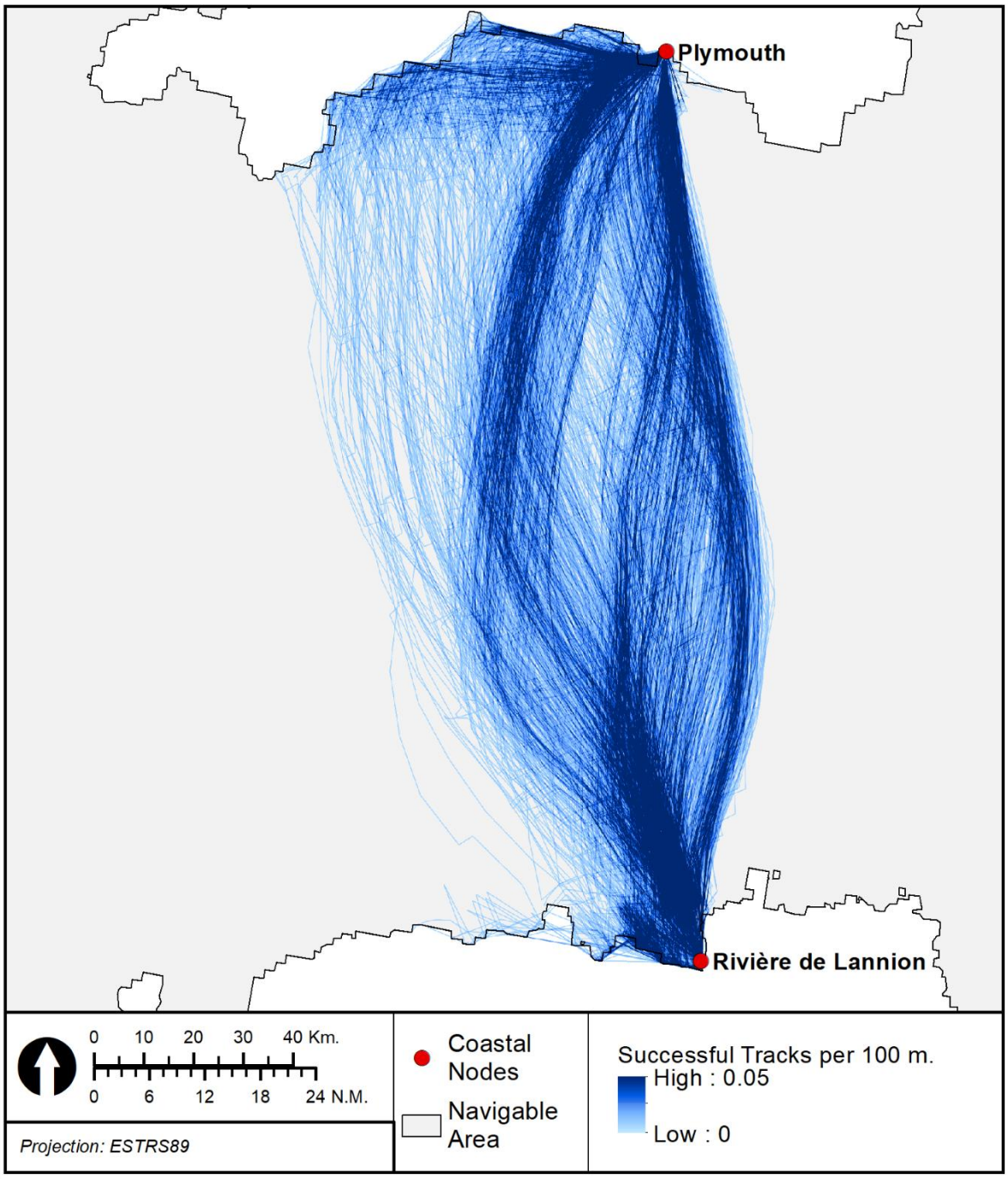


Figure 7.2: Ship track density results for all successful simulations performed for Case Study 2.

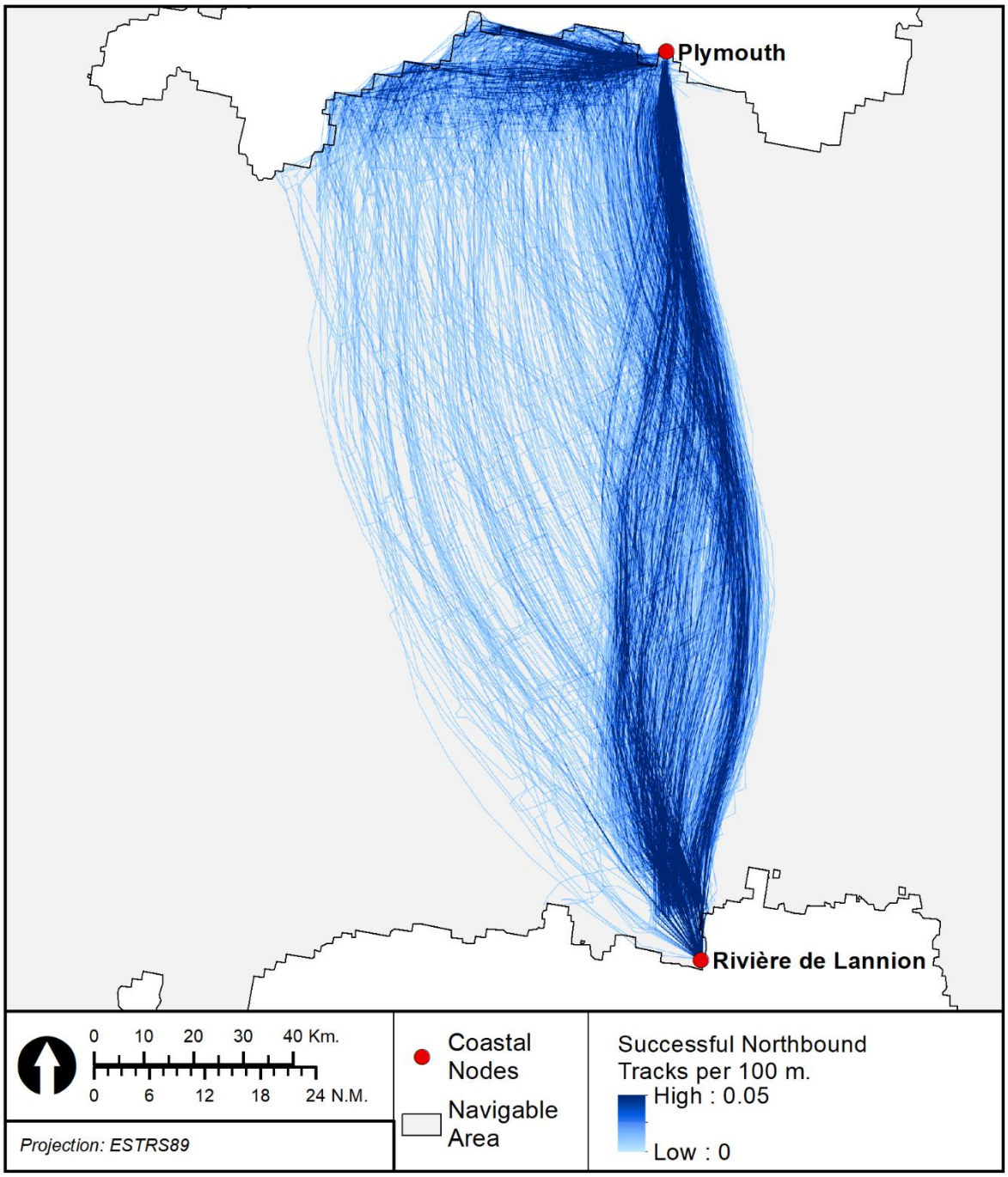


Figure 7.3: Ship track density results for all successful northbound simulations performed for Case Study 2.

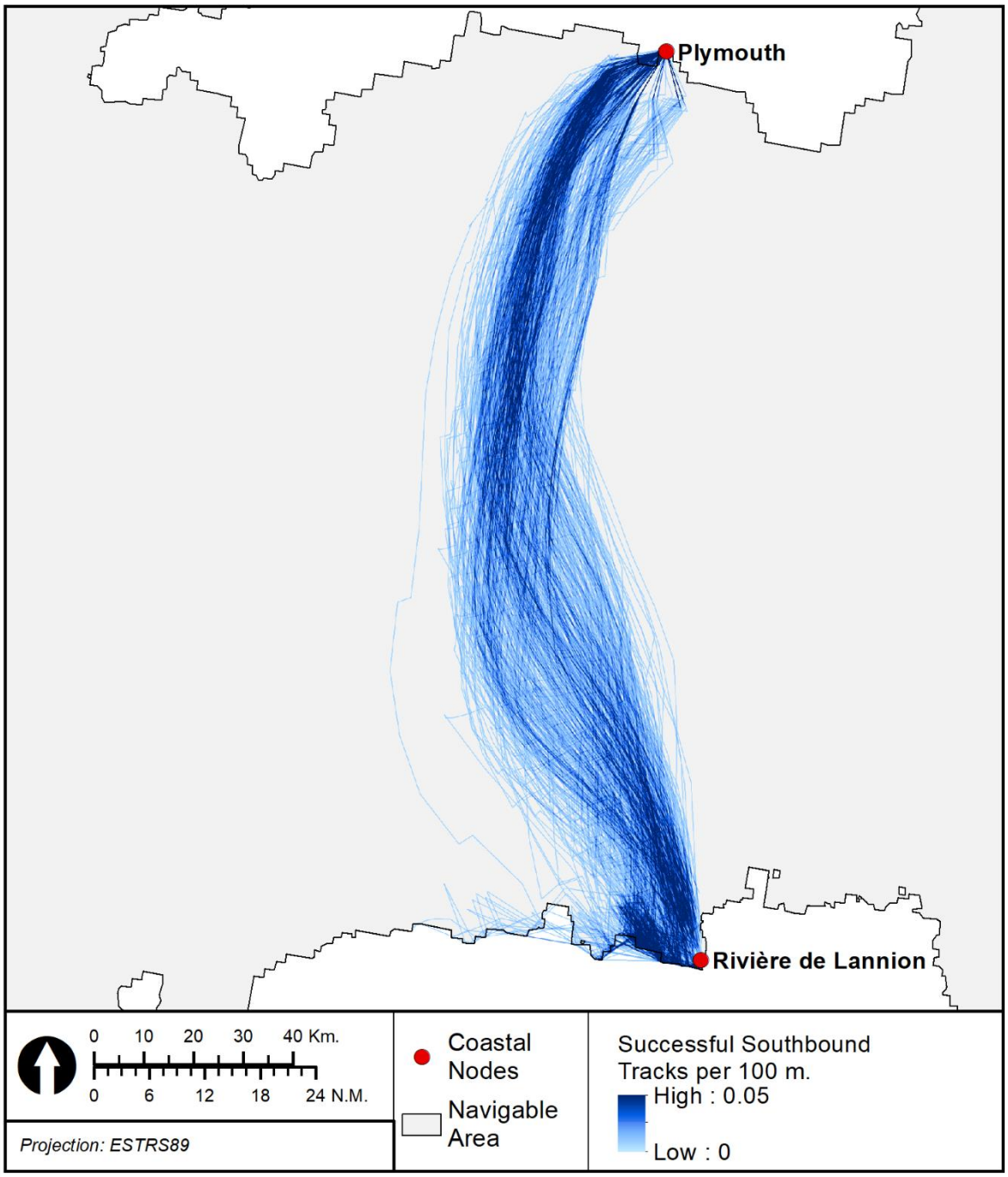


Figure 7.4: Ship track density results for all successful southbound simulations performed for Case Study 2.

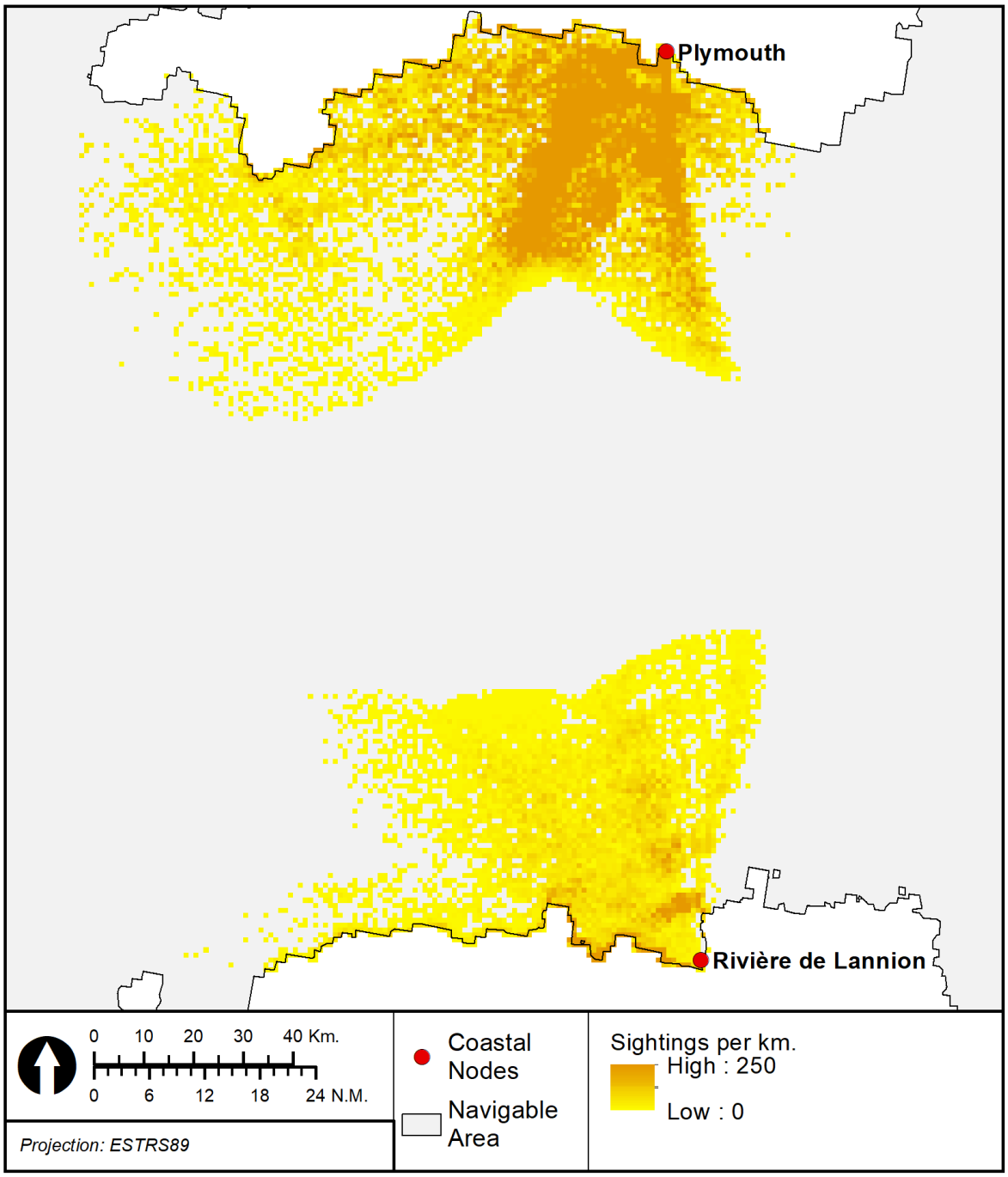


Figure 7.5: Sighting density results for all simulations performed for Case Study 2.

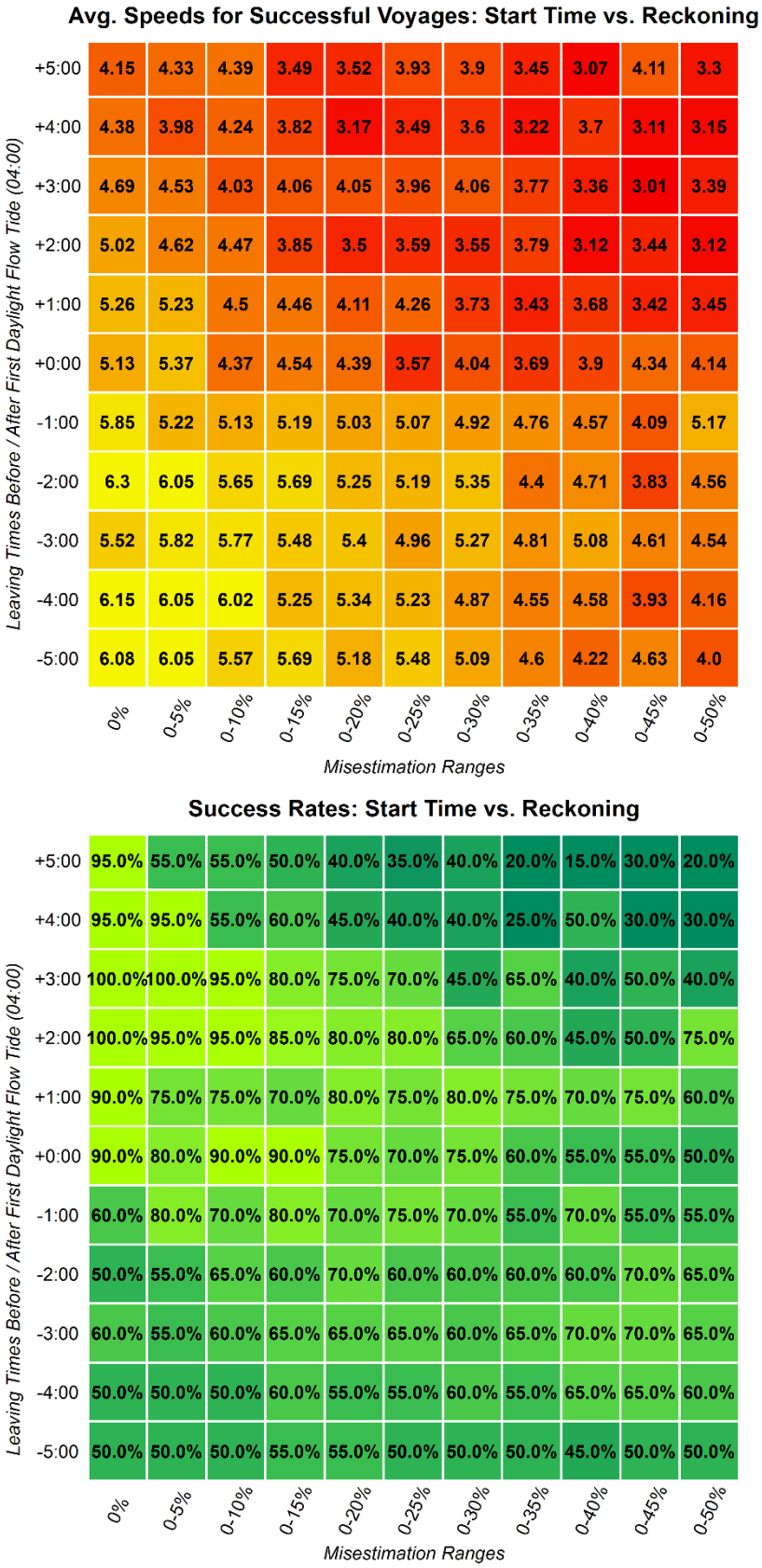


Figure 7.6: Average speeds and success rates for combinations of estimation ranges and leaving times in Case Study 2. Light and dark green indicate high and low success rates. Yellow and red indicate fast and slow speeds.

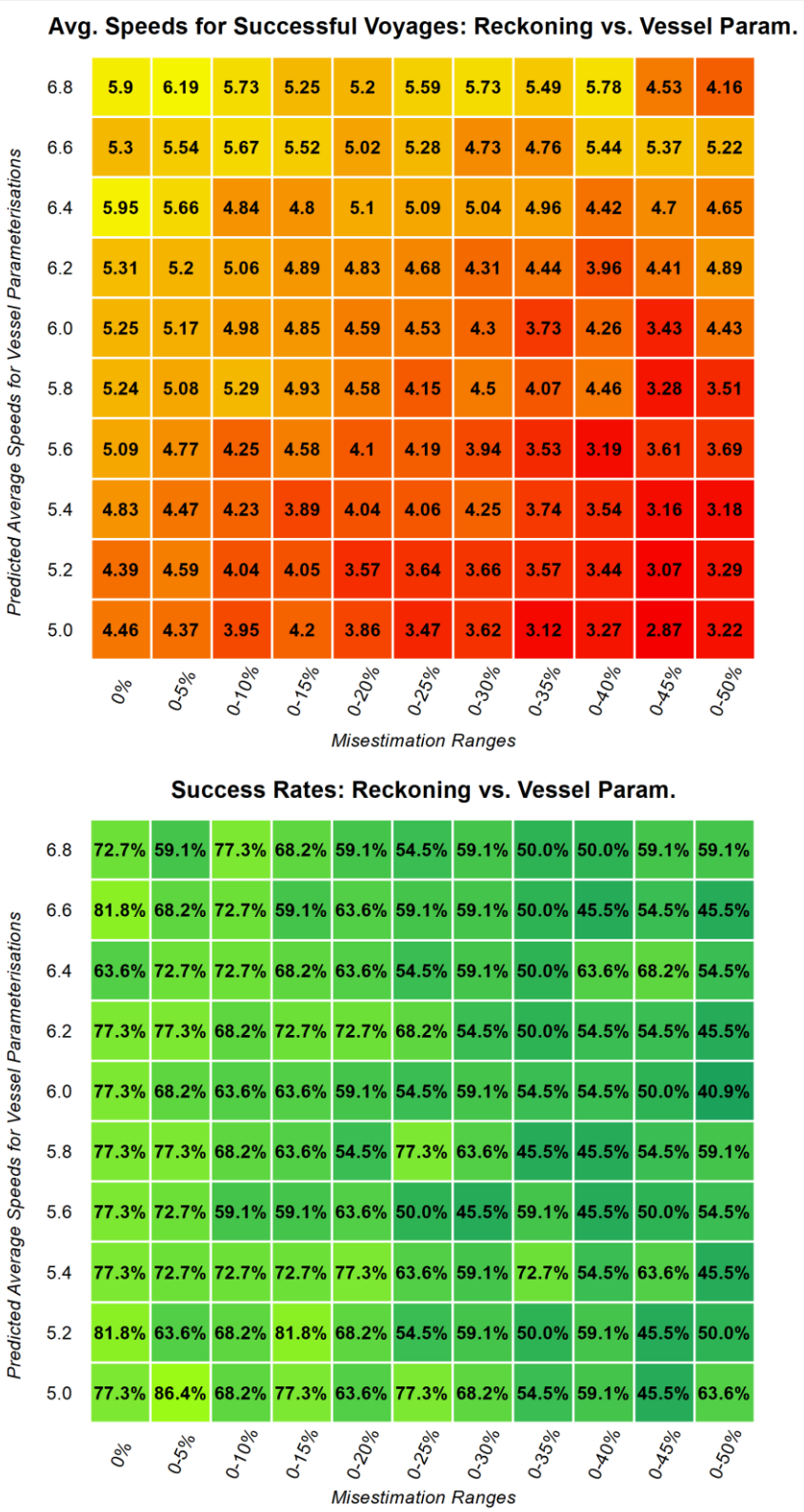


Figure 7.7: Average speeds and success rates for combinations of estimation ranges and vessel parameterisations in Case Study 2. Light and dark green indicate high and low success rates. Yellow and red indicate fast and slow speeds.

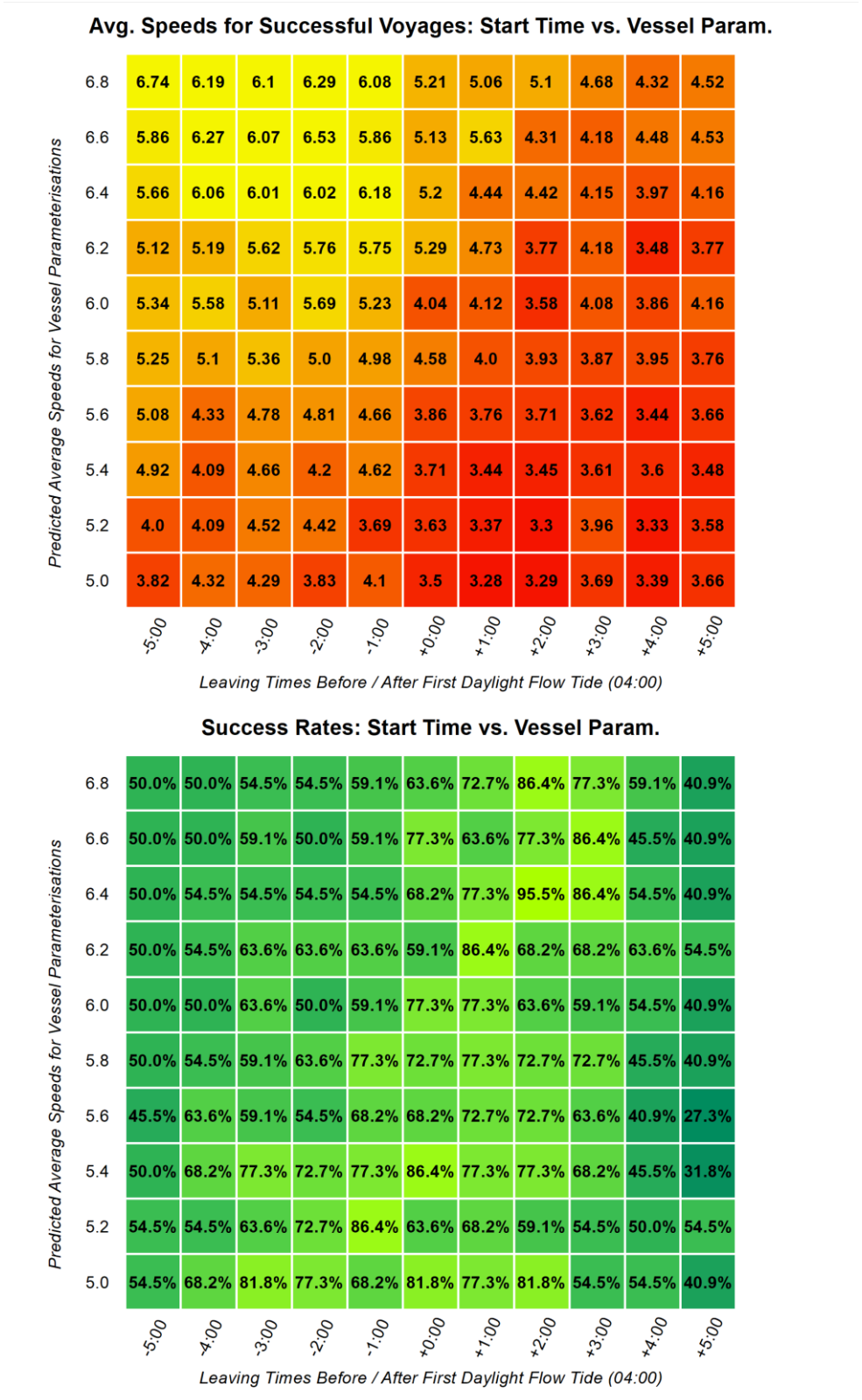


Figure 7.8: Average speeds and success rates for combinations of vessel parameterisations and leaving times in Case Study 2. Light and dark green indicate high and low success rates. Yellow and red indicate fast and slow speeds.

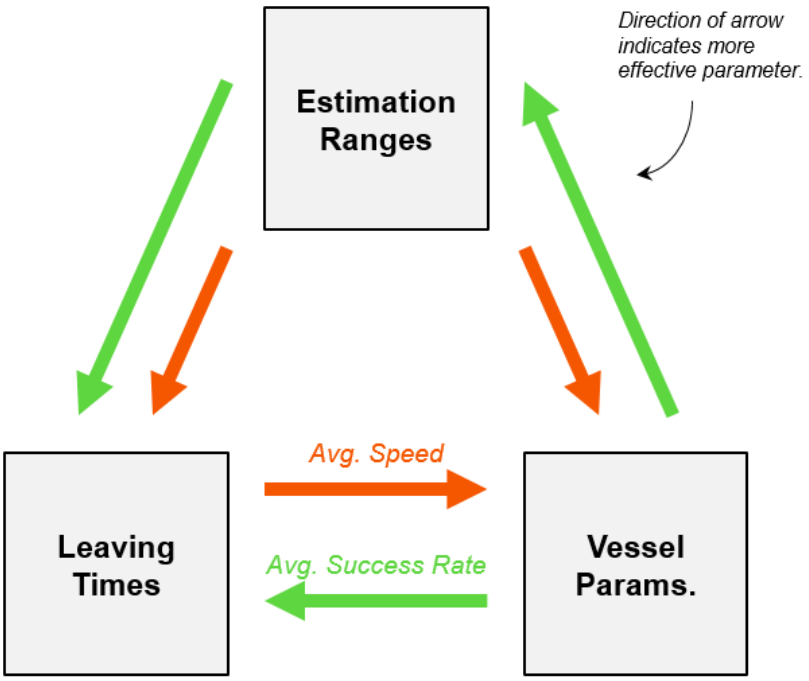


Figure 7.9: Summary of relative parameter effects in Case Study 2.

Chapter 8 Figures

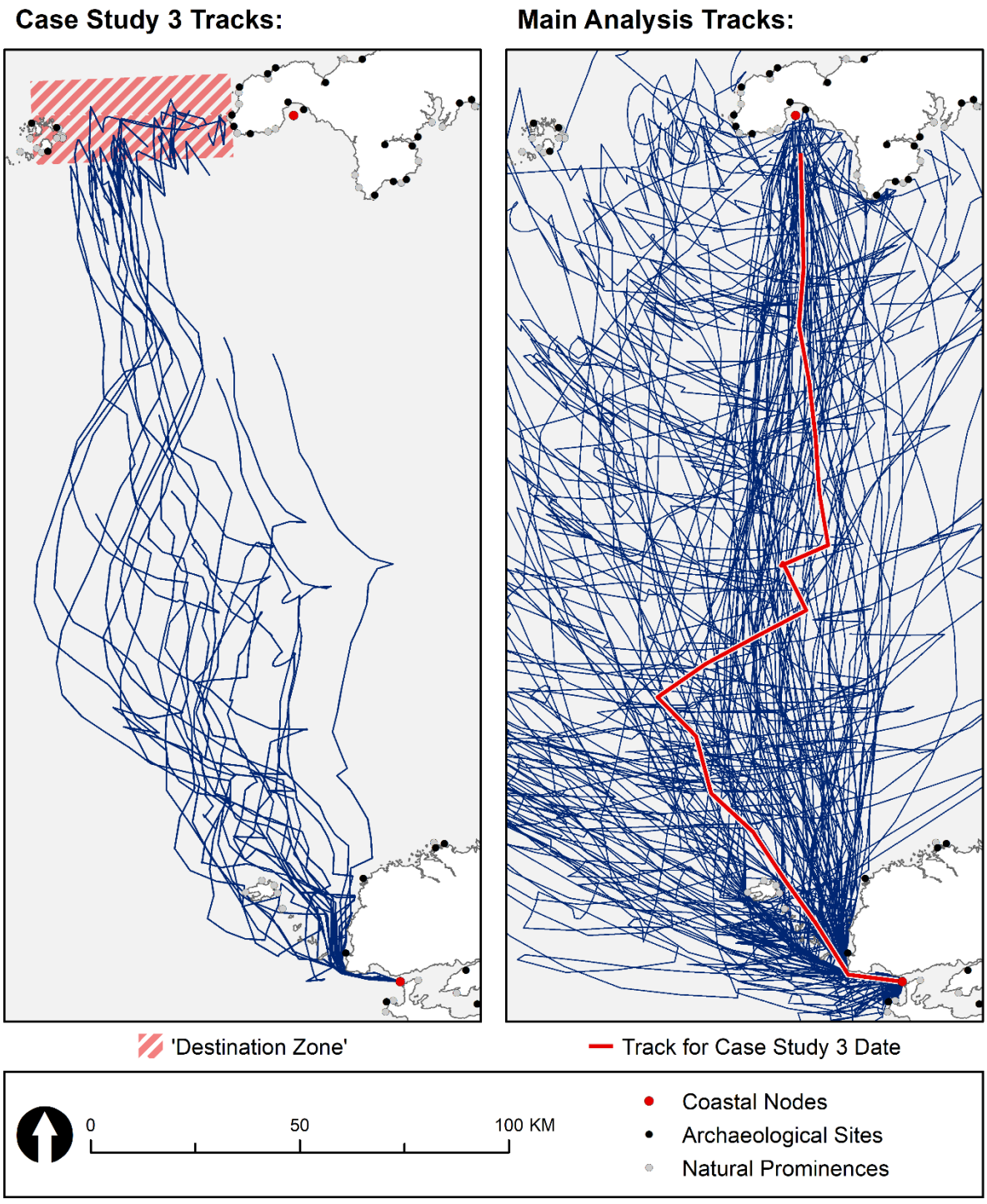


Figure 8.1: Simulated ship tracks for Case Study 3, and for the Brest-Penzance route from the Main Analysis.

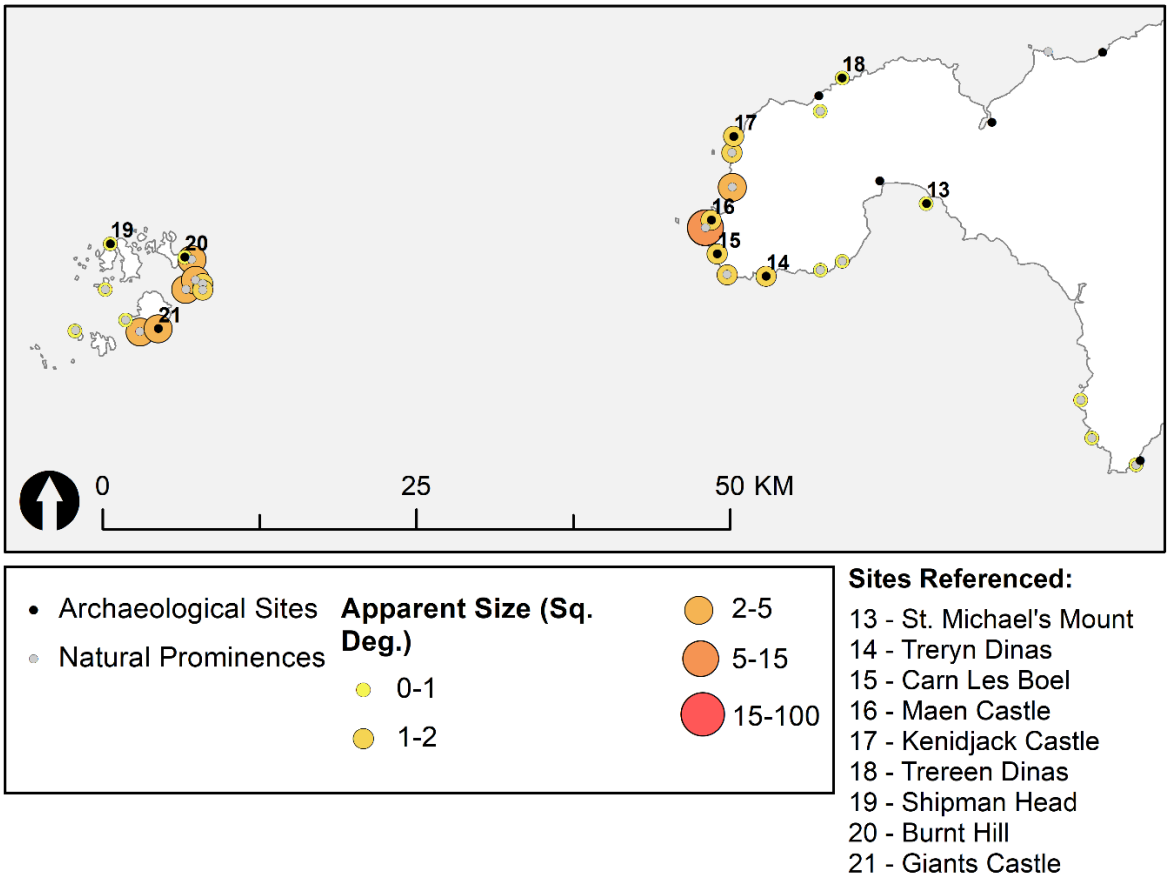


Figure 8.2: Apparent size of landmarks sighted on the northern shore of the western Channel in Case Study 3.

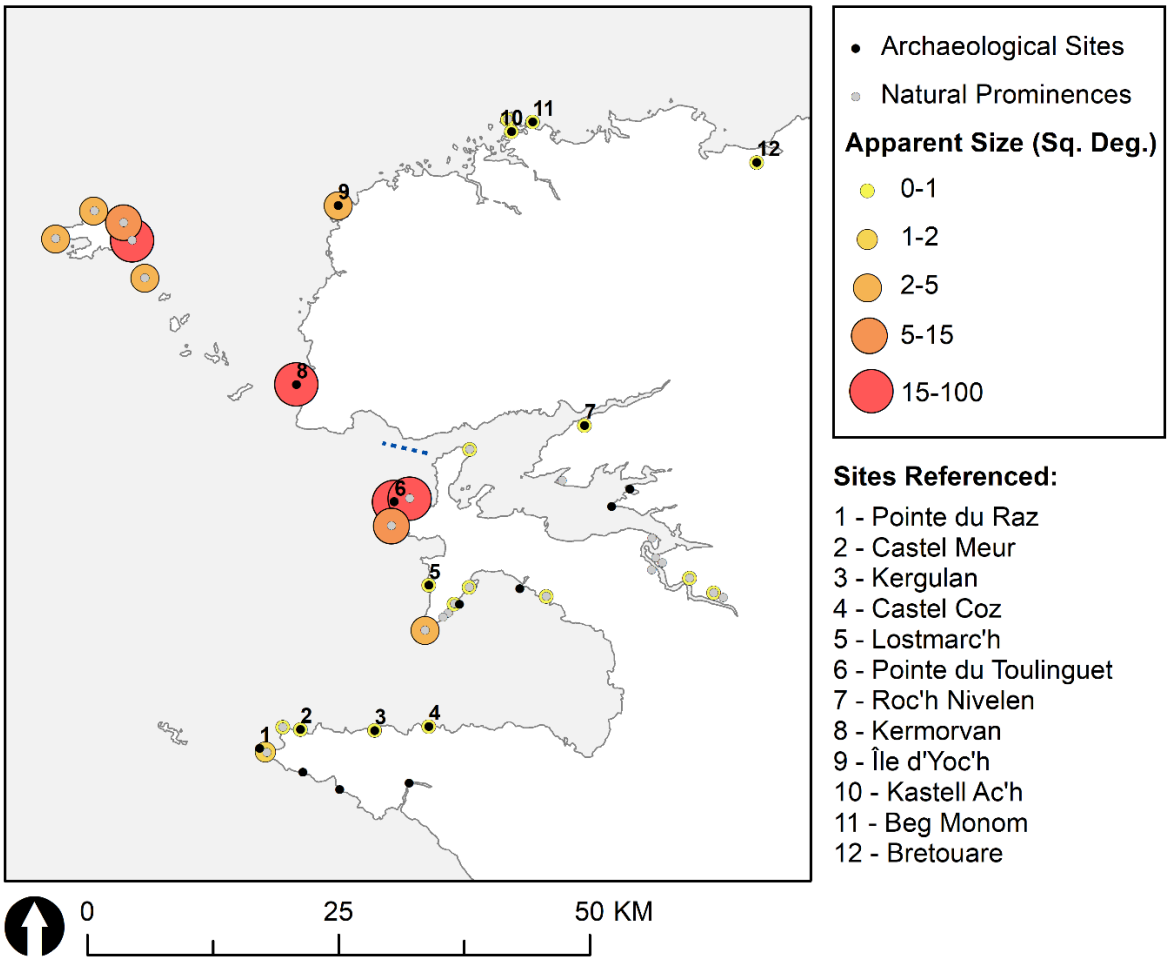


Figure 8.3: Apparent size of landmarks sighted on the southern shore of the western Channel in Case Study 3.

List of Tables

Table 4.1: Custom functions used in the navigation simulator. 76
Table 4.2: Script tools used to process navigation simulator outputs. 78
Table 4.3: Values required in parameter files. 80
Table 4.4: Values included in output logs by the navigation simulator 81
Table 4.5: Visibility categories according to the Shipping Forecast. 81
Table 5.1: Parameter spaces for analyses performed in this study. 82
Table 5.2: Vessel parameterisations used in analyses. 82
Table 5.3: Success and speed averages for nodes tested in the Main Analysis. Average speeds are in knots, which higher speeds shaded yellow. Success rates are in %, with higher percentages shaded lighter green. 83
Table 5.4: Node groups in the Main Analysis. Thresholds are derived from average values from Table 1. 84
Table 5.5: Visibility data for archaeological landmarks sighted during simulations in the Main Analysis. 85
Table 5.6: Comparison of travel times for routes evaluated by McGrail's (1983) model, and travel times recorded in the Main Analysis. 86
Table 6.1: Inbound and outbound averages for nodes in Case Study 1. Average speeds are in knots, which higher speeds shaded yellow. Success rates are in %, with higher percentages shaded lighter green. 87
Table 6.2: Sightings by landmark for Case Study 1. Archaeological sites are highlighted. 87
Table 7.1: Speed and success rates for parameters tested in Case Study 2. Average speeds are in knots, which higher speeds shaded yellow. Success rates are in %, with higher percentages shaded lighter green. 91
Table 7.2: Sighting counts for landmarks for Case Study 2. Potential landmarks identified with archaeological sites are highlighted: 92
Table 8.1: Success counts for simulations in Case Study 3. 95
Table 8.2: Number of sightings and apparent size for sites in Case Study 3: 95
Table 8.3: Speeds for 'successful' runs in Case Study 3. 96

Chapter 4 Tables

Table 4.1: Custom functions used in the navigation simulator.

Function Type	*Function Name*	*Description*	*ArcGIS Tools Used?*
Extraction	Raster_Clip	Creates / identifies raster subset.	*X*
Extraction	CSV_to_List	Reads CSV file to Python list object.	
Extraction	Extract_Raster_Value	Extracts value at coordinates.	X
Extraction	TXT_to_Dictionary	Reads textfile to Python dictionary object.	
Extraction	Extract_NetCDF	Extracts value from NetCDF at coordinates.	
Extraction	Raster_Mosaic	Mosaics raster datasets.	X
Extraction	Search_Nested_List	Retrieves value from Python list object.	
Extraction	Shipping_Forecast_Visibility	Reads vis. distance from Shipping Forecast.	
Visibility	Create_Observer_Point	Writes coordinates to shapefile.	X
Visibility	Check_Skyline_Intersection	Checks vector-skyline intrsection.	X
Visibility	Directed_Projective_Array	Generates radial array.	X
Visibility	Directed_Skyline	Generates constricted skyline.	X
Visibility	Intersect_3D_Line_With_Surface	Performs vector-DEM intersection.	X
Visibility	Check_Daylight	Checks solar azimuth at timestep/coordinate.	
Navigation	Angle_to_Compass_Bearing	Converts angle to compass bearing.	
Navigation	Coordinate_Polygon_Disjoint	Tests coordinate-polygon disjoint.	X
Navigation	Vector_Magnitude	Computes vector magnitude.	
Navigation	Clockwise_Angle	Calculates clockwise angle between vectors.	
Navigation	ETRS89_to_WGS84	Transforms coordinates to geographic coordinate system.	X
Navigation	WGS84_to_ETRS89	Transforms coordinates to projected coordinate system.	X
Navigation	Compute_Interior_Angle	Computes interior angle.	
Navigation	Convex_Path	Computes observer-target path distance.	X
Navigation	Knots_to_MPS	Converts from knots to metres per second.	
Navigation	Metres_to_NM	Converts from metres to nautical miles.	
Navigation	MPS_to_Knots	Converts from metres per second to knots.	
Navigation	MPS_to_Beaufort	Converts from metres per second to the Beaufort scale.	
Navigation	NM_to_Metres	Converts nautical miles to metres.	
Navigation	Translate_Point	Translates ESRI point object by offset.	
Navigation	Vector_to_Compass_Bearing	Calculates compass bearing.	
Navigation	Vectors_to_Relative_Bearing	Calculates relative bearing.	
Output	Save_Plot	Saves PyPlot plot to file.	

Output	Plot_From_Dictionary	Creates PyPlot plot from dictionary.	
Output	Plot_Shapefile	Adds shapefile to PyPlot plot.	X
Output	Plot_Geometry	Adds ESRI geometry object to PyPlot plot.	X
Output	Save_Textfile	Writes dictionary to text file.	
Output	Unique_Filename	Generates unique filename.	

Table 4.2: Script tools used to process navigation simulator outputs.

Folder	*Filename*	*Description*
navigation simulator	navigation_simulator	The primary script used to run the navigation simulation. Coordinates modules within the 'navigation_simulator' folder, and contains code for GUI.
navigation simulator	data: iterable	Contains list objects that are called into all simulations.
navigation simulator	functions: exception	Contains functions for error handling and reporting.
navigation simulator	functions: extraction	Contains functions for reading values from input datasets.
navigation simulator	functions: navigation	Contains functions for creating and evaluating headings, and for converting between units.
navigation simulator	functions: output	Contains functions for writing navigation simulator outputs.
navigation simulator	functions: visibility	Contains functions for performing all three stages of visibility analysis.
navigation simulator	main: alerts	Contains functions for sending email alerts to the user.
navigation simulator	main: analysis	Performs the navigation simulation for a single parameter file.
navigation simulator	main: recording	Produces outputs from the results of the navigation simulation.
navigation simulator	main: setup	Contains functions for importing modules.
data processing	generate_LRMs	Coordinates the Focal Statistics and Raster Calculator tools to generate a local relief model.
data_collection	scrape_shipping_forecasts	Scrapes shipping forecasts from the daily MET Office bulletin daily.
data_collection	scrape_SHOM_datasets	Scrapes hydrodynamic and aerodynamic datasets from the SHOM portal, weekly.
data_processing	build_parameters_files	Iterates through parameter ranges, generating parameter files for each unique combination. Assigns unique IDs to parameter files based on user input.
data_processing	extract_LRM_values	Extracts values from a set of local relief models to a set of points. Used to check local relief models against records from the Database of British and Irish Hills.
data_processing	generate_feature_grids	Generates 3D point grids for polygon extents corresponding to landmarks, using an input DEM.
data_processing	generate_netCDF_mask	Reads bins from a NetCDF file as points, and generates a polygon mask from the extent of said points.
data_processing	identify_parameters_files	Searches for duplicate parameter files. Used to coordinate analyses between PCs.

data_processing	output_aggregator	Reads navigation and visibility logs to a set of data tables. Validates logs and adds parameters for analysis.
data_processing	shipping_forecast_summarise	Validates records scraped from the Shipping forecast by performing a spell-check. Evaluates corrected records and assigns visibility values per record.
data_processing	validate_datasets	Checks NetCDF and Shipping Forecast records by querying a set of sample points for all days in the study period.

Table 4.3: Values required in parameter files.

Input Field Name	*Data Type*	*Value Description*
Destination Name	Coded Value	A code identifying the destination point in the Shipping Forecast.
Origin Name	Coded Value	A code identifying the origin point in the Shipping Forecast.
Simulation ID	Coded Value	An ID code used to identify simulation outputs.
Origin Coordinates	Coordinate Pair	Latitude / longitude coordinate pair for the simulated origin point.
Destination Coordinates	Coordinates	Latitude / longitude coordinate pair for the simulated destination point.
Simulation Date	Date String	The date on which the simulation is set to start.
Data Directory	Directory	A folder containing NetCDF files, and shipping forecast tables.
Landmarks Directory	Directory	Contains Polygon features and point grids for landmarks.
Output Directory	Directory	Creates a file system in this directory, into which script outputs are saved.
Overestimation Range	List of Numeric Values	Represents the amount (in percentage points) that a value may be overestimated by the script.
Underestimation Range	List of Numeric Values	Represents the amount (in percentage points) that a value may be underestimated by the script.
Maximum Time	Numeric Value	The maximum number of hours (timesteps) that the script will simulate.
Start Time	Numeric Value	The time at which the destination is set to start.
Obstacle Features	Polygon Features	Features representing 'obstacles' used in pathfinding.
Coastline Features	Polyline	Used to contextualise data in output plots.
DEM	Raster Image	An elevation model derived from terrain / bathymetry data.
Polar Diagram Table	Text File	Used to create heading envelopes.

Table 4.4: Values included in output logs by the navigation simulator.

Output Field Name	*Value Description*
Destination Easting / Northing	Coordinates for destination in ETRS89.
Destination ID	ID code for destination coastal node.
Destination Latitude / Longitude	Geographic coordinates for destination.
Landmark Count	Number of landmarks identified as visible.
Magnitude of Selected Heading	Magnitude (in metres) of the selected heading vector.
Maximum Visibility	Maximum visibility value derived from the Shipping Forecast.
Origin Easting / Northing	Coordinates for origin point in ETRS89.
Origin ID	ID code for origin coastal node.
Origin Latitude / Longitude	Geographic coordinates for origin point.
Real Distance to Destination	Distance to destination (in nautical miles).
Real Distance Travelled	Real distance travelled (in nautical miles).
Real Elevation	Real elevation above sea level (in metres).
Real End Easting / Northing	Real coordinates for endpoint in ETRS89.
Real End Latitude / Longitude	Real geographic coordinates for endpoint in ETRS89.
Real Hydrodynamic Bearing	Real current bearing at timestep.
Real Hydrodynamic Vector	Vector representing current direction / speed at timestep.
Real Hydrodynamic Velocity	Magnitude of Real Hydrodynamic Vector.
Real Vessel Speed	Simulated vessel speed in metres per second.
Real Start Easting / Northing	Real coordinates for start point in ETRS89.
Real Start Latitude / Longitude	Real geographic coordinates for start point.
Real Wind Bearing	Real wind bearing at timestep.
Real Wind Relative Bearing	Real wind bearing relative to selected heading.
Real Wind Speed in Beaufort	Real relative bearing classified by Beaufort Code.
Real Wind Speed	Magnitude of the Real Wind Vector.
Real Wind Vector	Vector representing wind direction / speed at timestep.
Reckoned End Easting / Northing	Reckoned end point coordinates in ETRS89.
Reckoned Hydrodynamic Bearing	Reckoned current bearing.
Reckoned Start Easting / Northing	Reckoned start point coordinates in ETRS89.
Reckoned Wind Vector	Vector representing reck. wind direction / speed at timestep.
Selected Heading	Heading selected for simulation.
Success	Results of success evaluation at timestep.
Timestep	Number of simulated hours elapsed since simulation start.

Table 4.5: Visibility categories according to the Shipping Forecast.

Shipping Forecast Code	*VISIBLE DISTANCE*
VERY POOR	< 1 kilometre
POOR	1 km. – 2 nautical miles (3.704 km.)
MODERATE	2 n.m. – 5 n.m. (9.26 km.)
GOOD	> 5 n.m.

** See: https://www.metoffice.gov.uk/guide/weather/marine/glossary*

Chapter 5 Tables

Table 5.1: Parameter spaces for analyses performed in this study.

Analysis	Days in Study Period	Simulated Routes	Landmark Sets	Vessel Params.	Ranges for 'Reckoning'	Sailings Per Day	Total Simulations
Main Analysis	212	419	1	1	1	1	88,828
Case Study 1	7	20	2	2	4	1	2,240
Case Study 2	1	2	1	10	11	11	2,420
Case Study 3	1	2	2	1	3	11	132
					Number of runs required to complete all analyses:		*93,620*
					Number of runs required to sweep combined parameter space:		*214,963,760*

Table 5.2: Vessel parameterisations used in analyses.

Name	*Maximum Speed*	*Average Speed*
McGrail-7m.*	10.56 kts.	5 kts.
McGrail-9m.*	13.96 kts.	6.8 kts.
Case Study 2.01	10.56 kts.	5 kts.
Case Study 2.02	10.94 kts.	5.2 kts.
Case Study 2.03	11.31 kts.	5.4 kts.
Case Study 2.04	11.69 kts.	5.6 kts.
Case Study 2.05	12.07 kts.	5.8 kts.
Case Study 2.06	12.45 kts.	6 kts.
Case Study 2.07	12.82 kts.	6.2 kts.
Case Study 2.08	13.2 kts.	6.4 kts.
Case Study 2.09	13.58 kts.	6.6 kts.
Case Study 2.10	13.96 kts.	6.8 kts.
Case Study 3.01	5 kts.	2.4 kts.
Case Study 3.02	7 kts.	3.3 kts.
Case Study 3.03	9 kts.	4.4 kts.

**Maximum speed values for params. inspired by McGrail are higher than he predicts (<<CALLBACK>>).*

Table 5.3: Success and speed averages for nodes tested in the Main Analysis. Average speeds are in knots, which higher speeds shaded yellow. Success rates are in %, with higher percentages shaded lighter green.

	Average Speed				*Success Rates*			
	Overall	*Inbound*	*Outbound*	*Diff.*	*Overall*	*Inbound*	*Outbound*	*Diff.*
Aber Wrac'h	3.94	4.38	3.58	IN+0.8	59.98	58.26	61.40	OUT+3.14
Anse de Kernic	4.12	4.34	3.92	IN+0.42	61.74	61.27	62.17	OUT+0.9
Bigbury Bay	3.87	3.60	4.19	OUT+0.59	62.39	59.64	65.41	OUT+5.77
Brest	4.58	4.05	5.26	OUT+1.21	35.36	38.33	32.46	IN+5.87
Budleigh Salterton	4.13	3.97	4.30	OUT+0.33	60.91	62.10	59.64	IN+2.46
Christchurch	3.84	3.86	3.83	IN+0.03	60.28	61.44	59.13	IN+2.31
Dartmouth	3.94	3.49	4.52	OUT+1.03	65.83	64.76	67.14	OUT+2.39
Fowey	4.09	3.78	4.45	OUT+0.66	57.93	53.72	62.13	OUT+8.4
Helford	3.98	3.52	4.58	OUT+1.07	53.34	46.49	60.44	OUT+13.96
Kérivoas	3.94	4.41	3.55	IN+0.86	61.21	60.27	62.05	OUT+1.78
Kimmeridge Bay	3.79	3.85	3.73	IN+0.12	61.94	63.07	60.80	IN+2.27
Le Légnét	4.62	5.08	4.25	IN+0.83	57.76	65.71	50.66	IN+15.05
Le Trieux	3.83	4.42	3.38	IN+1.04	64.02	66.63	61.69	IN+4.93
Lulworth Cove	4.06	3.85	4.28	OUT+0.43	58.86	61.58	55.80	IN+5.77
Mevagissey	4.17	3.75	4.70	OUT+0.95	56.83	51.45	62.45	OUT+11
Morlaix	4.21	4.47	3.99	IN+0.48	60.51	59.93	61.02	OUT+1.09
Mothecombe	4.07	3.67	4.56	OUT+0.88	61.14	57.96	64.72	OUT+6.77
Mullion	3.92	3.53	4.38	OUT+0.85	58.83	53.52	63.92	OUT+10.4
Nacqueville	3.41	3.73	3.14	IN+0.59	61.17	61.97	60.45	IN+1.52
Penzance	4.17	3.62	4.90	OUT+1.28	53.78	46.56	60.51	OUT+13.95
Plymouth	4.19	3.72	4.81	OUT+1.09	59.95	57.30	62.92	OUT+5.63
Poole	4.04	3.92	4.16	OUT+0.24	58.13	61.58	54.34	IN+7.24
Porthallow	4.09	3.83	4.39	OUT+0.56	59.92	55.49	64.29	OUT+8.8
Portland	4.32	3.80	5.00	OUT+1.19	57.57	60.89	53.29	IN+7.59
Rivière de Lannion	4.14	4.53	3.80	IN+0.73	59.61	61.96	57.57	IN+4.39
Salcombe	4.25	5.09	3.65	IN+1.44	58.98	67.05	51.77	IN+15.28
Seaton	3.86	3.55	4.23	OUT+0.68	63.27	62.07	64.70	OUT+2.63
Sidmouth	4.02	3.94	4.11	OUT+0.17	62.29	63.28	61.30	IN+1.98
St. Malo	4.01	3.88	4.15	OUT+0.27	62.06	61.88	62.24	OUT+0.36
St. Peter Port (N.)	3.23	3.64	2.86	IN+0.78	68.00	64.58	72.16	OUT+7.58
St. Peter Port (S.)	2.64	2.72	2.56	IN+0.15	63.35	60.63	66.83	OUT+6.19
Teignmouth	4.31	3.71	5.15	OUT+1.44	59.02	59.85	57.94	IN+1.92
Topsham	4.41	3.81	5.22	OUT+1.41	58.67	59.99	56.98	IN+3.01
Torquay	3.81	3.57	4.09	OUT+0.52	62.74	61.05	64.53	OUT+3.48

Table 5.4: Node groups in the Main Analysis. Thresholds are derived from average values from Table 1.

	Overall Speed > 4.00 kts.	Speed Difference < 0.74 kts.	Overall Success Rate > 59.63%	Success Rate Difference < 5.76%	Classification
Anse de Kernic	X	X	X	X	Generally Successful
Budleigh Salterton	X	X	X	X	Generally Successful
Morlaix	X	X	X	X	Generally Successful
Sidmouth	X	X	X	X	Generally Successful
St. Malo	X	X	X	X	Generally Successful
Helford					Generally Unsuccessful
Mullion					Generally Unsuccessful
Brest	X				Quick and Unsuccessful
Fowey	X	X			Quick and Unsuccessful
Le Légnét	X				Quick and Unsuccessful
Lulworth Cove	X	X			Quick and Unsuccessful
Mevagissey	X				Quick and Unsuccessful
Penzance	X				Quick and Unsuccessful
Poole	X	X			Quick and Unsuccessful
Portland	X				Quick and Unsuccessful
Rivière de Lannion	X	X		X	Quick and Unsuccessful
Salcombe	X				Quick and Unsuccessful
Teignmouth	X			X	Quick and Unsuccessful
Topsham	X			X	Quick and Unsuccessful
Aber Wrac'h			X	X	Slow and Successful
Bigbury Bay		X	X		Slow and Successful
Christchurch		X	X	X	Slow and Successful
Dartmouth			X	X	Slow and Successful
Kérivoas			X	X	Slow and Successful
Kimmeridge Bay		X	X	X	Slow and Successful
Le Trieux			X	X	Slow and Successful
Nacqueville		X	X	X	Slow and Successful
Seaton		X	X	X	Slow and Successful
St. Peter Port (N.)			X		Slow and Successful
St. Peter Port (S.)		X	X		Slow and Successful
Torquay		X	X	X	Slow and Successful
Mothecombe	X		X		Successful but Imbalanced
Plymouth	X		X	X	Successful but Imbalanced
Porthallow	X	X	X		Successful but Imbalanced

Table 5.5: Visibility data for archaeological landmarks sighted during simulations in the Main Analysis.

Landmark Name	*County / Département / Territory*	Total Sightings	Sightings from Successful Simulations	Sightings from Unsuccessful Simulations	Landmark within 5 km. with > 2,500 sightings?	Most sighted within 5 km.?
Rame Head	Cornwall	15,826	7237	8589	X	X
Bolt Tail Camp	Devon	15,147	7369	7778		X
Berry Cliff Camp	Devon	12,384	5197	7187		X
Pointe De Primel	Finistère	12,161	6295	5866	X	
Vaux Du Catel	Manche	11,822	5209	6613	X	X
Castle Head	Devon	11,673	6125	5548		X
Dodman Castle	Cornwall	10,920	4863	6057	X	X
Kerfiat	Finistère	9,495	5082	4413	X	
Ile Callot	Finistère	9,461	5015	4446	X	
Black Head	Cornwall	8,326	3726	4600	X	X
Bretouare	Finistère	8,132	4156	3976	X	
Jerbourg	Channel Islands	8,074	3567	4507		X
Chynhalls Point	Cornwall	8,008	3855	4153		X
Bantham Camp	Devon	7,844	3507	4337		X
Flowers Barrow	Dorset	7,730	3111	4619	X	X
Beg Monom	Finistère	7,380	3543	3837		X
Bindon Hill	Dorset	7,230	3053	4177		X
Rochan Evned	Côtes-d'Armor	7,086	3396	3690	X	
Erquy	Côtes-d'Armor	7,042	2985	4057	X	
Kastell Ach	Finistère	6,362	3000	3362		X
Les Fouaillages	Channel Islands	6,163	3379	2784	X	
Rosemullion Head	Cornwall	6,015	2828	3187	X	X
Le Voallas	Finistère	5,081	2692	2389	X	
Dingerein Castle	Cornwall	4,903	2313	2590		X
Le Catel De Rozel	Channel Islands	4,891	1703	3188		X
Pointe Roselier	Côtes-d'Armor	4,884	1932	2952	X	
Kilcobben Cove	Cornwall	4,836	2288	2548		X
Lankidden	Cornwall	4,661	2262	2399		X
Little Dennis	Cornwall	4,471	2051	2420		X
Ile D Yoch	Finistère	4,453	1856	2597	X	
Shorthorn Point	Cornwall	4,448	2073	2375		X
Le Minihic	Ille-et-Vilaine	3,990	1651	2339	X	
Pointe De Menga	Ille-et-Vilaine	3,894	1621	2273	X	
Treryn Dinas	Cornwall	3,325	1327	1998		X
Hengistbury Head	Dorset	3,223	1142	2081	X	
St Michaels Mount	Cornwall	3,040	1286	1754	X	
Pointe Du Grouin	Ille-et-Vilaine	2,878	1199	1679	X	
Coz Yaudet	Côtes-d'Armor	2,722	1228	1494	X	
Lescudjack Castle	Cornwall	2,620	1194	1426		X
Pointe Du Raz	Finistère	2,088	558	1530	X	
Pointe Du Toulinguet	Finistère	2,064	523	1541		
Castel Meur	Finistère	1,937	528	1409		
Carolles	Manche	1,764	792	972	X	
Kergulan	Finistère	1,706	452	1254	X	
Kermorvan	Finistère	1,521	430	1091	X	
Castel Coz	Finistère	1,513	401	1112	X	
Veryan Castle	Cornwall	1,463	615	848		X
Lostmarch	Finistère	1,360	371	989		
Holbury Camp	Devon	1,111	512	599		X

Landmark Name	*County / Département / Territory*	Total Sightings	Sightings from Successful Simulations	Sightings from Unsuccessful Simulations	Landmark within 5 km. with > 2,500 sightings?	Most sighted landmark within 5 km.?
Bonchurch	Isle of Wight	883	152	731		X
Carn Les Boel	Cornwall	775	178	597		X
Dinard	Ille-et-Vilaine	761	372	389	X	
Cour Baudouin	Ille-et-Vilaine	630	221	409	X	
Giants Castle	Cornwall	546	98	448		
Roch Nivelen	Finistère	422	93	329	X	
Yaverland	Isle of Wight	313	32	281		
Lavallot	Finistère	282	145	137	X	
Burnt Hill	Cornwall	239	48	191		
Kenidjack Castle	Cornwall	206	35	171		
Shipman Head	Cornwall	184	9	175		
Tourner Bury	Portsmouth	177	9	168	X	
Maen Castle	Cornwall	143	28	115		X
L Aber	Finistère	139	22	117		
Gear Farm	Cornwall	94	33	61	X	
Pointe Du Chateau	Finistère	47	15	32	X	
Pointe De Bendy	Finistère	43	15	28	X	
Belair	Finistère	39	16	23	X	
Trereen Dinas	Cornwall	37	1	36		
Bosigran Castle	Cornwall	34	1	33		
Pointe De Saint Hernot	Finistère	32	7	25		
Kerdugazul	Finistère	28	7	21	X	
Menei Castel	Finistère	28	7	21	X	
Saoutenet	Finistère	28	7	21		
Carnsew	Cornwall	16	1	15	X	
Tubbys Head	Cornwall	15	1	14		
Penhale Point	Cornwall	13	0	13	X	
Kelsey Head	Cornwall	11	0	11	X	
Crane Castle	Cornwall	10	0	10		
Hamble Common	Hampshire	3	0	3	X	
Porth Joke	Cornwall	1	0	1	X	
Griffins Point	Cornwall	1	0	1	X	
		Percent of total meeting criteria:			*53.01%*	*33.73%*

Table 5.6: Comparison of travel times for routes evaluated by McGrail's (1983) model, and travel times recorded in the Main Analysis.

Route from McGrail (1983)	*Equivalent Route in Main Analysis*	*Predicted Voyage Length for Ship with 2.5 kt. average speed*	*Predicted Voyage Length for Ship with 5 kt. average speed*	*Average Voyage Length in Simulations*	*Average Speed in Simulations*
Ushant to Mounts Bay	Brest to Penzance	38 hrs.	19 hrs.	25.73 hrs.	4.57 kts.
Ushant to Plymouth Sound	Brest to Plymouth	48 hrs.	24 hrs.	27.51 hrs.	4.47 kts.
River Rance to Christchurch	St. Malo to Christchurch	52 hrs.	26 hrs.	30.35 hrs.	5.1 kts.

Chapter 6 Tables

Table 6.1: Inbound and outbound averages for nodes in Case Study 1. Average speeds are in knots, which higher speeds shaded yellow. Success rates are in %, with higher percentages shaded lighter green.

	Average Speed				*Success Rates*			
	Overall	*Inbound*	*Outbound*	*Diff.*	*Overall*	*Inbound*	*Outbound*	*Diff.*
Christchurch	4.47	3.71	5.24	OUT+1.53	66.88	48.57	85.18	OUT+36.61
Le Légnét	3.94	5.20	2.69	IN+2.51	62.28	90.18	34.38	IN+55.8
Le Trieux	3.73	4.97	2.49	IN+2.48	70.31	91.52	49.11	IN+42.41
Nacqueville	4.24	4.57	3.90	IN+0.67	76.34	73.21	79.46	OUT+6.25
St. Malo	3.78	4.96	2.61	IN+2.34	64.06	91.07	37.05	IN+54.02
St. Peter Port (N.)	4.54	5.36	3.73	IN+1.63	83.04	91.96	74.11	IN+17.86
St. Peter Port (S.)	3.38	2.04	4.72	OUT+2.69	72.77	50.60	94.94	OUT+44.35
St. Peter Port (Overall)	3.96	3.70	4.23	OUT+0.53	77.90	71.28	84.52	OUT+13.24

Table 6.2: Sightings by landmark for Case Study 1. Archaeological sites are highlighted.

	Landmark Name	Landmark Type	Total Sightings	Sightings (Successful Voyages)	Sightings (Unsuccessful Voyages)
1.	Little Sark	Nat. Prom.	6,893	4,370	2,523
2.	St Martins Point	Nat. Prom.	6,803	4,308	2,495
3.	Herm	Nat. Prom.	6,409	4,265	2,144
4.	Jethou	Nat. Prom.	6,330	4,188	2,142
5.	La Coupee	Nat. Prom.	5,956	3,680	2,276
6.	L'etac	Nat. Prom.	5,918	3,525	2,393
7.	Brecqhou	Nat. Prom.	5,843	3,909	1,934
8.	Eperquerie	Nat. Prom.	5,414	3,480	1,934
9.	Icart	Nat. Prom.	5,204	3,056	2,148
10.	Jerbourg	Site	4,679	2,525	2,154
11.	Burhou	Nat. Prom.	4,671	3,693	978
12.	Clonque	Nat. Prom.	4,666	3,558	1,108
13.	La Valette	Nat. Prom.	4,620	2,911	1,709
14.	Longis Bay	Nat. Prom.	4,619	3,387	1,232
15.	La Forge	Nat. Prom.	4,245	2,473	1,772
16.	Houles Du Debarcadere	Nat. Prom.	4,209	2,150	2,059
17.	Telegraph Bay	Nat. Prom.	3,941	2,894	1,047
18.	Minard	Nat. Prom.	3,890	2,161	1,729
19.	Vaux Du Catel	Nat. Prom.	3,804	2,771	1,033
20.	Egypt	Nat. Prom.	3,783	2,064	1,719
21.	Grande Île 2	Nat. Prom.	3,751	1,698	2,053
22.	Erquy	Site	3,559	1,436	2,123
23.	Grande Île 5	Nat. Prom.	3,551	1,577	1,974
24.	Pors Pin	Nat. Prom.	3,525	1,967	1,558
25.	Tilly Whim Caves	Nat. Prom.	3,471	2,987	484
26.	Langton Matravers	Nat. Prom.	3,448	2,969	479

27.	Pointe De Plouha	Nat. Prom.	3,260	1,854	1,406
28.	Studland Hill	Nat. Prom.	3,123	2,707	416
29.	Grande Île 3	Nat. Prom.	2,967	1,290	1,677
30.	Belle Hougue	Nat. Prom.	2,955	1,867	1,088
31.	Grande Île 10	Nat. Prom.	2,953	1,269	1,684
32.	Grande Île 4	Nat. Prom.	2,949	1,273	1,676
33.	Le Minihic	Site	2,889	1,070	1,819
34.	Alum Bay	Nat. Prom.	2,887	2,507	380
35.	Flowers Barrow	Nat. Prom.	2,885	2,457	428
36.	Swyre Head	Nat. Prom.	2,882	2,425	457
37.	Winspit 2	Nat. Prom.	2,882	2,423	459
38.	Pointe De Menga	Nat. Prom.	2,868	1,031	1,837
39.	Winspit 1	Nat. Prom.	2,833	2,387	446
40.	Roch'an Evned	Site	2,744	1,162	1,582
41.	Emmetts Hill	Nat. Prom.	2,738	2,293	445
42.	Compton Down	Nat. Prom.	2,615	2,263	352
43.	Hameau Thiebot	Nat. Prom.	2,533	1,758	775
44.	Egmont Point	Nat. Prom.	2,526	2,103	423
45.	Hengistbury Head	Site	2,468	1,792	676
46.	Grande Île 1	Nat. Prom.	2,391	1,043	1,348
47.	Gore Down	Nat. Prom.	2,367	2,014	353
48.	Vaux Du Catel	Site	2,355	1,388	967
49.	Lowtherville	Nat. Prom.	2,277	1,927	350
50.	Pointe Du Grouin	Nat. Prom.	2,271	812	1,459
51.	Steeple 2	Nat. Prom.	2,248	1,871	377
52.	Hambury Tout	Nat. Prom.	2,091	1,727	364
53.	Pointe Roselier	Nat. Prom.	2,082	1,120	962
54.	Steeple 1	Nat. Prom.	2,080	1,760	320
55.	South Holworth	Nat. Prom.	2,038	1,690	348
56.	Le Catel De Rozel	Site	2,035	1,122	913
57.	St Boniface Down	Nat. Prom.	2,030	1,717	313
58.	Pointe Roselier	Nat. Prom.	2,027	805	1,222
59.	Lande Du Thot	Nat. Prom.	2,006	1,306	700
60.	Hurst Point	Nat. Prom.	1,965	1,748	217
61.	Bindon Hill	Nat. Prom.	1,956	1,605	351
62.	The Grove	Nat. Prom.	1,889	1,561	328
63.	Les Treize Vents	Nat. Prom.	1,887	1,215	672
64.	Portland Bill	Nat. Prom.	1,865	1,501	364
65.	Flowers Barrow	Site	1,840	1,235	605
66.	Bindon Hill	Site	1,821	1,212	609
67.	Fortuneswell	Nat. Prom.	1,719	1,374	345
68.	Castletown 1	Nat. Prom.	1,511	1,228	283
69.	Île Renote 4	Nat. Prom.	1,463	942	521
70.	Headon Warren	Nat. Prom.	1,345	1,190	155
71.	Carolles	Site	1,342	486	856
72.	Niton Undercliff	Nat. Prom.	1,285	1,049	236
73.	Île Renote	Nat. Prom.	1,255	800	455
74.	Osmington Mills	Nat. Prom.	1,138	888	250
75.	Île Renote 3	Nat. Prom.	1,118	707	411
76.	Osmington	Nat. Prom.	1,108	863	245

77.	Castletown	Nat. Prom.	1,094	900	194
78.	Les Fouaillages	Site	1,059	421	638
79.	Île Renote 1	Nat. Prom.	695	441	254
80.	Dinard	Site	670	292	378
81.	Weston 1	Nat. Prom.	495	354	141
82.	Cour Baudouin	Site	457	110	347
83.	Bonchurch	Site	328	167	161
84.	Swyre	Nat. Prom.	253	151	102
85.	Thorncombe Beacon	Nat. Prom.	214	123	91
86.	Golden Cap	Nat. Prom.	192	108	84
87.	Morcombelake	Nat. Prom.	167	94	73
88.	Black Ven	Nat. Prom.	158	87	71
89.	Pinhay Cliffs	Nat. Prom.	157	86	71
90.	Uplyme	Nat. Prom.	151	81	70
91.	Humble Point	Nat. Prom.	149	83	66
92.	Bembridge Down	Nat. Prom.	144	52	92
93.	Axe Cliff	Nat. Prom.	129	66	63
94.	Hooken Beach	Nat. Prom.	109	50	59
95.	Berry Cliff Camp	Nat. Prom.	89	41	48
96.	Luccombe	Nat. Prom.	89	12	77
97.	Dunscombe	Nat. Prom.	73	34	39
98.	Kingston	Nat. Prom.	70	33	37
99.	Kingston 1	Nat. Prom.	70	31	39
100.	Salcombe Mouth	Nat. Prom.	67	31	36
101.	Brownstone	Nat. Prom.	67	30	37
102.	Long Sands	Nat. Prom.	62	28	34
103.	Castle Head	Site	62	10	52
104.	Salcombe Hill	Nat. Prom.	61	29	32
105.	South Hallsands	Nat. Prom.	61	23	38
106.	Mew Stone	Nat. Prom.	60	24	36
107.	Higher Brixham	Nat. Prom.	59	25	34
108.	The Narrows	Nat. Prom.	58	20	38
109.	Woodcombe	Nat. Prom.	58	19	39
110.	Prawle Point	Nat. Prom.	55	15	40
111.	Castle Head	Nat. Prom.	54	23	31
112.	Hopes Nose	Nat. Prom.	49	17	32
113.	Torcross	Nat. Prom.	48	18	30
114.	Yaverland	Site	47	10	37
115.	Beesands	Nat. Prom.	46	19	27
116.	Mutters Moor	Nat. Prom.	46	18	28
117.	High Peak	Nat. Prom.	46	18	28
118.	Dartmouth	Nat. Prom.	46	18	28
119.	Boohay	Nat. Prom.	45	17	28
120.	Manor Gardens	Nat. Prom.	45	15	30
121.	Pointe De Primel	Nat. Prom.	41	4	37
122.	Strete	Nat. Prom.	40	16	24
123.	Wellswood	Nat. Prom.	40	12	28
124.	Berry Cliff Camp	Site	39	25	14
125.	Budleigh Salterton	Nat. Prom.	35	15	20
126.	Petit Tor	Nat. Prom.	34	7	27

127.	Giant Rock	Nat. Prom.	33	6	27
128.	Stokeinteignhead	Nat. Prom.	30	6	24
129.	Bolt Head	Nat. Prom.	30	3	27
130.	The Beacon	Nat. Prom.	28	6	22
131.	Steeple Cove	Nat. Prom.	26	3	23
132.	Sharp Tor	Nat. Prom.	26	3	23
133.	Down End	Nat. Prom.	25	9	16
134.	Tourner Bury	Site	20	0	20
135.	Île Callot	Site	18	3	15
136.	Bolberry Down	Nat. Prom.	17	0	17
137.	Shaws Corner	Nat. Prom.	16	1	15
138.	Bozomzeal	Nat. Prom.	15	3	12
139.	East Portlemouth	Nat. Prom.	14	0	14
140.	Ramillies Cove	Nat. Prom.	13	0	13
141.	Hook Bottom 1	Nat. Prom.	9	2	7
142.	Great Mewstone	Nat. Prom.	9	0	9
143.	Worswell Barton	Nat. Prom.	9	0	9
144.	Revelstoke	Nat. Prom.	9	0	9
145.	Netton	Nat. Prom.	9	0	9
146.	Netton 1	Nat. Prom.	9	0	9
147.	Netton 2	Nat. Prom.	9	0	9
148.	Mothecombe	Nat. Prom.	9	0	9
149.	Maker	Nat. Prom.	7	0	7
150.	Tregonhawke	Nat. Prom.	7	0	7
151.	Rame Head	Nat. Prom.	7	0	7
152.	Portwrinkle	Nat. Prom.	5	0	5
153.	Hendra	Nat. Prom.	5	0	5
154.	Down Thomas	Nat. Prom.	5	0	5
155.	Bigbury On Sea	Nat. Prom.	5	0	5
156.	Bantham 1	Nat. Prom.	5	0	5
157.	Polbathic	Nat. Prom.	4	0	4
158.	Crafthole	Nat. Prom.	4	0	4
159.	Bolt Tail Camp	Site	4	0	4
160.	Axmouth Harbour	Nat. Prom.	3	1	2
161.	Ashprington 1	Nat. Prom.	3	1	2
162.	Broadgates	Nat. Prom.	3	1	2
163.	Hook Bottom	Nat. Prom.	3	1	2
164.	Seaton	Nat. Prom.	3	0	3
165.	Aish	Nat. Prom.	2	1	1
166.	Ashprington	Nat. Prom.	2	1	1
167.	Bodigga	Nat. Prom.	2	0	2
168.	Seaford Head Camp	Nat. Prom.	2	0	2
169.	Newbarn	Nat. Prom.	2	0	2
170.	Old Town 1	Nat. Prom.	2	0	2
171.	Old Town 2	Nat. Prom.	2	0	2
172.	Kerfiat	Site	2	0	2
173.	Rame Head	Site	2	0	2

Chapter 7 Tables

Table 7.1: Speed and success rates for parameters tested in Case Study 2. Average speeds are in knots, which higher speeds shaded yellow. Success rates are in %, with higher percentages shaded lighter green.

Parameter	*Overall Speed (Knots)*	*Nbound. Speed (Knots)*	*Sbound. Speed (Knots)*	*N./S. Speed Diff.*	*Overall Success Rate (%)*	*Nbound. Success Rate (%)*	*Sbound. Success Rate (%)*	*N./S. Success Diff.*
All Simulations	4.52	4.75	4.07	N+0.68	62.15	81.57	42.73	N+38.84
Reckoning = 0%	5.15	5.35	4.80	N+0.55	76.36	98.18	54.55	N+43.64
Reckoning = 0-5%	5.07	5.17	4.89	N+0.28	71.82	94.55	49.09	N+45.45
Reckoning = 0-10%	4.82	5.03	4.46	N+0.57	69.09	88.18	50.00	N+38.18
Reckoning = 0-15%	4.66	4.92	4.22	N+0.71	68.64	86.36	50.91	N+35.45
Reckoning = 0-20%	4.47	4.79	3.92	N+0.87	64.55	81.82	47.27	N+34.55
Reckoning = 0-25%	4.43	4.60	4.09	N+0.51	61.36	80.00	42.73	N+37.27
Reckoning = 0-30%	4.41	4.76	3.77	N+0.99	58.64	75.45	41.82	N+33.64
Reckoning = 0-35%	4.10	4.36	3.58	N+0.77	53.64	71.82	35.45	N+36.36
Reckoning = 0-40%	4.14	4.42	3.53	N+0.89	53.18	73.64	32.73	N+40.91
Reckoning = 0-45%	3.89	4.18	3.32	N+0.86	54.55	72.73	36.36	N+36.36
Reckoning = 0-50%	3.98	4.30	3.16	N+1.14	51.82	74.55	29.09	N+45.45
Leaving Time = 23:00	5.16	5.19	3.27	N+1.92	50.45	99.09	1.82	N+97.27
Leaving Time = 00:00	5.04	5.27	3.51	N+1.76	56.82	99.09	14.55	N+84.55
Leaving Time = 01:00	5.19	5.63	3.56	N+2.07	63.64	100.00	27.27	N+72.73
Leaving Time = 02:00	5.14	5.62	3.14	N+2.48	61.36	99.09	23.64	N+75.45
Leaving Time = 03:00	5.02	5.48	3.68	N+1.8	67.27	100.00	34.55	N+65.45
Leaving Time = 04:00	4.38	4.54	4.01	N+0.53	71.82	98.18	45.45	N+52.73
Leaving Time = 05:00	4.17	4.41	3.70	N+0.71	75.00	99.09	50.91	N+48.18
Leaving Time = 06:00	3.93	3.70	4.23	S+0.53	75.45	83.64	67.27	N+16.36
Leaving Time = 07:00	4.03	3.12	4.74	S+1.62	69.09	60.91	77.27	S+16.36
Leaving Time = 08:00	3.78	3.06	4.19	S+1.13	51.36	37.27	65.45	S+28.18
Leaving Time = 09:00	3.93	3.06	4.22	S+1.17	41.36	20.91	61.82	S+40.91
Pred. Avg. Speed = 5.0 kts.	3.74	3.77	3.70	N+0.07	67.36	80.17	54.55	N+25.62
Pred. Avg. Speed = 5.2 kts.	3.82	3.86	3.76	N+0.1	61.98	76.86	47.11	N+29.75
Pred. Avg. Speed = 5.4 kts.	3.99	4.22	3.64	N+0.58	66.53	80.17	52.89	N+27.27
Pred. Avg. Speed = 5.6 kts.	4.16	4.26	3.93	N+0.34	57.85	80.17	35.54	N+44.63
Pred. Avg. Speed = 5.8 kts.	4.52	4.81	4.00	N+0.81	62.40	80.17	44.63	N+35.54
Pred. Avg. Speed = 6.0 kts.	4.56	4.74	4.19	N+0.55	58.68	79.34	38.02	N+41.32
Pred. Avg. Speed = 6.2 kts.	4.77	5.09	4.14	N+0.95	63.22	84.30	42.15	N+42.15
Pred. Avg. Speed = 6.4 kts.	5.02	5.22	4.60	N+0.62	62.81	86.78	38.84	N+47.93
Pred. Avg. Speed = 6.6 kts.	5.27	5.53	4.64	N+0.89	59.92	85.12	34.71	N+50.41
Pred. Avg. Speed = 6.8 kts.	5.42	5.85	4.52	N+1.33	60.74	82.64	38.84	N+43.8

Table 7.2: Sighting counts for landmarks for Case Study 2. Potential landmarks identified with archaeological sites are highlighted:

	Landmark Name	*Shoreline*	*Site?*	*Nat. Prom.?*	*Total Sightings*	*Sightings (Successful Voyages)*	*Sightings (Unsuccessful Voyages)*
1.	Pointe De Primel	South	X		16,682	8456	8226
2.	Rame Head	North	X	X	16,110	10312	5798
3.	Great Mewstone	North		X	15,602	10011	5591
4.	Netton	North		X	15,362	9907	5455
5.	Worswell Barton	North		X	15,245	9895	5350
6.	Dodman Castle	North	X	X	15,172	9153	6019
7.	Tregonhawke	North		X	14,954	9532	5422
8.	Lannear 1	North		X	14,952	9301	5651
9.	Talland	North		X	14,861	9324	5537
10.	Lannear	North		X	14,853	9231	5622
11.	Hannafore Point	North		X	14,803	9338	5465
12.	Giggen Cove	North		X	14,779	9216	5563
13.	Lansallos	North		X	14,375	8855	5520
14.	Trevarder	North		X	14,273	8768	5505
15.	Bolt Tail Camp	North	X		14,204	9268	4936
16.	Polruan	North		X	14,102	8668	5434
17.	Espace Yves Hamon	South		X	14,066	7538	6528
18.	Ramillies Cove	North		X	14,049	9172	4877
19.	Bolberry Down	North		X	14,037	9151	4886
20.	Steeple Cove	North		X	13,794	9051	4743
21.	Menabilly 1	North		X	13,773	8511	5262
22.	Looe	North		X	13,717	8467	5250
23.	Île Renote	South		X	13,613	7520	6093
24.	Hendra	North		X	13,574	8817	4757
25.	Chad Rock	North			13,538	8324	5214
26.	Netton 1	North		X	13,466	8754	4712
27.	Île Renote 4	South		X	13,462	7457	6005
28.	Seaton	North		X	13,444	8653	4791
29.	Drakes Island	North		X	13,426	8197	5229
30.	Bodigga	North		X	13,426	8484	4942
31.	Brodrugan Barton	North		X	13,393	8340	5053
32.	Menabilly	North		X	13,355	8299	5056
33.	Portwrinkle	North		X	13,223	8702	4521
34.	Île Callot	South	X		13,128	6220	6908
35.	Seaton 1	North		X	13,122	8376	4746
36.	Île Renote 3	South		X	13,075	7249	5826
37.	Down Thomas	North		X	13,061	8161	4900
38.	Crafthole	North		X	13,037	8699	4338
39.	Île Renote 1	South		X	12,946	7151	5795
40.	Plaidy	North		X	12,533	7637	4896
41.	Bantham 1	North		X	12,198	8035	4163
42.	Maker	North		X	12,192	7374	4818
43.	Black Head	North	X		12,147	7746	4401
44.	Garrans Point	North		X	11,969	7633	4336
45.	Bigbury On Sea	North		X	11,744	7667	4077
46.	Trewinney Barton	North		X	11,694	7488	4206

47.	Pentewan	North		X	11,588	7451	4137
48.	Mothecombe	North		X	11,340	7149	4191
49.	Mothecombe 1	North		X	11,336	7158	4178
50.	Bolt Head	North		X	11,262	7565	3697
51.	Nare Head	North		X	11,207	6380	4827
52.	Bantham Camp	North	X		11,010	7025	3985
53.	Revelstoke	North		X	9,865	5941	3924
54.	St Anthony Head	North		X	9,205	5251	3954
55.	Manacle Point	North		X	8,428	4392	4036
56.	Prawle Point	North		X	8,158	5414	2744
57.	Sharp Tor	North		X	8,013	5352	2661
58.	Pencra Head	North		X	7,974	4329	3645
59.	Kerfiat	South	X		7,956	3176	4780
60.	Carlyon Bay	North		X	7,881	4791	3090
61.	Pierre A Jean Rouzic	South		X	7,343	5088	2255
62.	Pedn Boar	North		X	7,219	3255	3964
63.	Chynhalls Point	North	X		7,193	3521	3672
64.	Polbathic	North		X	7,159	4436	2723
65.	Shag Rock	North		X	7,050	4825	2225
66.	Le Voallas	South	X		6,041	1881	4160
67.	Rosemullion Head	North	X		5,944	3526	2418
68.	Dingerein Castle	North	X		5,913	2934	2979
69.	St Mawes	North		X	5,907	3325	2582
70.	Shorthorn Point	North	X		5,868	3432	2436
71.	Caerhays Barton	North		X	5,863	2851	3012
72.	Bretouare	South	X		5,540	1525	4015
73.	Little Dennis	North	X		4,992	3127	1865
74.	Long Rock	North		X	4,891	2388	2503
75.	Pendennis Point	North		X	4,758	2335	2423
76.	Golant	North		X	4,475	2667	1808
77.	Pen Olver	North		X	4,395	1248	3147
78.	Coz Yaudet	South	X		4,263	1256	3007
79.	East Portlemouth	North		X	4,134	3515	619
80.	Meledan	South		X	3,865	175	3690
81.	Beg Monom	South	X		3,689	207	3482
82.	South Hallsands	North		X	3,455	2677	778
83.	Merafield	North		X	3,348	1977	1371
84.	Kilcobben Cove	North	X		3,252	1204	2048
85.	Kastell Ac'h 1	South		X	3,095	125	2970
86.	Woodcombe	North		X	3,036	2493	543
87.	The Narrows	North		X	2,806	2312	494
88.	Lankidden	North	X		2,590	505	2085
89.	Shaws Corner	North		X	2,476	2021	455
90.	Trefusis	North		X	2,397	1000	1397
91.	St Erney	North		X	2,278	1213	1065
92.	Kastell Ach	South	X		2,271	73	2198
93.	Collytown	North		X	1,977	1423	554
94.	Holly Park	North		X	1,938	1547	391
95.	Soapy Valley	North		X	1,872	111	1761
96.	Lamorna 1	North		X	1,485	20	1465
97.	Lamorna	North		X	1,475	15	1460
98.	Treryn Dinas	North	X		1,468	15	1453

99.	Penberth Cove	North		X	1,467	15	1452
100.	Raginnis	North		X	1,450	15	1435
101.	Gwennap Head	North		X	1,434	13	1421
102.	Veryan Castle	North	X		1,381	431	950
103.	Predannnack	North		X	1,362	21	1341
104.	Mousehole	North		X	1,361	11	1350
105.	St Michaels Mount	North	X		1,277	2	1275
106.	Holbury Camp	North	X		1,239	1018	221
107.	Lescudjack Castle	North	X		1,193	7	1186
108.	Beesands	North		X	1,145	869	276
109.	Watch Croft	North		X	1,131	10	1121
110.	Mer Melen	South		X	1,129	1026	103
111.	Le Chas De Laiguille	South		X	1,007	927	80
112.	Chyanvounder	North		X	911	2	909
113.	Torcross	North		X	863	554	309
114.	St Agnes Beacon	North		X	743	359	384
115.	Le Corps De Garde	South		X	592	562	30
116.	Lavallot	South	X		507	384	123
117.	Île D'Yoch	South	X		444	2	442
118.	Strete	North		X	368	237	131
119.	Belair	South	X		28	14	14
120.	Dartmouth	North		X	8	1	7
121.	Roch'an Evned	South	X		2	1	1

Chapter 8 Tables

Table 8.1: Success counts for simulations in Case Study 3.

	Success	*Qualified Success*	*Potential Success*	*Failure*	*Total*
All Runs	**3**	**14**	**10**	**11**	38
Landmarks = Sites	2	7	4	7	20
Landmarks = Nat. Proms.	1	7	6	4	18
Top Speed = 5 kts.	0	0	7	11	18
Top Speed = 7 kts.	1	7	2	0	10
Top Speed = 9 kts.	2	7	1	0	10
No Misestimation	3	14	10	3	30
Misestimation up to 50%	0	0	0	8	8
Start time -2 hrs.	1	3	2	2	8
Start time -1 hrs.	0	4	2	2	8
Start time + 0 hrs.	2	1	3	2	8
Start time + 1 hrs.	0	3	2	2	7
Start time + 2 hrs.	0	3	1	3	7

Table 8.2: Number of sightings and apparent size for sites in Case Study 3:

Landmark (Site)	*Total Sightings*	*Average Apparent Size (Sq. Degrees)*
Kermorvan	201	94.19
Pointe du Toulinguet	97	46.15
Giants Castle	160	2.25
Ile d'Yoc'h	228	2.22
Maen Castle	80	1.86
Kenidjack Castle	125	1.60
Treryn Dinas	123	1.56
Pointe du Raz	117	1.40
Carn les Boel	152	1.15
Roc'h Nivelen	21	0.85
Burnt Hill	6	0.80
St. Michael's Mount	1	0.70
Castel Meur	116	0.68
Castel Coz	81	0.34
Lostmarc'h	43	0.34
Trereen Dinas	3	0.33
Shipman Head	68	0.27
Kastell Ac'h	66	0.23
Kergulan	97	0.19
Beg Monom	20	0.11
Bretouare	1	0.02

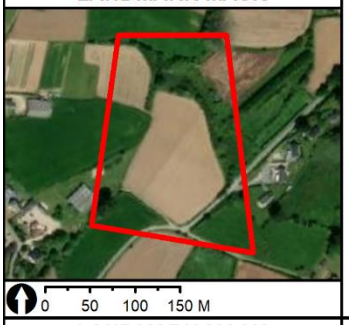
Table 8.3: Speeds for 'successful' runs in Case Study 3.

Simulation	*Max. Speed*	*Time to Dest.*	*Speed*
Simulation_01	5 kts.	48 hrs.	2.42 kts.
Simulation_06	5 kts.	48 hrs.	2.42 kts.
Simulation_12	7 kts.	43 hrs.	2.70 kts.
Simulation_13	7 kts.	38 hrs.	3.06 kts.
Simulation_14	7 kts.	41 hrs.	2.83 kts.
Simulation_15	7 kts.	44 hrs.	2.64 kts.
Simulation_17	7 kts.	43 hrs.	2.70 kts.
Simulation_20	7 kts.	44 hrs.	2.64 kts.
Simulation_21	9 kts.	31 hrs.	3.75 kts.
Simulation_22	9 kts.	31 hrs.	3.75 kts.
Simulation_23	9 kts.	33 hrs.	3.52 kts.
Simulation_24	9 kts.	30 hrs.	3.87 kts.
Simulation_26	9 kts.	31 hrs.	3.75 kts.
Simulation_27	9 kts.	31 hrs.	3.75 kts.
Simulation_28	9 kts.	33 hrs.	3.52 kts.
Simulation_29	9 kts.	30 hrs.	3.87 kts.
Simulation_30	9 kts.	31 hrs.	3.75 kts.
	Grand Average:	*37.06 hrs.*	*3.23 kts.*
	Average (5 kt. max.):	*48 hrs.*	*2.42 kts.*
	Average (7 kt. max.):	*42.17 hrs.*	*2.76 kts.*
	Average (9 kt. max.):	*31.22 hrs.*	*3.72 kts.*

Appendix I

This appendix contains records for each promontory fort used as a landmark in analyses in Chapters 5-8.

LANDMARK MASK



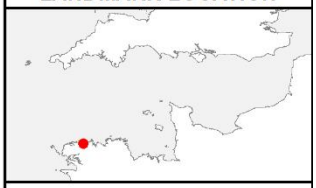
Brétouaré

Source: Geobretagne

Contextual Information:

Nearest Node:	Anse de Kernic
Km. to Nearest Node:	5.13
Mask Area (Hectares):	3.38
Sightings (Main Analysis):	8132

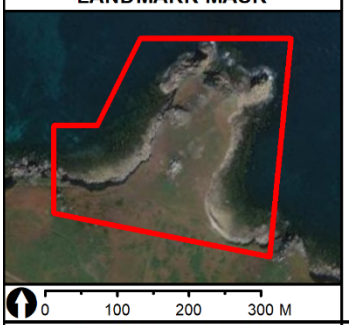
LANDMARK LOCATION



Longitude: 4° 13" 49' W
Latitude: 48° 38" 24' N

Source: Esri, DigitalGlobe, GeoEye, Earthstar Geographics, CNES/Airbus DS, USDA, USGS, AeroGRID, IGN, and the GIS User Community

LANDMARK MASK



Burnt Hill

Source: (Lock & Ralston 2017)

Contextual Information:

Nearest Node:	Penzance
Km. to Nearest Node:	56.6
Mask Area (Hectares):	7.47
Sightings (Main Analysis):	239

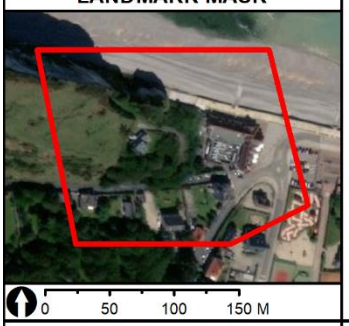
LANDMARK LOCATION



Longitude: 6° 16" 24' W
Latitude: 49° 57" 54' N

Source: Esri, DigitalGlobe, GeoEye, Earthstar Geographics, CNES/Airbus DS, USDA, USGS, AeroGRID, IGN, and the GIS User Community

LANDMARK MASK



Camp du Câtelier

Source: Bender (1986); Wheeler (1957)

Contextual Information:

Nearest Node:	Nacqueville
Km. to Nearest Node:	163.75
Mask Area (Hectares):	2.65
Sightings (Main Analysis):	0

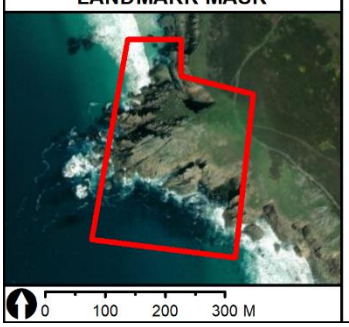
LANDMARK LOCATION



Longitude: 0° 35" 43' E
Latitude: 49° 51" 9' N

Source: Esri, DigitalGlobe, GeoEye, Earthstar Geographics, CNES/Airbus DS, USDA, USGS, AeroGRID, IGN, and the GIS User Community

LANDMARK MASK



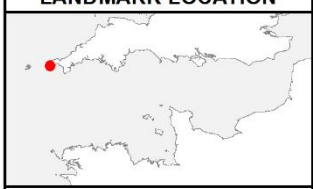
Carn Les Boel

Source: (Lock & Ralston 2017)

Contextual Information:

Nearest Node:	Penzance
Km. to Nearest Node:	14.34
Mask Area (Hectares):	7.07
Sightings (Main Analysis):	775

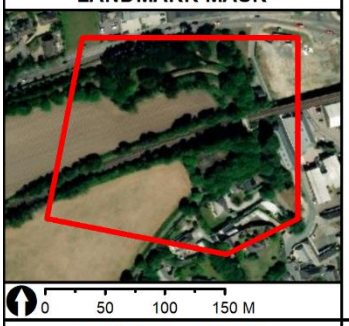
LANDMARK LOCATION



Longitude: 5° 41" 38' W
Latitude: 50° 3" 0' N

Source: Esri, DigitalGlobe, GeoEye, Earthstar Geographics, CNES/Airbus DS, USDA, USGS, AeroGRID, IGN, and the GIS User Community

LANDMARK MASK



Carnsew

Source: (Lock & Ralston 2017)

Contextual Information:

Nearest Node:	Penzance
Km. to Nearest Node:	10.83
Mask Area (Hectares):	3.24
Sightings (Main Analysis):	16

LANDMARK LOCATION



Longitude: 5° 25" 27' W
Latitude: 50° 11" 0' N

Source: Esri, DigitalGlobe, GeoEye, Earthstar Geographics, CNES/Airbus DS, USDA, USGS, AeroGRID, IGN, and the GIS User Community

LANDMARK MASK



Carolles

Source: Maguer (1996)

Contextual Information:

Nearest Node:	Saint Malo
Km. to Nearest Node:	34.55
Mask Area (Hectares):	18.77
Sightings (Main Analysis):	1764

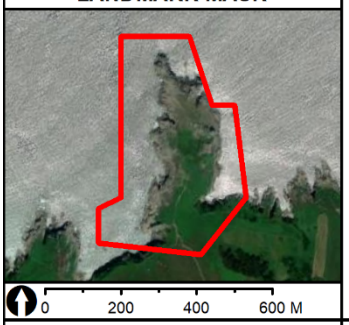
LANDMARK LOCATION



Longitude: 1° 34" 18' W
Latitude: 48° 44" 53' N

Source: Esri, DigitalGlobe, GeoEye, Earthstar Geographics, CNES/Airbus DS, USDA, USGS, AeroGRID, IGN, and the GIS User Community

LANDMARK MASK



Castel Coz

Source: Bender (1986)

Contextual Information:

Nearest Node:	Brest
Km. to Nearest Node:	26.9
Mask Area (Hectares):	15.79
Sightings (Main Analysis):	1513

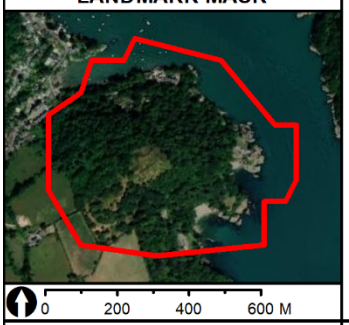
LANDMARK LOCATION



Longitude: 4° 31" 15' W
Latitude: 48° 5" 20' N

Source: Esri, DigitalGlobe, GeoEye, Earthstar Geographics, CNES/Airbus DS, USDA, USGS, AeroGRID, IGN, and the GIS User Community

LANDMARK MASK



Castle Head

Source: (Lock & Ralston 2017)

Contextual Information:

Nearest Node:	Dartmouth
Km. to Nearest Node:	3.38
Mask Area (Hectares):	31.27
Sightings (Main Analysis):	11673

LANDMARK LOCATION



Longitude: 3° 34" 8' W
Latitude: 50° 20" 29' N

Source: Esri, DigitalGlobe, GeoEye, Earthstar Geographics, CNES/Airbus DS, USDA, USGS, AeroGRID, IGN, and the GIS User Community

LANDMARK MASK



Castle Hill

Source: (Lock & Ralston 2017)

Contextual Information:

Nearest Node:	Christchurch
Km. to Nearest Node:	125.47
Mask Area (Hectares):	21.69
Sightings (Main Analysis):	0

LANDMARK LOCATION



Longitude: 0° 3" 5' E
Latitude: 50° 46" 56' N

Source: Esri, DigitalGlobe, GeoEye, Earthstar Geographics, CNES/Airbus DS, USDA, USGS, AeroGRID, IGN, and the GIS User Community

LANDMARK MASK



Chynhalls Point

Source: (Lock & Ralston 2017)

Contextual Information:

Nearest Node:	Helford
Km. to Nearest Node:	8.47
Mask Area (Hectares):	8.46
Sightings (Main Analysis):	8008

LANDMARK LOCATION



Longitude: 5° 5" 33' W
Latitude: 50° 0" 57' N

Source: Esri, DigitalGlobe, GeoEye, Earthstar Geographics, CNES/Airbus DS, USDA, USGS, AeroGRID, IGN, and the GIS User Community

LANDMARK MASK



Cité des Limes

Source: Bender (1986); Wheeler (1957)

Contextual Information:

Nearest Node:	Nacqueville
Km. to Nearest Node:	201.77
Mask Area (Hectares):	75.51
Sightings (Main Analysis):	0

LANDMARK LOCATION



Longitude: 1° 7" 21' E
Latitude: 49° 56" 28' N

Source: Esri, DigitalGlobe, GeoEye, Earthstar Geographics, CNES/Airbus DS, USDA, USGS, AeroGRID, IGN, and the GIS User Community

LANDMARK MASK



Cour Baudouin

Source: Maguer (1996)

Contextual Information:

Nearest Node:	Saint Malo
Km. to Nearest Node:	29.01
Mask Area (Hectares):	2.16
Sightings (Main Analysis):	630

LANDMARK LOCATION



Longitude: 1° 39" 31' W
Latitude: 48° 35" 10' N

Source: Esri, DigitalGlobe, GeoEye, Earthstar Geographics, CNES/Airbus DS, USDA, USGS, AeroGRID, IGN, and the GIS User Community

LANDMARK MASK



Crane Castle

Source: (Lock & Ralston 2017)

Contextual Information:

Nearest Node:	Penzance
Km. to Nearest Node:	21.07
Mask Area (Hectares):	5.49
Sightings (Main Analysis):	10

LANDMARK LOCATION



Longitude: 5° 19" 10' W
Latitude: 50° 14" 55' N

Source: Esri, DigitalGlobe, GeoEye, Earthstar Geographics, CNES/Airbus DS, USDA, USGS, AeroGRID, IGN, and the GIS User Community

LANDMARK MASK



Dinard

Source: Geobretagne

Contextual Information:

Nearest Node:	Saint Malo
Km. to Nearest Node:	7.48
Mask Area (Hectares):	21.29
Sightings (Main Analysis):	761

LANDMARK LOCATION



Longitude: 2° 1" 16' W
Latitude: 48° 36" 16' N

Source: Esri, DigitalGlobe, GeoEye, Earthstar Geographics, CNES/Airbus DS, USDA, USGS, AeroGRID, IGN, and the GIS User Community

LANDMARK MASK



Dingerein Castle

Source: (Lock & Ralston 2017)

Contextual Information:

Nearest Node:	Falmouth
Km. to Nearest Node:	8.74
Mask Area (Hectares):	2.97
Sightings (Main Analysis):	4903

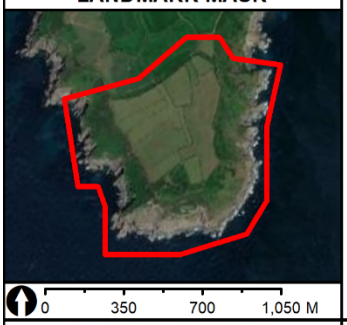
LANDMARK LOCATION



Longitude: 4° 58" 9' W
Latitude: 50° 11" 59' N

Source: Esri, DigitalGlobe, GeoEye, Earthstar Geographics, CNES/Airbus DS, USDA, USGS, AeroGRID, IGN, and the GIS User Community

LANDMARK MASK



Dodman Castle

Source: (Lock & Ralston 2017)

Contextual Information:

Nearest Node:	Mevagissey
Km. to Nearest Node:	5.26
Mask Area (Hectares):	66.87
Sightings (Main Analysis):	10920

LANDMARK LOCATION



Longitude: 4° 48" 7' W
Latitude: 50° 13" 19' N

Source: Esri, DigitalGlobe, GeoEye, Earthstar Geographics, CNES/Airbus DS, USDA, USGS, AeroGRID, IGN, and the GIS User Community

LANDMARK MASK



Dover Castle

Source: (Lock & Ralston 2017)

Contextual Information:

Nearest Node:	Christchurch
Km. to Nearest Node:	218.92
Mask Area (Hectares):	47.2
Sightings (Main Analysis):	0

LANDMARK LOCATION



Longitude: 1° 19" 21' E
Latitude: 51° 7" 43' N

Source: Esri, DigitalGlobe, GeoEye, Earthstar Geographics, CNES/Airbus DS, USDA, USGS, AeroGRID, IGN, and the GIS User Community

LANDMARK MASK



East Hill

Source: (Lock & Ralston 2017)

Contextual Information:

Nearest Node:	Christchurch
Km. to Nearest Node:	164.47
Mask Area (Hectares):	34.97
Sightings (Main Analysis):	0

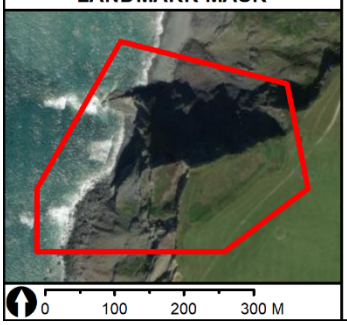
LANDMARK LOCATION



Longitude: 0° 36" 2' E
Latitude: 50° 51" 29' N

Source: Esri, DigitalGlobe, GeoEye, Earthstar Geographics, CNES/Airbus DS, USDA, USGS, AeroGRID, IGN, and the GIS User Community

LANDMARK MASK



Embury Beacon

Source: (Lock & Ralston 2017)

Contextual Information:

Nearest Node:	Fowey
Km. to Nearest Node:	71.46
Mask Area (Hectares):	8.78
Sightings (Main Analysis):	0

LANDMARK LOCATION



Longitude: 4° 32" 28' W
Latitude: 50° 56" 50' N

Source: Esri, DigitalGlobe, GeoEye, Earthstar Geographics, CNES/Airbus DS, USDA, USGS, AeroGRID, IGN, and the GIS User Community

LANDMARK MASK



Erquy

Source: Bender (1986), Geobretagne

Contextual Information:

Nearest Node:	Le Légnét
Km. to Nearest Node:	15.81
Mask Area (Hectares):	95.04
Sightings (Main Analysis):	7042

LANDMARK LOCATION



Longitude: 2° 28" 54' W
Latitude: 48° 38" 30' N

Source: Esri, DigitalGlobe, GeoEye, Earthstar Geographics, CNES/Airbus DS, USDA, USGS, AeroGRID, IGN, and the GIS User Community

LANDMARK MASK



Flower's Barrow

Source: (Lock & Ralston 2017)

Contextual Information:

Nearest Node:	Kimmeridge Bay
Km. to Nearest Node:	4.4
Mask Area (Hectares):	23.22
Sightings (Main Analysis):	7730

LANDMARK LOCATION



Longitude: 2° 11" 39' W
Latitude: 50° 37" 25' N

Source: Esri, DigitalGlobe, GeoEye, Earthstar Geographics, CNES/Airbus DS, USDA, USGS, AeroGRID, IGN, and the GIS User Community

LANDMARK MASK



Gear Farm

Source: (Lock & Ralston 2017)

Contextual Information:

Nearest Node:	Helford
Km. to Nearest Node:	7.5
Mask Area (Hectares):	12.33
Sightings (Main Analysis):	94

LANDMARK LOCATION



Longitude: 5° 11" 13' W
Latitude: 50° 4" 46' N

Source: Esri, DigitalGlobe, GeoEye, Earthstar Geographics, CNES/Airbus DS, USDA, USGS, AeroGRID, IGN, and the GIS User Community

LANDMARK MASK



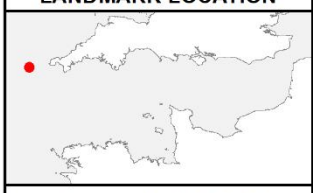
Giant's Castle

Source: (Lock & Ralston 2017)

Contextual Information:

Nearest Node:	Penzance
Km. to Nearest Node:	59.28
Mask Area (Hectares):	4.5
Sightings (Main Analysis):	546

LANDMARK LOCATION



Longitude: 6° 17" 5' W
Latitude: 49° 54" 40' N

Source: Esri, DigitalGlobe, GeoEye, Earthstar Geographics, CNES/Airbus DS, USDA, USGS, AeroGRID, IGN, and the GIS User Community

LANDMARK MASK



Griffin's Point

Source: (Lock & Ralston 2017)

Contextual Information:

Nearest Node:	Mevagissey
Km. to Nearest Node:	29.45
Mask Area (Hectares):	4.63
Sightings (Main Analysis):	1

LANDMARK LOCATION



Longitude: 5° 2" 33' W
Latitude: 50° 27" 30' N

Source: Esri, DigitalGlobe, GeoEye, Earthstar Geographics, CNES/Airbus DS, USDA, USGS, AeroGRID, IGN, and the GIS User Community

LANDMARK MASK



Hamble Common

Source: (Lock & Ralston 2017)

Contextual Information:

Nearest Node:	Christchurch
Km. to Nearest Node:	32.67
Mask Area (Hectares):	34.24
Sightings (Main Analysis):	3

LANDMARK LOCATION



Longitude: 1° 18" 50' W
Latitude: 50° 51" 3' N

Source: Esri, DigitalGlobe, GeoEye, Earthstar Geographics, CNES/Airbus DS, USDA, USGS, AeroGRID, IGN, and the GIS User Community

LANDMARK MASK



Hengistbury Head

Source: (Lock & Ralston 2017)

Contextual Information:

Nearest Node:	Christchurch
Km. to Nearest Node:	0.85
Mask Area (Hectares):	103.86
Sightings (Main Analysis):	3223

LANDMARK LOCATION



Longitude: 1° 45" 18' W
Latitude: 50° 42" 58' N

Source: Esri, DigitalGlobe, GeoEye, Earthstar Geographics, CNES/Airbus DS, USDA, USGS, AeroGRID, IGN, and the GIS User Community

LANDMARK MASK



Holbury Camp

Source: (Lock & Ralston 2017)

Contextual Information:

Nearest Node:	Bigbury Bay
Km. to Nearest Node:	10.07
Mask Area (Hectares):	6.12
Sightings (Main Analysis):	1111

LANDMARK LOCATION



Longitude: 3° 56" 6' W
Latitude: 50° 20" 17' N

Source: Esri, DigitalGlobe, GeoEye, Earthstar Geographics, CNES/Airbus DS, USDA, USGS, AeroGRID, IGN, and the GIS User Community

LANDMARK MASK



Ile Callot

Source: Geobretagne

Contextual Information:

Nearest Node:	Morlaix
Km. to Nearest Node:	2.45
Mask Area (Hectares):	22.09
Sightings (Main Analysis):	9461

LANDMARK LOCATION



Longitude: 3° 55" 30' W
Latitude: 48° 41" 51' N

Source: Esri, DigitalGlobe, GeoEye, Earthstar Geographics, CNES/Airbus DS, USDA, USGS, AeroGRID, IGN, and the GIS User Community

LANDMARK MASK



Île d'Yoc'h

Source: Maguer (1996)

Contextual Information:

Nearest Node:	Aber Wrac'h
Km. to Nearest Node:	15.46
Mask Area (Hectares):	30.42
Sightings (Main Analysis):	4453

LANDMARK LOCATION



Longitude: 4° 46" 30' W
Latitude: 48° 31" 44' N

Source: Esri, DigitalGlobe, GeoEye, Earthstar Geographics, CNES/Airbus DS, USDA, USGS, AeroGRID, IGN, and the GIS User Community

LANDMARK MASK



Jerbourg

Source: Burns (1988)

Contextual Information:

Nearest Node:	St. Peter Port
Km. to Nearest Node:	4.36
Mask Area (Hectares):	2.65
Sightings (Main Analysis):	8074

LANDMARK LOCATION



Longitude: 2° 31" 41' W
Latitude: 49° 25" 26' N

Source: Esri, DigitalGlobe, GeoEye, Earthstar Geographics, CNES/Airbus DS, USDA, USGS, AeroGRID, IGN, and the GIS User Community

LANDMARK MASK



Kastell Ac'h

Source: Geobretagne

Contextual Information:

Nearest Node:	Aber Wrac'h
Km. to Nearest Node:	3.39
Mask Area (Hectares):	17.14
Sightings (Main Analysis):	6362

LANDMARK LOCATION



Longitude: 4° 33" 51' W
Latitude: 48° 37" 27' N

Source: Esri, DigitalGlobe, GeoEye, Earthstar Geographics, CNES/Airbus DS, USDA, USGS, AeroGRID, IGN, and the GIS User Community

LANDMARK MASK



Kelsey Head

Source: (Lock & Ralston 2017)

Contextual Information:

Nearest Node:	Falmouth
Km. to Nearest Node:	31.43
Mask Area (Hectares):	5.22
Sightings (Main Analysis):	11

LANDMARK LOCATION



Longitude: 5° 8" 48' W
Latitude: 50° 24" 16' N

Source: Esri, DigitalGlobe, GeoEye, Earthstar Geographics, CNES/Airbus DS, USDA, USGS, AeroGRID, IGN, and the GIS User Community

LANDMARK MASK



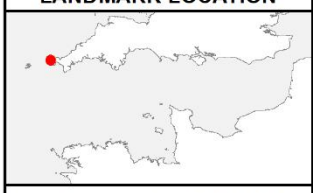
Kenidjack Castle

Source: (Lock & Ralston 2017)

Contextual Information:

Nearest Node:	Penzance
Km. to Nearest Node:	14.44
Mask Area (Hectares):	7.2
Sightings (Main Analysis):	206

LANDMARK LOCATION



Longitude: 5° 42" 13' W
Latitude: 50° 8" 4' N

Source: Esri, DigitalGlobe, GeoEye, Earthstar Geographics, CNES/Airbus DS, USDA, USGS, AeroGRID, IGN, and the GIS User Community

LANDMARK MASK



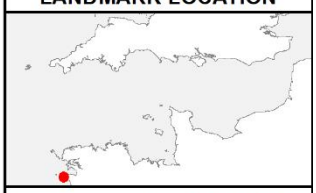
Kerdugazul

Source: Geobretagne

Contextual Information:

Nearest Node:	Brest
Km. to Nearest Node:	34.39
Mask Area (Hectares):	8.78
Sightings (Main Analysis):	28

LANDMARK LOCATION



Longitude: 4° 37" 19' W
Latitude: 48° 1" 5' N

Source: Esri, DigitalGlobe, GeoEye, Earthstar Geographics, CNES/Airbus DS, USDA, USGS, AeroGRID, IGN, and the GIS User Community

LANDMARK MASK



Kerfiat

Source: Geobretagne

Contextual Information:

Nearest Node:	Kerivoas
Km. to Nearest Node:	2.51
Mask Area (Hectares):	15.3
Sightings (Main Analysis):	9495

LANDMARK LOCATION



Longitude: 4° 5" 57' W
Latitude: 48° 41" 43' N

Source: Esri, DigitalGlobe, GeoEye, Earthstar Geographics, CNES/Airbus DS, USDA, USGS, AeroGRID, IGN, and the GIS User Community

LANDMARK MASK



Kergulan

Source: Geobretagne

Contextual Information:

Nearest Node:	Brest
Km. to Nearest Node:	27.94
Mask Area (Hectares):	4.72
Sightings (Main Analysis):	1706

LANDMARK LOCATION



Longitude: 4° 35" 27' W
Latitude: 48° 4" 33' N

Source: Esri, DigitalGlobe, GeoEye, Earthstar Geographics, CNES/Airbus DS, USDA, USGS, AeroGRID, IGN, and the GIS User Community

LANDMARK MASK



Kermorvan

Source: Maguer (1996)

Contextual Information:

Nearest Node:	Brest
Km. to Nearest Node:	14.05
Mask Area (Hectares):	66.28
Sightings (Main Analysis):	1521

LANDMARK LOCATION



Longitude: 4° 47" 1' W
Latitude: 48° 21" 53' N

Source: Esri, DigitalGlobe, GeoEye, Earthstar Geographics, CNES/Airbus DS, USDA, USGS, AeroGRID, IGN, and the GIS User Community

LANDMARK MASK



Kilcobben Cove

Source: (Lock & Ralston 2017)

Contextual Information:

Nearest Node:	Mullion
Km. to Nearest Node:	9.27
Mask Area (Hectares):	2.88
Sightings (Main Analysis):	4836

LANDMARK LOCATION



Longitude: 5° 11" 6' W
Latitude: 49° 58" 9' N

Source: Esri, DigitalGlobe, GeoEye, Earthstar Geographics, CNES/Airbus DS, USDA, USGS, AeroGRID, IGN, and the GIS User Community

LANDMARK MASK



L'Aber

Source: Maguer (1996)

Contextual Information:

Nearest Node:	Brest
Km. to Nearest Node:	16.09
Mask Area (Hectares):	21.82
Sightings (Main Analysis):	139

LANDMARK LOCATION



Longitude: 4° 26" 10' W
Latitude: 48° 13" 32' N

Source: Esri, DigitalGlobe, GeoEye, Earthstar Geographics, CNES/Airbus DS, USDA, USGS, AeroGRID, IGN, and the GIS User Community

LANDMARK MASK



Lankidden

Source: (Lock & Ralston 2017)

Contextual Information:

Nearest Node:	Helford
Km. to Nearest Node:	10.19
Mask Area (Hectares):	5.76
Sightings (Main Analysis):	4661

LANDMARK LOCATION



Longitude: 5° 8" 0' W
Latitude: 50° 0" 22' N

Source: Esri, DigitalGlobe, GeoEye, Earthstar Geographics, CNES/Airbus DS, USDA, USGS, AeroGRID, IGN, and the GIS User Community

LANDMARK MASK



Lavallot

Source: Geobretagne

Contextual Information:

Nearest Node:	Morlaix
Km. to Nearest Node:	9.48
Mask Area (Hectares):	18.68
Sightings (Main Analysis):	282

LANDMARK LOCATION



Longitude: 3° 51" 42' W
Latitude: 48° 36" 38' N

Source: Esri, DigitalGlobe, GeoEye, Earthstar Geographics, CNES/Airbus DS, USDA, USGS, AeroGRID, IGN, and the GIS User Community

LANDMARK MASK



Le Câtel de Rozel

Source: Bender (1986)

Contextual Information:

Nearest Node:	St. Peter Port
Km. to Nearest Node:	40.9
Mask Area (Hectares):	6.25
Sightings (Main Analysis):	4891

LANDMARK LOCATION



Longitude: 2° 3" 7' W
Latitude: 49° 14" 35' N

Source: Esri, DigitalGlobe, GeoEye, Earthstar Geographics, CNES/Airbus DS, USDA, USGS, AeroGRID, IGN, and the GIS User Community

LANDMARK MASK



Le Minihic

Source: Geobretagne

Contextual Information:

Nearest Node:	Saint Malo
Km. to Nearest Node:	2.99
Mask Area (Hectares):	26.5
Sightings (Main Analysis):	3990

LANDMARK LOCATION



Longitude: 1° 59" 18' W
Latitude: 48° 40" 54' N

Source: Esri, DigitalGlobe, GeoEye, Earthstar Geographics, CNES/Airbus DS, USDA, USGS, AeroGRID, IGN, and the GIS User Community

LANDMARK MASK



Le Voallas

Source: Geobretagne

Contextual Information:

Nearest Node:	Morlaix
Km. to Nearest Node:	6.14
Mask Area (Hectares):	2.25
Sightings (Main Analysis):	5081

LANDMARK LOCATION



Longitude: 3° 50" 27' W
Latitude: 48° 38" 0' N

Source: Esri, DigitalGlobe, GeoEye, Earthstar Geographics, CNES/Airbus DS, USDA, USGS, AeroGRID, IGN, and the GIS User Community

LANDMARK MASK



Le Yaudet

Source: Bender (1986)

Contextual Information:

Nearest Node:	Rivière De Lannion
Km. to Nearest Node:	4.44
Mask Area (Hectares):	17.5
Sightings (Main Analysis):	2722

LANDMARK LOCATION



Longitude: 3° 32" 13' W
Latitude: 48° 43" 53' N

Source: Esri, DigitalGlobe, GeoEye, Earthstar Geographics, CNES/Airbus DS, USDA, USGS, AeroGRID, IGN, and the GIS User Community

LANDMARK MASK



Les Fouaillages

Source: Bender (1986)

Contextual Information:

Nearest Node:	St. Peter Port
Km. to Nearest Node:	4.19
Mask Area (Hectares):	24.16
Sightings (Main Analysis):	6163

LANDMARK LOCATION



Longitude: 2° 32" 17' W
Latitude: 49° 29" 52' N

Source: Esri, DigitalGlobe, GeoEye, Earthstar Geographics, CNES/Airbus DS, USDA, USGS, AeroGRID, IGN, and the GIS User Community

LANDMARK MASK



Lescudjack Castle

Source: (Lock & Ralston 2017)

Contextual Information:

Nearest Node:	Penzance
Km. to Nearest Node:	3.29
Mask Area (Hectares):	4.68
Sightings (Main Analysis):	2620

LANDMARK LOCATION



Longitude: 5° 32" 0' W
Latitude: 50° 7" 32' N

Source: Esri, DigitalGlobe, GeoEye, Earthstar Geographics, CNES/Airbus DS, USDA, USGS, AeroGRID, IGN, and the GIS User Community

LANDMARK MASK



Little Dennis

Source: (Lock & Ralston 2017)

Contextual Information:

Nearest Node:	Helford
Km. to Nearest Node:	0.81
Mask Area (Hectares):	25.07
Sightings (Main Analysis):	4471

LANDMARK LOCATION



Longitude: 5° 5" 46' W
Latitude: 50° 5" 21' N

Source: Esri, DigitalGlobe, GeoEye, Earthstar Geographics, CNES/Airbus DS, USDA, USGS, AeroGRID, IGN, and the GIS User Community

LANDMARK MASK



Lostmarc'h

Source: Bender (1986), Geobretagne

Contextual Information:

Nearest Node:	Brest
Km. to Nearest Node:	13.01
Mask Area (Hectares):	8.23
Sightings (Main Analysis):	1360

LANDMARK LOCATION



Longitude: 4° 33" 25' W
Latitude: 48° 12" 45' N

Source: Esri, DigitalGlobe, GeoEye, Earthstar Geographics, CNES/Airbus DS, USDA, USGS, AeroGRID, IGN, and the GIS User Community

LANDMARK MASK



Maen Castle

Source: (Lock & Ralston 2017)

Contextual Information:

Nearest Node:	Penzance
Km. to Nearest Node:	14.62
Mask Area (Hectares):	3.96
Sightings (Main Analysis):	143

LANDMARK LOCATION



Longitude: 5° 42" 30' W
Latitude: 50° 4" 22' N

Source: Esri, DigitalGlobe, GeoEye, Earthstar Geographics, CNES/Airbus DS, USDA, USGS, AeroGRID, IGN, and the GIS User Community

LANDMARK MASK



Mastel Meur

Source: Bender (1986), Geobretagne

Contextual Information:

Nearest Node:	Brest
Km. to Nearest Node:	29.91
Mask Area (Hectares):	18.36
Sightings (Main Analysis):	1937

LANDMARK LOCATION



Longitude: 4° 41" 20' W
Latitude: 48° 3" 49' N

Source: Esri, DigitalGlobe, GeoEye, Earthstar Geographics, CNES/Airbus DS, USDA, USGS, AeroGRID, IGN, and the GIS User Community

LANDMARK MASK



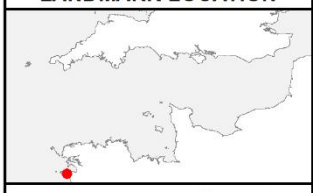
Menei-Castel

Source: Bender (1986), Geobretagne

Contextual Information:

Nearest Node:	Brest
Km. to Nearest Node:	32.74
Mask Area (Hectares):	6.25
Sightings (Main Analysis):	28

LANDMARK LOCATION



Longitude: 4° 31" 56' W
Latitude: 48° 2" 9' N

Source: Esri, DigitalGlobe, GeoEye, Earthstar Geographics, CNES/Airbus DS, USDA, USGS, AeroGRID, IGN, and the GIS User Community

LANDMARK MASK



Park Head

Source: (Lock & Ralston 2017)

Contextual Information:

Nearest Node:	Mevagissey
Km. to Nearest Node:	32.78
Mask Area (Hectares):	6.43
Sightings (Main Analysis):	0

LANDMARK LOCATION



Longitude: 5° 2" 41' W
Latitude: 50° 29" 49' N

Source: Esri, DigitalGlobe, GeoEye, Earthstar Geographics, CNES/Airbus DS, USDA, USGS, AeroGRID, IGN, and the GIS User Community

LANDMARK MASK



Penhale Point

Source: (Lock & Ralston 2017)

Contextual Information:

Nearest Node:	Falmouth
Km. to Nearest Node:	29.82
Mask Area (Hectares):	13.68
Sightings (Main Analysis):	13

LANDMARK LOCATION



Longitude: 5° 9" 20' W
Latitude: 50° 23" 19' N

Source: Esri, DigitalGlobe, GeoEye, Earthstar Geographics, CNES/Airbus DS, USDA, USGS, AeroGRID, IGN, and the GIS User Community

LANDMARK MASK



Pointe de Bendy

Source: Geobretagne

Contextual Information:

Nearest Node:	Brest
Km. to Nearest Node:	18.76
Mask Area (Hectares):	20.7
Sightings (Main Analysis):	43

LANDMARK LOCATION



Longitude: 4° 20" 8' W
Latitude: 48° 18" 47' N

Source: Esri, DigitalGlobe, GeoEye, Earthstar Geographics, CNES/Airbus DS, USDA, USGS, AeroGRID, IGN, and the GIS User Community

LANDMARK MASK



Pointe de Menga

Source: Bender (1986); Wheeler (1957)

Contextual Information:

Nearest Node:	Saint Malo
Km. to Nearest Node:	7.17
Mask Area (Hectares):	44.95
Sightings (Main Analysis):	3894

LANDMARK LOCATION



Longitude: 1° 56" 8' W
Latitude: 48° 41" 57' N

Source: Esri, DigitalGlobe, GeoEye, Earthstar Geographics, CNES/Airbus DS, USDA, USGS, AeroGRID, IGN, and the GIS User Community

LANDMARK MASK



Pointe de Primel

Source: Geobretagne

Contextual Information:

Nearest Node:	Morlaix
Km. to Nearest Node:	5.3
Mask Area (Hectares):	25.88
Sightings (Main Analysis):	12161

LANDMARK LOCATION



Longitude: 3° 49" 10' W
Latitude: 48° 43" 5' N

Source: Esri, DigitalGlobe, GeoEye, Earthstar Geographics, CNES/Airbus DS, USDA, USGS, AeroGRID, IGN, and the GIS User Community

LANDMARK MASK



Pointe de Saint-Hernot

Source: Geobretagne

Contextual Information:

Nearest Node:	Brest
Km. to Nearest Node:	15.23
Mask Area (Hectares):	7.47
Sightings (Main Analysis):	32

LANDMARK LOCATION



Longitude: 4° 30" 41' W
Latitude: 48° 12" 4' N

Source: Esri, DigitalGlobe, GeoEye, Earthstar Geographics, CNES/Airbus DS, USDA, USGS, AeroGRID, IGN, and the GIS User Community

LANDMARK MASK



Pointe du Château

Source: Geobretagne

Contextual Information:

Nearest Node:	Brest
Km. to Nearest Node:	20.29
Mask Area (Hectares):	9.86
Sightings (Main Analysis):	47

LANDMARK LOCATION



Longitude: 4° 18" 57' W
Latitude: 48° 19" 54' N

Source: Esri, DigitalGlobe, GeoEye, Earthstar Geographics, CNES/Airbus DS, USDA, USGS, AeroGRID, IGN, and the GIS User Community

LANDMARK MASK



Pointe du Grouin

Source: Geobretagne

Contextual Information:

Nearest Node:	Saint Malo
Km. to Nearest Node:	14.18
Mask Area (Hectares):	6.25
Sightings (Main Analysis):	2878

LANDMARK LOCATION



Longitude: 1° 50" 40' W
Latitude: 48° 42" 42' N

Source: Esri, DigitalGlobe, GeoEye, Earthstar Geographics, CNES/Airbus DS, USDA, USGS, AeroGRID, IGN, and the GIS User Community

LANDMARK MASK



Pointe du Raz

Source: Maguer (1996)

Contextual Information:

Nearest Node:	Brest
Km. to Nearest Node:	33.55
Mask Area (Hectares):	16.96
Sightings (Main Analysis):	2088

LANDMARK LOCATION



Longitude: 4° 44" 16' W
Latitude: 48° 2" 23' N

Source: Esri, DigitalGlobe, GeoEye, Earthstar Geographics, CNES/Airbus DS, USDA, USGS, AeroGRID, IGN, and the GIS User Community

LANDMARK MASK



Pointe du Toulinguet

Source: Geobretagne

Contextual Information:

Nearest Node:	Brest
Km. to Nearest Node:	5.52
Mask Area (Hectares):	37.71
Sightings (Main Analysis):	2064

LANDMARK LOCATION



Longitude: 4° 37" 26' W
Latitude: 48° 16" 46' N

Source: Esri, DigitalGlobe, GeoEye, Earthstar Geographics, CNES/Airbus DS, USDA, USGS, AeroGRID, IGN, and the GIS User Community

LANDMARK MASK



Pointe Roselier

Source: Geobretagne

Contextual Information:

Nearest Node:	Le Légnét
Km. to Nearest Node:	3.52
Mask Area (Hectares):	28.93
Sightings (Main Analysis):	4884

LANDMARK LOCATION



Longitude: 2° 42" 57' W
Latitude: 48° 33" 12' N

Source: Esri, DigitalGlobe, GeoEye, Earthstar Geographics, CNES/Airbus DS, USDA, USGS, AeroGRID, IGN, and the GIS User Community

LANDMARK MASK



Porth Joke

Source: (Lock & Ralston 2017)

Contextual Information:

Nearest Node:	Falmouth
Km. to Nearest Node:	31.29
Mask Area (Hectares):	2.97
Sightings (Main Analysis):	1

LANDMARK LOCATION



Longitude: 5° 8" 29' W
Latitude: 50° 24" 14' N

Source: Esri, DigitalGlobe, GeoEye, Earthstar Geographics, CNES/Airbus DS, USDA, USGS, AeroGRID, IGN, and the GIS User Community

LANDMARK MASK



Rame Head

Source: (Lock & Ralston 2017)

Contextual Information:

Nearest Node:	Plymouth
Km. to Nearest Node:	4.08
Mask Area (Hectares):	26.41
Sightings (Main Analysis):	15826

LANDMARK LOCATION



Longitude: 4° 13" 22' W
Latitude: 50° 18" 47' N

Source: Esri, DigitalGlobe, GeoEye, Earthstar Geographics, CNES/Airbus DS, USDA, USGS, AeroGRID, IGN, and the GIS User Community

LANDMARK MASK



Redcliff Castle

Source: (Lock & Ralston 2017)

Contextual Information:

Nearest Node:	Mevagissey
Km. to Nearest Node:	31.48
Mask Area (Hectares):	4.5
Sightings (Main Analysis):	0

LANDMARK LOCATION



Longitude: 5° 2" 1' W
Latitude: 50° 29" 12' N

Source: Esri, DigitalGlobe, GeoEye, Earthstar Geographics, CNES/Airbus DS, USDA, USGS, AeroGRID, IGN, and the GIS User Community

LANDMARK MASK



Roc'h Nivelen

Source: Geobretagne

Contextual Information:

Nearest Node:	Brest
Km. to Nearest Node:	15.75
Mask Area (Hectares):	5.08
Sightings (Main Analysis):	422

LANDMARK LOCATION



Longitude: 4° 23" 31' W
Latitude: 48° 22" 47' N

Source: Esri, DigitalGlobe, GeoEye, Earthstar Geographics, CNES/Airbus DS, USDA, USGS, AeroGRID, IGN, and the GIS User Community

LANDMARK MASK



Roch'an Evned

Source: Geobretagne

Contextual Information:

Nearest Node:	Le Trieux
Km. to Nearest Node:	7.96
Mask Area (Hectares):	8.23
Sightings (Main Analysis):	7086

LANDMARK LOCATION



Longitude: 3° 4" 20' W
Latitude: 48° 49" 10' N

Source: Esri, DigitalGlobe, GeoEye, Earthstar Geographics, CNES/Airbus DS, USDA, USGS, AeroGRID, IGN, and the GIS User Community

LANDMARK MASK



Rosemullion Head

Source: (Lock & Ralston 2017)

Contextual Information:

Nearest Node:	Helford
Km. to Nearest Node:	1.78
Mask Area (Hectares):	11.65
Sightings (Main Analysis):	6015

LANDMARK LOCATION



Longitude: 5° 4" 59' W
Latitude: 50° 6" 38' N

Source: Esri, DigitalGlobe, GeoEye, Earthstar Geographics, CNES/Airbus DS, USDA, USGS, AeroGRID, IGN, and the GIS User Community

LANDMARK MASK



Saoutenet

Source: Geobretagne

Contextual Information:

Nearest Node:	Brest
Km. to Nearest Node:	33.93
Mask Area (Hectares):	3.51
Sightings (Main Analysis):	28

LANDMARK LOCATION



Longitude: 4° 40" 28' W
Latitude: 48° 1" 36' N

Source: Esri, DigitalGlobe, GeoEye, Earthstar Geographics, CNES/Airbus DS, USDA, USGS, AeroGRID, IGN, and the GIS User Community

LANDMARK MASK



Seaford Head Camp

Source: (Lock & Ralston 2017)

Contextual Information:

Nearest Node:	Christchurch
Km. to Nearest Node:	130.16
Mask Area (Hectares):	12.6
Sightings (Main Analysis):	0

LANDMARK LOCATION



Longitude: 0° 7" 4' E
Latitude: 50° 45" 38' N

Source: Esri, DigitalGlobe, GeoEye, Earthstar Geographics, CNES/Airbus DS, USDA, USGS, AeroGRID, IGN, and the GIS User Community

LANDMARK MASK



Shipman Head

Source: (Lock & Ralston 2017)

Contextual Information:

Nearest Node:	Penzance
Km. to Nearest Node:	62.27
Mask Area (Hectares):	44.23
Sightings (Main Analysis):	184

LANDMARK LOCATION



Longitude: 6° 21" 27' W
Latitude: 49° 57" 45' N

Source: Esri, DigitalGlobe, GeoEye, Earthstar Geographics, CNES/Airbus DS, USDA, USGS, AeroGRID, IGN, and the GIS User Community

LANDMARK MASK



Shorthorn Point

Source: (Lock & Ralston 2017)

Contextual Information:

Nearest Node:	Fowey
Km. to Nearest Node:	7.35
Mask Area (Hectares):	3.6
Sightings (Main Analysis):	4448

LANDMARK LOCATION



Longitude: 4° 43" 39' W
Latitude: 50° 20" 15' N

Source: Esri, DigitalGlobe, GeoEye, Earthstar Geographics, CNES/Airbus DS, USDA, USGS, AeroGRID, IGN, and the GIS User Community

LANDMARK MASK



St. Michael's Mount

Source: Herring (2000)

Contextual Information:

Nearest Node:	Penzance
Km. to Nearest Node:	2.48
Mask Area (Hectares):	17.68
Sightings (Main Analysis):	3040

LANDMARK LOCATION



Longitude: 5° 28" 38' W
Latitude: 50° 7" 0' N

Source: Esri, DigitalGlobe, GeoEye, Earthstar Geographics, CNES/Airbus DS, USDA, USGS, AeroGRID, IGN, and the GIS User Community

LANDMARK MASK



The Rumps

Source: (Lock & Ralston 2017)

Contextual Information:

Nearest Node:	Fowey
Km. to Nearest Node:	37.59
Mask Area (Hectares):	17.14
Sightings (Main Analysis):	0

LANDMARK LOCATION



Longitude: 4° 55" 13' W
Latitude: 50° 35" 35' N

Source: Esri, DigitalGlobe, GeoEye, Earthstar Geographics, CNES/Airbus DS, USDA, USGS, AeroGRID, IGN, and the GIS User Community

LANDMARK MASK



Tourner Bury

Source: (Lock & Ralston 2017)

Contextual Information:

Nearest Node:	Christchurch
Km. to Nearest Node:	54.69
Mask Area (Hectares):	8.51
Sightings (Main Analysis):	177

LANDMARK LOCATION



Longitude: 0° 57" 46' W
Latitude: 50° 47" 36' N

Source: Esri, DigitalGlobe, GeoEye, Earthstar Geographics, CNES/Airbus DS, USDA, USGS, AeroGRID, IGN, and the GIS User Community

LANDMARK MASK



Trereen Dinas

Source: (Lock & Ralston 2017)

Contextual Information:

Nearest Node:	Penzance
Km. to Nearest Node:	11.98
Mask Area (Hectares):	10.89
Sightings (Main Analysis):	37

LANDMARK LOCATION



Longitude: 5° 35" 55' W
Latitude: 50° 11" 30' N

Source: Esri, DigitalGlobe, GeoEye, Earthstar Geographics, CNES/Airbus DS, USDA, USGS, AeroGRID, IGN, and the GIS User Community

LANDMARK MASK



Treryn Dinas

Source: (Lock & Ralston 2017)

Contextual Information:

Nearest Node:	Penzance
Km. to Nearest Node:	10.97
Mask Area (Hectares):	21.73
Sightings (Main Analysis):	3325

LANDMARK LOCATION



Longitude: 5° 38" 8' W
Latitude: 50° 2" 31' N

Source: Esri, DigitalGlobe, GeoEye, Earthstar Geographics, CNES/Airbus DS, USDA, USGS, AeroGRID, IGN, and the GIS User Community

LANDMARK MASK



Trevelgue Head

Source: (Lock & Ralston 2017)

Contextual Information:

Nearest Node:	Mevagissey
Km. to Nearest Node:	27.97
Mask Area (Hectares):	16.25
Sightings (Main Analysis):	0

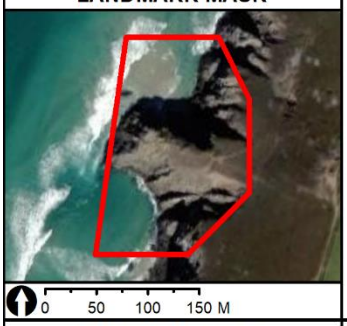
LANDMARK LOCATION



Longitude: 5° 3" 48' W
Latitude: 50° 25" 35' N

Source: Esri, DigitalGlobe, GeoEye, Earthstar Geographics, CNES/Airbus DS, USDA, USGS, AeroGRID, IGN, and the GIS User Community

LANDMARK MASK



Tubby's Head

Source: (Lock & Ralston 2017)

Contextual Information:

Nearest Node:	Falmouth
Km. to Nearest Node:	24.4
Mask Area (Hectares):	2.56
Sightings (Main Analysis):	15

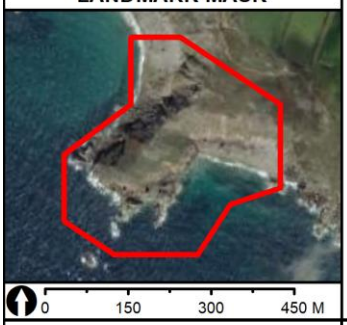
LANDMARK LOCATION



Longitude: 5° 14" 3' W
Latitude: 50° 18" 33' N

Source: Esri, DigitalGlobe, GeoEye, Earthstar Geographics, CNES/Airbus DS, USDA, USGS, AeroGRID, IGN, and the GIS User Community

LANDMARK MASK



Vaux du Catel

Source: Bender (1986)

Contextual Information:

Nearest Node:	Nacqueville
Km. to Nearest Node:	19.51
Mask Area (Hectares):	10.66
Sightings (Main Analysis):	11822

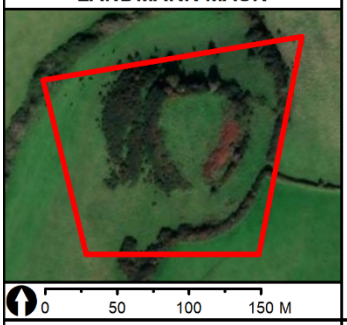
LANDMARK LOCATION



Longitude: 1° 56" 20' W
Latitude: 49° 40" 19' N

Source: Esri, DigitalGlobe, GeoEye, Earthstar Geographics, CNES/Airbus DS, USDA, USGS, AeroGRID, IGN, and the GIS User Community

LANDMARK MASK



Veryan Castle

Source: (Lock & Ralston 2017)

Contextual Information:

Nearest Node:	Falmouth
Km. to Nearest Node:	11.39
Mask Area (Hectares):	2.02
Sightings (Main Analysis):	1463

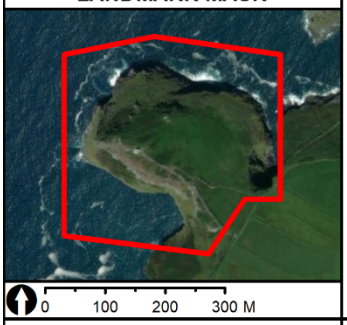
LANDMARK LOCATION



Longitude: 4° 55" 56' W
Latitude: 50° 12" 43' N

Source: Esri, DigitalGlobe, GeoEye, Earthstar Geographics, CNES/Airbus DS, USDA, USGS, AeroGRID, IGN, and the GIS User Community

LANDMARK MASK



Willapark

Source: (Lock & Ralston 2017)

Contextual Information:

Nearest Node:	Fowey
Km. to Nearest Node:	42.75
Mask Area (Hectares):	11.25
Sightings (Main Analysis):	0

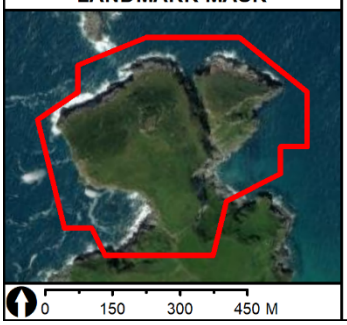
LANDMARK LOCATION



Longitude: 4° 42" 14' W
Latitude: 50° 41" 22' N

Source: Esri, DigitalGlobe, GeoEye, Earthstar Geographics, CNES/Airbus DS, USDA, USGS, AeroGRID, IGN, and the GIS User Community

LANDMARK MASK



Willapark Head

Source: (Lock & Ralston 2017)

Contextual Information:

Nearest Node:	Fowey
Km. to Nearest Node:	41.47
Mask Area (Hectares):	21.15
Sightings (Main Analysis):	0

LANDMARK LOCATION



Longitude: 4° 44" 35' W
Latitude: 50° 40" 29' N

Source: Esri, DigitalGlobe, GeoEye, Earthstar Geographics, CNES/Airbus DS, USDA, USGS, AeroGRID, IGN, and the GIS User Community

LANDMARK MASK



Winecove Point Complex

Source: (Lock & Ralston 2017)

Contextual Information:

Nearest Node:	Mevagissey
Km. to Nearest Node:	34.45
Mask Area (Hectares):	6.79
Sightings (Main Analysis):	0

LANDMARK LOCATION



Longitude: 5° 1" 42' W
Latitude: 50° 31" 20' N

Source: Esri, DigitalGlobe, GeoEye, Earthstar Geographics, CNES/Airbus DS, USDA, USGS, AeroGRID, IGN, and the GIS User Community

LANDMARK MASK



Yaverland

Source: (Lock & Ralston 2017)

Contextual Information:

Nearest Node:	Christchurch
Km. to Nearest Node:	42.29
Mask Area (Hectares):	11.74
Sightings (Main Analysis):	313

LANDMARK LOCATION



Longitude: 1° 7" 55' W
Latitude: 50° 40" 19' N

Source: Esri, DigitalGlobe, GeoEye, Earthstar Geographics, CNES/Airbus DS, USDA, USGS, AeroGRID, IGN, and the GIS User Community

LANDMARK MASK



Bantham Camp

Source: (Lock & Ralston 2017)

Contextual Information:

Nearest Node:	Bigbury Bay
Km. to Nearest Node:	3.08
Mask Area (Hectares):	22.05
Sightings (Main Analysis):	7844

LANDMARK LOCATION



Longitude: 3° 52" 38' W
Latitude: 50° 16" 45' N

Source: Esri, DigitalGlobe, GeoEye, Earthstar Geographics, CNES/Airbus DS, USDA, USGS, AeroGRID, IGN, and the GIS User Community

LANDMARK MASK



Beg Monom / Roc'h Pelguent

Source: Maguer (1996), Geobretagne

Contextual Information:

Nearest Node:	Aber Wrac'h
Km. to Nearest Node:	5.52
Mask Area (Hectares):	10.39
Sightings (Main Analysis):	7380

LANDMARK LOCATION



Longitude: 4° 32" 19' W
Latitude: 48° 38" 11' N

Source: Esri, DigitalGlobe, GeoEye, Earthstar Geographics, CNES/Airbus DS, USDA, USGS, AeroGRID, IGN, and the GIS User Community

LANDMARK MASK



Bel-air

Source: Geobretagne

Contextual Information:

Nearest Node:	Morlaix
Km. to Nearest Node:	9.32
Mask Area (Hectares):	8.91
Sightings (Main Analysis):	39

LANDMARK LOCATION



Longitude: 3° 48" 41' W
Latitude: 48° 37" 40' N

Source: Esri, DigitalGlobe, GeoEye, Earthstar Geographics, CNES/Airbus DS, USDA, USGS, AeroGRID, IGN, and the GIS User Community

LANDMARK MASK



Belle Tout

Source: (Lock & Ralston 2017)

Contextual Information:

Nearest Node:	Christchurch
Km. to Nearest Node:	136.29
Mask Area (Hectares):	39.69
Sightings (Main Analysis):	0

LANDMARK LOCATION



Longitude: 0° 12" 33' E
Latitude: 50° 44" 22' N

Source: Esri, DigitalGlobe, GeoEye, Earthstar Geographics, CNES/Airbus DS, USDA, USGS, AeroGRID, IGN, and the GIS User Community

LANDMARK MASK



Berry Cliff Camp

Source: (Lock & Ralston 2017)

Contextual Information:

Nearest Node:	Sidmouth
Km. to Nearest Node:	5.68
Mask Area (Hectares):	11.07
Sightings (Main Analysis):	12384

LANDMARK LOCATION



Longitude: 3° 9" 0' W
Latitude: 50° 41" 14' N

Source: Esri, DigitalGlobe, GeoEye, Earthstar Geographics, CNES/Airbus DS, USDA, USGS, AeroGRID, IGN, and the GIS User Community

LANDMARK MASK



Bindon Hill

Source: (Lock & Ralston 2017)

Contextual Information:

Nearest Node:	Lulworth Cove
Km. to Nearest Node:	2.64
Mask Area (Hectares):	167.53
Sightings (Main Analysis):	7230

LANDMARK LOCATION



Longitude: 2° 14" 2' W
Latitude: 50° 37" 10' N

Source: Esri, DigitalGlobe, GeoEye, Earthstar Geographics, CNES/Airbus DS, USDA, USGS, AeroGRID, IGN, and the GIS User Community

LANDMARK MASK



Black Head

Source: (Lock & Ralston 2017)

Contextual Information:

Nearest Node:	Mevagissey
Km. to Nearest Node:	3.52
Mask Area (Hectares):	12.02
Sightings (Main Analysis):	8326

LANDMARK LOCATION



Longitude: 4° 45" 15' W
Latitude: 50° 17" 57' N

Source: Esri, DigitalGlobe, GeoEye, Earthstar Geographics, CNES/Airbus DS, USDA, USGS, AeroGRID, IGN, and the GIS User Community

LANDMARK MASK



Bolt Tail Camp

Source: (Lock & Ralston 2017)

Contextual Information:

Nearest Node:	Bigbury Bay
Km. to Nearest Node:	1.8
Mask Area (Hectares):	18.36
Sightings (Main Analysis):	15147

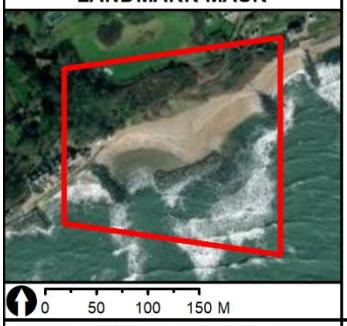
LANDMARK LOCATION



Longitude: 3° 52" 5' W
Latitude: 50° 14" 30' N

Source: Esri, DigitalGlobe, GeoEye, Earthstar Geographics, CNES/Airbus DS, USDA, USGS, AeroGRID, IGN, and the GIS User Community

LANDMARK MASK



Bonchurch

Source: (Lock & Ralston 2017)

Contextual Information:

Nearest Node:	Christchurch
Km. to Nearest Node:	40.66
Mask Area (Hectares):	3.78
Sightings (Main Analysis):	883

LANDMARK LOCATION



Longitude: 1° 10" 58' W
Latitude: 50° 35" 54' N

Source: Esri, DigitalGlobe, GeoEye, Earthstar Geographics, CNES/Airbus DS, USDA, USGS, AeroGRID, IGN, and the GIS User Community

LANDMARK MASK



Bosigran Castle

Source: (Lock & Ralston 2017)

Contextual Information:

Nearest Node:	Penzance
Km. to Nearest Node:	11.45
Mask Area (Hectares):	12.11
Sightings (Main Analysis):	34

LANDMARK LOCATION



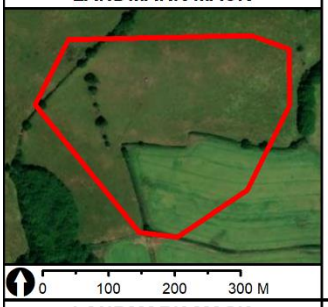
Longitude: 5° 37" 12' W
Latitude: 50° 10" 32' N

Source: Esri, DigitalGlobe, GeoEye, Earthstar Geographics, CNES/Airbus DS, USDA, USGS, AeroGRID, IGN, and the GIS User Community

Appendix II

This appendix contains records for each natural prominence used as a landmark in analyses in Chapters 5-8.

LANDMARK MASK



Aish

Identified as natural prominence.
Identified as site: No

Contextual Information:

Nearest Node:	Torquay
Km. to Nearest Node:	9.73
Mask Area (Hectares):	8.42
Sightings (Main Analysis):	2588

LANDMARK LOCATION



Longitude: 3° 3" 30' W
Latitude: 50° 25" 5' N

Source: Esri, DigitalGlobe, GeoEye, Earthstar Geographics, CNES/Airbus DS, USDA, USGS, AeroGRID, IGN, and the GIS User Community

LANDMARK MASK



Alum Bay

Identified as natural prominence.
Identified as site: No

Contextual Information:

Nearest Node:	Christchurch
Km. to Nearest Node:	11.87
Mask Area (Hectares):	141.41
Sightings (Main Analysis):	3820

LANDMARK LOCATION



Longitude: 1° 1" 11' W
Latitude: 50° 40" 4' N

Source: Esri, DigitalGlobe, GeoEye, Earthstar Geographics, CNES/Airbus DS, USDA, USGS, AeroGRID, IGN, and the GIS User Community

LANDMARK MASK



Ar Grill

Identified as natural prominence.
Identified as site: No

Contextual Information:

Nearest Node:	Brest
Km. to Nearest Node:	4.61
Mask Area (Hectares):	13.64
Sightings (Main Analysis):	1898

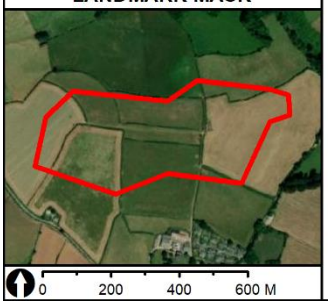
LANDMARK LOCATION



Longitude: 4° 4" 16' W
Latitude: 48° 17" 7' N

Source: Esri, DigitalGlobe, GeoEye, Earthstar Geographics, CNES/Airbus DS, USDA, USGS, AeroGRID, IGN, and the GIS User Community

LANDMARK MASK



Ashprington

Identified as natural prominence.
Identified as site: No

Contextual Information:

Nearest Node:	Torquay
Km. to Nearest Node:	11.53
Mask Area (Hectares):	16.86
Sightings (Main Analysis):	3011

LANDMARK LOCATION



Longitude: 3° 3" 1' W
Latitude: 50° 24" 20' N

Source: Esri, DigitalGlobe, GeoEye, Earthstar Geographics, CNES/Airbus DS, USDA, USGS, AeroGRID, IGN, and the GIS User Community

LANDMARK MASK



Ashprington 1

Identified as natural prominence.
Identified as site: No

Contextual Information:

Nearest Node:	Torquay
Km. to Nearest Node:	10.56
Mask Area (Hectares):	37.3
Sightings (Main Analysis):	3526

LANDMARK LOCATION



Longitude: 3° 3" 5' W
Latitude: 50° 24" 8' N

Source: Esri, DigitalGlobe, GeoEye, Earthstar Geographics, CNES/Airbus DS, USDA, USGS, AeroGRID, IGN, and the GIS User Community

LANDMARK MASK



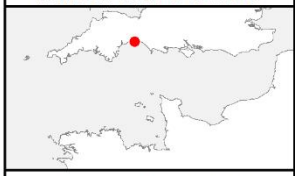
Axmouth Harbour

Identified as natural prominence.
Identified as site: No

Contextual Information:

Nearest Node:	Seaton
Km. to Nearest Node:	3.43
Mask Area (Hectares):	57.58
Sightings (Main Analysis):	11444

LANDMARK LOCATION



Longitude: 3° 3" 12' W
Latitude: 50° 42" 19' N

Source: Esri, DigitalGlobe, GeoEye, Earthstar Geographics, CNES/Airbus DS, USDA, USGS, AeroGRID, IGN, and the GIS User Community

LANDMARK MASK



Bantham 1

Identified as natural prominence.
Identified as site: No

Contextual Information:

Nearest Node:	Bigbury Bay
Km. to Nearest Node:	2.74
Mask Area (Hectares):	11.11
Sightings (Main Analysis):	11005

LANDMARK LOCATION



Longitude: 3° 3" 26' W
Latitude: 50° 16" 24' N

Source: Esri, DigitalGlobe, GeoEye, Earthstar Geographics, CNES/Airbus DS, USDA, USGS, AeroGRID, IGN, and the GIS User Community

LANDMARK MASK



Beeny

Identified as natural prominence.
Identified as site: No

Contextual Information:

Nearest Node:	Fowey
Km. to Nearest Node:	43.83
Mask Area (Hectares):	50.77
Sightings (Main Analysis):	0

LANDMARK LOCATION



Longitude: 4° 4" 22' W
Latitude: 50° 42" 13' N

Source: Esri, DigitalGlobe, GeoEye, Earthstar Geographics, CNES/Airbus DS, USDA, USGS, AeroGRID, IGN, and the GIS User Community

LANDMARK MASK



Beesands

Identified as natural prominence.
Identified as site: No

Contextual Information:

Nearest Node:	Salcombe
Km. to Nearest Node:	9.45
Mask Area (Hectares):	31.3
Sightings (Main Analysis):	12911

LANDMARK LOCATION



Longitude: 3° 3" 14' W
Latitude: 50° 15" 8' N

Source: Esri, DigitalGlobe, GeoEye, Earthstar Geographics, CNES/Airbus DS, USDA, USGS, AeroGRID, IGN, and the GIS User Community

LANDMARK MASK



Belle Hougue

Identified as natural prominence.
Identified as site: No

Contextual Information:

Nearest Node:	St Peter Port South
Km. to Nearest Node:	37.43
Mask Area (Hectares):	14.7
Sightings (Main Analysis):	6085

LANDMARK LOCATION



Longitude: 2° 2" 9' W
Latitude: 49° 15" 6' N

Source: Esri, DigitalGlobe, GeoEye, Earthstar Geographics, CNES/Airbus DS, USDA, USGS, AeroGRID, IGN, and the GIS User Community

LANDMARK MASK



Bellevue

Identified as natural prominence.
Identified as site: No

Contextual Information:

Nearest Node:	Brest
Km. to Nearest Node:	28.59
Mask Area (Hectares):	20.39
Sightings (Main Analysis):	201

LANDMARK LOCATION



Longitude: 4° 4" 7' W
Latitude: 48° 16" 9' N

Source: Esri, DigitalGlobe, GeoEye, Earthstar Geographics, CNES/Airbus DS, USDA, USGS, AeroGRID, IGN, and the GIS User Community

LANDMARK MASK



Bembridge Down

Identified as natural prominence.
Identified as site: No

Contextual Information:

Nearest Node:	Christchurch
Km. to Nearest Node:	43.24
Mask Area (Hectares):	55.75
Sightings (Main Analysis):	420

LANDMARK LOCATION



Longitude: 1° 1" 24' W
Latitude: 50° 40" 7' N

Source: Esri, DigitalGlobe, GeoEye, Earthstar Geographics, CNES/Airbus DS, USDA, USGS, AeroGRID, IGN, and the GIS User Community

LANDMARK MASK



Berry Cliff Camp

Identified as natural prominence.
Identified as site: Yes

Contextual Information:

Nearest Node:	Sidmouth
Km. to Nearest Node:	4.31
Mask Area (Hectares):	117.65
Sightings (Main Analysis):	12384

LANDMARK LOCATION



Longitude: 3° 3" 28' W
Latitude: 50° 41" 18' N

Source: Esri, DigitalGlobe, GeoEye, Earthstar Geographics, CNES/Airbus DS, USDA, USGS, AeroGRID, IGN, and the GIS User Community

LANDMARK MASK



Bigbury On Sea

Identified as natural prominence.
Identified as site: No

Contextual Information:

Nearest Node:	Bigbury Bay
Km. to Nearest Node:	3.98
Mask Area (Hectares):	28.96
Sightings (Main Analysis):	11100

LANDMARK LOCATION



Longitude: 3° 3" 4' W
Latitude: 50° 17" 18' N

Source: Esri, DigitalGlobe, GeoEye, Earthstar Geographics, CNES/Airbus DS, USDA, USGS, AeroGRID, IGN, and the GIS User Community

LANDMARK MASK



Bindon Hill

Identified as natural prominence.
Identified as site: Yes

Contextual Information:

Nearest Node:	Lulworth Cove
Km. to Nearest Node:	2.64
Mask Area (Hectares):	184.33
Sightings (Main Analysis):	7230

LANDMARK LOCATION



Longitude: 2° 2" 2' W
Latitude: 50° 37" 11' N

Source: Esri, DigitalGlobe, GeoEye, Earthstar Geographics, CNES/Airbus DS, USDA, USGS, AeroGRID, IGN, and the GIS User Community

LANDMARK MASK



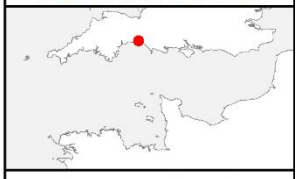
Black Ven

Identified as natural prominence.
Identified as site: No

Contextual Information:

Nearest Node:	Seaton
Km. to Nearest Node:	10.93
Mask Area (Hectares):	70.5
Sightings (Main Analysis):	7244

LANDMARK LOCATION



Longitude: 2° 2" 19' W
Latitude: 50° 44" 15' N

Source: Esri, DigitalGlobe, GeoEye, Earthstar Geographics, CNES/Airbus DS, USDA, USGS, AeroGRID, IGN, and the GIS User Community

LANDMARK MASK



Bodigga

Identified as natural prominence.
Identified as site: No

Contextual Information:

Nearest Node:	Porthallow
Km. to Nearest Node:	7.59
Mask Area (Hectares):	58.09
Sightings (Main Analysis):	9933

LANDMARK LOCATION



Longitude: 4° 4" 11' W
Latitude: 50° 22" 1' N

Source: Esri, DigitalGlobe, GeoEye, Earthstar Geographics, CNES/Airbus DS, USDA, USGS, AeroGRID, IGN, and the GIS User Community

LANDMARK MASK



Bolberry Down

Identified as natural prominence.
Identified as site: No

Contextual Information:

Nearest Node:	Bigbury Bay
Km. to Nearest Node:	3.32
Mask Area (Hectares):	54.26
Sightings (Main Analysis):	16347

LANDMARK LOCATION



Longitude: 3° 3" 24' W
Latitude: 50° 14" 0' N

Source: Esri, DigitalGlobe, GeoEye, Earthstar Geographics, CNES/Airbus DS, USDA, USGS, AeroGRID, IGN, and the GIS User Community

LANDMARK MASK



Bollowall Cliff

Identified as natural prominence.
Identified as site: No

Contextual Information:

Nearest Node:	Penzance
Km. to Nearest Node:	13.93
Mask Area (Hectares):	12.83
Sightings (Main Analysis):	229

LANDMARK LOCATION



Longitude: 5° 5" 6' W
Latitude: 50° 7" 23' N

Source: Esri, DigitalGlobe, GeoEye, Earthstar Geographics, CNES/Airbus DS, USDA, USGS, AeroGRID, IGN, and the GIS User Community

LANDMARK MASK



Bolt Head

Identified as natural prominence.
Identified as site: No

Contextual Information:

Nearest Node:	Salcombe
Km. to Nearest Node:	2.13
Mask Area (Hectares):	32.37
Sightings (Main Analysis):	16809

LANDMARK LOCATION



Longitude: 3° 3" 30' W
Latitude: 50° 13" 12' N

Source: Esri, DigitalGlobe, GeoEye, Earthstar Geographics, CNES/Airbus DS, USDA, USGS, AeroGRID, IGN, and the GIS User Community

LANDMARK MASK



Boohay

Identified as natural prominence.
Identified as site: No

Contextual Information:

Nearest Node:	Dartmouth
Km. to Nearest Node:	5.37
Mask Area (Hectares):	46.05
Sightings (Main Analysis):	15297

LANDMARK LOCATION



Longitude: 3° 3" 14' W
Latitude: 50° 22" 5' N

Source: Esri, DigitalGlobe, GeoEye, Earthstar Geographics, CNES/Airbus DS, USDA, USGS, AeroGRID, IGN, and the GIS User Community

LANDMARK MASK



Bozomzeal

Identified as natural prominence.
Identified as site: No

Contextual Information:

Nearest Node:	Dartmouth
Km. to Nearest Node:	7.09
Mask Area (Hectares):	42.47
Sightings (Main Analysis):	8231

LANDMARK LOCATION



Longitude: 3° 3" 26' W
Latitude: 50° 22" 22' N

Source: Esri, DigitalGlobe, GeoEye, Earthstar Geographics, CNES/Airbus DS, USDA, USGS, AeroGRID, IGN, and the GIS User Community

LANDMARK MASK



Brecqhou

Identified as natural prominence.
Identified as site: No

Contextual Information:

Nearest Node:	St Peter Port South
Km. to Nearest Node:	8.81
Mask Area (Hectares):	12.75
Sightings (Main Analysis):	12379

LANDMARK LOCATION



Longitude: 2° 2" 15' W
Latitude: 49° 26" 4' N

Source: Esri, DigitalGlobe, GeoEye, Earthstar Geographics, CNES/Airbus DS, USDA, USGS, AeroGRID, IGN, and the GIS User Community

LANDMARK MASK



Broadgates

Identified as natural prominence.
Identified as site: No

Contextual Information:

Nearest Node:	Dartmouth
Km. to Nearest Node:	10.29
Mask Area (Hectares):	27.63
Sightings (Main Analysis):	4040

LANDMARK LOCATION



Longitude: 3° 3" 3' W
Latitude: 50° 23" 17' N

Source: Esri, DigitalGlobe, GeoEye, Earthstar Geographics, CNES/Airbus DS, USDA, USGS, AeroGRID, IGN, and the GIS User Community

LANDMARK MASK



Brodrugan Barton

Identified as natural prominence.
Identified as site: No

Contextual Information:

Nearest Node:	Mevagissey
Km. to Nearest Node:	1.65
Mask Area (Hectares):	10.41
Sightings (Main Analysis):	9383

LANDMARK LOCATION



Longitude: 4° 4" 24' W
Latitude: 50° 15" 9' N

Source: Esri, DigitalGlobe, GeoEye, Earthstar Geographics, CNES/Airbus DS, USDA, USGS, AeroGRID, IGN, and the GIS User Community

LANDMARK MASK



Brownstone

Identified as natural prominence.
Identified as site: No

Contextual Information:

Nearest Node:	Dartmouth
Km. to Nearest Node:	2.21
Mask Area (Hectares):	76.61
Sightings (Main Analysis):	15300

LANDMARK LOCATION



Longitude: 3° 3" 30' W
Latitude: 50° 20" 29' N

Source: Esri, DigitalGlobe, GeoEye, Earthstar Geographics, CNES/Airbus DS, USDA, USGS, AeroGRID, IGN, and the GIS User Community

LANDMARK MASK



Budleigh Salterton

Identified as natural prominence.
Identified as site: No

Contextual Information:

Nearest Node:	Budleigh Salterton
Km. to Nearest Node:	3.41
Mask Area (Hectares):	23.77
Sightings (Main Analysis):	13187

LANDMARK LOCATION



Longitude: 3° 3" 3' W
Latitude: 50° 37" 24' N

Source: Esri, DigitalGlobe, GeoEye, Earthstar Geographics, CNES/Airbus DS, USDA, USGS, AeroGRID, IGN, and the GIS User Community

LANDMARK MASK



Burhou

Identified as natural prominence.
Identified as site: No

Contextual Information:

Nearest Node:	St Peter Port North
Km. to Nearest Node:	27.81
Mask Area (Hectares):	57.55
Sightings (Main Analysis):	16607

LANDMARK LOCATION



Longitude: 2° 2" 16' W
Latitude: 49° 44" 11' N

Source: Esri, DigitalGlobe, GeoEye, Earthstar Geographics, CNES/Airbus DS, USDA, USGS, AeroGRID, IGN, and the GIS User Community

LANDMARK MASK



Butte De Houlgate

Identified as natural prominence.
Identified as site: No

Contextual Information:

Nearest Node:	Nacqueville
Km. to Nearest Node:	122.68
Mask Area (Hectares):	39.04
Sightings (Main Analysis):	5

LANDMARK LOCATION



Longitude: 0° 0" 15' W
Latitude: 49° 18" 13' N

Source: Esri, DigitalGlobe, GeoEye, Earthstar Geographics, CNES/Airbus DS, USDA, USGS, AeroGRID, IGN, and the GIS User Community

LANDMARK MASK



Caerhays Barton

Identified as natural prominence.
Identified as site: No

Contextual Information:

Nearest Node:	Mevagissey
Km. to Nearest Node:	7.39
Mask Area (Hectares):	15.8
Sightings (Main Analysis):	5133

LANDMARK LOCATION



Longitude: 4° 4" 20' W
Latitude: 50° 14" 18' N

Source: Esri, DigitalGlobe, GeoEye, Earthstar Geographics, CNES/Airbus DS, USDA, USGS, AeroGRID, IGN, and the GIS User Community

LANDMARK MASK



Cap Blanc Nez

Identified as natural prominence.
Identified as site: No

Contextual Information:

Nearest Node:	Christchurch
Km. to Nearest Node:	243.06
Mask Area (Hectares):	26.55
Sightings (Main Analysis):	0

LANDMARK LOCATION



Longitude: 1° 1" 18' E
Latitude: 50° 56" 27' N

Source: Esri, DigitalGlobe, GeoEye, Earthstar Geographics, CNES/Airbus DS, USDA, USGS, AeroGRID, IGN, and the GIS User Community

LANDMARK MASK



Carn Irish

Identified as natural prominence.
Identified as site: No

Contextual Information:

Nearest Node:	Penzance
Km. to Nearest Node:	65.69
Mask Area (Hectares):	31.37
Sightings (Main Analysis):	138

LANDMARK LOCATION



Longitude: 6° 6" 29' W
Latitude: 49° 54" 13' N

Source: Esri, DigitalGlobe, GeoEye, Earthstar Geographics, CNES/Airbus DS, USDA, USGS, AeroGRID, IGN, and the GIS User Community

LANDMARK MASK



Castle Head

Identified as natural prominence.
Identified as site: Yes

Contextual Information:

Nearest Node:	Dartmouth
Km. to Nearest Node:	3.24
Mask Area (Hectares):	66.11
Sightings (Main Analysis):	11673

LANDMARK LOCATION



Longitude: 3° 3" 16' W
Latitude: 50° 20" 18' N

Source: Esri, DigitalGlobe, GeoEye, Earthstar Geographics, CNES/Airbus DS, USDA, USGS, AeroGRID, IGN, and the GIS User Community

LANDMARK MASK



Castletown

Identified as natural prominence.
Identified as site: No

Contextual Information:

Nearest Node:	Portland
Km. to Nearest Node:	0.88
Mask Area (Hectares):	24.22
Sightings (Main Analysis):	5121

LANDMARK LOCATION



Longitude: 2° 2" 28' W
Latitude: 50° 35" 24' N

Source: Esri, DigitalGlobe, GeoEye, Earthstar Geographics, CNES/Airbus DS, USDA, USGS, AeroGRID, IGN, and the GIS User Community

LANDMARK MASK



Castletown 1

Identified as natural prominence.
Identified as site: No

Contextual Information:

Nearest Node:	Portland
Km. to Nearest Node:	0.58
Mask Area (Hectares):	30.06
Sightings (Main Analysis):	6330

LANDMARK LOCATION



Longitude: 2° 2" 6' W
Latitude: 50° 35" 19' N

Source: Esri, DigitalGlobe, GeoEye, Earthstar Geographics, CNES/Airbus DS, USDA, USGS, AeroGRID, IGN, and the GIS User Community

LANDMARK MASK



Church Hougham

Identified as natural prominence.
Identified as site: No

Contextual Information:

Nearest Node:	Christchurch
Km. to Nearest Node:	209.57
Mask Area (Hectares):	280.77
Sightings (Main Analysis):	0

LANDMARK LOCATION



Longitude: 1° 1" 14' E
Latitude: 51° 6" 25' N

Source: Esri, DigitalGlobe, GeoEye, Earthstar Geographics, CNES/Airbus DS, USDA, USGS, AeroGRID, IGN, and the GIS User Community

LANDMARK MASK



Cleave

Identified as natural prominence.
Identified as site: No

Contextual Information:

Nearest Node:	Fowey
Km. to Nearest Node:	64.14
Mask Area (Hectares):	46.04
Sightings (Main Analysis):	0

LANDMARK LOCATION



Longitude: 4° 4" 27' W
Latitude: 50° 53" 6' N

Source: Esri, DigitalGlobe, GeoEye, Earthstar Geographics, CNES/Airbus DS, USDA, USGS, AeroGRID, IGN, and the GIS User Community

LANDMARK MASK



Cligga Head

Identified as natural prominence.
Identified as site: No

Contextual Information:

Nearest Node:	Falmouth
Km. to Nearest Node:	25.08
Mask Area (Hectares):	16.56
Sightings (Main Analysis):	12

LANDMARK LOCATION



Longitude: 5° 5" 29' W
Latitude: 50° 20" 20' N

Source: Esri, DigitalGlobe, GeoEye, Earthstar Geographics, CNES/Airbus DS, USDA, USGS, AeroGRID, IGN, and the GIS User Community

LANDMARK MASK



Clonque

Identified as natural prominence.
Identified as site: No

Contextual Information:

Nearest Node:	St Peter Port North
Km. to Nearest Node:	27.48
Mask Area (Hectares):	21.37
Sightings (Main Analysis):	15651

LANDMARK LOCATION



Longitude: 2° 2" 15' W
Latitude: 49° 43" 29' N

Source: Esri, DigitalGlobe, GeoEye, Earthstar Geographics, CNES/Airbus DS, USDA, USGS, AeroGRID, IGN, and the GIS User Community

LANDMARK MASK



Coad Trez Bihan

Identified as natural prominence.
Identified as site: No

Contextual Information:

Nearest Node:	Brest
Km. to Nearest Node:	18.11
Mask Area (Hectares):	24.02
Sightings (Main Analysis):	278

LANDMARK LOCATION



Longitude: 4° 4" 3' W
Latitude: 48° 13" 25' N

Source: Esri, DigitalGlobe, GeoEye, Earthstar Geographics, CNES/Airbus DS, USDA, USGS, AeroGRID, IGN, and the GIS User Community

LANDMARK MASK



Collytown

Identified as natural prominence.
Identified as site: No

Contextual Information:

Nearest Node:	Plymouth
Km. to Nearest Node:	15.83
Mask Area (Hectares):	11.91
Sightings (Main Analysis):	1035

LANDMARK LOCATION



Longitude: 4° 4" 28' W
Latitude: 50° 28" 2' N

Source: Esri, DigitalGlobe, GeoEye, Earthstar Geographics, CNES/Airbus DS, USDA, USGS, AeroGRID, IGN, and the GIS User Community

LANDMARK MASK



Compton Down

Identified as natural prominence.
Identified as site: No

Contextual Information:

Nearest Node:	Christchurch
Km. to Nearest Node:	17.13
Mask Area (Hectares):	105.58
Sightings (Main Analysis):	3345

LANDMARK LOCATION



Longitude: 1° 1" 17' W
Latitude: 50° 40" 7' N

Source: Esri, DigitalGlobe, GeoEye, Earthstar Geographics, CNES/Airbus DS, USDA, USGS, AeroGRID, IGN, and the GIS User Community

LANDMARK MASK



Crafthole

Identified as natural prominence.
Identified as site: No

Contextual Information:

Nearest Node:	Plymouth
Km. to Nearest Node:	10.09
Mask Area (Hectares):	10.71
Sightings (Main Analysis):	9380

LANDMARK LOCATION



Longitude: 4° 4" 21' W
Latitude: 50° 22" 18' N

Source: Esri, DigitalGlobe, GeoEye, Earthstar Geographics, CNES/Airbus DS, USDA, USGS, AeroGRID, IGN, and the GIS User Community

LANDMARK MASK



Criel Sur Mer

Identified as natural prominence.
Identified as site: No

Contextual Information:

Nearest Node:	Nacqueville
Km. to Nearest Node:	216.4
Mask Area (Hectares):	12.02
Sightings (Main Analysis):	0

LANDMARK LOCATION



Longitude: 1° 1" 10' E
Latitude: 50° 1" 8' N

Source: Esri, DigitalGlobe, GeoEye, Earthstar Geographics, CNES/Airbus DS, USDA, USGS, AeroGRID, IGN, and the GIS User Community

LANDMARK MASK



Dartmouth

Identified as natural prominence.
Identified as site: No

Contextual Information:

Nearest Node:	Dartmouth
Km. to Nearest Node:	4.25
Mask Area (Hectares):	36.45
Sightings (Main Analysis):	11661

LANDMARK LOCATION



Longitude: 3° 3" 1' W
Latitude: 50° 21" 20' N

Source: Esri, DigitalGlobe, GeoEye, Earthstar Geographics, CNES/Airbus DS, USDA, USGS, AeroGRID, IGN, and the GIS User Community

LANDMARK MASK



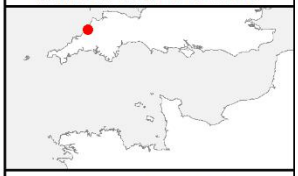
Dizzard

Identified as natural prominence.
Identified as site: No

Contextual Information:

Nearest Node:	Fowey
Km. to Nearest Node:	50.18
Mask Area (Hectares):	48.87
Sightings (Main Analysis):	0

LANDMARK LOCATION



Longitude: 4° 4" 9' W
Latitude: 50° 46" 23' N

Source: Esri, DigitalGlobe, GeoEye, Earthstar Geographics, CNES/Airbus DS, USDA, USGS, AeroGRID, IGN, and the GIS User Community

LANDMARK MASK



Dodman Castle

Identified as natural prominence.
Identified as site: Yes

Contextual Information:

Nearest Node:	Mevagissey
Km. to Nearest Node:	3.62
Mask Area (Hectares):	127.12
Sightings (Main Analysis):	10920

LANDMARK LOCATION



Longitude: 4° 4" 2' W
Latitude: 50° 14" 22' N

Source: Esri, DigitalGlobe, GeoEye, Earthstar Geographics, CNES/Airbus DS, USDA, USGS, AeroGRID, IGN, and the GIS User Community

LANDMARK MASK



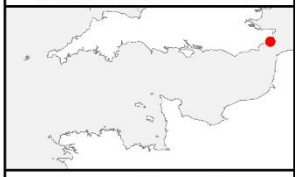
Dover Castle

Identified as natural prominence.
Identified as site: Yes

Contextual Information:

Nearest Node:	Christchurch
Km. to Nearest Node:	218.92
Mask Area (Hectares):	47.34
Sightings (Main Analysis):	0

LANDMARK LOCATION



Longitude: 1° 1" 22' E
Latitude: 51° 8" 17' N

Source: Esri, DigitalGlobe, GeoEye, Earthstar Geographics, CNES/Airbus DS, USDA, USGS, AeroGRID, IGN, and the GIS User Community

LANDMARK MASK



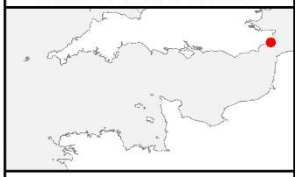
Dover Harbour

Identified as natural prominence.
Identified as site: No

Contextual Information:

Nearest Node:	Christchurch
Km. to Nearest Node:	220.46
Mask Area (Hectares):	15.54
Sightings (Main Analysis):	0

LANDMARK LOCATION



Longitude: 1° 1" 29' E
Latitude: 51° 8" 1' N

Source: Esri, DigitalGlobe, GeoEye, Earthstar Geographics, CNES/Airbus DS, USDA, USGS, AeroGRID, IGN, and the GIS User Community

LANDMARK MASK



Down End

Identified as natural prominence.
Identified as site: No

Contextual Information:

Nearest Node:	Dartmouth
Km. to Nearest Node:	3.85
Mask Area (Hectares):	26.17
Sightings (Main Analysis):	10460

LANDMARK LOCATION



Longitude: 3° 3" 23' W
Latitude: 50° 21" 0' N

Source: Esri, DigitalGlobe, GeoEye, Earthstar Geographics, CNES/Airbus DS, USDA, USGS, AeroGRID, IGN, and the GIS User Community

LANDMARK MASK



Down Thomas

Identified as natural prominence.
Identified as site: No

Contextual Information:

Nearest Node:	Plymouth
Km. to Nearest Node:	3.16
Mask Area (Hectares):	40.66
Sightings (Main Analysis):	8872

LANDMARK LOCATION



Longitude: 4° 4" 20' W
Latitude: 50° 20" 29' N

Source: Esri, DigitalGlobe, GeoEye, Earthstar Geographics, CNES/Airbus DS, USDA, USGS, AeroGRID, IGN, and the GIS User Community

LANDMARK MASK



Dunscombe

Identified as natural prominence.
Identified as site: No

Contextual Information:

Nearest Node:	Sidmouth
Km. to Nearest Node:	3.77
Mask Area (Hectares):	10.07
Sightings (Main Analysis):	12045

LANDMARK LOCATION



Longitude: 3° 3" 30' W
Latitude: 50° 41" 15' N

Source: Esri, DigitalGlobe, GeoEye, Earthstar Geographics, CNES/Airbus DS, USDA, USGS, AeroGRID, IGN, and the GIS User Community

LANDMARK MASK



East Hill

Identified as natural prominence.
Identified as site: Yes

Contextual Information:

Nearest Node:	Christchurch
Km. to Nearest Node:	164.47
Mask Area (Hectares):	34.99
Sightings (Main Analysis):	0

LANDMARK LOCATION



Longitude: 0° 0" 3' E
Latitude: 50° 51" 30' N

Source: Esri, DigitalGlobe, GeoEye, Earthstar Geographics, CNES/Airbus DS, USDA, USGS, AeroGRID, IGN, and the GIS User Community

LANDMARK MASK



East Portlemouth

Identified as natural prominence.
Identified as site: No

Contextual Information:

Nearest Node:	Salcombe
Km. to Nearest Node:	3.88
Mask Area (Hectares):	19.89
Sightings (Main Analysis):	10887

LANDMARK LOCATION



Longitude: 3° 3" 26' W
Latitude: 50° 14" 9' N

Source: Esri, DigitalGlobe, GeoEye, Earthstar Geographics, CNES/Airbus DS, USDA, USGS, AeroGRID, IGN, and the GIS User Community

LANDMARK MASK



Ecole Decalade De Pen Hir

Identified as natural prominence.
Identified as site: No

Contextual Information:

Nearest Node:	Brest
Km. to Nearest Node:	7.43
Mask Area (Hectares):	31.41
Sightings (Main Analysis):	2118

LANDMARK LOCATION



Longitude: 4° 4" 17' W
Latitude: 48° 15" 29' N

Source: Esri, DigitalGlobe, GeoEye, Earthstar Geographics, CNES/Airbus DS, USDA, USGS, AeroGRID, IGN, and the GIS User Community

LANDMARK MASK



Egmont Point

Identified as natural prominence.
Identified as site: No

Contextual Information:

Nearest Node:	Kimmeridge Bay
Km. to Nearest Node:	5.19
Mask Area (Hectares):	28.58
Sightings (Main Analysis):	7192

LANDMARK LOCATION



Longitude: 2° 2" 16' W
Latitude: 50° 36" 7' N

Source: Esri, DigitalGlobe, GeoEye, Earthstar Geographics, CNES/Airbus DS, USDA, USGS, AeroGRID, IGN, and the GIS User Community

LANDMARK MASK



Egypt

Identified as natural prominence.
Identified as site: No

Contextual Information:

Nearest Node:	St Peter Port South
Km. to Nearest Node:	38.49
Mask Area (Hectares):	11.63
Sightings (Main Analysis):	6624

LANDMARK LOCATION



Longitude: 2° 2" 24' W
Latitude: 49° 15" 17' N

Source: Esri, DigitalGlobe, GeoEye, Earthstar Geographics, CNES/Airbus DS, USDA, USGS, AeroGRID, IGN, and the GIS User Community

LANDMARK MASK



Elmscott

Identified as natural prominence.
Identified as site: No

Contextual Information:

Nearest Node:	Porthallow
Km. to Nearest Node:	73.72
Mask Area (Hectares):	19.79
Sightings (Main Analysis):	0

LANDMARK LOCATION



Longitude: 4° 4" 11' W
Latitude: 50° 58" 15' N

Source: Esri, DigitalGlobe, GeoEye, Earthstar Geographics, CNES/Airbus DS, USDA, USGS, AeroGRID, IGN, and the GIS User Community

LANDMARK MASK



Embury Beacon

Identified as natural prominence.
Identified as site: Yes

Contextual Information:

Nearest Node:	Fowey
Km. to Nearest Node:	70.37
Mask Area (Hectares):	121.28
Sightings (Main Analysis):	0

LANDMARK LOCATION



Longitude: 4° 4" 18' W
Latitude: 50° 57" 2' N

Source: Esri, DigitalGlobe, GeoEye, Earthstar Geographics, CNES/Airbus DS, USDA, USGS, AeroGRID, IGN, and the GIS User Community

LANDMARK MASK



Emmetts Hill

Identified as natural prominence.
Identified as site: No

Contextual Information:

Nearest Node:	Kimmeridge Bay
Km. to Nearest Node:	6.16
Mask Area (Hectares):	17.23
Sightings (Main Analysis):	7506

LANDMARK LOCATION



Longitude: 2° 2" 29' W
Latitude: 50° 35" 16' N

Source: Esri, DigitalGlobe, GeoEye, Earthstar Geographics, CNES/Airbus DS, USDA, USGS, AeroGRID, IGN, and the GIS User Community

LANDMARK MASK



Eperquerie

Identified as natural prominence.
Identified as site: No

Contextual Information:

Nearest Node:	St Peter Port South
Km. to Nearest Node:	10.35
Mask Area (Hectares):	29.52
Sightings (Main Analysis):	13336

LANDMARK LOCATION



Longitude: 2° 2" 20' W
Latitude: 49° 27" 28' N

Source: Esri, DigitalGlobe, GeoEye, Earthstar Geographics, CNES/Airbus DS, USDA, USGS, AeroGRID, IGN, and the GIS User Community

LANDMARK MASK



Escalls Cliff

Identified as natural prominence.
Identified as site: No

Contextual Information:

Nearest Node:	Penzance
Km. to Nearest Node:	13.17
Mask Area (Hectares):	10.69
Sightings (Main Analysis):	160

LANDMARK LOCATION



Longitude: 5° 5" 24' W
Latitude: 50° 6" 4' N

Source: Esri, DigitalGlobe, GeoEye, Earthstar Geographics, CNES/Airbus DS, USDA, USGS, AeroGRID, IGN, and the GIS User Community

LANDMARK MASK



Exmansworthy

Identified as natural prominence.
Identified as site: No

Contextual Information:

Nearest Node:	Porthallow
Km. to Nearest Node:	78.88
Mask Area (Hectares):	119.7
Sightings (Main Analysis):	0

LANDMARK LOCATION



Longitude: 4° 4" 27' W
Latitude: 51° 1" 4' N

Source: Esri, DigitalGlobe, GeoEye, Earthstar Geographics, CNES/Airbus DS, USDA, USGS, AeroGRID, IGN, and the GIS User Community

LANDMARK MASK



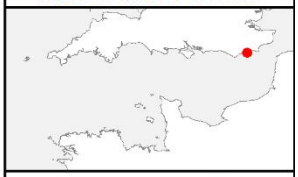
Fairlight Glen

Identified as natural prominence.
Identified as site: No

Contextual Information:

Nearest Node:	Christchurch
Km. to Nearest Node:	165.95
Mask Area (Hectares):	16.14
Sightings (Main Analysis):	0

LANDMARK LOCATION



Longitude: 0° 0" 14' E
Latitude: 50° 52" 12' N

Source: Esri, DigitalGlobe, GeoEye, Earthstar Geographics, CNES/Airbus DS, USDA, USGS, AeroGRID, IGN, and the GIS User Community

LANDMARK MASK



Firehills

Identified as natural prominence.
Identified as site: No

Contextual Information:

Nearest Node:	Christchurch
Km. to Nearest Node:	167.82
Mask Area (Hectares):	54.29
Sightings (Main Analysis):	0

LANDMARK LOCATION



Longitude: 0° 0" 16' E
Latitude: 50° 52" 25' N

Source: Esri, DigitalGlobe, GeoEye, Earthstar Geographics, CNES/Airbus DS, USDA, USGS, AeroGRID, IGN, and the GIS User Community

LANDMARK MASK



Flowers Barrow

Identified as natural prominence.
Identified as site: Yes

Contextual Information:

Nearest Node:	Kimmeridge Bay
Km. to Nearest Node:	3.94
Mask Area (Hectares):	241.92
Sightings (Main Analysis):	7730

LANDMARK LOCATION



Longitude: 2° 2" 16' W
Latitude: 50° 38" 7' N

Source: Esri, DigitalGlobe, GeoEye, Earthstar Geographics, CNES/Airbus DS, USDA, USGS, AeroGRID, IGN, and the GIS User Community

LANDMARK MASK



Fontaine Saint Mathieu

Identified as natural prominence.
Identified as site: No

Contextual Information:

Nearest Node:	Brest
Km. to Nearest Node:	30.6
Mask Area (Hectares):	16.33
Sightings (Main Analysis):	2048

LANDMARK LOCATION



Longitude: 4° 4" 15' W
Latitude: 48° 4" 15' N

Source: Esri, DigitalGlobe, GeoEye, Earthstar Geographics, CNES/Airbus DS, USDA, USGS, AeroGRID, IGN, and the GIS User Community

LANDMARK MASK



Fortuneswell

Identified as natural prominence.
Identified as site: No

Contextual Information:

Nearest Node:	Portland
Km. to Nearest Node:	2.88
Mask Area (Hectares):	48.0
Sightings (Main Analysis):	11376

LANDMARK LOCATION



Longitude: 2° 2" 4' W
Latitude: 50° 34" 19' N

Source: Esri, DigitalGlobe, GeoEye, Earthstar Geographics, CNES/Airbus DS, USDA, USGS, AeroGRID, IGN, and the GIS User Community

LANDMARK MASK



Garrans Point

Identified as natural prominence.
Identified as site: No

Contextual Information:

Nearest Node:	Mevagissey
Km. to Nearest Node:	4.01
Mask Area (Hectares):	11.87
Sightings (Main Analysis):	8131

LANDMARK LOCATION



Longitude: 4° 4" 25' W
Latitude: 50° 18" 14' N

Source: Esri, DigitalGlobe, GeoEye, Earthstar Geographics, CNES/Airbus DS, USDA, USGS, AeroGRID, IGN, and the GIS User Community

LANDMARK MASK



Giant Rock

Identified as natural prominence.
Identified as site: No

Contextual Information:

Nearest Node:	Teignmouth
Km. to Nearest Node:	4.75
Mask Area (Hectares):	26.0
Sightings (Main Analysis):	12082

LANDMARK LOCATION



Longitude: 3° 3" 25' W
Latitude: 50° 30" 0' N

Source: Esri, DigitalGlobe, GeoEye, Earthstar Geographics, CNES/Airbus DS, USDA, USGS, AeroGRID, IGN, and the GIS User Community

LANDMARK MASK



Giggen Cove

Identified as natural prominence.
Identified as site: No

Contextual Information:

Nearest Node:	Porthallow
Km. to Nearest Node:	3.07
Mask Area (Hectares):	37.43
Sightings (Main Analysis):	12293

LANDMARK LOCATION



Longitude: 4° 4" 25' W
Latitude: 50° 20" 1' N

Source: Esri, DigitalGlobe, GeoEye, Earthstar Geographics, CNES/Airbus DS, USDA, USGS, AeroGRID, IGN, and the GIS User Community

LANDMARK MASK



Godrevy Towans

Identified as natural prominence.
Identified as site: No

Contextual Information:

Nearest Node:	Penzance
Km. to Nearest Node:	17.86
Mask Area (Hectares):	10.02
Sightings (Main Analysis):	103

LANDMARK LOCATION



Longitude: 5° 5" 15' W
Latitude: 50° 14" 28' N

Source: Esri, DigitalGlobe, GeoEye, Earthstar Geographics, CNES/Airbus DS, USDA, USGS, AeroGRID, IGN, and the GIS User Community

LANDMARK MASK



Golden Cap

Identified as natural prominence.
Identified as site: No

Contextual Information:

Nearest Node:	Seaton
Km. to Nearest Node:	15.43
Mask Area (Hectares):	71.24
Sightings (Main Analysis):	9459

LANDMARK LOCATION



Longitude: 2° 2" 17' W
Latitude: 50° 44" 15' N

Source: Esri, DigitalGlobe, GeoEye, Earthstar Geographics, CNES/Airbus DS, USDA, USGS, AeroGRID, IGN, and the GIS User Community

LANDMARK MASK



Gore Down

Identified as natural prominence.
Identified as site: No

Contextual Information:

Nearest Node:	Christchurch
Km. to Nearest Node:	32.68
Mask Area (Hectares):	93.59
Sightings (Main Analysis):	3233

LANDMARK LOCATION



Longitude: 1° 1" 14' W
Latitude: 50° 35" 19' N

Source: Esri, DigitalGlobe, GeoEye, Earthstar Geographics, CNES/Airbus DS, USDA, USGS, AeroGRID, IGN, and the GIS User Community

LANDMARK MASK



Goret

Identified as natural prominence.
Identified as site: No

Contextual Information:

Nearest Node:	Brest
Km. to Nearest Node:	61.3
Mask Area (Hectares):	22.56
Sightings (Main Analysis):	0

LANDMARK LOCATION



Longitude: 4° 4" 25' W
Latitude: 47° 48" 23' N

Source: Esri, DigitalGlobe, GeoEye, Earthstar Geographics, CNES/Airbus DS, USDA, USGS, AeroGRID, IGN, and the GIS User Community

LANDMARK MASK



Gorreker

Identified as natural prominence.
Identified as site: No

Contextual Information:

Nearest Node:	Brest
Km. to Nearest Node:	22.98
Mask Area (Hectares):	32.5
Sightings (Main Analysis):	67

LANDMARK LOCATION



Longitude: 4° 4" 17' W
Latitude: 48° 18" 27' N

Source: Esri, DigitalGlobe, GeoEye, Earthstar Geographics, CNES/Airbus DS, USDA, USGS, AeroGRID, IGN, and the GIS User Community

LANDMARK MASK



Grande Île 1

Identified as natural prominence.
Identified as site: No

Contextual Information:

Nearest Node:	Saint Malo
Km. to Nearest Node:	29.09
Mask Area (Hectares):	12.74
Sightings (Main Analysis):	3114

LANDMARK LOCATION



Longitude: 1° 1" 10' W
Latitude: 48° 53" 23' N

Source: Esri, DigitalGlobe, GeoEye, Earthstar Geographics, CNES/Airbus DS, USDA, USGS, AeroGRID, IGN, and the GIS User Community

LANDMARK MASK



Grande Île 2

Identified as natural prominence.
Identified as site: No

Contextual Information:

Nearest Node:	Saint Malo
Km. to Nearest Node:	25.87
Mask Area (Hectares):	47.32
Sightings (Main Analysis):	4986

LANDMARK LOCATION



Longitude: 1° 1" 9' W
Latitude: 48° 53" 4' N

Source: Esri, DigitalGlobe, GeoEye, Earthstar Geographics, CNES/Airbus DS, USDA, USGS, AeroGRID, IGN, and the GIS User Community

LANDMARK MASK



Grande Île 3

Identified as natural prominence.
Identified as site: No

Contextual Information:

Nearest Node:	Saint Malo
Km. to Nearest Node:	28.27
Mask Area (Hectares):	13.96
Sightings (Main Analysis):	4092

LANDMARK LOCATION



Longitude: 1° 1" 13' W
Latitude: 48° 53" 20' N

Source: Esri, DigitalGlobe, GeoEye, Earthstar Geographics, CNES/Airbus DS, USDA, USGS, AeroGRID, IGN, and the GIS User Community

LANDMARK MASK



Grande Île 4

Identified as natural prominence.
Identified as site: No

Contextual Information:

Nearest Node:	Saint Malo
Km. to Nearest Node:	28.97
Mask Area (Hectares):	27.62
Sightings (Main Analysis):	3957

LANDMARK LOCATION



Longitude: 1° 1" 6' W
Latitude: 48° 52" 22' N

Source: Esri, DigitalGlobe, GeoEye, Earthstar Geographics, CNES/Airbus DS, USDA, USGS, AeroGRID, IGN, and the GIS User Community

LANDMARK MASK



Grande Île 5

Identified as natural prominence.
Identified as site: No

Contextual Information:

Nearest Node:	Saint Malo
Km. to Nearest Node:	28.74
Mask Area (Hectares):	11.23
Sightings (Main Analysis):	4593

LANDMARK LOCATION



Longitude: 1° 1" 23' W
Latitude: 48° 54" 20' N

Source: Esri, DigitalGlobe, GeoEye, Earthstar Geographics, CNES/Airbus DS, USDA, USGS, AeroGRID, IGN, and the GIS User Community

LANDMARK MASK



Great Arthur

Identified as natural prominence.
Identified as site: No

Contextual Information:

Nearest Node:	Penzance
Km. to Nearest Node:	56.57
Mask Area (Hectares):	33.04
Sightings (Main Analysis):	615

LANDMARK LOCATION



Longitude: 6° 6" 4' W
Latitude: 49° 57" 17' N

Source: Esri, DigitalGlobe, GeoEye, Earthstar Geographics, CNES/Airbus DS, USDA, USGS, AeroGRID, IGN, and the GIS User Community

LANDMARK MASK



Great Ganilly

Identified as natural prominence.
Identified as site: No

Contextual Information:

Nearest Node:	Penzance
Km. to Nearest Node:	55.78
Mask Area (Hectares):	21.37
Sightings (Main Analysis):	640

LANDMARK LOCATION



Longitude: 6° 6" 23' W
Latitude: 49° 57" 3' N

Source: Esri, DigitalGlobe, GeoEye, Earthstar Geographics, CNES/Airbus DS, USDA, USGS, AeroGRID, IGN, and the GIS User Community

LANDMARK MASK



Great Ganilly 1

Identified as natural prominence.
Identified as site: No

Contextual Information:

Nearest Node:	Penzance
Km. to Nearest Node:	55.21
Mask Area (Hectares):	13.74
Sightings (Main Analysis):	663

LANDMARK LOCATION



Longitude: 6° 6" 9' W
Latitude: 49° 57" 1' N

Source: Esri, DigitalGlobe, GeoEye, Earthstar Geographics, CNES/Airbus DS, USDA, USGS, AeroGRID, IGN, and the GIS User Community

LANDMARK MASK



Great Mewstone

Identified as natural prominence.
Identified as site: No

Contextual Information:

Nearest Node:	Mothecombe
Km. to Nearest Node:	1.66
Mask Area (Hectares):	12.79
Sightings (Main Analysis):	15883

LANDMARK LOCATION



Longitude: 4° 4" 25' W
Latitude: 50° 18" 23' N

Source: Esri, DigitalGlobe, GeoEye, Earthstar Geographics, CNES/Airbus DS, USDA, USGS, AeroGRID, IGN, and the GIS User Community

LANDMARK MASK



Greenaway

Identified as natural prominence.
Identified as site: No

Contextual Information:

Nearest Node:	Mevagissey
Km. to Nearest Node:	36.07
Mask Area (Hectares):	20.51
Sightings (Main Analysis):	0

LANDMARK LOCATION



Longitude: 4° 4" 4' W
Latitude: 50° 34" 0' N

Source: Esri, DigitalGlobe, GeoEye, Earthstar Geographics, CNES/Airbus DS, USDA, USGS, AeroGRID, IGN, and the GIS User Community

LANDMARK MASK



Grotte Du Charivari

Identified as natural prominence.
Identified as site: No

Contextual Information:

Nearest Node:	Brest
Km. to Nearest Node:	17.0
Mask Area (Hectares):	85.08
Sightings (Main Analysis):	1577

LANDMARK LOCATION



Longitude: 4° 4" 1' W
Latitude: 48° 10" 21' N

Source: Esri, DigitalGlobe, GeoEye, Earthstar Geographics, CNES/Airbus DS, USDA, USGS, AeroGRID, IGN, and the GIS User Community

LANDMARK MASK



Gwennap Head

Identified as natural prominence.
Identified as site: No

Contextual Information:

Nearest Node:	Penzance
Km. to Nearest Node:	13.86
Mask Area (Hectares):	11.54
Sightings (Main Analysis):	3244

LANDMARK LOCATION



Longitude: 5° 5" 18' W
Latitude: 50° 2" 14' N

Source: Esri, DigitalGlobe, GeoEye, Earthstar Geographics, CNES/Airbus DS, USDA, USGS, AeroGRID, IGN, and the GIS User Community

LANDMARK MASK



Hambury Tout

Identified as natural prominence.
Identified as site: No

Contextual Information:

Nearest Node:	Lulworth Cove
Km. to Nearest Node:	3.04
Mask Area (Hectares):	17.31
Sightings (Main Analysis):	7341

LANDMARK LOCATION



Longitude: 2° 2" 15' W
Latitude: 50° 37" 20' N

Source: Esri, DigitalGlobe, GeoEye, Earthstar Geographics, CNES/Airbus DS, USDA, USGS, AeroGRID, IGN, and the GIS User Community

LANDMARK MASK



Hameau Thiebot

Identified as natural prominence.
Identified as site: No

Contextual Information:

Nearest Node:	Nacqueville
Km. to Nearest Node:	17.51
Mask Area (Hectares):	25.05
Sightings (Main Analysis):	8555

LANDMARK LOCATION



Longitude: 1° 1" 10' W
Latitude: 49° 40" 6' N

Source: Esri, DigitalGlobe, GeoEye, Earthstar Geographics, CNES/Airbus DS, USDA, USGS, AeroGRID, IGN, and the GIS User Community

LANDMARK MASK



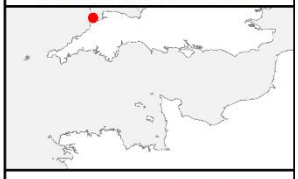
Hartland Point

Identified as natural prominence.
Identified as site: No

Contextual Information:

Nearest Node:	Porthallow
Km. to Nearest Node:	79.19
Mask Area (Hectares):	15.47
Sightings (Main Analysis):	0

LANDMARK LOCATION



Longitude: 4° 4" 22' W
Latitude: 51° 1" 6' N

Source: Esri, DigitalGlobe, GeoEye, Earthstar Geographics, CNES/Airbus DS, USDA, USGS, AeroGRID, IGN, and the GIS User Community

LANDMARK MASK



Headon Warren

Identified as natural prominence.
Identified as site: No

Contextual Information:

Nearest Node:	Christchurch
Km. to Nearest Node:	12.57
Mask Area (Hectares):	16.48
Sightings (Main Analysis):	2015

LANDMARK LOCATION



Longitude: 1° 1" 24' W
Latitude: 50° 40" 19' N

Source: Esri, DigitalGlobe, GeoEye, Earthstar Geographics, CNES/Airbus DS, USDA, USGS, AeroGRID, IGN, and the GIS User Community

LANDMARK MASK



Hendra

Identified as natural prominence.
Identified as site: No

Contextual Information:

Nearest Node:	Porthallow
Km. to Nearest Node:	11.25
Mask Area (Hectares):	48.07
Sightings (Main Analysis):	10549

LANDMARK LOCATION



Longitude: 4° 4" 22' W
Latitude: 50° 22" 11' N

Source: Esri, DigitalGlobe, GeoEye, Earthstar Geographics, CNES/Airbus DS, USDA, USGS, AeroGRID, IGN, and the GIS User Community

LANDMARK MASK



Herm

Identified as natural prominence.
Identified as site: No

Contextual Information:

Nearest Node:	St Peter Port South
Km. to Nearest Node:	4.04
Mask Area (Hectares):	28.39
Sightings (Main Analysis):	14953

LANDMARK LOCATION



Longitude: 2° 2" 11' W
Latitude: 49° 28" 6' N

Source: Esri, DigitalGlobe, GeoEye, Earthstar Geographics, CNES/Airbus DS, USDA, USGS, AeroGRID, IGN, and the GIS User Community

LANDMARK MASK



High Cliff

Identified as natural prominence.
Identified as site: No

Contextual Information:

Nearest Node:	Fowey
Km. to Nearest Node:	45.47
Mask Area (Hectares):	28.24
Sightings (Main Analysis):	0

LANDMARK LOCATION



Longitude: 4° 4" 7' W
Latitude: 50° 43" 6' N

Source: Esri, DigitalGlobe, GeoEye, Earthstar Geographics, CNES/Airbus DS, USDA, USGS, AeroGRID, IGN, and the GIS User Community

LANDMARK MASK



High Peak

Identified as natural prominence.
Identified as site: No

Contextual Information:

Nearest Node:	Sidmouth
Km. to Nearest Node:	3.62
Mask Area (Hectares):	22.97
Sightings (Main Analysis):	12330

LANDMARK LOCATION



Longitude: 3° 3" 17' W
Latitude: 50° 40" 0' N

Source: Esri, DigitalGlobe, GeoEye, Earthstar Geographics, CNES/Airbus DS, USDA, USGS, AeroGRID, IGN, and the GIS User Community

LANDMARK MASK



Higher Brixham

Identified as natural prominence.
Identified as site: No

Contextual Information:

Nearest Node:	Dartmouth
Km. to Nearest Node:	6.35
Mask Area (Hectares):	70.8
Sightings (Main Analysis):	15252

LANDMARK LOCATION



Longitude: 3° 3" 7' W
Latitude: 50° 23" 19' N

Source: Esri, DigitalGlobe, GeoEye, Earthstar Geographics, CNES/Airbus DS, USDA, USGS, AeroGRID, IGN, and the GIS User Community

LANDMARK MASK



Holly Park

Identified as natural prominence.
Identified as site: No

Contextual Information:

Nearest Node:	Plymouth
Km. to Nearest Node:	11.82
Mask Area (Hectares):	10.37
Sightings (Main Analysis):	1037

LANDMARK LOCATION



Longitude: 4° 4" 20' W
Latitude: 50° 26" 15' N

Source: Esri, DigitalGlobe, GeoEye, Earthstar Geographics, CNES/Airbus DS, USDA, USGS, AeroGRID, IGN, and the GIS User Community

LANDMARK MASK



Honfleur

Identified as natural prominence.
Identified as site: No

Contextual Information:

Nearest Node:	Nacqueville
Km. to Nearest Node:	138.94
Mask Area (Hectares):	21.42
Sightings (Main Analysis):	0

LANDMARK LOCATION



Longitude: 0° 0" 21' E
Latitude: 49° 25" 19' N

Source: Esri, DigitalGlobe, GeoEye, Earthstar Geographics, CNES/Airbus DS, USDA, USGS, AeroGRID, IGN, and the GIS User Community

LANDMARK MASK



Hook Bottom

Identified as natural prominence.
Identified as site: No

Contextual Information:

Nearest Node:	Dartmouth
Km. to Nearest Node:	8.0
Mask Area (Hectares):	8.31
Sightings (Main Analysis):	4926

LANDMARK LOCATION



Longitude: 3° 3" 7' W
Latitude: 50° 23" 0' N

Source: Esri, DigitalGlobe, GeoEye, Earthstar Geographics, CNES/Airbus DS, USDA, USGS, AeroGRID, IGN, and the GIS User Community

LANDMARK MASK



Hook Bottom 1

Identified as natural prominence.
Identified as site: No

Contextual Information:

Nearest Node:	Dartmouth
Km. to Nearest Node:	6.71
Mask Area (Hectares):	32.9
Sightings (Main Analysis):	8202

LANDMARK LOCATION



Longitude: 3° 3" 15' W
Latitude: 50° 23" 25' N

Source: Esri, DigitalGlobe, GeoEye, Earthstar Geographics, CNES/Airbus DS, USDA, USGS, AeroGRID, IGN, and the GIS User Community

LANDMARK MASK



Hooken Beach

Identified as natural prominence.
Identified as site: No

Contextual Information:

Nearest Node:	Seaton
Km. to Nearest Node:	3.6
Mask Area (Hectares):	91.5
Sightings (Main Analysis):	12472

LANDMARK LOCATION



Longitude: 3° 3" 28' W
Latitude: 50° 41" 24' N

Source: Esri, DigitalGlobe, GeoEye, Earthstar Geographics, CNES/Airbus DS, USDA, USGS, AeroGRID, IGN, and the GIS User Community

LANDMARK MASK



Hopes Nose

Identified as natural prominence.
Identified as site: No

Contextual Information:

Nearest Node:	Torquay
Km. to Nearest Node:	2.06
Mask Area (Hectares):	43.42
Sightings (Main Analysis):	14356

LANDMARK LOCATION



Longitude: 3° 3" 29' W
Latitude: 50° 28" 16' N

Source: Esri, DigitalGlobe, GeoEye, Earthstar Geographics, CNES/Airbus DS, USDA, USGS, AeroGRID, IGN, and the GIS User Community

LANDMARK MASK



Houles Du Debarcadere

Identified as natural prominence.
Identified as site: No

Contextual Information:

Nearest Node:	Saint Malo
Km. to Nearest Node:	20.78
Mask Area (Hectares):	27.54
Sightings (Main Analysis):	6960

LANDMARK LOCATION



Longitude: 2° 2" 1' W
Latitude: 48° 41" 1' N

Source: Esri, DigitalGlobe, GeoEye, Earthstar Geographics, CNES/Airbus DS, USDA, USGS, AeroGRID, IGN, and the GIS User Community

LANDMARK MASK



Humble Point

Identified as natural prominence.
Identified as site: No

Contextual Information:

Nearest Node:	Seaton
Km. to Nearest Node:	5.71
Mask Area (Hectares):	17.43
Sightings (Main Analysis):	11616

LANDMARK LOCATION



Longitude: 2° 2" 20' W
Latitude: 50° 43" 24' N

Source: Esri, DigitalGlobe, GeoEye, Earthstar Geographics, CNES/Airbus DS, USDA, USGS, AeroGRID, IGN, and the GIS User Community

LANDMARK MASK



Hurst Point

Identified as natural prominence.
Identified as site: No

Contextual Information:

Nearest Node:	Christchurch
Km. to Nearest Node:	12.2
Mask Area (Hectares):	31.79
Sightings (Main Analysis):	2311

LANDMARK LOCATION



Longitude: 1° 1" 9' W
Latitude: 50° 42" 27' N

Source: Esri, DigitalGlobe, GeoEye, Earthstar Geographics, CNES/Airbus DS, USDA, USGS, AeroGRID, IGN, and the GIS User Community

LANDMARK MASK



Icart

Identified as natural prominence.
Identified as site: No

Contextual Information:

Nearest Node:	St Peter Port South
Km. to Nearest Node:	5.82
Mask Area (Hectares):	17.48
Sightings (Main Analysis):	8809

LANDMARK LOCATION



Longitude: 2° 2" 16' W
Latitude: 49° 25" 15' N

Source: Esri, DigitalGlobe, GeoEye, Earthstar Geographics, CNES/Airbus DS, USDA, USGS, AeroGRID, IGN, and the GIS User Community

LANDMARK MASK



Île Renote

Identified as natural prominence.
Identified as site: No

Contextual Information:

Nearest Node:	Rivière De Lannion
Km. to Nearest Node:	18.88
Mask Area (Hectares):	13.99
Sightings (Main Analysis):	16466

LANDMARK LOCATION



Longitude: 3° 3" 30' W
Latitude: 48° 53" 17' N

Source: Esri, DigitalGlobe, GeoEye, Earthstar Geographics, CNES/Airbus DS, USDA, USGS, AeroGRID, IGN, and the GIS User Community

LANDMARK MASK



Île Renote 1

Identified as natural prominence.
Identified as site: No

Contextual Information:

Nearest Node:	Rivière De Lannion
Km. to Nearest Node:	18.09
Mask Area (Hectares):	13.14
Sightings (Main Analysis):	14189

LANDMARK LOCATION



Longitude: 3° 3" 22' W
Latitude: 48° 53" 29' N

Source: Esri, DigitalGlobe, GeoEye, Earthstar Geographics, CNES/Airbus DS, USDA, USGS, AeroGRID, IGN, and the GIS User Community

LANDMARK MASK



Île Renote 3

Identified as natural prominence.
Identified as site: No

Contextual Information:

Nearest Node:	Rivière De Lannion
Km. to Nearest Node:	18.94
Mask Area (Hectares):	30.59
Sightings (Main Analysis):	15841

LANDMARK LOCATION



Longitude: 3° 3" 2' W
Latitude: 48° 53" 3' N

Source: Esri, DigitalGlobe, GeoEye, Earthstar Geographics, CNES/Airbus DS, USDA, USGS, AeroGRID, IGN, and the GIS User Community

LANDMARK MASK



Île Renote 4

Identified as natural prominence.
Identified as site: No

Contextual Information:

Nearest Node:	Rivière De Lannion
Km. to Nearest Node:	19.54
Mask Area (Hectares):	30.95
Sightings (Main Analysis):	17024

LANDMARK LOCATION



Longitude: 3° 3" 13' W
Latitude: 48° 53" 2' N

Source: Esri, DigitalGlobe, GeoEye, Earthstar Geographics, CNES/Airbus DS, USDA, USGS, AeroGRID, IGN, and the GIS User Community

LANDMARK MASK



Île Vierge

Identified as natural prominence.
Identified as site: No

Contextual Information:

Nearest Node:	Brest
Km. to Nearest Node:	14.97
Mask Area (Hectares):	18.78
Sightings (Main Analysis):	1497

LANDMARK LOCATION



Longitude: 4° 4" 8' W
Latitude: 48° 12" 2' N

Source: Esri, DigitalGlobe, GeoEye, Earthstar Geographics, CNES/Airbus DS, USDA, USGS, AeroGRID, IGN, and the GIS User Community

LANDMARK MASK



Jethou

Identified as natural prominence.
Identified as site: No

Contextual Information:

Nearest Node:	St Peter Port South
Km. to Nearest Node:	3.01
Mask Area (Hectares):	12.99
Sightings (Main Analysis):	14440

LANDMARK LOCATION



Longitude: 2° 2" 15' W
Latitude: 49° 28" 29' N

Source: Esri, DigitalGlobe, GeoEye, Earthstar Geographics, CNES/Airbus DS, USDA, USGS, AeroGRID, IGN, and the GIS User Community

LANDMARK MASK



Kastell Ac'h 1

Identified as natural prominence.
Identified as site: No

Contextual Information:

Nearest Node:	Aber Wrac'h
Km. to Nearest Node:	3.1
Mask Area (Hectares):	10.08
Sightings (Main Analysis):	7384

LANDMARK LOCATION



Longitude: 4° 4" 21' W
Latitude: 48° 38" 3' N

Source: Esri, DigitalGlobe, GeoEye, Earthstar Geographics, CNES/Airbus DS, USDA, USGS, AeroGRID, IGN, and the GIS User Community

LANDMARK MASK



Kervenan

Identified as natural prominence.
Identified as site: No

Contextual Information:

Nearest Node:	Brest
Km. to Nearest Node:	32.58
Mask Area (Hectares):	10.04
Sightings (Main Analysis):	21

LANDMARK LOCATION



Longitude: 4° 4" 4' W
Latitude: 48° 15" 11' N

Source: Esri, DigitalGlobe, GeoEye, Earthstar Geographics, CNES/Airbus DS, USDA, USGS, AeroGRID, IGN, and the GIS User Community

LANDMARK MASK



Kingston

Identified as natural prominence.
Identified as site: No

Contextual Information:

Nearest Node:	Dartmouth
Km. to Nearest Node:	3.63
Mask Area (Hectares):	33.93
Sightings (Main Analysis):	18379

LANDMARK LOCATION



Longitude: 3° 3" 13' W
Latitude: 50° 21" 9' N

Source: Esri, DigitalGlobe, GeoEye, Earthstar Geographics, CNES/Airbus DS, USDA, USGS, AeroGRID, IGN, and the GIS User Community

LANDMARK MASK



Kingston 1

Identified as natural prominence.
Identified as site: No

Contextual Information:

Nearest Node:	Dartmouth
Km. to Nearest Node:	3.15
Mask Area (Hectares):	10.12
Sightings (Main Analysis):	17548

LANDMARK LOCATION



Longitude: 3° 3" 24' W
Latitude: 50° 21" 11' N

Source: Esri, DigitalGlobe, GeoEye, Earthstar Geographics, CNES/Airbus DS, USDA, USGS, AeroGRID, IGN, and the GIS User Community

LANDMARK MASK



L'etac

Identified as natural prominence.
Identified as site: No

Contextual Information:

Nearest Node:	St Peter Port South
Km. to Nearest Node:	11.96
Mask Area (Hectares):	8.17
Sightings (Main Analysis):	9752

LANDMARK LOCATION



Longitude: 2° 2" 3' W
Latitude: 49° 24" 4' N

Source: Esri, DigitalGlobe, GeoEye, Earthstar Geographics, CNES/Airbus DS, USDA, USGS, AeroGRID, IGN, and the GIS User Community

LANDMARK MASK



La Butte De Caumont

Identified as natural prominence.
Identified as site: No

Contextual Information:

Nearest Node:	Nacqueville
Km. to Nearest Node:	121.72
Mask Area (Hectares):	22.82
Sightings (Main Analysis):	5

LANDMARK LOCATION



Longitude: 0° 0" 9' W
Latitude: 49° 17" 27' N

Source: Esri, DigitalGlobe, GeoEye, Earthstar Geographics, CNES/Airbus DS, USDA, USGS, AeroGRID, IGN, and the GIS User Community

LANDMARK MASK



La Coupee

Identified as natural prominence.
Identified as site: No

Contextual Information:

Nearest Node:	St Peter Port South
Km. to Nearest Node:	10.93
Mask Area (Hectares):	9.83
Sightings (Main Analysis):	11514

LANDMARK LOCATION



Longitude: 2° 2" 8' W
Latitude: 49° 25" 24' N

Source: Esri, DigitalGlobe, GeoEye, Earthstar Geographics, CNES/Airbus DS, USDA, USGS, AeroGRID, IGN, and the GIS User Community

LANDMARK MASK



La Forge

Identified as natural prominence.
Identified as site: No

Contextual Information:

Nearest Node:	St Peter Port South
Km. to Nearest Node:	11.86
Mask Area (Hectares):	14.7
Sightings (Main Analysis):	7605

LANDMARK LOCATION



Longitude: 2° 2" 7' W
Latitude: 49° 26" 17' N

Source: Esri, DigitalGlobe, GeoEye, Earthstar Geographics, CNES/Airbus DS, USDA, USGS, AeroGRID, IGN, and the GIS User Community

LANDMARK MASK



La Valette

Identified as natural prominence.
Identified as site: No

Contextual Information:

Nearest Node:	St Peter Port South
Km. to Nearest Node:	11.66
Mask Area (Hectares):	15.58
Sightings (Main Analysis):	9852

LANDMARK LOCATION



Longitude: 2° 2" 8' W
Latitude: 49° 26" 3' N

Source: Esri, DigitalGlobe, GeoEye, Earthstar Geographics, CNES/Airbus DS, USDA, USGS, AeroGRID, IGN, and the GIS User Community

LANDMARK MASK



Lamorna

Identified as natural prominence.
Identified as site: No

Contextual Information:

Nearest Node:	Penzance
Km. to Nearest Node:	5.0
Mask Area (Hectares):	18.56
Sightings (Main Analysis):	3459

LANDMARK LOCATION



Longitude: 5° 5" 21' W
Latitude: 50° 4" 9' N

Source: Esri, DigitalGlobe, GeoEye, Earthstar Geographics, CNES/Airbus DS, USDA, USGS, AeroGRID, IGN, and the GIS User Community

LANDMARK MASK



Lamorna 1

Identified as natural prominence.
Identified as site: No

Contextual Information:

Nearest Node:	Penzance
Km. to Nearest Node:	6.96
Mask Area (Hectares):	12.2
Sightings (Main Analysis):	3421

LANDMARK LOCATION



Longitude: 5° 5" 20' W
Latitude: 50° 3" 16' N

Source: Esri, DigitalGlobe, GeoEye, Earthstar Geographics, CNES/Airbus DS, USDA, USGS, AeroGRID, IGN, and the GIS User Community

LANDMARK MASK



Lande Du Thot

Identified as natural prominence.
Identified as site: No

Contextual Information:

Nearest Node:	Nacqueville
Km. to Nearest Node:	13.12
Mask Area (Hectares):	9.23
Sightings (Main Analysis):	7222

LANDMARK LOCATION



Longitude: 1° 1" 16' W
Latitude: 49° 38" 13' N

Source: Esri, DigitalGlobe, GeoEye, Earthstar Geographics, CNES/Airbus DS, USDA, USGS, AeroGRID, IGN, and the GIS User Community

LANDMARK MASK



Langton Matravers

Identified as natural prominence.
Identified as site: No

Contextual Information:

Nearest Node:	Poole
Km. to Nearest Node:	9.56
Mask Area (Hectares):	15.48
Sightings (Main Analysis):	6122

LANDMARK LOCATION



Longitude: 1° 1" 21' W
Latitude: 50° 36" 22' N

Source: Esri, DigitalGlobe, GeoEye, Earthstar Geographics, CNES/Airbus DS, USDA, USGS, AeroGRID, IGN, and the GIS User Community

LANDMARK MASK



Lann Penn Arland

Identified as natural prominence.
Identified as site: No

Contextual Information:

Nearest Node:	Aber Wrac'h
Km. to Nearest Node:	35.64
Mask Area (Hectares):	31.14
Sightings (Main Analysis):	4393

LANDMARK LOCATION



Longitude: 5° 5" 20' W
Latitude: 48° 28" 19' N

Source: Esri, DigitalGlobe, GeoEye, Earthstar Geographics, CNES/Airbus DS, USDA, USGS, AeroGRID, IGN, and the GIS User Community

LANDMARK MASK



Lann Penn Arland 1

Identified as natural prominence.
Identified as site: No

Contextual Information:

Nearest Node:	Brest
Km. to Nearest Node:	32.86
Mask Area (Hectares):	13.18
Sightings (Main Analysis):	3334

LANDMARK LOCATION



Longitude: 5° 5" 15' W
Latitude: 48° 26" 13' N

Source: Esri, DigitalGlobe, GeoEye, Earthstar Geographics, CNES/Airbus DS, USDA, USGS, AeroGRID, IGN, and the GIS User Community

LANDMARK MASK



Lannear

Identified as natural prominence.
Identified as site: No

Contextual Information:

Nearest Node:	Porthallow
Km. to Nearest Node:	4.26
Mask Area (Hectares):	38.28
Sightings (Main Analysis):	12276

LANDMARK LOCATION



Longitude: 4° 4" 22' W
Latitude: 50° 20" 22' N

Source: Esri, DigitalGlobe, GeoEye, Earthstar Geographics, CNES/Airbus DS, USDA, USGS, AeroGRID, IGN, and the GIS User Community

LANDMARK MASK



Lannear 1

Identified as natural prominence.
Identified as site: No

Contextual Information:

Nearest Node:	Porthallow
Km. to Nearest Node:	3.61
Mask Area (Hectares):	33.43
Sightings (Main Analysis):	12417

LANDMARK LOCATION



Longitude: 4° 4" 19' W
Latitude: 50° 20" 15' N

Source: Esri, DigitalGlobe, GeoEye, Earthstar Geographics, CNES/Airbus DS, USDA, USGS, AeroGRID, IGN, and the GIS User Community

LANDMARK MASK



Lansallos

Identified as natural prominence.
Identified as site: No

Contextual Information:

Nearest Node:	Fowey
Km. to Nearest Node:	5.09
Mask Area (Hectares):	24.65
Sightings (Main Analysis):	10991

LANDMARK LOCATION



Longitude: 4° 4" 1' W
Latitude: 50° 20" 4' N

Source: Esri, DigitalGlobe, GeoEye, Earthstar Geographics, CNES/Airbus DS, USDA, USGS, AeroGRID, IGN, and the GIS User Community

LANDMARK MASK



Le Chaudron

Identified as natural prominence.
Identified as site: No

Contextual Information:

Nearest Node:	Nacqueville
Km. to Nearest Node:	134.89
Mask Area (Hectares):	57.01
Sightings (Main Analysis):	10

LANDMARK LOCATION



Longitude: 0° 0" 8' E
Latitude: 49° 43" 6' N

Source: Esri, DigitalGlobe, GeoEye, Earthstar Geographics, CNES/Airbus DS, USDA, USGS, AeroGRID, IGN, and the GIS User Community

LANDMARK MASK



Le Chien Intrepide

Identified as natural prominence.
Identified as site: No

Contextual Information:

Nearest Node:	Nacqueville
Km. to Nearest Node:	149.39
Mask Area (Hectares):	13.93
Sightings (Main Analysis):	0

LANDMARK LOCATION



Longitude: 0° 0" 28' E
Latitude: 49° 47" 22' N

Source: Esri, DigitalGlobe, GeoEye, Earthstar Geographics, CNES/Airbus DS, USDA, USGS, AeroGRID, IGN, and the GIS User Community

LANDMARK MASK



Le Mat Du Pavillon

Identified as natural prominence.
Identified as site: No

Contextual Information:

Nearest Node:	Nacqueville
Km. to Nearest Node:	206.66
Mask Area (Hectares):	20.55
Sightings (Main Analysis):	0

LANDMARK LOCATION



Longitude: 1° 1" 2' E
Latitude: 49° 58" 8' N

Source: Esri, DigitalGlobe, GeoEye, Earthstar Geographics, CNES/Airbus DS, USDA, USGS, AeroGRID, IGN, and the GIS User Community

LANDMARK MASK



Le Mont De Vassonville

Identified as natural prominence.
Identified as site: No

Contextual Information:

Nearest Node:	Nacqueville
Km. to Nearest Node:	208.65
Mask Area (Hectares):	9.79
Sightings (Main Analysis):	0

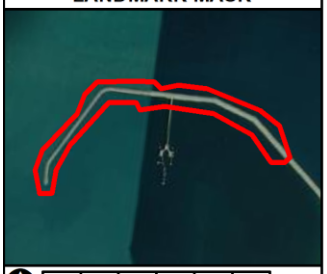
LANDMARK LOCATION



Longitude: 1° 1" 20' E
Latitude: 49° 58" 16' N

Source: Esri, DigitalGlobe, GeoEye, Earthstar Geographics, CNES/Airbus DS, USDA, USGS, AeroGRID, IGN, and the GIS User Community

LANDMARK MASK



Le Presbytere

Identified as natural prominence.
Identified as site: No

Contextual Information:

Nearest Node:	Nacqueville
Km. to Nearest Node:	128.47
Mask Area (Hectares):	50.84
Sightings (Main Analysis):	22

LANDMARK LOCATION



Longitude: 0° 0" 11' E
Latitude: 49° 40" 6' N

Source: Esri, DigitalGlobe, GeoEye, Earthstar Geographics, CNES/Airbus DS, USDA, USGS, AeroGRID, IGN, and the GIS User Community

LANDMARK MASK



Le Presbytere 1

Identified as natural prominence.
Identified as site: No

Contextual Information:

Nearest Node:	Nacqueville
Km. to Nearest Node:	131.35
Mask Area (Hectares):	10.8
Sightings (Main Analysis):	16

LANDMARK LOCATION



Longitude: 0° 0" 29' E
Latitude: 49° 40" 19' N

Source: Esri, DigitalGlobe, GeoEye, Earthstar Geographics, CNES/Airbus DS, USDA, USGS, AeroGRID, IGN, and the GIS User Community

LANDMARK MASK



Le Stiff

Identified as natural prominence.
Identified as site: No

Contextual Information:

Nearest Node:	Brest
Km. to Nearest Node:	3.89
Mask Area (Hectares):	32.18
Sightings (Main Analysis):	1010

LANDMARK LOCATION



Longitude: 4° 4" 16' W
Latitude: 48° 20" 19' N

Source: Esri, DigitalGlobe, GeoEye, Earthstar Geographics, CNES/Airbus DS, USDA, USGS, AeroGRID, IGN, and the GIS User Community

LANDMARK MASK



Le Treport

Identified as natural prominence.
Identified as site: No

Contextual Information:

Nearest Node:	Nacqueville
Km. to Nearest Node:	223.77
Mask Area (Hectares):	10.99
Sightings (Main Analysis):	0

LANDMARK LOCATION



Longitude: 1° 1" 24' E
Latitude: 50° 4" 26' N

Source: Esri, DigitalGlobe, GeoEye, Earthstar Geographics, CNES/Airbus DS, USDA, USGS, AeroGRID, IGN, and the GIS User Community

LANDMARK MASK



Le Treport 1

Identified as natural prominence.
Identified as site: No

Contextual Information:

Nearest Node:	Nacqueville
Km. to Nearest Node:	220.46
Mask Area (Hectares):	25.16
Sightings (Main Analysis):	0

LANDMARK LOCATION



Longitude: 1° 1" 28' E
Latitude: 50° 3" 24' N

Source: Esri, DigitalGlobe, GeoEye, Earthstar Geographics, CNES/Airbus DS, USDA, USGS, AeroGRID, IGN, and the GIS User Community

LANDMARK MASK



Les Pres Sales

Identified as natural prominence.
Identified as site: No

Contextual Information:

Nearest Node:	Nacqueville
Km. to Nearest Node:	216.35
Mask Area (Hectares):	21.83
Sightings (Main Analysis):	0

LANDMARK LOCATION



Longitude: 1° 1" 4' E
Latitude: 50° 2" 22' N

Source: Esri, DigitalGlobe, GeoEye, Earthstar Geographics, CNES/Airbus DS, USDA, USGS, AeroGRID, IGN, and the GIS User Community

LANDMARK MASK



Les Treize Vents

Identified as natural prominence.
Identified as site: No

Contextual Information:

Nearest Node:	Nacqueville
Km. to Nearest Node:	15.29
Mask Area (Hectares):	10.56
Sightings (Main Analysis):	7077

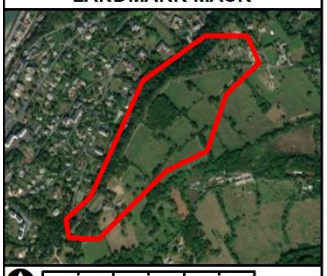
LANDMARK LOCATION



Longitude: 1° 1" 7' W
Latitude: 49° 40" 18' N

Source: Esri, DigitalGlobe, GeoEye, Earthstar Geographics, CNES/Airbus DS, USDA, USGS, AeroGRID, IGN, and the GIS User Community

LANDMARK MASK



Les Trois Etangs

Identified as natural prominence.
Identified as site: No

Contextual Information:

Nearest Node:	Nacqueville
Km. to Nearest Node:	131.36
Mask Area (Hectares):	18.82
Sightings (Main Analysis):	0

LANDMARK LOCATION



Longitude: 0° 0" 23' E
Latitude: 49° 22" 21' N

Source: Esri, DigitalGlobe, GeoEye, Earthstar Geographics, CNES/Airbus DS, USDA, USGS, AeroGRID, IGN, and the GIS User Community

LANDMARK MASK



Leurarbouar

Identified as natural prominence.
Identified as site: No

Contextual Information:

Nearest Node:	Brest
Km. to Nearest Node:	24.44
Mask Area (Hectares):	50.67
Sightings (Main Analysis):	178

LANDMARK LOCATION



Longitude: 4° 4" 21' W
Latitude: 48° 16" 30' N

Source: Esri, DigitalGlobe, GeoEye, Earthstar Geographics, CNES/Airbus DS, USDA, USGS, AeroGRID, IGN, and the GIS User Community

LANDMARK MASK



Little Sark

Identified as natural prominence.
Identified as site: No

Contextual Information:

Nearest Node:	St Peter Port South
Km. to Nearest Node:	10.49
Mask Area (Hectares):	75.72
Sightings (Main Analysis):	13676

LANDMARK LOCATION



Longitude: 2° 2" 24' W
Latitude: 49° 25" 9' N

Source: Esri, DigitalGlobe, GeoEye, Earthstar Geographics, CNES/Airbus DS, USDA, USGS, AeroGRID, IGN, and the GIS User Community

LANDMARK MASK



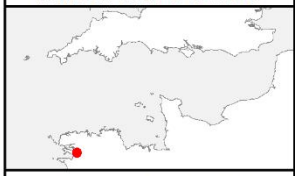
Loguivy

Identified as natural prominence.
Identified as site: No

Contextual Information:

Nearest Node:	Brest
Km. to Nearest Node:	31.41
Mask Area (Hectares):	28.23
Sightings (Main Analysis):	130

LANDMARK LOCATION



Longitude: 4° 4" 15' W
Latitude: 48° 15" 19' N

Source: Esri, DigitalGlobe, GeoEye, Earthstar Geographics, CNES/Airbus DS, USDA, USGS, AeroGRID, IGN, and the GIS User Community

LANDMARK MASK



Long Sands

Identified as natural prominence.
Identified as site: No

Contextual Information:

Nearest Node:	Dartmouth
Km. to Nearest Node:	4.79
Mask Area (Hectares):	36.83
Sightings (Main Analysis):	14151

LANDMARK LOCATION



Longitude: 3° 3" 27' W
Latitude: 50° 22" 10' N

Source: Esri, DigitalGlobe, GeoEye, Earthstar Geographics, CNES/Airbus DS, USDA, USGS, AeroGRID, IGN, and the GIS User Community

LANDMARK MASK



Longis Bay

Identified as natural prominence.
Identified as site: No

Contextual Information:

Nearest Node:	St Peter Port North
Km. to Nearest Node:	30.86
Mask Area (Hectares):	15.08
Sightings (Main Analysis):	14591

LANDMARK LOCATION



Longitude: 2° 2" 21' W
Latitude: 49° 43" 0' N

Source: Esri, DigitalGlobe, GeoEye, Earthstar Geographics, CNES/Airbus DS, USDA, USGS, AeroGRID, IGN, and the GIS User Community

LANDMARK MASK



Looe

Identified as natural prominence.
Identified as site: No

Contextual Information:

Nearest Node:	Porthallow
Km. to Nearest Node:	4.82
Mask Area (Hectares):	17.04
Sightings (Main Analysis):	10864

LANDMARK LOCATION



Longitude: 4° 4" 29' W
Latitude: 50° 21" 6' N

Source: Esri, DigitalGlobe, GeoEye, Earthstar Geographics, CNES/Airbus DS, USDA, USGS, AeroGRID, IGN, and the GIS User Community

LANDMARK MASK



Lowtherville

Identified as natural prominence.
Identified as site: No

Contextual Information:

Nearest Node:	Christchurch
Km. to Nearest Node:	35.68
Mask Area (Hectares):	143.7
Sightings (Main Analysis):	2766

LANDMARK LOCATION



Longitude: 1° 1" 10' W
Latitude: 50° 36" 21' N

Source: Esri, DigitalGlobe, GeoEye, Earthstar Geographics, CNES/Airbus DS, USDA, USGS, AeroGRID, IGN, and the GIS User Community

LANDMARK MASK



Luccombe

Identified as natural prominence.
Identified as site: No

Contextual Information:

Nearest Node:	Christchurch
Km. to Nearest Node:	40.14
Mask Area (Hectares):	27.3
Sightings (Main Analysis):	359

LANDMARK LOCATION



Longitude: 1° 1" 20' W
Latitude: 50° 37" 1' N

Source: Esri, DigitalGlobe, GeoEye, Earthstar Geographics, CNES/Airbus DS, USDA, USGS, AeroGRID, IGN, and the GIS User Community

LANDMARK MASK



Maker

Identified as natural prominence.
Identified as site: No

Contextual Information:

Nearest Node:	Plymouth
Km. to Nearest Node:	2.62
Mask Area (Hectares):	136.9
Sightings (Main Analysis):	11673

LANDMARK LOCATION



Longitude: 4° 4" 8' W
Latitude: 50° 21" 14' N

Source: Esri, DigitalGlobe, GeoEye, Earthstar Geographics, CNES/Airbus DS, USDA, USGS, AeroGRID, IGN, and the GIS User Community

LANDMARK MASK



Manor Gardens

Identified as natural prominence.
Identified as site: No

Contextual Information:

Nearest Node:	Torquay
Km. to Nearest Node:	1.87
Mask Area (Hectares):	23.5
Sightings (Main Analysis):	13808

LANDMARK LOCATION



Longitude: 3° 3" 24' W
Latitude: 50° 28" 16' N

Source: Esri, DigitalGlobe, GeoEye, Earthstar Geographics, CNES/Airbus DS, USDA, USGS, AeroGRID, IGN, and the GIS User Community

LANDMARK MASK



Menabilly

Identified as natural prominence.
Identified as site: No

Contextual Information:

Nearest Node:	Fowey
Km. to Nearest Node:	3.43
Mask Area (Hectares):	10.92
Sightings (Main Analysis):	9465

LANDMARK LOCATION



Longitude: 4° 4" 16' W
Latitude: 50° 19" 17' N

Source: Esri, DigitalGlobe, GeoEye, Earthstar Geographics, CNES/Airbus DS, USDA, USGS, AeroGRID, IGN, and the GIS User Community

LANDMARK MASK



Menabilly 1

Identified as natural prominence.
Identified as site: No

Contextual Information:

Nearest Node:	Fowey
Km. to Nearest Node:	2.8
Mask Area (Hectares):	17.16
Sightings (Main Analysis):	9850

LANDMARK LOCATION



Longitude: 4° 4" 24' W
Latitude: 50° 19" 1' N

Source: Esri, DigitalGlobe, GeoEye, Earthstar Geographics, CNES/Airbus DS, USDA, USGS, AeroGRID, IGN, and the GIS User Community

LANDMARK MASK



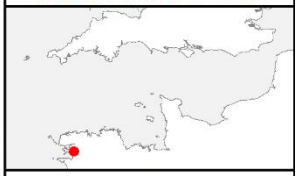
Mene Ar Chaor

Identified as natural prominence.
Identified as site: No

Contextual Information:

Nearest Node:	Brest
Km. to Nearest Node:	24.94
Mask Area (Hectares):	10.33
Sightings (Main Analysis):	94

LANDMARK LOCATION



Longitude: 4° 4" 1' W
Latitude: 48° 16" 7' N

Source: Esri, DigitalGlobe, GeoEye, Earthstar Geographics, CNES/Airbus DS, USDA, USGS, AeroGRID, IGN, and the GIS User Community

LANDMARK MASK



Menesguen

Identified as natural prominence.
Identified as site: No

Contextual Information:

Nearest Node:	Brest
Km. to Nearest Node:	16.18
Mask Area (Hectares):	10.49
Sightings (Main Analysis):	438

LANDMARK LOCATION



Longitude: 4° 4" 11' W
Latitude: 48° 11" 14' N

Source: Esri, DigitalGlobe, GeoEye, Earthstar Geographics, CNES/Airbus DS, USDA, USGS, AeroGRID, IGN, and the GIS User Community

LANDMARK MASK



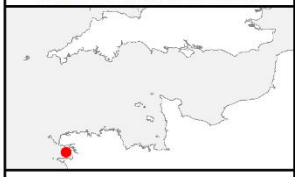
Menez Kador

Identified as natural prominence.
Identified as site: No

Contextual Information:

Nearest Node:	Brest
Km. to Nearest Node:	13.73
Mask Area (Hectares):	48.92
Sightings (Main Analysis):	1298

LANDMARK LOCATION



Longitude: 4° 4" 11' W
Latitude: 48° 13" 4' N

Source: Esri, DigitalGlobe, GeoEye, Earthstar Geographics, CNES/Airbus DS, USDA, USGS, AeroGRID, IGN, and the GIS User Community

LANDMARK MASK



Merafield

Identified as natural prominence.
Identified as site: No

Contextual Information:

Nearest Node:	Plymouth
Km. to Nearest Node:	9.13
Mask Area (Hectares):	27.86
Sightings (Main Analysis):	1338

LANDMARK LOCATION



Longitude: 4° 4" 4' W
Latitude: 50° 23" 5' N

Source: Esri, DigitalGlobe, GeoEye, Earthstar Geographics, CNES/Airbus DS, USDA, USGS, AeroGRID, IGN, and the GIS User Community

LANDMARK MASK



Mew Stone

Identified as natural prominence.
Identified as site: No

Contextual Information:

Nearest Node:	Torquay
Km. to Nearest Node:	4.87
Mask Area (Hectares):	30.38
Sightings (Main Analysis):	17099

LANDMARK LOCATION



Longitude: 3° 3" 21' W
Latitude: 50° 24" 8' N

Source: Esri, DigitalGlobe, GeoEye, Earthstar Geographics, CNES/Airbus DS, USDA, USGS, AeroGRID, IGN, and the GIS User Community

LANDMARK MASK



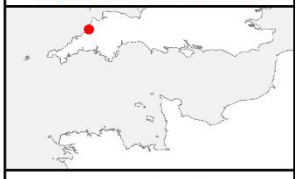
Millook

Identified as natural prominence.
Identified as site: No

Contextual Information:

Nearest Node:	Fowey
Km. to Nearest Node:	52.09
Mask Area (Hectares):	15.38
Sightings (Main Analysis):	0

LANDMARK LOCATION



Longitude: 4° 4" 8' W
Latitude: 50° 46" 28' N

Source: Esri, DigitalGlobe, GeoEye, Earthstar Geographics, CNES/Airbus DS, USDA, USGS, AeroGRID, IGN, and the GIS User Community

LANDMARK MASK



Millook 1

Identified as natural prominence.
Identified as site: No

Contextual Information:

Nearest Node:	Fowey
Km. to Nearest Node:	51.1
Mask Area (Hectares):	21.35
Sightings (Main Analysis):	0

LANDMARK LOCATION



Longitude: 4° 4" 2' W
Latitude: 50° 46" 2' N

Source: Esri, DigitalGlobe, GeoEye, Earthstar Geographics, CNES/Airbus DS, USDA, USGS, AeroGRID, IGN, and the GIS User Community

LANDMARK MASK



Minard

Identified as natural prominence.
Identified as site: No

Contextual Information:

Nearest Node:	Le Trieux
Km. to Nearest Node:	16.07
Mask Area (Hectares):	10.44
Sightings (Main Analysis):	9045

LANDMARK LOCATION



Longitude: 2° 2" 1' W
Latitude: 48° 45" 17' N

Source: Esri, DigitalGlobe, GeoEye, Earthstar Geographics, CNES/Airbus DS, USDA, USGS, AeroGRID, IGN, and the GIS User Community

LANDMARK MASK



Mont Canisy

Identified as natural prominence.
Identified as site: No

Contextual Information:

Nearest Node:	Nacqueville
Km. to Nearest Node:	128.62
Mask Area (Hectares):	44.58
Sightings (Main Analysis):	0

LANDMARK LOCATION



Longitude: 0° 0" 26' E
Latitude: 49° 20" 21' N

Source: Esri, DigitalGlobe, GeoEye, Earthstar Geographics, CNES/Airbus DS, USDA, USGS, AeroGRID, IGN, and the GIS User Community

LANDMARK MASK



Morcombelake

Identified as natural prominence.
Identified as site: No

Contextual Information:

Nearest Node:	Seaton
Km. to Nearest Node:	13.31
Mask Area (Hectares):	107.44
Sightings (Main Analysis):	9321

LANDMARK LOCATION



Longitude: 2° 2" 12' W
Latitude: 50° 44" 13' N

Source: Esri, DigitalGlobe, GeoEye, Earthstar Geographics, CNES/Airbus DS, USDA, USGS, AeroGRID, IGN, and the GIS User Community

LANDMARK MASK



Morwenstow

Identified as natural prominence.
Identified as site: No

Contextual Information:

Nearest Node:	Fowey
Km. to Nearest Node:	67.6
Mask Area (Hectares):	17.73
Sightings (Main Analysis):	0

LANDMARK LOCATION



Longitude: 4° 4" 30' W
Latitude: 50° 55" 10' N

Source: Esri, DigitalGlobe, GeoEye, Earthstar Geographics, CNES/Airbus DS, USDA, USGS, AeroGRID, IGN, and the GIS User Community

LANDMARK MASK



Morwenstow 1

Identified as natural prominence.
Identified as site: No

Contextual Information:

Nearest Node:	Fowey
Km. to Nearest Node:	66.88
Mask Area (Hectares):	10.13
Sightings (Main Analysis):	0

LANDMARK LOCATION



Longitude: 4° 4" 19' W
Latitude: 50° 54" 26' N

Source: Esri, DigitalGlobe, GeoEye, Earthstar Geographics, CNES/Airbus DS, USDA, USGS, AeroGRID, IGN, and the GIS User Community

LANDMARK MASK



Morwenstow 2

Identified as natural prominence.
Identified as site: No

Contextual Information:

Nearest Node:	Fowey
Km. to Nearest Node:	65.65
Mask Area (Hectares):	18.0
Sightings (Main Analysis):	0

LANDMARK LOCATION



Longitude: 4° 4" 23' W
Latitude: 50° 54" 9' N

Source: Esri, DigitalGlobe, GeoEye, Earthstar Geographics, CNES/Airbus DS, USDA, USGS, AeroGRID, IGN, and the GIS User Community

LANDMARK MASK



Mothecombe

Identified as natural prominence.
Identified as site: No

Contextual Information:

Nearest Node:	Bigbury Bay
Km. to Nearest Node:	6.06
Mask Area (Hectares):	18.43
Sightings (Main Analysis):	11858

LANDMARK LOCATION



Longitude: 3° 3" 19' W
Latitude: 50° 18" 2' N

Source: Esri, DigitalGlobe, GeoEye, Earthstar Geographics, CNES/Airbus DS, USDA, USGS, AeroGRID, IGN, and the GIS User Community

LANDMARK MASK



Mouth Mill

Identified as natural prominence.
Identified as site: No

Contextual Information:

Nearest Node:	Porthallow
Km. to Nearest Node:	78.47
Mask Area (Hectares):	24.57
Sightings (Main Analysis):	0

LANDMARK LOCATION



Longitude: 4° 4" 4' W
Latitude: 51° 1" 22' N

Source: Esri, DigitalGlobe, GeoEye, Earthstar Geographics, CNES/Airbus DS, USDA, USGS, AeroGRID, IGN, and the GIS User Community

LANDMARK MASK



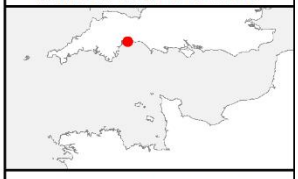
Mutters Moor

Identified as natural prominence.
Identified as site: No

Contextual Information:

Nearest Node:	Sidmouth
Km. to Nearest Node:	3.29
Mask Area (Hectares):	49.01
Sightings (Main Analysis):	12002

LANDMARK LOCATION



Longitude: 3° 3" 21' W
Latitude: 50° 41" 20' N

Source: Esri, DigitalGlobe, GeoEye, Earthstar Geographics, CNES/Airbus DS, USDA, USGS, AeroGRID, IGN, and the GIS User Community

LANDMARK MASK



Nare Head

Identified as natural prominence.
Identified as site: No

Contextual Information:

Nearest Node:	Falmouth
Km. to Nearest Node:	10.7
Mask Area (Hectares):	36.18
Sightings (Main Analysis):	7594

LANDMARK LOCATION



Longitude: 4° 4" 1' W
Latitude: 50° 12" 0' N

Source: Esri, DigitalGlobe, GeoEye, Earthstar Geographics, CNES/Airbus DS, USDA, USGS, AeroGRID, IGN, and the GIS User Community

LANDMARK MASK



Netton

Identified as natural prominence.
Identified as site: No

Contextual Information:

Nearest Node:	Mothecombe
Km. to Nearest Node:	3.31
Mask Area (Hectares):	23.46
Sightings (Main Analysis):	15768

LANDMARK LOCATION



Longitude: 4° 4" 16' W
Latitude: 50° 18" 10' N

Source: Esri, DigitalGlobe, GeoEye, Earthstar Geographics, CNES/Airbus DS, USDA, USGS, AeroGRID, IGN, and the GIS User Community

LANDMARK MASK



Netton 1

Identified as natural prominence.
Identified as site: No

Contextual Information:

Nearest Node:	Mothecombe
Km. to Nearest Node:	4.2
Mask Area (Hectares):	25.67
Sightings (Main Analysis):	14936

LANDMARK LOCATION



Longitude: 4° 4" 19' W
Latitude: 50° 18" 8' N

Source: Esri, DigitalGlobe, GeoEye, Earthstar Geographics, CNES/Airbus DS, USDA, USGS, AeroGRID, IGN, and the GIS User Community

LANDMARK MASK



Newbarn

Identified as natural prominence.
Identified as site: No

Contextual Information:

Nearest Node:	Christchurch
Km. to Nearest Node:	133.24
Mask Area (Hectares):	16.87
Sightings (Main Analysis):	0

LANDMARK LOCATION



Longitude: 0° 0" 19' E
Latitude: 50° 46" 29' N

Source: Esri, DigitalGlobe, GeoEye, Earthstar Geographics, CNES/Airbus DS, USDA, USGS, AeroGRID, IGN, and the GIS User Community

LANDMARK MASK



Niton Undercliff

Identified as natural prominence.
Identified as site: No

Contextual Information:

Nearest Node:	Christchurch
Km. to Nearest Node:	35.63
Mask Area (Hectares):	18.66
Sightings (Main Analysis):	1685

LANDMARK LOCATION



Longitude: 1° 1" 10' W
Latitude: 50° 35" 10' N

Source: Esri, DigitalGlobe, GeoEye, Earthstar Geographics, CNES/Airbus DS, USDA, USGS, AeroGRID, IGN, and the GIS User Community

LANDMARK MASK



Old Town 1

Identified as natural prominence.
Identified as site: No

Contextual Information:

Nearest Node:	Christchurch
Km. to Nearest Node:	138.48
Mask Area (Hectares):	91.26
Sightings (Main Analysis):	0

LANDMARK LOCATION



Longitude: 0° 0" 3' E
Latitude: 50° 44" 27' N

Source: Esri, DigitalGlobe, GeoEye, Earthstar Geographics, CNES/Airbus DS, USDA, USGS, AeroGRID, IGN, and the GIS User Community

LANDMARK MASK



Osmington

Identified as natural prominence.
Identified as site: No

Contextual Information:

Nearest Node:	Portland
Km. to Nearest Node:	6.58
Mask Area (Hectares):	10.92
Sightings (Main Analysis):	7862

LANDMARK LOCATION



Longitude: 2° 2" 5' W
Latitude: 50° 39" 24' N

Source: Esri, DigitalGlobe, GeoEye, Earthstar Geographics, CNES/Airbus DS, USDA, USGS, AeroGRID, IGN, and the GIS User Community

LANDMARK MASK



Osmington Mills

Identified as natural prominence.
Identified as site: No

Contextual Information:

Nearest Node:	Portland
Km. to Nearest Node:	6.59
Mask Area (Hectares):	13.79
Sightings (Main Analysis):	7311

LANDMARK LOCATION



Longitude: 2° 2" 4' W
Latitude: 50° 38" 21' N

Source: Esri, DigitalGlobe, GeoEye, Earthstar Geographics, CNES/Airbus DS, USDA, USGS, AeroGRID, IGN, and the GIS User Community

LANDMARK MASK



Pedn Boar

Identified as natural prominence.
Identified as site: No

Contextual Information:

Nearest Node:	Helford
Km. to Nearest Node:	9.42
Mask Area (Hectares):	38.03
Sightings (Main Analysis):	8624

LANDMARK LOCATION



Longitude: 5° 5" 24' W
Latitude: 50° 0" 23' N

Source: Esri, DigitalGlobe, GeoEye, Earthstar Geographics, CNES/Airbus DS, USDA, USGS, AeroGRID, IGN, and the GIS User Community

LANDMARK MASK



Pen Olver

Identified as natural prominence.
Identified as site: No

Contextual Information:

Nearest Node:	Mullion
Km. to Nearest Node:	9.19
Mask Area (Hectares):	21.65
Sightings (Main Analysis):	7382

LANDMARK LOCATION



Longitude: 5° 5" 20' W
Latitude: 49° 58" 4' N

Source: Esri, DigitalGlobe, GeoEye, Earthstar Geographics, CNES/Airbus DS, USDA, USGS, AeroGRID, IGN, and the GIS User Community

LANDMARK MASK



Pencra Head

Identified as natural prominence.
Identified as site: No

Contextual Information:

Nearest Node:	Helford
Km. to Nearest Node:	3.62
Mask Area (Hectares):	12.16
Sightings (Main Analysis):	8137

LANDMARK LOCATION



Longitude: 5° 5" 4' W
Latitude: 50° 4" 24' N

Source: Esri, DigitalGlobe, GeoEye, Earthstar Geographics, CNES/Airbus DS, USDA, USGS, AeroGRID, IGN, and the GIS User Community

LANDMARK MASK



Pendennis Point

Identified as natural prominence.
Identified as site: No

Contextual Information:

Nearest Node:	Falmouth
Km. to Nearest Node:	1.7
Mask Area (Hectares):	13.7
Sightings (Main Analysis):	4972

LANDMARK LOCATION



Longitude: 5° 5" 11' W
Latitude: 50° 9" 10' N

Source: Esri, DigitalGlobe, GeoEye, Earthstar Geographics, CNES/Airbus DS, USDA, USGS, AeroGRID, IGN, and the GIS User Community

LANDMARK MASK



Penhale Point

Identified as natural prominence.
Identified as site: Yes

Contextual Information:

Nearest Node:	Falmouth
Km. to Nearest Node:	29.6
Mask Area (Hectares):	21.26
Sightings (Main Analysis):	13

LANDMARK LOCATION



Longitude: 5° 5" 16' W
Latitude: 50° 23" 18' N

Source: Esri, DigitalGlobe, GeoEye, Earthstar Geographics, CNES/Airbus DS, USDA, USGS, AeroGRID, IGN, and the GIS User Community

LANDMARK MASK



Peninnis Head

Identified as natural prominence.
Identified as site: No

Contextual Information:

Nearest Node:	Penzance
Km. to Nearest Node:	60.64
Mask Area (Hectares):	28.31
Sightings (Main Analysis):	489

LANDMARK LOCATION



Longitude: 6° 6" 16' W
Latitude: 49° 54" 23' N

Source: Esri, DigitalGlobe, GeoEye, Earthstar Geographics, CNES/Airbus DS, USDA, USGS, AeroGRID, IGN, and the GIS User Community

LANDMARK MASK



Penn Ar Ru Meur

Identified as natural prominence.
Identified as site: No

Contextual Information:

Nearest Node:	Aber Wrac'h
Km. to Nearest Node:	38.58
Mask Area (Hectares):	23.74
Sightings (Main Analysis):	2761

LANDMARK LOCATION



Longitude: 5° 5" 8' W
Latitude: 48° 29" 10' N

Source: Esri, DigitalGlobe, GeoEye, Earthstar Geographics, CNES/Airbus DS, USDA, USGS, AeroGRID, IGN, and the GIS User Community

LANDMARK MASK



Pentire Point

Identified as natural prominence.
Identified as site: No

Contextual Information:

Nearest Node:	Fowey
Km. to Nearest Node:	37.39
Mask Area (Hectares):	36.2
Sightings (Main Analysis):	0

LANDMARK LOCATION



Longitude: 4° 4" 23' W
Latitude: 50° 35" 17' N

Source: Esri, DigitalGlobe, GeoEye, Earthstar Geographics, CNES/Airbus DS, USDA, USGS, AeroGRID, IGN, and the GIS User Community

LANDMARK MASK



Petit Tor

Identified as natural prominence.
Identified as site: No

Contextual Information:

Nearest Node:	Torquay
Km. to Nearest Node:	5.16
Mask Area (Hectares):	16.31
Sightings (Main Analysis):	12116

LANDMARK LOCATION



Longitude: 3° 3" 3' W
Latitude: 50° 29" 28' N

Source: Esri, DigitalGlobe, GeoEye, Earthstar Geographics, CNES/Airbus DS, USDA, USGS, AeroGRID, IGN, and the GIS User Community

LANDMARK MASK



Pinhay Cliffs

Identified as natural prominence.
Identified as site: No

Contextual Information:

Nearest Node:	Seaton
Km. to Nearest Node:	6.67
Mask Area (Hectares):	23.76
Sightings (Main Analysis):	11183

LANDMARK LOCATION



Longitude: 2° 2" 27' W
Latitude: 50° 43" 12' N

Source: Esri, DigitalGlobe, GeoEye, Earthstar Geographics, CNES/Airbus DS, USDA, USGS, AeroGRID, IGN, and the GIS User Community

LANDMARK MASK



Plage De St Adresse

Identified as natural prominence.
Identified as site: No

Contextual Information:

Nearest Node:	Nacqueville
Km. to Nearest Node:	126.33
Mask Area (Hectares):	12.73
Sightings (Main Analysis):	18

LANDMARK LOCATION



Longitude: 0° 0" 15' E
Latitude: 49° 31" 23' N

Source: Esri, DigitalGlobe, GeoEye, Earthstar Geographics, CNES/Airbus DS, USDA, USGS, AeroGRID, IGN, and the GIS User Community

LANDMARK MASK



Plaidy

Identified as natural prominence.
Identified as site: No

Contextual Information:

Nearest Node:	Porthallow
Km. to Nearest Node:	6.04
Mask Area (Hectares):	29.3
Sightings (Main Analysis):	8966

LANDMARK LOCATION



Longitude: 4° 4" 11' W
Latitude: 50° 22" 20' N

Source: Esri, DigitalGlobe, GeoEye, Earthstar Geographics, CNES/Airbus DS, USDA, USGS, AeroGRID, IGN, and the GIS User Community

LANDMARK MASK



Pointe De Bachaol

Identified as natural prominence.
Identified as site: No

Contextual Information:

Nearest Node:	Aber Wrac'h
Km. to Nearest Node:	36.02
Mask Area (Hectares):	21.33
Sightings (Main Analysis):	4728

LANDMARK LOCATION



Longitude: 5° 5" 18' W
Latitude: 48° 29" 29' N

Source: Esri, DigitalGlobe, GeoEye, Earthstar Geographics, CNES/Airbus DS, USDA, USGS, AeroGRID, IGN, and the GIS User Community

LANDMARK MASK



Pointe De Pern

Identified as natural prominence.
Identified as site: No

Contextual Information:

Nearest Node:	Brest
Km. to Nearest Node:	42.53
Mask Area (Hectares):	14.87
Sightings (Main Analysis):	1089

LANDMARK LOCATION



Longitude: 5° 5" 27' W
Latitude: 48° 27" 4' N

Source: Esri, DigitalGlobe, GeoEye, Earthstar Geographics, CNES/Airbus DS, USDA, USGS, AeroGRID, IGN, and the GIS User Community

LANDMARK MASK



Pointe De Plouha

Identified as natural prominence.
Identified as site: No

Contextual Information:

Nearest Node:	Le Légnét
Km. to Nearest Node:	21.7
Mask Area (Hectares):	14.69
Sightings (Main Analysis):	7775

LANDMARK LOCATION



Longitude: 2° 2" 16' W
Latitude: 48° 41" 21' N

Source: Esri, DigitalGlobe, GeoEye, Earthstar Geographics, CNES/Airbus DS, USDA, USGS, AeroGRID, IGN, and the GIS User Community

LANDMARK MASK



Pointe Du Fourquet

Identified as natural prominence.
Identified as site: No

Contextual Information:

Nearest Node:	Nacqueville
Km. to Nearest Node:	132.22
Mask Area (Hectares):	9.72
Sightings (Main Analysis):	15

LANDMARK LOCATION



Longitude: 0° 0" 19' E
Latitude: 49° 41" 24' N

Source: Esri, DigitalGlobe, GeoEye, Earthstar Geographics, CNES/Airbus DS, USDA, USGS, AeroGRID, IGN, and the GIS User Community

LANDMARK MASK



Pointe Du Raz

Identified as natural prominence.
Identified as site: Yes

Contextual Information:

Nearest Node:	Brest
Km. to Nearest Node:	33.45
Mask Area (Hectares):	75.48
Sightings (Main Analysis):	2088

LANDMARK LOCATION



Longitude: 4° 4" 16' W
Latitude: 48° 2" 17' N

Source: Esri, DigitalGlobe, GeoEye, Earthstar Geographics, CNES/Airbus DS, USDA, USGS, AeroGRID, IGN, and the GIS User Community

LANDMARK MASK



Pointe Du Toulinguet

Identified as natural prominence.
Identified as site: Yes

Contextual Information:

Nearest Node:	Brest
Km. to Nearest Node:	5.52
Mask Area (Hectares):	37.44
Sightings (Main Analysis):	2064

LANDMARK LOCATION



Longitude: 4° 4" 27' W
Latitude: 48° 17" 14' N

Source: Esri, DigitalGlobe, GeoEye, Earthstar Geographics, CNES/Airbus DS, USDA, USGS, AeroGRID, IGN, and the GIS User Community

LANDMARK MASK



Pointe Roselier

Identified as natural prominence.
Identified as site: Yes

Contextual Information:

Nearest Node:	Le Légnét
Km. to Nearest Node:	3.52
Mask Area (Hectares):	29.55
Sightings (Main Analysis):	4884

LANDMARK LOCATION



Longitude: 2° 2" 2' W
Latitude: 48° 33" 13' N

Source: Esri, DigitalGlobe, GeoEye, Earthstar Geographics, CNES/Airbus DS, USDA, USGS, AeroGRID, IGN, and the GIS User Community

LANDMARK MASK



Polbathic

Identified as natural prominence.
Identified as site: No

Contextual Information:

Nearest Node:	Plymouth
Km. to Nearest Node:	12.72
Mask Area (Hectares):	9.27
Sightings (Main Analysis):	3785

LANDMARK LOCATION



Longitude: 4° 4" 3' W
Latitude: 50° 23" 2' N

Source: Esri, DigitalGlobe, GeoEye, Earthstar Geographics, CNES/Airbus DS, USDA, USGS, AeroGRID, IGN, and the GIS User Community

LANDMARK MASK



Polruan

Identified as natural prominence.
Identified as site: No

Contextual Information:

Nearest Node:	Fowey
Km. to Nearest Node:	1.96
Mask Area (Hectares):	77.07
Sightings (Main Analysis):	10114

LANDMARK LOCATION



Longitude: 4° 4" 16' W
Latitude: 50° 20" 19' N

Source: Esri, DigitalGlobe, GeoEye, Earthstar Geographics, CNES/Airbus DS, USDA, USGS, AeroGRID, IGN, and the GIS User Community

LANDMARK MASK



Popes Hole

Identified as natural prominence.
Identified as site: No

Contextual Information:

Nearest Node:	Penzance
Km. to Nearest Node:	56.0
Mask Area (Hectares):	18.49
Sightings (Main Analysis):	601

LANDMARK LOCATION



Longitude: 6° 6" 5' W
Latitude: 49° 58" 7' N

Source: Esri, DigitalGlobe, GeoEye, Earthstar Geographics, CNES/Airbus DS, USDA, USGS, AeroGRID, IGN, and the GIS User Community

LANDMARK MASK



Pors Pin

Identified as natural prominence.
Identified as site: No

Contextual Information:

Nearest Node:	Le Trieux
Km. to Nearest Node:	17.74
Mask Area (Hectares):	15.18
Sightings (Main Analysis):	8244

LANDMARK LOCATION



Longitude: 2° 2" 16' W
Latitude: 48° 44" 12' N

Source: Esri, DigitalGlobe, GeoEye, Earthstar Geographics, CNES/Airbus DS, USDA, USGS, AeroGRID, IGN, and the GIS User Community

LANDMARK MASK



Porte A La Reine

Identified as natural prominence.
Identified as site: No

Contextual Information:

Nearest Node:	Nacqueville
Km. to Nearest Node:	146.68
Mask Area (Hectares):	103.89
Sightings (Main Analysis):	0

LANDMARK LOCATION



Longitude: 0° 0" 2' E
Latitude: 49° 46" 6' N

Source: Esri, DigitalGlobe, GeoEye, Earthstar Geographics, CNES/Airbus DS, USDA, USGS, AeroGRID, IGN, and the GIS User Community

LANDMARK MASK



Portland Bill

Identified as natural prominence.
Identified as site: No

Contextual Information:

Nearest Node:	Portland
Km. to Nearest Node:	7.5
Mask Area (Hectares):	8.79
Sightings (Main Analysis):	11655

LANDMARK LOCATION



Longitude: 2° 2" 24' W
Latitude: 50° 31" 17' N

Source: Esri, DigitalGlobe, GeoEye, Earthstar Geographics, CNES/Airbus DS, USDA, USGS, AeroGRID, IGN, and the GIS User Community

LANDMARK MASK



Portwrinkle

Identified as natural prominence.
Identified as site: No

Contextual Information:

Nearest Node:	Plymouth
Km. to Nearest Node:	11.9
Mask Area (Hectares):	10.03
Sightings (Main Analysis):	9623

LANDMARK LOCATION



Longitude: 4° 4" 6' W
Latitude: 50° 22" 4' N

Source: Esri, DigitalGlobe, GeoEye, Earthstar Geographics, CNES/Airbus DS, USDA, USGS, AeroGRID, IGN, and the GIS User Community

LANDMARK MASK



Prawle Point

Identified as natural prominence.
Identified as site: No

Contextual Information:

Nearest Node:	Salcombe
Km. to Nearest Node:	3.44
Mask Area (Hectares):	11.51
Sightings (Main Analysis):	18467

LANDMARK LOCATION



Longitude: 3° 3" 20' W
Latitude: 50° 12" 18' N

Source: Esri, DigitalGlobe, GeoEye, Earthstar Geographics, CNES/Airbus DS, USDA, USGS, AeroGRID, IGN, and the GIS User Community

LANDMARK MASK



Predannnack

Identified as natural prominence.
Identified as site: No

Contextual Information:

Nearest Node:	Mullion
Km. to Nearest Node:	2.29
Mask Area (Hectares):	17.76
Sightings (Main Analysis):	3986

LANDMARK LOCATION



Longitude: 5° 5" 11' W
Latitude: 50° 0" 9' N

Source: Esri, DigitalGlobe, GeoEye, Earthstar Geographics, CNES/Airbus DS, USDA, USGS, AeroGRID, IGN, and the GIS User Community

LANDMARK MASK



Ragged Island

Identified as natural prominence.
Identified as site: No

Contextual Information:

Nearest Node:	Penzance
Km. to Nearest Node:	55.33
Mask Area (Hectares):	9.54
Sightings (Main Analysis):	670

LANDMARK LOCATION



Longitude: 6° 6" 14' W
Latitude: 49° 57" 17' N

Source: Esri, DigitalGlobe, GeoEye, Earthstar Geographics, CNES/Airbus DS, USDA, USGS, AeroGRID, IGN, and the GIS User Community

LANDMARK MASK



Rame Head

Identified as natural prominence.
Identified as site: Yes

Contextual Information:

Nearest Node:	Plymouth
Km. to Nearest Node:	1.93
Mask Area (Hectares):	168.0
Sightings (Main Analysis):	15826

LANDMARK LOCATION



Longitude: 4° 4" 29' W
Latitude: 50° 19" 11' N

Source: Esri, DigitalGlobe, GeoEye, Earthstar Geographics, CNES/Airbus DS, USDA, USGS, AeroGRID, IGN, and the GIS User Community

LANDMARK MASK



Ramillies Cove

Identified as natural prominence.
Identified as site: No

Contextual Information:

Nearest Node:	Bigbury Bay
Km. to Nearest Node:	2.34
Mask Area (Hectares):	8.56
Sightings (Main Analysis):	15709

LANDMARK LOCATION



Longitude: 3° 3" 11' W
Latitude: 50° 14" 22' N

Source: Esri, DigitalGlobe, GeoEye, Earthstar Geographics, CNES/Airbus DS, USDA, USGS, AeroGRID, IGN, and the GIS User Community

LANDMARK MASK



Revelstoke

Identified as natural prominence.
Identified as site: No

Contextual Information:

Nearest Node:	Mothecombe
Km. to Nearest Node:	6.12
Mask Area (Hectares):	15.2
Sightings (Main Analysis):	11972

LANDMARK LOCATION



Longitude: 4° 4" 25' W
Latitude: 50° 18" 18' N

Source: Esri, DigitalGlobe, GeoEye, Earthstar Geographics, CNES/Airbus DS, USDA, USGS, AeroGRID, IGN, and the GIS User Community

LANDMARK MASK



Round Hole

Identified as natural prominence.
Identified as site: No

Contextual Information:

Nearest Node:	Mevagissey
Km. to Nearest Node:	36.89
Mask Area (Hectares):	28.24
Sightings (Main Analysis):	0

LANDMARK LOCATION



Longitude: 5° 5" 9' W
Latitude: 50° 33" 6' N

Source: Esri, DigitalGlobe, GeoEye, Earthstar Geographics, CNES/Airbus DS, USDA, USGS, AeroGRID, IGN, and the GIS User Community

LANDMARK MASK



Rusey Beach

Identified as natural prominence.
Identified as site: No

Contextual Information:

Nearest Node:	Fowey
Km. to Nearest Node:	44.58
Mask Area (Hectares):	57.71
Sightings (Main Analysis):	0

LANDMARK LOCATION



Longitude: 4° 4" 17' W
Latitude: 50° 43" 24' N

Source: Esri, DigitalGlobe, GeoEye, Earthstar Geographics, CNES/Airbus DS, USDA, USGS, AeroGRID, IGN, and the GIS User Community

LANDMARK MASK



Saint Jouin Bruneval

Identified as natural prominence.
Identified as site: No

Contextual Information:

Nearest Node:	Nacqueville
Km. to Nearest Node:	130.5
Mask Area (Hectares):	22.48
Sightings (Main Analysis):	16

LANDMARK LOCATION



Longitude: 0° 0" 10' E
Latitude: 49° 38" 5' N

Source: Esri, DigitalGlobe, GeoEye, Earthstar Geographics, CNES/Airbus DS, USDA, USGS, AeroGRID, IGN, and the GIS User Community

LANDMARK MASK



Saint Norgard

Identified as natural prominence.
Identified as site: No

Contextual Information:

Nearest Node:	Brest
Km. to Nearest Node:	15.85
Mask Area (Hectares):	13.16
Sightings (Main Analysis):	467

LANDMARK LOCATION



Longitude: 4° 4" 28' W
Latitude: 48° 11" 30' N

Source: Esri, DigitalGlobe, GeoEye, Earthstar Geographics, CNES/Airbus DS, USDA, USGS, AeroGRID, IGN, and the GIS User Community

LANDMARK MASK



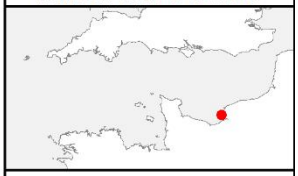
Sainte Adresse

Identified as natural prominence.
Identified as site: No

Contextual Information:

Nearest Node:	Nacqueville
Km. to Nearest Node:	126.33
Mask Area (Hectares):	36.91
Sightings (Main Analysis):	17

LANDMARK LOCATION



Longitude: 0° 0" 19' E
Latitude: 49° 31" 22' N

Source: Esri, DigitalGlobe, GeoEye, Earthstar Geographics, CNES/Airbus DS, USDA, USGS, AeroGRID, IGN, and the GIS User Community

LANDMARK MASK



Salcombe Hill

Identified as natural prominence.
Identified as site: No

Contextual Information:

Nearest Node:	Sidmouth
Km. to Nearest Node:	2.69
Mask Area (Hectares):	106.47
Sightings (Main Analysis):	12067

LANDMARK LOCATION



Longitude: 3° 3" 2' W
Latitude: 50° 41" 20' N

Source: Esri, DigitalGlobe, GeoEye, Earthstar Geographics, CNES/Airbus DS, USDA, USGS, AeroGRID, IGN, and the GIS User Community

LANDMARK MASK



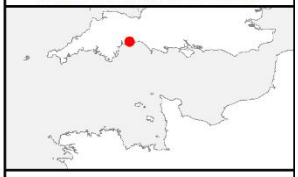
Salcombe Mouth

Identified as natural prominence.
Identified as site: No

Contextual Information:

Nearest Node:	Sidmouth
Km. to Nearest Node:	3.08
Mask Area (Hectares):	38.99
Sightings (Main Analysis):	12211

LANDMARK LOCATION



Longitude: 3° 3" 1' W
Latitude: 50° 41" 9' N

Source: Esri, DigitalGlobe, GeoEye, Earthstar Geographics, CNES/Airbus DS, USDA, USGS, AeroGRID, IGN, and the GIS User Community

LANDMARK MASK



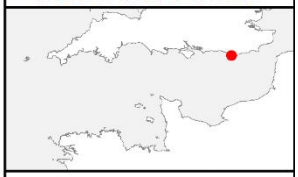
Seaford Head Camp

Identified as natural prominence.
Identified as site: Yes

Contextual Information:

Nearest Node:	Christchurch
Km. to Nearest Node:	130.16
Mask Area (Hectares):	61.27
Sightings (Main Analysis):	0

LANDMARK LOCATION



Longitude: 0° 0" 29' E
Latitude: 50° 46" 23' N

Source: Esri, DigitalGlobe, GeoEye, Earthstar Geographics, CNES/Airbus DS, USDA, USGS, AeroGRID, IGN, and the GIS User Community

LANDMARK MASK



Seaton

Identified as natural prominence.
Identified as site: No

Contextual Information:

Nearest Node:	Porthallow
Km. to Nearest Node:	9.87
Mask Area (Hectares):	24.81
Sightings (Main Analysis):	9674

LANDMARK LOCATION



Longitude: 4° 4" 18' W
Latitude: 50° 22" 1' N

Source: Esri, DigitalGlobe, GeoEye, Earthstar Geographics, CNES/Airbus DS, USDA, USGS, AeroGRID, IGN, and the GIS User Community

LANDMARK MASK



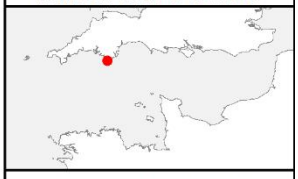
Sharp Tor

Identified as natural prominence.
Identified as site: No

Contextual Information:

Nearest Node:	Salcombe
Km. to Nearest Node:	2.55
Mask Area (Hectares):	39.09
Sightings (Main Analysis):	15658

LANDMARK LOCATION



Longitude: 3° 3" 10' W
Latitude: 50° 13" 10' N

Source: Esri, DigitalGlobe, GeoEye, Earthstar Geographics, CNES/Airbus DS, USDA, USGS, AeroGRID, IGN, and the GIS User Community

LANDMARK MASK



Shaws Corner

Identified as natural prominence.
Identified as site: No

Contextual Information:

Nearest Node:	Salcombe
Km. to Nearest Node:	4.2
Mask Area (Hectares):	24.31
Sightings (Main Analysis):	9609

LANDMARK LOCATION



Longitude: 3° 3" 24' W
Latitude: 50° 14" 4' N

Source: Esri, DigitalGlobe, GeoEye, Earthstar Geographics, CNES/Airbus DS, USDA, USGS, AeroGRID, IGN, and the GIS User Community

LANDMARK MASK



Soapy Valley

Identified as natural prominence.
Identified as site: No

Contextual Information:

Nearest Node:	Mullion
Km. to Nearest Node:	5.28
Mask Area (Hectares):	16.18
Sightings (Main Analysis):	4936

LANDMARK LOCATION



Longitude: 5° 5" 26' W
Latitude: 49° 59" 20' N

Source: Esri, DigitalGlobe, GeoEye, Earthstar Geographics, CNES/Airbus DS, USDA, USGS, AeroGRID, IGN, and the GIS User Community

LANDMARK MASK



South Hallsands

Identified as natural prominence.
Identified as site: No

Contextual Information:

Nearest Node:	Salcombe
Km. to Nearest Node:	8.22
Mask Area (Hectares):	92.62
Sightings (Main Analysis):	20987

LANDMARK LOCATION



Longitude: 3° 3" 23' W
Latitude: 50° 14" 29' N

Source: Esri, DigitalGlobe, GeoEye, Earthstar Geographics, CNES/Airbus DS, USDA, USGS, AeroGRID, IGN, and the GIS User Community

LANDMARK MASK



South Hill

Identified as natural prominence.
Identified as site: No

Contextual Information:

Nearest Node:	Penzance
Km. to Nearest Node:	63.04
Mask Area (Hectares):	13.76
Sightings (Main Analysis):	226

LANDMARK LOCATION



Longitude: 6° 6" 7' W
Latitude: 49° 56" 12' N

Source: Esri, DigitalGlobe, GeoEye, Earthstar Geographics, CNES/Airbus DS, USDA, USGS, AeroGRID, IGN, and the GIS User Community

LANDMARK MASK



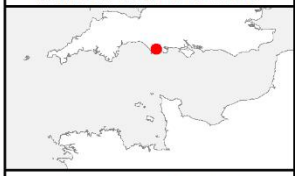
South Holworth

Identified as natural prominence.
Identified as site: No

Contextual Information:

Nearest Node:	Lulworth Cove
Km. to Nearest Node:	4.58
Mask Area (Hectares):	122.0
Sightings (Main Analysis):	8348

LANDMARK LOCATION



Longitude: 2° 2" 12' W
Latitude: 50° 38" 15' N

Source: Esri, DigitalGlobe, GeoEye, Earthstar Geographics, CNES/Airbus DS, USDA, USGS, AeroGRID, IGN, and the GIS User Community

LANDMARK MASK



Squiffiec

Identified as natural prominence.
Identified as site: No

Contextual Information:

Nearest Node:	Brest
Km. to Nearest Node:	13.22
Mask Area (Hectares):	30.19
Sightings (Main Analysis):	71

LANDMARK LOCATION



Longitude: 4° 4" 28' W
Latitude: 48° 20" 21' N

Source: Esri, DigitalGlobe, GeoEye, Earthstar Geographics, CNES/Airbus DS, USDA, USGS, AeroGRID, IGN, and the GIS User Community

LANDMARK MASK



St Agnes Beacon

Identified as natural prominence.
Identified as site: No

Contextual Information:

Nearest Node:	Falmouth
Km. to Nearest Node:	23.48
Mask Area (Hectares):	17.5
Sightings (Main Analysis):	922

LANDMARK LOCATION



Longitude: 5° 5" 4' W
Latitude: 50° 19" 27' N

Source: Esri, DigitalGlobe, GeoEye, Earthstar Geographics, CNES/Airbus DS, USDA, USGS, AeroGRID, IGN, and the GIS User Community

LANDMARK MASK



St Agnes Head 1

Identified as natural prominence.
Identified as site: No

Contextual Information:

Nearest Node:	Falmouth
Km. to Nearest Node:	24.67
Mask Area (Hectares):	22.99
Sightings (Main Analysis):	15

LANDMARK LOCATION



Longitude: 5° 5" 8' W
Latitude: 50° 19" 2' N

Source: Esri, DigitalGlobe, GeoEye, Earthstar Geographics, CNES/Airbus DS, USDA, USGS, AeroGRID, IGN, and the GIS User Community

LANDMARK MASK



St Anthony Head

Identified as natural prominence.
Identified as site: No

Contextual Information:

Nearest Node:	Falmouth
Km. to Nearest Node:	1.67
Mask Area (Hectares):	22.2
Sightings (Main Analysis):	7953

LANDMARK LOCATION



Longitude: 5° 5" 24' W
Latitude: 50° 9" 28' N

Source: Esri, DigitalGlobe, GeoEye, Earthstar Geographics, CNES/Airbus DS, USDA, USGS, AeroGRID, IGN, and the GIS User Community

LANDMARK MASK



St Boniface Down

Identified as natural prominence.
Identified as site: No

Contextual Information:

Nearest Node:	Christchurch
Km. to Nearest Node:	37.89
Mask Area (Hectares):	235.04
Sightings (Main Analysis):	2132

LANDMARK LOCATION



Longitude: 1° 1" 4' W
Latitude: 50° 36" 30' N

Source: Esri, DigitalGlobe, GeoEye, Earthstar Geographics, CNES/Airbus DS, USDA, USGS, AeroGRID, IGN, and the GIS User Community

LANDMARK MASK



St Erney

Identified as natural prominence.
Identified as site: No

Contextual Information:

Nearest Node:	Plymouth
Km. to Nearest Node:	12.79
Mask Area (Hectares):	9.91
Sightings (Main Analysis):	1057

LANDMARK LOCATION



Longitude: 4° 4" 25' W
Latitude: 50° 24" 20' N

Source: Esri, DigitalGlobe, GeoEye, Earthstar Geographics, CNES/Airbus DS, USDA, USGS, AeroGRID, IGN, and the GIS User Community

LANDMARK MASK



St Gennys

Identified as natural prominence.
Identified as site: No

Contextual Information:

Nearest Node:	Fowey
Km. to Nearest Node:	48.39
Mask Area (Hectares):	34.49
Sightings (Main Analysis):	0

LANDMARK LOCATION



Longitude: 4° 4" 15' W
Latitude: 50° 45" 22' N

Source: Esri, DigitalGlobe, GeoEye, Earthstar Geographics, CNES/Airbus DS, USDA, USGS, AeroGRID, IGN, and the GIS User Community

LANDMARK MASK



St Margarets At Cliffe

Identified as natural prominence.
Identified as site: No

Contextual Information:

Nearest Node:	Christchurch
Km. to Nearest Node:	224.13
Mask Area (Hectares):	26.7
Sightings (Main Analysis):	0

LANDMARK LOCATION



Longitude: 1° 1" 26' E
Latitude: 51° 9" 22' N

Source: Esri, DigitalGlobe, GeoEye, Earthstar Geographics, CNES/Airbus DS, USDA, USGS, AeroGRID, IGN, and the GIS User Community

LANDMARK MASK



St Margarets At Cliffe 1

Identified as natural prominence.
Identified as site: No

Contextual Information:

Nearest Node:	Christchurch
Km. to Nearest Node:	221.41
Mask Area (Hectares):	61.95
Sightings (Main Analysis):	0

LANDMARK LOCATION



Longitude: 1° 1" 3' E
Latitude: 51° 8" 20' N

Source: Esri, DigitalGlobe, GeoEye, Earthstar Geographics, CNES/Airbus DS, USDA, USGS, AeroGRID, IGN, and the GIS User Community

LANDMARK MASK



St Martins Point

Identified as natural prominence.
Identified as site: No

Contextual Information:

Nearest Node:	St Peter Port South
Km. to Nearest Node:	4.2
Mask Area (Hectares):	44.42
Sightings (Main Analysis):	13019

LANDMARK LOCATION



Longitude: 2° 2" 5' W
Latitude: 49° 25" 26' N

Source: Esri, DigitalGlobe, GeoEye, Earthstar Geographics, CNES/Airbus DS, USDA, USGS, AeroGRID, IGN, and the GIS User Community

LANDMARK MASK



Steeple 1

Identified as natural prominence.
Identified as site: No

Contextual Information:

Nearest Node:	Kimmeridge Bay
Km. to Nearest Node:	2.47
Mask Area (Hectares):	76.22
Sightings (Main Analysis):	7291

LANDMARK LOCATION



Longitude: 2° 2" 30' W
Latitude: 50° 37" 4' N

Source: Esri, DigitalGlobe, GeoEye, Earthstar Geographics, CNES/Airbus DS, USDA, USGS, AeroGRID, IGN, and the GIS User Community

LANDMARK MASK



Steeple Cove

Identified as natural prominence.
Identified as site: No

Contextual Information:

Nearest Node:	Salcombe
Km. to Nearest Node:	3.58
Mask Area (Hectares):	53.1
Sightings (Main Analysis):	18435

LANDMARK LOCATION



Longitude: 3° 3" 4' W
Latitude: 50° 13" 9' N

Source: Esri, DigitalGlobe, GeoEye, Earthstar Geographics, CNES/Airbus DS, USDA, USGS, AeroGRID, IGN, and the GIS User Community

LANDMARK MASK



Strete

Identified as natural prominence.
Identified as site: No

Contextual Information:

Nearest Node:	Dartmouth
Km. to Nearest Node:	7.08
Mask Area (Hectares):	55.63
Sightings (Main Analysis):	12015

LANDMARK LOCATION



Longitude: 3° 3" 13' W
Latitude: 50° 18" 27' N

Source: Esri, DigitalGlobe, GeoEye, Earthstar Geographics, CNES/Airbus DS, USDA, USGS, AeroGRID, IGN, and the GIS User Community

LANDMARK MASK



Studland Hill

Identified as natural prominence.
Identified as site: No

Contextual Information:

Nearest Node:	Poole
Km. to Nearest Node:	3.79
Mask Area (Hectares):	96.55
Sightings (Main Analysis):	4528

LANDMARK LOCATION



Longitude: 1° 1" 1' W
Latitude: 50° 38" 6' N

Source: Esri, DigitalGlobe, GeoEye, Earthstar Geographics, CNES/Airbus DS, USDA, USGS, AeroGRID, IGN, and the GIS User Community

LANDMARK MASK



Swyre

Identified as natural prominence.
Identified as site: No

Contextual Information:

Nearest Node:	Portland
Km. to Nearest Node:	22.9
Mask Area (Hectares):	10.47
Sightings (Main Analysis):	8425

LANDMARK LOCATION



Longitude: 2° 2" 1' W
Latitude: 50° 42" 28' N

Source: Esri, DigitalGlobe, GeoEye, Earthstar Geographics, CNES/Airbus DS, USDA, USGS, AeroGRID, IGN, and the GIS User Community

LANDMARK MASK



Swyre Head

Identified as natural prominence.
Identified as site: No

Contextual Information:

Nearest Node:	Kimmeridge Bay
Km. to Nearest Node:	3.56
Mask Area (Hectares):	81.95
Sightings (Main Analysis):	7579

LANDMARK LOCATION



Longitude: 2° 2" 1' W
Latitude: 50° 37" 18' N

Source: Esri, DigitalGlobe, GeoEye, Earthstar Geographics, CNES/Airbus DS, USDA, USGS, AeroGRID, IGN, and the GIS User Community

LANDMARK MASK



Talland

Identified as natural prominence.
Identified as site: No

Contextual Information:

Nearest Node:	Porthallow
Km. to Nearest Node:	3.17
Mask Area (Hectares):	43.25
Sightings (Main Analysis):	12550

LANDMARK LOCATION



Longitude: 4° 4" 15' W
Latitude: 50° 20" 15' N

Source: Esri, DigitalGlobe, GeoEye, Earthstar Geographics, CNES/Airbus DS, USDA, USGS, AeroGRID, IGN, and the GIS User Community

LANDMARK MASK



Telegraph Bay

Identified as natural prominence.
Identified as site: No

Contextual Information:

Nearest Node:	St Peter Port North
Km. to Nearest Node:	27.3
Mask Area (Hectares):	19.54
Sightings (Main Analysis):	13857

LANDMARK LOCATION



Longitude: 2° 2" 22' W
Latitude: 49° 42" 16' N

Source: Esri, DigitalGlobe, GeoEye, Earthstar Geographics, CNES/Airbus DS, USDA, USGS, AeroGRID, IGN, and the GIS User Community

LANDMARK MASK



The Beacon

Identified as natural prominence.
Identified as site: No

Contextual Information:

Nearest Node:	Teignmouth
Km. to Nearest Node:	1.57
Mask Area (Hectares):	112.31
Sightings (Main Analysis):	11804

LANDMARK LOCATION



Longitude: 3° 3" 23' W
Latitude: 50° 32" 25' N

Source: Esri, DigitalGlobe, GeoEye, Earthstar Geographics, CNES/Airbus DS, USDA, USGS, AeroGRID, IGN, and the GIS User Community

LANDMARK MASK



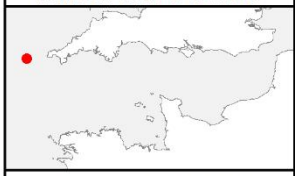
The Garrison

Identified as natural prominence.
Identified as site: No

Contextual Information:

Nearest Node:	Penzance
Km. to Nearest Node:	61.65
Mask Area (Hectares):	27.11
Sightings (Main Analysis):	429

LANDMARK LOCATION



Longitude: 6° 6" 20' W
Latitude: 49° 55" 17' N

Source: Esri, DigitalGlobe, GeoEye, Earthstar Geographics, CNES/Airbus DS, USDA, USGS, AeroGRID, IGN, and the GIS User Community

LANDMARK MASK



The Grove

Identified as natural prominence.
Identified as site: No

Contextual Information:

Nearest Node:	Portland
Km. to Nearest Node:	3.4
Mask Area (Hectares):	43.57
Sightings (Main Analysis):	9359

LANDMARK LOCATION



Longitude: 2° 2" 20' W
Latitude: 50° 33" 4' N

Source: Esri, DigitalGlobe, GeoEye, Earthstar Geographics, CNES/Airbus DS, USDA, USGS, AeroGRID, IGN, and the GIS User Community

LANDMARK MASK



The Narrows

Identified as natural prominence.
Identified as site: No

Contextual Information:

Nearest Node:	Salcombe
Km. to Nearest Node:	7.51
Mask Area (Hectares):	24.25
Sightings (Main Analysis):	16730

LANDMARK LOCATION



Longitude: 3° 3" 12' W
Latitude: 50° 13" 28' N

Source: Esri, DigitalGlobe, GeoEye, Earthstar Geographics, CNES/Airbus DS, USDA, USGS, AeroGRID, IGN, and the GIS User Community

LANDMARK MASK



Theuville

Identified as natural prominence.
Identified as site: No

Contextual Information:

Nearest Node:	Nacqueville
Km. to Nearest Node:	131.55
Mask Area (Hectares):	54.9
Sightings (Main Analysis):	16

LANDMARK LOCATION



Longitude: 0° 0" 11' E
Latitude: 49° 41" 23' N

Source: Esri, DigitalGlobe, GeoEye, Earthstar Geographics, CNES/Airbus DS, USDA, USGS, AeroGRID, IGN, and the GIS User Community

LANDMARK MASK



Thorncombe Beacon

Identified as natural prominence.
Identified as site: No

Contextual Information:

Nearest Node:	Seaton
Km. to Nearest Node:	17.35
Mask Area (Hectares):	75.81
Sightings (Main Analysis):	9427

LANDMARK LOCATION



Longitude: 2° 2" 3' W
Latitude: 50° 43" 22' N

Source: Esri, DigitalGlobe, GeoEye, Earthstar Geographics, CNES/Airbus DS, USDA, USGS, AeroGRID, IGN, and the GIS User Community

LANDMARK MASK



Tilly Whim Caves

Identified as natural prominence.
Identified as site: No

Contextual Information:

Nearest Node:	Poole
Km. to Nearest Node:	8.47
Mask Area (Hectares):	31.19
Sightings (Main Analysis):	6227

LANDMARK LOCATION



Longitude: 1° 1" 26' W
Latitude: 50° 36" 15' N

Source: Esri, DigitalGlobe, GeoEye, Earthstar Geographics, CNES/Airbus DS, USDA, USGS, AeroGRID, IGN, and the GIS User Community

LANDMARK MASK



Tintagel

Identified as natural prominence.
Identified as site: No

Contextual Information:

Nearest Node:	Fowey
Km. to Nearest Node:	39.93
Mask Area (Hectares):	26.53
Sightings (Main Analysis):	0

LANDMARK LOCATION



Longitude: 4° 4" 19' W
Latitude: 50° 40" 23' N

Source: Esri, DigitalGlobe, GeoEye, Earthstar Geographics, CNES/Airbus DS, USDA, USGS, AeroGRID, IGN, and the GIS User Community

LANDMARK MASK



Titchberry

Identified as natural prominence.
Identified as site: No

Contextual Information:

Nearest Node:	Porthallow
Km. to Nearest Node:	79.46
Mask Area (Hectares):	14.69
Sightings (Main Analysis):	0

LANDMARK LOCATION



Longitude: 4° 4" 18' W
Latitude: 51° 1" 12' N

Source: Esri, DigitalGlobe, GeoEye, Earthstar Geographics, CNES/Airbus DS, USDA, USGS, AeroGRID, IGN, and the GIS User Community

LANDMARK MASK



Torcross

Identified as natural prominence.
Identified as site: No

Contextual Information:

Nearest Node:	Dartmouth
Km. to Nearest Node:	10.51
Mask Area (Hectares):	30.09
Sightings (Main Analysis):	12909

LANDMARK LOCATION



Longitude: 3° 3" 22' W
Latitude: 50° 16" 10' N

Source: Esri, DigitalGlobe, GeoEye, Earthstar Geographics, CNES/Airbus DS, USDA, USGS, AeroGRID, IGN, and the GIS User Community

LANDMARK MASK



Tregonhawke

Identified as natural prominence.
Identified as site: No

Contextual Information:

Nearest Node:	Plymouth
Km. to Nearest Node:	4.33
Mask Area (Hectares):	57.5
Sightings (Main Analysis):	14665

LANDMARK LOCATION



Longitude: 4° 4" 13' W
Latitude: 50° 20" 18' N

Source: Esri, DigitalGlobe, GeoEye, Earthstar Geographics, CNES/Airbus DS, USDA, USGS, AeroGRID, IGN, and the GIS User Community

LANDMARK MASK



Trevalga

Identified as natural prominence.
Identified as site: No

Contextual Information:

Nearest Node:	Fowey
Km. to Nearest Node:	42.17
Mask Area (Hectares):	8.52
Sightings (Main Analysis):	0

LANDMARK LOCATION



Longitude: 4° 4" 24' W
Latitude: 50° 41" 3' N

Source: Esri, DigitalGlobe, GeoEye, Earthstar Geographics, CNES/Airbus DS, USDA, USGS, AeroGRID, IGN, and the GIS User Community

LANDMARK MASK



Trevarder

Identified as natural prominence.
Identified as site: No

Contextual Information:

Nearest Node:	Fowey
Km. to Nearest Node:	2.99
Mask Area (Hectares):	46.77
Sightings (Main Analysis):	10495

LANDMARK LOCATION



Longitude: 4° 4" 7' W
Latitude: 50° 20" 12' N

Source: Esri, DigitalGlobe, GeoEye, Earthstar Geographics, CNES/Airbus DS, USDA, USGS, AeroGRID, IGN, and the GIS User Community

LANDMARK MASK



Trevescan Cliff

Identified as natural prominence.
Identified as site: No

Contextual Information:

Nearest Node:	Penzance
Km. to Nearest Node:	14.99
Mask Area (Hectares):	13.22
Sightings (Main Analysis):	838

LANDMARK LOCATION



Longitude: 5° 5" 13' W
Latitude: 50° 4" 0' N

Source: Esri, DigitalGlobe, GeoEye, Earthstar Geographics, CNES/Airbus DS, USDA, USGS, AeroGRID, IGN, and the GIS User Community

LANDMARK MASK



Trevigue Cottage

Identified as natural prominence.
Identified as site: No

Contextual Information:

Nearest Node:	Fowey
Km. to Nearest Node:	46.62
Mask Area (Hectares):	57.16
Sightings (Main Analysis):	0

LANDMARK LOCATION



Longitude: 4° 4" 16' W
Latitude: 50° 44" 4' N

Source: Esri, DigitalGlobe, GeoEye, Earthstar Geographics, CNES/Airbus DS, USDA, USGS, AeroGRID, IGN, and the GIS User Community

LANDMARK MASK



Trewinney Barton

Identified as natural prominence.
Identified as site: No

Contextual Information:

Nearest Node:	Mevagissey
Km. to Nearest Node:	2.17
Mask Area (Hectares):	13.04
Sightings (Main Analysis):	7551

LANDMARK LOCATION



Longitude: 4° 4" 1' W
Latitude: 50° 17" 15' N

Source: Esri, DigitalGlobe, GeoEye, Earthstar Geographics, CNES/Airbus DS, USDA, USGS, AeroGRID, IGN, and the GIS User Community

LANDMARK MASK



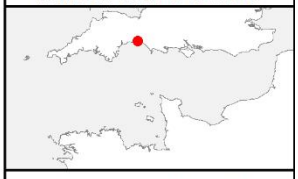
Uplyme

Identified as natural prominence.
Identified as site: No

Contextual Information:

Nearest Node:	Seaton
Km. to Nearest Node:	8.98
Mask Area (Hectares):	25.97
Sightings (Main Analysis):	7080

LANDMARK LOCATION



Longitude: 2° 2" 11' W
Latitude: 50° 44" 20' N

Source: Esri, DigitalGlobe, GeoEye, Earthstar Geographics, CNES/Airbus DS, USDA, USGS, AeroGRID, IGN, and the GIS User Community

LANDMARK MASK



Vattetot Sur Mer

Identified as natural prominence.
Identified as site: No

Contextual Information:

Nearest Node:	Nacqueville
Km. to Nearest Node:	139.88
Mask Area (Hectares):	14.09
Sightings (Main Analysis):	4

LANDMARK LOCATION



Longitude: 0° 0" 11' E
Latitude: 49° 44" 5' N

Source: Esri, DigitalGlobe, GeoEye, Earthstar Geographics, CNES/Airbus DS, USDA, USGS, AeroGRID, IGN, and the GIS User Community

LANDMARK MASK



Vaux Du Catel

Identified as natural prominence.
Identified as site: Yes

Contextual Information:

Nearest Node:	Nacqueville
Km. to Nearest Node:	19.31
Mask Area (Hectares):	54.98
Sightings (Main Analysis):	11822

LANDMARK LOCATION



Longitude: 1° 1" 23' W
Latitude: 49° 41" 27' N

Source: Esri, DigitalGlobe, GeoEye, Earthstar Geographics, CNES/Airbus DS, USDA, USGS, AeroGRID, IGN, and the GIS User Community

LANDMARK MASK



Watch Croft

Identified as natural prominence.
Identified as site: No

Contextual Information:

Nearest Node:	Penzance
Km. to Nearest Node:	10.36
Mask Area (Hectares):	27.79
Sightings (Main Analysis):	2372

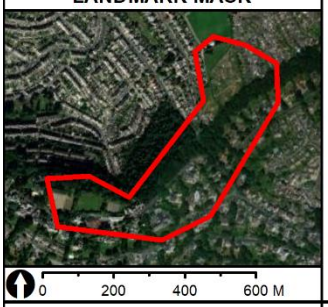
LANDMARK LOCATION



Longitude: 5° 5" 6' W
Latitude: 50° 10" 5' N

Source: Esri, DigitalGlobe, GeoEye, Earthstar Geographics, CNES/Airbus DS, USDA, USGS, AeroGRID, IGN, and the GIS User Community

LANDMARK MASK



Wellswood

Identified as natural prominence.
Identified as site: No

Contextual Information:

Nearest Node:	Torquay
Km. to Nearest Node:	2.85
Mask Area (Hectares):	14.99
Sightings (Main Analysis):	13210

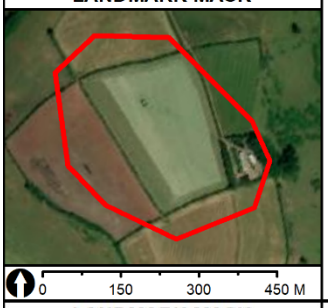
LANDMARK LOCATION



Longitude: 3° 3" 9' W
Latitude: 50° 28" 13' N

Source: Esri, DigitalGlobe, GeoEye, Earthstar Geographics, CNES/Airbus DS, USDA, USGS, AeroGRID, IGN, and the GIS User Community

LANDMARK MASK



Weston

Identified as natural prominence.
Identified as site: No

Contextual Information:

Nearest Node:	Torquay
Km. to Nearest Node:	10.79
Mask Area (Hectares):	11.24
Sightings (Main Analysis):	530

LANDMARK LOCATION



Longitude: 3° 3" 27' W
Latitude: 50° 25" 8' N

Source: Esri, DigitalGlobe, GeoEye, Earthstar Geographics, CNES/Airbus DS, USDA, USGS, AeroGRID, IGN, and the GIS User Community

LANDMARK MASK



Weston 1

Identified as natural prominence.
Identified as site: No

Contextual Information:

Nearest Node:	Portland
Km. to Nearest Node:	5.24
Mask Area (Hectares):	14.67
Sightings (Main Analysis):	8600

LANDMARK LOCATION



Longitude: 2° 2" 9' W
Latitude: 50° 33" 24' N

Source: Esri, DigitalGlobe, GeoEye, Earthstar Geographics, CNES/Airbus DS, USDA, USGS, AeroGRID, IGN, and the GIS User Community

LANDMARK MASK



Winspit 1

Identified as natural prominence.
Identified as site: No

Contextual Information:

Nearest Node:	Kimmeridge Bay
Km. to Nearest Node:	6.38
Mask Area (Hectares):	43.98
Sightings (Main Analysis):	7796

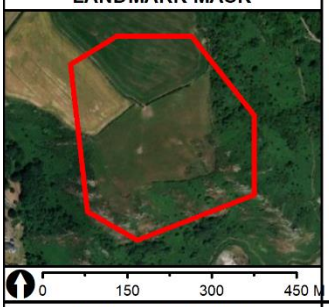
LANDMARK LOCATION



Longitude: 2° 2" 5' W
Latitude: 50° 35" 8' N

Source: Esri, DigitalGlobe, GeoEye, Earthstar Geographics, CNES/Airbus DS, USDA, USGS, AeroGRID, IGN, and the GIS User Community

LANDMARK MASK



Woodcombe

Identified as natural prominence.
Identified as site: No

Contextual Information:

Nearest Node:	Salcombe
Km. to Nearest Node:	5.86
Mask Area (Hectares):	9.16
Sightings (Main Analysis):	14705

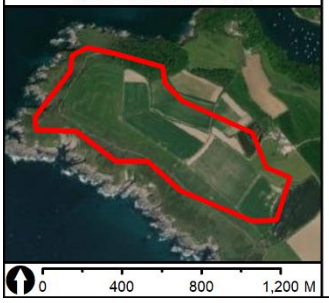
LANDMARK LOCATION



Longitude: 3° 3" 22' W
Latitude: 50° 13" 5' N

Source: Esri, DigitalGlobe, GeoEye, Earthstar Geographics, CNES/Airbus DS, USDA, USGS, AeroGRID, IGN, and the GIS User Community

LANDMARK MASK



Worswell Barton

Identified as natural prominence.
Identified as site: No

Contextual Information:

Nearest Node:	Mothecombe
Km. to Nearest Node:	2.1
Mask Area (Hectares):	51.18
Sightings (Main Analysis):	14924

LANDMARK LOCATION



Longitude: 4° 4" 6' W
Latitude: 50° 18" 18' N

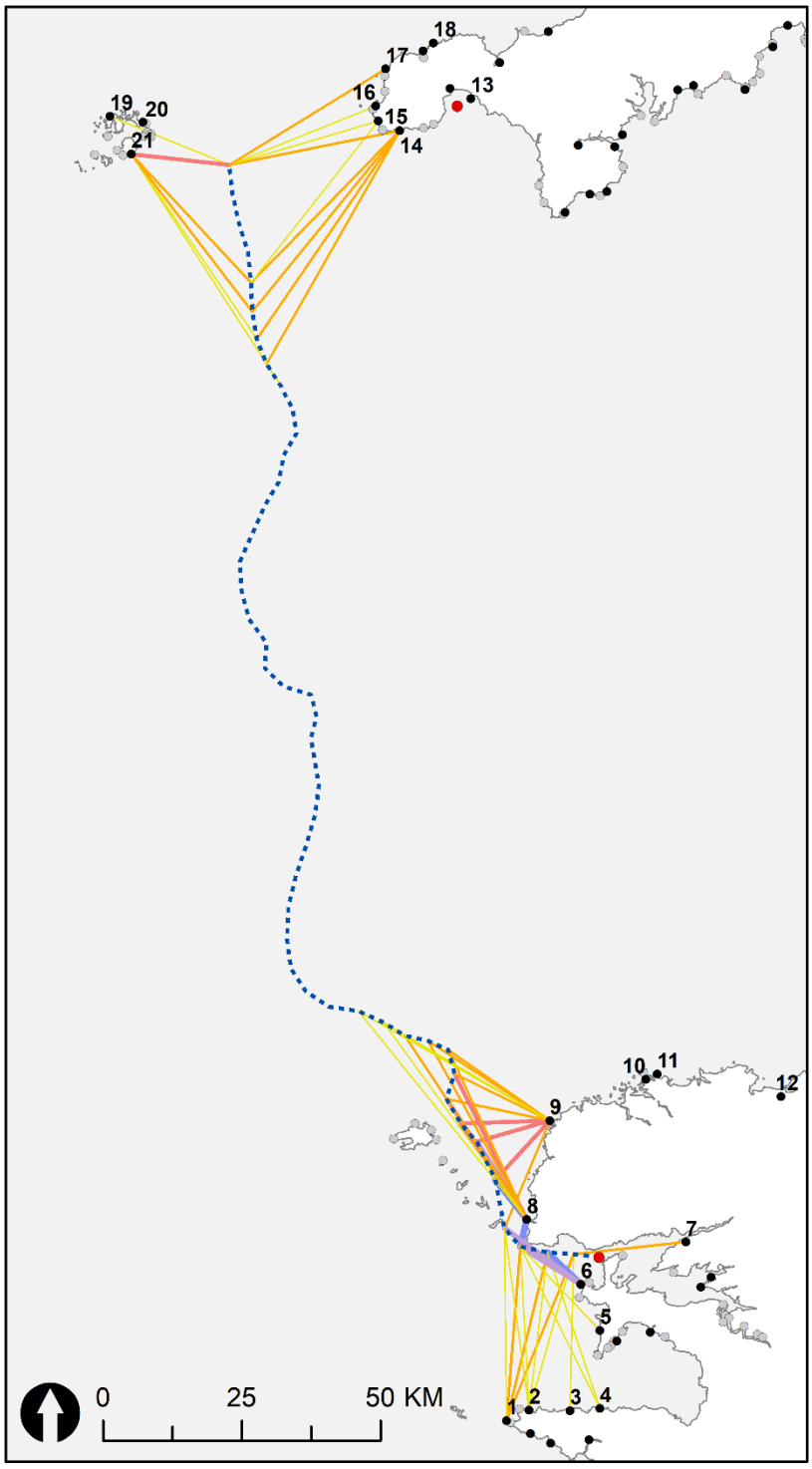
Source: Esri, DigitalGlobe, GeoEye, Earthstar Geographics, CNES/Airbus DS, USDA, USGS, AeroGRID, IGN, and the GIS User Community

APPENDIX III

This appendix contains plots showing the results of Case Study 3. In each plot relevant parameters are summarised in the box in the upper left. The map area shows the track of the simulated vessel, and sight-lines graded by the apparent size of the landmark being sighted. Archaeological sites are symbolised by a black circle, and are labelled; natural prominences are not labelled and are symbolised by a grey circle. Only landmarks that were sighted in this Case Study are shown.

Plots in this appendix are summarised in the following table:

Name	Landmark Type	Estimation	Start Time	Result
Simulation 01	Archaeological Sites	No Misestimation	-2	Potential Success
Simulation 02	Archaeological Sites	No Misestimation	-1	Potential Success
Simulation 03	Archaeological Sites	No Misestimation	+0	Potential Success
Simulation 04	Archaeological Sites	No Misestimation	+1	Failure
Simulation 05	Archaeological Sites	No Misestimation	+2	Failure
Simulation 06	Natural Prominences	No Misestimation	-2	Potential Success
Simulation 07	Natural Prominences	No Misestimation	-1	Potential Success
Simulation 08	Natural Prominences	No Misestimation	+0	Potential Success
Simulation 09	Natural Prominences	No Misestimation	+1	Potential Success
Simulation 10	Natural Prominences	No Misestimation	+2	Failure
Simulation 11	Archaeological Sites	No Misestimation	-2	Qualified Success
Simulation 12	Archaeological Sites	No Misestimation	-1	Qualified Success
Simulation 13	Archaeological Sites	No Misestimation	+0	Success
Simulation 14	Archaeological Sites	No Misestimation	+1	Qualified Success
Simulation 15	Archaeological Sites	No Misestimation	+2	Qualified Success
Simulation 16	Natural Prominences	No Misestimation	-2	Qualified Success
Simulation 17	Natural Prominences	No Misestimation	-1	Qualified Success
Simulation 18	Natural Prominences	No Misestimation	+0	Potential Success
Simulation 19	Natural Prominences	No Misestimation	+1	Potential Success
Simulation 20	Natural Prominences	No Misestimation	+2	Qualified Success
Simulation 21	Archaeological Sites	No Misestimation	-2	Qualified Success
Simulation 22	Archaeological Sites	No Misestimation	-1	Qualified Success
Simulation 23	Archaeological Sites	No Misestimation	+0	Success
Simulation 24	Archaeological Sites	No Misestimation	+1	Qualified Success
Simulation 25	Archaeological Sites	No Misestimation	+2	Potential Success
Simulation 26	Natural Prominences	No Misestimation	-2	Success
Simulation 27	Natural Prominences	No Misestimation	-1	Qualified Success
Simulation 28	Natural Prominences	No Misestimation	+0	Qualified Success
Simulation 29	Natural Prominences	No Misestimation	+1	Qualified Success
Simulation 30	Natural Prominences	No Misestimation	+2	Qualified Success
Simulation 31	Archaeological Sites	Up to 50%	-2	Failure
Simulation 32	Archaeological Sites	Up to 50%	-1	Failure
Simulation 33	Archaeological Sites	Up to 50%	+0	Failure
Simulation 34	Archaeological Sites	Up to 50%	+1	Failure
Simulation 35	Archaeological Sites	Up to 50%	+2	Failure
Simulation 36	Natural Prominences	Up to 50%	-2	Failure
Simulation 37	Natural Prominences	Up to 50%	-1	Failure
Simulation 38	Natural Prominences	Up to 50%	+0	Failure



Simulation 01

Max speed: 5 kts.
Lmark. type: Arch. sites
Estimation: No misest.
Starting time: -2 hrs.
Result: Potential Success

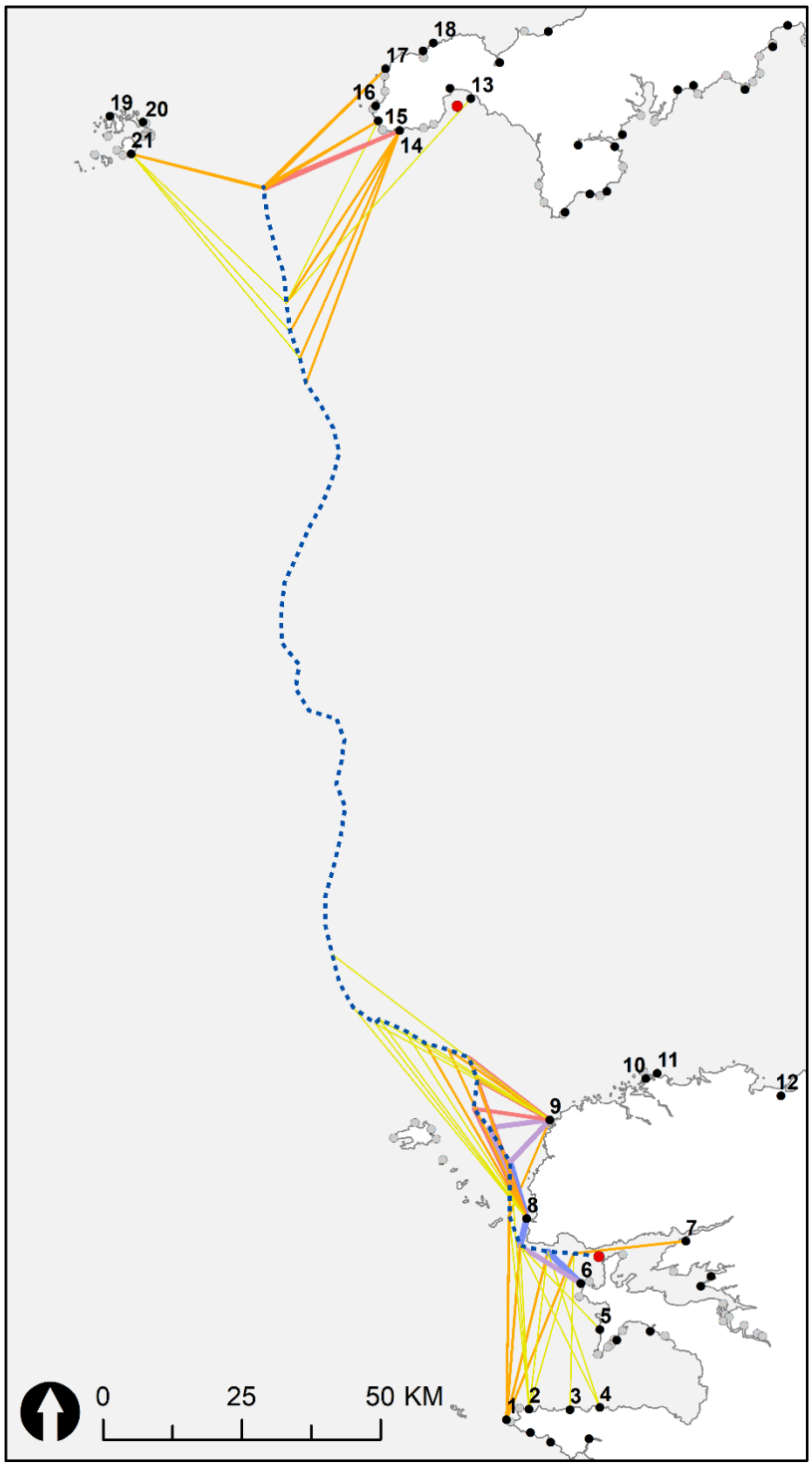
- Coastal Nodes
- Archaeological Sites
- Natural Prominences
- Simulation Track

Sightlines (by Apparent Size)

- 0-1 sq. deg.
- 1-2 sq. deg.
- 2-5 sq. deg.
- 5-15 sq. deg.
- 15-100 sq. deg.

Sites Referenced:

1 - Pointe du Raz
2 - Castel Meur
3 - Kergulan
4 - Castel Coz
5 - Lostmarc'h
6 - Pointe du Toulinguet
7 - Roc'h Nivelen
8 - Kermorvan
9 - Île d'Yoc'h
10 - Kastell Ac'h
11 - Beg Monom
12 - Bretouare
13 - St. Michael's Mount
14 - Treryn Dinas
15 - Carn Les Boel
16 - Maen Castle
17 - Kenidjack Castle
18 - Trereen Dinas
19 - Shipman Head
20 - Burnt Hill
21 - Giants Castle



Simulation 02

Max speed: 5 kts.
Lmark. type: Arch. sites
Estimation: No misest.
Starting time: -1 hrs.
Result: Potential Success

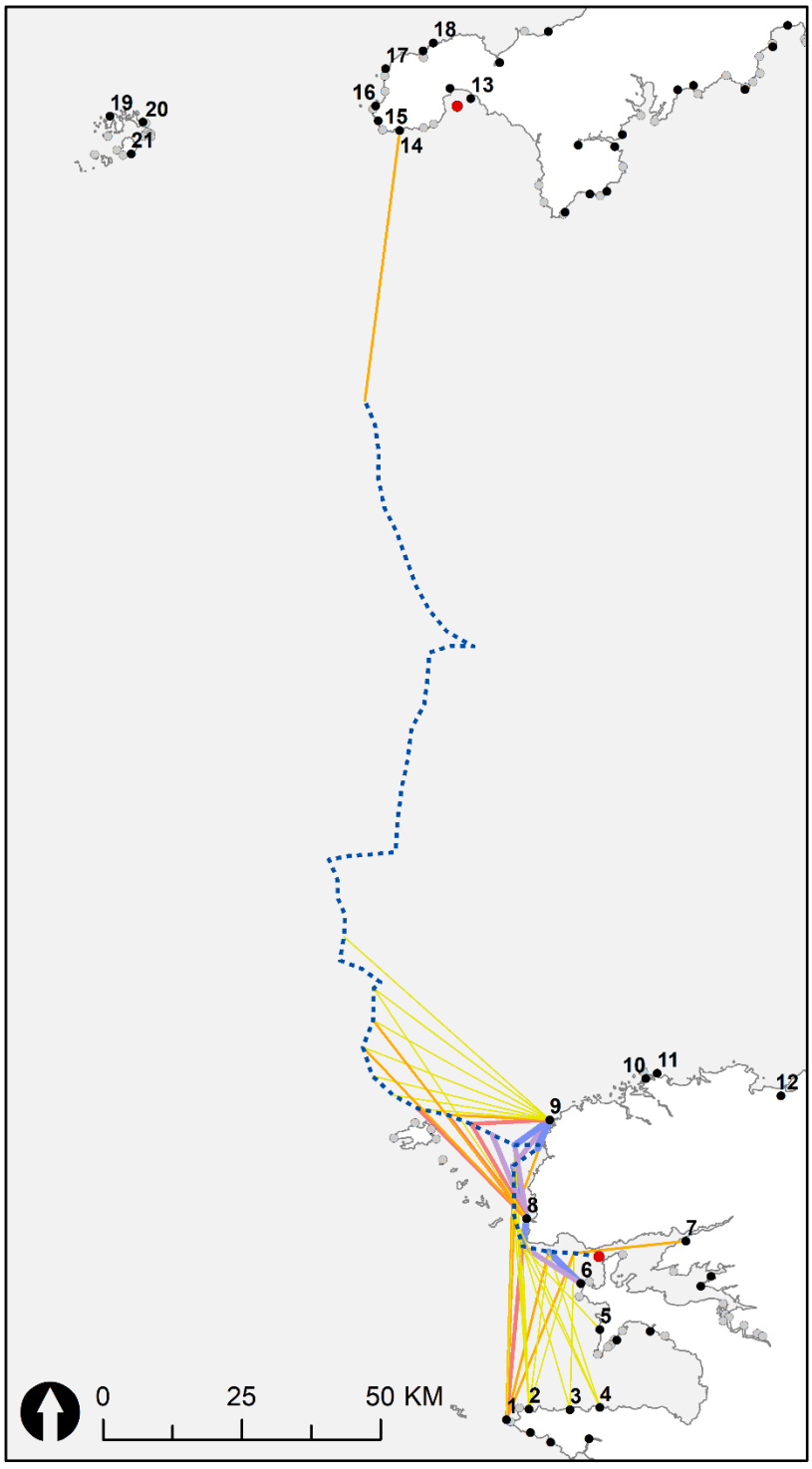
- Coastal Nodes
- Archaeological Sites
- Natural Prominences
- Simulation Track

Sightlines (by Apparent Size)

- 0-1 sq. deg.
- 1-2 sq. deg.
- 2-5 sq. deg.
- 5-15 sq. deg.
- 15-100 sq. deg.

Sites Referenced:

1 - Pointe du Raz
2 - Castel Meur
3 - Kergulan
4 - Castel Coz
5 - Lostmarc'h
6 - Pointe du Toulinguet
7 - Roc'h Nivelen
8 - Kermorvan
9 - Île d'Yoc'h
10 - Kastell Ac'h
11 - Beg Monom
12 - Bretouare
13 - St. Michael's Mount
14 - Treryn Dinas
15 - Carn Les Boel
16 - Maen Castle
17 - Kenidjack Castle
18 - Trereen Dinas
19 - Shipman Head
20 - Burnt Hill
21 - Giants Castle



Simulation 03

Max speed: 5 kts.
Lmark. type: Arch. sites
Estimation: No misest.
Starting time: +0 hrs.
Result: Potential Success

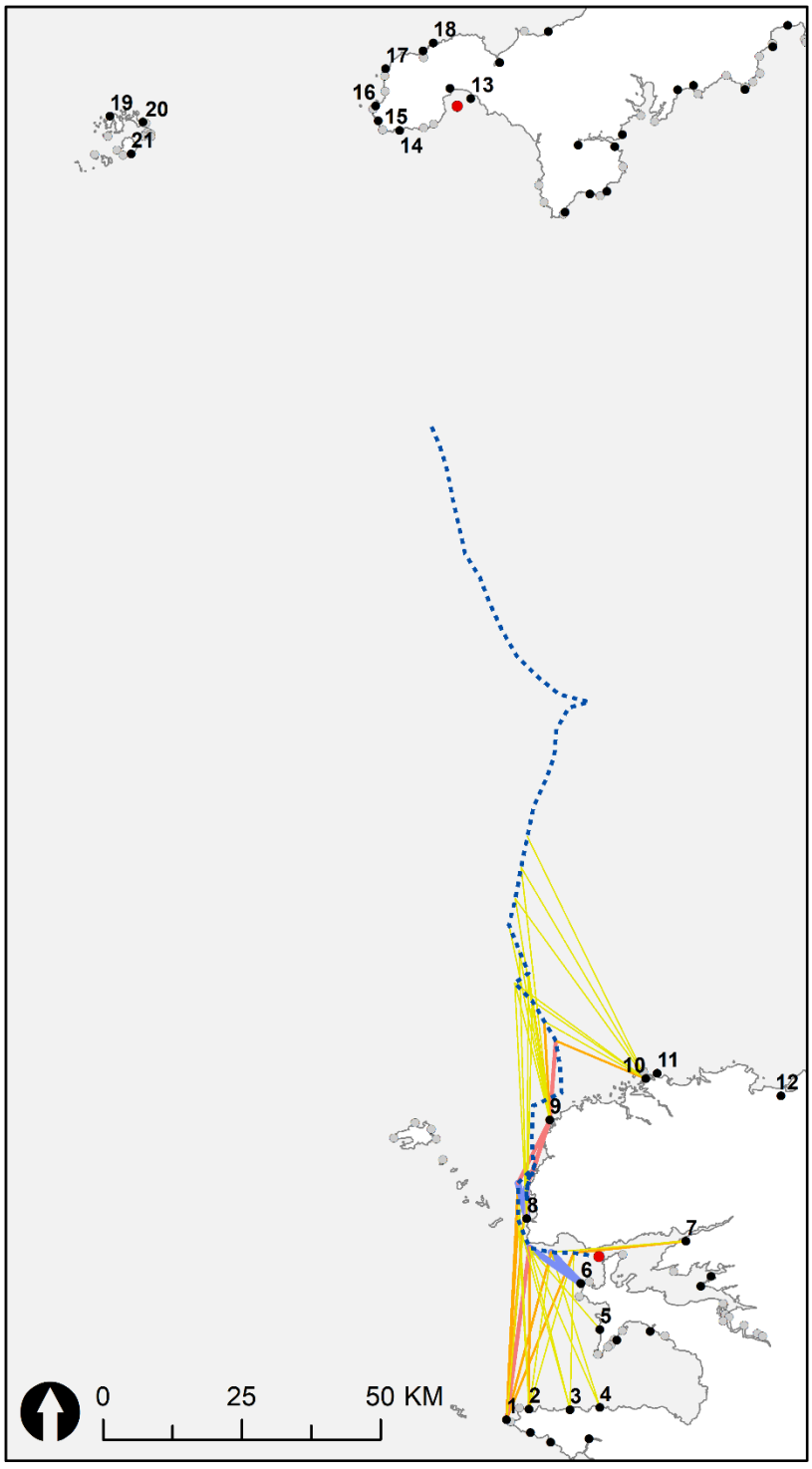
- Coastal Nodes
- Archaeological Sites
- Natural Prominences
- Simulation Track

Sightlines (by Apparent Size)

- 0-1 sq. deg.
- 1-2 sq. deg.
- 2-5 sq. deg.
- 5-15 sq. deg.
- 15-100 sq. deg.

Sites Referenced:

1 - Pointe du Raz
2 - Castel Meur
3 - Kergulan
4 - Castel Coz
5 - Lostmarc'h
6 - Pointe du Toulinguet
7 - Roc'h Nivelen
8 - Kermorvan
9 - Île d'Yoc'h
10 - Kastell Ac'h
11 - Beg Monom
12 - Bretouare
13 - St. Michael's Mount
14 - Treryn Dinas
15 - Carn Les Boel
16 - Maen Castle
17 - Kenidjack Castle
18 - Trereen Dinas
19 - Shipman Head
20 - Burnt Hill
21 - Giants Castle



Simulation 04

Max speed: 5 kts.
Lmark. type: Arch. sites
Estimation: No misest.
Starting time: +1 hrs.
Result: Failure

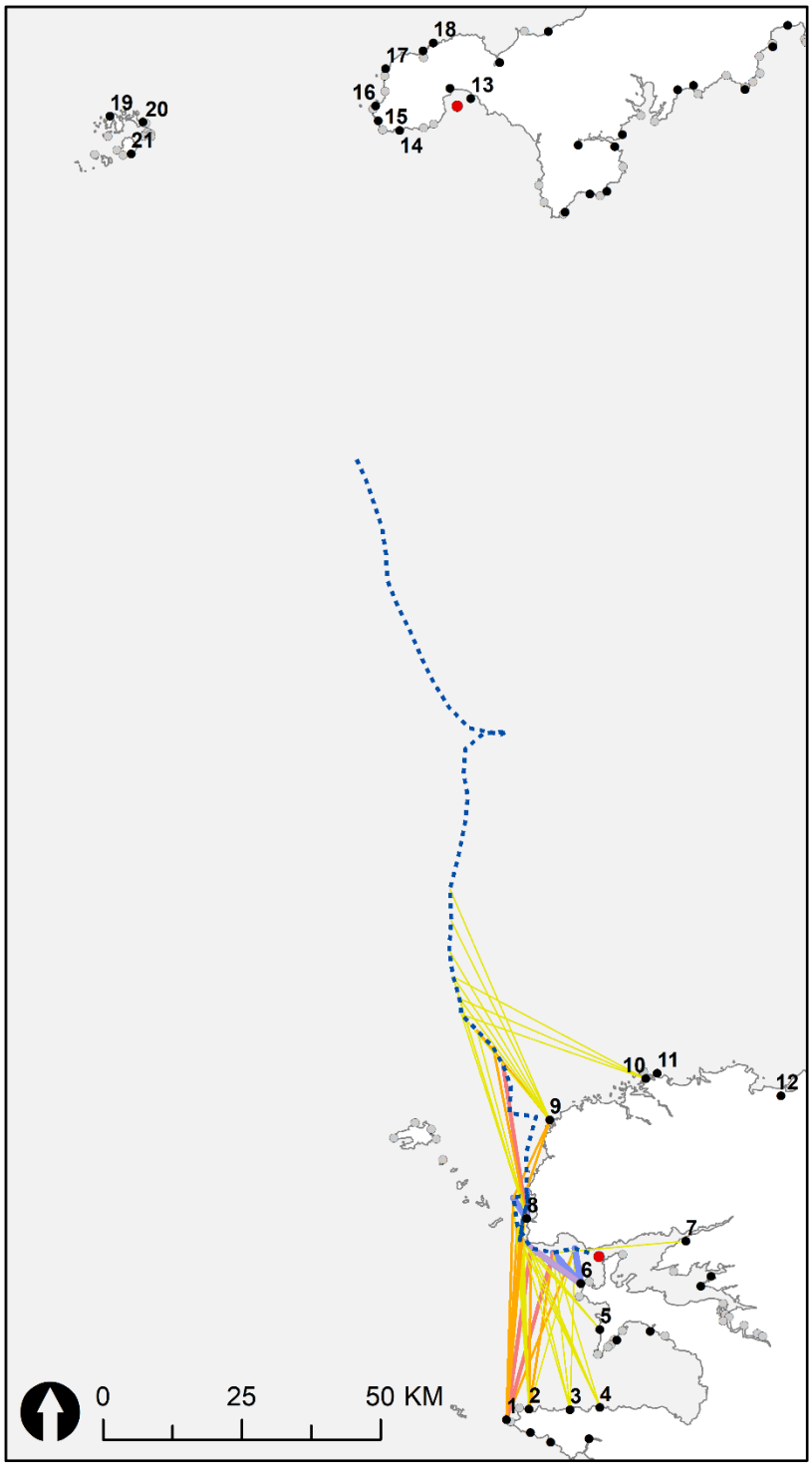
- Coastal Nodes
- Archaeological Sites
- Natural Prominences
- Simulation Track

Sightlines (by Apparent Size)

- 0-1 sq. deg.
- 1-2 sq. deg.
- 2-5 sq. deg.
- 5-15 sq. deg.
- 15-100 sq. deg.

Sites Referenced:

1 - Pointe du Raz
2 - Castel Meur
3 - Kergulan
4 - Castel Coz
5 - Lostmarc'h
6 - Pointe du Toulinguet
7 - Roc'h Nivelen
8 - Kermorvan
9 - Île d'Yoc'h
10 - Kastell Ac'h
11 - Beg Monom
12 - Bretouare
13 - St. Michael's Mount
14 - Treryn Dinas
15 - Carn Les Boel
16 - Maen Castle
17 - Kenidjack Castle
18 - Trereen Dinas
19 - Shipman Head
20 - Burnt Hill
21 - Giants Castle



Simulation 05

Max speed: 5 kts.
Lmark. type: Arch. sites
Estimation: No misest.
Starting time: +2 hrs.
Result: Failure

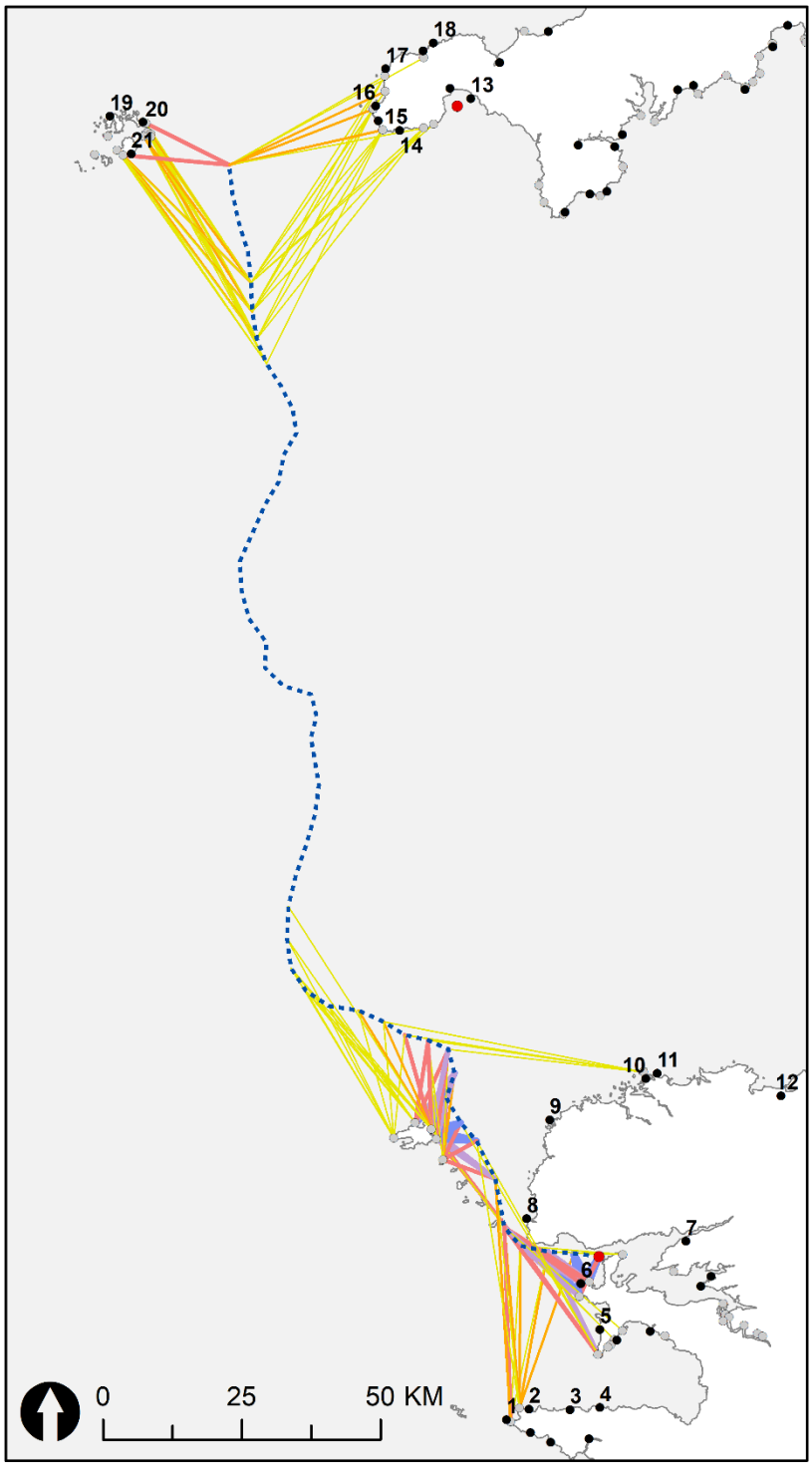
- Coastal Nodes
- Archaeological Sites
- Natural Prominences
- Simulation Track

Sightlines (by Apparent Size)

- 0-1 sq. deg.
- 1-2 sq. deg.
- 2-5 sq. deg.
- 5-15 sq. deg.
- 15-100 sq. deg.

Sites Referenced:

1 - Pointe du Raz
2 - Castel Meur
3 - Kergulan
4 - Castel Coz
5 - Lostmarc'h
6 - Pointe du Toulinguet
7 - Roc'h Nivelen
8 - Kermorvan
9 - Île d'Yoc'h
10 - Kastell Ac'h
11 - Beg Monom
12 - Bretouare
13 - St. Michael's Mount
14 - Treryn Dinas
15 - Carn Les Boel
16 - Maen Castle
17 - Kenidjack Castle
18 - Trereen Dinas
19 - Shipman Head
20 - Burnt Hill
21 - Giants Castle



Simulation 06

Max speed: 5 kts.
Lmark. type: Nat. proms.
Estimation: No misest.
Starting time: -2 hrs.
Result: Potential Success

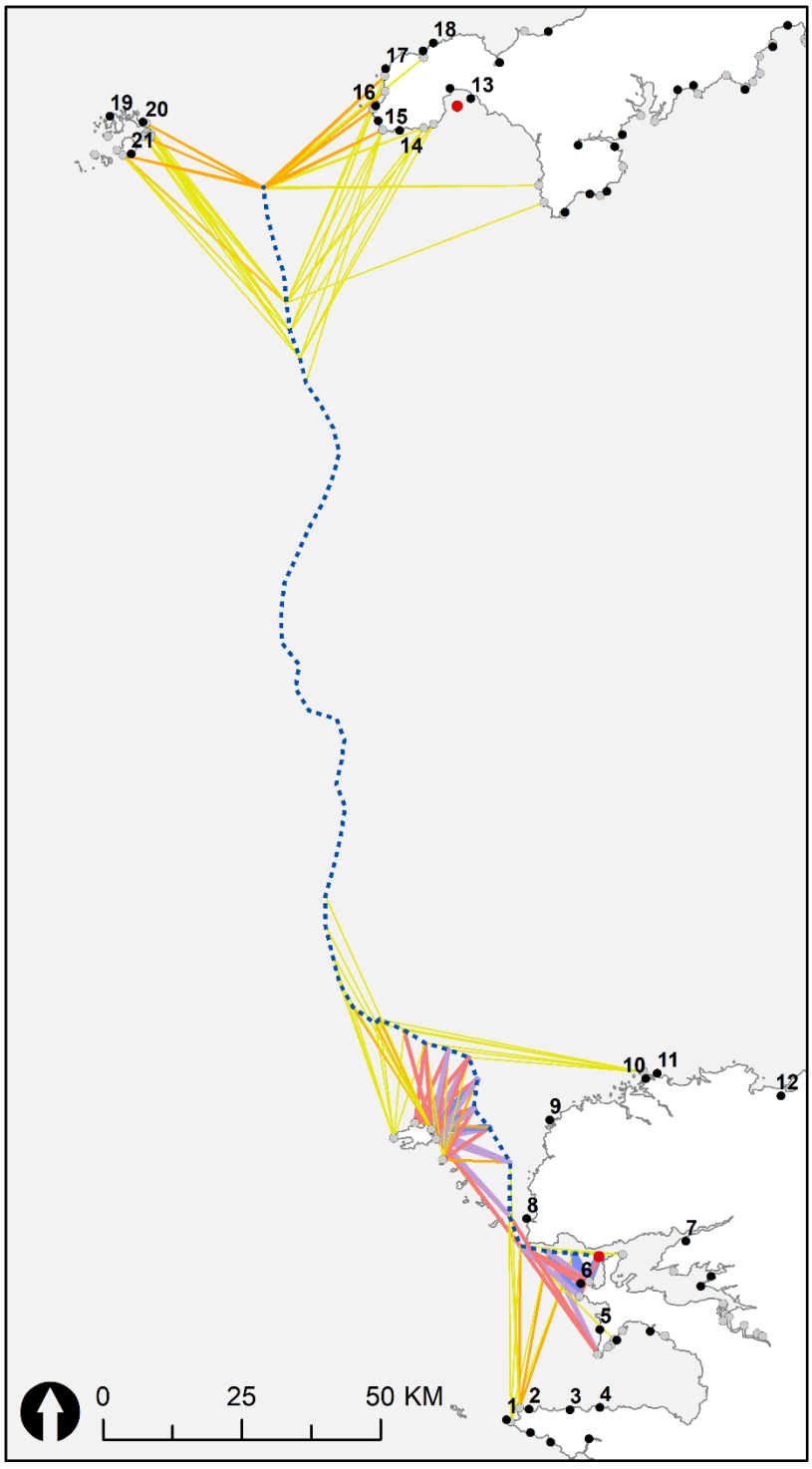
- Coastal Nodes
- Archaeological Sites
- Natural Prominences
- Simulation Track

Sightlines (by Apparent Size)

- 0-1 sq. deg.
- 1-2 sq. deg.
- 2-5 sq. deg.
- 5-15 sq. deg.
- 15-100 sq. deg.

Sites Referenced:

1 - Pointe du Raz
2 - Castel Meur
3 - Kergulan
4 - Castel Coz
5 - Lostmarc'h
6 - Pointe du Toulinguet
7 - Roc'h Nivelen
8 - Kermorvan
9 - Île d'Yoc'h
10 - Kastell Ac'h
11 - Beg Monom
12 - Bretouare
13 - St. Michael's Mount
14 - Treryn Dinas
15 - Carn Les Boel
16 - Maen Castle
17 - Kenidjack Castle
18 - Trereen Dinas
19 - Shipman Head
20 - Burnt Hill
21 - Giants Castle



Simulation 07

Max speed: 5 kts.
Lmark. type: Nat. proms.
Estimation: No misest.
Starting time: -1 hrs.
Result: Potential Success

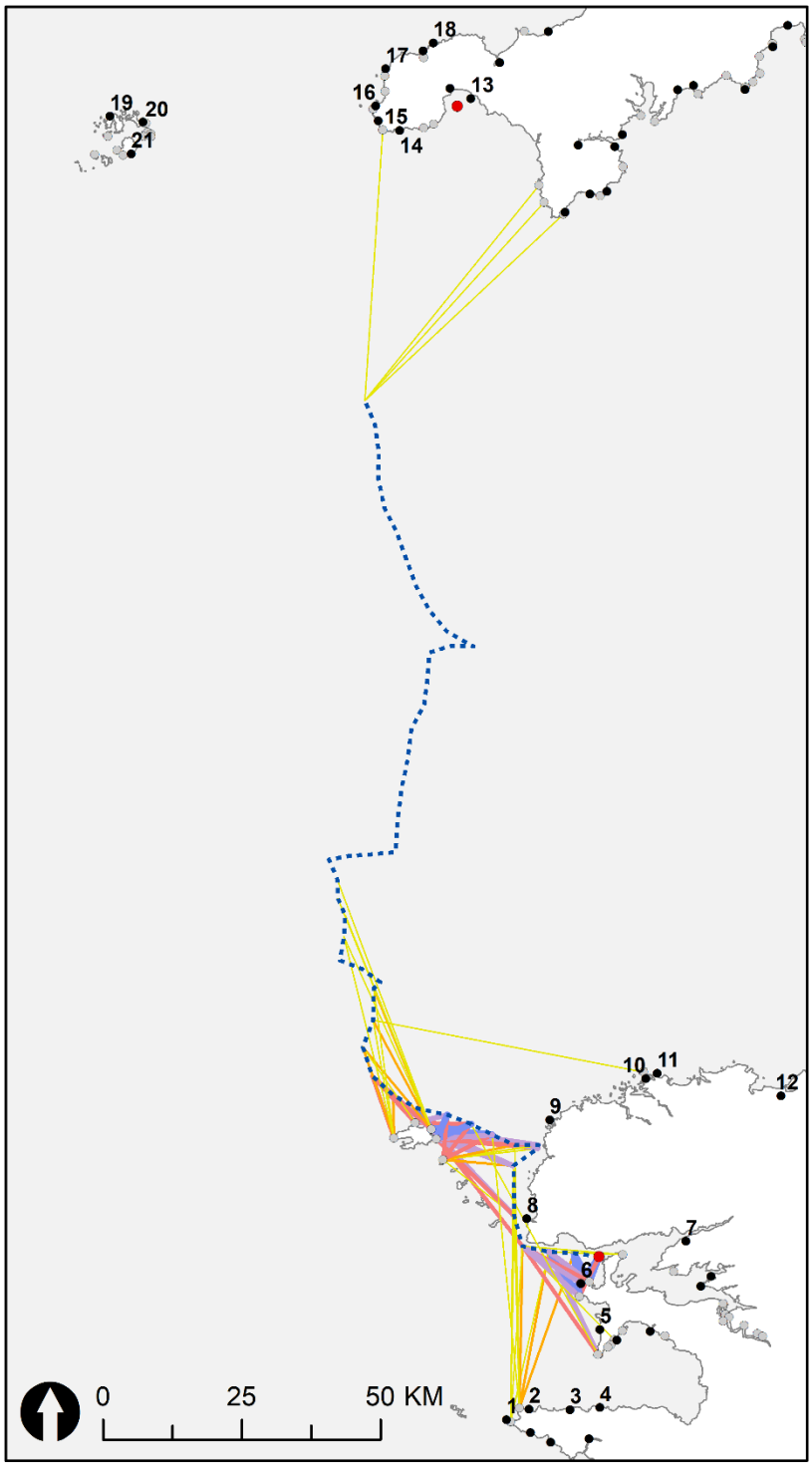
- Coastal Nodes
- Archaeological Sites
- Natural Prominences
- Simulation Track

Sightlines (by Apparent Size)

- 0-1 sq. deg.
- 1-2 sq. deg.
- 2-5 sq. deg.
- 5-15 sq. deg.
- 15-100 sq. deg.

Sites Referenced:

1 - Pointe du Raz
2 - Castel Meur
3 - Kergulan
4 - Castel Coz
5 - Lostmarc'h
6 - Pointe du Toulinguet
7 - Roc'h Nivelen
8 - Kermorvan
9 - Île d'Yoc'h
10 - Kastell Ac'h
11 - Beg Monom
12 - Bretouare
13 - St. Michael's Mount
14 - Treryn Dinas
15 - Carn Les Boel
16 - Maen Castle
17 - Kenidjack Castle
18 - Trereen Dinas
19 - Shipman Head
20 - Burnt Hill
21 - Giants Castle



Simulation 08

Max speed: 5 kts.
Lmark. type: Nat. proms.
Estimation: No misest.
Starting time: 0 hrs.
Result: Potential Success

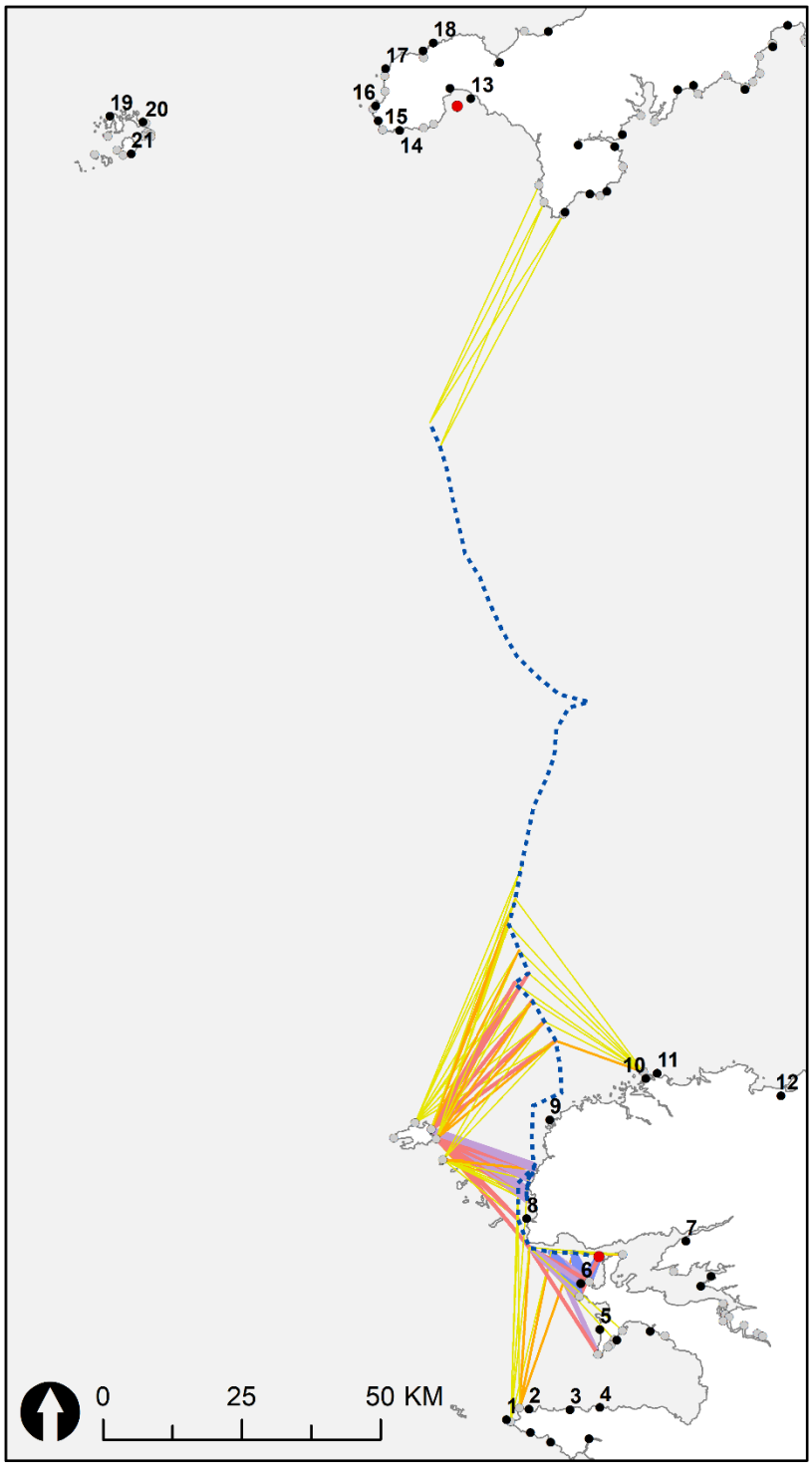
- Coastal Nodes
- Archaeological Sites
- Natural Prominences
- Simulation Track

Sightlines (by Apparent Size)

- 0-1 sq. deg.
- 1-2 sq. deg.
- 2-5 sq. deg.
- 5-15 sq. deg.
- 15-100 sq. deg.

Sites Referenced:

1 - Pointe du Raz
2 - Castel Meur
3 - Kergulan
4 - Castel Coz
5 - Lostmarc'h
6 - Pointe du Toulinguet
7 - Roc'h Nivelen
8 - Kermorvan
9 - Île d'Yoc'h
10 - Kastell Ac'h
11 - Beg Monom
12 - Bretouare
13 - St. Michael's Mount
14 - Treryn Dinas
15 - Carn Les Boel
16 - Maen Castle
17 - Kenidjack Castle
18 - Trereen Dinas
19 - Shipman Head
20 - Burnt Hill
21 - Giants Castle



Simulation 09

Max speed: 5 kts.
Lmark. type: Nat. proms.
Estimation: No misest.
Starting time: +1 hrs.
Result: Potential Success

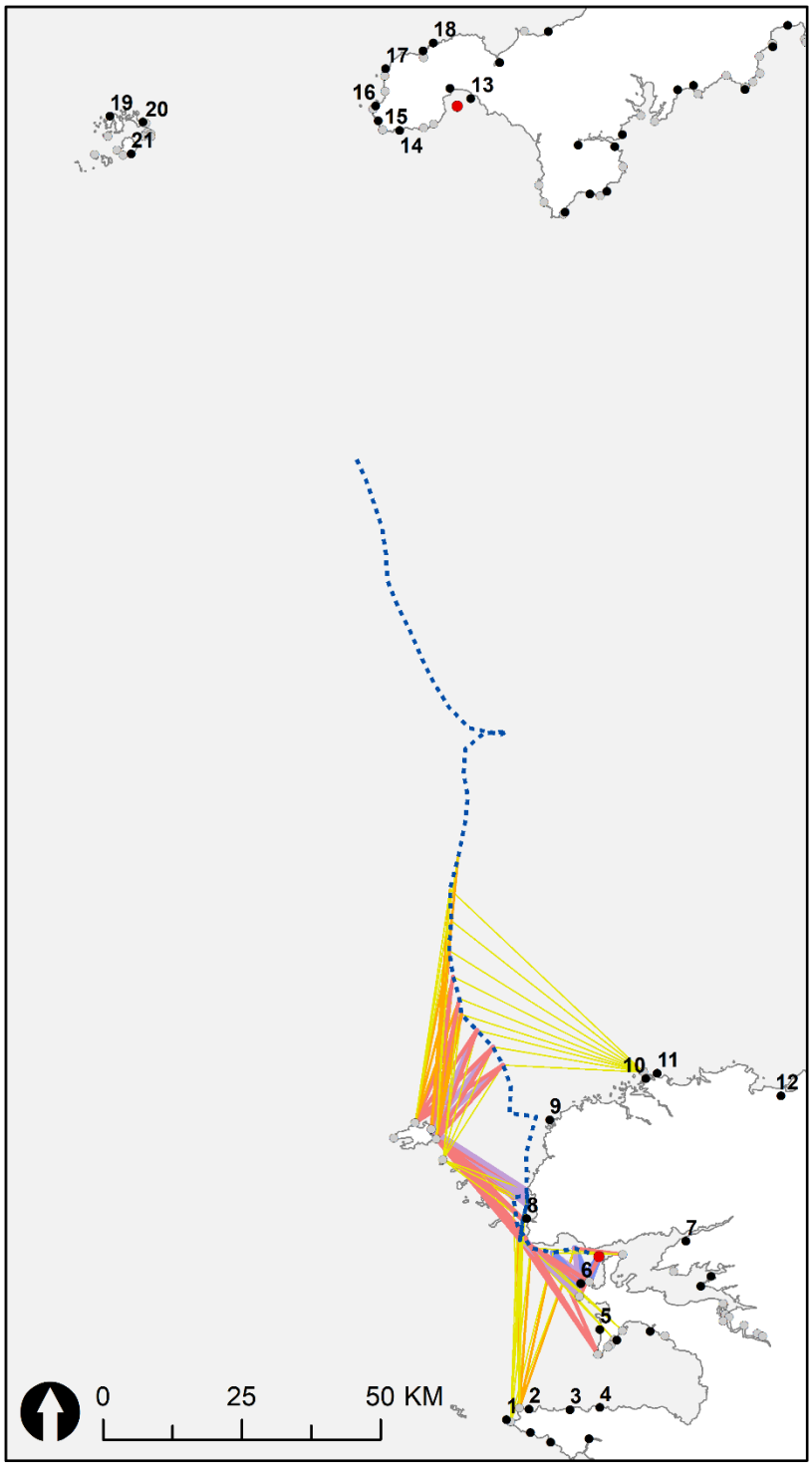
- Coastal Nodes
- Archaeological Sites
- Natural Prominences
- Simulation Track

Sightlines (by Apparent Size)

- 0-1 sq. deg.
- 1-2 sq. deg.
- 2-5 sq. deg.
- 5-15 sq. deg.
- 15-100 sq. deg.

Sites Referenced:

1 - Pointe du Raz
2 - Castel Meur
3 - Kergulan
4 - Castel Coz
5 - Lostmarc'h
6 - Pointe du Toulinguet
7 - Roc'h Nivelen
8 - Kermorvan
9 - Île d'Yoc'h
10 - Kastell Ac'h
11 - Beg Monom
12 - Bretouare
13 - St. Michael's Mount
14 - Treryn Dinas
15 - Carn Les Boel
16 - Maen Castle
17 - Kenidjack Castle
18 - Trereen Dinas
19 - Shipman Head
20 - Burnt Hill
21 - Giants Castle



Simulation 10

Max speed: 5 kts.
Lmark. type: Nat. proms.
Estimation: No misest.
Starting time: +2 hrs.
Result: Potential Success

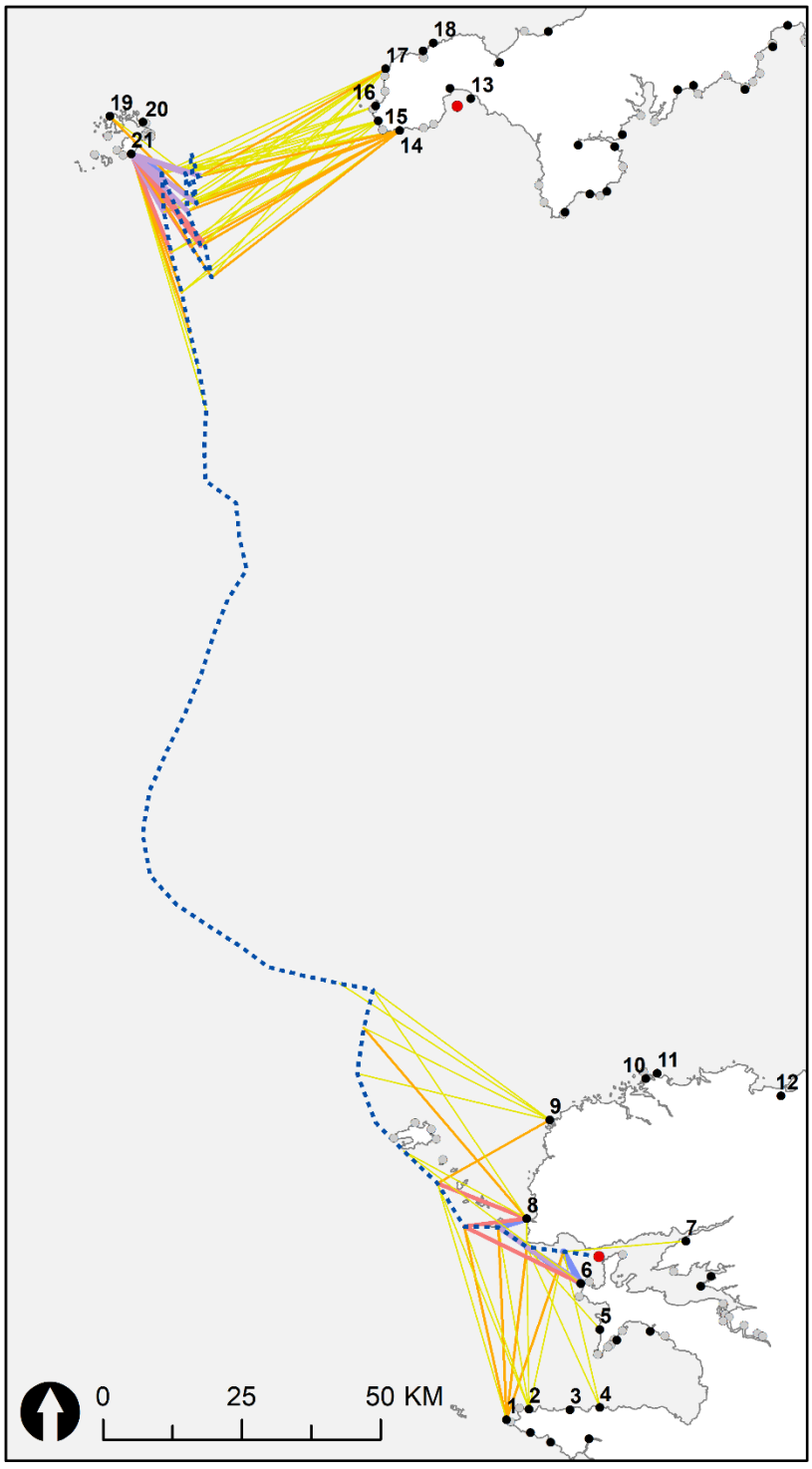
- Coastal Nodes
- Archaeological Sites
- Natural Prominences
- Simulation Track

Sightlines (by Apparent Size)

- 0-1 sq. deg.
- 1-2 sq. deg.
- 2-5 sq. deg.
- 5-15 sq. deg.
- 15-100 sq. deg.

Sites Referenced:

1 - Pointe du Raz
2 - Castel Meur
3 - Kergulan
4 - Castel Coz
5 - Lostmarc'h
6 - Pointe du Toulinguet
7 - Roc'h Nivelen
8 - Kermorvan
9 - Île d'Yoc'h
10 - Kastell Ac'h
11 - Beg Monom
12 - Bretouare
13 - St. Michael's Mount
14 - Treryn Dinas
15 - Carn Les Boel
16 - Maen Castle
17 - Kenidjack Castle
18 - Trereen Dinas
19 - Shipman Head
20 - Burnt Hill
21 - Giants Castle



Simulation 11

Max speed: 7 kts.
Lmark. type: Arch. sites.
Estimation: No misest.
Starting time: -2 hrs.
Result: Qualified Success

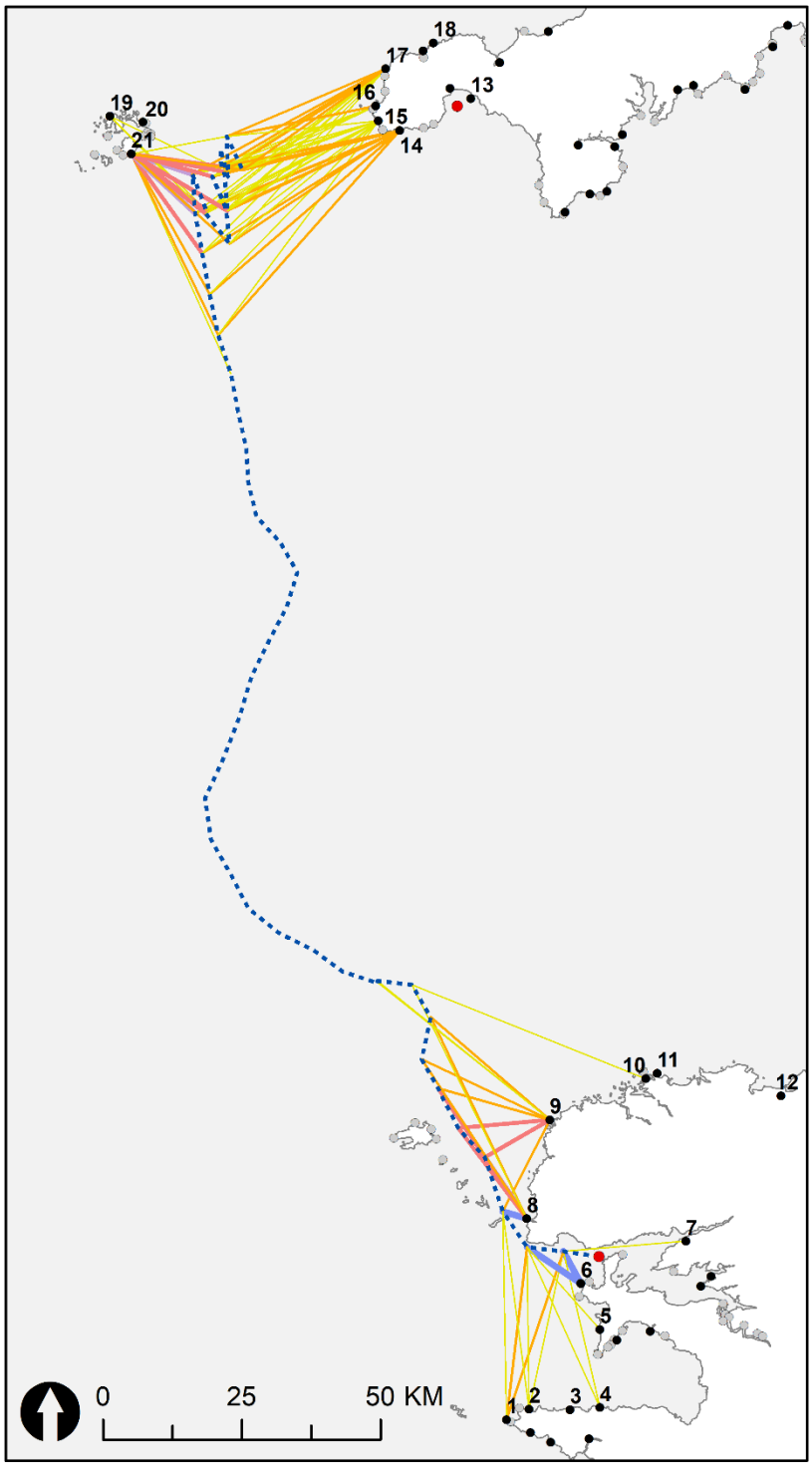
- Coastal Nodes
- Archaeological Sites
- Natural Prominences
- Simulation Track

Sightlines (by Apparent Size)

- 0-1 sq. deg.
- 1-2 sq. deg.
- 2-5 sq. deg.
- 5-15 sq. deg.
- 15-100 sq. deg.

Sites Referenced:

1 - Pointe du Raz
2 - Castel Meur
3 - Kergulan
4 - Castel Coz
5 - Lostmarc'h
6 - Pointe du Toulinguet
7 - Roc'h Nivelen
8 - Kermorvan
9 - Île d'Yoc'h
10 - Kastell Ac'h
11 - Beg Monom
12 - Bretouare
13 - St. Michael's Mount
14 - Treryn Dinas
15 - Carn Les Boel
16 - Maen Castle
17 - Kenidjack Castle
18 - Trereen Dinas
19 - Shipman Head
20 - Burnt Hill
21 - Giants Castle



Simulation 12

Max speed: 7 kts.
Lmark. type: Arch. sites.
Estimation: No misest.
Starting time: -1 hrs.
Result: Qualified Success

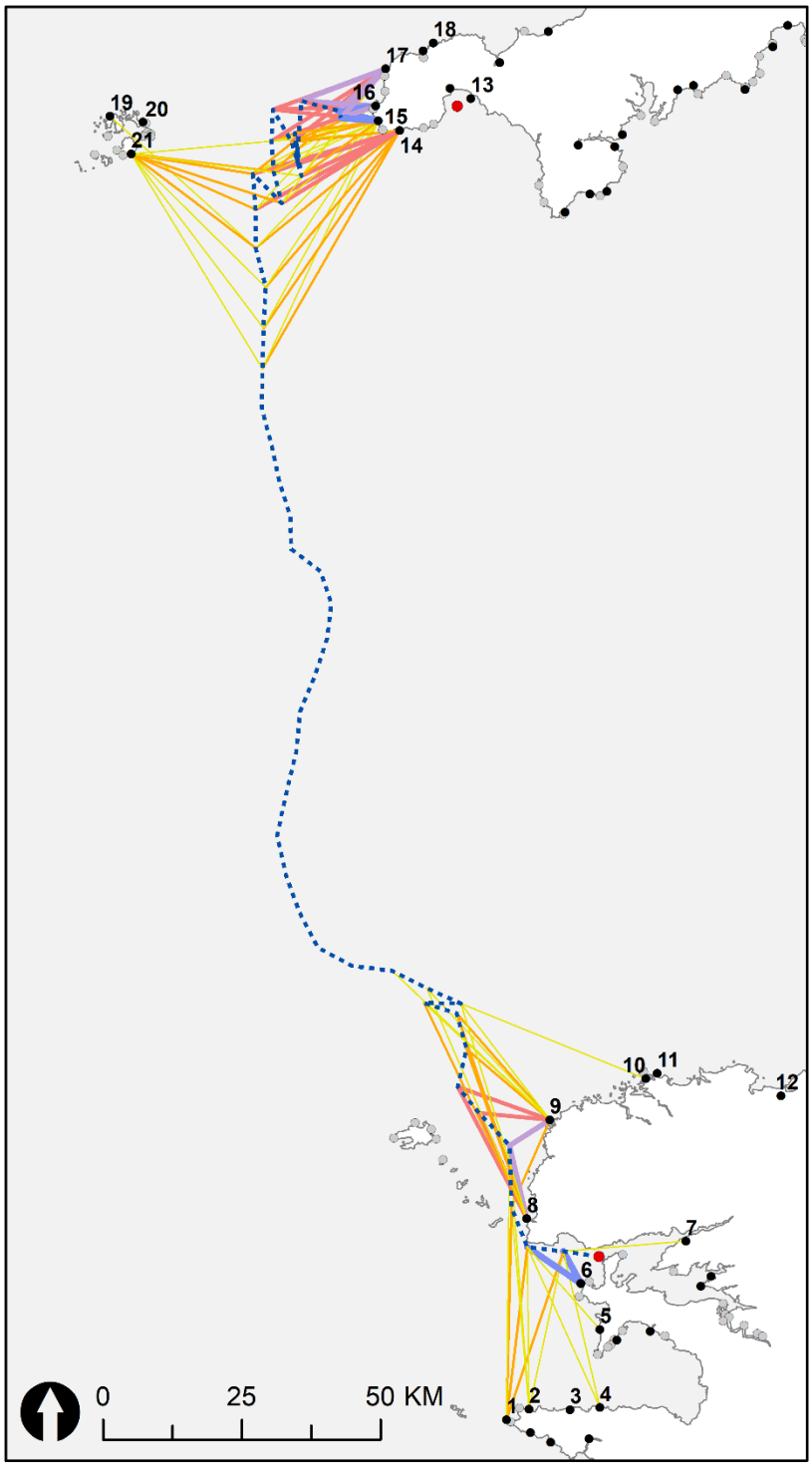
- Coastal Nodes
- Archaeological Sites
- Natural Prominences
- Simulation Track

Sightlines (by Apparent Size)

- 0-1 sq. deg.
- 1-2 sq. deg.
- 2-5 sq. deg.
- 5-15 sq. deg.
- 15-100 sq. deg.

Sites Referenced:

1 - Pointe du Raz
2 - Castel Meur
3 - Kergulan
4 - Castel Coz
5 - Lostmarc'h
6 - Pointe du Toulinguet
7 - Roc'h Nivelen
8 - Kermorvan
9 - Île d'Yoc'h
10 - Kastell Ac'h
11 - Beg Monom
12 - Bretouare
13 - St. Michael's Mount
14 - Treryn Dinas
15 - Carn Les Boel
16 - Maen Castle
17 - Kenidjack Castle
18 - Trereen Dinas
19 - Shipman Head
20 - Burnt Hill
21 - Giants Castle



Simulation 13

Max speed: 7 kts.
Lmark. type: Arch. sites.
Estimation: No misest.
Starting time: 0 hrs.
Result: Success

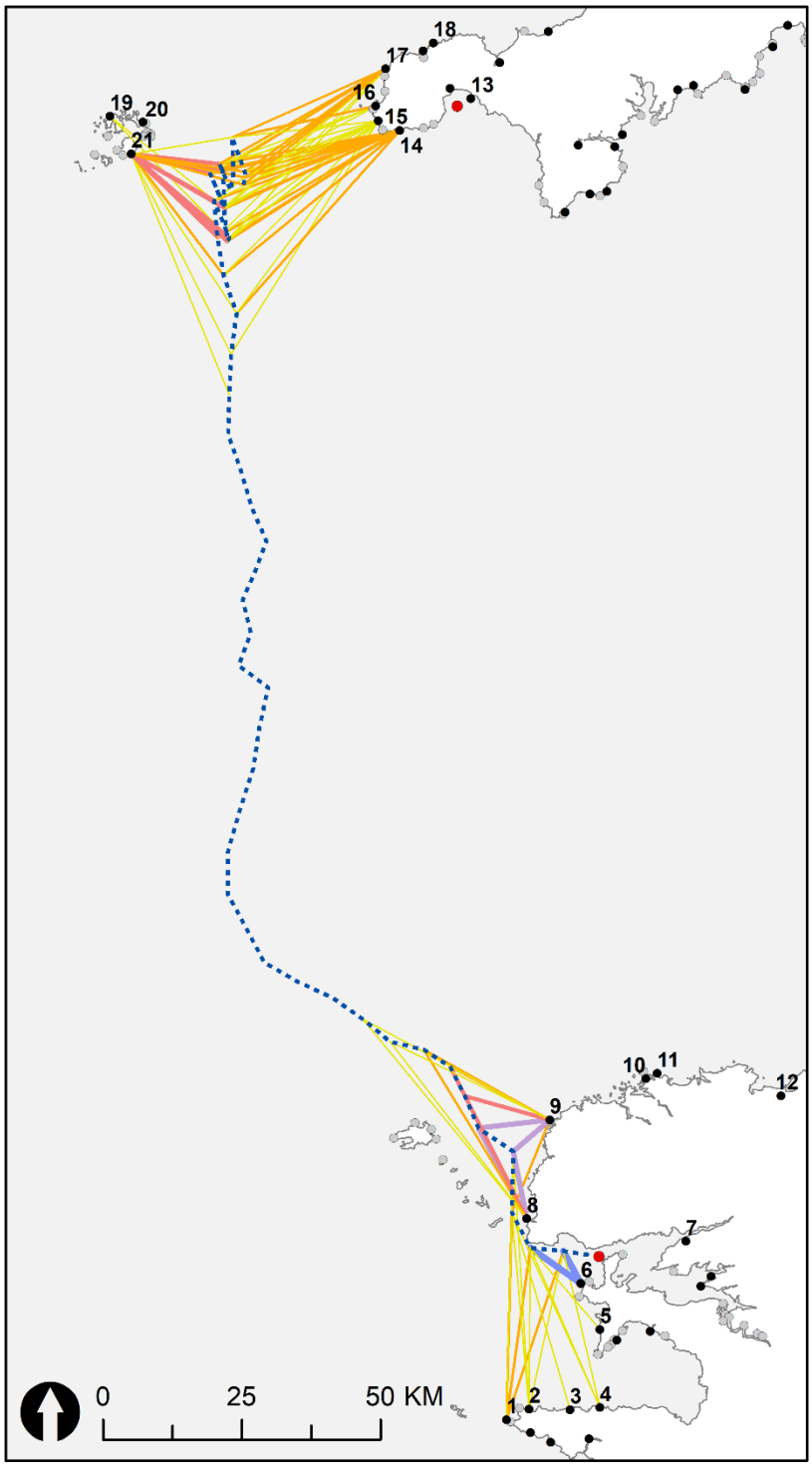
- Coastal Nodes
- Archaeological Sites
- Natural Prominences
- Simulation Track

Sightlines (by Apparent Size)

- 0-1 sq. deg.
- 1-2 sq. deg.
- 2-5 sq. deg.
- 5-15 sq. deg.
- 15-100 sq. deg.

Sites Referenced:

1 - Pointe du Raz
2 - Castel Meur
3 - Kergulan
4 - Castel Coz
5 - Lostmarc'h
6 - Pointe du Toulinguet
7 - Roc'h Nivelen
8 - Kermorvan
9 - Île d'Yoc'h
10 - Kastell Ac'h
11 - Beg Monom
12 - Bretouare
13 - St. Michael's Mount
14 - Treryn Dinas
15 - Carn Les Boel
16 - Maen Castle
17 - Kenidjack Castle
18 - Trereen Dinas
19 - Shipman Head
20 - Burnt Hill
21 - Giants Castle



Simulation 14

Max speed: 7 kts.
Lmark. type: Arch. sites.
Estimation: No misest.
Starting time: +1 hrs.
Result: Qualified Success

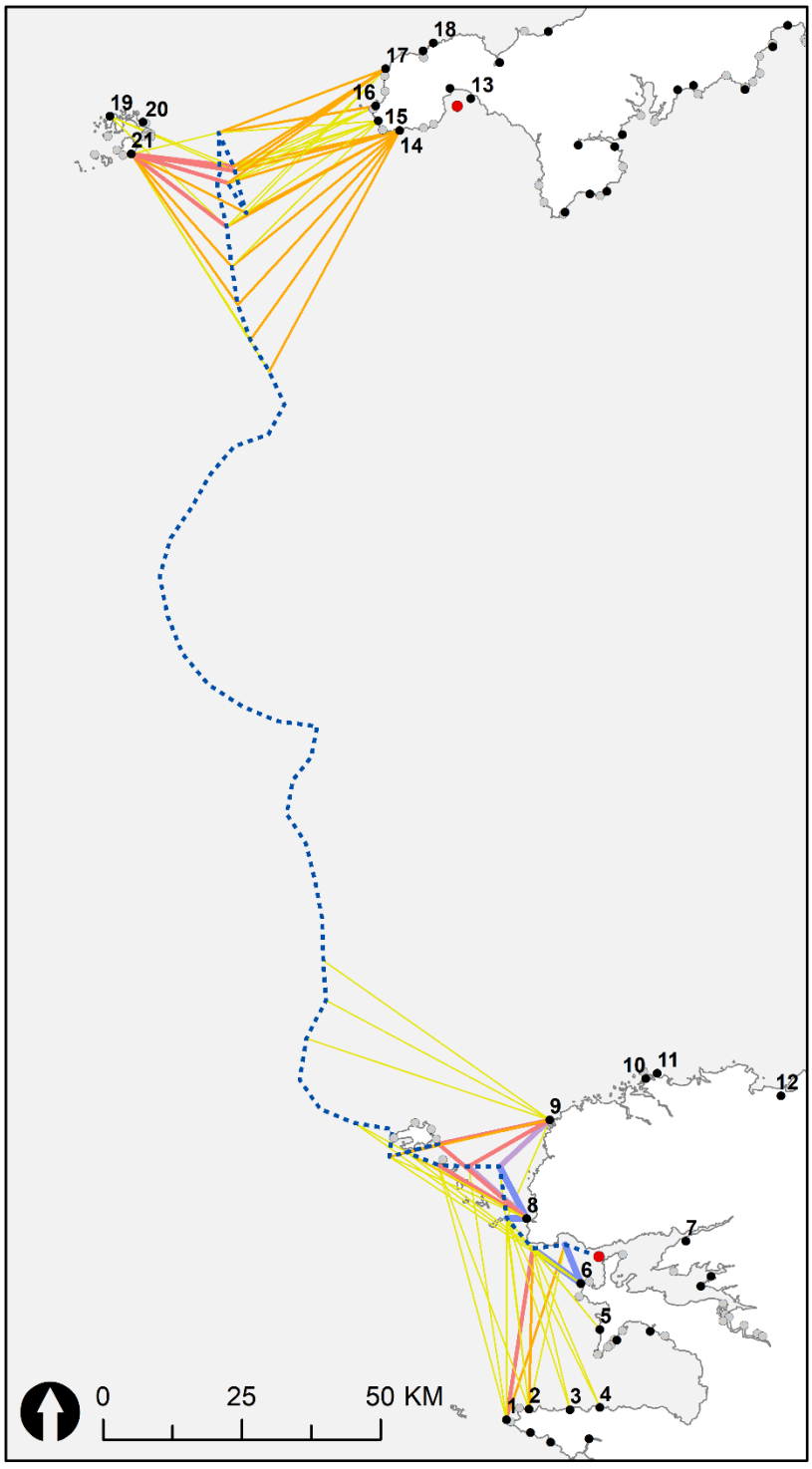
- Coastal Nodes
- Archaeological Sites
- Natural Prominences
- Simulation Track

Sightlines (by Apparent Size)

- 0-1 sq. deg.
- 1-2 sq. deg.
- 2-5 sq. deg.
- 5-15 sq. deg.
- 15-100 sq. deg.

Sites Referenced:

1 - Pointe du Raz
2 - Castel Meur
3 - Kergulan
4 - Castel Coz
5 - Lostmarc'h
6 - Pointe du Toulinguet
7 - Roc'h Nivelen
8 - Kermorvan
9 - Île d'Yoc'h
10 - Kastell Ac'h
11 - Beg Monom
12 - Bretouare
13 - St. Michael's Mount
14 - Treryn Dinas
15 - Carn Les Boel
16 - Maen Castle
17 - Kenidjack Castle
18 - Trereen Dinas
19 - Shipman Head
20 - Burnt Hill
21 - Giants Castle



Simulation 15

Max speed: 7 kts.
Lmark. type: Arch. sites.
Estimation: No misest.
Starting time: +2 hrs.
Result: Qualified Success

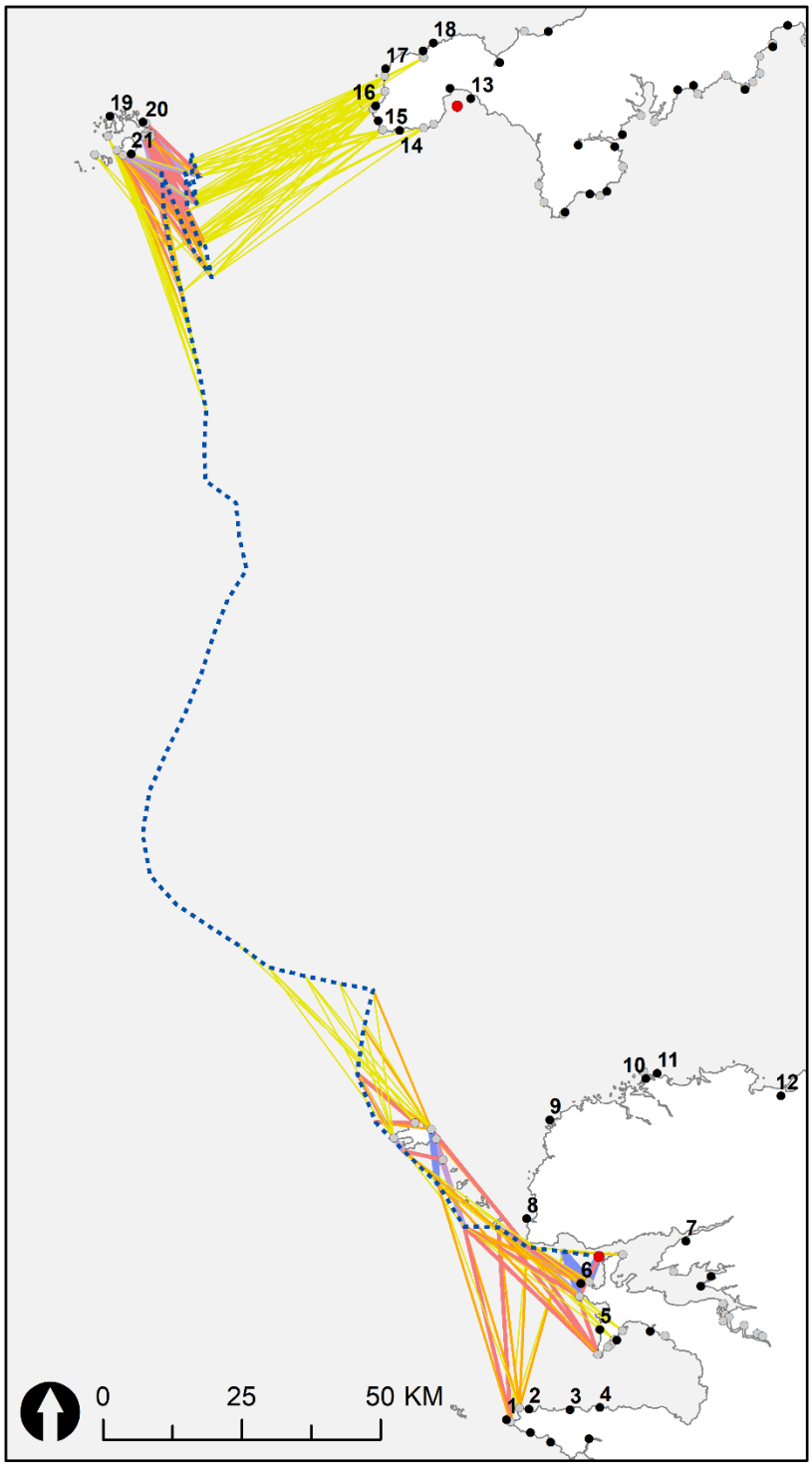
- Coastal Nodes
- Archaeological Sites
- Natural Prominences
- Simulation Track

Sightlines (by Apparent Size)

- 0-1 sq. deg.
- 1-2 sq. deg.
- 2-5 sq. deg.
- 5-15 sq. deg.
- 15-100 sq. deg.

Sites Referenced:

1 - Pointe du Raz
2 - Castel Meur
3 - Kergulan
4 - Castel Coz
5 - Lostmarc'h
6 - Pointe du Toulinguet
7 - Roc'h Nivelen
8 - Kermorvan
9 - Île d'Yoc'h
10 - Kastell Ac'h
11 - Beg Monom
12 - Bretouare
13 - St. Michael's Mount
14 - Treryn Dinas
15 - Carn Les Boel
16 - Maen Castle
17 - Kenidjack Castle
18 - Trereen Dinas
19 - Shipman Head
20 - Burnt Hill
21 - Giants Castle



Simulation 16

Max speed: 7 kts.
Lmark. type: Nat. proms.
Estimation: No misest.
Starting time: -2 hrs.
Result: Qualified Success

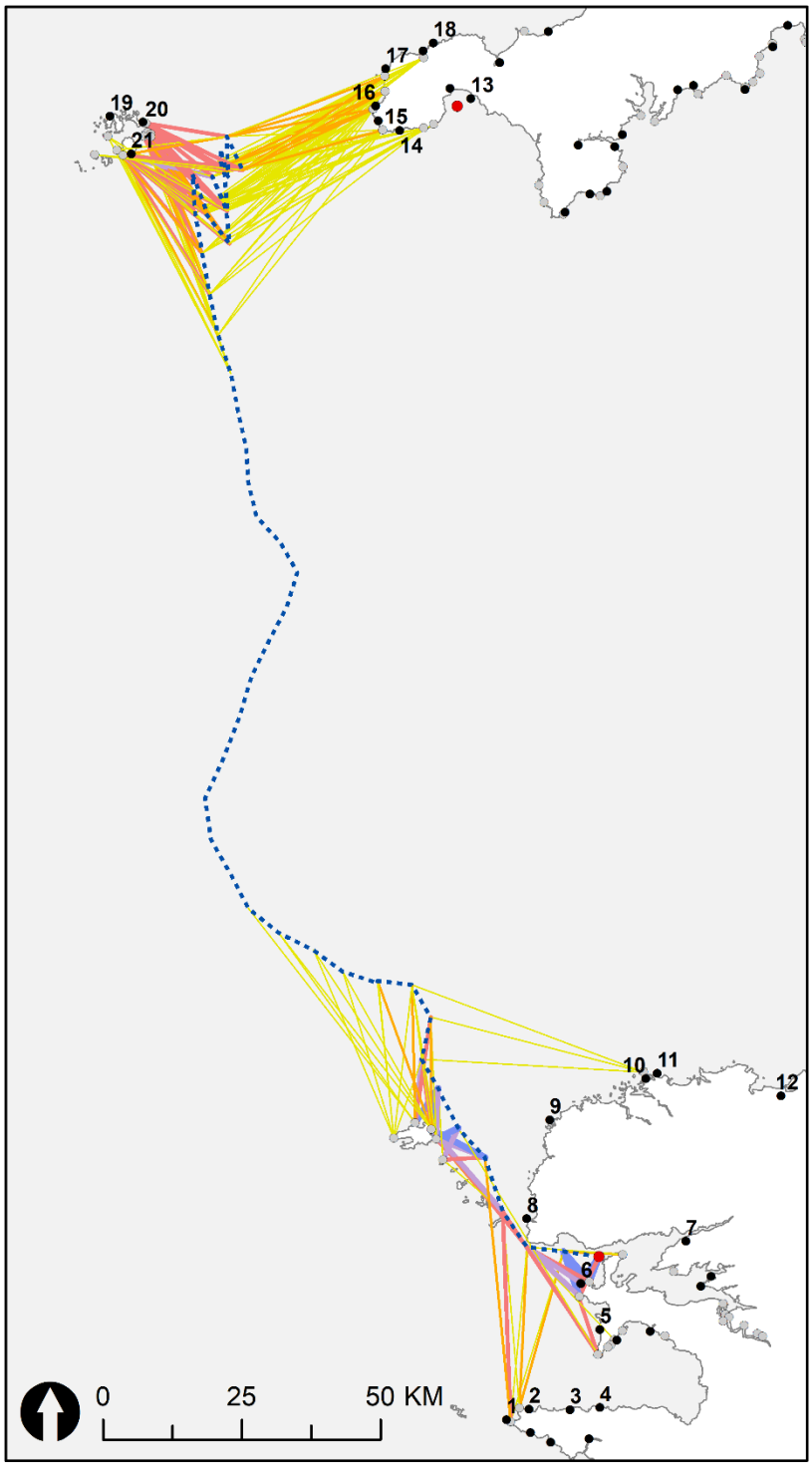
- Coastal Nodes
- Archaeological Sites
- Natural Prominences
- Simulation Track

Sightlines (by Apparent Size)

- 0-1 sq. deg.
- 1-2 sq. deg.
- 2-5 sq. deg.
- 5-15 sq. deg.
- 15-100 sq. deg.

Sites Referenced:

1 - Pointe du Raz
2 - Castel Meur
3 - Kergulan
4 - Castel Coz
5 - Lostmarc'h
6 - Pointe du Toulinguet
7 - Roc'h Nivelen
8 - Kermorvan
9 - Île d'Yoc'h
10 - Kastell Ac'h
11 - Beg Monom
12 - Bretouare
13 - St. Michael's Mount
14 - Treryn Dinas
15 - Carn Les Boel
16 - Maen Castle
17 - Kenidjack Castle
18 - Trereen Dinas
19 - Shipman Head
20 - Burnt Hill
21 - Giants Castle



Simulation 17

Max speed: 7 kts.
Lmark. type: Nat. proms.
Estimation: No misest.
Starting time: -1 hrs.
Result: Qualified Success

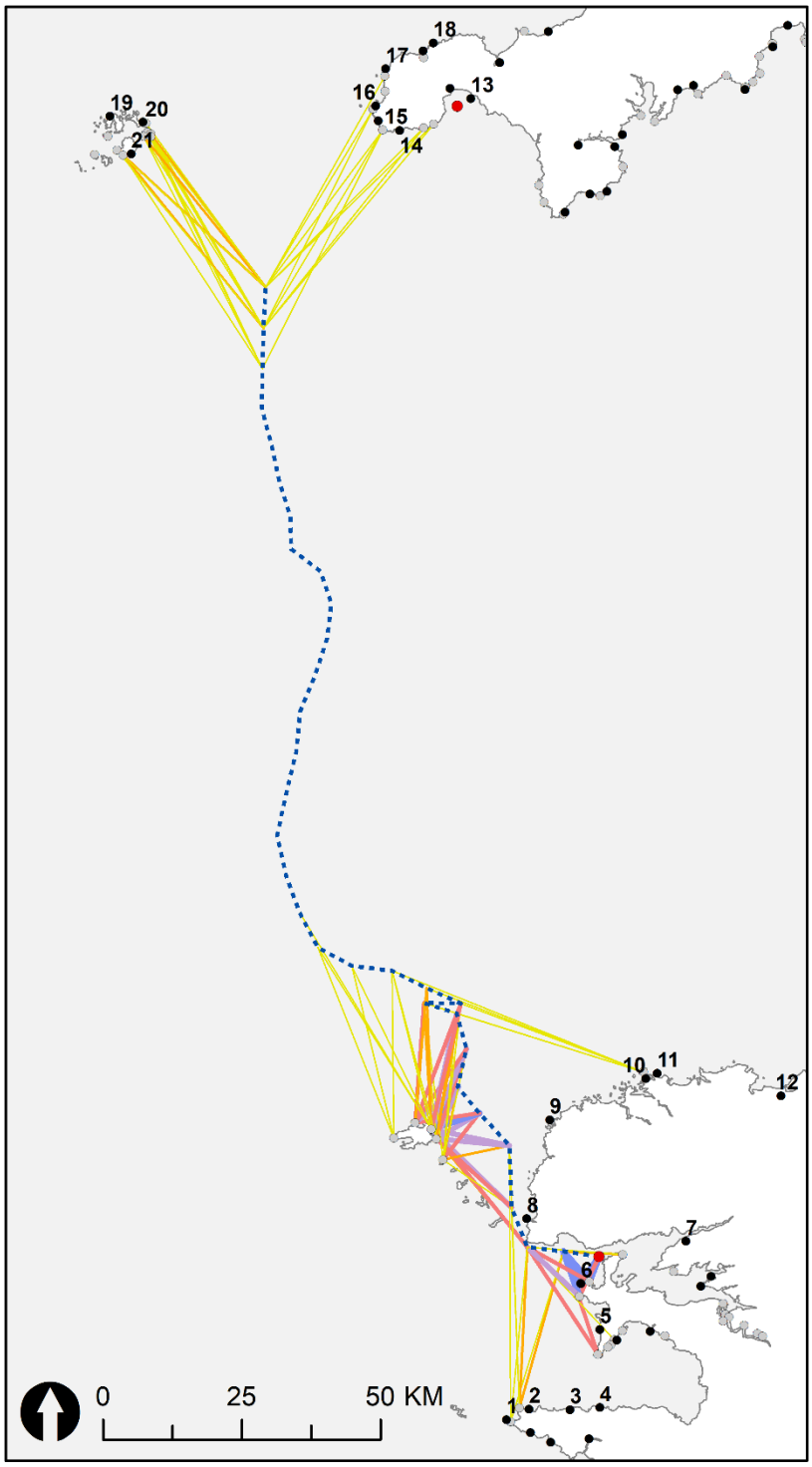
- Coastal Nodes
- Archaeological Sites
- Natural Prominences
- Simulation Track

Sightlines (by Apparent Size)

- 0-1 sq. deg.
- 1-2 sq. deg.
- 2-5 sq. deg.
- 5-15 sq. deg.
- 15-100 sq. deg.

Sites Referenced:

1 - Pointe du Raz
2 - Castel Meur
3 - Kergulan
4 - Castel Coz
5 - Lostmarc'h
6 - Pointe du Toulinguet
7 - Roc'h Nivelen
8 - Kermorvan
9 - Île d'Yoc'h
10 - Kastell Ac'h
11 - Beg Monom
12 - Bretouare
13 - St. Michael's Mount
14 - Treryn Dinas
15 - Carn Les Boel
16 - Maen Castle
17 - Kenidjack Castle
18 - Trereen Dinas
19 - Shipman Head
20 - Burnt Hill
21 - Giants Castle



Simulation 18

Max speed: 7 kts.
Lmark. type: Nat. proms.
Estimation: No misest.
Starting time: +0 hrs.
Result: Potential Success

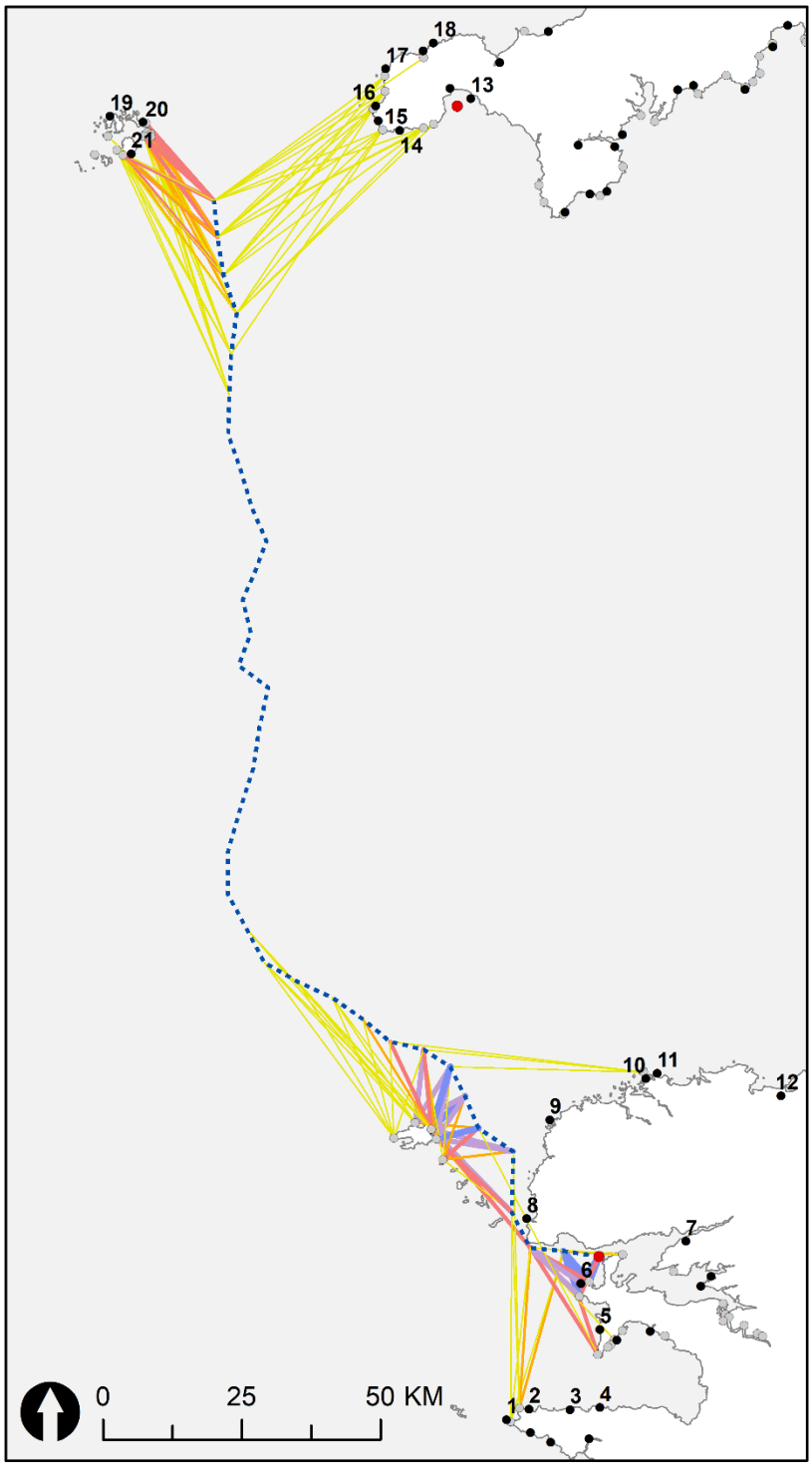
- Coastal Nodes
- Archaeological Sites
- Natural Prominences
- Simulation Track

Sightlines (by Apparent Size)

- 0-1 sq. deg.
- 1-2 sq. deg.
- 2-5 sq. deg.
- 5-15 sq. deg.
- 15-100 sq. deg.

Sites Referenced:

1 - Pointe du Raz
2 - Castel Meur
3 - Kergulan
4 - Castel Coz
5 - Lostmarc'h
6 - Pointe du Toulinguet
7 - Roc'h Nivelen
8 - Kermorvan
9 - Île d'Yoc'h
10 - Kastell Ac'h
11 - Beg Monom
12 - Bretouare
13 - St. Michael's Mount
14 - Treryn Dinas
15 - Carn Les Boel
16 - Maen Castle
17 - Kenidjack Castle
18 - Trereen Dinas
19 - Shipman Head
20 - Burnt Hill
21 - Giants Castle



Simulation 19

Max speed: 7 kts.
Lmark. type: Nat. proms.
Estimation: No misest.
Starting time: +1 hrs.
Result: Potential Success

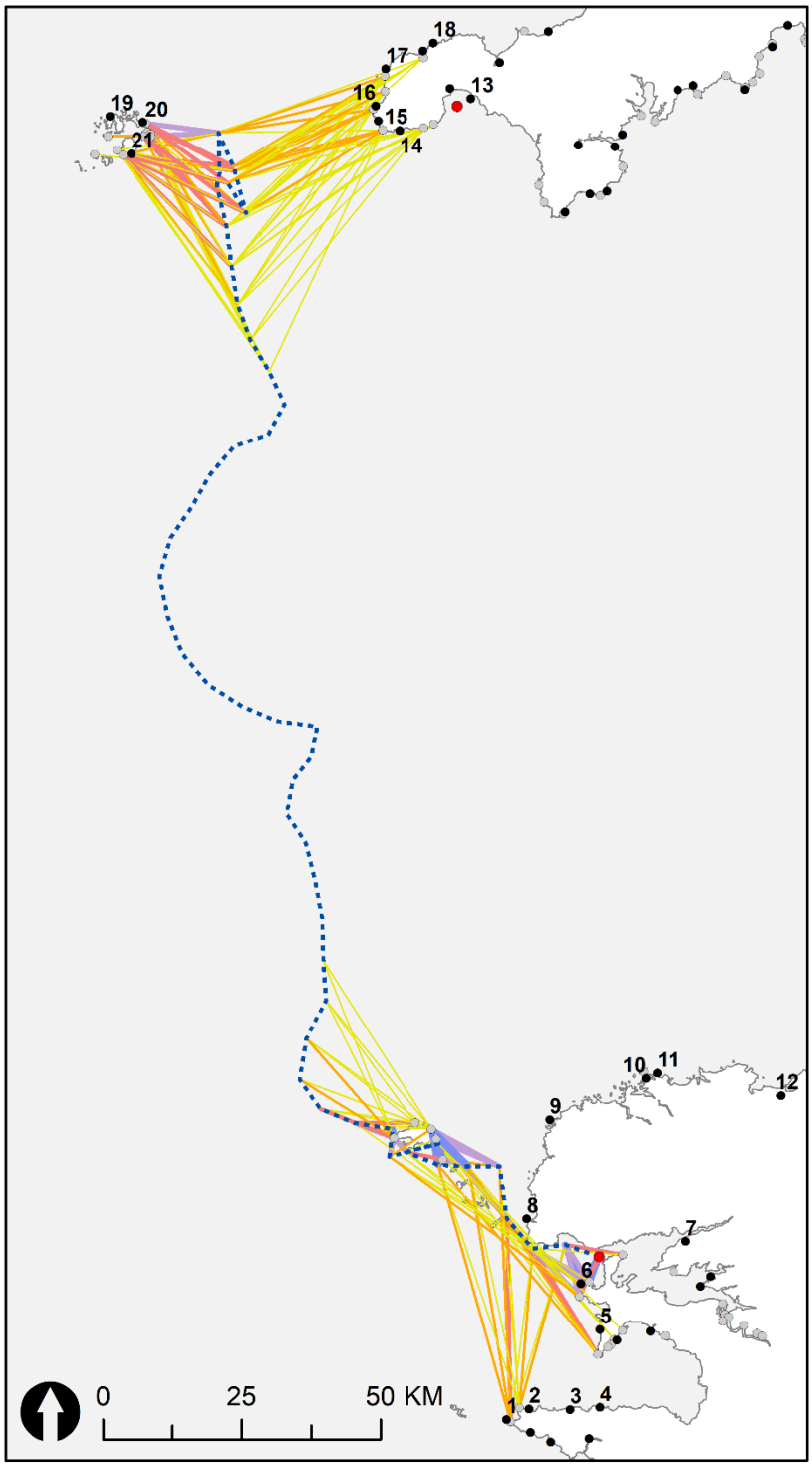
- Coastal Nodes
- Archaeological Sites
- Natural Prominences
- Simulation Track

Sightlines (by Apparent Size)

- 0-1 sq. deg.
- 1-2 sq. deg.
- 2-5 sq. deg.
- 5-15 sq. deg.
- 15-100 sq. deg.

Sites Referenced:

1 - Pointe du Raz
2 - Castel Meur
3 - Kergulan
4 - Castel Coz
5 - Lostmarc'h
6 - Pointe du Toulinguet
7 - Roc'h Nivelen
8 - Kermorvan
9 - Île d'Yoc'h
10 - Kastell Ac'h
11 - Beg Monom
12 - Bretouare
13 - St. Michael's Mount
14 - Treryn Dinas
15 - Carn Les Boel
16 - Maen Castle
17 - Kenidjack Castle
18 - Trereen Dinas
19 - Shipman Head
20 - Burnt Hill
21 - Giants Castle



Simulation 20

Max speed: 7 kts.
Lmark. type: Nat. proms.
Estimation: No misest.
Starting time: +2 hrs.
Result: Qualified Success

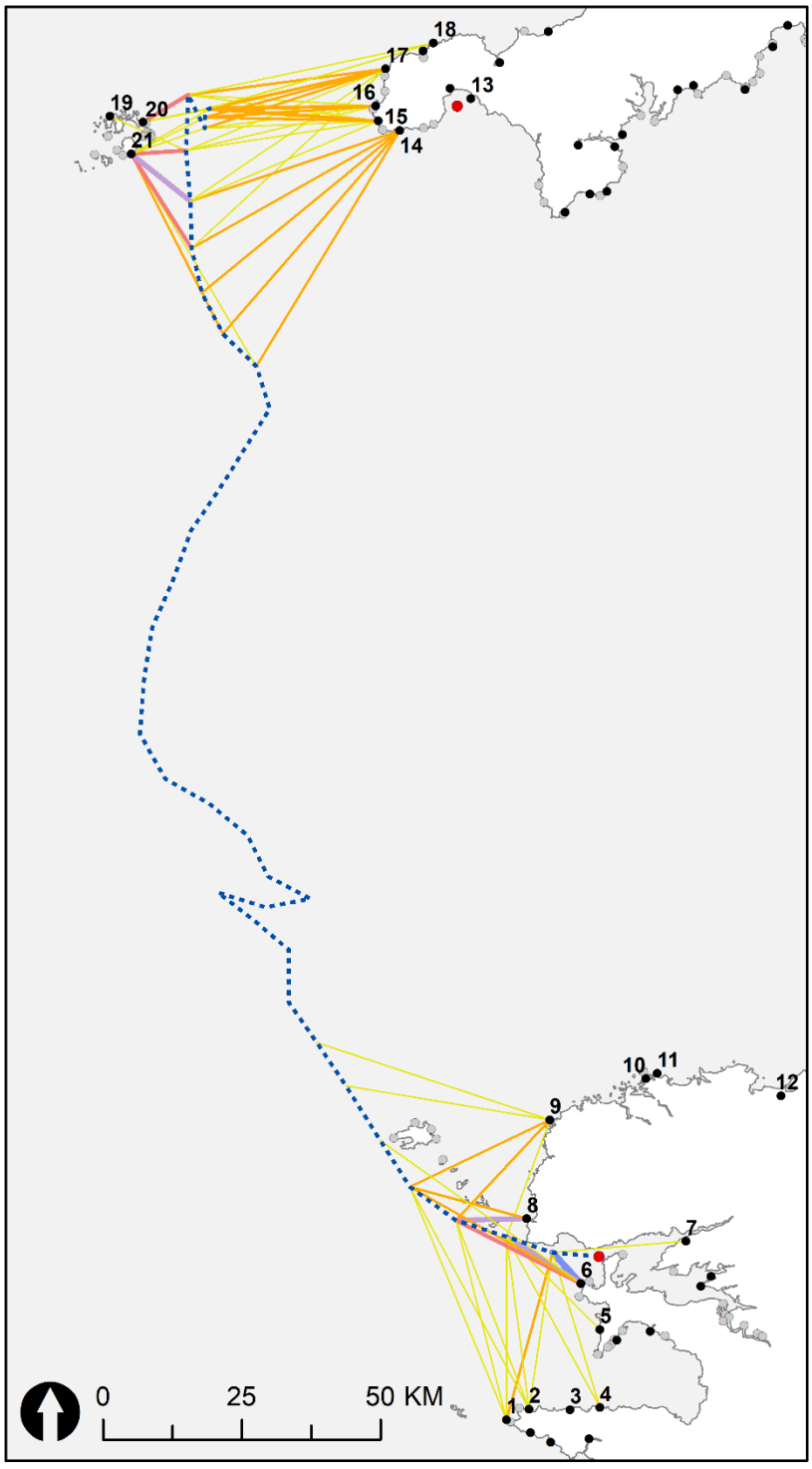
- Coastal Nodes
- Archaeological Sites
- Natural Prominences
- Simulation Track

Sightlines (by Apparent Size)

- 0-1 sq. deg.
- 1-2 sq. deg.
- 2-5 sq. deg.
- 5-15 sq. deg.
- 15-100 sq. deg.

Sites Referenced:

1 - Pointe du Raz
2 - Castel Meur
3 - Kergulan
4 - Castel Coz
5 - Lostmarc'h
6 - Pointe du Toulinguet
7 - Roc'h Nivelen
8 - Kermorvan
9 - Île d'Yoc'h
10 - Kastell Ac'h
11 - Beg Monom
12 - Bretouare
13 - St. Michael's Mount
14 - Treryn Dinas
15 - Carn Les Boel
16 - Maen Castle
17 - Kenidjack Castle
18 - Trereen Dinas
19 - Shipman Head
20 - Burnt Hill
21 - Giants Castle



Simulation 21

Max speed: 9 kts.
Lmark. type: Arch. Sites
Estimation: No misest.
Starting time: -2 hrs.
Result: Qualified Success

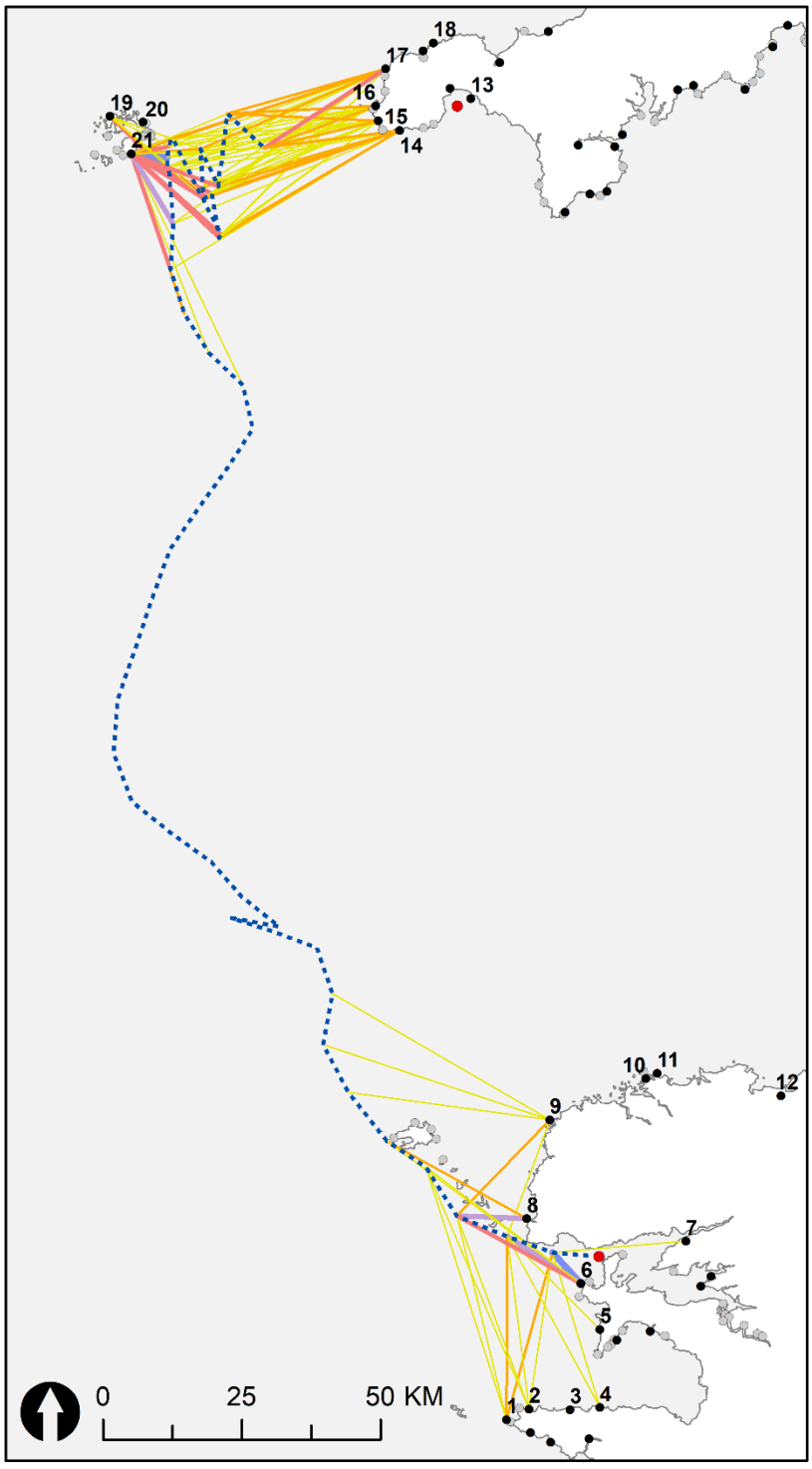
- Coastal Nodes
- Archaeological Sites
- Natural Prominences
- Simulation Track

Sightlines (by Apparent Size)

- 0-1 sq. deg.
- 1-2 sq. deg.
- 2-5 sq. deg.
- 5-15 sq. deg.
- 15-100 sq. deg.

Sites Referenced:

1 - Pointe du Raz
2 - Castel Meur
3 - Kergulan
4 - Castel Coz
5 - Lostmarc'h
6 - Pointe du Toulinguet
7 - Roc'h Nivelen
8 - Kermorvan
9 - Île d'Yoc'h
10 - Kastell Ac'h
11 - Beg Monom
12 - Bretouare
13 - St. Michael's Mount
14 - Treryn Dinas
15 - Carn Les Boel
16 - Maen Castle
17 - Kenidjack Castle
18 - Trereen Dinas
19 - Shipman Head
20 - Burnt Hill
21 - Giants Castle



Simulation 22

Max speed: 9 kts.
Lmark. type: Arch. Sites
Estimation: No misest.
Starting time: -1 hrs.
Result: Qualified Success

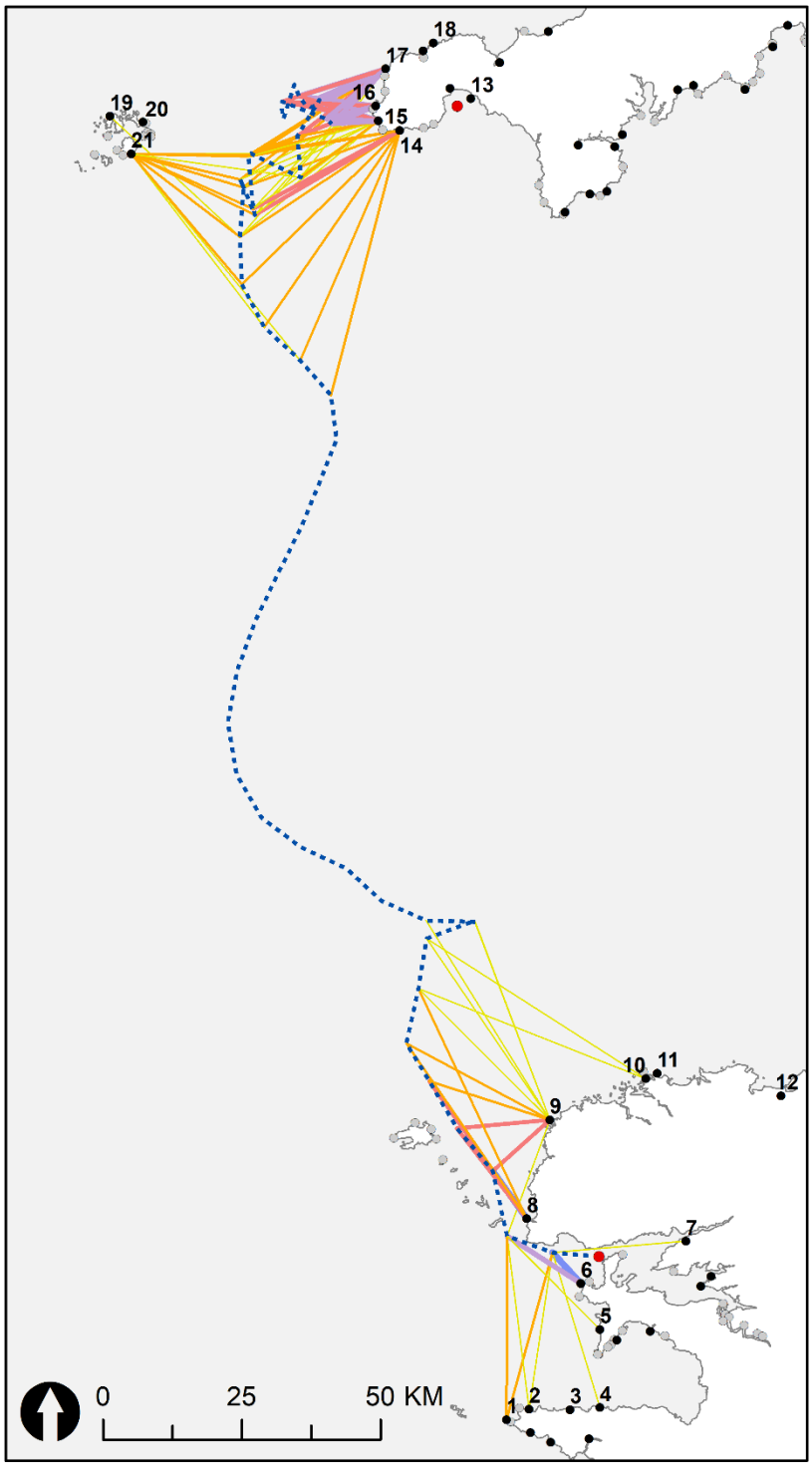
- Coastal Nodes
- Archaeological Sites
- Natural Prominences
- Simulation Track

Sightlines (by Apparent Size)

- 0-1 sq. deg.
- 1-2 sq. deg.
- 2-5 sq. deg.
- 5-15 sq. deg.
- 15-100 sq. deg.

Sites Referenced:

1 - Pointe du Raz
2 - Castel Meur
3 - Kergulan
4 - Castel Coz
5 - Lostmarc'h
6 - Pointe du Toulinguet
7 - Roc'h Nivelen
8 - Kermorvan
9 - Île d'Yoc'h
10 - Kastell Ac'h
11 - Beg Monom
12 - Bretouare
13 - St. Michael's Mount
14 - Treryn Dinas
15 - Carn Les Boel
16 - Maen Castle
17 - Kenidjack Castle
18 - Trereen Dinas
19 - Shipman Head
20 - Burnt Hill
21 - Giants Castle



Simulation 23

Max speed: 9 kts.
Lmark. type: Arch. Sites
Estimation: No misest.
Starting time: +0 hrs.
Result: Success

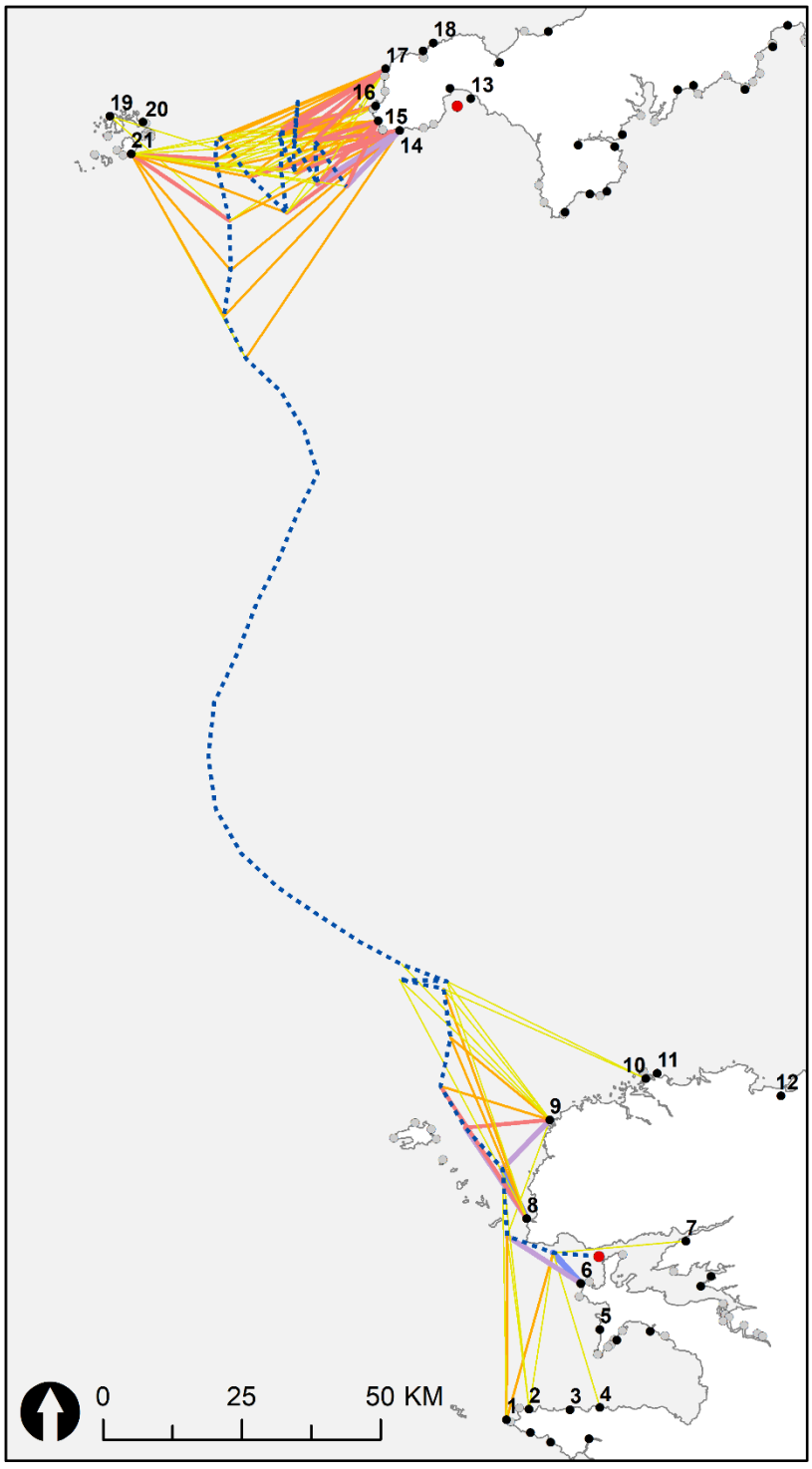
- Coastal Nodes
- Archaeological Sites
- Natural Prominences
- Simulation Track

Sightlines (by Apparent Size)

- 0-1 sq. deg.
- 1-2 sq. deg.
- 2-5 sq. deg.
- 5-15 sq. deg.
- 15-100 sq. deg.

Sites Referenced:

1 - Pointe du Raz
2 - Castel Meur
3 - Kergulan
4 - Castel Coz
5 - Lostmarc'h
6 - Pointe du Toulinguet
7 - Roc'h Nivelen
8 - Kermorvan
9 - Île d'Yoc'h
10 - Kastell Ac'h
11 - Beg Monom
12 - Bretouare
13 - St. Michael's Mount
14 - Treryn Dinas
15 - Carn Les Boel
16 - Maen Castle
17 - Kenidjack Castle
18 - Trereen Dinas
19 - Shipman Head
20 - Burnt Hill
21 - Giants Castle



Simulation 24

Max speed: 9 kts.
Lmark. type: Arch. Sites
Estimation: No misest.
Starting time: +1 hrs.
Result: Qualified Success

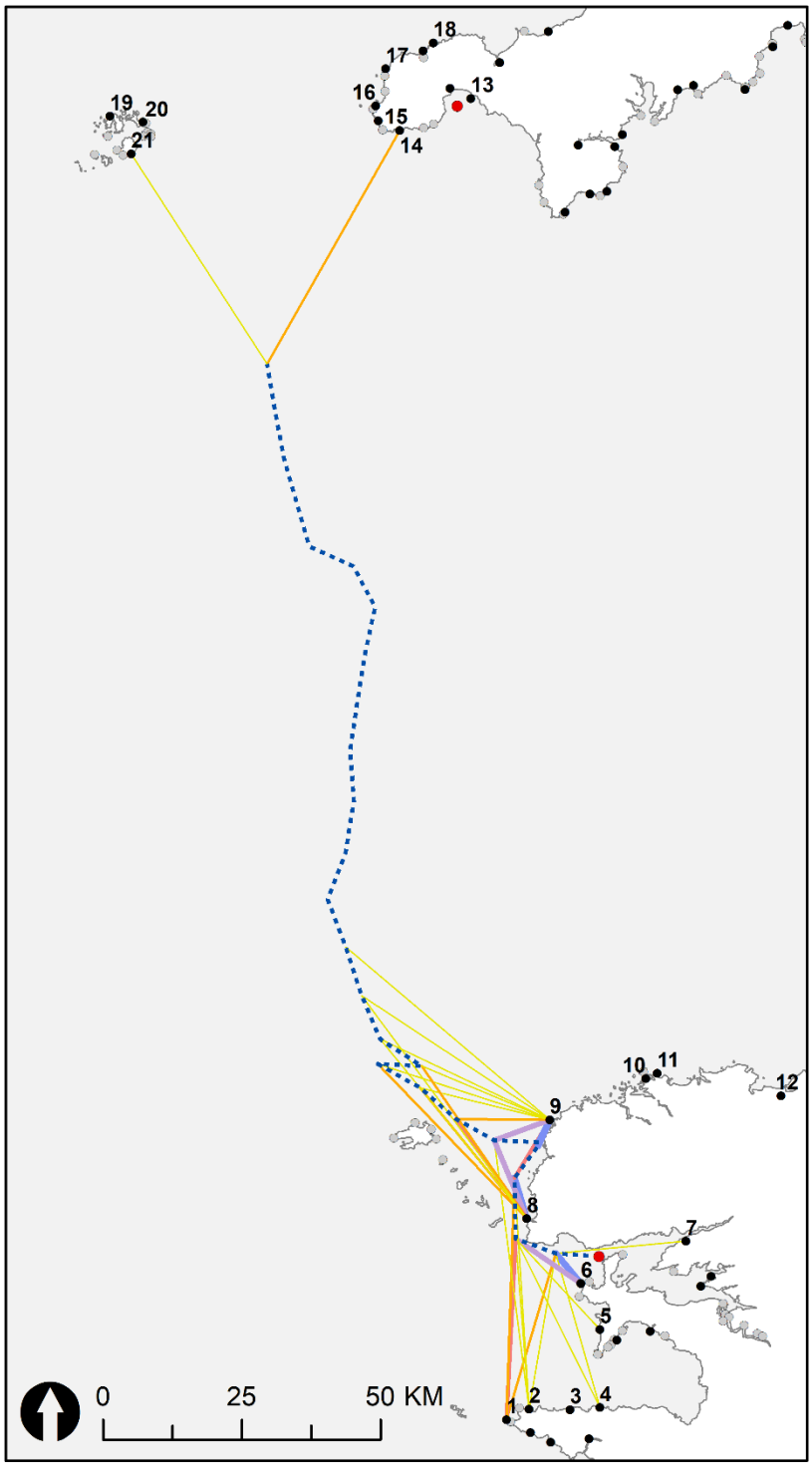
- Coastal Nodes
- Archaeological Sites
- Natural Prominences
- Simulation Track

Sightlines (by Apparent Size)

- 0-1 sq. deg.
- 1-2 sq. deg.
- 2-5 sq. deg.
- 5-15 sq. deg.
- 15-100 sq. deg.

Sites Referenced:

1 - Pointe du Raz
2 - Castel Meur
3 - Kergulan
4 - Castel Coz
5 - Lostmarc'h
6 - Pointe du Toulinguet
7 - Roc'h Nivelen
8 - Kermorvan
9 - Île d'Yoc'h
10 - Kastell Ac'h
11 - Beg Monom
12 - Bretouare
13 - St. Michael's Mount
14 - Treryn Dinas
15 - Carn Les Boel
16 - Maen Castle
17 - Kenidjack Castle
18 - Trereen Dinas
19 - Shipman Head
20 - Burnt Hill
21 - Giants Castle



Simulation 25

Max speed: 9 kts.
Lmark. type: Arch. Sites
Estimation: No misest.
Starting time: +2 hrs.
Result: Potential Success

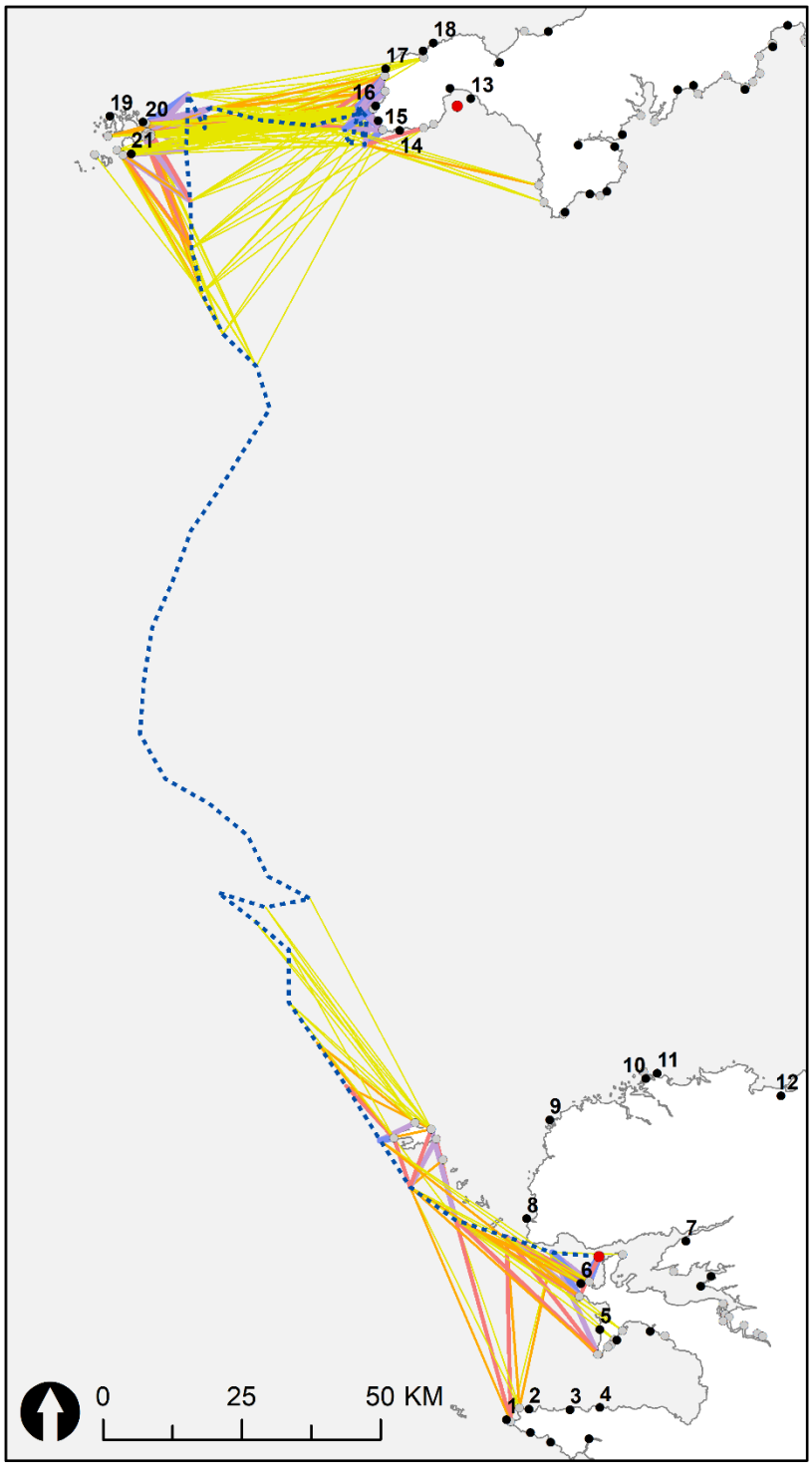
- Coastal Nodes
- Archaeological Sites
- Natural Prominences
- Simulation Track

Sightlines (by Apparent Size)

- 0-1 sq. deg.
- 1-2 sq. deg.
- 2-5 sq. deg.
- 5-15 sq. deg.
- 15-100 sq. deg.

Sites Referenced:

1 - Pointe du Raz
2 - Castel Meur
3 - Kergulan
4 - Castel Coz
5 - Lostmarc'h
6 - Pointe du Toulinguet
7 - Roc'h Nivelen
8 - Kermorvan
9 - Île d'Yoc'h
10 - Kastell Ac'h
11 - Beg Monom
12 - Bretouare
13 - St. Michael's Mount
14 - Treryn Dinas
15 - Carn Les Boel
16 - Maen Castle
17 - Kenidjack Castle
18 - Trereen Dinas
19 - Shipman Head
20 - Burnt Hill
21 - Giants Castle



Simulation 26

Max speed: 9 kts.
Lmark. type: Nat. Proms.
Estimation: No misest.
Starting time: -2 hrs.
Result: Success

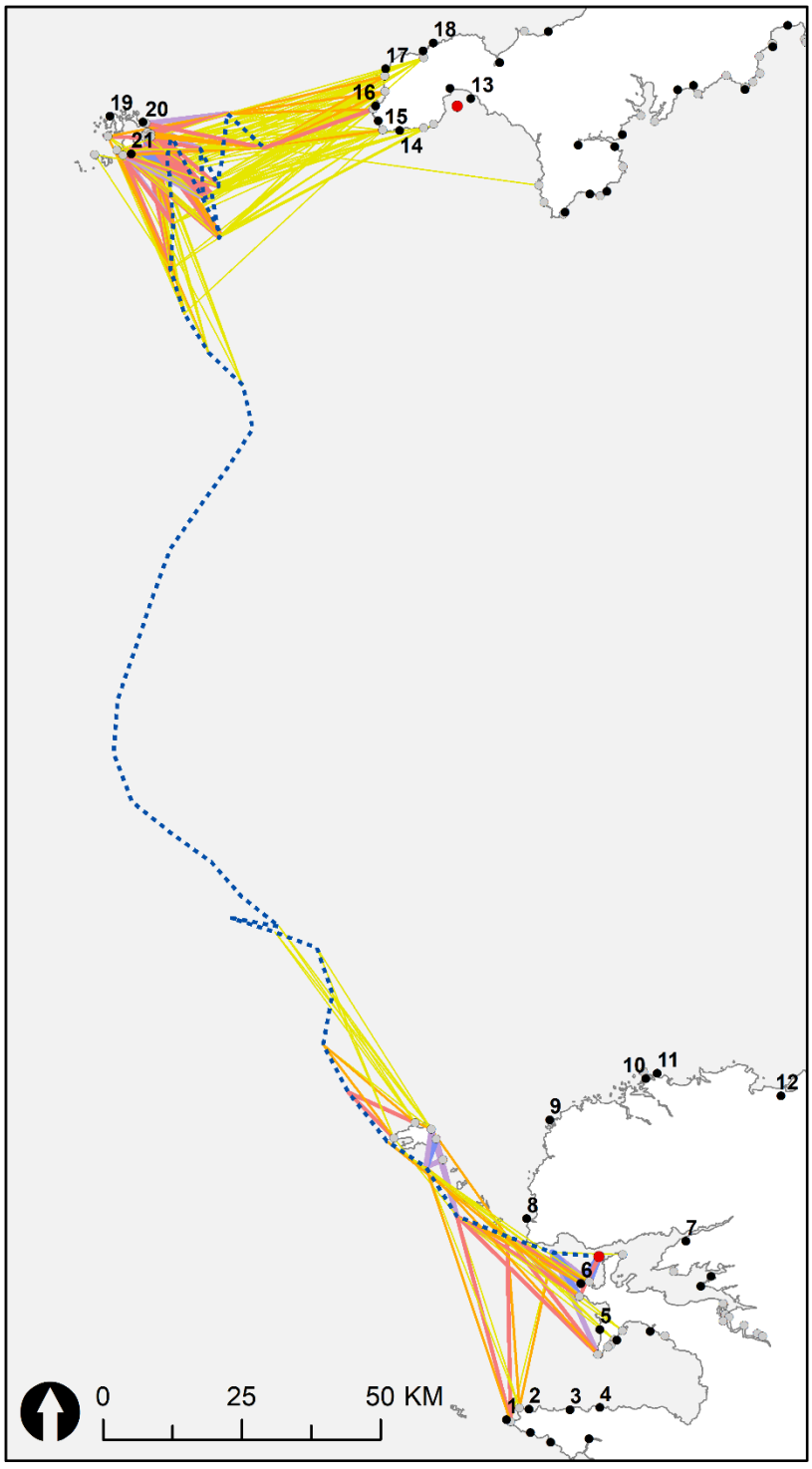
- Coastal Nodes
- Archaeological Sites
- Natural Prominences
- Simulation Track

Sightlines (by Apparent Size)

- 0-1 sq. deg.
- 1-2 sq. deg.
- 2-5 sq. deg.
- 5-15 sq. deg.
- 15-100 sq. deg.

Sites Referenced:

1 - Pointe du Raz
2 - Castel Meur
3 - Kergulan
4 - Castel Coz
5 - Lostmarc'h
6 - Pointe du Toulinguet
7 - Roc'h Nivelen
8 - Kermorvan
9 - Île d'Yoc'h
10 - Kastell Ac'h
11 - Beg Monom
12 - Bretouare
13 - St. Michael's Mount
14 - Treryn Dinas
15 - Carn Les Boel
16 - Maen Castle
17 - Kenidjack Castle
18 - Trereen Dinas
19 - Shipman Head
20 - Burnt Hill
21 - Giants Castle



Simulation 27

Max speed: 9 kts.
Lmark. type: Nat. Proms.
Estimation: No misest.
Starting time: -1 hrs.
Result: Qualified Success

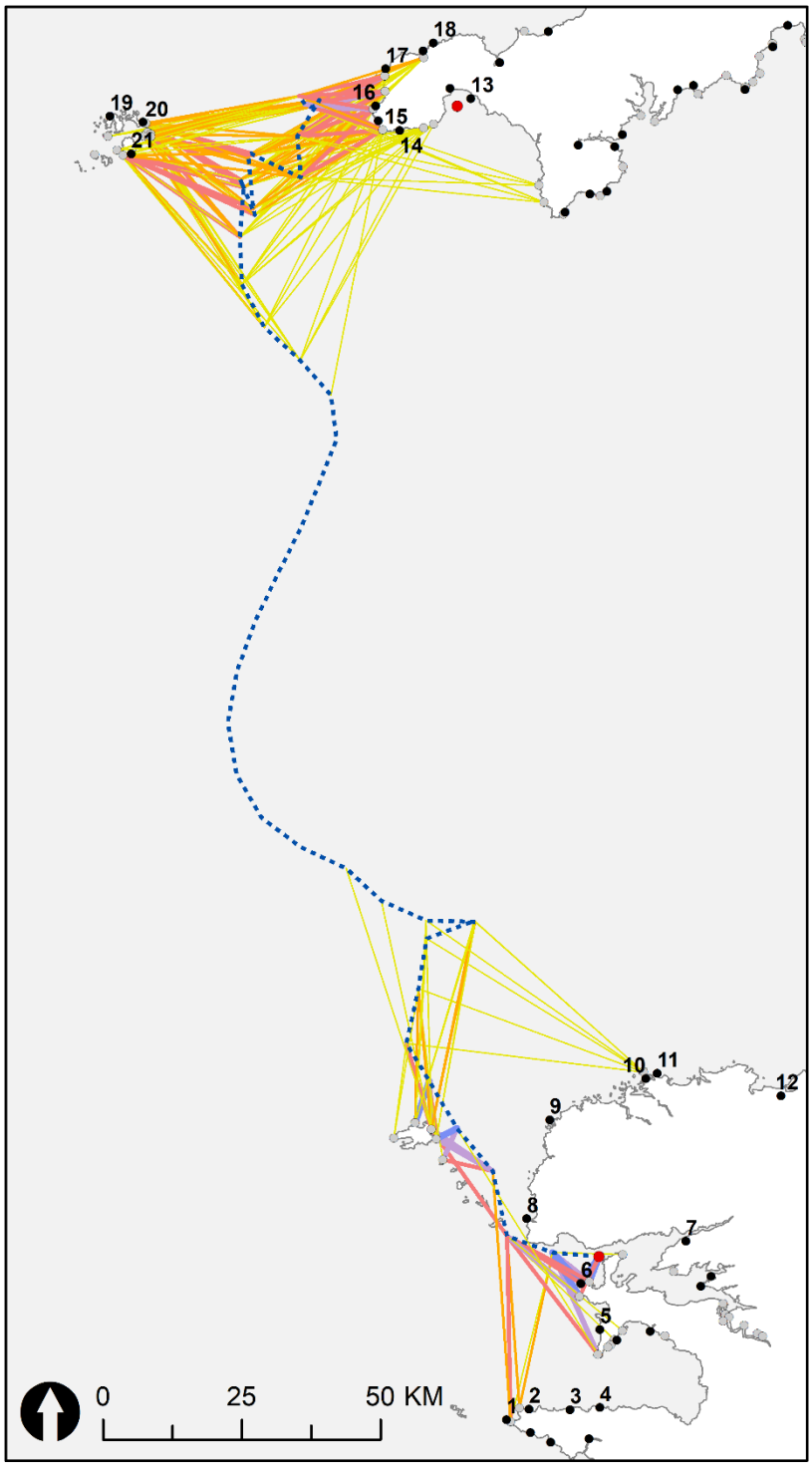
- Coastal Nodes
- Archaeological Sites
- Natural Prominences
- Simulation Track

Sightlines (by Apparent Size)

- 0-1 sq. deg.
- 1-2 sq. deg.
- 2-5 sq. deg.
- 5-15 sq. deg.
- 15-100 sq. deg.

Sites Referenced:

1 - Pointe du Raz
2 - Castel Meur
3 - Kergulan
4 - Castel Coz
5 - Lostmarc'h
6 - Pointe du Toulinguet
7 - Roc'h Nivelen
8 - Kermorvan
9 - Île d'Yoc'h
10 - Kastell Ac'h
11 - Beg Monom
12 - Bretouare
13 - St. Michael's Mount
14 - Treryn Dinas
15 - Carn Les Boel
16 - Maen Castle
17 - Kenidjack Castle
18 - Trereen Dinas
19 - Shipman Head
20 - Burnt Hill
21 - Giants Castle



Simulation 28

Max speed: 9 kts.
Lmark. type: Nat. Proms.
Estimation: No misest.
Starting time: +0 hrs.
Result: Qualified Success

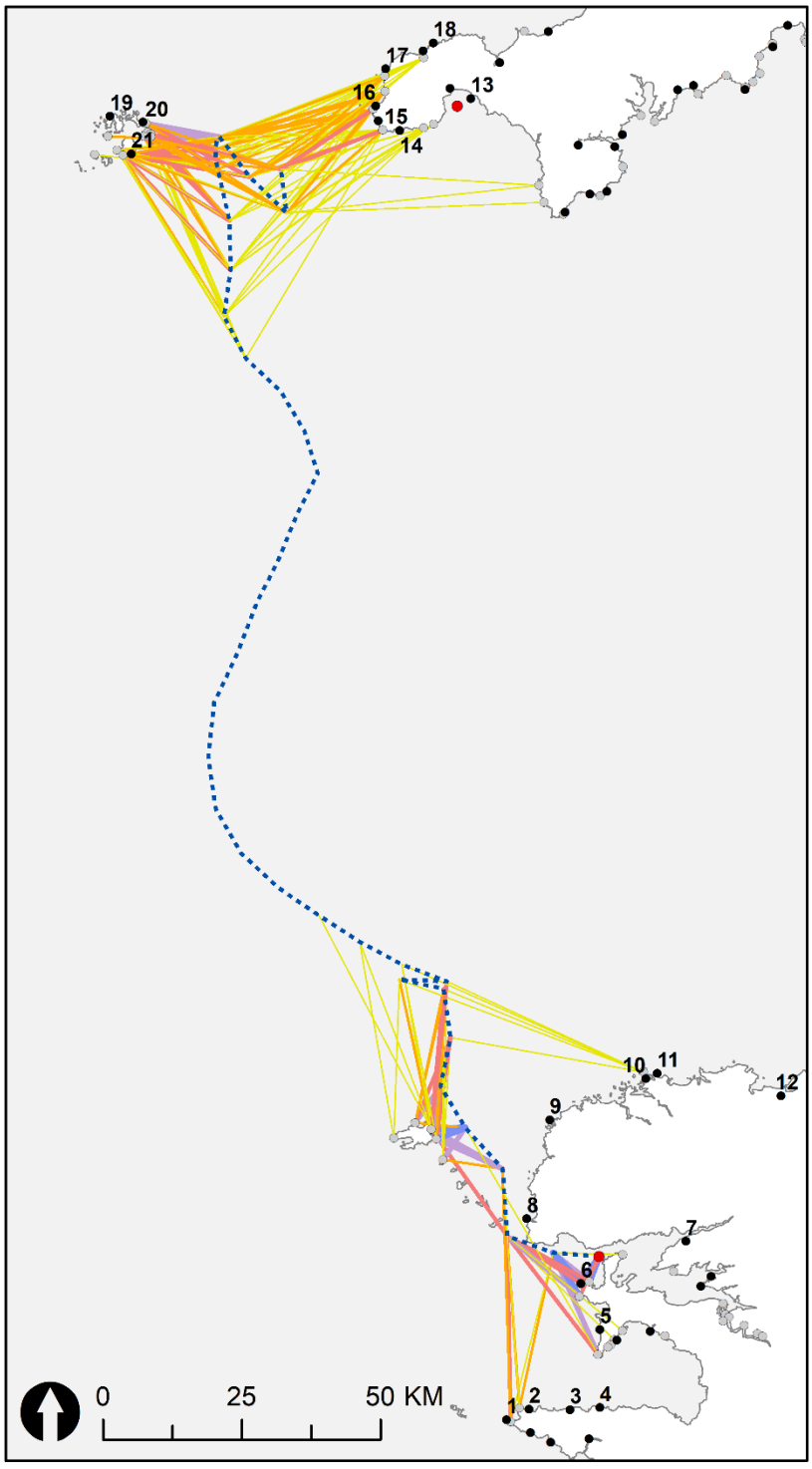
- Coastal Nodes
- Archaeological Sites
- Natural Prominences
- Simulation Track

Sightlines (by Apparent Size)

- 0-1 sq. deg.
- 1-2 sq. deg.
- 2-5 sq. deg.
- 5-15 sq. deg.
- 15-100 sq. deg.

Sites Referenced:

1 - Pointe du Raz
2 - Castel Meur
3 - Kergulan
4 - Castel Coz
5 - Lostmarc'h
6 - Pointe du Toulinguet
7 - Roc'h Nivelen
8 - Kermorvan
9 - Île d'Yoc'h
10 - Kastell Ac'h
11 - Beg Monom
12 - Bretouare
13 - St. Michael's Mount
14 - Treryn Dinas
15 - Carn Les Boel
16 - Maen Castle
17 - Kenidjack Castle
18 - Trereen Dinas
19 - Shipman Head
20 - Burnt Hill
21 - Giants Castle



Simulation 29

Max speed: 9 kts.
Lmark. type: Nat. Proms.
Estimation: No misest.
Starting time: +1 hrs.
Result: Qualified Success

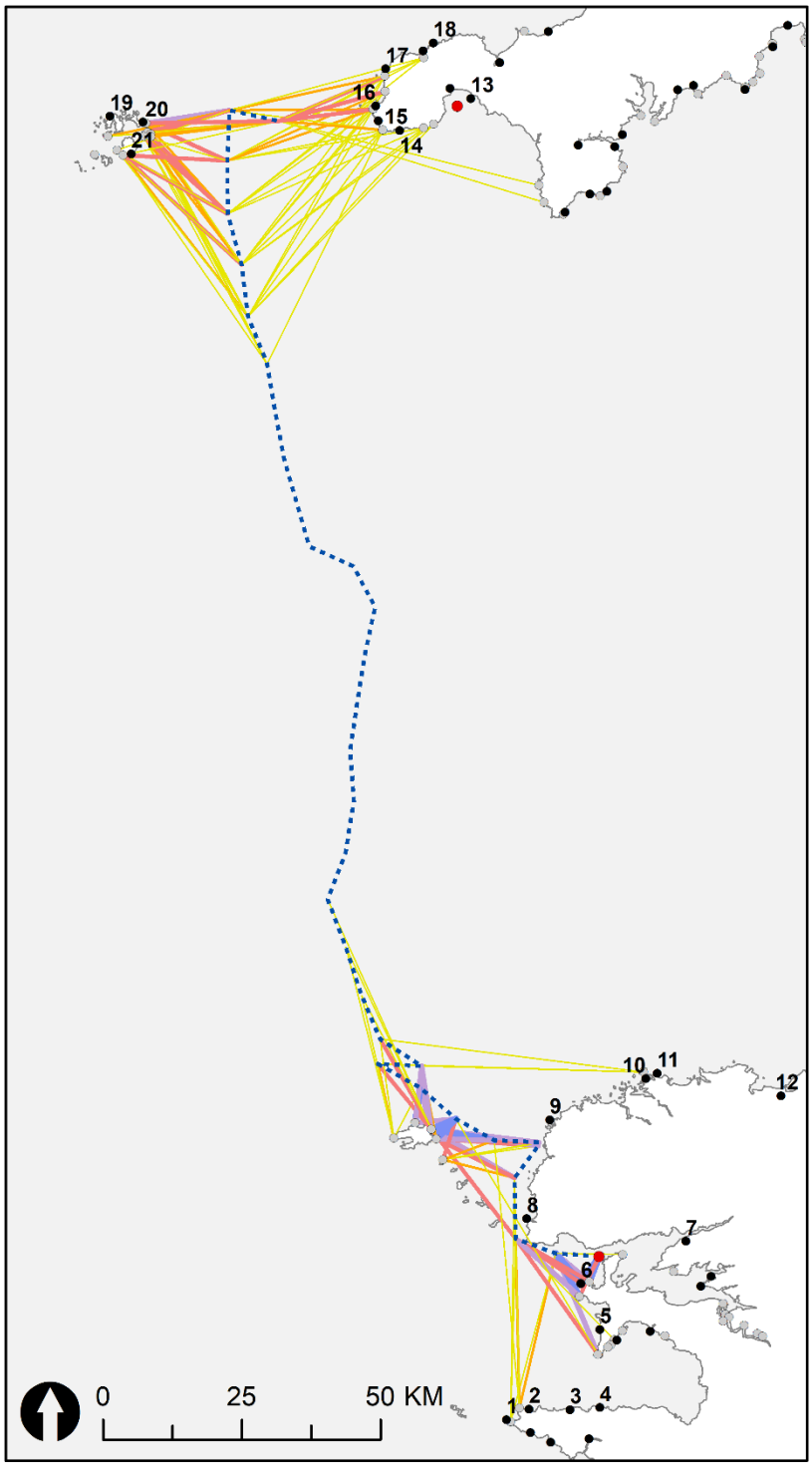
- Coastal Nodes
- Archaeological Sites
- Natural Prominences
- Simulation Track

Sightlines (by Apparent Size)

- 0-1 sq. deg.
- 1-2 sq. deg.
- 2-5 sq. deg.
- 5-15 sq. deg.
- 15-100 sq. deg.

Sites Referenced:

1 - Pointe du Raz
2 - Castel Meur
3 - Kergulan
4 - Castel Coz
5 - Lostmarc'h
6 - Pointe du Toulinguet
7 - Roc'h Nivelen
8 - Kermorvan
9 - Île d'Yoc'h
10 - Kastell Ac'h
11 - Beg Monom
12 - Bretouare
13 - St. Michael's Mount
14 - Treryn Dinas
15 - Carn Les Boel
16 - Maen Castle
17 - Kenidjack Castle
18 - Trereen Dinas
19 - Shipman Head
20 - Burnt Hill
21 - Giants Castle



Simulation 30

Max speed: 9 kts.
Lmark. type: Nat. Proms.
Estimation: No misest.
Starting time: +2 hrs.
Result: Qualified Success

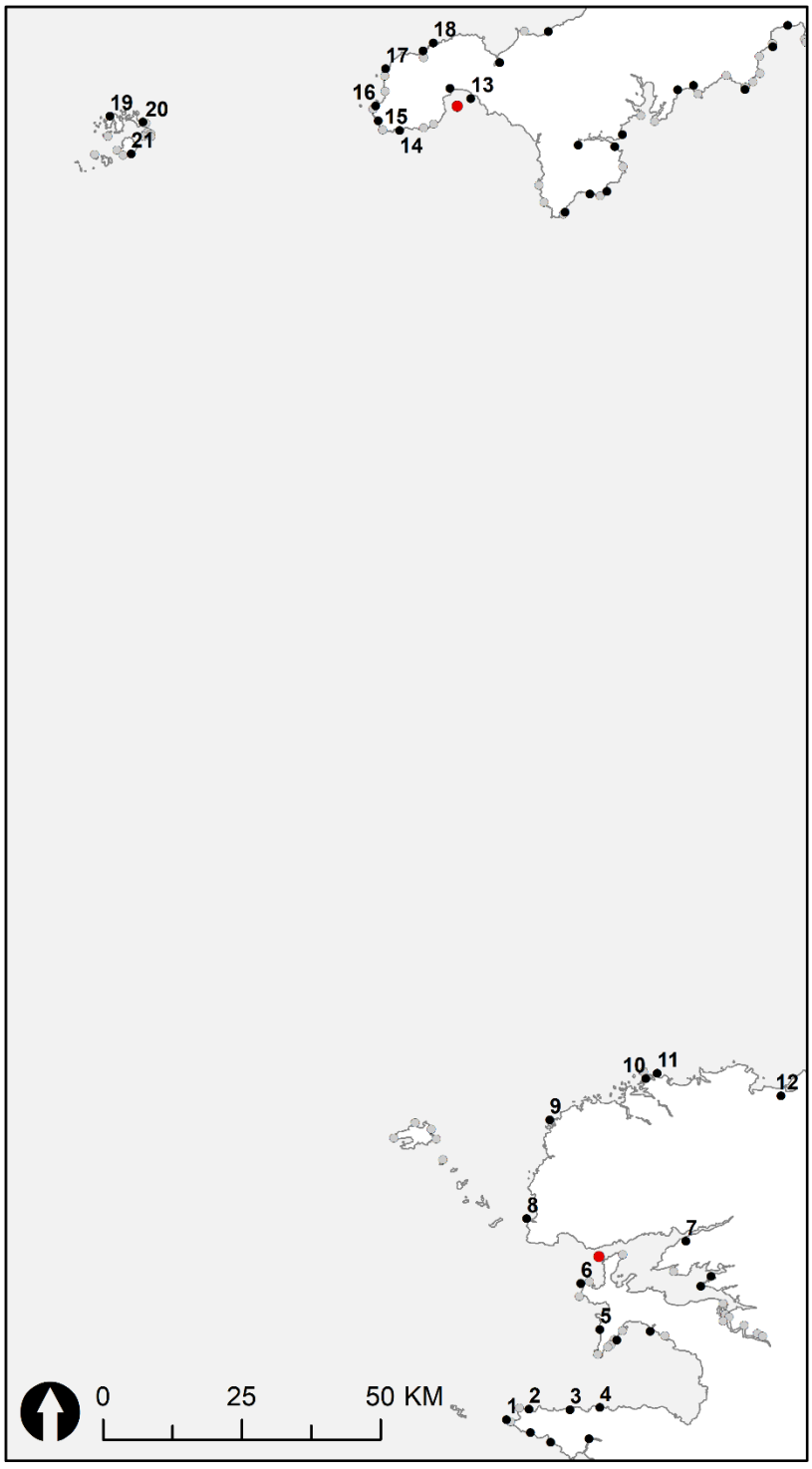
- Coastal Nodes
- Archaeological Sites
- Natural Prominences
- Simulation Track

Sightlines (by Apparent Size)

- 0-1 sq. deg.
- 1-2 sq. deg.
- 2-5 sq. deg.
- 5-15 sq. deg.
- 15-100 sq. deg.

Sites Referenced:

1 - Pointe du Raz
2 - Castel Meur
3 - Kergulan
4 - Castel Coz
5 - Lostmarc'h
6 - Pointe du Toulinguet
7 - Roc'h Nivelen
8 - Kermorvan
9 - Île d'Yoc'h
10 - Kastell Ac'h
11 - Beg Monom
12 - Bretouare
13 - St. Michael's Mount
14 - Treryn Dinas
15 - Carn Les Boel
16 - Maen Castle
17 - Kenidjack Castle
18 - Trereen Dinas
19 - Shipman Head
20 - Burnt Hill
21 - Giants Castle



Simulation 31

Max speed: 5 kts.
Lmark. type: Arch. Sites
Estimation: Up to 50%
Starting time: -2 hrs.
Result: Failure

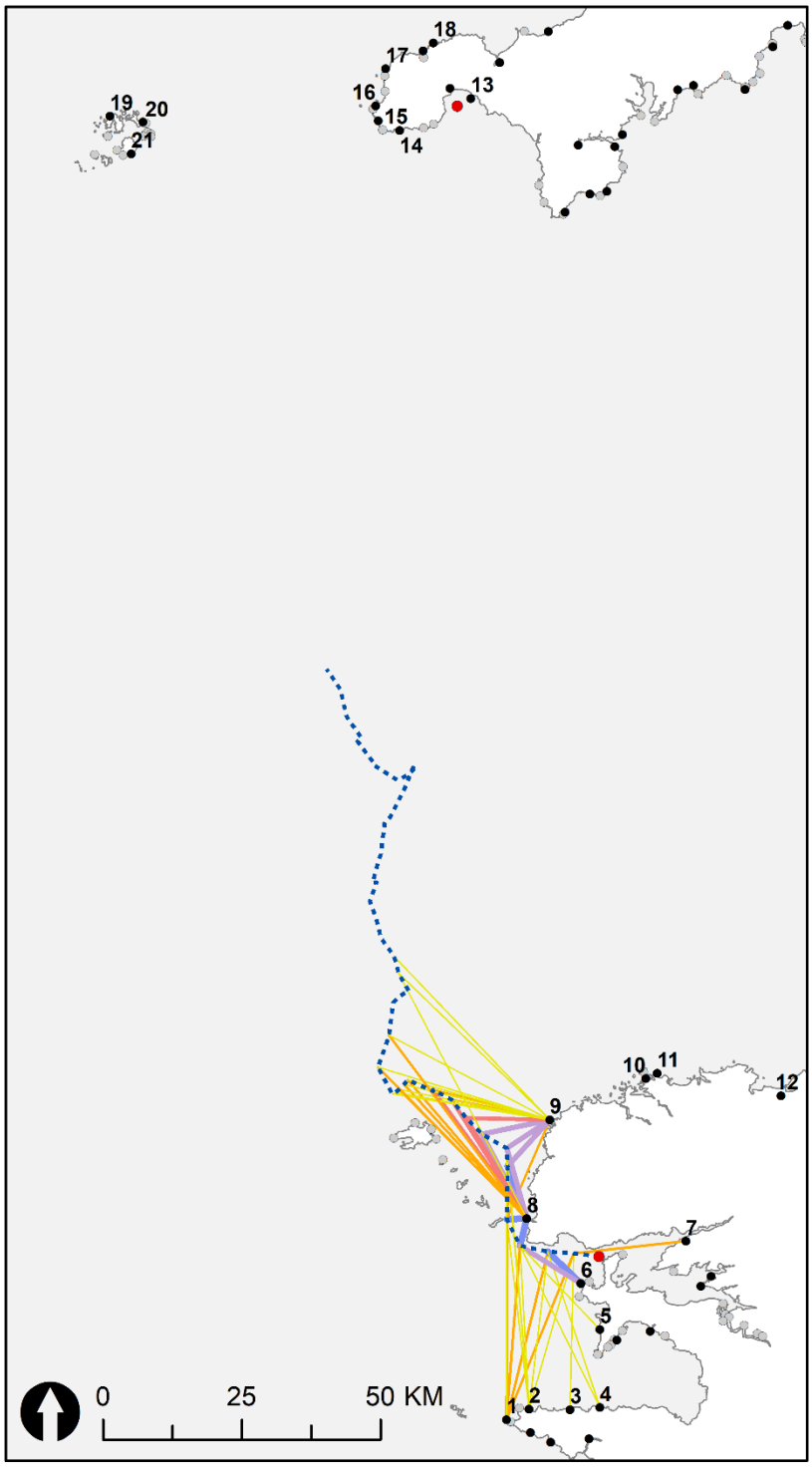
- Coastal Nodes
- Archaeological Sites
- Natural Prominences
- Simulation Track

Sightlines (by Apparent Size)

- 0-1 sq. deg.
- 1-2 sq. deg.
- 2-5 sq. deg.
- 5-15 sq. deg.
- 15-100 sq. deg.

Sites Referenced:

1 - Pointe du Raz
2 - Castel Meur
3 - Kergulan
4 - Castel Coz
5 - Lostmarc'h
6 - Pointe du Toulinguet
7 - Roc'h Nivelen
8 - Kermorvan
9 - Île d'Yoc'h
10 - Kastell Ac'h
11 - Beg Monom
12 - Bretouare
13 - St. Michael's Mount
14 - Treryn Dinas
15 - Carn Les Boel
16 - Maen Castle
17 - Kenidjack Castle
18 - Trereen Dinas
19 - Shipman Head
20 - Burnt Hill
21 - Giants Castle



Simulation 32

Max speed: 5 kts.
Lmark. type: Arch. Sites
Estimation: Up to 50%
Starting time: -1 hrs.
Result: Failure

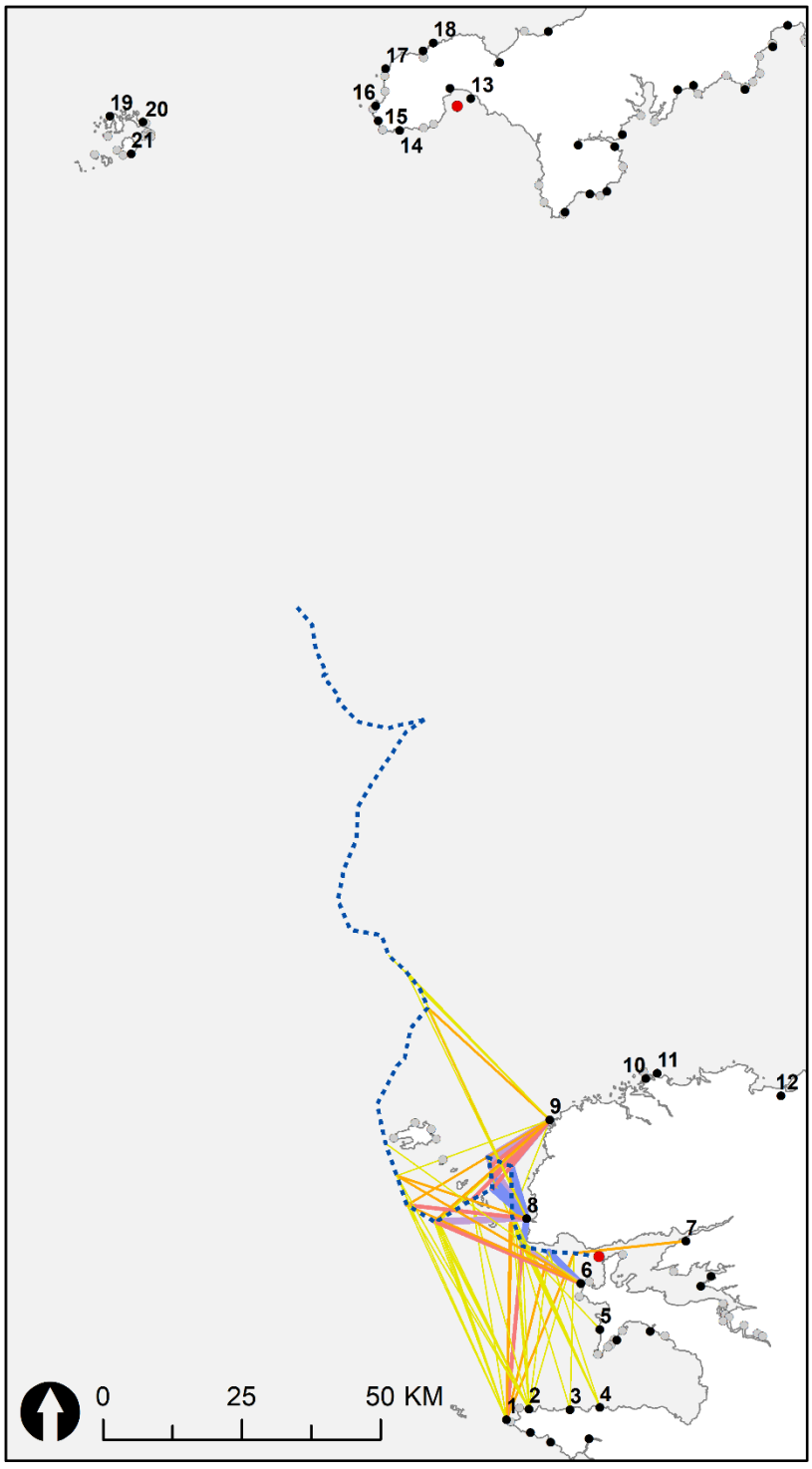
- Coastal Nodes
- Archaeological Sites
- Natural Prominences
- Simulation Track

Sightlines (by Apparent Size)

- 0-1 sq. deg.
- 1-2 sq. deg.
- 2-5 sq. deg.
- 5-15 sq. deg.
- 15-100 sq. deg.

Sites Referenced:

1 - Pointe du Raz
2 - Castel Meur
3 - Kergulan
4 - Castel Coz
5 - Lostmarc'h
6 - Pointe du Toulinguet
7 - Roc'h Nivelen
8 - Kermorvan
9 - Île d'Yoc'h
10 - Kastell Ac'h
11 - Beg Monom
12 - Bretouare
13 - St. Michael's Mount
14 - Treryn Dinas
15 - Carn Les Boel
16 - Maen Castle
17 - Kenidjack Castle
18 - Trereen Dinas
19 - Shipman Head
20 - Burnt Hill
21 - Giants Castle



Simulation 33

Max speed: 5 kts.
Lmark. type: Arch. Sites
Estimation: Up to 50%
Starting time: +0 hrs.
Result: Failure

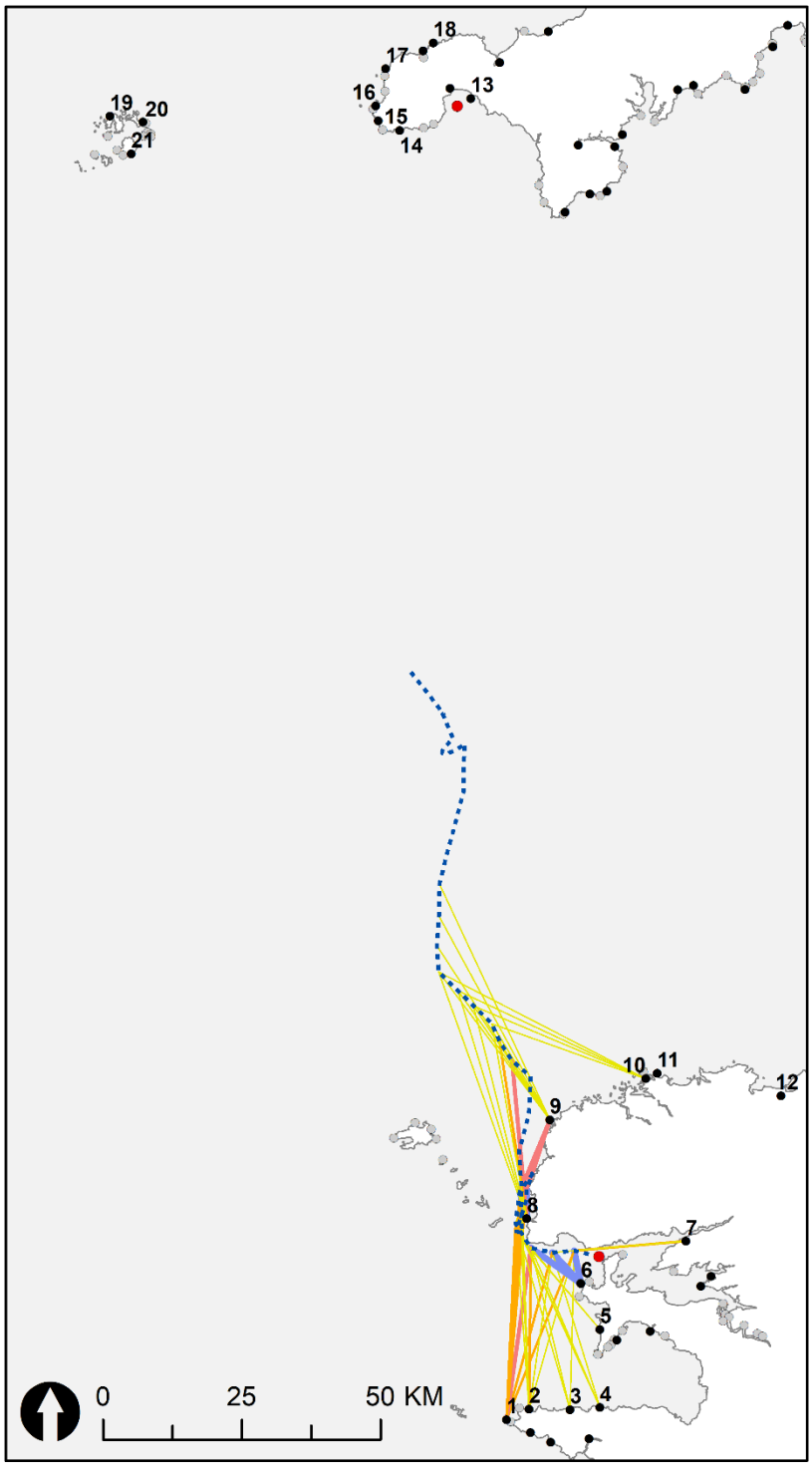
- Coastal Nodes
- Archaeological Sites
- Natural Prominences
- Simulation Track

Sightlines (by Apparent Size)

- 0-1 sq. deg.
- 1-2 sq. deg.
- 2-5 sq. deg.
- 5-15 sq. deg.
- 15-100 sq. deg.

Sites Referenced:

1 - Pointe du Raz
2 - Castel Meur
3 - Kergulan
4 - Castel Coz
5 - Lostmarc'h
6 - Pointe du Toulinguet
7 - Roc'h Nivelen
8 - Kermorvan
9 - Île d'Yoc'h
10 - Kastell Ac'h
11 - Beg Monom
12 - Bretouare
13 - St. Michael's Mount
14 - Treryn Dinas
15 - Carn Les Boel
16 - Maen Castle
17 - Kenidjack Castle
18 - Trereen Dinas
19 - Shipman Head
20 - Burnt Hill
21 - Giants Castle



Simulation 34

Max speed: 5 kts.
Lmark. type: Arch. Sites
Estimation: Up to 50%
Starting time: +1 hrs.
Result: Failure

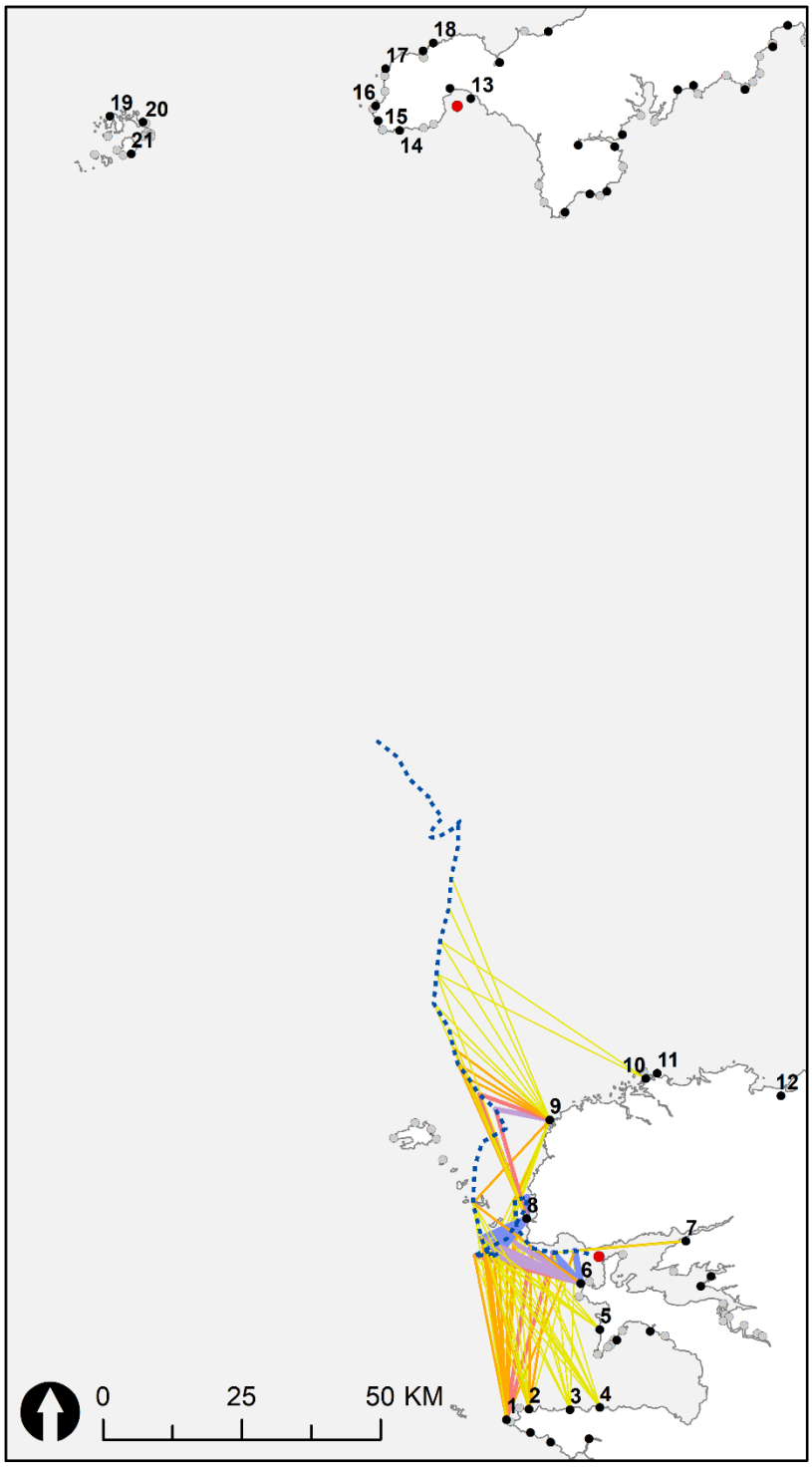
- Coastal Nodes
- Archaeological Sites
- Natural Prominences
- Simulation Track

Sightlines (by Apparent Size)

- 0-1 sq. deg.
- 1-2 sq. deg.
- 2-5 sq. deg.
- 5-15 sq. deg.
- 15-100 sq. deg.

Sites Referenced:

1 - Pointe du Raz
2 - Castel Meur
3 - Kergulan
4 - Castel Coz
5 - Lostmarc'h
6 - Pointe du Toulinguet
7 - Roc'h Nivelen
8 - Kermorvan
9 - Île d'Yoc'h
10 - Kastell Ac'h
11 - Beg Monom
12 - Bretouare
13 - St. Michael's Mount
14 - Treryn Dinas
15 - Carn Les Boel
16 - Maen Castle
17 - Kenidjack Castle
18 - Trereen Dinas
19 - Shipman Head
20 - Burnt Hill
21 - Giants Castle



Simulation 35

Max speed: 5 kts.
Lmark. type: Arch. Sites
Estimation: Up to 50%
Starting time: +2 hrs.
Result: Failure

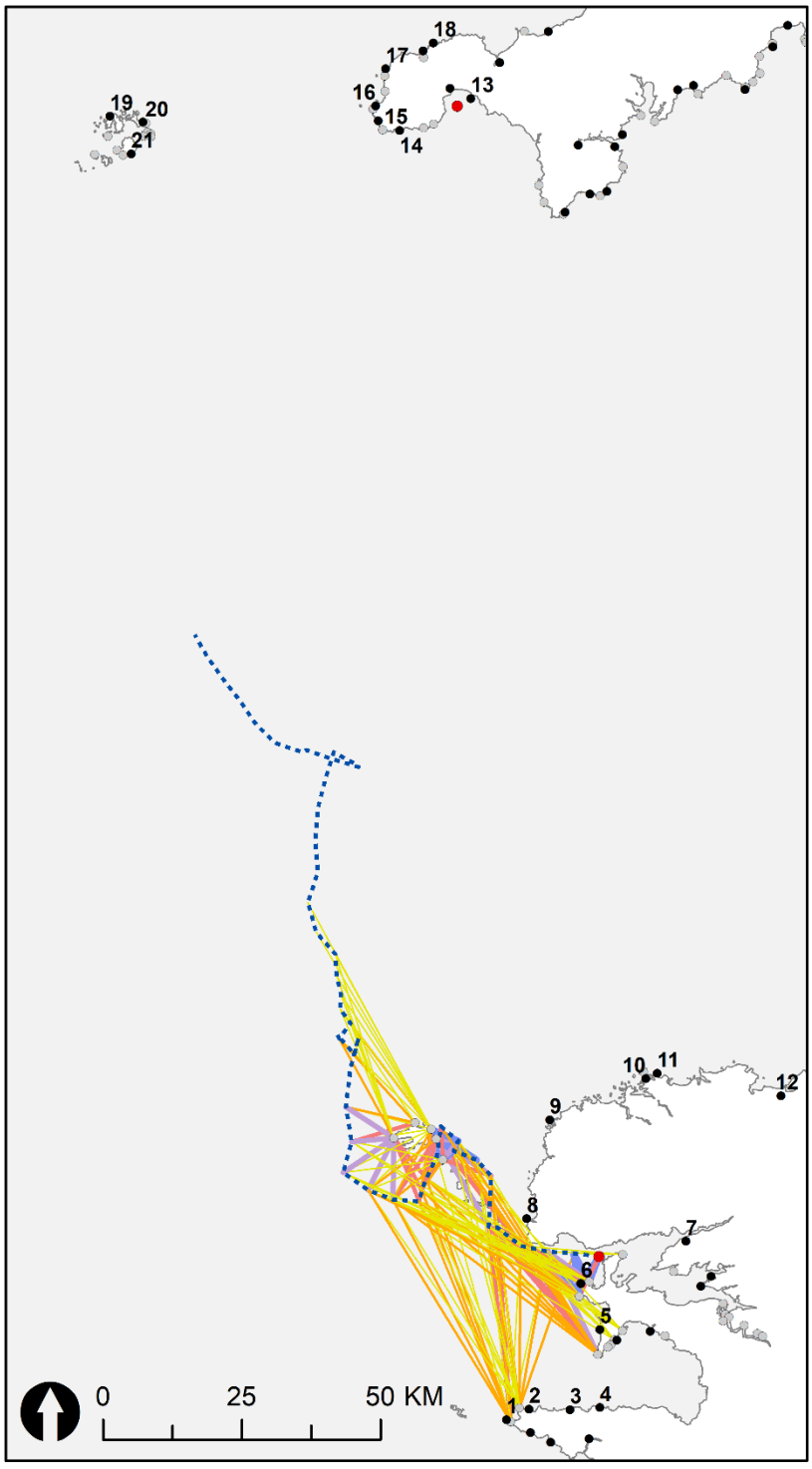
- Coastal Nodes
- Archaeological Sites
- Natural Prominences
- Simulation Track

Sightlines (by Apparent Size)

- 0-1 sq. deg.
- 1-2 sq. deg.
- 2-5 sq. deg.
- 5-15 sq. deg.
- 15-100 sq. deg.

Sites Referenced:

1 - Pointe du Raz
2 - Castel Meur
3 - Kergulan
4 - Castel Coz
5 - Lostmarc'h
6 - Pointe du Toulinguet
7 - Roc'h Nivelen
8 - Kermorvan
9 - Île d'Yoc'h
10 - Kastell Ac'h
11 - Beg Monom
12 - Bretouare
13 - St. Michael's Mount
14 - Treryn Dinas
15 - Carn Les Boel
16 - Maen Castle
17 - Kenidjack Castle
18 - Trereen Dinas
19 - Shipman Head
20 - Burnt Hill
21 - Giants Castle



Simulation 36

Max speed: 5 kts.
Lmark. type: Nat. Proms.
Estimation: Up to 50%
Starting time: -2 hrs.
Result: Failure

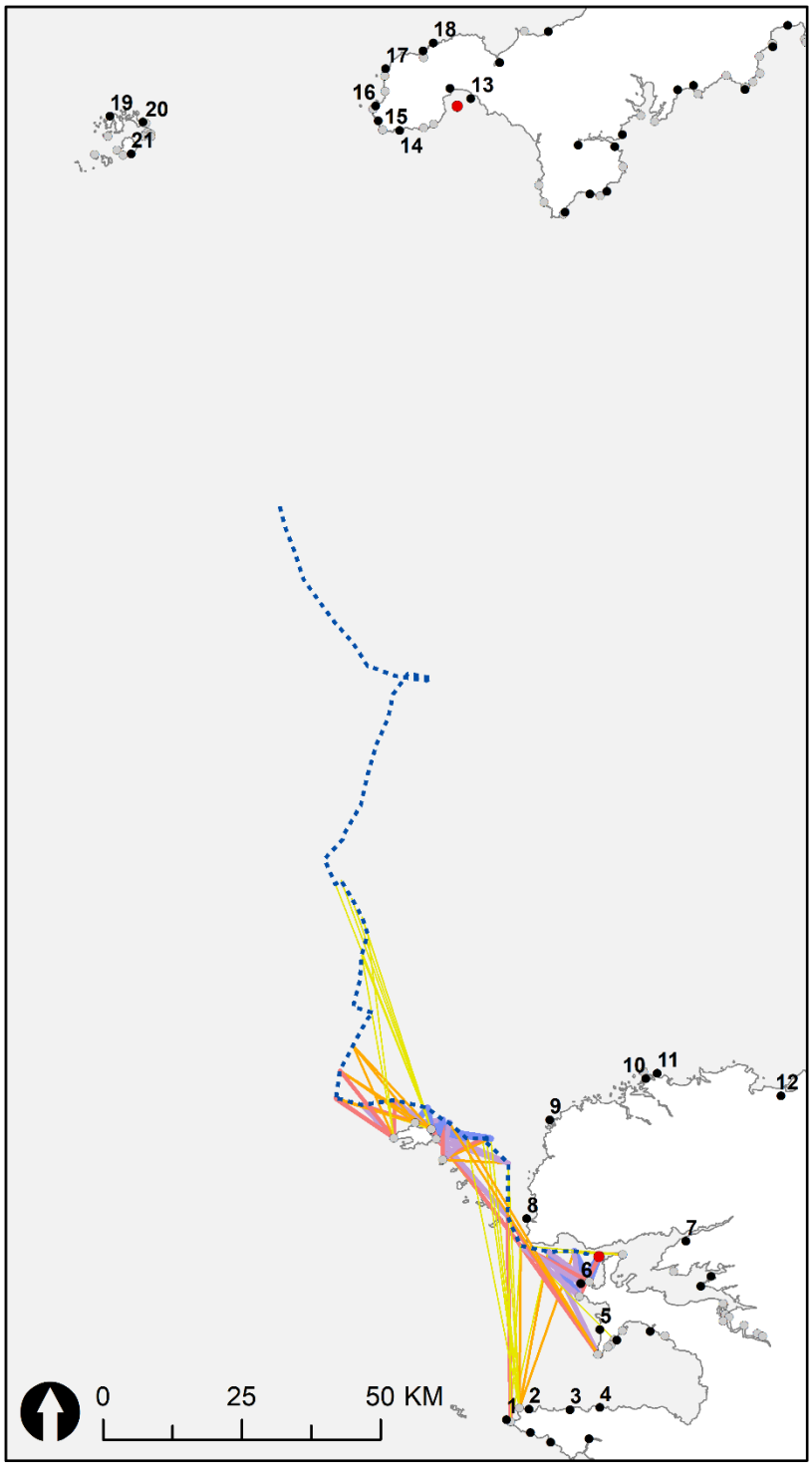
- Coastal Nodes
- Archaeological Sites
- Natural Prominences
- Simulation Track

Sightlines (by Apparent Size)

- 0-1 sq. deg.
- 1-2 sq. deg.
- 2-5 sq. deg.
- 5-15 sq. deg.
- 15-100 sq. deg.

Sites Referenced:

1 - Pointe du Raz
2 - Castel Meur
3 - Kergulan
4 - Castel Coz
5 - Lostmarc'h
6 - Pointe du Toulinguet
7 - Roc'h Nivelen
8 - Kermorvan
9 - Île d'Yoc'h
10 - Kastell Ac'h
11 - Beg Monom
12 - Bretouare
13 - St. Michael's Mount
14 - Treryn Dinas
15 - Carn Les Boel
16 - Maen Castle
17 - Kenidjack Castle
18 - Trereen Dinas
19 - Shipman Head
20 - Burnt Hill
21 - Giants Castle



Simulation 37

Max speed: 5 kts.
Lmark. type: Nat. Proms.
Estimation: Up to 50%
Starting time: -1 hrs.
Result: Failure

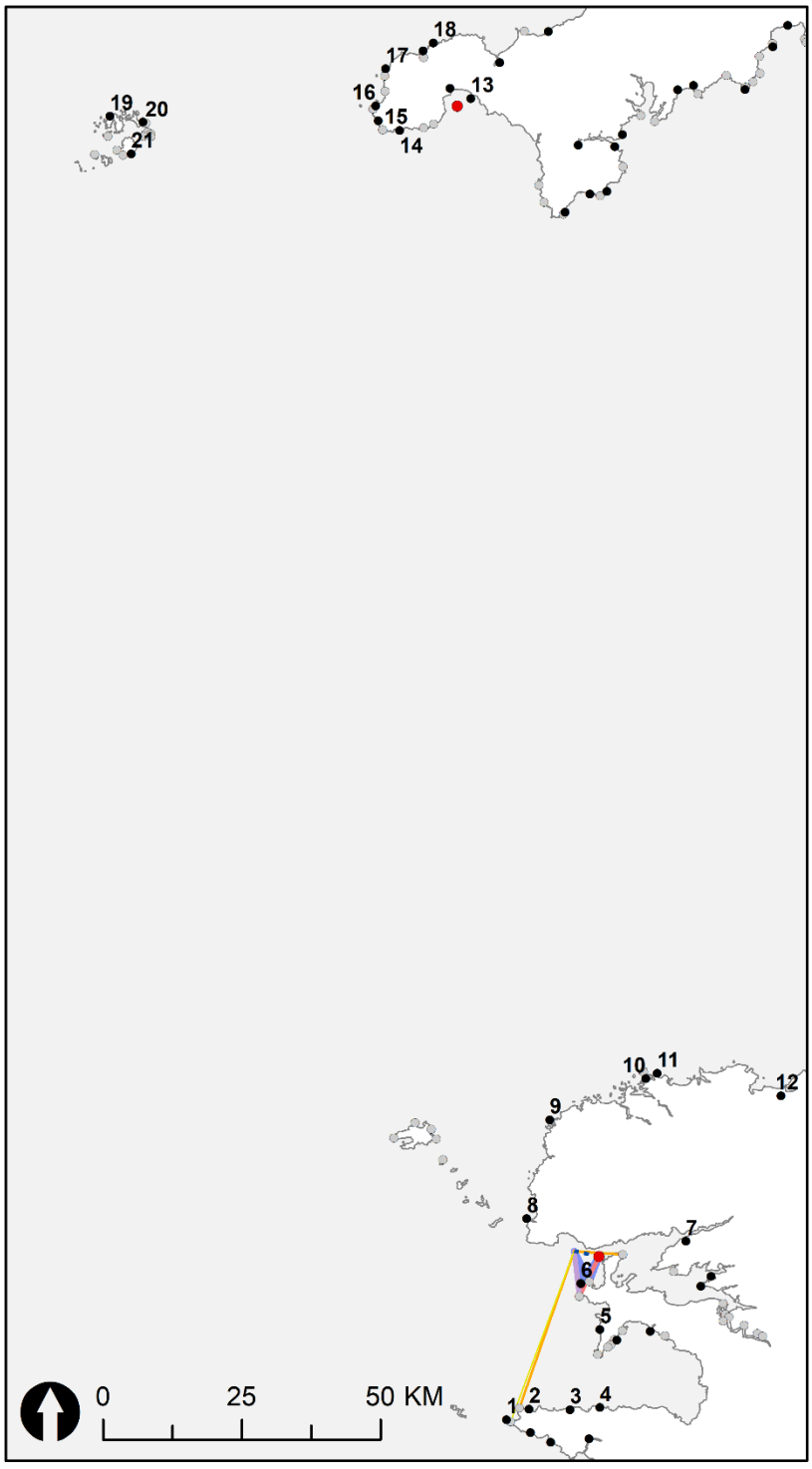
- Coastal Nodes
- Archaeological Sites
- Natural Prominences
- Simulation Track

Sightlines (by Apparent Size)

- 0-1 sq. deg.
- 1-2 sq. deg.
- 2-5 sq. deg.
- 5-15 sq. deg.
- 15-100 sq. deg.

Sites Referenced:

1 - Pointe du Raz
2 - Castel Meur
3 - Kergulan
4 - Castel Coz
5 - Lostmarc'h
6 - Pointe du Toulinguet
7 - Roc'h Nivelen
8 - Kermorvan
9 - Île d'Yoc'h
10 - Kastell Ac'h
11 - Beg Monom
12 - Bretouare
13 - St. Michael's Mount
14 - Treryn Dinas
15 - Carn Les Boel
16 - Maen Castle
17 - Kenidjack Castle
18 - Trereen Dinas
19 - Shipman Head
20 - Burnt Hill
21 - Giants Castle



Simulation 38

Max speed: 5 kts.
Lmark. type: Nat. Proms.
Estimation: Up to 50%
Starting time: +0 hrs.
Result: Failure

- Coastal Nodes
- Archaeological Sites
- Natural Prominences
- Simulation Track

Sightlines (by Apparent Size)

- 0-1 sq. deg.
- 1-2 sq. deg.
- 2-5 sq. deg.
- 5-15 sq. deg.
- 15-100 sq. deg.

Sites Referenced:

1 - Pointe du Raz
2 - Castel Meur
3 - Kergulan
4 - Castel Coz
5 - Lostmarc'h
6 - Pointe du Toulinguet
7 - Roc'h Nivelen
8 - Kermorvan
9 - Île d'Yoc'h
10 - Kastell Ac'h
11 - Beg Monom
12 - Bretouare
13 - St. Michael's Mount
14 - Treryn Dinas
15 - Carn Les Boel
16 - Maen Castle
17 - Kenidjack Castle
18 - Trereen Dinas
19 - Shipman Head
20 - Burnt Hill
21 - Giants Castle